

## AN ABSTRACT OF THE DISSERTATION OF

Jonathan C. Huffman for the degree of Doctor of Philosophy in Civil Engineering presented on October 23, 2020.

Title: Reliability-based Serviceability Limit State Design Procedures for Shallow Foundations.

Abstract approved:

---

Armin W. Stuedlein

Reliability-based geotechnical foundation design focusses on soil and structure analysis that meets necessary safety, performance and/or serviceability criteria, calibrated based on probabilistic analyses and an accepted level of risk. As the civil engineering community seeks to better harmonize geotechnical and structural design methodologies, reliability-based design is being incorporated more into geotechnical limit states analysis, for example ultimate limit state (ULS; e.g., bearing capacity) and serviceability limit state (SLS; e.g., settlement) foundation design. However, additional work is required to develop robust design procedures that can be easily implemented in practice.

The main objective of this study is to advance the underlying knowledge of reliability-based serviceability limit state (RBSLS) design for shallow foundations. Particularly, this study focusses on foundations supported on plastic, fine-grained soil (e.g., clay) and aggregate pier-improved plastic, fine-grained soil.

As part of this work, two new RBLS models were developed for footings supported on clay and aggregate pier-reinforced clay. Both SLS models were developed and calibrated using probabilistic analyses and databases compiled from the literature for high-quality footing loading tests with immediate (undrained) settlement. The new models capture the nonlinear bearing pressure-displacement behavior that is typical of footings on plastic, fine-grained soils, even at relatively small (e.g., service-level) loads. A calibrated, lumped load and resistance factor is also introduced for both models that can be easily implemented in conjunction with a pre-selected level of risk and/or reliability index.

The study continues with further discussion of calibration procedures, with focus on the impact of the correlation structure of individual load-displacement parameters and suitable factors to account for the propagation of model error and other sources of uncertainty. This phase of work also focused on re-evaluating the calibrated SLS model for footings supported on aggregate pier-reinforced clay and providing an independent evaluation using additional full-scale loading tests completed at the Oregon State University geotechnical engineering field research site (OSU GEFRS).

Finally, the calibrated load-displacement model for a footing supported on fine-grained soil was used to develop a non-linear soil-spring model within the computer program OpenSees. The foundation spring model was used in combination with a previously developed 3-story steel moment frame building model to complete a series of Monte Carlo simulations with varying levels of soil variability to investigate the role of both inherent soil variability and soil-structure interaction on foundation and structural performance.

©Copyright by Jonathan C. Huffman  
October 23, 2020  
All Rights Reserved

Reliability-based Serviceability Limit State Design Procedures for Shallow  
Foundations

by  
Jonathan C. Huffman

A DISSERTATION

submitted to

Oregon State University

in partial fulfillment of  
the requirements for the  
degree of

Doctor of Philosophy

Presented October 23, 2020  
Commencement June 2021

Doctor of Philosophy dissertation of Jonathan C. Huffman presented on  
October 23, 2020

APPROVED:

---

Major Professor, representing Civil Engineering

---

Head of the School of Civil and Construction Engineering

---

Dean of the Graduate School

I understand that my dissertation will become part of the permanent collection of Oregon State University libraries. My signature below authorizes release of my dissertation to any reader upon request.

---

Jonathan C. Huffman, Author

## ACKNOWLEDGEMENTS

This journey took quite a bit longer than I originally anticipated. So, first and foremost, I thank my advisor, Dr. Armin W. Stuedlein, for sticking through this with me. Armin continuously provided encouragement, inspirational thoughts, considerate review, and gentle to moderate prodding as the time suited to help get me through. I joined Armin as one of his first PhD students and will likely be his longest tenured student considering this has taken more than 10 years to complete. So, Armin, I hope you do not miss me too much and still find meaning in academia now that I have moved on.

I would also like to express sincere appreciation to the members of my committee that include Dr. Andre R. Barbosa, Dr. Ben Leshchinsky, Dr. Erdem Coleri, and Dr. Yuan Jiang for providing thoughtful comments and review. Special thanks also go to Dr. Barbosa and graduated members of his research group that include Dr. Andre Belejo and Dr. Mohammad Shafiqul Alam for providing significant collaboration for the structural analysis component documented in Chapter 7 of this dissertation.

I would also like to thank graduated members of the Stuedlein Research Group that include Dr. Andrew Strahler, Mr. John Martin, Dr. Seth Reddy, and Dr. Tadesse Meskele; each of whom provided collaboration, review, discussion, or some combination thereof that helped with the development of this dissertation.

My coworkers at Foundation Engineering, Inc. deserve thanks for sometimes understanding when I was less available. Although, it is within reason that they questioned if I was “really” getting a PhD after I continued to use the excuse for well

over 5 years. I also could not have pursued this goal without being gainfully employed for the duration.

And, of course, all the thanks and all the love to my wonderful, wonderful, wonderful wife, Rebecca. We both went back to school at the same time, but she became Dr. Huffman long before me. Thanks for understanding; thanks for humoring me; thanks for keeping me grounded and humble as needed; thanks for your sacrifice; and thanks for continuing this journey with me. You are an amazing wife, mother, and all-around person. I'm blessed to have you, Henry, and Eloise.

## CONTRIBUTION OF AUTHORS

Dr. Armin W. Stuedlein provided review, edits, and commentary and is listed as second or third author on journal papers that comprise Chapters 4, 5 and 6 of this dissertation. Dr. Stuedlein will also be included as a co-author on future journal papers that are developed from the research documented in Chapter 7.

Dr. Andrew Strahler is included as second author for the journal paper that comprises Chapter 5 of this dissertation. Dr. Strahler's contribution included vetting and compiling a load test database as part of his master's thesis, which was later used for data fitting and probabilistic analysis in Chapter 5.

Mr. John Martin is included as second author for the journal paper that comprises Chapter 6 of this dissertation. Mr. Martin's contribution included leading the effort to document soil conditions and complete new loading tests that were used for independent evaluation of the revised RBSLS model in Chapter 6.

Dr. Andre Barbosa and his previous graduate students, Dr. Andre Belejo and Dr. Mohammad Shafiqul Alam, provided collaboration for the structural analysis component documented in Chapter 7. They will be included as co-authors for upcoming journal papers that are developed from this work.



# TABLE OF CONTENTS

	<u>Page</u>
1 INTRODUCTION .....	1
1.1 Statement of Problem.....	1
1.2 Purpose and Scope .....	3
1.3 Organization of Dissertation.....	4
2 LITERATURE REVIEW .....	9
2.1 Introduction.....	9
2.2 Limit State Design .....	11
2.2.1 Ultimate Limit State (ULS) Design .....	12
2.2.1.1 Bearing Capacity of Spread Footings .....	13
2.2.1.2 Estimation of Bearing Capacity Based on Footing Loading Tests .....	20
2.2.1.3 Bearing Capacity of Footings on Aggregate Pier-Improved Soil.....	21
2.2.2 Serviceability Limit State (SLS) Design.....	30
2.2.2.1 Immediate (Distortion) Settlement of Spread Footings .....	34
2.2.2.2 Distortion Settlement of Footings on Aggregate Pier-Improved Soil .....	38
2.2.2.3 Nonlinear Models for Bearing Pressure-Displacement Response .....	43
2.3 Reliability Based Design.....	46
2.3.1 Performance Function and Statistical Characterization .....	48
2.3.2 Reliability Index.....	49
2.3.3 Spatial Variability and Random Field Theory .....	51
2.3.4 Correlation of Soil and Model Parameters.....	54
2.3.4.1 General Discussion and Correlation Coefficients.....	54

## TABLE OF CONTENTS (Continued)

	<u>Page</u>
2.3.4.2 Copula Functions .....	54
2.3.5 Soil-Structure Interaction.....	58
2.3.5.1 General Discussion .....	58
2.3.5.2 Soil-Structure Interaction within RBD Framework.....	62
2.3.6 Calibration of Limit State Load and Resistance Factors using RBD.....	64
2.3.6.1 Closed-Form Solutions .....	64
2.3.6.2 Monte Carlo Simulations .....	66
2.4 Summary of Literature Review.....	67
2.4.1 Summary.....	67
2.4.2 Outstanding Issues .....	67
<b>3 RESEARCH OBJECTIVES AND PROGRAM.....</b>	<b>70</b>
3.1 Research Objectives.....	70
3.2 Research Program .....	71
<b>4 RELIABILITY-BASED SERVICEABILITY LIMIT STATE DESIGN OF SPREAD FOOTINGS ON AGGREGATE PIER REINFORCED CLAY.....</b>	<b>73</b>
4.1 Abstract.....	74
4.2 Introduction.....	75
4.3 Load Test Database and Selected Bearing Capacity Model .....	77
4.4 Serviceability Limit State Design Model.....	79
4.5 Monte Carlo-Based Reliability Simulations .....	84
4.5.1 Model Selection and Resistance Model Parameter.....	84

## TABLE OF CONTENTS (Continued)

	<u>Page</u>
4.5.2 Bearing Pressure-Displacement Model Parameter Correlation and Simulation .....	87
4.5.3 Assessment and Incorporation of Lower-Bound Capacity .....	93
4.5.4 Characterization of Allowable Displacement and Applied Bearing Pressure .....	94
4.5.5 Reliability Simulations and LRFD Calibration.....	96
4.6 Application of the Reliability Calibrations and Discussion.....	101
4.7 Conclusion .....	104
4.8 Acknowledgements.....	105
4.9 Supplemental Data .....	106
4.10 References.....	106
5 RELIABILITY-BASED SERVICEABILITY LIMIT STATE DESIGN FOR IMMEDIATE SETTLEMENT OF SPREAD FOOTINGS ON CLAY .....	109
5.1 Abstract.....	110
5.2 Introduction.....	111
5.3 Load Test Database and ULS Bearing Capacity Model .....	114
5.4 Bearing Pressure-Displacement Model.....	119
5.5 Application of Bearing Pressure-Displacement Model to Reliability-Based Design .....	124
5.6 Simulation-Based Serviceability Limit State Design Calibrations.....	126
5.6.1 Characterization of Resistance Parameters .....	126
5.6.2 Resistance Parameter Dependence and Copula Analysis .....	129
5.6.3 Assessment of Lower-Bound Resistance.....	133

## TABLE OF CONTENTS (Continued)

	<u>Page</u>
5.6.4 Characterization of Applied Bearing Pressure.....	135
5.6.5 Characterization of Allowable Displacement .....	135
5.6.6 Reliability Simulations and Lumped Factor Calibration .....	137
5.6.7 Comparison of MCS Results and Closed-Form Model .....	142
5.7 Application of the Reliability Calibrations .....	144
5.7.1 Design Example .....	144
5.7.2 Discussion .....	146
5.8 Summary .....	148
5.9 References .....	150
6 CALIBRATION AND ASSESSMENT OF RELIABILITY-BASED SERVICEABILITY LIMIT STATE PROCEDURES FOR FOUNDATION ENGINEERING .....	155
6.1 Abstract .....	156
6.2 Introduction .....	157
6.3 Review of RBSLS Framework and Selected Procedure .....	158
6.3.1 Selected Ultimate and Serviceability Limit State Models .....	158
6.3.2 Monte Carlo Simulation-based Performance Function Simulation .....	161
6.4 Factors Affecting Calibration of RBSLS Models .....	163
6.4.1 Assessment of Correlation Structure model and Impact on Reliability...163	
6.4.1.1 Fitting of Copulas for Monte Carlo Simulation of Bivariate $q$ - $\delta$ Model Parameters .....	163
6.4.1.2 Impact of Correlation Structure Model on Calibrated Load and Resistance Factor .....	167

## TABLE OF CONTENTS (Continued)

	<u>Page</u>
6.4.1.3 Impact of Correlation Structure Model on Allowable Bearing Pressure, $q_{all}$ .....	171
6.4.2 Assessment of Normalization Protocol for Bearing Pressure-Displacement Curves and Impact on Computed Reliability.....	172
6.4.2.1 Impact of Normalization Protocol on Scatter in $q$ - $\delta$ Curves.....	172
6.4.2.2 Decision Framework for Selection of Appropriate Normalization Protocol.....	175
6.4.2.3 Comparison of Previous and Updated RBSLS Procedure.....	182
6.5 Assessment of RBSLS Models.....	184
6.5.1 Need to Re-visit and Assess RBSLS Models.....	184
6.5.2 New Full-Scale Loading Test Data: Test Site and Subsurface Conditions.....	184
6.5.3 Comparison of Original and Revised Models to Footing Performance...188	
6.5.4 Implications for Future RBSLS Procedure.....	191
6.6 Summary and Conclusions.....	192
6.7 References.....	193
<b>7 RELIABILITY-BASED ASSESSMENT OF FOUNDATION AND STRUCTURE PERFORMANCE WITH SPATIALLY VARIABLE SOIL.....</b>	<b>195</b>
7.1 Introduction.....	195
7.2 Building and Soil Model.....	201
7.2.1 Building Model and Foundations.....	201
7.2.1.1 SAC Building Model.....	201
7.2.1.2 Foundations.....	204

## TABLE OF CONTENTS (Continued)

	<u>Page</u>
7.2.2 Nonlinear Soil-Foundation Springs .....	206
7.2.2.1 Vertical and Rotational Resistance .....	206
7.2.2.2 Horizontal Resistance .....	213
7.2.3 Soil Spatial Variability and Random Field Model.....	215
7.2.4 Inter-site vs Intra-site Bearing Pressure-Displacement Response .....	219
7.3 Reliability Analysis and Monte Carlo Simulations .....	224
7.3.1 Case 1: Soil-Foundation Response (Inter-site Soil Parameters).....	229
7.3.2 Case 2: Soil-Foundation Response (Intra-site Soil Parameters).....	242
7.3.3 Case 3: Soil-Foundation-Structure Response (Inter-site Soil Parameters) .....	252
7.3.3.1 Soil-Foundation Performance .....	253
7.3.3.2 Structural Performance .....	261
7.3.4 Case 4: Soil-Foundation-Structure Response (Intra-site Soil Parameters) .....	298
7.3.4.1 Soil-Foundation Performance .....	298
7.3.4.2 Structural Performance .....	307
7.4 Summary and Conclusions .....	315
7.5 References.....	321
8 SUMMARY AND CONCLUSIONS .....	328
8.1 Summary of Work Completed.....	328
8.1.1 Reliability-based SLS Design of Spread Footings on Aggregate Pier Reinforced Clay .....	328

## TABLE OF CONTENTS (Continued)

	<u>Page</u>
8.1.2 Reliability-based SLS Design for Immediate Settlement of Spread Footings on Clay .....	330
8.1.3 Calibration and Assessment of Reliability-based SLS Procedures for Foundation Engineering.....	331
8.1.4 Reliability-based Assessment of Foundation and Structure Performance with Spatially Variable Soil .....	332
8.2 Conclusions Drawn from this Work .....	333
8.2.1 Reliability-based SLS Design of Spread Footings on Aggregate Pier Reinforced Clay .....	333
8.2.2 Reliability-based SLS Design for Immediate Settlement of Spread Footings on Clay .....	334
8.2.3 Calibration and Assessment of Reliability-based SLS Procedures for Foundation Engineering.....	336
8.2.4 Reliability-based Assessment of Foundation and Structure Performance with Spatially Variable Soil .....	337
8.3 Suggestions for Future Research .....	340
COMPLETE LIST OF REFERENCES.....	343
APPENDIX A: CHAPTER 4 SUPPLEMENTAL DATA .....	357
APPENDIX B: EXAMPLE CODE .....	379
APPENDIX C: TABULATED FOOTING RESPONSE FROM OPENSEES ANALYSIS.....	442

## LIST OF FIGURES

<u>Figure</u>	<u>Page</u>
Chapter 2	
2.1 Models of bearing capacity failure and shear plane development in soil (adapted from Das 1984, originally from Vesic 1973).....	15
2.2 Typical shallow footing with notes on design assumptions based on Terzaghi (1943) model (adapted from Bowles 1988).....	17
2.3 Modes of failure for footings supported on single aggregate piers: (a) bulging failure, (b) shear failure, and (c) punching failure (adapted from Barksdale and Bachus 1983) .....	22
2.4 Modes of failure for footings supported on multiple aggregate piers: (a) bulging failure and (b) punching failure (adapted from Barksdale and Bachus 1983)....	24
2.5 Schematic showing cavity expansion and shear failure plane approximation used for estimating the ultimate bearing resistance of footings supported on multiple aggregate piers (from Barksdale and Bachus 1983) .....	26
2.6 Foundation with typical aggregate pier layout and idealized unit cell model (adapted from Barksdale and Bachus 1983) .....	27
2.7 Schematic of total settlement, differential settlement, and angular distortion across a building area (adapted from Grant et al. 1974).....	31
2.8 Stress distribution for estimating displacement from foundation load, $P$ , for an aggregate pier-supported footing (adapted from Sehn and Blackburn 2008).....	41
2.9 Hyperbolic load-displacement curve and general equation (adapted from Duncan and Mokwa 2001) .....	44
2.10 Example of hyperbolic and power law functions fit to normalized footing loading test data reported by Stuedlein and Holtz (2013, 2014).....	46
2.11 Generalized concept of load and resistance (capacity) probability distribution with reliability-based design (adapted from Kulhawy and Phoon 2006) .....	47
2.12 Probability density of performance function, $P$ , with reliability index, $\beta$ (adapted from Allen et al. 2005).....	50
2.13 Example of soil spatial variability with depth, $z$ , for soil layer $j$ (from Phoon and Kulhawy 1999a).....	52



## LIST OF FIGURES (Continued)

<u>Figure</u>	<u>Page</u>
2.14 Example of estimate for the scale of fluctuation, $\delta$ , with depth for a soil property with trend function, $t(z)$ (adapted from Phoon and Kulhawy 1999a, originally from Spry et al. 1988) .....	54
2.15 Examples of simulated values with bivariate correlation structure based on different copula functions (adapted from Bhat and Eluru 2009) .....	56
2.16 Idealized soil-foundation response for typical SSI analysis, with (a) foundation loads and uncoupled vertical, horizontal, and rotational springs; (b) Winkler spring model; and (c) typical elasto-plastic load and deformation response (adapted from Buckle et al. 2006).....	61
2.17 Example equations to calculate uncoupled vertical, horizontal, and rotational spring stiffnesses (from Buckle et al. 2006, originally from Gazetas 1991) .....	62
2.18 Upper and lower-bound approach to define soil-foundation stiffness and capacity (from Buckle et al. 2006) .....	64
 Chapter 4	
4.1 Example of hyperbolic and power law models fitted to normalized load test data (Footing G1, data from Stuedlein and Holtz 2013a, 2013b).....	81
4.2 Variation of bearing pressure with displacement for loading tests in the load test database: (a) raw data, and (b) normalized data .....	82
4.3 Cumulative distribution of the observed power law model parameters (a) $k_3$ and (b) $k_4$ with fitted lognormal CDFs .....	86
4.4 Regressed power law model $k_3 - k_4$ pairs from load test database plotted versus design variables in the ultimate limit state capacity model .....	88
4.5 Variation of power law model parameters $k_3$ and $k_4$ derived from fitting to the normalized bearing pressure – normalized displacement data .....	89
4.6 Example simulations of normalized bearing pressure-normalized displacement of spread footings on aggregate pier reinforced clay: (a) observed and simulated $k_3 - k_4$ pairs derived using the fitted Gumbel copula model, and (b) associated normalized bearing pressure-normalized displacement curves .....	92

## LIST OF FIGURES (Continued)

<u>Figure</u>	<u>Page</u>
4.7	Variation of load and resistance factor, $\psi_q$ , and reliability index, $\beta$ , for various magnitudes of normalized displacement, $\eta$ , for $\text{COV}(q_{app}) = 0.10$ and (a and e) $\text{COV}(\delta_a) = 0$ , (b and f) $\text{COV}(\delta_a) = 20$ percent, (c and g) $\text{COV}(\delta_a) = 40$ percent, and (d and h) $\text{COV}(\delta_a) = 60$ percent. Two-parameter logarithmic curves have been fit to simulations pairs for $\beta > 0$ and $\psi_q \leq 10$ are plotted in (e) through (h) .....97
4.8	Variation of the best fit coefficient and constant: (a) $p_1$ , and (b) $p_2$ with normalized displacement for use with Eq. 4.14 for $\text{COV}(q^*_{app}) = 10$ percent and $\text{COV}(\delta_a) = 0$ .....100
Chapter 5	
5.1	Variation of bearing pressure with displacement for footings in the load test database: (a) observed $q$ - $\delta$ response, (b) normalized $q$ - $\delta$ response using $q_{ult,i}$ and (c) normalized $q$ - $\delta$ response using $q_{STC}$ .....121
5.2	Variation of the reference slope tangent capacity with the interpreted bearing capacity .....124
5.3	Variation of normalized bearing pressure-displacement model parameters $k_1$ and $k_2$ , and model factor $M_{STC}$ with geometric and soil properties influencing bearing capacity .....129
5.4	Comparison of observed and simulated ( $n = 1,000$ ) normalized bearing pressure-displacement model parameters $k_1$ and $k_2$ , and model factor $M_{STC}$ .....130
5.5	Load and resistance factor, $\psi_q$ , and reliability index, $\beta$ , varying with normalized displacement, $\eta$ , for $\text{COV}(q_{app}) = 0.10$ and (a and e) $\text{COV}(\delta_a) = 0$ , (b and f) $\text{COV}(\delta_a) = 20$ percent, (c and g) $\text{COV}(\delta_a) = 40$ percent, and (d and h) $\text{COV}(\delta_a) = 60$ percent. Note, logarithmic-fitted curves shown in (e) through (h) are limited to $\beta > 0$ .....139
5.6	Variation of regressed coefficients (a) $p_1$ and (b) $p_2$ with normalized displacement. Curves shown for $\text{COV}(q_{app}) = 10$ percent and $\text{COV}(\delta_a) = 0$ ..141
5.7	Comparison of MCS-based load and resistance factor, $\psi_q$ and predicted load and resistance factor, $\psi_{q,p}$ using Eq. 5.17, along with 95 percent prediction interval. Comparisons in (a) through (d) represent $\text{COV}(q^*_{app}) = 10$ percent, whereas comparisons in (e) through (h) represent $\text{COV}(q^*_{app}) = 20$ percent .....143

## LIST OF FIGURES (Continued)

<u>Figure</u>	<u>Page</u>
5.8 Procedure for implementation of the proposed reliability-based serviceability limit state methodology for immediate settlements of spread footings on plastic, fine-grained soils.....	146
Chapter 6	
6.1 Comparison of 1,000 $c_1$ - $c_2$ pairs simulated using various copula models fitted to the sample pairs derived from the load test database of footings on aggregate pier-reinforced ground.....	164
6.2 Impact of correlation structure model selection on the lumped load and resistance factor as a function of probability of exceeding the serviceability limit state for $COV(\delta_a) = 0$ and $COV(q'_{app}) = 10\%$ .....	168
6.3 Impact of correlation structure model selection on the allowable bearing pressure considering allowable immediate displacement .....	173
6.4 Comparison of raw and normalized bearing pressure-displacement curves in the footing loading test database: (a) raw q-d curves, (b) bearing pressure normalized by ultimate resistance, (c) bearing pressure normalized by the slope tangent capacity with 0.01B offset, and (d) bearing pressure normalized by the slope tangent capacity with 0.02B offset.....	175
6.5 Comparison of sample and fitted continuous lognormal distributions for power law model parameters (a) $c_1$ , and (b) $c_2$ .....	177
6.6 Comparison of correlation between the bivariate power law parameters reported by Huffman and Stuedlein (2014) using $q_{ult,p}$ -normalized $q_{mob}$ versus (a) $q_{STC,0.01B}$ -normalized and (b) $q_{STC,0.02B}$ -normalized $q_{mob}$ .....	179
6.7 Correlation and variability between bearing capacity and the slope tangent capacities for (a) spread footings resting on unreinforced clayey soils reported by Huffman et al. (2015), and (b) spread footings resting on reinforced clayey soils considered in this study.....	180
6.8 Comparison of 5,000 $c_1$ - $c_2$ pairs simulated using the Gumbel copula model (rotated 180°) fitted to the sample pairs derived from the load test database of footings on aggregate pier-reinforced ground.....	182

## LIST OF FIGURES (Continued)

<u>Figure</u>	<u>Page</u>
6.9 Variation of load and resistance factor, $\psi_q$ , and reliability index, $\beta$ , for various magnitudes of normalized allowable displacement, $\eta_a$ , for $\text{COV}(q_{app}) = 0.10$ and $\text{COV}(\delta_a) = 0$ .....	183
6.10 Test site for new footing loading tests: (a) the site and exploration plan, and (b) Section A-A', indicating the results of mud rotary borings with standard penetration tests (SPT) and cone penetration tests (CPTs).....	187
6.11 Normalized bearing pressure-displacement curves associated with the RBSLS procedures: (a) comparison of Huffman and Stuedlein (2014) with the revised RBSLS procedure revised in this study, and (b) comparison of new full-scale loading tests to the revised RBSLS procedure.....	189
6.12 Comparison of the observed and expected cumulative distribution functions (CDFs) of the normalized resistance at $\eta = \delta/B'$ of (a) 0.01, (b) 0.02, (c) 0.03, and (d) 0.05.....	190
6.13 Comparison of bias and COV in bias for calibrated model and sample CDFs for the original and revised RBSLS procedures.....	191
Chapter 7	
7.1 Example of structure and foundation response in spatially variable soil.....	197
7.2 Structural model used with OpenSees analysis for MCS. Based on SE 3-story building per FEMA-355C (2000) and Barbosa et al. (2017).....	202
7.3 General moment-rotation backbone curve for structural members (adapted from Lignos and Krawinkler 2011, Ribeiro et al. 2014).....	204
7.4 Normalized global dataset footing loading test results and mean bearing pressure-displacement curve based on Eq. 7.1.....	207
7.5 Footing model with vertical and horizontal soil-foundation springs.....	210
7.6 Moment versus displacement for varying number of equally-spaced vertical footing springs.....	212
7.7 Horizontal load versus deflection curve based on Eq. 7.5 (adapted from Duncan and Mokwa 2001).....	214

## LIST OF FIGURES (Continued)

<u>Figure</u>	<u>Page</u>
7.8 Examples of undrained shear strength across horizontal building footprints with varying $COV_{w,h}$ and $\delta_h$ values .....	219
7.9 Normalized bearing pressure-displacement factors from the global and OSU GEFRS datasets plotted versus each other for a) $k_1-k_2$ , b) $k_1-M_{STC}$ , and c) $k_2-M_{STC}$ .....	222
7.10 Normalized bearing pressure-displacement factors from the global and OSU GEFRS datasets with $n = 1,000$ simulated values based on a) global dataset characteristics distributions and dependencies and b) OSU GEFRS characteristics distributions and dependencies .....	224
7.11 Distribution of vertical footing displacement for selected Case 1 MCS results for Footing 2 .....	234
7.12 Distribution of differential footing displacement for selected Case 1 MCS results for Bay 1 .....	239
7.13 Case 1 MCS results for Bay1. Probability of exceedance of selected limit state angular distortion for varying horizontal scale of fluctuation .....	240
7.14 Calculated bearing pressure-displacement response for footings using mean values for inter- and intra-site parameters .....	244
7.15 Distribution of differential footing displacement for selected Case 1 and 2 MCS results for Bay 1 .....	250
7.16 Case 1 (inter-site) and Case 2 (intra-site) MCS results for Bay 1. Probability of exceedance of selected limit state angular distortion for varying horizontal scale of fluctuation.....	251
7.17 Distribution of differential footing displacement for selected Case 1 and 3 MCS results for Bay 1 .....	260
7.18 Case 1 and Case 3 MCS results for Bay 1. Probability of exceedance of selected limit state angular distortion for varying horizontal scale of fluctuation.....	261
7.19 Case 3 MCS. Probability density of angular distortion versus beam yield rotation at Bay 1 for $COV_{w,h}(s_u) = 5$ percent and $\delta_h(s_u) = 5$ m .....	263
7.20 Case 3 MCS. Probability density of angular distortion versus beam yield rotation at Bay 1 for $COV_{w,h}(s_u) = 5$ percent and $\delta_h(s_u) = 50$ m .....	264

## LIST OF FIGURES (Continued)

<u>Figure</u>	<u>Page</u>
7.21 Case 3 MCS. Probability density of angular distortion versus beam yield rotation at Bay 1 for $COV_{w,h}(s_u) = 30$ percent and $\delta_h(s_u) = 50$ m .....	265
7.22 Case 3 MCS. Probability density of angular distortion versus beam yield rotation at Bay 1 for $COV_{w,h}(s_u) = 50$ percent and $\delta_h(s_u) = 5$ m .....	266
7.23 Case 3 MCS. Probability density of angular distortion versus beam yield rotation at Bay 1 for $COV_{w,h}(s_u) = 50$ percent and $\delta_h(s_u) = 50$ m .....	267
7.24 Case 3 MCS. Probability of beam end rotation exceeding $\theta_y$ for selected values of angular distortion and combinations of $COV_{w,h}(s_u)$ and $\delta_h(s_u)$ , and conditioned with a) all data is included, b) data is limited to instances where $\Delta s/l > 1/500$ , c) data is limited to instances where $\Delta s/l > 1/300$ , and d) data is limited to instances where $\Delta s/l > 1/150$ .....	269
7.25 Case 3 MCS results. Probability of beam end rotation exceeding $\theta_y$ or portion of $\theta_y$ for selected values of angular distortion and combinations of $COV_{w,h}(s_u)$ and $\delta_h(s_u)$ , and conditioned with a) all data is included, b) data is limited to instances where $\Delta s/l > 1/500$ , c) data is limited to instances where $\Delta s/l > 1/300$ , and d) data is limited to instances where $\Delta s/l > 1/150$ .....	270
7.26 Case 3 MCS. Probability of beam end rotation exceeding $\theta_y$ for selected values of angular distortion and where $COV_{w,h}(s_u) = 0$ to 100% and $\delta_h(s_u) = 50$ m ....	272
7.27 Case 3 MCS. Probability of beam end rotation exceeding $\theta_y$ for selected values of angular distortion and where $COV_{w,h}(s_u) = 30\%$ and $\delta_h(s_u) = 1$ to 100 m ....	273
7.28 Case 3 MCS results. Probability of beam end rotation exceeding $\theta_y$ or portion of $\theta_y$ for selected values of angular distortion and where $COV_{w,h}(s_u) = 30\%$ and $\delta_h(s_u) = 1$ to 100 m .....	276
7.29 Case 3 MCS results for Bay 1. Probability of exceedance of beam yield rotation for $COV_{w,h}(s_u) = 30\%$ with varying horizontal scale of fluctuation.....	279
7.30 Case 3 MCS results for Bay 1. Probability of exceedance of beam yield rotation for $COV_{w,h}(s_u) = 50\%$ with varying horizontal scale of fluctuation.....	280
7.31 Selected Case 3 MCS realizations for $COV_{w,h}(s_u) = 5\%$ and $\delta_h(s_u) = 5$ m where mean $\Delta s/l$ between footings is equal to a) median value, b) median plus 1 standard deviation, c) median plus 2 standard deviations .....	282

## LIST OF FIGURES (Continued)

<u>Figure</u>	<u>Page</u>
7.32 Selected Case 3 MCS realizations for $COV_{w,h}(s_u) = 5\%$ and $\delta_h(s_u) = 50$ m where mean $\Delta s/l$ between footings is equal to a) median value, b) median plus 1 standard deviation, c) median plus 2 standard deviations .....	283
7.33 Selected Case 3 MCS realizations for $COV_{w,h}(s_u) = 30\%$ and $\delta_h(s_u) = 50$ m where mean $\Delta s/l$ between footings is equal to a) median value, b) median plus 1 standard deviation, c) median plus 2 standard deviations .....	284
7.34 Selected Case 3 MCS realizations for $COV_{w,h}(s_u) = 50\%$ and $\delta_h(s_u) = 5$ m where mean $\Delta s/l$ between footings is equal to a) median value, b) median plus 1 standard deviation, c) median plus 2 standard deviations .....	285
7.35 Selected Case 3 MCS realizations for $COV_{w,h}(s_u) = 50\%$ and $\delta_h(s_u) = 50$ m where mean $\Delta s/l$ between footings is equal to a) median value, b) median plus 1 standard deviation, c) median plus 2 standard deviations .....	286
7.36 Case 3 MCS. Median angular distortion across each bay at occurrences when beam rotation, $\theta > \theta_y$ . $COV_{w,h}(s_u) = 30$ m .....	288
7.37 Selected Case 3 MCS realizations for $COV_{w,h}(s_u) = 30\%$ and $\delta_h(s_u) = 50$ m where beam rotation exceeded $\theta_y$ at multiple beam ends .....	295
7.38 Selected Case 3 MCS realizations for $COV_{w,h}(s_u) = 50\%$ and $\delta_h(s_u) = 5$ m where beam rotation exceeded $\theta_y$ at multiple beam ends .....	296
7.39 Selected Case 3 MCS realizations for $COV_{w,h}(s_u) = 50\%$ and $\delta_h(s_u) = 50$ m where beam rotation exceeded $\theta_y$ at multiple beam ends .....	297
7.40 Distribution of differential footing displacement for each MCS case. Results for Bay 1 where $COV_{w,h}(s_u) = 30$ percent and $\delta_h = 50$ m .....	303
7.41 Case 2 and Case 4 MCS results for Bay 1. Probability of exceedance of selected limit state angular distortion for varying horizontal scale of fluctuation.....	304
7.42 Case 3 and Case 4 MCS results for Bay 1. Probability of exceedance of selected limit state angular distortion for varying horizontal scale of fluctuation.....	305
7.43 Case 4 MCS. Probability of beam end rotation exceeding $\theta_y$ for selected values of angular distortion and where $COV_{w,h}(s_u) = 30\%$ and $\delta_h(s_u) = 1$ to 100 m ....	308

## LIST OF FIGURES (Continued)

<u>Figure</u>	<u>Page</u>
7.44 Case 4 MCS results. Probability of beam end rotation exceeding $\theta_y$ or portion of $\theta_y$ for selected values of angular distortion and where $COV_{w,h}(s_u) = 30\%$ and $\delta_h(s_u) = 1$ to 100 m .....	309
7.45 Case 3 and Case 4 MCS results for Bay 1. Probability of exceedance of beam yield rotation for $COV_{w,h}(s_u) = 30\%$ with varying horizontal scale of fluctuation .....	312
7.46 Case 3 and Case 4 MCS results for Bay 1. Probability of exceedance of beam yield rotation for $COV_{w,h}(s_u) = 50\%$ with varying horizontal scale of fluctuation .....	313
7.47 Case 4 MCS. Median angular distortion across each bay at occurrences when beam rotation, $\theta > \theta_y$ . $COV_{w,h}(s_u) = 30\%$ .....	314



## LIST OF TABLES

<u>Table</u>	<u>Page</u>
Chapter 2	
2.1 Summary of bearing capacity factors for spread footings .....	19
2.2 Summary of bearing capacity coefficients for Eq. 2.26 (after Stuedlein and Holtz 2013a) .....	30
2.3 Allowable average settlement for different building types (after Das 1984).....	32
2.4 Allowable angular distortion for different building types (after Coduto 2001)..	33
2.5 Relationship between reliability index, probability of failure, and expected performance level (after US Army Corps of Engineers 1997) .....	50
2.6 Summary of dependence structure characteristics and probability functions for various bivariate copulas (adapted from Bhat and Eluru 2009) .....	58
Chapter 4	
4.1 Summary of Fitted Bearing Pressure Displacement Model Parameters .....	85
4.2 Summary of Copula Fitting Analyses for the Power Law $q$ - $\delta$ Model Parameters. Note that Kendall's Tau Rank Correlation $\rho_\tau = 0.43$ for all copulas investigated .....	92
4.3 Summary of Load and Displacement Parameters Used for MCS Analysis.....	95
4.4 Summary of Best-fit Coefficients for Eqs. 4.15 and 4.16, valid for $\beta > 0$ and $\psi_q \leq 10$ .....	100
Chapter 5	
5.1 Summary of load test database .....	116
5.2 Comparison of interpreted, calculated, and slope tangent capacities with corresponding ratios.....	118
5.3 Summary of bearing pressure-displacement model coefficients and goodness-of-fit parameters .....	122

## LIST OF TABLES (Continued)

<u>Table</u>	<u>Page</u>
5.4 Summary of AIC and BIC values for selected distributions fit to normalized resistance model parameters .....	128
5.5 Summary of fitted normalized resistance model parameters .....	128
5.6 Summary of best-fit copula functions representing bivariate dependence in the vine copula .....	133
5.7 Summary of assumed normalized bearing pressure and displacement parameters .....	136
5.8 Summary of best-fit coefficient for Eqs. 5.16 and 5.17 and multiplying factor, $M_{\psi,95}$ .....	142
Chapter 6	
6.1 Summary of statistical distributions describing ULS and SLS model parameters used in the demonstration procedure (modified from Huffman and Stuedlein 2014) .....	161
6.2 Selected copula functions, copula parameters, and goodness-of-fit outcomes (modified from Huffman and Stuedlein 2014) .....	166
6.3 Summary of best-fit coefficients for Eq. 6.8, valid for $\beta > 0$ and $\psi_Q \leq 10$ .....	167
6.4 Summary of pertinent soil information, ground improvement geometry, and footing dimensions .....	186
Chapter 7	
7.1 Summary of Seattle (SE) three-story building steel beam section members and strength parameters .....	203
7.2 Summary of footing dimensions and nominal loads and resistances .....	205
7.3 Summary of assumed or fitted soil resistance parameters for MCS .....	208
7.4 Summary of copula functions representing bivariate dependence in the vine copula used for MCS .....	221

## LIST OF TABLES (Continued)

<u>Table</u>	<u>Page</u>
7.5 Calculated vertical footing displacements and corresponding differential displacement and distortion across each bay based on mean resistance parameters .....	230
7.6 Summary of vertical footing displacement for selected Case 1 MCS results with $COV_{w,h}(s_u)$ values of 10 and 30 percent .....	232
7.7 Summary of differential displacement and angular distortion at selected building bay for Case 1 MCS .....	237
7.8 Summary of vertical footing displacement for selected Case 2 MCS results with $COV_{w,h}(s_u)$ values of 10 and 30 percent .....	245
7.9 Summary of differential displacement and angular distortion at selected building bay for Case 2 MCS .....	247
7.10 Summary of vertical footing displacement for selected Case 3 MCS results with $COV_{w,h}(s_u)$ values of 10 and 30 percent .....	255
7.11 Summary of differential displacement and angular distortion at selected building bay for Case 3 MCS .....	257
7.12 Case 3 MCS for $COV_{w,h}(s_u) = 30$ percent and $\delta_h(s_u) = 50$ m. Summary of beam rotation at each beam end for varying footing angular distortion limits .....	277
7.13 Case 3 MCS for selected combinations of $COV_{w,h}(s_u)$ and $\delta_h(s_u)$ . Yield rotation occurrences for each beam at the beam ends and summary of median footing angular distortion across each bay when beam yield rotation occurs .....	289
7.14 Case 3 MCS for $COV_{w,h}(s_u) = 30$ percent and $\delta_h(s_u) = 1$ to 100 m. Yield rotation occurrences for each beam at the beam ends and summary of median footing angular distortion across each bay when beam yield rotation occurs .....	290
7.15 Summary of vertical footing displacement for selected Case 4 MCS results with $COV_{w,h}(s_u)$ values of 10 and 30 percent .....	299
7.16 Summary of differential displacement and angular distortion at selected building bay for Case 4 MCS .....	301

## DEDICATION

*Henry and Eloise, perhaps you will someday get inspiration from the work put into this.*

*Maybe you'll even read a few of these pages. But probably not, and that's okay too.*

*I love you both.*

## CHAPTER 1: INTRODUCTION

### 1.1 STATEMENT OF PROBLEM

Geotechnical engineers routinely make assumptions or generalizations of subsurface properties when completing foundation analyses, and must design with uncertainties stemming from multiple, related sources. Some of the most obvious and common uncertainties include the *modeled* versus *actual* soil response to foundation loads, inherent soil variability (both horizontally and with depth), and soil-structure interaction. Quantifying each uncertainty and its relative impact is difficult and can be cost-prohibitive for routine foundation design. For example, the cost for geotechnical explorations such as borings or cone penetrometer tests often require collecting limited subsurface data relative to the overall extent of a project area. As a result, soil parameters are interpolated over a wide area where soil spatial variability may be high. In addition, foundation loading tests are not completed for most projects, leading to a relative scarcity of large-scale high-quality loading test data from which to calibrate soil response and soil-structure interaction.

The noted uncertainties are particularly acute for foundations supported on plastic, fine-grained soils (i.e., clay and clayey silt) because these soils are generally weaker and prone to greater distortion compared to granular soils (e.g., sands and gravels) under similar footing loads. In addition, the response of plastic, fine-grained soils depend on loading rate and whether soil shear resistance develops under drained or undrained conditions.

To account for these uncertainties, foundation analysis and design for all soil types has historically been completed by applying relatively arbitrary factors of safety coupled with

experience or rule-of-thumb guidelines. The intent of this approach is to reduce foundation loads enough to limit the risk of unsatisfactory foundation and structure performance, both at an ultimate limit state (e.g., bearing capacity failure) and serviceability limit state (e.g., excessive footing displacement). However, using this approach as an umbrella to cover all aspects of risk or uncertainty can lead to unnecessarily expensive designs if overly-conservative assumptions are made. Conversely, it may lead to unsatisfactory or dangerous structural performance if one or more of these interrelated uncertainties are not properly accounted for. Overall, with this methodology, the design engineer does not have an accurate sense of variability, risk or reliability associated with their design.

Recent efforts have been made by the engineering community to adopt reliability-based design (RBD) methods for geotechnical applications to better quantify the multiple uncertainties and provide cost-effective design for an accepted level of risk based on probabilistic analysis. For example, Load and Resistance Factor Design (LRFD) has been incorporated in national codes such as AASHTO specifications, and it is routinely used to evaluate both shallow and deep foundations at the ultimate and serviceability limit states. This approach follows methods used successfully by structural engineering designers for some time.

Despite the noted advancements, there are still on-going challenges to improving RBD methods for geotechnical foundation design. Three related items are identified herein. First, soil resistance factors used with most code-based design are not often calibrated based on probabilistic analyses with accepted risk levels or inherent soil variability, but instead selected to provide equivalent FS values comparable to previously-accepted design standards. As a result, this approach provides no more insight to measurable and

acceptable foundation performance compared to previous design methods and should be updated. Concurrently, code-based serviceability limit state (SLS) models (i.e., displacement-based foundation analyses) for plastic, fine-grained soils typically only evaluate consolidation-induced settlement while ignoring potentially significant immediate settlement from undrained loading. Evaluation for SLS must account for the multiple sources of foundation displacement. Third, SLS models for foundation analysis must be harmonized with SLS models for structural analysis to ensure acceptable performance of the entire structure-foundation-soil system. For example, the consequence of soil and foundation movement should be better understood in terms of structural performance to better calibrate serviceability limit states.

## 1.2 PURPOSE AND SCOPE

Reliability-based geotechnical foundation design focusses on soil and structure analysis that meets necessary safety, performance and/or serviceability criteria, calibrated based on probabilistic analyses and accepted level of risk. The main objective of this study is to advance the underlying knowledge of reliability-based SLS design for shallow foundations. Particularly, this study focusses on foundations supported on plastic, fine-grained soil and aggregate pier-improved plastic, fine-grained soil.

As part of this work, serviceability limit state models were developed for footings supported on plastic, fine-grained soil and aggregate pier-improved fine-grained soil. Both SLS models were developed and calibrated using probabilistic analyses and databases compiled from the literature for high-quality footing loading tests with immediate

(undrained) settlement. These models were later re-evaluated using additional full-scale loading tests completed at the OSU geotechnical field test site.

The study continues with further discussion of calibration procedures, with focus on the impact of the correlation structure of individual load-displacement parameters and suitable factors to account for the propagation of model error and other sources of uncertainty. This phase of work also focused on revising the calibrated SLS model for footings supported on aggregate pier-improved fine-grained soil.

Finally, the calibrated footing load-displacement model on fine-grained soil was used to develop a non-linear soil-spring model within the computer program OpenSees. The foundation spring model was used in combination with a previously developed 3-story steel moment frame building model to complete a series of Monte Carlo simulations with varying levels of soil variability to investigate the role of both inherent soil variability and soil-structure interaction on foundation and structural performance.

### 1.3 ORGANIZATION OF DISSERTATION

The research documented herein was completed to advance reliability-based serviceability limit state design for shallow foundations supported on plastic, fine-grained soil and aggregate pier-improved fine-grained soil. Chapter 2 provides a review of current limit state design methods for shallow foundations supported on such strata, followed by a review of reliability theory with respect to limit state design. The review of reliability theory includes a discussion of Monte Carlo simulations (MCS) accounting for correlation structure of pertinent design parameters, and calibration of resistance factors. An overview of inherent soil variability and random field theory is also provided with focus on



characterizing the uncertainty of soil properties. The literature review also includes a discussion of recent foundation models used for structure-foundation-soil analysis. Following the literature review, the chapter concludes by identifying limitations with current reliability-based design for shallow footings.

Chapter 3 provides an overview of the research objectives and the program of study developed for the advancement of reliability-based serviceability limit state design for shallow foundations supported on plastic, fine-grained soil and aggregate pier-improved fine-grained soil.

Chapter 4 focuses on reliability-based serviceability limit state design of spread footings on aggregate pier reinforced clay. The study summarized in this chapter proposes a simple RBD procedure for assessing the allowable bearing pressure for aggregate pier reinforced clay in consideration of the desired serviceability limit state. A bivariate bearing pressure-displacement model was calibrated using a high quality full-scale load test database and incorporated with a recently-established bearing capacity model developed by Stuedlein and Holtz (2013). Following the generation of an appropriate performance function, a combined load and resistance factor was calibrated in consideration of the uncertainty in the bearing pressure-displacement model, bearing capacity, applied bearing pressure, allowable displacement, and footing width using Monte Carlo simulations seeded with the respective source distributions.

Chapter 5 focuses on reliability-based serviceability limit state design for immediate settlement of spread footings on clay. Following similar guidelines used in chapter 4, this study proposes an RBD procedure for assessing the allowable immediate displacement of a spread footing supported on clay in consideration of a desired serviceability limit state.

A relationship between the traditional spread footing bearing capacity equation and slope tangent capacity is established, then incorporated into a bivariate normalized bearing pressure-displacement model to estimate the mobilized resistance associated with a given displacement. The model was calibrated using a high-quality database of full-scale loading tests compiled from various sources. The loading test data was used to characterize the uncertainty associated with the model and incorporated into an appropriate reliability-based performance function. Monte Carlo simulations were then used to calibrate a resistance factor with consideration of the uncertainty in the bearing pressure-displacement model, bearing capacity, applied bearing pressure, allowable displacement, and footing width.

Chapter 6 provides a discussion of the critical elements in the calibration and assessment of reliability-based serviceability limit state procedures for foundation engineering. This chapter summarizes the framework used in developing the SLS models discussed in Chapters 4 and 5. It further provides a discussion of common correlation structures observed within pertinent model parameters and the selection of appropriate copula models to account for these correlations within the reliability simulations. This chapter later describes recent full-scale loading tests completed at the OSU geotechnical field site and compares the observed loading test results to those predicted from the SLS model. Finally, a revised SLS model for footings supported on aggregate pier-reinforced clay is proposed that incorporates the new loading tests and a revised procedure calibrated to a reference slope tangent capacity.

Chapter 7 presents the framework and preliminary results for reliability analysis of spread footings supporting a 3-story, 4-bay steel moment frame structure. The finite

element-based computer program OpenSees was used in combination with Monte Carlo simulations to analyze probabilistic soil-foundation-structure response with respect to inherent soil variability modeled with a range of undrained shear strength ( $s_u$ ) horizontal scale of fluctuation ( $\delta_h$ ) and coefficient of variability ( $COV$ ) values. The two-dimensional building model used in the simulations corresponds to the SAC steel moment frame building (FEMA 2000) designed using pre-Northridge codes. The foundation soil resistance was modeled as a nonlinear inelastic spring with bearing pressure-displacement response calibrated using the results presented in Chapter 5. To account for foundation rotational stiffness, the vertical spring was modified using the beam-on-nonlinear-Winkler-foundation (BNWF) approach with multiple springs providing partial resistance over a defined area of influence. Horizontal soil resistance was modeled as a single nonlinear spring based on Duncan and Mokwa (2001). The analyses focused on evaluating probabilistic differential foundation settlements with respect to soil variability, the role of the structure in reducing total and differential foundation displacements (i.e., structural stiffness), and service-level structural response versus differential foundation displacements.

The conclusions and significant findings are summarized in Chapter 8. Recommendations for future work are also provided in this chapter. References for the different studies are presented at the end of each chapter. A complete list of references is provided in Chapter 9. The appendices provide additional information related to the different analyses completed as part of this dissertation: Appendix A provides supplemental data for Chapter 4 that was requested during the journal review to give additional background using the copula function for generating dependent, random

coefficients,  $k_3$  and  $k_4$ ; Appendix B provides examples of code written for the program R used to evaluate best-fit copula functions, complete Monte Carlo simulations for various reliability analyses, and generate horizontal soil profiles with variable soil strength (based on random field theory) and soil-foundation spring parameters; Appendix C provides a summary of selected output from Chapter 7 analyses for calculated settlement at five footing locations due to applied foundation loads.

## CHAPTER 2: LITERATURE REVIEW

### 2.1 INTRODUCTION

Reliability-based design (RBD) provides a means to quantify the risk of exceeding selected performance criteria for engineering systems, then calibrating design factors to reduce those risks to an acceptable level. Limit state design procedures used with current codes such as AASHTO (2017) are increasingly utilizing RBD as more data becomes available and methods are developed to better calibrate system response and risk. While RBD concepts may be applied to a broad range of geotechnical systems, the current research focused on the serviceability design for shallow footings supported on plastic, fine-grained soils (i.e., clay and clayey silt) and aggregate pier-improved fine-grained soils subject to undrained loading conditions, as described below.

Shallow spread or continuous footings are the most common foundation type, owing to their relative low cost and ease of construction, and are used to support all types and sizes of structures (e.g., Coduto 2001, Peck et al. 1974). Properly designed shallow footing systems transfer structural loads to the underlying foundation soils while limiting the risk of excessive settlement or other movement that could damage the structure. Shallow footings are typically defined as a foundation element having a width,  $B$ , greater than 3 to 4 times the embedment depth,  $D_f$ , below the ground surface (e.g., Bowles 1988; Das 2011). Present-day shallow footings are often constructed of reinforced concrete and can be built to different size and shape specifications to accommodate structural elements and design loads.

Where the foundation soils are too soft or compressible or the loads from a proposed structure are relatively large for standard shallow footings, aggregate piers may be installed below the foundations, providing a means of ground improvement wherein bearing resistance is increased and foundation settlement is reduced. Aggregate piers are an alternative to deep foundations (e.g., driven piles, drilled shafts, micropiles or similar) or other types of ground improvement that may include overexcavation and replacement of weaker soils, surcharging, dynamic compaction, or other methods. The term “aggregate pier” as discussed herein encompasses a range of construction techniques wherein compacted granular material, typically crushed gravel or rock, is introduced into a weaker soil stratum such as soft to stiff fine-grained soil (i.e., silt and clay) to improve the bearing resistance and reduce settlement. Aggregate piers are typically installed to a predetermined depth, diameter and spacing that is dictated by the subsurface conditions, foundation loads, and construction methods and equipment. Detailed descriptions of typical construction techniques and design methodology for stone column aggregate piers is provided in Barksdale and Bachus (1983). Stuedlein (2008) provides an updated review, including a review of newer construction methods such as vibropiers and rammed aggregate piers.

This chapter first provides a review of limit state design concepts and how they apply to the design of spread footings supported on fine-grained soil and on aggregate pier-improved fine-grained soils under undrained loading. Next, distortion displacement models are reviewed as it applies to the foundation loading response on undrained soils. Then, a review of the reliability-based design framework is provided in the context of serviceability limit state analysis. The review of reliability theory includes a discussion of Monte Carlo simulations (MCS) accounting for correlation structure of pertinent design

parameters, and calibration of resistance factors. An overview of inherent soil variability and random field theory is also provided with focus on characterizing the uncertainty of soil properties, such as undrained shear strength. The literature review concludes with a summary and discussion of current limitations for reliability-based serviceability limit state design for spread footings supported on fine-grained soil and on aggregate pier-improved fine-grained soils.

## 2.2 LIMIT STATE DESIGN

A limit state is defined as the point at which a combination of one or more loads has reached or exceeded the available resistance in one or multiple elements of a structure, resulting in “failure” that is defined by a specific failure criterion (Baecher and Christian 2003, Scott et al. 2003, Paikowsky 2004, Allen et al. 2005). A given limit state may be represented as:

$$\Sigma \gamma_i \cdot Q_{ni} \leq \varphi \cdot R_n \quad (2.1)$$

where:

$\gamma_i$	= load factor applied to a specific load component;
$Q_{ni}$	= a specific nominal load component;
$\Sigma \gamma_i Q_{ni}$	= the total factored load for the group applicable to the limit state being considered;
$\varphi$	= the resistance factor; and
$R_n$	= the nominal resistance available

Phoon et al. (1995) describes the philosophy of limit state design for engineering structures as following three basic requirements:

1. Identify all potential failure modes or limit states.
2. Apply separate checks on each limit state.
3. Show that occurrence of each limit state is sufficiently improbable.

For geotechnical design of shallow foundations, the applicable limit state checks on potential modes of failure typically include those for the ultimate or strength limit state (ULS) and serviceability limit state (SLS) (e.g., AASHTO 2017). The nominal resistance,  $R_n$ , for ULS is calculated as the bearing capacity or strength limit of the foundation soil. The nominal resistance for SLS is typically determined as the equilibrium between applied load and mobilized soil resistance that results in an acceptable level of deformation or displacement (e.g., foundation settlement). The load factors ( $\gamma \geq 1.0$ ) and resistance factor ( $\phi \leq 1.0$ ) in Eq. 2.1 are calibrated to reduce the risk of exceeding the selected limit state to an acceptable level (or “sufficiently improbable” as described by Phoon et al. 1995).

A review of geotechnical foundation design in terms of ULS and SLS for spread footings supported on plastic, fine-grained soils and aggregate pier-improved fine-grained soils is provided below. Further discussion of load and resistance factors and suitable calibration methods is provided later in this chapter in the RBD summary.

### 2.2.1 Ultimate Limit State (ULS) Design

Geotechnical ULS design for shallow foundations is based on the bearing capacity of the foundation soil, which may be estimated from bearing capacity equations or inferred from load testing. Bearing capacity analysis for shallow footings is discussed, followed by interpretation of bearing resistance from loading tests results, then a review of ULS design for spread footings supported on aggregate pier-improved soil.



### 2.2.1.1 Bearing Capacity of Spread Footings

The bearing capacity of a footing is the point at which the shear strength of the foundation soil is met or exceeded. Soil shear strength is defined based on Mohr-Coulomb criteria as (e.g., Terzaghi 1943):

$$\text{shear strength} = \tau = c' + (\sigma - u)\tan\phi' \quad (2.2)$$

where:

$\tau$	= shear stress on the shear plane at failure;
$c'$	= effective soil cohesion;
$\sigma$	= normal stress on the shear plane;
$u$	= pore pressure
$\phi'$	= effective soil friction angle

If the foundation soil consists of saturated, plastic fine-grained soil loaded in an undrained manor (i.e., without dissipation of pore pressures), the strength becomes independent of increasing confining pressure ( $\phi = 0$  condition) and the strength equation is reduced to (e.g., Terzaghi 1943):

$$\text{shear strength} = c = s_u \quad (2.3)$$

where  $c$  is the cohesion along the shear plane at total stress and  $s_u$  is defined as the soil undrained shear strength.

As a foundation reaches its bearing capacity, the shear plane develops according to one of three principal modes defined as (Vesić 1973): 1) general shear failure, 2) local shear failure, or 3) punching shear failure. A schematic of each is failure mode is included in Figure 2.1 (adapted from Vesić 1973). General shear failure typically includes a well-defined, continuous failure plane from one edge of the footing to the ground surface. Unless the footing is constrained, general shear is accompanied by tilting or footing rotation. Local shear failure is similar to general shear, but the failure plane is more

constrained and may not reach the ground surface. Punching shear failure occurs directly below the footing without the failure plane extending beyond the sides of the footing. Different soil types and/or soil layering profiles may be more prone to a particular mode of failure. For undrained loading of plastic, fine-grained soils consistent with those included throughout this study, general shear failure typically governs (e.g., Coduto 2001). Therefore, reference bearing capacities used in later chapters of this dissertation are calculated using equations that assume general shear failure.

The shear plane that develops when a footing reaches bearing capacity is not only a function of the soil, but also the footing dimensions and depth. Because of the complicated and variable nature of the shear plane, there is currently no method for calculating foundation bearing capacity other than as an estimate (e.g., Bowles 1988, Terzaghi et al. 1996). An early and widely accepted formula for estimating bearing capacity was developed by Terzaghi (1943) based on initial work by Prandtl (1920) and others. Several bearing capacity models have been developed since then using similar criteria, including those by Meyerhof (1951, 1963), Hansen (1970) and Vesic (1973, 1974). Each of these models is based on limit-equilibrium analysis that estimates the soil strength relative to the applied foundation load but does not explicitly include soil deformation in the analysis.

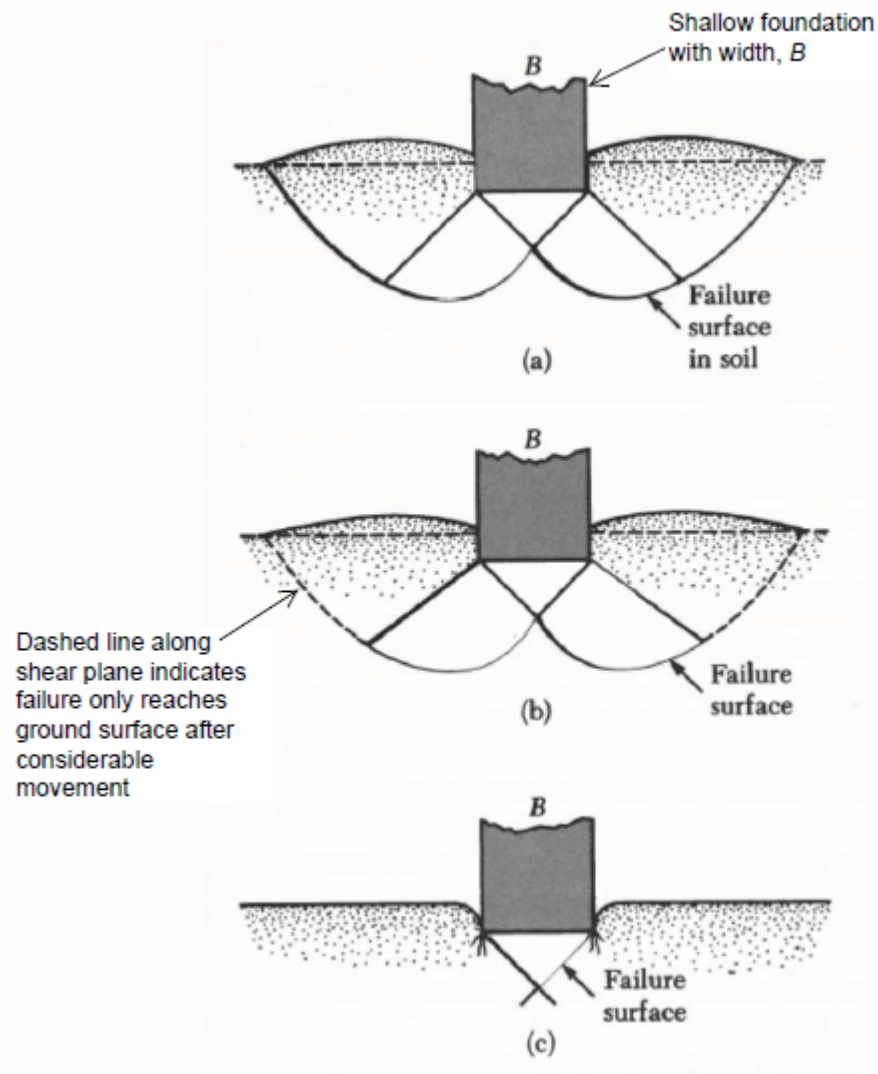


**Figure 2.1** Models of bearing capacity failure and shear plane development in soil: (a) general shear failure, (b) local shear failure, and (c) punching shear failure (adapted from Das 1984, originally from Vesic 1973).

Figure 2.2 includes a schematic of a typical spread footing element and general shear failure plane model with noted components used to develop various bearing capacity equations. Models developed by Terzaghi (1946), Hansen (1970), and Vesic (1973, 1974) assume three separate zones acting along the failure shear plane. From Fig. 2.2b, these zones include I) the active wedge zone that moves downward in response to the foundation load, II) the radial shear zone that extends from either side of the wedge and takes the shape

of a logarithmic spiral, and III) the passive shear zone that extends linearly from the radial zone. These models neglect resistance along the shear plane extending through the surcharge zone (i.e., soil above the bottom of the footing) to the ground surface. Because of this, Terzaghi (1943) proposed his bearing capacity model apply only to footings where the footing depth,  $D_f$ , is less than or equal to the footing width,  $B$ , as indicated in Fig. 2.2a. Later bearing capacity models include a depth factor to account for deeper footings. Meyerhof (1951, 1963) proposed a similar model to those developed by Terzaghi (1943), Hansen (1970), and Vesíć (1973, 1974), but extended the log spiral radial shear zone to the ground surface (and through the surcharge zone), as shown in Fig. 2.2b.

Terzaghi (1943) developed bearing capacity equations for general shear based on three components: 1) capacity derived from soil cohesive strength, 2) capacity derived from surcharge (i.e., confining) resistance, and 3) capacity derived from frictional passive soil pressure. Each of the three capacity components are modified using bearing capacity factors, identified as  $N_c$ ,  $N_q$  and  $N_\gamma$ . The bearing capacity factors account for the geometry of the shear failure surface and are a function of the effective friction angle,  $\phi'$ , of the foundation soil. Terzaghi (1943) developed three separate equations; one for a continuous strip footing based on two-dimensional analysis, and two separate equations with empirical coefficients to account for three-dimensional effects for square or circular foundations.

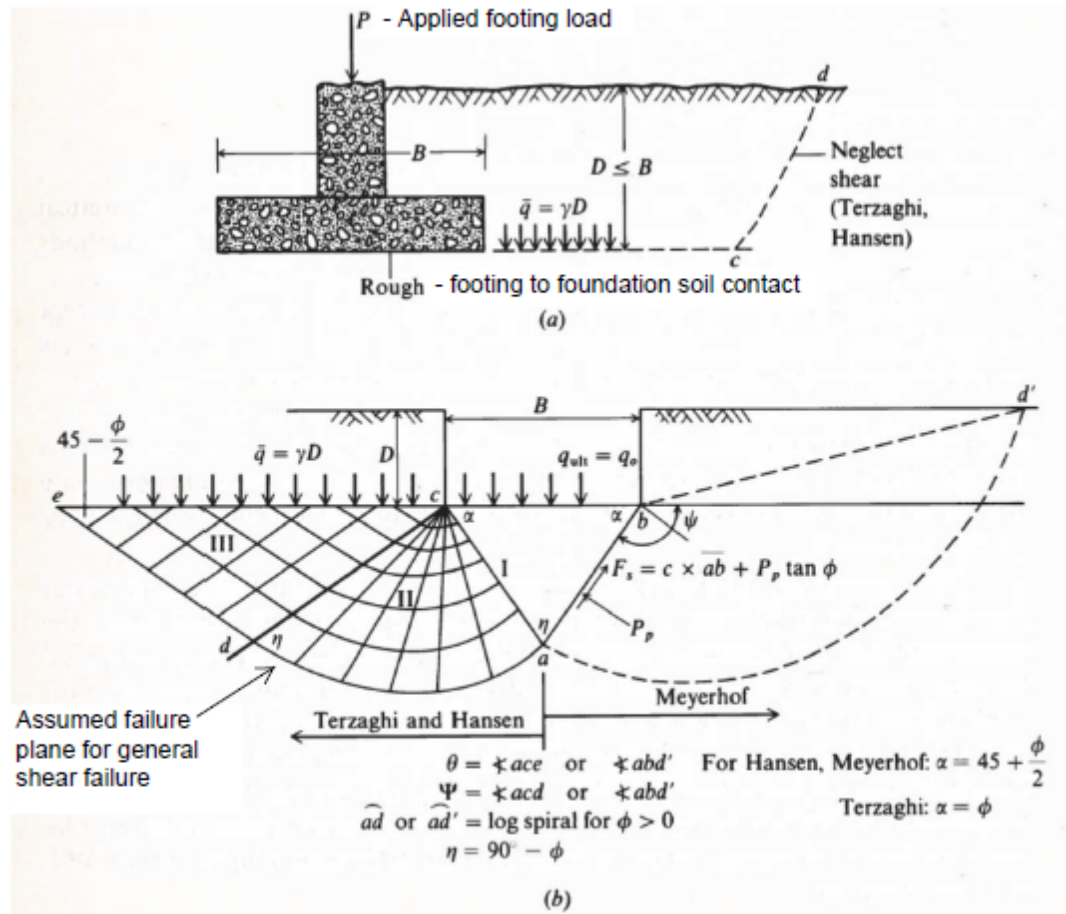


**Figure 2.2** (a) Typical shallow footing, with notes on design assumptions based on Terzaghi (1943) model.  
 (b) Footing-soil interaction models used to develop shear bearing capacity equations. Terzaghi (1943) and Hansen (1970) models shown on left, and Meyerhof (1951, 1963) models shown on right (adapted from Bowles 1988).

The Terzaghi (1943) equations for estimating bearing capacity,  $q_{ult}$ , are as follows:

$$\text{Continuous footing:} \quad q_{ult} = c'N_c + q_s N_q + \frac{1}{2} \gamma B N_\gamma \quad (2.4)$$

$$\text{Square footing:} \quad q_{ult} = 1.3c'N_c + q_s N_q + 0.4\gamma B N_\gamma \quad (2.5)$$

$$\text{Circular footing:} \quad q_{ult} = 1.3c'N_c + q_s N_q + 0.3\gamma B N_\gamma \quad (2.6)$$

where  $\gamma$  is the soil unit weight and  $q_s$  is the surcharge or confining stress acting above Zone III in the bearing capacity model (Fig. 2.2b), calculated as the soil unit weight multiplied

by the footing embedment depth ( $\gamma \cdot D_f$ ). Equations for calculating the bearing capacity factors are summarized in Table 2.1. For undrained ( $\phi = 0$ ) loading conditions where the soil shear strength is defined in terms of  $s_u$ , the bearing capacity factors are  $N_c = 5.7$ ,  $N_q = 1.0$  and  $N_\gamma = 0$ , and the equations are revised as follows:

$$\text{Continuous footing:} \quad q_{ult} = 5.7s_u + q_s \quad (2.7)$$

$$\text{Square/circular footing:} \quad q_{ult} = 7.4s_u + q_s \quad (2.8)$$

The bearing capacity equations developed by Meyerhof (1951, 1963) Hansen (1970) and Vesić (1973, 1974) generally follow similar methods as those used by Terzaghi (1943) with a few noted exceptions. For example, Terzaghi (1943) assumed the angle of the active wedge (identified as  $\alpha$  in Fig. 2.2b) to be equal to  $\phi$ , whereas later researchers found it to be more accurately estimated as  $45 + \phi'/2$  (where  $\phi'$  is measured in degrees). Also, later methods have been developed to provide a single, general equation that incorporate three-dimensional shape effects along with modifications to account for footing depth, load inclination, and ground slope. Hansen (1970) proposed the following general bearing capacity equation:

$$q_{ult} = c'N_c\lambda_{cs}\lambda_{cd}\lambda_{ci}\lambda_{cg}\lambda_{cb} + q_sN_q\lambda_{qs}\lambda_{qd}\lambda_{qi}\lambda_{qg}\lambda_{qb} + \frac{1}{2}\gamma B N_\gamma\lambda_{\gamma s}\lambda_{\gamma d}\lambda_{\gamma i}\lambda_{\gamma g}\lambda_{\gamma b} \quad (2.9)$$

where  $\lambda^*_s$ ,  $\lambda^*_d$ ,  $\lambda^*_i$ ,  $\lambda^*_g$ , and  $\lambda^*_b$  are factors to account for shape, depth, inclination, ground slope, and base slope, respectively.

**Table 2.1. Summary of bearing capacity factors for spread footings.**

Applicable Bearing Capacity Equation	Factors	
	$N_c = 5.7 \text{ for } \phi' = 0$	$N_c = \frac{N_q}{\tan\phi'} \text{ for } \phi' > 0$
Eqs. 2.4 to 2.6	$N_q = \frac{[\exp(\pi(0.75 - \phi'/360)\tan\phi')]^2}{2\cos^2(45 + \phi'/2)}$	
	$N_\gamma = \frac{\tan\phi'}{2} \left( \frac{K_{py}}{\cos^2\phi'} - 1 \right)$	$N_\gamma \approx \frac{2(N_q + 1)\tan\phi'}{1 + 0.4\sin(4\phi')}$
	$N_c = 5.14 \text{ for } \phi' = 0$	$N_c = \frac{N_q - 1}{\tan\phi'} \text{ for } \phi' > 0$
	$N_q = \exp(\pi\tan\phi')\tan^2(45 + \phi'/2)$	
	$N_\gamma = 2(N_q + 1)\tan\phi'$	
Eqs. 2.9 and 2.10	$\lambda_{cs} = 1 + 0.2 \left( \frac{B}{L} \right)$	
	$\lambda_{qs} = 1$	
	$\lambda_{cd} = 1 + 0.4 \left( \frac{D_f}{B} \right) \quad \frac{D_f}{B} \leq 1$	$\lambda_{cd} = 1 + 0.4 \left( \tan^{-1} \frac{D_f}{B} \right) \quad \frac{D_f}{B} > 1$
	$\lambda_{qd} = 1$	

- Notes:**
1. Effective soil friction angle,  $\phi'$ , is measured in degrees for all equations.
  2. Coefficient  $K_{py}$  in  $N_\gamma$  equation is estimated based on chart solutions presented in Terzaghi (1943).
  3. Approximate  $N_\gamma$  solution for Terzaghi (1943) equation is provided in Coduto (2001).
  4. Bearing capacity factors  $N_c$  and  $N_q$  for general bearing capacity equation (i.e., Eqs. 2.9 and 2.10) are relatively consistent among most formulas. Bearing capacity factor  $N_\gamma$  included herein is based on Vesić (1973, 1974).
  5. Shape and depth factors,  $\lambda_{cs}$ ,  $\lambda_{qs}$ ,  $\lambda_{cd}$  and  $\lambda_{qd}$ , are based on those provided in Hansen (1970).
  6. Parameter  $L$  used in the equation to calculate  $\lambda_{cs}$  is the footing length.
  7. For the equation calculating  $\lambda_{cd}$  using  $\tan^{-1}(D_f/B)$ , the parameter  $D_f/B$  is in radians.

Equations for calculating the bearing capacity factors  $N_c$ ,  $N_q$  and  $N_\gamma$  in Eq. 2.9 are summarized in Table 2.1. These factors are not equal the Terzaghi (1943) factors included in Eqs. 2.4 through 2.6 because of the modified assumptions used to estimate the shear failure plane. For undrained ( $\phi = 0$ ) loading conditions where the soil shear strength is

defined in terms of  $s_u$ , and where load inclination and ground slope are not a consideration, the general bearing capacity equation reduces to:

$$q_{ult} = s_u N_c \lambda_{cs} \lambda_{cd} + q_s N_q \lambda_{qs} \lambda_{qd} \quad (2.10)$$

where bearing capacity factors  $N_c$  and  $N_q$  are equal to 5.14 and 1.0, respectively.

Table 2.1 includes a summary of formulas for calculating  $\lambda^*_s$  and  $\lambda^*_d$ .

### 2.2.1.2 *Estimation of Bearing Capacity Based on Footing Loading Tests*

Whereas bearing capacity calculations based on accepted formulas provide only an estimate of the true bearing capacity, full-scale footing loading tests may be used to determine the bearing capacity of a footing more accurately at a given location. Such tests typically include loading a footing or plate in increments and measuring vertical soil deformation,  $\delta$ , versus incremental load,  $q$ . Bearing capacity and/or ultimate resistance is typically defined as the point at which deformation occurs with little or no additional load (i.e., plastic deformation). However, it may also be defined based on a predetermined amount of deformation (e.g., Bowles 1988), such as 25 or 50 mm of vertical displacement.

Loading tests can be used to determine bearing resistance for shallow footings and footings supported on aggregate piers. However, the use of loading tests for routine foundation design is rare because of the high relative costs, limited application for a single test, and large loads that are typically required to induce bearing failure (e.g., Bowles 1988, Coduto 2001). Bowles (1988) notes that scaled tests may be performed, but extrapolation to full-scale design is difficult because of interrelated issues that include variability in the depth of influence, variation in confining (and/or overburden) pressures, and the influence of footing dimensions on bearing capacity.



Even when full-scale footing loading tests are performed, the loading often does not reach the level to induce failure and bearing capacity must be estimated by extrapolating from the measured results. Hirany and Kulhawy (1988) and Paikowsky and Tolosko (1999) provide a summary of several methods used to estimate foundation bearing capacity from loading test data, primarily focusing on deep foundations. Chin (1971) and Jeon and Kulhawy (2001) both proposed fitting loading-displacement ( $q$ - $\delta$ ) data to a hyperbolic curve and estimating the ultimate bearing resistance as the asymptote of the curve. Hyperbolic fitting and interpretation of  $q$ - $\delta$  data is also important for SLS design, as discussed in subsequent sections of this chapter.

### *2.2.1.3 Bearing Capacity of Footings on Aggregate Pier-Improved Soil*

Foundations supported on aggregate pier-improved soil mobilize bearing resistance in different ways that depend on factors such as the depth of ground improvement (i.e., pier length), the stiffness or density of the surrounding matrix soil, depth of firm bearing stratum (if present), the number and spacing of aggregate piers beneath the footing, and the tributary stresses that develop between the piers and matrix soil. Figures 2.3 and 2.4 (adapted from Barksdale and Bachus 1983) show potential failure mechanisms for different scenarios with footings supported on single or multiple aggregate piers.

Barksdale and Bachus (1983) identify three potential failure modes for a footing supported on a single aggregate pier. The most common method is for relatively long piers, where bearing capacity is reached as the pier bulges and capacity is dictated by the confining strength of the surrounding soil (Fig. 2.3a). For relatively short piers extending to a firm bearing stratum (Fig. 2.3b), the bearing capacity is typically consistent with a

general shear failure model, much like the general shear failure of footings on unimproved soils discussed above. For relatively short piers that do not extend to a firm bearing stratum (Fig. 2.3c), a punching failure can occur, where capacity is developed similar to deep foundations (e.g., driven pile or drilled shaft) with resistance provided by side friction along the length of the aggregate pier and end bearing at the base.

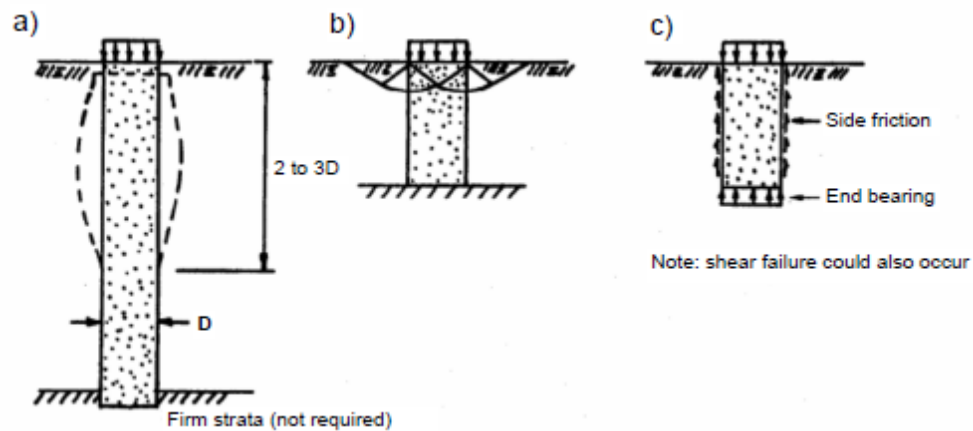


**Figure 2.3** Modes of failure for footings supported on single aggregate piers: (a) bulging failure, (b) shear failure, and (c) punching failure (adapted from Barksdale and Bachus 1983).

When bearing capacity of a footing supported on a single aggregate pier is controlled by pier bulging, several researchers (e.g., Hughes and Withers 1974, Hughes et al. 1975, Wong 1975, Aboshi et al. 1979, Goughnour and Bayuk 1979, Datye and Nagaraju 1983) have recommended assuming a triaxial state of stress where the strength of both the aggregate pier and surrounding matrix soil is fully mobilized. The resulting ultimate bearing pressure,  $q_{ult}$ , is calculated as:

$$q_{ult} = \sigma_1 = \sigma_3 \frac{1 + \sin \phi_s}{1 - \sin \phi_s} \quad (2.11)$$

where  $\sigma_l$  is the vertical stress and/or axial resistance provided by the aggregate pier,  $\sigma_3$  is the maximum confining pressure from the matrix soil, and  $\phi_s$  is the soil friction angle of the granular pier material. Hughes and Withers (1974) and Vesic (1972) proposed calculating the confining pressure,  $\sigma_3$ , based on cavity expansion theory to approximate the bulging of the pier into the matrix soil. Hughes and Withers (1974) proposed the following to estimate confining pressure provided by fine-grained matrix soil:

$$\sigma_3 = \sigma_{ro} + c \left[ 1 + \exp\left(\frac{E_c}{2c(1+\nu)}\right) \right] \quad (2.12)$$

where:

$\sigma_{ro}$	= total initial (in-situ) lateral stress;
$c$	= soil cohesion (also defined as $s_u$ );
$E_c$	= elastic modulus of the matrix soil;
$\nu$	= Poisson's Ratio

Vesic (1972) proposed estimating the confining pressure as:

$$\sigma_3 = cF'_c + qF'_q \quad (2.13)$$

where  $c$  is cohesion and/or undrained shear strength of the matrix soil,  $q$  is the mean isotropic stress at the estimated failure depth, and  $F'_c$  and  $F'_q$  are cavity expansion factors. The cavity expansion factors are estimated from chart solutions provided by Vesic (1973) and based on the internal friction angle of the matrix soil, and a Rigidity Index,  $I_r$ , that is a function of the matrix soil stiffness properties. Solutions for either Eq. 2.12 or 2.13 may be incorporated into Eq. 2.11.

For short columns where general shear failure controls, Madhav and Vitkar (1978) proposed estimating the bearing resistance as:

$$q_{ult} = cN_c + D_f\gamma_c N_q + \frac{1}{2}\gamma_c B N_\gamma \quad (2.14)$$

where  $N_c$ ,  $N_q$  and  $N_\gamma$  are bearing capacity factors similar to the factors used for general bearing capacity calculations in Eqs. 2.4 through 2.10. The bearing capacity factors are obtained from chart solutions in Madhav and Vitkar (1978) that assume mobilization of a general shear failure plane through the matrix soil and aggregate pier. The unit weight of the matrix soil is defined as  $\gamma_c$ , and other variables are consistent with definitions provided above.

Footings supported on multiple aggregate piers have similar modes of failure compared to footings on single piers. Barksdale and Bachus (1983) indicate bulging failures are likely to occur for groups of deep piers (Fig. 2.4a) and punching failures are likely for groups of shorter piers that do not extend to a firm bearing soil (Fig. 2.4b). However, the mechanism for developing confining pressure to resist bulging (Fig. 2.4a) is much more complicated for footings on multiples aggregate piers compared to single pier systems as the confining pressure for each pier is influenced by the pier spacing, the size of the footing relative to the improvement area, and mobilization of the composite shear strengths of the piers and matrix soil (Stuedlein 2008; Stuedlein and Holtz 2013, 2014).

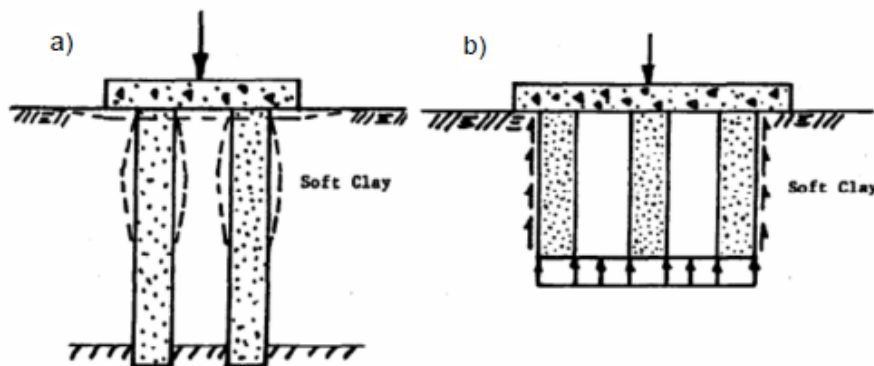


**Figure 2.4** Modes of failure for footings supported in multiple aggregate piers: (a) bulging failure and (b) punching failure (adapted from Barksdale and Bachus 1983).

Barksdale and Bachus (1983) proposed estimating the bearing capacity for footings underlain by multiple piers by combining principles from cavity expansion with a shear failure plane that forms a wedge extending through the matrix soil and pier group. A schematic of this approach is shown in Fig. 2.5 (from Barksdale and Bachus 1983). The ultimate bearing capacity is estimated as:

$$q_{ult} = \sigma_3 \tan^2 \beta + 2c_{ave} \tan \beta \quad (2.15)$$

where  $\sigma_3$  is the confining pressure acting against the failure wedge and  $\beta$  is the failure surface (i.e., shear plane) as shown in Fig. 2.5. The failure plane,  $\beta$ , is calculated as:

$$\beta = 45 + \frac{\phi_{ave}}{2} \quad (2.16)$$

The average or composite soil strength parameters,  $c_{ave}$  and  $\phi_{ave}$ , are calculated based on the strength parameters of the granular pier soil and matrix soil acting across the shear plane, with:

$$c_{ave} = (1 - a_s)c \quad (2.17)$$

$$\phi_{ave} = \tan^{-1}(\mu_s a_r \tan \phi_s) \quad (2.18)$$

where  $c$  is the cohesion (or undrained shear strength,  $s_u$ ) of the matrix soil and  $\phi_s$  is the internal friction angle of the granular aggregate pier material. The term  $a_r$  in both Eqs. 2.17 and 2.18 is defined as the area replacement ratio and equal to:

$$a_r = A_s/A \quad (2.19)$$

where  $A_s$  is the surface area of an aggregate pier in plan (i.e., the top of the pier) and  $A$  is the area of a unit cell. The unit cell is defined as the approximate area of influence encompassed by each pier element and is used to estimate stresses applied to the aggregate pier and the matrix soil (Aboshi et al. 1979). A schematic of the unit cell concept is shown

in Fig. 2.6 (after Barksdale and Bachus 1983). With pier elements spaced in a typical equilateral triangle spacing (Fig. 2.6a), the area replacement ratio may be estimated as:

$$a_r = 0.907 \left( \frac{d_p}{s} \right)^2 \quad (2.20)$$

where  $d_p$  is the pier diameter and  $s$  is the center-to-center spacing between piers.

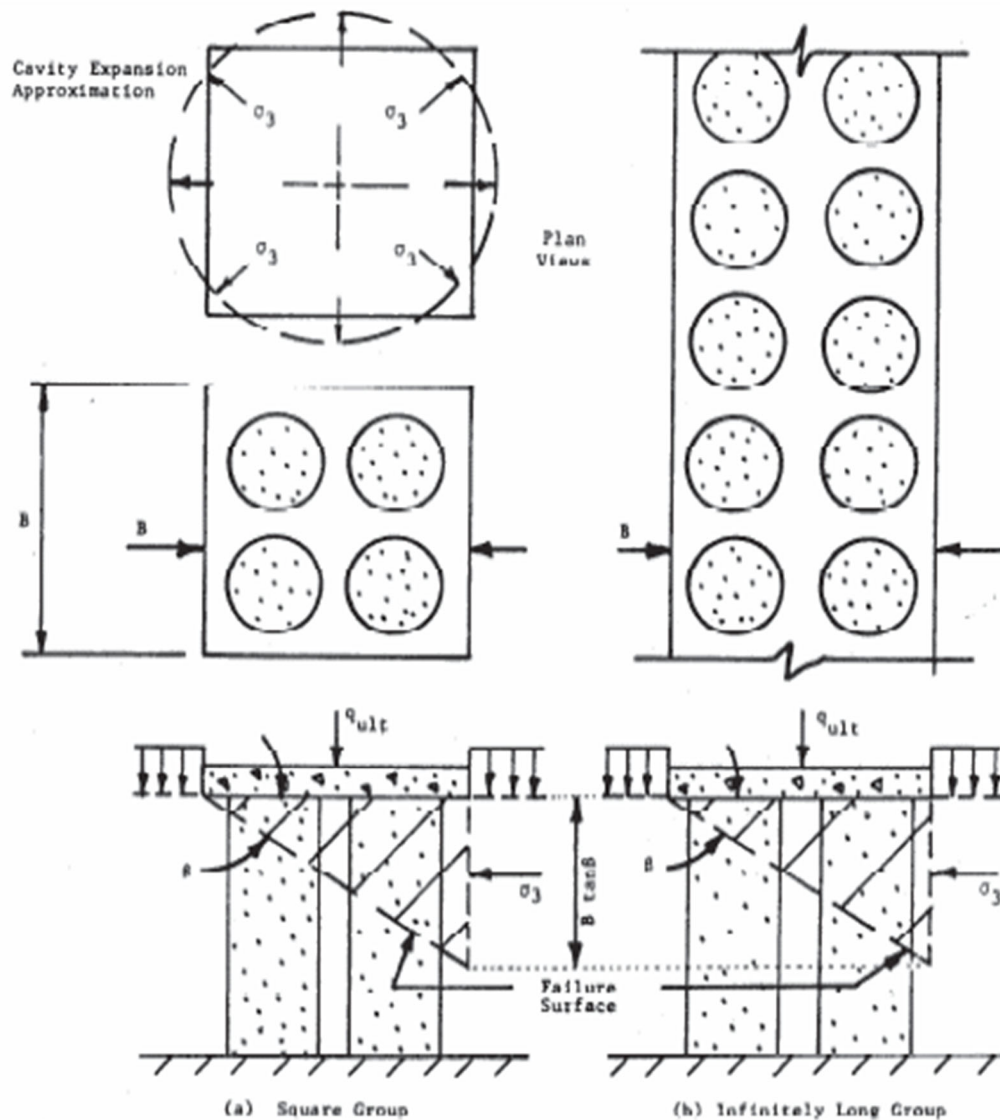


**Figure 2.5** Schematic showing cavity expansion and shear failure plane approximation used for estimating the ultimate bearing resistance of footings supported on multiple aggregate piers (from Barksdale and Bachus 1983).

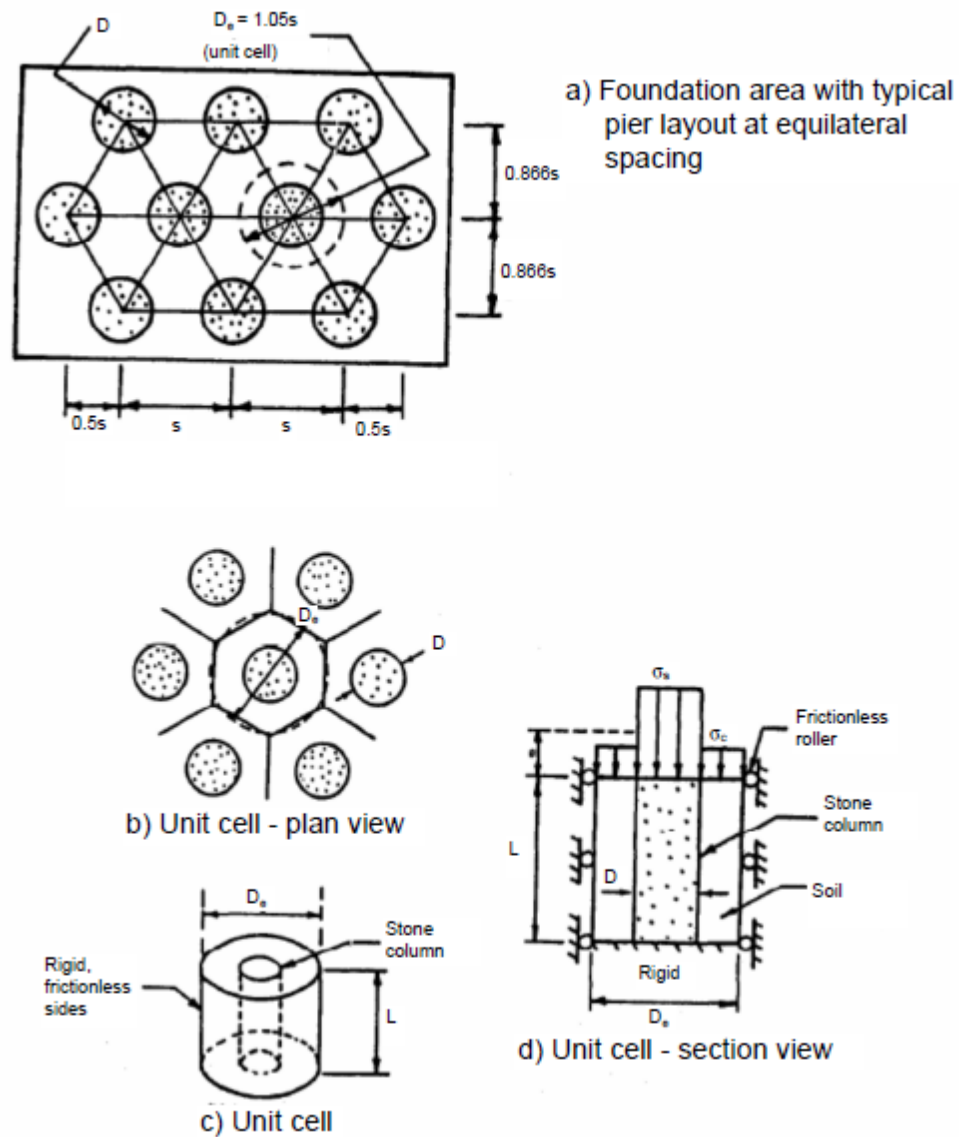


**Figure 2.6** Foundation with typical aggregate pier layout and idealized unit cell model (adapted from Barksdale and Bachus 1983).

The ratio between the bearing pressure applied to the aggregate pier and the matrix soil within a unit cell must be estimated to calculate bearing capacity using Eq. 2.15. As shown in Fig. 2.6d, the stress applied to the pier is defined as  $\sigma_s$  and the stress applied to the matrix soil is defined as  $\sigma_c$ . The stress concentration ratio or factor,  $n$ , is then defined as:

$$n = \sigma_s / \sigma_c \quad (2.21)$$

For total bearing pressure,  $\sigma$ , acting over the unit cell, the stress components for the pier and the matrix soil is calculated as (Aboshi et al. 1979):

$$\sigma_c = \mu_c \sigma = \sigma / [1 + (n - 1)a_r] \quad (2.22)$$

and

$$\sigma_s = \mu_s \sigma = n\sigma / [1 + (n - 1)a_r] \quad (2.23)$$

and  $\sigma$  is calculated as:

$$\sigma = \sigma_s a_s + \sigma_c (1 - a_r) \quad (2.24)$$

The stress concentration ratio,  $n$ , is a function of the stiffness of the pier element and the stiffness of the matrix soil, but is also influenced by pier spacing, confining stress imparted by the foundation, foundation loading rate, drainage (and/or consolidation), and similar factors (e.g., Goughnour and Bayuk 1979, Juran and Guermazi 1988, Han and Ye 1991). Barksdale and Bachus (1983) reported  $n$  in the range of 1.5 to 8.5 from case histories and recommended a typical range of 4 to 5 for settlement analysis. Others have suggested a much larger range of values for  $n$ . For example, Lawton and Warner (2004) reported test results showing  $n$  in the range of 8 to 40. The range of possible stress concentration between the pier and matrix soil introduces some uncertainty in using Eq. 2.15 to estimate bearing capacity.

Mitchell (1981) proposed a simple model for bearing capacity that could be applied to footings supported on either a single pier or multiple piers:

$$q_{ult} = cN_{sc} \quad (2.25)$$

where  $c$  is the cohesion (or undrained shear strength,  $s_u$ ) of the matrix soil and  $N_{sc}$  is an empirical bearing capacity factor. Mitchell (1981) recommended  $N_{sc} = 25$ , while Barksdale and Bachus (1983) recommend a range of  $N_{sc} = 18$  to 22 based on field test results. Others



(e.g., Datye et al. 1982, Wallays 1981) recommended other ranges of  $N_{sc}$  based on types of piers and construction techniques. While the bearing capacity equation proposed by Mitchell (1981) provides a concise way to estimate bearing resistance, it does not specifically take into account important factors that can affect bearing resistance, such as pier spacing, pier depth, and similar factors noted above.

Stuedlein (2008) and Stuedlein and Holtz (2013) analyzed the results from several new and previous loading tests for footings supported on single and multiple aggregate piers. Bearing capacity from the loading tests was typically estimated based on hyperbolic extrapolation. Using this data, they proposed empirical modifications to existing bearing capacity equations using best-fit approximations to reduce bias between the calculated and observed bearing capacities. Stuedlein and Holtz (2013) also proposed a new bearing capacity equation using the loading test results and multi-linear regression (MLR) modeling. They proposed the following:

$$\ln(q_{ult}) = b_0 + b_1 S_{rp} + b_2 a_r + b_3 D_f S_{rp} + b_4 \tau_{mp}^{-1} + b_5 \tau_{mp} \quad (2.26)$$

where  $b_0$  through  $b_5$  are regression coefficients. The best-fit coefficient values determined by Stuedlein and Holtz (2013) are summarized in Table 2.2.  $S_{rp}$  is the pier slenderness ratio, equal to pier length divided by pier diameter ( $L_p/d_p$ ). Stuedlein and Holtz (2013) also incorporated a new term,  $\tau_{mp}$ , identified as the matrix soil shear mass participation factor, equal the ratio of the matrix soil undrained shear strength and the area replacement ratio ( $s_u/a_r$ ). For Eq. 2.26, the area replacement ratio,  $a_r$ , was defined as the ratio of the pier area to the foundation footprint, which is slightly modified compared to the definition in Eq. 2.19 for a typical unit cell.

**Table 2.2. Summary of bearing capacity coefficients for Eq. 2.26 (after Stuedlein and Holtz 2013a).**

Variable	Coefficient Designation	Fitted Coefficient Value
Intercept	$b_0$	4.756
$S_{rp}$	$b_1$	0.013
$a_r$	$b_2$	1.914
$D_f \cdot S_{rp}$	$b_3$	0.070
$\tau_{mp}^{-1}$	$b_4$	-13.71
$\tau_{mp}$	$b_5$	0.005

Stuedlein and Holtz (2013) provide a comparison of the MLR approach (Eq. 2.26) to previous methods for calculating bearing capacity of footings supported on single or multiple aggregate piers. Based on the results from several full-scale loading tests, the MLR model provided an overall closer approximation and less bias for estimating the bearing capacity.

### 2.2.2 Serviceability Limit State (SLS) Design

Geotechnical SLS design for shallow foundations focuses primarily on limiting foundation settlement to acceptable levels to accommodate service-level performance of the structure. Performance criteria may be controlled by total settlement,  $s$ . But it is often based on differential settlement,  $\Delta s$ , and angular distortion,  $\Delta s/l$ , between individual footings or columns (e.g., Coduto 2001). A schematic illustrating these concepts is provided in Fig. 2.7 (modified from Grant et al. 1974).

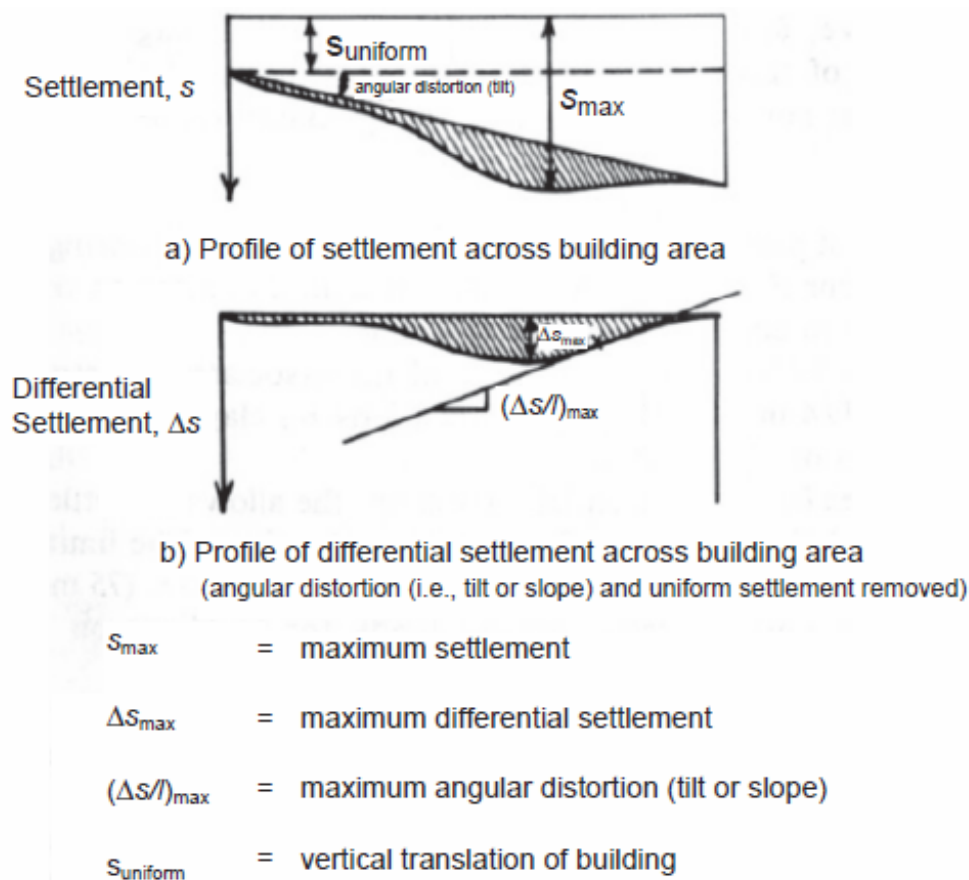


**Figure 2.7** Schematic of total settlement, differential settlement, and angular distortion across a building area (adapted from Grant et al. 1974).

Different structure types have different performance limits. Skempton and MacDonald (1956) and Polshkin and Tokar (1957) initially proposed guidelines based on observed foundation settlements (total and differential) and corresponding building performance. Those studies were later reviewed and updated with work documented in Grant et al. (1974), Burland and Wroth (1974) and Wahls (1981) to help establish guidelines for allowable or tolerable building foundation settlements and angular distortion. Table 2.3 provides a summary of allowable average settlements for different structure types, as compiled by Das (1984) (after Wahls 1981). Table 2.4 summarizes average allowable

angular distortion for varying structures, as compiled by Coduto (2001) (after Wahls 1981, AASHTO 1996, and other sources).

**Table 2.3. Allowable average settlement for different building types (after Das 1984).**

<b>Structure type</b>	<b>Allowable average settlement (mm)</b>
Building with plain brick walls; length/height $\geq 2.5$	80
Building with plain brick walls; length/height $\leq 2.5$	100
Building with brick walls, reinforced with reinf. concrete or reinf. brick	150
Framed building	100
Solid reinforced concrete foundations of smokestacks, silos, towers, etc.	300

The settlement,  $s$ , from foundation loading has three components: immediate (distortion), primary consolidation, and secondary, given as:

$$s = s_i + s_c + s_s \quad (2.27)$$

where  $s_i$  is immediate settlement,  $s_c$  is consolidation settlement, and  $s_s$  is secondary settlement. Immediate settlement is the expression of shear strains that develop below and adjacent to a loaded shallow foundation and is associated with the mobilization of the shear strength of the soil (e.g., Lambe and Whitman 1969, D'Appolonia et al. 1971). As the name implies, immediate settlement occurs relatively rapidly, at least relative to the hydraulic conductivity of the foundation soil, and is associated with an undrained response for plastic, fine-grained soil. Consolidation settlement occurs due to the expulsion of pore water from the soil voids and transfer of the foundation load to the soil skeleton (e.g., Terzaghi 1943). The time for consolidation settlement can range from almost instantaneous for clean sands and gravels to several years for fine-grained soils with low

hydraulic conductivity. Consolidation settlement is influenced strongly by the depositional and stress history of the foundation soil. Secondary settlement (also referred to as creep) occurs from multiple factors that include reorientation of soil particles under a steady-state foundation load over a long period of time, and decomposition of organics in highly organic soils (e.g., Coduto 2001).

**Table 2.4. Allowable angular distortion for different building types (after Coduto 2001).**

<b>Structure type</b>	<b>Allowable angular distortion</b>
Steel tanks	1/25
Bridges with simply supported spans	1/125
Bridges with continuous spans	1/250
Buildings that are tolerant of differential settlements (e.g., industrial buildings with corrugated steel siding and no sensitive interior walls)	1/250
Typical commercial and residential buildings	1/500
Overhead traveling crane rails	1/500
Buildings that are especially intolerant of differential settlement (e.g., those with sensitive wall or floor finishes)	1/1,000
Machinery (general)	1/1,500
Buildings with unreinforced masonry load-bearing walls; length/height $\leq 3$	1/2,500
Buildings with unreinforced masonry load-bearing walls; length/height $\geq 5$	1/1,250

Consolidation settlement,  $s_c$ , is generally the prime concern for foundations supported on plastic fine-grained soils as it typically provides the largest portion of settlement (e.g., AASHTO 2017). However, D'Appolonia and Lambe (1970), D'Appolonia et al. (1971), Osman and Bolton (2005), and Foye et al. (2008), among others, note the importance of quantifying immediate settlement as well. D'Appalonia et al. (1971) identifies three critical reasons as follows:

1. Initial (immediate) settlement may constitute a large portion of the total final settlement, depending on the nature of the soil, loading geometry, and thickness of the compressible layer.
2. Analysis of the initial settlement is an integral part of the analysis of the overall time-settlement behavior of foundations.
3. Initial settlement is closely related to the undrained stability of a foundation, and excessive initial settlement may be a warning of impending failure.

The research in this dissertation focused on the evaluation of immediate foundation settlement for serviceability limit state design, both for foundations supported on plastic fine-grained soil and aggregate pier-improved fine-grained soil. A review is provided below. Further discussion of consolidation theory and creep may be found in most geotechnical and/or foundation design textbooks.

### 2.2.2.1 *Immediate (Distortion) Settlement of Spread Footings*

Immediate settlement is often interpreted as elastic settlement,  $s_e$ , and estimated based on the Young's modulus,  $E_s$ , of the foundation soil. Janbu et al. (1956) recommended calculating elastic settlement for saturated clay (with assumed Poisson's ratio,  $\nu = 0.5$ ) as:

$$s_e = A_1 A_2 \frac{q_0 B}{E_s} \quad (2.28)$$

where  $q_0$  is the applied foundation bearing pressure and  $A_1$  and  $A_2$  are coefficients to account for foundation shape and depth, respectively. Christian and Carrier (1978) later proposed an updated model with revised coefficients. AASHTO (2017) recommends a similar approach that is applicable for all soil types:

$$s_e = \frac{q_0(1-\nu^2)\sqrt{A'} }{E_s \beta_z} \quad (2.29)$$

where  $A'$  is the effective footing area, modified to account for eccentricity, and  $\beta_z$  is a coefficient to account for footing shape and stiffness. The coefficient  $\beta_z$  assumes the footing is either “flexible” or “rigid”.

Despite the ease of using elastic solutions for immediate settlement of plastic fine-grained soils, many researchers have pointed out the shortcomings of this approach. Jardine et al. (1986) identify field and laboratory studies that show soils exhibiting non-linear behavior even at very small strains for foundation loading and other applications. D’Appolonia et al. (1971) showed that local yielding can occur beneath loaded footings, causing stress redistribution and strains (i.e., settlement) that cannot be predicted from elastic theory. Foye et al. (2008) notes that the selection of a representative Young’s modulus (and/or secant modulus) is highly dependent on the level of loading. Therefore, to accurately model immediate settlement with undrained loading, it is desirable to have a representative non-linear solution.

D’Appolonia et al. (1971) performed finite element analysis (FEA) using a linear elastic-perfectly plastic constitutive model that incorporates local yielding of the soil. They proposed estimating immediate settlement using an elastic solution modified with a settlement ratio,  $S_R$ , representing the ratio of the elastic solution compared to the FEA results where:

$$S_i = \frac{s_e}{S_R} \quad (2.30)$$

The settlement ratio,  $S_R$ , is a function of the ratio of applied stress to ultimate stress (i.e., bearing capacity),  $q/q_{ult}$ , the ratio of soil layer depth to footing width,  $H/B$ , and the initial shear stress ratio, defined as:

$$f = \frac{\sigma'_{vo} - \sigma'_{ho}}{2s_u} = \frac{1 - K_0}{2s_u / \sigma'_{vo}} \quad (2.31)$$

where  $\sigma'_{vo}$  and  $\sigma'_{ho}$  are the initial effective vertical and horizontal stresses (before foundation loading) at the depth of interest, and  $K_0$  is the at-rest earth pressure coefficient. Chart solutions are provided in D'Appolonia et al. (1971) for estimating  $S_R$ . This approach gives a better representation of bearing pressure-settlement response for undrained loading compared to elastic theory alone. However, Stuedlein and Holtz (2010) reported that it provided an overly stiff response and underpredicted immediate settlements from full-scale loading tests at modest strain levels.

Foye et al. (2008) provide a similar approach, using an influence factor,  $I_q$ , calibrated from FEA to scale elastic solution results as follows:

$$s_i = I_q \frac{q_{o,net} B}{E_s} \quad (2.32)$$

where  $q_{o,net}$  is the net applied bearing pressure (i.e., bearing pressure minus overburden). Foye et al. (2008) use the initial and/or undrained elastic modulus to represent  $E_s$ . They provide chart solutions for  $I_q$ , which is a function of the ratio of applied bearing pressure to undrained shear strength ( $q_{o,net}/s_u$ ), footing shape, and the thickness of compressible soil stratum extending below the footing.

Elhakim and Mayne (2006) provide a closed-form, hyperbolic-type solution, calibrated using a database of full-scale and laboratory loading tests under both drained and undrained conditions. They proposed estimating immediate settlement as:

$$s_i = \frac{q_o \cdot B \cdot I}{2 \cdot G_{max}(1+\nu) \left[ 1 - 0.99 \left( \frac{q_o}{q_{ult}} \right)^{\left( \frac{14.29}{x_L^{1.05}} - 0.034 \right)} \right]} \quad (2.33)$$



where  $I$  is a displacement influence factor,  $G_{max}$  is the small-strain (and/or initial strain) soil shear modulus within the zone of influence beneath the footing, and  $\nu$  is the Poisson's ratio (assumed equal to 0.5 for undrained loading). The term  $x_L$  is identified as the normalized limiting strain, set equal to:

$$x_L = \gamma_f G_{max} / s_u \quad (2.34)$$

where  $\gamma_f$  is the shear strain at failure. A limiting factor for using this approach is that while  $\gamma_f$  can be estimated from laboratory triaxial strength tests or in-situ methods, doing so is not routine for typical shallow foundation design.

Strahler and Stuedlein (2013) used a database of footing loading tests initially compiled and vetted by Strahler (2012) to evaluate both linear-elastic and nonlinear distortion displacement models. They concluded that linear models (similar to Eqs. 2.28 and 2.29) may be relatively accurate at low displacement levels but increase in error at higher displacements. They evaluated a constitutive nonlinear displacement model based on the Duncan-Chang hyperbolic solution (Duncan and Chang 1970, Duncan et al. 1980) with the principal stress difference beneath the footing represented as:

$$\sigma_1 - \sigma_3 = \frac{\epsilon}{\frac{1}{E_{in}} + \frac{\epsilon}{(\sigma_1 - \sigma_3)_{ult}}} \quad (2.35)$$

where the effective vertical stress,  $\sigma_1$ , and confining stress,  $\sigma_3$ , were defined previously;  $\epsilon$  is the vertical strain; and  $E_{in}$  is the initial undrained Young's modulus. The principal stress difference at failure for undrained loading is defined as:

$$(\sigma_1 - \sigma_3)_{ult} = 2s_u \quad (2.36)$$

To better predict footing response, Strahler and Stuedlein (2013) also proposed estimating the Young's modulus based on a relationship to overconsolidation ratio (OCR) as:

$$E_{in}/p_{atm} = 11(OCR) + 33 \quad (2.37)$$

where  $p_{atm}$  is the atmospheric pressure.  $OCR$  is defined as the ratio of the maximum past soil overburden pressure to existing overburden pressure and is routinely estimated from one-dimensional consolidation testing. They concluded the nonlinear model with revised estimate of  $E_{in}$  better predicts footing loading-displacement behavior for a wider range of bearing pressures. There was still uncertainty in modeled versus observed response, which they attributed to inherent soil variability, transformation error associated with correlations, and model error.

Despite the limitations identified by Strahler and Stuedlein (2013), their work identified an improvement in evaluating and estimating nonlinear footing response using full-scale data. However, additional studies are required to calibrate such a model for suitable reliability-based limit state design.

#### 2.2.2.2 *Distortion Settlement of Footings on Aggregate Pier-Improved Soil*

Several methods have been developed to model settlements of foundations supported on aggregate pier-improved soils. Priebe (1976), Balaam et al. (1977), Aboshi et al. (1979), Goughnour and Bayuk (1979), Balaam and Booker (1981, 1985), Van Impe and De Beer (1983), and Alamgir et al. (1996) used the unit cell concept to evaluate the distribution of pressure to the aggregate piers and matrix soil using the area replacement ratio,  $a_r$ , and stress concentration ratio,  $n$ , as defined and used in Eqs. 2.19 through 2.24 above. With this concept, strain compatibility between the piers and matrix soil is harmonized by adjusting  $n$  based on the estimated stiffness of the piers versus the stiffness of the matrix soil. Most of these models assume elastic behavior for both the piers and the matrix soil.

Barksdale and Bachus (1983) provide a summary of settlement calculations using unit cell idealization. The first step is to estimate settlement of unimproved ground using one-dimensional consolidation theory. For normally consolidated soil, this is estimated as:

$$S_t = \left( \frac{C_c}{1+e_0} \right) \log_{10} \left( \frac{\sigma'_{v0} + \Delta\sigma_v}{\sigma'_{v0}} \right) H \quad (2.38)$$

where:

- $S_t$  = consolidation settlement of unimproved ground to a depth,  $H$ , equal to the stone column treatment depth (approximately equal to  $s_c$  in Eq. 2.27);
- $H$  = vertical height (or depth) of stone column treated ground over which settlement is being calculated;
- $\sigma'_{v0}$  = average initial vertical effective stress in the unimproved soil layer;
- $\Delta\sigma_v$  = change in vertical stress due to the applied load (e.g., foundation load);
- $e_0$  = initial void ratio of the unimproved soil;
- $C_c$  = compression index of the unimproved soil (estimated from one-dimensional consolidation testing)

Then, the ratio of settlements of the aggregate pier-improved soil to the unimproved soil can be estimated as:

$$\frac{S_t}{S} = \frac{\log_{10} \left( \frac{\sigma'_{v0} + \mu_c \sigma}{\sigma'_{v0}} \right)}{\log_{10} \left( \frac{\sigma'_{v0} + \sigma}{\sigma'_{v0}} \right)} = \frac{1}{[1+(n-1)a_s]} = \mu_c \quad (2.39)$$

where the total stress on the unit cell,  $\sigma$ , the area replacement ratio,  $a_s$ , and the stress ratio in the matrix soil,  $\mu_c$ , have all been defined previously. Barksdale and Bachus (1983) suggest a typical range for  $n$  between 2 and 5. However, the different methods using the unit cell concept provide varying means to estimate  $n$  and/or the accompanying settlement

reduction ratio,  $S_i/S$ . For example, Priebe (1976) developed chart solutions to estimate  $S_i/S$  based on  $a_s$  and the internal friction angle of the pier material,  $\phi_s$ .

Lawton et al. (1994), Fox and Cowell (1998), and Sehn and Blackburn (2008) among others proposed methods that include a unit cell model in combination with elastic modulus of subgrade reaction and/or analogous soil springs. The methods by Lawton et al. (1994) and Fox and Cowell (1998) assume a soil profile that includes an upper zone with soil thickness  $d_{uz}$ , and lower zone with soil thickness  $d_{lz}$ . The upper zone extends below the footing to a depth equal to the aggregate pier length plus one pier diameter. The thickness of the lower zone is dependent on the footing size and is equal to four times the footing width minus  $d_{uz}$  (continuous footing), two times the footing width minus  $d_{uz}$  (square footings), or two times the root sum of the squared footing length and width minus  $d_{uz}$  (rectangular footings).

Within the upper zone, the settlement is assumed to be a function of independent elastic springs, with stiffness constants,  $k_s$  and  $k_p$ , representing the matrix soil and piers, respectively, and stress concentration ratio,  $n$ , equal to the ratio of spring stiffnesses, or  $k_p/k_s$ . Using the unit cell concept, the stress on the pier is equal to:

$$\sigma_p = \frac{n\sigma}{a_r(n-1)+1} = \frac{\frac{k_p}{k_s}\sigma}{a_r\left(\frac{k_p}{k_s}-1\right)+1} \quad (2.40)$$

and the settlement in the upper zone is estimated as an elastic displacement equal to:

$$\delta_{uz} = \frac{\sigma_p}{k_p} = \frac{\sigma_s}{k_s} \quad (2.41)$$

Fox and Cowell (1998) recommended estimating the spring constants (i.e., modulus of subgrade reaction) as a function of SPT N-values and unconfined compressive strength.

The pier spring stiffness,  $k_p$ , may also be back calculated from site-specific load tests on single piers.

Settlement in the lower zone is calculated using elastic (e.g., Eq. 2.28 or 2.29) or consolidation (e.g., Eq. 2.37) based analysis. The stress increase within the lower zone is estimated based on typical stress distribution models (e.g., Westergaard stress distribution) with stress reduction from the transfer of foundation load within the upper zone.

The method proposed by Sehn and Blackburn (2008) is similar to Lawton et al. (1994) and Fox and Cowell (1998), with the exceptions that softer spring constants be used to calculate settlement in the upper zone and the stress distribution in the lower zone be calculated assuming a 4:1 (vertical to horizontal) distribution to two-thirds the pier depth,  $L_p$ , then a 2:1 distribution below that. An illustrated example of this concept is provided in Fig. 2.8.

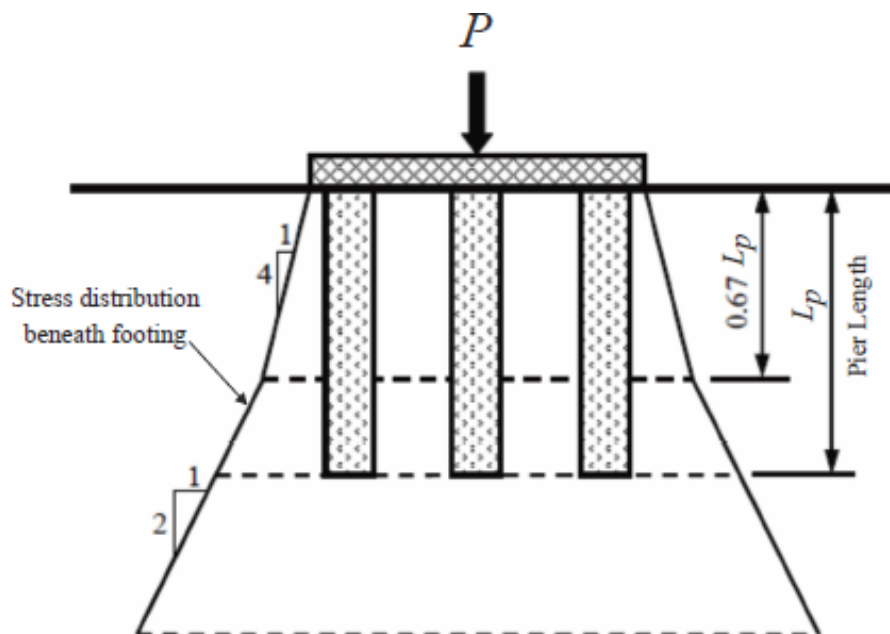


**Figure 2.8** Stress distribution for estimating displacement from foundation load,  $P$ , for an aggregate pier-supported footing (adapted from Sehn and Blackburn 2008).

Stuedlein and Holtz (2014) compared settlement estimates based on unit cell and modulus of subgrade reaction springs to a database of full-scale footing load test. The database included 30 full-scale load tests of spread footings supported on various configurations of aggregate piers in cohesive soils. Fifteen of the load tests were initially completed by Stuedlein (2008). The remaining portion of the database consisted of load tests reported by Greenwood (1975), Hughes et al. (1975), Baumann and Bauer (1974), Bergado and Lam (1987), Han and Ye (1991), Lillis et al. (2004), and White et al. (2007). The comparison showed the existing unit cell and soil spring models typically have a high degree of bias and prediction uncertainty that depend on the magnitude to footing displacement. Stuedlein and Holtz (2014) suggest this uncertainty is due in part to the unit cell concept being more suited to model flexible embankment loads over a wide area, but a poorer predictor of the soil response beneath rigid footing loads with smaller footprint and greater dependence on boundary conditions.

Stuedlein and Holtz (2014) proposed a footing bearing equation for different levels of displacement using the loading test results and non-linear MLR modeling. They proposed the following:

$$\ln(q_\delta) = b_{\delta 0} + b_{\delta 1}a_r + b_{\delta 2}L_p + b_{\delta 3}S_{rp} + b_{\delta 4}\tau_{mp} + b_{\delta 5}D_f S_{rp} \quad (2.42)$$

where  $q_\delta$  is the footing bearing pressure at a selected displacement (e.g.,  $\delta = 2, 5, 10, 17, 25, 35,$  or  $50$  mm). Regression coefficients  $b_{\delta 0}$  through  $b_{\delta 5}$  are best fit based on the selected magnitude of footing displacement. Other variables have been defined (see Eq. 2.26). Stuedlein and Holtz (2014) report the MLR equation showed significant improvement compared to equations using unit cell and/or soil spring models with a reduction in bias and uncertainty.

The work in Stuedlein and Holtz (2014) provides significant contribution using a high-quality database and statistical analysis of variability in foundation load-displacement response. However, the reliance on different regression coefficients for selected displacements creates some limitations for implementing the MLR model with more varied levels of displacement and for incorporating it into global RBD analysis.

### 2.2.2.3 *Nonlinear Models for Bearing Pressure-Displacement Response*

As discussed in the preceding sections, immediate settlement of shallow footings typically follows a nonlinear path in response to applied bearing pressure. This is particularly true for footings on weaker, unimproved fine-grained soils, as reported by D'Appolonia et al. (1971), Jardine et al. (1986), Foye et al. (2008), Stuedlein and Holtz (2010), and Strahler and Stuedlein (2013), among others. It is also true for footings supported on aggregate pier-improved fine-grained soil (e.g., Stuedlein 2008, Stuedlein and Holtz 2013, 2014).

Nonlinear foundation load-displacement response has been studied by several researchers. Duncan and Chang (1970), Chin (1971), Duncan et al. (1980), Duncan and Mokwa (2001), and Jeon and Kulhawy (2001) proposed hyperbolic models to represent the nonlinear stress-strain or load-displacement response for foundations subject to vertical or lateral loading conditions. A general form of the hyperbolic function used for foundation loading is:

$$Q = \frac{\delta}{\left[ \frac{1}{K_{max}} + R_f \frac{\delta}{Q_{ult}} \right]} \quad (2.43)$$

where  $Q$  is the foundation load at a given displacement,  $\delta$ ,  $K_{max}$  is the initial slope of the load-displacement curve and is analogous to the initial soil modulus at very small strain

defined above as  $E_{in}$ ,  $Q_{ult}$  represents the ultimate soil resistance, and  $R_f$  is a factor identified as the “failure ratio” and is equal to  $Q_{ult}$  divided by the hyperbolic asymptote. Duncan and Chang (1970) suggested values for  $R_f$  in the range of 0.75 to 0.95 based on observation and curve fitting to loading test data. Figure 2.9 (adapted from Duncan and Mokwa 2001) includes a typical load-displacement curve generated using a hyperbolic model.

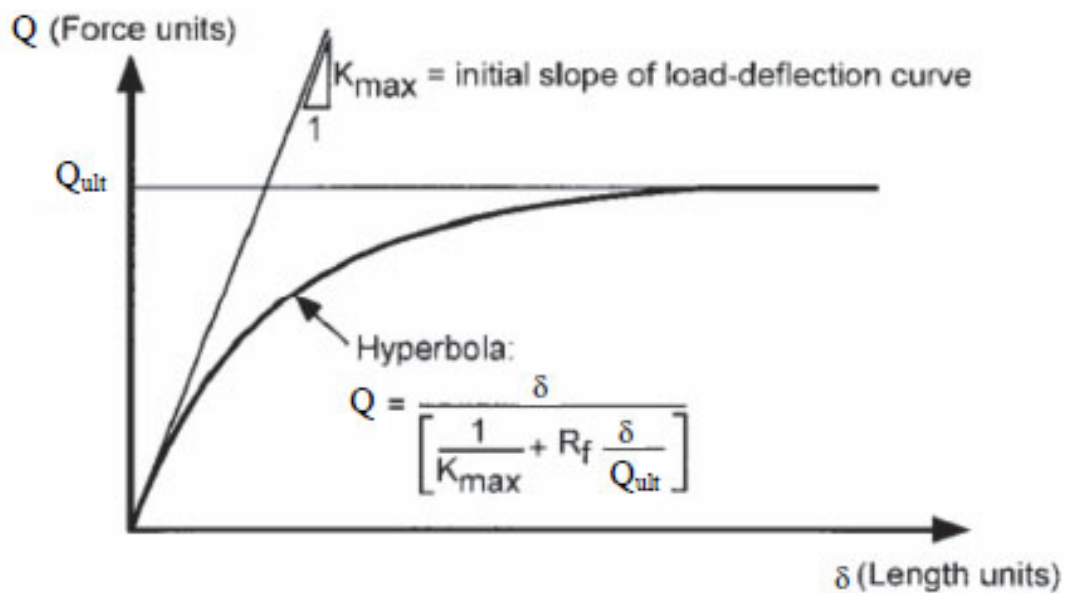


**Figure 2.9** Hyperbolic load-displacement curve and general equation (adapted from Duncan and Mokwa 2001).

Phoon and Kulhawy (2008), Akbas and Kulhawy (2009), Dithinde et al. (2011), and Uzielli and Mayne (2011), among others, proposed fitting bearing pressure-displacement ( $q$ - $\delta$ ) loading test results to normalized hyperbolic or power law functions to provide best-fit curves modeling a range of conditions. For these cases, the footing displacement is normalized by a reference length such as footing width or equivalent diameter. The mobilized bearing pressure at a given displacement,  $q_{mob}$ , is normalized with a reference soil resistance,  $q_{ref}$ , that may represent the calculated bearing capacity, the interpreted



capacity from a footing loading test, or another reference capacity (e.g., slope-tangent capacity; Hirany and Kulhawy 1988). The normalized hyperbolic model is:

$$\frac{q_{mob}}{q_{ref}} = \frac{(\delta/B)}{[k_1 + k_2(\delta/B)]} \quad (2.44)$$

The normalized power law model is:

$$\frac{q_{mob}}{q_{ref}} = k_3 \left( \delta/B \right)^{k_4} \quad (2.45)$$

where  $B$  is the normalizing reference length (e.g., footing width or diameter) and  $k_1$  through  $k_4$  are equation coefficient optimized to provide best-fit solutions for the range of  $q$ - $\delta$  data, typically determined using least squares regression with the given dataset. An example of best-fit normalized curves for both hyperbolic and power law functions is plotted in Fig. 2.10 with a selected example of loading test data from Stuedlein and Holts (2013, 2014). Other curve-fitting functions are available to model the nonlinear  $q$ - $\delta$  behavior (e.g., McConville 2008). The curve-fitting function used to model the observed foundation response is selected to provide the least error between observed and calculated displacement data. With suitable calibration, these nonlinear models can provide good prediction of mobilized bearing resistance and footing displacement at a range of service level displacements. However, their incorporation into SLS design of shallow footings is currently limited.

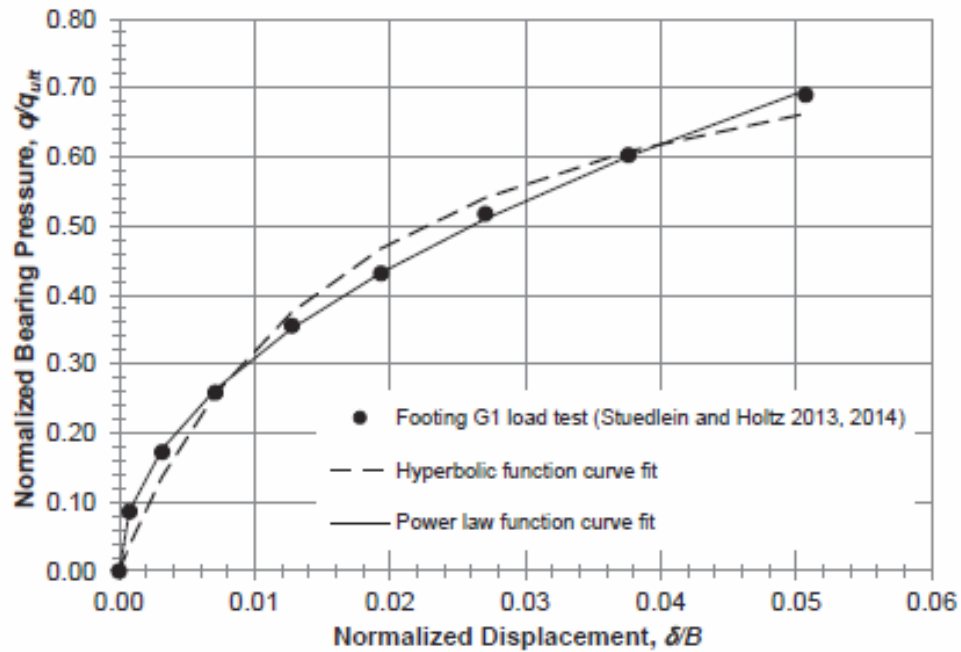


**Figure 2.10** Example of hyperbolic and power law functions fit to normalized footing loading test data reported by Stuedlein and Holtz (2013, 2014).

### 2.3 RELIABILITY BASED DESIGN

Kulhawy and Phoon (2002) broadly define reliability-based design (RBD) as any design methodology that is firmly founded on a rigorous reliability basis. Gilbert (1997) notes the objective of RBD is to assure satisfactory system performance within the constraint of economy. In terms of limit state design and Eq. 2.1, RBD is used to calibrate the load and resistance factors ( $\gamma$  and  $\phi$ ) to reduce the risk of the nominal load,  $Q_n$ , exceeding the nominal resistance,  $R_n$ , to an “acceptable” level, concurrently recognizing the uncertainty associated with the design input parameters (e.g., Phoon et al. 1995, Gilbert 1997, Kulhawy and Phoon 2002, Baecher and Christian 2003, Scott et al. 2003, Paikowsky 2004, Allen et al. 2005). A concise illustration of this concept, including probability

density functions for load and resistance of a typical engineering system is shown in Figure 2.11.

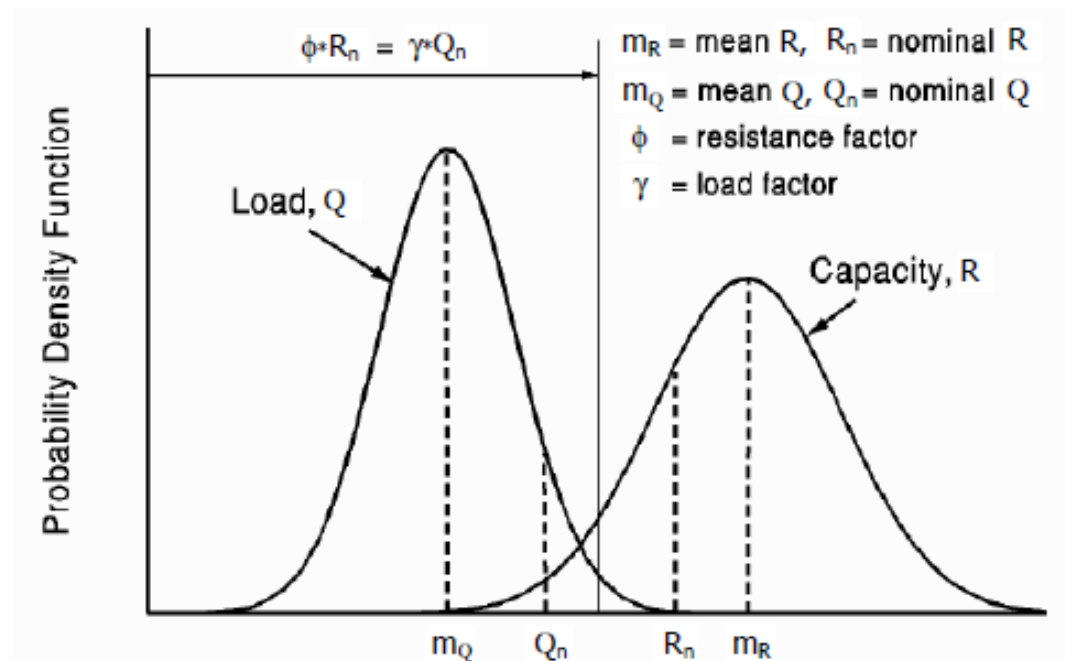


**Figure 2.11** Generalized concept of load and resistance (capacity) probability distribution with reliability-based design (adapted from Kulhawy and Phoon 2006).

Nominal values of load and resistance are calculated using accepted standards of practice. For example, in geotechnical design of spread footings, the nominal soil resistance (i.e., bearing capacity) for ULS may be calculated using Eq. 2.10 for a footing on clay or Eq. 2.26 for a footing on aggregate pier-improved clay. However, the design engineer must also recognize that the actual resistance can vary from the calculated resistance with probabilistic distribution of resistance,  $R$ , as shown in Figure 2.11. For geotechnical engineering applications, uncertainty in resistance is associated with three primary sources that include inherent soil variability, measurement error, and transformation (model) uncertainty (e.g., Phoon et al. 1995; Phoon and Kulhawy 1999a,

1999b). Phoon and Kulhawy (1999a) further note that the first two items are collectively described as “data scatter”. A robust RBD analysis for foundation design requires suitable characterization of the uncertainty (i.e., probability distribution) of the pertinent soil strength parameters and calibration to limit the risk of the resistance being less than the load, or the area of  $Q$  overlapping  $R$  in Figure 2.11. These items are discussed further below.

### 2.3.1 Performance Function and Statistical Characterization

Calibration for RBD analysis is generally framed in the context of the performance function,  $P$ , as (Baecher and Christian 2003, Phoon 2003, Allen et al. 2005, Phoon 2008):

$$p_f = Prob(R - Q < 0) = Prob(P < 0) \leq p_T \quad (2.46)$$

where  $Prob(*)$  is the probability of any particular combination of resistance and load occurring and  $p_T$  = the accepted target probability that the load will be greater than the resistance. The variables  $Q$  and  $R$  have previously been defined as load and resistance. The resistance,  $R$ , may represent an ultimate resistance or serviceability (i.e., mobilized) resistance depending on which limit state is being evaluated. The probability of  $P < 0$  is defined as the probability of failure,  $p_f$ , of exceeding a particular limit state and is not necessarily a structural or foundation failure.

The load and resistance are calculated with random variables that must be characterized statistically, typically in terms of the mean value,  $\mu$ , standard deviation,  $\sigma$ , or coefficient of variation (i.e.,  $COV = \sigma/\mu$ ), and the characteristic distribution (e.g., normal, lognormal, or other). The parameter statistics are developed by compiling a database of measured results (e.g., foundation loading test data), developing performance predictors such as a

ULS equation, and comparing the bias between the predicted versus measured behavior (e.g., Paikowsky et al. 2004, Allen et al. 2005, Dithinde et al. 2011). Characteristic distributions may be evaluated based on goodness-of-fit methods and/or hypothesis tests (e.g., Baecher and Christian 2003) such as Anderson-Darling (Anderson and Darling 1952), Akaike information criterion (AIC) (Akaike 1974) or Bayesian Information Criterion (BIC) (Schwarz 1978).

### 2.3.2 Reliability Index

The probability of failure,  $p_f$ , is often described in terms of the reliability index,  $\beta$ , defined as (e.g., Phoon et al. 1995, Baecher and Christian 2003, Phoon 2003, Allen et al. 2005):

$$\beta = -\Phi^{-1}(p_f) \quad (2.47)$$

where  $\Phi^{-1}$  is the inverse standard normal probability distribution function. Figure 2.12 illustrates the definition of  $\beta$ , equal to the distance measured in standard deviations,  $\sigma$ , between the mean value of  $P$  and  $P = 0$  (i.e., the upper limit for the failure region). Phoon et al. (1995) and Kulhawy and Phoon (2006, 2009) note that  $\beta$  is more convenient than  $p_f$  to use in reliability analyses because the probability of failure is cumbersome when values are very small and  $p_f$  has the negative connotation associated with “failure”, particularly problematic for SLS evaluations. Additionally, the reliability index has been adopted by various codes, and typical values are well understood in terms of performance. For example, the US Army Corp of Engineers (1997) developed general levels of expected performance versus a range of  $\beta$  values, as summarized in Table 2.5. It should be noted

the performance levels noted in Table 2.5 are subjective and can change depending on application, design requirements, and the limit state being analyzed.

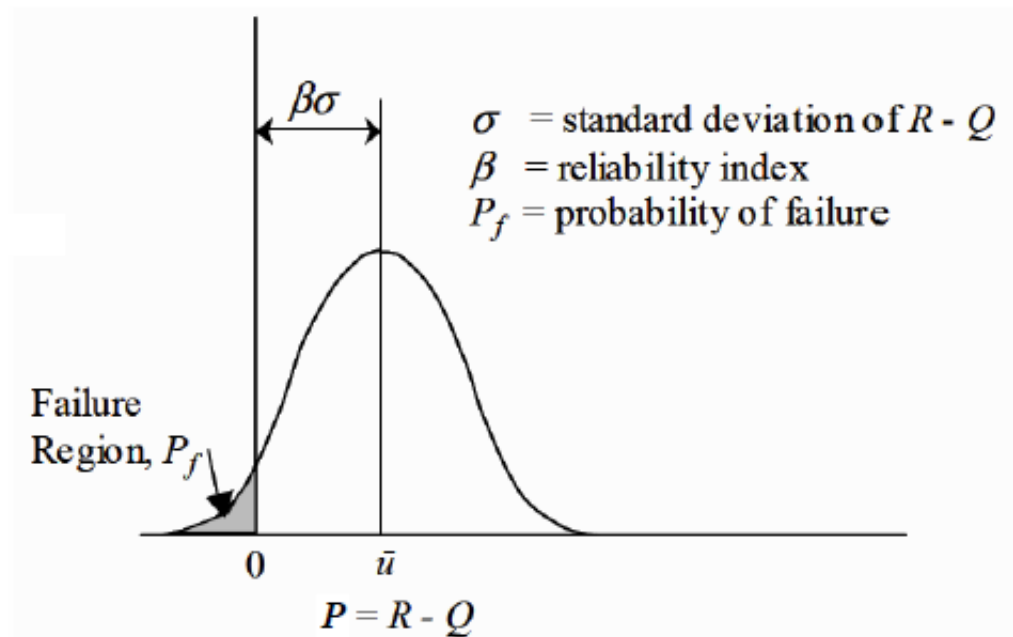


**Figure 2.12** Probability density of performance function,  $P$ , with reliability index,  $\beta$  (adapted from Allen et al. 2005).

**Table 2.5. Relationship between reliability index, probability of failure, and expected performance level (after US Army Corps of Engineers 1997).**

Reliability Index, $\beta$	Probability of Failure, $p_r = \Phi(-\beta)$	Expected Performance Level
1.0	0.16	Hazardous
1.5	0.07	Unsatisfactory
2.0	0.023	Poor
2.5	0.006	Below average
3.0	0.001	Above average
4.0	0.00003	Good
5.0	0.000003	High

Uzielli and Mayne (2011) identified another beneficial aspect of using the reliability index,  $\beta$ , wherein relationships can be developed to calculate load and resistance factors used in limit state analysis based on the desired  $\beta$  value. As part of a study for SLS design of shallow footings on sand, Uzielli and Mayne (2011) identified a logarithmic relationship as follows:

$$\beta = p_1 \cdot \ln(\psi_q) + p_2 \quad (2.48)$$

where  $\psi_q$  is a lumped load and resistance factor that combines the  $\gamma$  and  $\phi$  factors used in Eq. 2.1. The coefficients  $p_1$  and  $p_2$  vary based on allowable displacement and are fitted to the results of Monte Carlo simulations. Up to now, similar relationships have not been explored for developing reliability based SLS design for footings supported on plastic, fine-grained soils or aggregate-improved fine-grained soils.

### 2.3.3 Spatial Variability and Random Field Theory

Inherent soil spatial variability provides a significant portion of the uncertainty when estimating soil resistance,  $R$ , and therefore should be accounted for in a robust RBD analysis. Phoon and Kulhawy (1999a), Elktab et al. (2002), Uzielli et al. (2007), Stuedlein et al. (2012), and Bong and Stuedlein (2017), among others note that this variability arises because soil properties are affected by how the soil layer was deposited, and the loading and weathering history thereafter, which can lead to additional heterogeneity in the soil structure or fabric. Phoon and Kulhawy (1999a) suggest that geotechnical soil properties can generally be decomposed into a trend function,  $t(z)$ , and fluctuating component,  $w(z)$ , represented as:

$$\xi(z) = t(z) + w(z) \quad (2.49)$$

where  $\zeta$  is an in-situ soil property that varies with depth,  $z$ . Spatial variability is represented by the randomly fluctuating component of the soil property,  $w(z)$ . Figure 2.13 provides an example of this concept of soil variability with depth. Similar trends may be observed for horizontal variations in a soil property within a given deposit (e.g.,  $\zeta(x)$  or  $\zeta(y)$ ).

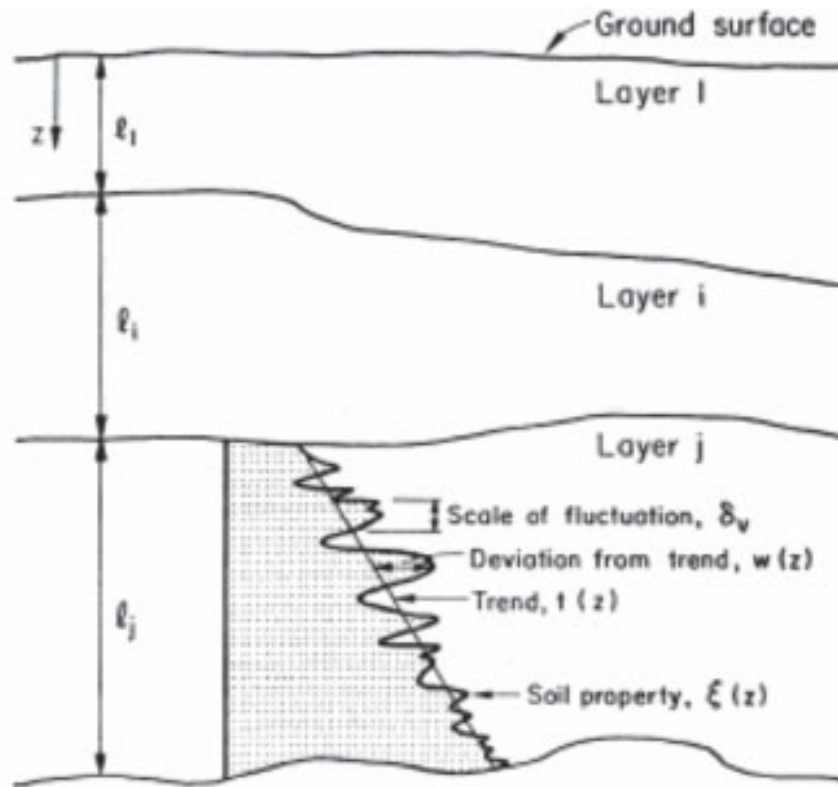


**Figure 2.13** Example of soil spatial variability with depth,  $z$ , for soil layer  $j$  (from Phoon and Kulhawy 1999a).

Random Field Theory (RFT; Vanmarcke 1977, 1983) provides a method to characterize soil spatial variability and the function,  $w(z)$ , and recognizes that a soil property, for example shear strength, does not vary randomly in any direction but exhibits autocorrelation. That is, the closer in distance between measurements of a selected property, the more likely the measurements will be similar. If we can assume  $w(z)$  has



constant mean and variance and the variability between two locations (say  $d_1$  and  $d_2$ ) is a function of distance between  $d_1$  and  $d_2$  but not absolute position, then  $w(z)$  may be considered statistically homogeneous (Vanmarcke 1983, Phoon and Kulhawy 1999a). In that case, variability may be defined in terms of the coefficient of variation of inherent variability,  $COV_w$ , and the scale of fluctuation,  $\delta$ . The coefficient of variation represents the magnitude of deviation about the trend function and is defined as (e.g., Phoon and Kulhawy 1999a):

$$COV_w = \frac{\sigma_w(z)}{t(z)} \quad (2.50)$$

where  $\sigma_w$  is the standard deviation of  $w$ . The scale of fluctuation is defined as (Vanmarcke 1977, 1983):

$$\delta = \int_{-\infty}^{+\infty} \rho_{\Delta z} d(\Delta z) = 2 \int_0^{+\infty} \rho_{\Delta z} d(\Delta z) \quad (2.51)$$

where  $\rho_{\Delta z}$  is the autocorrelation between incremental points with depth,  $z$ . The scale of fluctuation is generally defined as the distance within which a soil exhibits strong correlation. A small  $\delta$  value indicates rapid fluctuation above and below the trend value  $t(z)$ , while a large  $\delta$  value indicates a longer distance between the observed values crossing  $t(z)$ . Figure 2.14 provides an illustration of the estimation of  $\delta$  with depth  $z$ . Vanmarcke (1977) provides an approximate method of estimating  $\delta$  as:

$$\delta \approx 0.8d_{ave} \quad (2.52)$$

where  $d_{ave}$  is the average distance between points where the measured soil property intersects the trend function (e.g., see Fig. 2.14). Typical autocorrelation models used for geotechnical applications include single-exponential, binary noise, cosine exponential, second-order Markov, and squared exponential (Stuedlein et al. 2012).

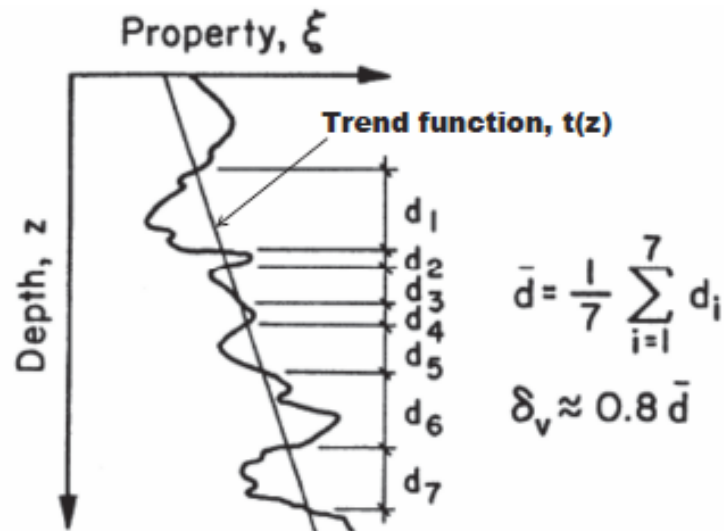


**Figure 2.14** Example of estimate for the scale of fluctuation,  $\delta$ , with depth for a soil property with trend function,  $t(z)$  (adapted from Phoon and Kulhawy 1999a, originally from Spry et al. 1988).

## 2.3.4 Correlation of Soil and Model Parameters

### 2.3.4.1 General Discussion and Correlation Coefficients

In addition to spatial correlation of a single soil parameter (Section 2.3.3), multiple soil parameters used to estimate resistance,  $R$ , can exhibit correlation structure. For example, Griffiths et al. (2009), Le (2014), and Javankhoshdel and Bathurst (2014, 2015), identified negative correlation structure between soil strength parameters  $c'$  and  $\phi'$  (e.g., see Eq. 2.2) wherein greater cohesive strength typically corresponds with lower soil friction angle, and vice-versa. Model parameters used to calculate soil response for specific geotechnical applications can also exhibit correlation. For example, Phoon and Kulhawy (2008), Dithinde et al. (2011), Uzielli and Mayne (2011, 2012), Wang (2011), and Li et al. (2013) identified correlation in foundation spring parameters similar to the nonlinear hyperbolic (Eq. 2.44) and power law (Eq. 2.45) models wherein  $k_1$  and  $k_2$  or  $k_3$  and  $k_4$  are

correlated. Such correlation or dependence structures must be accounted for to accurately assess the probabilistic distributions of the variables affecting RBD analysis (e.g., Phoon and Kulhawy 2008; Uzielli and Mayne 2011, 2012; Stuedlein et al. 2012; Tang et al. 2013).

The strength and direction of correlation between two parameters can be evaluated in terms of a correlation coefficient, such as Pearson's product-moment correlation or the more robust nonparametric Kendall's rank tau, among others. For two variables within a dataset (e.g.,  $k_1$  and  $k_2$  from Eq. 2.44) Pearson's correlation is calculated as:

$$r(k_1, k_2) = \frac{\sum_{i=1}^n (k_{1i} - \mu(k_1))(k_{2i} - \mu(k_2))}{\sqrt{\sum_{i=1}^n (k_{1i} - \mu(k_1))^2} \sqrt{\sum_{i=1}^n (k_{2i} - \mu(k_2))^2}} \quad (2.53)$$

where  $n$  is the number of values in the dataset for each variable ( $k_1$  and  $k_2$ ) and  $\mu$  was previously defined as the mean value of a given parameter. Kendall's rank tau is calculated as:

$$\tau(k_1, k_2) = \frac{2}{n(n-1)} \sum_{i < j} \text{sgn}(k_{1i} - k_{1j}) \text{sgn}(k_{2i} - k_{2j}) \quad (2.54)$$

A value of -1 or +1 for either of these correlation statistics indicates a perfect correlation, whereas a value of or close to zero indicates zero correlation. However, additional information is required beyond just these statistics to fully describe the correlation structure and develop accurate probabilistic distributions of each parameter for RBD analysis.

#### 2.3.4.2 Copula Functions

Copula functions provide a means to fully characterize the dependence structure between two or more variables. Their use is gaining wider acceptance for geotechnical applications with RBD for soil-foundation response (e.g., Uzielli and Mayne 2011, 2012; Li et al. 2013) and characterization of soil strength parameters (e.g., Tang et al. 2013, 2015;

Wu 2013, 2015). Copula functions rely on the rank values of variables for a given dataset and describe the probable rank values of one variable given the rank values of the other, correlated variable (Nelson 2006). Different copula types are available to account for possible trends in correlation structures, including linear or nonlinear correlations, elliptical correlations, and tail-dependent correlations, among others. Figure 2.15 provides an example of simulated values with bivariate correlation structure based on five common copula functions: Gaussian, Clayton, Gumbel, Frank, and Joe.

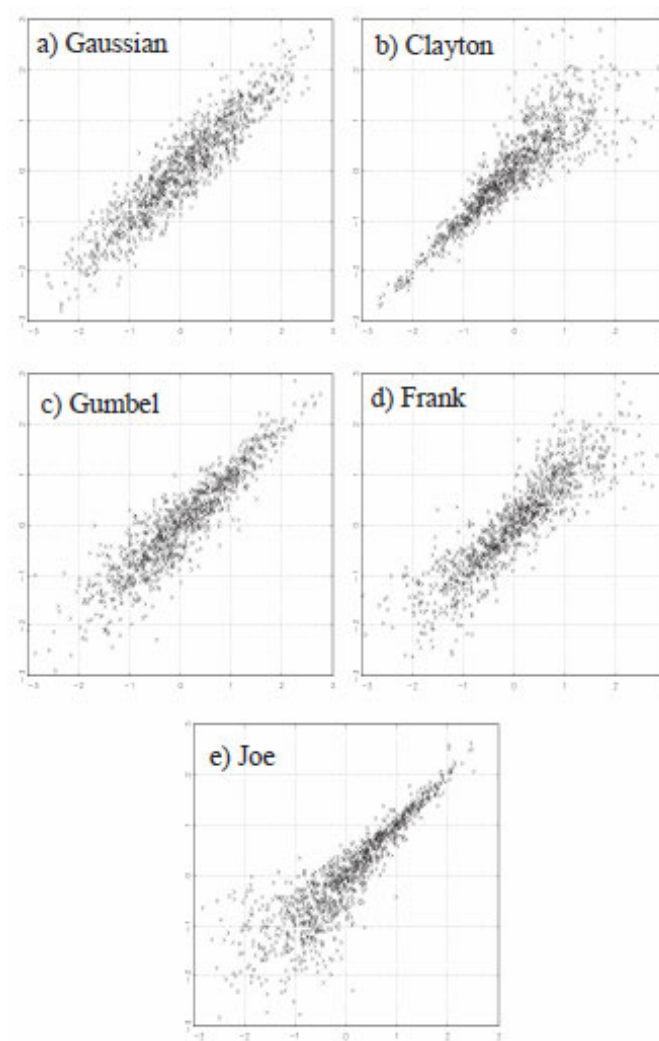


**Figure 2.15** Examples of simulated values with bivariate correlation structure based on different copula functions (adapted from Bhat and Eluru 2009).

Copula functions are typically calibrated using a single copula parameter,  $\theta$ , to define the dependence structure between rank values of different variables in  $[0,1]$  space. The copula parameter is used to calculate the copula probability function,  $C(u_1, u_2)$ , where  $u_1$  and  $u_2$  represent rank values in  $[0,1]$  space of individual variables within a bivariate dataset. The probability functions are unique to the different copula types; examples of bivariate probability functions are provided in Table 2.6. The copula parameter and probability density function can be calibrated based on a relationship with the Kendall's rank tau (i.e., Eq. 2.54). For a bivariate dataset with parameters  $k_1$  and  $k_2$  and corresponding  $[0,1]$  rank  $u_1$  and  $u_2$  values this relationship is (e.g., Nelson 2006, Li et al. 2013):

$$\tau(k_1, k_2) = 4 \int_0^1 \int_0^1 C_{k_1, k_2}(u_1, u_2) d C_{k_1, k_2}(u_1, u_2) - 1 \quad (2.55)$$

Once copula probability distributions have been calculated for a range of copula functions, the most appropriate copula function is selected based on goodness-of-fit statistics such as AIC or BIC to best characterize the correlation strength, direction, and shape (e.g., Li et al. 2013). Then, the rank values can be transposed back to actual values based on the marginal distribution of each variable to fully establish probabilistic distributions with suitable dependence structure.

When more than two variables exhibit correlation structure, the dependence can be accounted for using a multivariate copula function or a string of bivariate copula functions known as a vine copula (e.g., Joe 1996, Aas et al. 2009, Brechmann and Schepsmeier 2013). Brechmann and Schepsmeier (2013) suggest the vine copula approach is typically preferable to using a multivariate copula function because the vine copula is not limited to a single dependence structure and, therefore, generally provides better representation of the correlation between individual variables within the multivariable set.

**Table 2.6. Summary of dependence structure characteristics and probability functions for various bivariate copulas (adapted from Bhat and Eluru 2009).**

Copula	Dependence Structure Characteristics	Probability Function, $C(u_1, u_2)$
Gaussian	Radially symmetric, weak tail dependencies, left and right tail dependencies go to zero at extremes	$\Phi_\theta(\Phi^{-1}(u_1), \Phi^{-1}(u_2))$
Clayton	Radially asymmetric, strong left tail dependence and weak right tail dependence, right tail dependence goes to zero at right extreme	$u_1 - (u_1^{-\theta} + (1 - u_2)^{-\theta} - u_1^{-\theta}(1 - u_2)^{-\theta})^{\frac{1}{\theta}}$
Gumbel	Radially asymmetric, weak left tail dependence, strong right tail dependence, left tail dependence goes to zero at left extreme	$\exp \left[ - \left( (-\log(u_1))^\theta - (-\log(u_2))^\theta \right)^{\frac{1}{\theta}} \right]$
Frank	Radially symmetric, very weak tail dependencies (even weaker than Gaussian), left and right tail dependencies go to zero at extremes	$-\frac{1}{\theta} \ln \left[ 1 + \frac{(e^{-\theta u_1} - 1)(e^{-\theta u_2} - 1)}{e^{-\theta} - 1} \right]$
Joe	Radially asymmetric, weak left tail dependence and very strong right tail dependence (stronger than Gumbel), left tail dependence goes to zero at left extreme	$u_1 + u_2 - 1 - \left( 1 - ((1 - u_1)^{-\theta} + (1 - u_2)^{-\theta} - 1)^{\frac{1}{\theta}} \right)$

- Notes:**
1. Copula parameter,  $\theta$ , is based on best-fit for selected copula type and relationship to Kendall's rank tau (Eq. 2.55).
  2. Variables  $u_1$  and  $u_2$  are the rank values from a bivariate dataset.
  3. Function  $\Phi^{-1}$  is the inverse standard normal cumulative distribution function (e.g., Eq. 2.47).

## 2.3.5 Soil-Structure Interaction

### 2.3.5.1 General Discussion

The distribution of load,  $Q$ , depends in part on the stiffness of the structure and soil resistance,  $R$ , at individual foundation locations. Therefore,  $Q$  and  $R$  are not independent of each other, but instead must act in a compatible manner influenced by soil-structure interaction (SSI; French 1999). Such interaction may also induce moments and/or

rotational loading on the foundations and at the soil-foundation interface, which was not previously discussed in the preceding sections reviewing ULS and SLS foundation design.

Soil-structure interaction is often evaluated as part of the seismic analysis (i.e., extreme limit state) for a structure (also referred to as soil-foundation-structure interaction), where a design free-field ground motion acts on the structure, which in turn acts on the foundations that are supporting the structure (inertial interaction) and may also affect the free-field motion (kinematic interaction) (e.g., Stewart et al. 1999, Buckle et al. 2006, Kavazanjian 2011, NEHRP 2012). However, soil-structure interaction is also important for SLS design because the stiffness of the structure (or components of the structure) in combination with the stiffness of the soil beneath individual foundations affects the potential for differential settlement and angular distortion, and overall structure performance.

When considering SSI, the soil-foundation model for spread footings is often idealized as a set of linear or nonlinear springs that may be coupled or uncoupled (e.g., Buckle et al. 2006, Kavazanjian 2011). Figure 2.16 illustrates an example of foundation loads imparted from a rigid spread footing and spring models for either a) uncoupled vertical, horizontal, and rotational springs, or b) a Winkler spring model. The Winkler spring model in Fig. 2.16b replaces the rotational spring in Fig. 2.16a with a series of vertical springs acting across the bottom of the foundation. The soil spring stiffnesses may be evaluated using different methods; for example Gazetas (1991) developed a series of equations accompanying the springs shown in Fig. 2.16a based on the theory of a rigid plate acting on the surface of, or embedded into, a homogenous elastic half-space. Figure 2.17 provides a summary of the equations proposed by Gazetas (1991) and illustration of accompanying

foundation plan and section view. The spring equations summarized in Fig. 2.17 typically accompany a linear elastic-plastic model, where plastic behavior corresponds to the foundation loads reaching bearing capacity and/or the ultimate limit state (e.g., Fig 2.16c). The spring stiffness in the elastic phase is calculated using typical mechanics of material properties that include elastic and shear moduli and Poisson's ratio ( $E$ ,  $G$  and  $\nu$ ), and which may be estimated from correlations to in-situ or laboratory soil strength measurements. Other soil-foundation spring models may be used for spread footings or mat foundations (e.g., Horvath 1993, Stavridis 2002, Allotey and El Naggar 2008, Horvath and Colasanti 2011). Idealized springs for deep foundations such as driven piles or drilled shafts are often developed using nonlinear  $p$ - $y$  (lateral load versus deflection) or  $t$ - $z$  (axial load versus deflection) analysis (e.g., Georgiadis 1983, Reese 1984, Fellenius and Rahman 2019).

The idealized foundations springs are incorporated into a structural model that can range in complexity from a few elements to the entire structure with 2-dimensional or 3-dimensional analysis. Load distribution and redistribution occurs due to the transfer of loads in accordance with the governing stiffness of the structure and foundation elements. Stiffer springs attract more load, but such stiffness may be limited by the yield stress (or accompanying yield rotation) within structural members and bearing resistance of the foundation soil, or softening in nonlinear elements. Moderate to complex structural systems typically require finite element model (FEM) programs such SAP2000 (Computers and Structures, Inc.) or OpenSees (McKenna et al. 2010) to complete the analysis that require harmonization of load versus deflection or rotation for each of the structure and foundation components, and may require several iterations.



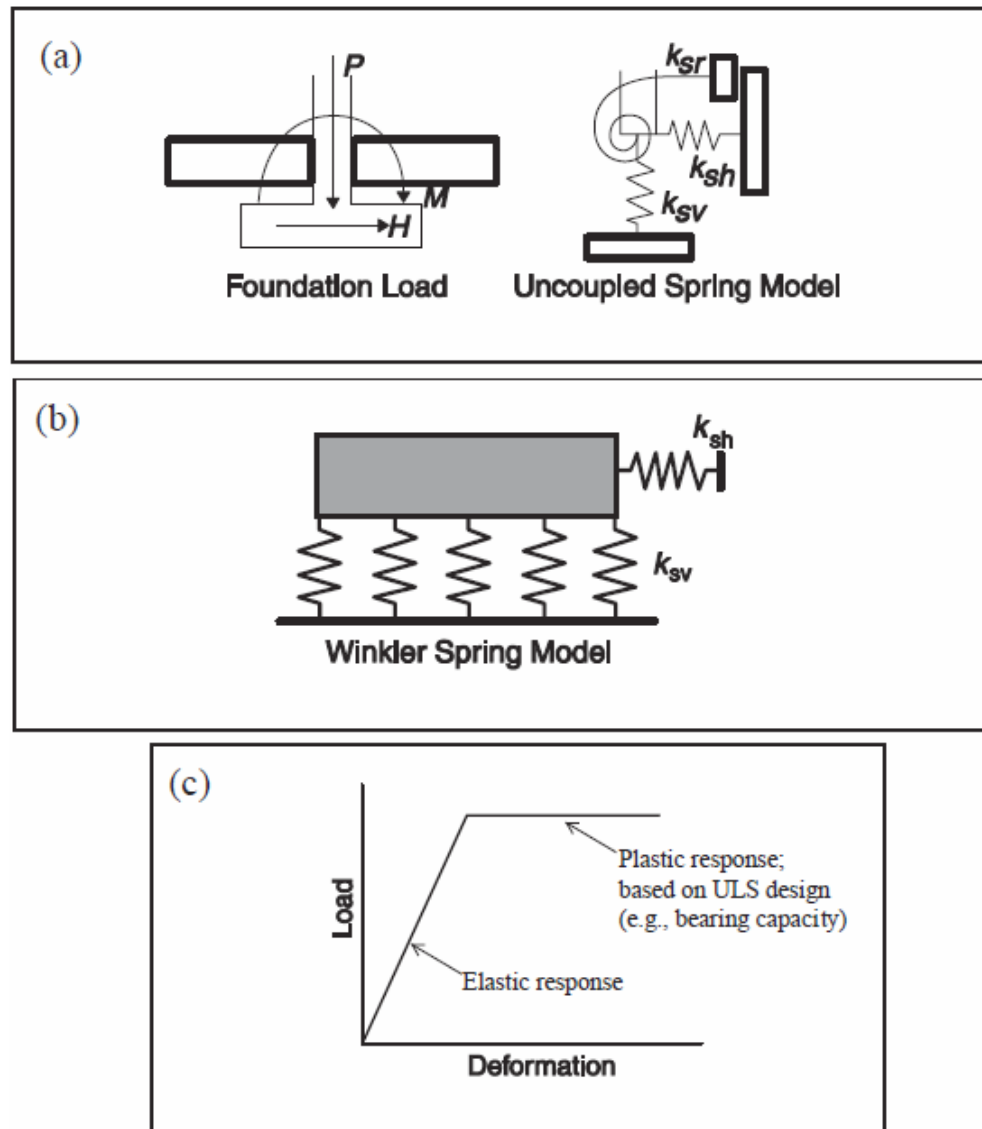


**Figure 2.16** Idealized soil-foundation response for typical SSI analysis, with (a) foundation loads and uncoupled vertical, horizontal, and rotational springs; (b) Winkler spring model; and (c) typical elasto-plastic load and deformation response (adapted from Buckle et al. 2006).

Stiffness Parameter	Rigid Plate Stiffness at Surface, $K_i'$
Vertical Translation, $K_z'$	$\frac{GL}{(1-\nu)} \left[ 0.73 + 1.54 \left( \frac{B}{L} \right)^{0.75} \right]$
Horizontal Translation, $K_y'$ (toward long side)	$\frac{GL}{(2-\nu)} \left[ 2 + 2.5 \left( \frac{B}{L} \right)^{0.85} \right]$
Horizontal Translation, $K_x'$ (toward short side)	$\frac{GL}{(2-\nu)} \left[ 2 + 2.5 \left( \frac{B}{L} \right)^{0.85} \right] - \frac{GL}{(0.75-\nu)} \left[ 0.1 \left( 1 - \frac{B}{L} \right) \right]$
Rotation, $K_{\theta x}'$ (about x axis)	$\frac{G}{(1-\nu)} I_x^{0.75} \left( \frac{L}{B} \right)^{0.25} \left( 2.4 + 0.5 \frac{B}{L} \right)$
Rotation, $K_{\theta y}'$ (about y axis)	$\frac{G}{(1-\nu)} I_y^{0.75} \left[ 3 \left( \frac{L}{B} \right)^{0.15} \right]$
<div style="display: flex; justify-content: space-between;"> <div style="width: 45%;"> <p style="text-align: center;"><b>Plan</b></p> <p style="text-align: center;"><b>Section</b></p> </div> <div style="width: 50%;"> <ol style="list-style-type: none"> <li>1. Determine the uncoupled total surface stiffnesses, <math>K_i'</math>, of the foundation element by assuming it to be a rigid plate bearing at the surface of a semi-infinite elastic half-space (see above).</li> <li>2. Adjust the uncoupled total surface stiffnesses, <math>K_i'</math>, for the effect of the depth of bearing by multiplying by embedment factors (see Table 6-2), <math>e_i</math>, to generate the uncoupled total embedded stiffnesses, <math>K_i</math>. <math>K_i = e_i K_i'</math></li> </ol> </div> </div>	
<p><b>Note:</b> <math>I_x, I_y</math> are moments of inertia of the footing about the x- and y-axes, respectively.</p>	

**Figure 2.17** Example equations to calculate uncoupled vertical, horizontal, and rotational spring stiffnesses (from Buckle et al. 2006, originally from Gazetas 1991).

### 2.3.5.2 Soil-Structure Interaction within RBD Framework

The state of practice for incorporating SSI affects into reliability-based probabilistic foundation analysis is currently limited. For example, Buckle et al. (2006) suggest selecting upper- and lower-bound stiffnesses to define soil-foundation spring elements, as

shown in Fig. 2.18, as a means to bracket the potential soil-foundation response. This approach is intended account for uncertainties in the foundation soil stiffness and/or resistance, and to help characterize the structures sensitivity to this variability. Both the geotechnical and structural designers are recommended to provide input, but a more detailed framework to establish these bounds, particularly in a probabilistic manner, is not provided. Breysse et al. (2004) opine that the fields of soil variability and soil-structure interaction seem to be addressed independently even though they are quite interrelated. Generally, SSI analysis tends to incorporate deterministic soil-foundation models or uses a limited probabilistic approach to address soil variability.

Fenton and Griffiths (2002, 2005) and Ahmed and Soubra (2014) completed studies to evaluate the response of adjacent footings supported on spatially variable foundation soils. However, those studies did not incorporate stiffness from a structure connecting the footing, thereby neglecting the effect of SSI on the footing response. These studies also generally limited the soil response based on an assumed soil Young's modulus,  $E_s$ , which does not account for nonlinear soil behavior. Stuart (1962), Das and Larbi-Cherif (1983), Wang and Jao (2002), Kumar and Ghosh (2007), Mabrouki et al. (2010), and Lavasan and Ghazavi (2012) analyzed the response of adjacent footings based primarily on the influence of the footings on each other, but not the structural response or within a variable soil profile. Breysse et al. (2004) completed probabilistic analysis of a structure over spatially variable soil, but limited the analysis to continuous structures such as buried pipes, concrete slabs, and structural walls with homogenous material properties to simplify analyses and develop generic evaluations based on structure stiffness versus variable soil stiffness. Furthermore, Breysse et al. (2004) implemented elastic soil properties for the purposes of investigating

the effects of soil variability. Bathurst and Javankhoshdel (2017) explored soil variability and bias for relatively simple limit states analysis that could be solved with a closed-form solution within the context of MSE wall design. Overall, there appears to be a lack of data in the literature that addresses nonlinear soil-foundation response across multiple footings with spatially variable soil, and which also accounts for SSI.

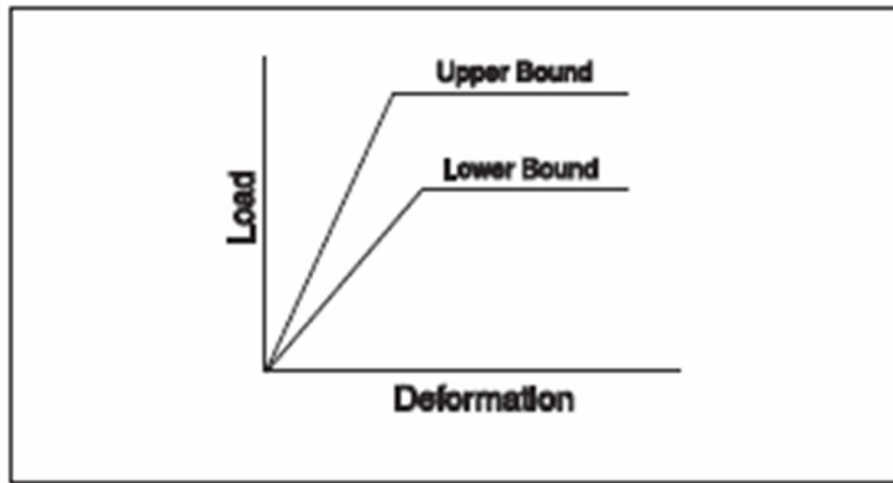


**Figure 2.18** Upper and lower-bound approach to define soil-foundation stiffness and capacity (from Buckle et al. 2006).

## 2.3.6 Calibration of Limit State Load and Resistance Factors using RBD

### 2.3.6.1 Closed-Form Solutions

A closed-form solution such as First-Order, Second-Moment (FOSM) can be used to calibrate load and resistance factors based on a target  $\beta$  value if  $Q$  and  $R$  can be represented as single or lumped, normal- or lognormal-distributed functions (e.g., see Fig. 2.11). For normally distributed functions, the relationship is (Barker et al. 1991, Paikowsky et al. 2004, Allen et al. 2005):

$$\beta = \frac{R_n \lambda_R - Q_n \lambda_Q}{\sqrt{(COV_R R_n \lambda_R)^2 + (COV_Q Q_n \lambda_Q)^2}} = \frac{(\gamma_Q / \varphi_R) \lambda_R - \lambda_Q}{\sqrt{(COV_R (\gamma_Q / \varphi_R) \lambda_R)^2 + (COV_Q \lambda_Q)^2}} \quad (2.56)$$

and for lognormally distributed functions, the relationship is (Barker et al. 1991, Paikowsky et al. 2004, Allen et al. 2005):

$$\beta = \frac{\ln\left[\frac{R_n\lambda_R}{Q_n\lambda_Q} - \sqrt{(1+COV_Q^2)/(1+COV_R^2)}\right]}{\sqrt{\ln[(1+COV_Q^2)(1+COV_R^2)]}} = \frac{\ln\left[\frac{\gamma_Q\lambda_R}{\varphi_R\lambda_Q} - \sqrt{(1+COV_Q^2)/(1+COV_R^2)}\right]}{\sqrt{\ln[(1+COV_Q^2)(1+COV_R^2)]}} \quad (2.57)$$

All values have previously been defined (see Eqs. 2.1, 2.46 and 2.47, and Section 2.3.1) except  $\lambda$ , which is the bias between the nominal (i.e., predicted) values of  $Q$  and  $R$  and the measured values (e.g., from a dataset), and represented as (Allen et al. 2005):

$$\lambda_R = \mu_R / R_n \quad (2.58)$$

$$\lambda_Q = \mu_Q / Q_n \quad (2.59)$$

Equations 2.56 and 2.57 can be solved for  $\beta$  by varying the load and resistance factors,  $\gamma_Q$  and  $\varphi_R$ . Alternatively, if  $\gamma_Q$  is known and  $\beta$  is selected based on a target performance level (e.g., see Table 2.5), the equations can be rearranged to solve for the required resistance factor,  $\varphi_R$ .

The closed-form FOSM solution is easy to apply but has limited application for solving the performance function when the resistance,  $R$ , is comprised of multiple parameters with different marginal distributions and potential correlation structure, as described in the preceding sections. Other solutions are available, such as the First-Order Reliability Method (FORM), originally developed by Hasofer and Lind (1974) and used more extensively in structural engineering applications (Paikowsky 2004). FORM uses an iterative process to solve the performance function and estimate  $\beta$ , which can be complicated or impractical for  $R$  comprised of multiple parameters with different marginal distributions and correlation structure.

### 2.3.6.2 Monte Carlo Simulations

Monte Carlo simulation (MCS) is a relatively simple concept that provides a robust and adaptable technique for solving the performance function and calibrating limit state factors using RBD. Allen et al. (2005) note that MCS is generally more rigorous and adaptable for reliability-based design compared to using closed-form solutions.

The overall concept for MCS is to generate random realizations for each input parameter based on their estimated or known characteristic distributions and dependence structure. In the context of limit state analysis (e.g., Eq. 2.1), the realizations generated for each parameter are used to calculate individual values of load,  $Q$ , and resistance,  $R$ . The performance function is then evaluated based on  $Q$  and  $R$  generated from each realization and the probability of occurrence (and/or probability of failure,  $p_f$ ) for the selected limit state is estimated by dividing the number of responses for a particular occurrence by the total number of simulations (e.g., Allen et al 2005, Fenton and Griffiths 2008, Uzielli and Mayne 2011). MCS can be completed using Excel or similar spreadsheet programs for limited numbers of realizations with relatively simple distribution and dependence structure. MCS with greater numbers of realizations and with more complex distribution or dependence (e.g., dependence requiring copula functions) can be completed using Matlab, R, or similar programs with more robust statistical packages.

The accuracy for MCS analysis depends on the accuracy of each input parameter as well as the number of simulations. Broding et al. (1964) recommended the following for determining the minimum number of simulations:

$$N \geq -\frac{\ln(1-\alpha)}{P_f} \cdot X \quad (2.60)$$

where  $N$  is the number of MCS simulations (and/or realizations of each input parameter),  $X$  is the number of input parameters,  $\alpha$  is the desired confidence level, and  $p_f$  was previously defined as the target probability of failure. A greater number of simulations should, in theory, provide more accurate results with greater confidence level. However, the selected number of simulations must also be tempered by the required computing time and effort.

## 2.4 SUMMARY OF LITERATURE REVIEW

### 2.4.1 Summary

This literature review focused on geotechnical design for spread footings supported on fine-grained soils and aggregate pier-improved fine-grained soils in the context of reliability-based limit state design. The review included: (1) limit state design concepts focusing on bearing capacity analysis at the ultimate limit state and vertical deformation at the serviceability limit state, (2) linear and nonlinear distortion displacement models related to immediate settlement under foundation loads, (3) reliability-based design and the calibration of suitable resistance factors. Particular attention was given to the implementation of nonlinear distortion models for serviceability limit state design and how the parameters used in these models are calibrated for robust RBD analysis.

### 2.4.2 Outstanding Issues

This review identified outstanding issues that should be addressed to advance geotechnical design of spread footings supported on fine-grained soils and on aggregate-improved fine-grained soil, particularly in the context of serviceability limit state design:

1. Serviceability limit state design for spread footings supported on fine-grained soils typically focusses on consolidation settlement within a deterministic framework

and neglects the contribution in foundation movement from immediate settlement (i.e., distortion or undrained displacement). Further, if immediate settlement is considered, it is often evaluated in terms of elastic (linear) displacement even though plastic fine-grained soils mobilize resistance with a nonlinear response. Finally, the use of deterministic-only analysis overlooks inherent uncertainties that are better addressed with a probabilistic approach. Therefore, updated SLS design is necessary for footings on plastic, fine-grained soils that utilizes a more accurate nonlinear soil-foundation response while incorporating probabilistic analysis within a reliability-based design framework.

2. For footings supported on aggregate pier-improved fine-grained soil, several methods have been developed over the years to evaluate foundation settlement, but none has been widely adopted or incorporated into code for SLS design. Recent improvements have been made to better estimate nonlinear load-displacement response for footings underlain by single or multiple piers (e.g., Stuedlein and Holtz 2014). However, even the updated methods do not include soil and model uncertainties inherent in foundation design. Therefore, consistent with footings on unimproved fine-grained soil (Item 1), additional work is needed to provide an improved nonlinear soil-foundation response that incorporates probabilistic analysis within a reliability-based design framework.
3. Significant work has been completed over the past 25 years by researchers and in practice to improve reliability-based design and incorporate it into geotechnical limit state analysis. However, some limitations still exist that need to be explored, particularly as it applies to single versus multiple footings and soil-structure



interaction (SSI). Traditional foundation analysis that focuses on single footings neglects inherent soil spatial variability across multiple footings. However, it is the response across multiple footings (e.g., differential displacement) that typically dictates foundation performance. Congruently, soil-structure interaction between the building and multiple footings (e.g., structural stiffness) affects the foundation response. These items have been addressed in previous research, but analysis within the framework of probabilistic RBD is limited.

4. Soil-structure interaction within the context of building performance (e.g., structure member response) and its relation to limit state foundation design is not well understood and should be addressed with additional research.

## CHAPTER 3: RESEARCH OBJECTIVES AND PROGRAM

### 3.1 RESEARCH OBJECTIVES

The objective of this study is to further develop and improve reliability-based Serviceability Limit State (SLS) design procedures for shallow foundations supported on fine-grain soil and aggregate pier-improved fine-grain soil under undrained loading conditions. More specifically, the objectives include:

1. Evaluation of the nonlinear bearing pressure-displacement behavior of shallow foundations supported on fine-grain soil and aggregate pier-improved fine-grain soil under undrained loading;
2. Generation of methods for predicting bearing pressure-displacement behavior for shallow foundations, particularly with regard to SLS design and in relation to the ultimate limit state (i.e., bearing capacity) of the foundation;
3. Evaluation and characterization of the variability and dependence structure of the parameters associated with the new bearing pressure-displacement models;
4. Calibration of appropriate SLS load-resistance factors for the bearing pressure-displacement models within the framework of reliability-based design methodologies;
5. Evaluation of inter- versus intra-site variability with respect to bearing pressure-displacement model parameter dependence, and its effect on model error and appropriate limit state factors; and,

6. Evaluation of total and differential displacement between foundation elements supporting a multi-story structure, and the resulting structural performance, accounting for the soil-structure interaction, nonlinear soil bearing resistance, and the spatial variability of the foundation soil.

### 3.2 RESEARCH PROGRAM

The research program undertaken to achieve the objectives noted herein includes:

1. The development of a nonlinear bearing pressure-displacement model for the SLS design of shallow footings supported on aggregate pier-improved fine-grain soil with undrained loading conditions, based on the results of full-scale loading tests reported in the literature, within a reliability-based design framework using Monte Carlo simulations, while accounting for a bivariate model parameter correlation structure using an appropriate copula;
2. The development of a nonlinear bearing pressure-displacement model for the SLS design of shallow footings supported on fine-grain soil with undrained loading conditions, based on the results of full-scale loading tests reported in the literature, within a reliability-based design framework using Monte Carlo simulations, while accounting for a multivariate model parameter correlation structure using appropriate copulas;
3. A step-by-step description of an appropriate reliability-based design framework, and recalibration of the SLS design model for shallow footings supported on aggregate pier-improved fine-grain soil that includes new full-scale loading tests completed at the OSU field test site; and,

4. The probabilistic characterization of total and differential foundation displacement and the resulting structure performance at the serviceability limit state based on analyses using OpenSEES software and Monte Carlo-based simulations to model the soil-structure response. The analyses used a non-linear finite element model to represent a 3-story steel moment frame building. The foundations and soil were modeled using a Beam-on-nonlinear-Winkler-foundation (BNWF) with nonlinear vertical spring elements developed using the reliability-based bearing pressure-displacement model for spread footings on fine-grained soil with undrained loading conditions. Varying degrees of spatial soil variability were evaluated, particularly variability in the undrained shear strength over horizontal distances, to characterize its influence on differential foundation displacement. Inter-site and intra-site variability was evaluated by assuming a dependence structure for the multivariate bearing pressure-displacement model parameters being based either on a single site from the loading test database or from the entire loading test database.

**CHAPTER 4:  
RELIABILITY-BASED SERVICEABILITY LIMIT STATE DESIGN  
OF SPREAD FOOTINGS ON AGGREGATE PIER REINFORCED  
CLAY**

Authors:

Jonathan C. Huffman, P.E. and Armin W. Stuedlein, Ph.D., P.E., M.ASCE

Journal:

Journal of Geotechnical and Geoenvironmental Engineering  
American Society of Civil Engineers (ASCE)  
1801 Alexander Bell Drive  
Reston, VA 20191-4400

Volume 140, Issue 10 (October 2014)

## 4.1 ABSTRACT

Despite the availability of numerous methods to predict the load-displacement response of aggregate pier reinforced clay, accurately modeling the non-linear displacement response remains challenging. Moreover, the uncertainty in the bearing pressure-displacement prediction has not been satisfactorily estimated, preventing the generation of reliability-based design (RBD) procedures. This study proposes a simple RBD procedure for assessing the allowable bearing pressure for aggregate pier reinforced clay in consideration of the desired serviceability limit state. A recently established bearing capacity model for aggregate pier reinforced clay, and its uncertainty, is incorporated into a bivariate bearing pressure-displacement model appropriate for a wide range in displacement, and calibrated using a high quality full-scale load test database. Several copulas were then evaluated for goodness of fit to the measured dependence structure between the coefficients of the selected two-parameter bearing pressure-displacement model. Following the generation of an appropriate performance function, a combined load and resistance factor is calibrated in consideration of the uncertainty in the bearing pressure-displacement model, bearing capacity, applied bearing pressure, allowable displacement, and footing width using Monte Carlo simulations of the respective source distributions. An example is provided to illustrate the application of the proposed procedure to estimate the bearing pressure for an allowable displacement at the desired serviceability limit probability.

## 4.2 INTRODUCTION

Aggregate piers, or stone columns, are often used as a means to provide in-situ ground improvement, helping to transfer light, medium, and heavy foundation loads from shallow spread footings to deeper strata, thereby increasing the allowable bearing pressure and reducing settlement as compared to the unimproved ground. The performance of spread footings supported on aggregate pier reinforced clay is influenced by several factors, including the footing size, the diameter and length of the aggregate piers, the percent of ground improved, and the stiffness of the matrix soil (Barksdale and Bachus 1983; Stuedlein and Holtz 2012; 2013a; 2013b). Modeling the performance of aggregate pier reinforced clay is difficult due to the complex distribution of stress and load transfer that develop between the aggregate piers and the matrix soil, particularly for footings underlain by multiple piers. However, several empirical and semi-empirical methods have been recently developed to estimate bearing capacity and displacement.

Stuedlein and Holtz (2013a, 2013b) provide an overview of methods that have been used in practice to estimate bearing capacity and displacement, respectively, of spread footings supported by single and multiple pier systems. Most methods used to estimate displacement of aggregate pier reinforced soil are not directly applicable for use with rigid spread footings because they rely on the unit cell concept developed by Aboshi et al. (1979), which is more appropriate for uniform pressures applied over a large area (e.g., embankment loads). Moreover, existing methods typically assume a soil-pier stiffness with linear bearing pressure-displacement ( $q$ - $\delta$ ) relationship that does not accurately capture the non-linear  $q$ - $\delta$  response of footings supported on aggregate pier reinforced clay. As a result, there is often significant uncertainty associated with estimating

the displacement of spread footings supported on aggregate pier reinforced clay (Stuedlein and Holtz 2013b). However, the quantification of the uncertainty in the  $q$ - $\delta$  response in aggregate pier reinforced ground has heretofore been considered impractical given the lack of suitable data and accurate ultimate and serviceability level design models.

With the increasing implementation of reliability-based design (RBD) in engineering practice, there is greater emphasis on characterizing design uncertainty and quantifying the probability of exceeding a particular limit state (e.g., Phoon 2003; Allen et al. 2005; Phoon 2008; Phoon and Kulhawy 2008; Li et al. 2011; Uzielli and Mayne 2011). To meet the requirements for serviceability limit state (SLS) design, there is a need to develop procedures that can accurately and reliably predict the displacement of foundations supported on aggregate pier reinforced clay with regard to the multiple sources of uncertainty that contribute to the prediction variability.

This paper uses an existing full-scale load test database and associated ultimate limit state (ULS; e.g, bearing capacity) model to investigate the reliability-based SLS design of spread footings on aggregate pier reinforced clay. First, the statistical regression-based bearing capacity model and supporting load test database generated by Stuedlein and Holtz (2013a) is reviewed. Then the methodology for the probabilistic SLS calibration is described in the context of selected two-parameter bearing pressure-displacement models. The bivariate  $q$ - $\delta$  model parameters determined from least squares regression of the load test data are then characterized using copula theory accounting for parameter correlation structure. Unreasonably low values of randomly generated bearing capacity are avoided by truncating the distribution of the capacity through the use of the estimated remolded shear strength of the clayey soils described in the database. Monte Carlo simulations are



then used to simulate the combined uncertainty in the ULS and the selected  $q$ - $\delta$  model, including variability in the applied bearing pressure (i.e., load), allowable displacement, and footing width. Finally, a procedure is described to estimate the allowable bearing pressure of a spread footing supported on aggregate pier reinforced clay with a given service level displacement and acceptable probability of exceeding the SLS. The procedure proposed herein can be used to estimate the reliability of spread footing displacement for aggregate pier-reinforced clay.

### 4.3 LOAD TEST DATABASE AND SELECTED BEARING CAPACITY MODEL

The database used by Stuedlein and Holtz (2013a) to develop the selected bearing capacity model consisted of 30 full scale load tests of spread footings supported on various configurations of aggregate piers in cohesive soil. Fifteen of the load tests were performed by Stuedlein (2008) and described by Stuedlein and Holtz (2012). The remaining portion of the database consisted of load tests reported by Greenwood (1975), Hughes et al. (1975), Baumann and Bauer (1974), Bergado and Lam (1987), Han and Ye (1991), Lillis et al. (2004), and White et al. (2007). The criteria for including the selected cases were: (1) satisfactory soil characterization and relatively uniform profile within the assumed failure zone, (2) adequate load test and pier geometry description, (3) the matrix soil being comprised predominantly of fine-grained soil with undrained shear response, and (4) the load test being conducted in a rapid continuous manner (Stuedlein, 2008; Stuedlein and Holtz, 2013a; 2013b). Each load test provided bearing pressure-displacement ( $q$ - $\delta$ ) curves that were used to estimate the bearing capacity of the footing. The  $q$ - $\delta$  curves represent distortion (i.e., immediate) displacement due to shear strains

within a depth of approximately  $1B$ , where  $B$  is the footing width or diameter (Stuedlein and Holtz 2013b). Owing to the danger associated with collapse of full-scale loading tests, the true capacity of footings can rarely be achieved experimentally; therefore, the interpreted bearing capacity,  $q_{ult,i}$ , of each load test was determined by weighted least squares regression on several asymptotic curves to the observed  $q-\delta$  as described in Stuedlein and Holtz (2013a).

The bearing capacity model selected for the analyses described herein was developed using multiple non-linear regression analysis of the estimated capacity and parameters controlling the performance of the footing and comprising the database. The predicted capacity,  $q_{ult,p}$ , of an isolated spread footing resting on aggregate pier reinforced clay, measured in kPa, was determined equal to (Stuedlein and Holtz 2013a):

$$\ln(q_{ult,p}) = b_0 + b_1 S_r + b_2 a_r + b_3 d_f S_r + b_4 \tau_m^{-1} + b_5 \tau_m \quad (4.1)$$

in which  $S_r$  is the slenderness ratio of the aggregate pier(s) given by  $S_r = L_p/d_p$  (i.e., ratio of pier length to pier diameter),  $a_r$  is the area replacement ratio beneath the footing and equal to ratio of pier area to foundation footprint;  $d_f$  is the depth of footing embedment (m); and  $\tau_m$  is the matrix soil shear mass participation factor given by  $\tau_m = s_u/a_r$ , where  $s_u$  is the undrained shear strength of the matrix soil (kPa). Optimally fitted model coefficients were determined equal to  $b_0 = 4.756$ ,  $b_1 = 0.013$ ,  $b_2 = 1.914$ ,  $b_3 = 0.070$ ,  $b_4 = -13.71$ , and  $b_5 = 0.005$ .

The accuracy of the bearing capacity predicted by Eq. 4.1,  $q_{ult,p}$ , was compared to the interpreted bearing capacity,  $q_{ult,i}$ , using several metrics, including the adjusted coefficient of determination ( $R^2$ ), mean bias (defined as the average ratio of measured to predicted capacity), and coefficient of variation (COV) in point bias, yielding 0.94, 1.00, and

13.1 percent, respectively, illustrative of a satisfactory model (Stuedlein and Holtz 2013a). The bearing capacity model represented the average footing response after controlling for variability in pier length, diameter, embedment, undrained shear strength, and area replacement ratio and was independent of the aggregate pier construction method (Stuedlein and Holtz 2013a). This capacity model was selected as a reference capacity for the serviceability limit state analyses described in the remainder of this work.

#### 4.4 SERVICEABILITY LIMIT STATE DESIGN MODEL

Reliability-based design recognizes the sources of uncertainty that can contribute to design decisions and uses probability theory to propagate error through a design procedure. Probability theory provides a means to estimate the probability of failure,  $p_f$ , where *failure* is defined as exceeding a given limit state, and to determine whether the resulting probability is acceptably small (Phoon 2008). A suitable framework is described concisely by the margin of safety performance function,  $P$  (e.g., Baecher and Christian 2003):

$$p_f = \Pr(R - Q < 0) = \Pr(P < 0) \leq p_T \quad (4.2)$$

in which  $R$  equals the ultimate or allowable resistance, as desired,  $Q$  is the applied load, and  $p_T$  is the target probability of failure. For foundation design, the ULS is met when the applied bearing pressure equals the bearing capacity, whereas the SLS is typically defined by the exceedance of a prescribed allowable displacement. The load and resistance terms in the performance function (i.e.,  $R$  and  $Q$ ) are both represented by a deterministic, nominal (i.e., predicted) value coupled with its assumed or known dispersion. Use of the performance function and estimation of the corresponding associated parameters for SLS design of a spread footing on aggregate pier reinforced clay is described subsequently.

Phoon and Kulhawy (2008), Dithinde et al. (2011), and Uzielli and Mayne (2011) showed that non-linear  $q$ - $\delta$  behavior normalized by a reference bearing capacity and footing diameter, respectively, can be well represented by hyperbolic and power law models, given by:

$$q^* = \frac{q_{mob}}{q_{ult,i}} = \frac{(\delta / B')}{k_1 + k_2(\delta / B')} \quad (4.3)$$

and:

$$q^* = \frac{q_{mob}}{q_{ult,i}} = k_3(\delta / B')^{k_4} \quad (4.4)$$

respectively, where  $q_{mob}$  is the mobilized resistance at a given displacement,  $\delta$ , which is normalized by the equivalent footing diameter,  $B'$ , defined as the equivalent circular footing diameter resulting from an area balance (e.g., Mayne and Poulos 1999). The coefficients  $k_1$ ,  $k_2$ ,  $k_3$  and  $k_4$  are determined using least squares optimization.

Figure 4.1 presents a typical comparison of an observed and fitted normalized  $q$ - $\delta$  curve (referred to hereafter as  $q^*$ - $\eta$  curves where  $\eta = \delta/B'$ ) from the load test database. Normalization of the mobilized resistance and displacement allows the scatter in the  $q$ - $\delta$  behavior of geometrically and physically different footings to be reduced. Figure 2a shows the  $q$ - $\delta$  curves comprising the database of spread footings supported on aggregate pier reinforced clay and represents single isolated, intermediate single and groups, and groups of aggregate piers, as defined in Stuedlein and Holtz (2013a, 2013b). Figure 2b presents the  $q^*$ - $\eta$  curves; although non-trivial scatter remains in the normalized curves, the magnitude of the scatter is significantly reduced in comparison to the raw  $q$ - $\delta$  curves.

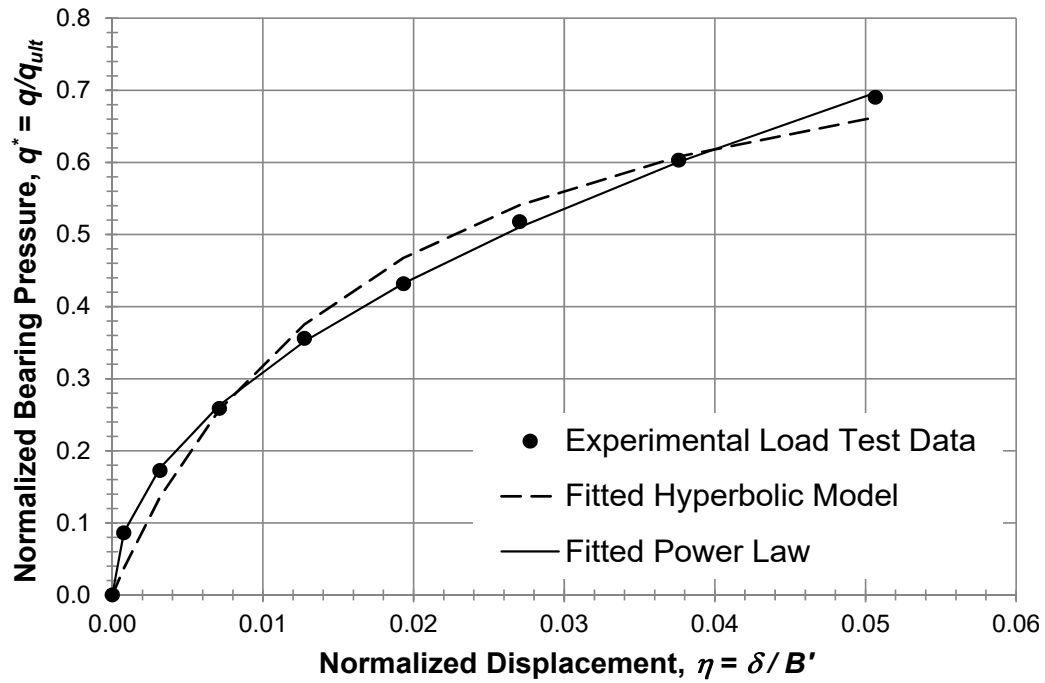


**Figure 4.1** Example of hyperbolic and power law models fitted to normalized load test data (Footing G1, data from Stuedlein and Holtz 2013a, 2013b).

The hyperbolic and power law models may be rewritten in terms of the mobilized resistance for use with the performance function (e.g., Dithinde et al. 2011):

$$q_{mob} = \frac{\eta}{k_1 + k_2\eta} q_{ult,i} = M_s q_{ult,i} \quad (4.5)$$

$$q_{mob} = k_3 \eta^{k_4} q_{ult,i} = M_s q_{ult,i} \quad (4.6)$$

where  $M_s$  is the appropriate factor used to scale the ultimate resistance to a mobilized resistance based on the allowable (i.e., service level) normalized footing displacement,  $\eta$ .

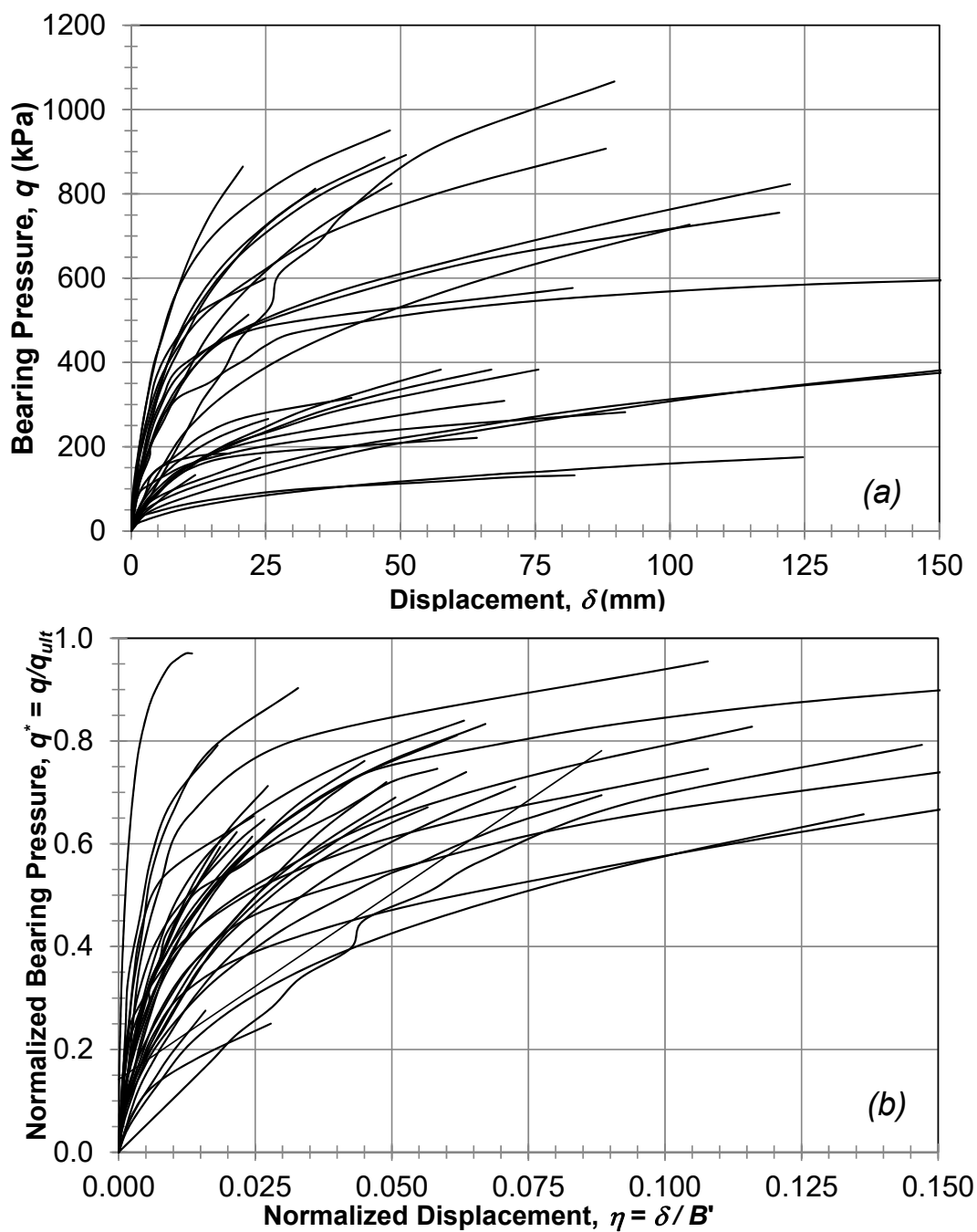


**Figure 4.2** Variation of bearing pressure with displacement for loading tests in the load test database: (a) raw data, and (b) normalized data.

In the absence of site-specific load tests,  $q_{ult,i}$  may be replaced with the predicted bearing capacity,  $q_{ult,p}$  (Eq. 4.1), provided the associated dispersion is incorporated into the SLS characterization. The predicted capacity provides the nominal resistance for the performance function (Eq. 4.2), while its dispersion is represented by the statistical distribution associated with fitting Eq. 4.1 to the load test results (i.e., the distribution of the capacity model point biases). The reliability of footing behavior at the SLS is then calibrated by solving the performance function in terms of the applied bearing pressure,  $q_{app}$ , and the mobilized bearing resistance,  $q_{mob}$ , computed using Eq. 4.5 or Eq. 4.6. The performance function,  $P$ , may then be restated as the difference between the mobilized resistance and the applied bearing pressure:

$$p_f = \Pr(M_s q_{ult,p} - q_{app} < 0) = \Pr(M_s < \frac{q_{app}}{q_{ult,p}}) \leq p_T \quad (4.7)$$

By defining the ultimate and applied bearing pressures in terms of a deterministic nominal value (i.e.,  $q_{app,n}$  and  $q_{ult,n}$ ) and the corresponding normalized random variable (i.e.,  $q_{app}^*$  and  $q_{ult}^*$ ) representing the statistical distribution of the bearing pressure and resistance, Eq. 4.7 can be rewritten as (Uzielli and Mayne 2011):

$$p_f = \Pr(M_s < \frac{q_{app,n} \cdot q_{app}^*}{q_{ult,n} \cdot q_{ult}^*}) = \Pr(M_s < \frac{1}{\psi_q} \frac{q_{app}^*}{q_{ult}^*}) \leq p_T \quad (4.8)$$

where  $\psi_q$  is the combined (i.e., lumped) load and resistance factor assigned to provide an acceptable probability of failure and is similar to a global factor of safety used in allowable stress design (Phoon and Kulhawy 2008). Note again that the random variable representing the statistical distribution of the resistance ( $q_{ult}^*$ ) has been established based on the

dispersion associated with fitting Eq. 4.1 to the load test results. The distribution of the applied bearing pressure ( $q^*_{app}$ ) is discussed subsequently.

In this study, the probability of failure and the accompanying reliability index,  $\beta$ , were estimated based on a prescribed interval of  $\psi_q$  that ranged from one (i.e., no reduction in applied bearing pressure) to 20. The reliability index was computed using:

$$\beta = -\Phi^{-1}(p_f) \quad (4.9)$$

where  $\Phi^{-1}$  represents the inverse standard normal cumulative function, and  $\beta$  is the number of standard deviations separating the mobilized resistance from the applied load. Monte Carlo simulations were used to estimate  $p_f$  and  $\beta$  for the range in  $\psi_q$  to investigate possible relationships between the parameters in the performance function to provide a simplified procedure for SLS design.

## 4.5 MONTE CARLO-BASED RELIABILITY SIMULATIONS

Monte Carlo simulations were used to incorporate multiple sources of uncertainty and generate numerous estimations of the performance function,  $P$ , and accompanying probability of failure,  $p_f$ . This was accomplished by selecting the appropriate resistance model, simulating variables for normalized resistances and normalized bearing pressures using estimated or assumed distributions and parameter correlations, and then comparing the normalized resistances at a prescribed normalized service level displacement to the normalized bearing pressures. The details of the simulations are described below.

### 4.5.1 Model Selection and Resistance Model Parameters

Hyperbolic and power law models were evaluated for suitability in representing the observed load test data by fitting to each of the  $q^*-\eta$  curves. Table 4.1 presents the



statistical summary of the  $q^*-\eta$  model parameters (i.e.,  $k_1, \dots, k_4$ ) determined from the least squares optimization. Selected goodness-of-fit metrics for both  $q^*-\eta$  models are also summarized in Table 4.1, including the cumulative root mean squared error (RMSE), average  $R^2$ , average bias, and average COV in bias computed from the fitting to the entire load test dataset. The lower RMSE value for the hyperbolic model suggests a slightly better fit, on average, relative to the power law model. The average  $R^2$  values of 0.99 and 0.98 for the hyperbolic and power law models, respectively, indicate that the curvature of the bearing pressure-displacement curves is satisfactorily captured, with just slightly better performance provided by the hyperbolic model. The model biases also indicate that both models closely predict the  $q^*-\eta$  response relative to the observed data, although the power law model is slightly more accurate than the hyperbolic model with an average bias closer to one. The COV in the model bias was greater for the hyperbolic model, pointing to a wider dispersion in inaccuracy as compared to the power law model.

**Table 4.1. Summary of Fitted Bearing Pressure Displacement Model Parameters**

Parameter	Mean	COV (%)	Cumulative Root Mean Squared Error (RMSE)	Average $R^2$	Average Mean Bias	Average COV in Bias (%)
$k_1$	0.020	78.7	461.5	0.99	1.087	23.1
$k_2$	1.148	24.7				
$k_3$	3.088	40.7	576.5	0.98	0.966	12.2
$k_4$	0.454	23.3				

**Note:** Mean and COV reported for individual parameters. RMSE,  $R^2$ , mean bias, and COV in bias reported for combined  $k_1$  and  $k_2$  or  $k_3$  and  $k_4$  parameters based on curve fit to database of load test results.

The goodness-of-fit metrics indicate both models sufficiently capture the average  $q^*-\eta$  response of the load test data. However, the power law model was ultimately selected for the reliability analyses owing primarily to the observation that the dispersion of the model prediction bias and the model parameters is significantly less when compared to the hyperbolic model. The power law model parameters ( $k_3$  and  $k_4$ ) were not inconsistent with a lognormal distribution at a significance level of 5 percent using the Anderson-Darling goodness of fit test (e.g., Anderson and Darling 1952); therefore, the resistance model parameters were simulated using a lognormal distribution. Figure 4.3 shows the cumulative distribution of the  $k_3$  and  $k_4$  parameters along with the fitted lognormal cumulative distribution functions (CDF) for each model parameter.

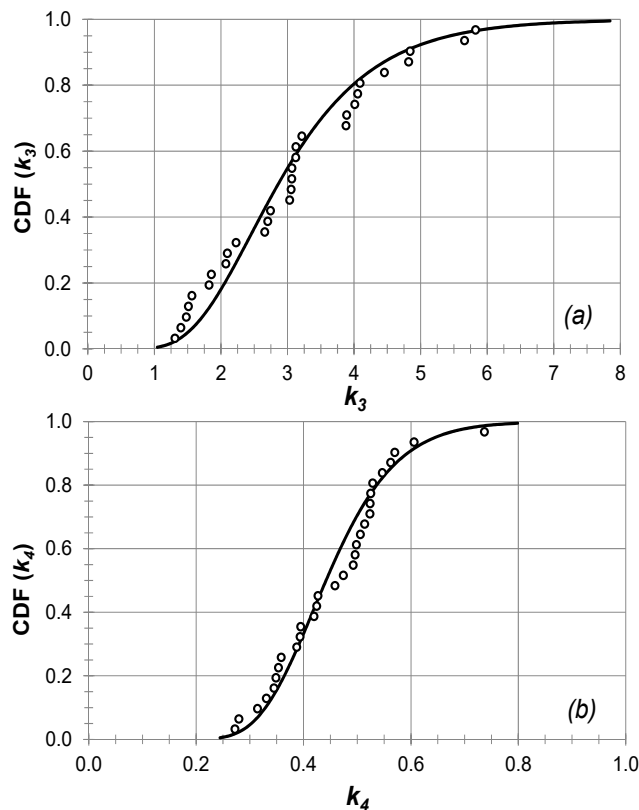


**Figure 4.3** Cumulative distribution of the observed power law model parameters (a)  $k_3$  and (b)  $k_4$  with fitted lognormal CDFs.

#### 4.5.2 Bearing Pressure-Displacement Model Parameter Correlation and Simulation

In order to avoid bias in the reliability calculations, the dependence, or correlation between model parameters must be incorporated in the simulations (e.g., Phoon and Kulhawy 2008; Dithinde et al. 2011; Uzielli and Mayne 2011; 2012; Tang et al. 2013). Therefore, the possible dependence of the regressed  $q^*$ - $\eta$  model parameters,  $k_3$  and  $k_4$ , was investigated between each other and the bearing capacity variables (i.e.,  $s_u$ ,  $a_r$ ,  $L_p$ ,  $B$ ,  $d_p$ , and  $d_f$ ). Figure 4.4 shows the bearing capacity variables plotted versus  $k_3$  and  $k_4$ , in which no apparent correlations can be observed. However, it is important to note that a single data pair can give the appearance of dependence in datasets with small sample sizes; therefore, it is critical that the randomness of these factors with respect to  $k_3$  and  $k_4$  be re-evaluated should additional data become available. Figure 4.5 shows the variation of  $k_3$  with  $k_4$ , wherein a moderate, positive linear correlation between these parameters can be observed, corresponding to a Pearson product-moment correlation,  $\rho$ , of 0.62 and Kendall's Tau rank correlation,  $\rho_\tau$  of 0.43.

Copulas, which are functions that couple multivariate functions to their marginal distributions and may represent any number of correlated random variables (Nelson 2006), were used to simulate the bivariate correlation structure of the load-displacement model parameters  $k_3$  and  $k_4$ . Copulas are used in many applications, ranging from complex financial forecasts to hydrological forecasts, and are becoming more frequently used in geotechnical analyses. For example, Tang et al. (2013) used copulas to account for the negative correlation between cohesion and the internal friction angle for the purpose of estimating factors of safety and the associated probabilities of failure for simple slope

stability and retaining wall applications. Other approaches previously used to simulate correlated geotechnical model parameters include the translation-based probability model and rank correlation method (e.g., Phoon and Kulhawy 2008; Dithinde et al. 2011). These approaches represent a special Gaussian-type copula, but use the less robust Pearson product-moment and Spearman rank correlations, respectively, instead of  $\rho_\tau$  to generate the copula parameter as discussed below. Additionally, Li et al. (2013) indicated that the translation method was unsatisfactory when the multivariate correlations exhibit nonlinearity.

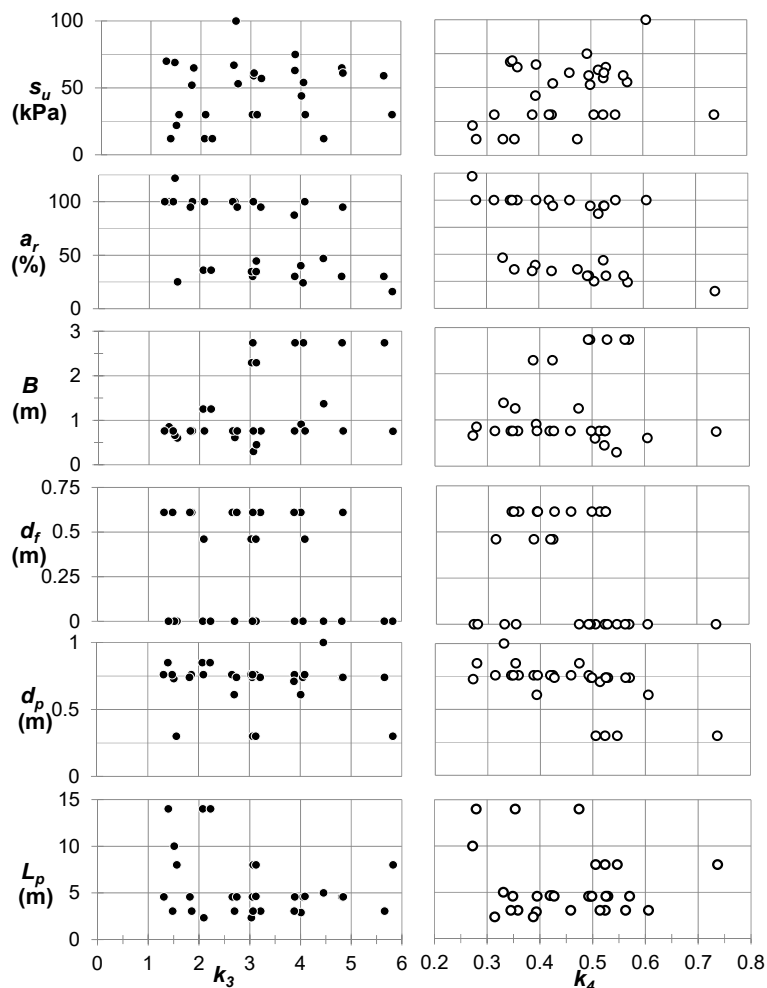


**Figure 4.4** Regressed power law model  $k_3 - k_4$  pairs from load test database plotted versus design variables in the ultimate limit state capacity model.

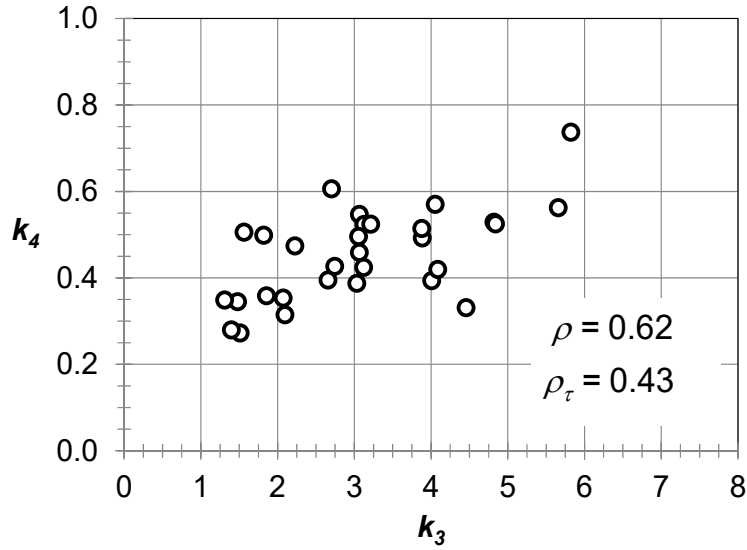


**Figure 4.5** Variation of power law model parameters  $k_3$  and  $k_4$  derived from fitting to the normalized bearing pressure – normalized displacement data.

Many copula types are available to account for trends in parameter correlations, including linear or nonlinear correlations and tail-dependent or tail-independent correlations, among others, and are therefore well-suited for parameter simulation where sparse data, such as full-scale load test data exists. In similar work, Uzielli and Mayne (2011, 2012) and Li et al. (2013) used copulas to account for load-displacement model parameter dependence. The Gaussian, Frank, Clayton and Gumbel copula functions (e.g., Nelson 2006), given by:

$$C(u_1, u_2) = \Phi_\theta(\Phi^{-1}(u_1), \Phi^{-1}(u_2)) \quad (4.10a)$$

$$C(u_1, u_2) = -\frac{1}{\theta} \ln \left[ 1 + \frac{(e^{-\theta u_1} - 1)(e^{-\theta u_2} - 1)}{e^{-\theta} - 1} \right] \quad (4.10b)$$

$$C(u_1, u_2) = (u_1^{-\theta} + u_2^{-\theta} - 1)^{-1/\theta} \quad (4.10c)$$

$$C(u_1, u_2) = \exp\{-[(-\ln u_1)^\theta + (-\ln u_2)^\theta]^{1/\theta}\} \quad (4.10d)$$

respectively, where  $u_1$  and  $u_2$  are standardized ranked values of correlated parameters transposed into the  $[0,1]$  space, determined by dividing the ranked values by the total number of pairs in the dataset, and  $\theta$  is the copula parameter computed as described below, represent a range of possible trends in the dependence between variables and were evaluated for possible use in representing the correlation structure of load-displacement model parameters. Note that these copula functions reference the rank of the model parameters rather than the model parameters themselves for the purposes of parameter simulation. The relationship between  $k_3$  and  $k_4$  and the copula function,  $C_{k_3, k_4}$ , can be determined by fitting to  $\rho_\tau$  using (e.g., Nelson 2006, Li et al. 2013):

$$\rho_\tau(k_3, k_4) = 4 \int_0^1 \int_0^1 C_{k_3, k_4}(u_3, u_4) dC_{k_3, k_4}(u_3, u_4) - 1 \quad (4.11)$$

where  $u_3$  and  $u_4$  are the corresponding standardized ranked values of the  $k_3 - k_4$  dataset. The copula parameters,  $\theta$ , used in Eqs. 4.10a to 4.10d, were calculated using  $\rho_\tau$  as described by Nelson (2006) and Li et al. (2013). The best fit copula was determined by evaluating the Akaike Information Criterion (*AIC*) (Akaike 1974) and Bayesian Information Criterion (*BIC*) (Schwarz 1978). The *AIC* and *BIC* are defined as:

$$AIC = -2 \sum_{i=1}^N \ln c(u_{3i}, u_{4i}) + 2k \quad (4.12)$$

$$BIC = -2 \sum_{i=1}^N \ln c(u_{3i}, u_{4i}) + k \ln N \quad (4.13)$$

respectively, where  $N$  is the sample size of the data (i.e., number of  $k_3 - k_4$  pairs),  $c$  equals the copula density function for the respective copula type, given by:

$$c(u_1, u_2) = \frac{\partial^2}{\partial u_1 \partial u_2} C(u_1, u_2) \quad (4.14)$$

and  $u_{3i}$  and  $u_{4i}$  are the standardized ranked values of each  $k_3 - k_4$  pair from the dataset, and  $k$  is the number of copula parameters (equal to unity for the selected single parameter copulas evaluated herein).

Table 4.2 summarizes the goodness-of-fit of the sample  $k_3 - k_4$  bivariate distribution to the selected copulas assessed using the AIC and BIC. The optimal (i.e., lowest) AIC and BIC values were obtained using the Gumbel copula function, and therefore it was selected for the reliability simulations. The  $k_3 - k_4$  pairs fitted to the observed bearing pressure-displacement curves are compared against 1,000 pairs simulated using the fitted distributions for  $k_3$  and  $k_4$  (Fig. 4.3) and the fitted Gumbel copula (Table 4.2) in Fig. 4.6a. Appendix S1 in the Supplemental Online Data (and Appendix A in this dissertation) summarizes the procedure and calculations associated with simulating random correlated  $k_3 - k_4$  pairs. The simulated power law model parameters are shown to qualitatively capture the scatter associated with the fitted bearing pressure-displacement model parameters. Quantitatively, the Kendall's Tau rank correlation corresponding to the simulated  $k_3 - k_4$  pairs equals 0.41, similar to that obtained for the fitted  $k_3 - k_4$  pairs. The resulting  $q^* - \eta$  curves using the power law model and  $k_3 - k_4$  pairs are plotted in Fig. 4.6b and indicate that the observed spread in  $q^* - \eta$  behavior is satisfactorily captured, indicating that the selected statistical models satisfactorily represent the observed footing performance in the reliability simulations.

**Table 4.2. Summary of Copula Fitting Analyses for the Power Law  $q$ - $\delta$  Model Parameters. Note that Kendall's Tau Rank Correlation  $\rho_\tau = 0.43$  for all copulas investigated.**

Copula Type	Copula Parameter, $\theta$	AIC	BIC
Gaussian	0.626	-12.9	-11.5
Frank	4.593	-12.0	-10.6
Clayton	1.510	-11.0	-9.6
Gumbel	1.755	-14.4	-13.0

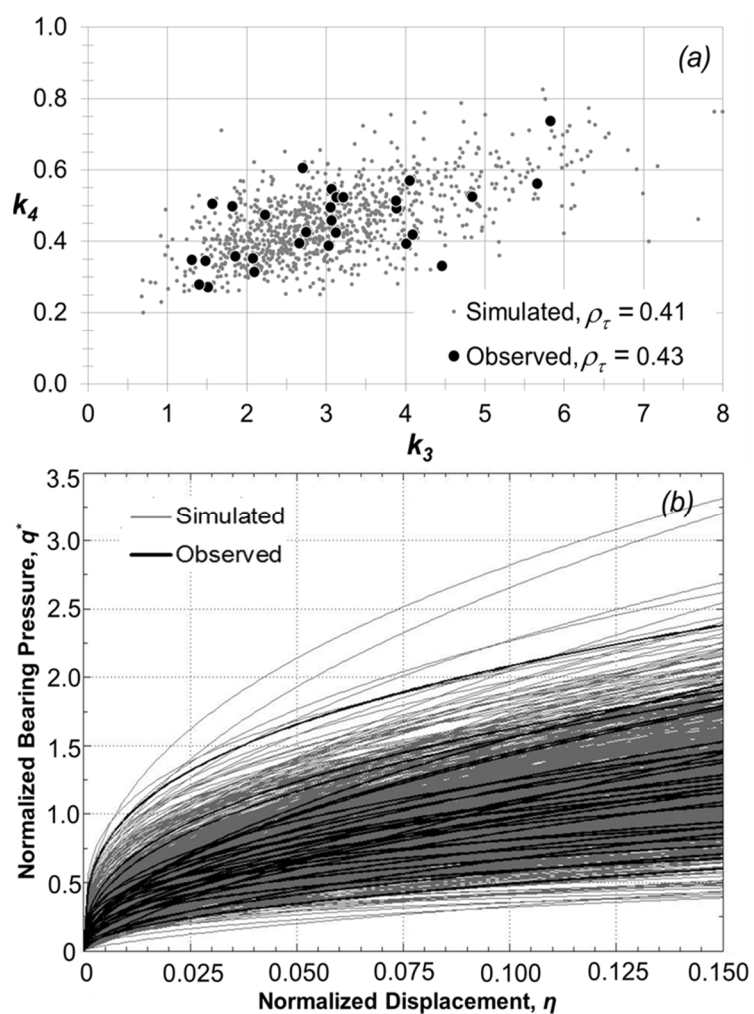


**Figure 4.6** Example simulations of normalized bearing pressure-normalized displacement of spread footings on aggregate pier reinforced clay: (a) observed and simulated  $k_3 - k_4$  pairs derived using the fitted Gumbel copula model, and (b) associated normalized bearing pressure-normalized displacement curves.



### 4.5.3 Assessment and Incorporation of Lower-Bound Capacity

The normalized bearing capacity,  $q^*_{ult}$ , is statistically characterized with a normalized mean bias of 1.00, COV in bias of 13.1 percent, and lognormal point bias distribution (Table 3). Although random samples of capacity could be simulated or drawn from the lognormal distribution, Najjar (2005) and Najjar and Gilbert (2009) found significant evidence pointing to the need to limit conservative bias values (i.e., unreasonably high biases associated with large under-prediction of capacity) for the purposes of accurately modeling reliability. Najjar and Gilbert (2009) used a closed-form solution for reliability analysis, modified to reflect a truncation in the lower-bound portion of the capacity distribution. In this study, the lower-bound normalized capacities resulting from unrealistic lower-bound undrained shear strengths simulated from the source distribution were avoided using a truncated distribution.

To estimate lower-bound capacity, the bearing capacity was recalculated for each data set using Eq. 4.1 with residual undrained shear strength,  $s_{ur}$ , values in place of  $s_u$ . Triaxial test data reported by Stuedlein (2008) indicated average soil sensitivity ( $s_u/s_{ur}$ ) of 1.24, which was used to estimate the residual undrained shear strength for the matrix soil surrounding the aggregate piers reported by Stuedlein (2008) and Stuedlein and Holtz (2012). Similarly, the piers evaluated by Han and Ye (1991) were installed within soil with a sensitivity of 3.9. For the remaining portion of the database,  $s_{ur}$  was estimated based on a correlation to the liquidity index,  $LI$ , recommended by Najjar (2005):

$$s_{ur} = 170e^{-(4.6LI)} \quad (4.15)$$

where  $s_{ur}$  is in kPa. Comparing the bearing capacity values calculated using  $s_u$  to the bearing capacity values calculated using  $s_{ur}$  (i.e., the lower-bound capacity) indicated a

mean ratio of lower-bound bearing capacity to predicted mean bearing capacity of approximately 0.66. Therefore, a minimum normalized bearing capacity,  $q^{*}_{ult, min}$ , of 0.66 was specified as the lower bound capacity truncating the lognormal capacity distribution for use in the reliability simulations. The inclusion of the lower-bound capacity did not significantly affect the reliability simulations because the uncertainty associated with the bearing capacity model,  $COV(q^{*}_{ult})$ , was relatively small (13.1 percent). Nonetheless, it is important to include the lower bound truncation in the simulations in order to produce as accurate and physically meaningful reliability estimates as possible.

#### 4.5.4 Characterization of Allowable Displacement and Applied Bearing Pressure

Reliability analysis for the SLS using Eq. 4.8 required the characterization of the allowable displacement,  $\delta_a$ , and applied bearing pressure, including expected values and their distribution. An informed geotechnical workflow requires the close collaboration with the structural engineer in order to confirm the true allowable structural displacement. To provide a generalized framework, this study specified a range of values to statistically characterize the applied bearing pressure and allowable displacement in lieu of employing specific structural loads and displacements. The loading was modeled using a unit mean normalized applied bearing pressure,  $q^{*}_{app}$ , equal to 1.00 and  $COV(q^{*}_{app})$  equal to 10 and 20 percent for dead and live loads, respectively. The unit mean normalized applied bearing pressure was modeled using a lognormal distribution, consistent with national codes (e.g., AASHTO 2012) and similar reliability analyses performed by others (e.g., Phoon and Kuhawy 2008, Uzielli and Mayne 2011, and Li et al. 2013).

Table 4.3 summarizes the bearing pressure and displacement parameters used in the reliability simulations. Normalized allowable displacements,  $\eta_a$ , ranging from 0.005 to 0.20 were specified, based on an assumed range of mean  $\delta_a$  of 2.5 mm to 600 mm and equivalent footing diameters,  $B'$ , ranging from 0.5 m to 3 m. The dispersion of  $\delta_a$  may be considered a desirable random variable in the estimate of reliability; however, the dispersion in  $\delta_a$  has not been adequately characterized in previous studies. Phoon and Kulhawy (2008) assumed a *COV* of 60 percent for  $\delta_a$  based on research by Zhang and Ng (2005) for structures supported on deep foundations. Likewise, Uzielli and Mayne (2011) assumed a *COV* of 60 percent for  $\delta_a$  and lognormal distribution when analyzing the SLS for spread footings on sand. However, it is not clear as to why such a large variability in allowable displacement exists. For this study,  $\delta_a$  was modeled using a lognormal distribution with *COV* ranging from 0 to 60 percent, in order to allow the user judgment in the selection of the appropriate *COV*( $\delta_a$ ). The dispersion in footing width,  $B'$ , was modeled using a *COV* of 2 percent and a normal distribution.

**Table 4.3. Summary of Load and Displacement Parameters Used for MCS Analysis**

Parameter	Nominal Value	COV (%)	Modeled Distribution
$q_{ult}^*$	1.00	13.1	lognormal
$q_{app}^*$	1.00	10, 20	lognormal
$\delta_a$ (mm)	2.5, 5, 7.5, 10, 12.5, 15, 20, 25, 30, 37.5, 50, 75, 100, 112.5, 125, 150, 187.5, 200, 225, 250, 300, 400, 500, 600	0, 20, 40, 60	lognormal
$B'$ (m)	0.5, 1.0, 1.5, 2.0, 2.5, 3.0	2	normal
$\eta$	0.005, 0.01, 0.025, 0.05, 0.075, 0.10, 0.20	-	-

#### 4.5.5 Reliability Simulations and LRFD Calibration

The objective of this work was to calibrate the lumped load and resistance factor,  $\psi_q$ , to an estimate of the reliability index,  $\beta$ , and corresponding probability of exceeding the SLS. Monte Carlo simulations (MCS) were employed to generate random samples from each of the random variable distributions. The calibrations employed  $5 \times 10^6$  simulations for each  $\psi_q$ , in which each random variable, including  $k_3$ ,  $k_4$ ,  $\delta_a$ ,  $B'$ ,  $q^*_{ult}$  and  $q^*_{app}$ , was randomly sampled from their source distributions. The final number of simulations used for computing  $p_f$  was slightly smaller than  $5 \times 10^6$ , as simulations associated with  $q^*_{ult, min}$  less than 0.66 were rejected. The MCS was repeated approximately 3,600 times in order to estimate  $\beta$  and  $p_f$  for different combinations of  $\delta_a$  (ranging from 2.5 mm to 600 mm),  $B'$  (ranging from 0.5 to 3 m),  $COV(q^*_{app})$  (ranging from 10 to 20 percent), and  $\psi_q$  (ranging from 1 to 20).

The results of the reliability simulations indicated strong non-linear relationships between  $\psi_q$  and  $\beta$  at any given  $\eta_a$ . Figure 4.7 presents the  $\psi_q$  calibration for the case of  $COV(q^*_{app}) = 10$  percent and  $COV(\delta_a)$  ranging from 0 to 60 percent. For ease of interpretation, trend lines were fit to the  $\psi_q$ - $\beta$  pairs resulting from the Monte Carlo simulations. The reliability index decreases as  $COV(\delta_a)$  increases for a given value of  $\psi_q$ . Figure 4.7 also shows that there is significant probability of exceeding any displacement value when  $q^*_{app}$  is unfactored (i.e.,  $\psi_q = 1$ ). However, moderate increases in  $\psi_q$  result in large increases in the reliability index. For example, for the case of  $COV(\delta_a) = 0$  (Fig. 4.7a), the probability of exceeding  $\eta_a$  of 5 percent at  $\psi_q = 3$ , is approximately 1 percent.

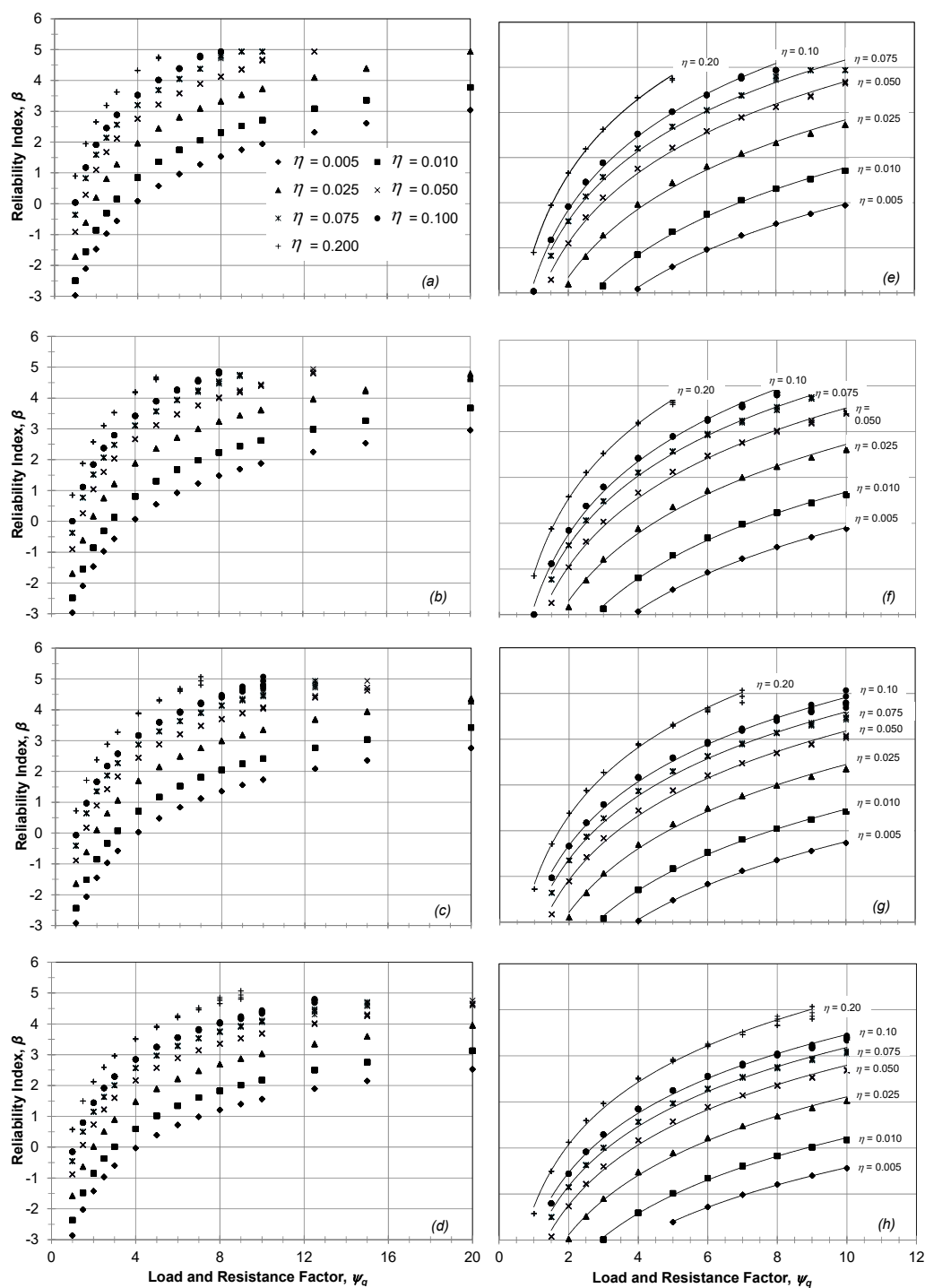


**Figure 4.7** Variation of load and resistance factor,  $\psi_q$ , and reliability index,  $\beta$ , for various magnitudes of normalized displacement,  $\eta$ , for  $\text{COV}(q_{app}) = 0.10$  and (a and e)  $\text{COV}(\delta_a) = 0$ , (b and f)  $\text{COV}(\delta_a) = 20$  percent, (c and g)  $\text{COV}(\delta_a) = 40$  percent, and (d and h)  $\text{COV}(\delta_a) = 60$  percent. Two-parameter logarithmic curves have been fit to simulations pairs for  $\beta > 0$  and  $\psi_q \leq 10$  are plotted in (e) through (h).

The load and resistance factor calibrations shown in Fig. 4.7 also indicated that the reliability in allowable bearing pressures increases as the allowable displacement increases. The relationships of  $\beta$  and  $\psi_q$  were nearly identical regardless of the  $\delta_a$  and  $B'$  values used to define  $\eta_a$ , consistent with the findings of Uzielli and Mayne (2011). The reliability simulations corresponding to  $\text{COV}(q^*_{app}) = 20$  percent resulted in similar trends in the variation of  $\psi_q$  with  $\beta$ .

Uzielli and Mayne (2011) suggested that the  $\psi_q$  vs.  $\beta$  relationship could be characterized with a logarithmic model of the form:

$$\beta = p_1 \ln(\psi_q) + p_2 \quad (4.16)$$

where  $p_1$  and  $p_2$  are best fit coefficients, and the simulations herein followed the same functional form. The simulations resulted in  $\beta$  ranging from approximately -3 to greater than 5. However, fitting of the regression coefficients and constants was limited to  $\beta > 0$  and  $\psi_q \leq 10$  in order to discourage the use of these simulations when  $p_f = 50$  percent or larger and to improve the accuracy of the reliability procedures, as shown in Fig. 4.7e through 4.7h.

Uzielli and Mayne (2011) also found that the fitting coefficients,  $p_1$  and  $p_2$ , vary with the normalized allowable displacement,  $\eta_a$ , in a linear and logarithmic trend, respectively, and eliminated the need to calculate new  $p_1$  and  $p_2$  coefficients for each value of  $\eta_a$ . For this study, logarithmic models were found to provide a relatively good fit for both  $p_1$  and  $p_2$ . Figure 4.8 shows the regressed, best-fit curves for estimating  $p_1$  and  $p_2$  corresponding to  $\text{COV}(q^*_{app}) = 10$  percent and  $\text{COV}(\delta_a) = 0$ . Similar results were observed for the other

combinations of  $\text{COV}(q^*_{app})$  and  $\text{COV}(\delta_a)$  investigated. Combining the logarithmic models used to predict  $p_1$  and  $p_2$  with Eq. 4.14 yields:

$$\beta = (a \ln(\eta_a) + b) \ln(\psi_q) + c \ln(\eta_a) + d \quad (4.17)$$

where  $a$  and  $b$  are the best-fit coefficients used to estimate  $p_1$ , and  $c$  and  $d$  are the best-fit coefficients used to estimate  $p_2$ . Table 4.4 provides a summary of the best-fit coefficients  $a$ ,  $b$ ,  $c$  and  $d$  to estimate the reliability index associated with any  $\eta_a$  and  $\psi_q$  and Eq. 4.15. Alternatively, the load and resistance factor associated with any  $\beta$  and  $\eta_a$  may be computed by inverting Eq. 4.15:

$$\psi_q = \exp \left[ \frac{\beta - c \ln(\eta_a) - d}{a \ln(\eta_a) + b} \right] \quad (18)$$

Note the coefficients  $a, \dots, d$  will vary based on the selected  $\text{COV}(q^*_{app})$  and  $\text{COV}(\delta_a)$ , as indicated in Table 4.4. Owing to the fitting procedure,  $\beta$  and  $\psi_q$  computed using Eq. 4.15 and 4.16 and the fitting parameters will produce error as  $\beta$  approaches zero; however, for  $\beta > 1$  ( $p_f < 16$  percent), the average error is approximately 2 percent. The coefficients vary smoothly with  $\text{COV}(\delta_a)$ , and further compression of the expression for  $\psi_q$  could be realized though at the expense of increased complexity and error in Eqs. 4.15 and 4.16. Because the reliability simulations were based on specific ranges of the dependent variables, extrapolation of  $\beta$  less than 0 and  $\psi_q$  greater than 10 is not recommended.

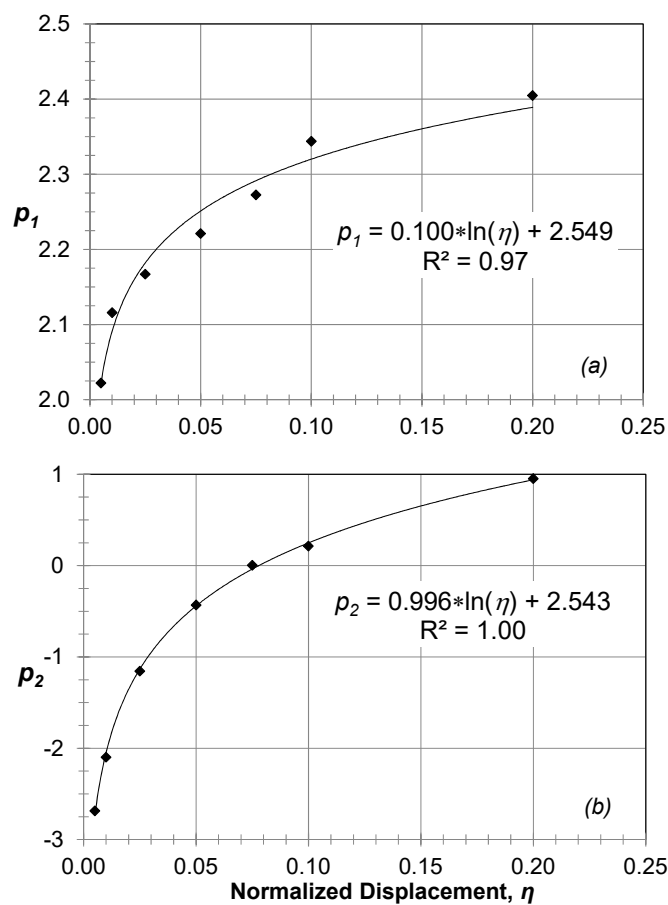


**Figure 4.8** Variation of the best fit coefficient and constant: (a)  $p_1$ , and (b)  $p_2$  with normalized displacement for use with Eq. 4.14 for  $\text{COV}(q_{app}^*) = 10$  percent and  $\text{COV}(\delta_a) = 0$ .

**Table 4.4. Summary of Best-fit Coefficients for Eqs. 4.15 and 4.16, valid for  $\beta > 0$  and  $\psi_q \leq 10$ .**

$\text{COV}(\delta_a)$	$\text{COV}(q_{app}^*)$	$a$	$b$	$c$	$d$
0	0.10	0.100	2.549	0.996	2.543
0.20	0.10	0.096	2.478	0.972	2.465
0.40	0.10	0.064	2.212	0.935	2.359
0.60	0.10	0.059	2.041	0.846	2.048
0	0.20	0.079	2.365	0.946	2.408
0.20	0.20	0.080	2.319	0.923	2.330
0.40	0.20	0.066	2.153	0.879	2.183
0.60	0.20	0.061	1.994	0.803	1.921



## 4.6 APPLICATION OF THE RELIABILITY CALIBRATIONS AND DISCUSSION

The results of the preceding analyses are illustrated using a typical design scenario where a structure is supported on a footing or multiple footings underlain by aggregate pier-reinforced clay. For a typical equivalent footing diameter of 1 meter and nominal allowable footing displacement of 25 mm, the following steps are required for SLS estimation of the allowable bearing pressure associated with a 1 percent probability of exceedance ( $\beta = 2.33$ ):

1. Estimate the nominal bearing capacity,  $q_{ult}$ , using Eq. 4.1. This requires additional design input such as establishing aggregate pier length and spacing, and may require multiple iterations depending on the results of the following analysis.
2. Establish the mobilized resistance,  $q_{mob}$ , using Eq. 4.6. For this example, the normalized allowable displacement,  $\eta_a$ , is 0.025 based the criteria indicated above. The coefficients  $k_3$  and  $k_4$  provided in Table 4.1 are 3.088 and 0.454, respectively. Therefore, the factor,  $M_s$ , used in Eq. 4.6 is 0.579.
3. For reliability-based SLS design, an appropriate load and resistance factor,  $\psi_q$ , must be applied to  $q_{ult}$  based on the selected target probability of failure. Eq. 4.16 is used to estimate  $\psi_q$  with coefficients  $a$ ,  $b$ ,  $c$ , and  $d$  from Table 4.4 based on the allowable displacement. For this example, a  $COV(\delta_a)$  and  $COV(q_{app}^*)$  of 0 and 10 percent were assumed, respectively. For a  $p_f = 1$  percent ( $\beta = 2.33$ ),  $\psi_q$  equals approximately 4.9 using Eq. 4.16.

4. The allowable bearing pressure that limits undrained displacement to 25 mm or less with probability of exceeding the allowable undrained displacement of 1 percent may then be computed using  $(1/\psi_q)(M_s)(q_{ult})$ , or  $0.118q_{ult}$ .

For comparison, if larger variation of the allowable displacement and/or applied bearing pressure is anticipated, the given example could be altered assuming, for example,  $COV(\delta_a)$  and  $COV(q_{app}^*)$  of 60 and 20 percent, respectively, corresponding to the highest amount of variability investigated herein. The steps followed are the same with the exception that the coefficients selected from Table 4.4 ( $a, \dots, d$ ) will reflect the change in  $COV(\delta_a)$  and  $COV(q_{app}^*)$ . For  $p_f = 1$  percent, Eq. 4.16 returns  $\psi_q = 6.7$ , and corresponds to an allowable bearing pressure of  $0.086q_{ult}$ . This represents a 27 percent reduction as compared to the bearing pressure calculated for  $COV(\delta_a) = 0$  percent and  $COV(q_{app}^*) = 10$  percent.

For designers accustomed to allowable stress design (ASD) standards using a global factor of safety, the reduction in  $q_{ult}$  may seem quite high compared to typical factors of safety in the range of 2.5 to 4 for design of most foundation systems. However, it should be pointed out that the definition of  $q_{ult}$  (and its uncertainty) plays a strong role in the resulting calibrated load and resistance factor. For example, Phoon and Kulhawy (2008) and Dithinde et al. (2011) estimated nominal bearing capacity with a slope-tangent method that usually returns a capacity that was significantly less than a plunging or near-plunging capacity. In contrast, Eq. 4.1 assumed a capacity representative of a true collapse capacity (Stuedlein and Holtz 2012). Therefore, the mobilized resistance at a given displacement (e.g., 25 mm used in the example) represents a relatively small fraction of  $q_{ult}$  as estimated using Eq. 4.1. The mobilized resistance estimated using, for example, the slope-tangent

method (e.g., Phoon and Kulhawy 2008) would be significantly less than that using Eq. 4.1, and therefore require a lower lumped load and resistance factor for the same allowable displacement. In other words, it would be acceptable to design with an allowable bearing pressure closer to  $q_{ult}$  if  $q_{ult}$  was estimated using a more conservative approach.

In order to illustrate the effect of bearing pressure-displacement model correlation structure, a comparison of  $\psi_q$  generated using the other copulas, as well as that generated assuming no correlation, to the approach selected herein is performed. The entire simulation exercise was repeated as previously described except that the other copulas (i.e., Gaussian, Clayton, or Frank) were used to simulate the dependence structure between  $k_3$  and  $k_4$ . For the example presented above assuming  $\text{COV}(\delta_a) = 0$  and  $\text{COV}(q^*_{app}) = 10$  percent, the resulting lumped load and resistance factor,  $\psi_q$ , equaled 4.7, 5.6, and 5.3 for the Gaussian, Clayton, or Frank copulas, respectively, indicating slightly unconservative to slightly conservative  $\psi_q$  as compared to the value of 4.9 estimated from simulations using the Gumbel copula. The similarity in  $\psi_q$  is attributed to the moderate correlation observed ( $\rho_\tau = 0.43$ ) and the relatively linear correlation between the power law model parameters. The performance of a given copula could have been more disparate if the correlation was stronger or if a different correlation structure was evident between the rank values (e.g., non-linear or tail-dependent). Additional high-quality load test data, when available, could provide additional refinement to the analyses and dependence structure between bearing pressure-displacement model parameters.

Simulations were also completed without incorporating the power law model parameter correlation (i.e., without the use of a copula), representing an assumed independence between the model parameters. For the example described above, the assumption of

independence yields  $\psi_q = 7.9$ . This value is significantly more conservative than those produced assuming an appropriate magnitude of dependence, and provides a potentially uneconomical design. Therefore, reliability simulations incorporating model parameter correlation structure, if existing, are preferred to those that assume no correlation structure.

#### 4.7 CONCLUSION

Many existing methods to predict the load-displacement response of aggregate pier reinforced clay rely on the unit cell concept for widely distributed loads or a linear soil-pier spring for isolated footing loads to compute the bearing pressure-displacement response. These methods do not accurately model the response of rigid spread footings supported on aggregate pier reinforced clay, nor are they appropriate for reliability-based design because the variability associated with the required model parameters have not been quantified. Heretofore, no reliability-based serviceability limit state (SLS) approach for allowable bearing pressures for spread footings on aggregate pier reinforced clay has been available.

In this paper, a reliability-based SLS procedure for computing the allowable bearing pressure at a given displacement and target probability of exceeding the SLS has been developed for use with spread footings resting on aggregate pier-reinforced clay. The allowable bearing pressure is linked to a reference capacity predicted using an existing bearing capacity model. Two load-displacement models were evaluated for suitability in predicting the normalized bearing pressure-normalized displacement,  $q^*-\eta$ , response by comparing the predicted behavior to the behavior in a full scale load test database, and resulted in the selection of a power law to represent the variation of  $q^*$  with  $\eta$ . The  $q^*-\eta$

model accurately predicted service level spread footing displacements over the range in applied bearing pressures for individual loading tests. In order to account for  $q^*$ - $\eta$  model parameter correlation in the reliability simulations, various bivariate copula functions were assessed for quality of fit to the load test database. Statistical distributions representing the uncertainty in the reference capacity, allowable displacement, applied bearing pressure,  $q^*$ - $\eta$  model parameters, and equivalent footing diameter were generated for use the Monte Carlo-based reliability simulations, which were conducted to calibrate a combined load and resistance factor,  $\psi_q$ . Concise equations were proposed to provide the  $\psi_q$  associated with a target probability of exceeding the SLS given specified levels of uncertainty in the independent design variables. Finally, an example of the application of the proposed reliability-based SLS procedure is provided to illustrate the intended workflow.

Owing to the relatively small number of load tests in the source database (i.e., thirty), the analyses presented herein could be improved as more data become available. For example, the bearing capacity equation (Eq. 1) or dispersion of the capacity model relative to load test data could be further refined. Similarly, the dependence structure between the model parameters, including selection of the appropriate copula, could be reevaluated with the inclusion of additional data. Application of the proposed procedure should not be performed for design scenarios that fall outside the footing load test database or for levels of reliability or load and resistance factors greater than those evaluated herein.

#### 4.8 ACKNOWLEDGEMENTS

The authors would like to acknowledge Marco Uzielli of Georisk Engineering S.r.l. for the helpful and interesting discussions regarding the reliability simulations. The work

performed herein was strengthened by discussions with graduate student Seth C. Reddy, and Dr. Tadesse Meskele, as well as the anonymous reviewers.

#### 4.9 SUPPLEMENTAL DATA

Appendix S1 summarizes the procedure for simulation of random correlated  $k_3 - k_4$  pairs and is available online in the ASCE Library ([www.ascelibrary.com](http://www.ascelibrary.com)). The information is also included as Appendix A of this dissertation.

#### 4.10 REFERENCES

- AASHTO (2012) *AASHTO LRFD Bridge Design Specifications, 6<sup>th</sup> Ed.*, American Association of State Highway and Transportation Officials, Washington, DC.
- Aboshi, H., Ichimoto, E., Enoki, M., and Harada, K. (1979) "The Composer – A Method to Improve Characteristics of Soft Clays by Inclusion of Large Diameter Sand Columns," *Proceedings, Reinforced Earth and Other Techniques*, Vol. 1, Paris, France.
- Akaike, H. (1974) "A New Look at the Statistical Model Identification," *Transactions on Automatic Control*, IEEE, Vol. 19, No. 6, pp. 716-723.
- Anderson, T.W., Darling, D.A. (1952) "Asymptotic theory of certain 'goodness-of-fit' criteria based on stochastic processes," *Annals of Mathematical Statistics*, Vol. 23, No. 2 pp. 193-212.
- Allen, T.A., Nowak, A.S., and Bathurst, R.J. (2005) "Calibration to Determine Load and Resistance Factors for Geotechnical and Structural Design," *Transportation Research Circular E-C079*, Transportation Research Board of the National Academies, Washington D.C., 93 p.
- Baecher, G.B. and Christian, J.T. (2003) Reliability and Statistics in Geotechnical Engineering, John Wiley and Sons, Ltd., London and New York, 605 pp.
- Baumann, V., and Bauer, G.E.A. (1974) "The Performance of Foundation on Various Soils Stabilized by Vibrocompaction Method," *Canadian Geotechnical Journal*, Vol. 11, pp. 509-530.
- Barksdale, R. D., and Bachus, R. C. (1983) "Design and Construction of Stone Columns," *Report No. FHWA/RD 83/026*, Federal Highway Administration.
- Bergado, D.T., and Lam, F.L. (1987) "Full Scale Load Test of Granular Piles with Different Densities and Different Proportions of Gravel and Sand in the Soft Bangkok Clay," *Soils and Foundations Journal*, Vol. 27, No. 1, Japan, pp. 86-93.

- Dithinde, M., Phoon, K.K., De Wet, M., and Retief, J.V. (2011) "Characterization of Model Uncertainty in the Static Pile Design Formula," *Journal of Geotechnical and Geoenvironmental Engineering*, ASCE, Vol. 137, No. 1, pp. 70-85.
- Greenwood, D.A. (1975) "Vibroflotation: Rationale for Design and Practice," *Methods of Treatment of Unstable Ground*, F. G. Bell, ed., Newness-Buttersworth, London, UK, pp. 189-209.
- Han, J., and Ye, S. (1991) "Field Tests of Soft Clay Stabilized by Stone Columns in Coastal Areas of China," *Proceedings, 4th International Deep Foundations Institute Conference*, Vol. 1, Balkema Press, Rotterdam, The Netherlands.
- Hughes, J.M.O., Withers, N.J., and Greenwood, D.A. (1975) "A Field Trial of the Reinforcing Effect of a Stone Column in Soil," *Geotechnique*, Vol. 25, No. 1, Thomas Telford Ltd., London, UK.
- Mayne, P.W., Poulos, H.G. (1999) "Approximate Displacement Influence Factors for Elastic Shallow Foundations," *Journal of Geotechnical and Geoenvironmental Engineering*, ASCE, Vol. 125, No. 6, pp. 453-460.
- Li, D.Q., Tang, X.S., Phoon, K.K., Chen, Y.F., Zhou, C.B. (2013) "Bivariate Simulation Using Copula and its Application to Probabilistic Pile Settlement Analysis," *International Journal for Numerical and Analytical Methods in Geomechanics*, John Wiley & Sons, Vol. 37, No. 6, pp. 597-617.
- Lillis, C., Lutenecker, A. J., Adams, M. (2004) "Performance of a Group of GeoPier Elements Loaded in Compression Compared to Single GeoPier Elements and Unreinforced Soil," *Report No. UUCVEEN 04-12*, University of Utah, Salt Lake City, UT, pp. 257.
- Najjar, S.S. (2005) "The Importance of Lower-Bound Capacities in Geotechnical Reliability Assessments," *Ph.D. Thesis*, University of Texas at Austin, 317 p.
- Najjar, S.S., and Gilbert, R.B. (2009) "Importance of Lower-Bound Capacities in the Design of Deep Foundations," *Journal of Geotechnical and Geoenvironmental Engineering*, ASCE, Vol. 135, No. 7, pp. 890-900.
- Nelson, R.B. (2006) *An Introduction to Copulas: Second Ed.*, Springer, New York, 269 p.
- Phoon, K.K. (2003). "Practical Guidelines for Reliability-Based Design Calibration," *Paper presented at Session TC 23 (1) "Advances in Geotechnical Limit State Design"*, 12th Asian Regional Conference on SMGE, August 7-8, 2003, Singapore.
- Phoon, K.K. (2008) "Numerical Recipes for Reliability Analysis – A Primer," *Reliability-Based Design in Geotechnical Engineering: Computations and Applications*, Taylor and Francis, London, pp. 1-75.
- Phoon, K.K., and Kulhawy, F.H. (2008) "Serviceability Limit State Reliability-Based Design," *Reliability-Based Design in Geotechnical Engineering: Computations and Applications*, Taylor and Francis, London, pp. 344-384.
- Stuedlein, A.W. (2008) "Bearing Capacity and Displacement of Spread Footings on Aggregate Pier Reinforced Clay," *Ph.D. Thesis*, University of Washington, 585 p.

- Stuedlein, A.W., and Holtz, R.D. (2012) "Analysis of Footing Load Tests on Aggregate Pier Reinforced Clay," *Journal of Geotechnical and Geoenvironmental Engineering*, ASCE, Vol. 138, No. 9, pp. 1091-1103.
- Stuedlein, A.W. and Holtz, R.D. (2013a) "Bearing Capacity of Spread Footings on Aggregate Pier Reinforced Clay," *Journal of Geotechnical and Geoenvironmental Engineering*, ASCE, Vol. 139, No. 1, pp. 49-58.
- Stuedlein, A.W. and Holtz, R.D. (2013b) "Displacement of Spread Footings on Aggregate Pier Reinforced Clay," *Journal of Geotechnical and Geoenvironmental Engineering*, ASCE.
- Schwarz, G. (1978) "Estimating the Dimension of a Model," *The Annals of Statistics*, Vol. 6, No. 2, pp. 461-464.
- Tang, X.S., Li, D.Q., Rong, G., Phoon, K.K., Zhou, C.B. (2013) "Impact of Copula Selection on Geotechnical Reliability Under Incomplete Probability Information," *Computers and Geotechnics*, Elsevier, Vol. 49, pp. 264-278.
- Uzielli, M. and Mayne, P., (2011) "Serviceability Limit State CPT-based Design for Vertically Loaded Shallow Footings on Sand," *Geomechanics and Geoengineering: An International Journal*, Taylor and Francis, Vol. 6, No. 2, pp. 91-107.
- Uzielli, M. and Mayne, P., (2012) "Load-Displacement Uncertainty of Vertically Loaded Shallow Footings on Sands and Effects on Probabilistic Settlement," *Georisk*, Vol. 6, No. 1, pp. 50-69.
- White, D.J., Pham, H.T., and Hoevelkamp, K.K., (2007) "Support Mechanisms of Rammed Aggregate Piers. I - Experimental Results," *Journal of Geotechnical and Geoenvironmental Engineering*, Vol. 133, No. 12, pp. 1503-1511.
- Zhang, L.M., Ng, A.M.Y., (2005) "Probabilistic Limiting Tolerable Displacements for Serviceability Limit State Design of Foundations," *Geotechnique*, Vol. 55, No. 2, pp. 151-161.



**CHAPTER 5:  
RELIABILITY-BASED SERVICEABILITY LIMIT STATE DESIGN  
FOR IMMEDIATE SETTLEMENT OF SPREAD FOOTINGS ON  
CLAY**

Authors:

Jonathan C. Huffman, Andrew W. Strahler, and Armin W. Stuedlein

Journal:

Soils and Foundations  
The Japanese Geotechnical Society (JGS)  
4-38-2 Sengoku, Bunkyo-ku, Tokyo, 112-0011, Japan

Volume 55, Issue 4 (August 2015)

## 5.1 ABSTRACT

While many spread footings constructed on clayey soils are designed using consolidation settlement analyses for the serviceability limit state (SLS), immediate settlement, or undrained displacement, of the footing may also contribute a significant portion of the total and/or differential settlement. Owing to possible magnitudes in immediate settlement, and with regard to stress history, assessment of the contribution of immediate settlement comprises an essential task for the understanding of the performance of a foundation system. This study proposes a simple reliability-based design (RBD) procedure for assessing the allowable immediate displacement of a spread footing supported on clay in consideration of a desired serviceability limit state. A relationship between the traditional spread footing bearing capacity equation and slope tangent capacity is established, then incorporated into a bivariate normalized bearing pressure-displacement model to estimate the mobilized resistance associated with a given displacement. The model was calibrated using a high quality database of full-scale loading tests compiled from various sources. The loading test data was used to characterize the uncertainty associated with the model and incorporated into an appropriate reliability-based performance function. Monte Carlo simulations were then used to calibrate a resistance factor with consideration of the uncertainty in the bearing pressure-displacement model, bearing capacity, applied bearing pressure, allowable displacement, and footing width. An example is provided to illustrate the application of the proposed procedure to estimate the bearing pressure for an allowable immediate displacement of a footing at the targeted probability and serviceability limit state.

## 5.2 INTRODUCTION

Geotechnical limit state design for spread footings requires the estimation of the bearing capacity, or the resistance at the ultimate limit state (ULS), while limiting excessive displacement to meet serviceability limit state (SLS) requirements. Bearing capacity models (e.g., Terzaghi 1943, Brinch Hansen 1970, Vesic 1973, among others) for the ULS are well established for a range of soil types, and generally requires the selection or development of a limited number of design variables. The analysis for the SLS is more complicated since footing displacements consist of one or more components, including initial or immediate settlement (i.e., distortion or undrained displacement), consolidation, and secondary compression (D'Appolonia and Lambe 1970). The contribution from each component depends on various factors such as the soil plasticity, the hydraulic conductivity, and loading rates, geometries, and magnitudes.

It is common for practicing engineers to focus on the consolidation component of settlement with SLS design for spread footings resting on plastic, fine-grained soils since it often provides the largest portion of the total settlement. However, immediate settlement should also be considered a critical design component for footings on plastic soils as it may comprise a significant portion of the total settlement and is essential to understanding the overall displacement behavior and undrained stability of the foundation (D'Appolonia and Lambe 1970, D'Appolonia et al. 1971, Foye et al. 2008). Consideration of short-term construction or rapidly applied loads (e.g., live loads or seismic loads) that act quickly relative to the hydraulic conductivity of the soil are of particular concern.

Immediate settlement is the expression of shear strains that develop below and adjacent to a loaded shallow foundation and is associated with the mobilization of the shear strength

of the soil (e.g., Lambe and Whitman 1969, D'Appolonia et al. 1971). Unlike primary consolidation and secondary compression, there is significant uncertainty associated with available analytical methods for use with plastic fine-grained soils (Strahler and Stuedlein 2013). Although accepted immediate settlement models often assume an elastic soil response (e.g., AASHTO 2012, Eurocode 7 [Orr and Breysse 2008]), the stress-strain characteristics of soils follow a nonlinear path at relatively small footing displacements (e.g., D'Appolonia et al. 1971, Jardine et al. 1986, Foye et al. 2008, Stuedlein and Holtz 2010, Strahler and Stuedlein 2013). The nonlinear behavior must be incorporated into an appropriate analytical model to predict the footing response.

Separately, the uncertainty associated with an appropriate analytical model must be characterized if the transition to a reliability-based limit state design and harmonization with existing design codes will be achieved. This requires that the multiple sources of uncertainty associated with the SLS be characterized including model uncertainty (e.g., Phoon 2003, 2008; Li et al. 2011; Uzielli and Mayne 2011; Wang 2011; Huffman and Stuedlein 2014), and incorporate the uncertainty within a probabilistic framework to estimate the displacement of footings with a pre-determined reliability. Fenton et al. (2005) presents a reliability approach for immediate settlements in consideration of spatial variability using the random finite element method and linear elastic constitutive laws, and Wang (2011) presented an expanded RBD approach for spread foundations that considers cost-optimization. The benefit of the approach by Fenton et al. (2005) is that the autocorrelation distance and inherent variability of the elastic stiffness may be incorporated directly; however, the true nonlinear behavior of foundations undergoing distortion settlement is not captured by either Fenton et al. (2005) or Wang (2011), which could result

in significant error for heavily loaded foundations in plastic fine-grained soils. Roberts and Misra (2010) present an SLS design methodology for spread footings, but this approach was limited to elastic-plastic bearing pressure-displacement response.

Huffman and Stuedlein (2014) described a reliability-based SLS procedure for shallow foundations resting on aggregate pier (or stone column) reinforced clayey soils that accounted for soil nonlinearity. However, such a framework does not presently exist for unreinforced plastic, fine-grained soils. To address the potential shortcomings in available methods for the estimation of immediate settlement for serviceability design of shallow foundations bearing on saturated, plastic fine-grained soils, this study uses the results from 30 full-scale loading tests on unreinforced clayey subgrades and a selected bearing capacity (ULS) model to develop a novel reliability-based SLS design procedure for nonlinear, inelastic immediate settlement. First, the loading test database compiled by Strahler (2012) and characterized by Strahler and Stuedlein (2014) is described, and the capacity inferred from each loading test,  $q_{ult,i}$ , is compared to the capacity calculated using a traditional bearing capacity model,  $q_{ult,p}$ , to estimate the model bias and uncertainty associated with the ULS. A relationship between the ULS and a new reference capacity is then established to reduce the dispersion of the bearing pressure-displacement ( $q-\delta$ ) response. Bivariate hyperbolic and power law models are then investigated for possible use for simulating the normalized  $q-\delta$  response over a range of typical bearing pressures and displacements. Owing to the multi-dimensional correlation between the normalized  $q-\delta$  parameters representing the hyperbolic model and the selected reference capacity, a computationally efficient vine copula approach is implemented in the reliability simulations. To improve the estimate of SLS reliability, a suitable lower bound ULS capacity to limit unreasonably

low values of capacity is imposed by considering the remolded shear strength of typical fine-grained soils. Monte Carlo simulations (MCS) are then used to formulate a procedure to generate the calibrated, lumped load-and-resistance factor used to estimate the bearing pressure associated with a given displacement and its probability of exceedance. The MCS accounts for the uncertainty in the ULS capacity, normalized  $q$ - $\delta$  model, applied bearing pressure, allowable displacement, and footing width. The new procedure developed herein is appropriate for the reliability-based assessment of nonlinear, inelastic immediate settlement resulting from rapid loading of rigid footings on saturated, plastic fine-grained soils.

### 5.3 LOAD TEST DATABASE AND ULS BEARING CAPACITY MODEL

Reliability analyses using a high-quality loading test database allows the assessment of design model bias and uncertainty across a range of differing geologic conditions, construction techniques, and other relevant design variables (Stuedlein et al. 2012). The new and original database compiled by Strahler (2012) and Strahler and Stuedlein (2014) included 30 loading tests of various-sized spread footings supported on soft to very stiff, plastic, fine-grained soil at twelve different sites located throughout Asia, Europe and North America. The criteria for the selection of cases for the database included: (1) a relatively uniform soil profile to at least  $2B$  below the base of the footing (where  $B$  is the footing width or diameter) consisting of plastic, fine-grained soil acting in an undrained manner during loading, (2) adequate in-situ and/or laboratory data to determine representative soil conditions (e.g., undrained shear strength,  $s_u$ ), (3) sufficient description of the load test setup and loading protocol, (4) footing embedment depth less than  $4B$  to

ensure a shallow failure mechanism, (5) a rigid footing response, and (6) sufficient footing displacement to estimate the non-linear response of the soil (Strahler and Stuedlein 2014).

The new load test database is summarized in Table 5.1.

Importantly, the database assembled for this study consisted of footing loading tests with various kinds of instrumentation, and not all case histories were characterized with sufficient instrumentation to confirm that the subgrade acted in an undrained manner. However, several well-instrumented loading tests provided evidence of undrained displacements and were used as a basis for comparison of cases and evaluation of admissibility to the database. For example, the pore pressure response exhibited by the saturated, medium stiff clay subgrade ( $s_u = 48$  kPa) reported by Andersen and Stenhamar (1982) and saturated, soft clay subgrade ( $s_u = 21$  kPa) reported by Jardine et al. (1995) indicated undrained responses. Stuedlein and Holtz (2010) compared the vertical and lateral displacements measured to the theoretical displacements assuming zero volume change, and showed that an undrained response was achieved at large displacements (Stuedlein and Holtz 2010). Such responses are anticipated for footing loading tests conducted rapidly in plastic, fine-grained deposits owing to their low hydraulic conductivities and coefficients of consolidation. The database did not include those high-quality case histories with layered soil conditions (e.g., Consoli, et al. 1998), with possible drainage paths within  $2B$  of the footing base. Additionally, each test admitted to the database was conducted over a period of minutes or hours, rather than months. Thus, the footing subgrades admitted into the loading test database may be assumed to respond in a relatively undrained manner, and are representative of typical immediate settlement scenarios.

**Table 5.1. Summary of load test database**

Source	Test	Footing Shape	B (m) <sup>a</sup>	B' (m) <sup>b</sup>	D <sub>f</sub> (m) <sup>c</sup>	D <sub>w</sub> (m) <sup>d</sup>	s <sub>u</sub> (kPa) <sup>e</sup>	γ <sub>m</sub> (kN/m <sup>3</sup> ) <sup>f</sup>
Andersen & Stenhamar (1982)	HA-1	Square	1.00	1.13	0.0	10.0	48	22.0
	HA-2	Square	1.00	1.13	0.0	10.0	48	22.0
Bauer et al. (1976)	OB-1	Circle	0.46	0.46	2.60	1.75	74	17.9
	OB-2	Square	3.10	3.50	0.66	1.75	108	17.9
Bergado et al. (1984)	RB-1	Circle	0.30	0.30	0.0	1.00	37	14.9
Brand et al. (1972)	BB-1	Square	1.05	1.18	1.60	0.90	20	19.5
	BB-2	Square	0.90	1.02	1.60	0.90	20	19.5
	BB-3	Square	0.75	0.85	1.60	0.90	20	19.5
	BB-4	Square	0.67	0.76	1.60	0.90	21	19.5
	BB-5	Square	0.60	0.68	1.60	0.90	21	19.5
Deshmukh & Ganpule (1984)	BD-1	Square	0.60	0.68	0.60	0.60	20	17.7
	BD-2	Square	0.60	0.68	0.60	0.60	20	17.7
Greenwood (1975)	GG-1	Square	0.91	1.03	0.61	>10.	44	18.5
Jardine et al. (1995)	BH-1	Square	2.20	2.48	0.78	0.90	21	16.0
Lehane (2003)	BL-1	Square	2.00	2.26	1.60	1.40	20	17.0
Marsland & Powell (1980)	CM-1	Circle	0.87	0.87	0.0	>10.	139	19.5
Newton (1975)	ON-1	Circle	0.60	0.60	0.38	0.31	20	18.5
	ON-2	Circle	0.49	0.49	0.38	0.31	20	18.5
	ON-3	Circle	0.34	0.34	0.38	0.31	20	18.5
Stuedlein & Holtz (2010)	TS-1	Circle	0.76	0.76	0.61	2.40	70	19.7
	TS-2	Circle	0.76	0.76	0.61	2.40	70	19.7
	TS-3	Square	2.74	3.09	0.0	2.40	85	19.7
Tand & Funegard (2005)	TT-1	Circle	0.58	0.58	1.50	0.90	44	20.0
	TT-2	Circle	0.58	0.58	1.50	0.90	44	20.0
	TT-3	Circle	0.58	0.58	1.50	0.90	44	20.0
	TT-4	Circle	0.58	0.58	1.50	0.90	45	20.0
	TT-5	Circle	0.58	0.58	1.50	0.90	45	20.0
	TT-6	Circle	0.58	0.58	1.50	1.10	67	20.0
	TT-7	Circle	0.58	0.58	1.50	1.10	67	20.0
	TT-8	Circle	0.58	0.58	1.50	1.10	67	20.0

<sup>a</sup> Footing width or diameter<sup>d</sup> Ground water depth<sup>b</sup> Equivalent footing width<sup>e</sup> Soil undrained shear strength<sup>c</sup> Footing embedment depth<sup>f</sup> Soil unit weight



Bearing pressure-displacement ( $q$ - $\delta$ ) data were compiled from the individual tests and the ultimate resistance (i.e., bearing capacity) was determined by extrapolation of the  $q$ - $\delta$  data using fitted hyperbolic curves. The interpreted capacity,  $q_{ult,i}$ , was set equal to the estimated asymptote resulting from the fitted hyperbolic relationship. A predicted capacity,  $q_{ult,p}$ , was calculated for each test using the general bearing capacity equation (e.g., Terzaghi 1943) with Meyerhof (1963) bearing capacity factors, and shape and depth factors proposed by Brinch Hansen (1970). Assuming undrained loading conditions, the bearing capacity equation for a general shear failure for the footings in the database considered equals:

$$q_{ult,p} = s_u N_c \lambda_{cs} \lambda_{cd} + \gamma D_f N_q \lambda_{qs} \lambda_{qd} \quad (5.1)$$

where  $s_u$  = undrained shear strength,  $\gamma$  = unit weight,  $D_f$  = footing embedment depth,  $N_c$  and  $N_q$  represent bearing capacity factors (assumed equal to 5.14 and 1.0, respectively, for the  $\phi = 0$  condition), and  $\lambda_{cs}$ ,  $\lambda_{qs}$ ,  $\lambda_{cd}$  and  $\lambda_{qd}$  are the Hansen (1970) shape and depth factors, respectively. The factors  $\lambda_{qs}$  and  $\lambda_{qd}$  were assumed to be 1.0 for  $\phi = 0$  soil, and shape factors were computed in accordance with the relevant geometry (i.e., circular or square). The interpreted and predicted bearing capacities for each loading test are summarized in Table 5.2. The bias for each test, defined as the ratio of the interpreted and predicted bearing capacity, is also summarized Table 5.2. The mean bias was equal to  $M_{ult} = 1.25$ , indicating Eq. 5.1 under-predicted the interpreted capacity by 25 percent on average. The coefficient of variation ( $COV$ ) in bias was equal to 37 percent, indicating moderate to significant variability. The capacity model error is typical in geotechnical

applications, and underscores the need to appropriately characterize model uncertainty for reliability-based limit state design.

**Table 5.2. Comparison of interpreted, calculated, and slope tangent capacities with corresponding ratios**

Test	Interpreted Capacity, $q_{ult,i}$ (kPa)	Calculated Capacity, $q_{ult,p}$ (kPa)	Bias $q_{ult,i}/q_{ult,p}$	Slope Tangent Capacity, $q_{STC}$ (kPa)	$q_{STC}/q_{ult,i}$
HA-1	343	298	1.15	342	1.00
HA-2	378	298	1.27	-	-
OB-1	560	746	0.75	305	0.54
OB-2	515	735	0.70	-	-
RB-1	180	231	0.78	125	0.69
BB-1	177	191	0.93	-	-
BB-2	213	196	1.09	171	0.80
BB-3	228	204	1.12	177	0.78
BB-4	227	209	1.09	-	-
BB-5	271	211	1.28	-	-
BD-1	262	175	1.50	-	-
BD-2	365	175	2.09	-	-
GG-1	313	347	0.90	217	0.69
BH-1	205	160	1.28	118	0.58
BL-1	120	186	0.64	91	0.76
CM-1	539	858	0.63	-	-
ON-1	415	162	2.56	187	0.45
ON-2	221	169	1.31	125	0.57
ON-3	342	172	1.99	-	-
TS-1	754	582	1.29	477	0.63
TS-2	774	582	1.33	458	0.59
TS-3	568	527	1.08	384	0.68
TT-1	750	429	1.75	426	0.57
TT-2	734	429	1.71	414	0.56
TT-3	684	429	1.59	443	0.65
TT-4	382	436	0.88	176	0.46
TT-5	225	436	0.52	158	0.70
TT-6	1021	640	1.59	607	0.59
TT-7	963	640	1.50	599	0.62
TT-8	844	640	1.32	494	0.59
			<b>Mean = 1.25</b>		<b>Mean = 0.643</b>
			<b>COV = 0.367</b>		<b>COV = 0.187</b>

**Note:** Values of  $q_{STC}$  are reported only for load tests taken to a footing displacement of at least  $0.03B'$ .

## 5.4 BEARING PRESSURE-DISPLACEMENT MODEL

Serviceability limit state design of spread footings is controlled by the allowable displacement. The undrained loading of plastic fine-grained soils follow a nonlinear path even at relatively small foundation displacements. Akbas and Kulhawy (2009) and Uzieli and Mayne (2011), among others, showed that nonlinear  $q$ - $\delta$  behavior for spread footings, with applied pressure normalized by a reference capacity or in-situ measurement,  $q_{ref}$ , respectively, and displacement normalized by footing size, can be represented using a hyperbolic model:

$$q^* = \frac{q_{mob}}{q_{ref}} = \frac{\eta}{k_1 + k_2 \cdot \eta} \quad (5.2)$$

or power law:

$$q^* = \frac{q_{mob}}{q_{ref}} = k_3 \cdot \eta^{k_4} \quad (5.3)$$

respectively, where  $q_{mob}$  is the mobilized resistance at a given displacement,  $\delta$ ,  $\eta = \delta/B'$  is the normalized displacement, and  $B'$  is the equivalent footing diameter, defined as the diameter that produces the same area as that of a square footing (e.g., Mayne and Poulos 1999).

The reference capacity,  $q_{ref}$ , is used as a means to both normalize the resistance and reduce scatter inherent with load test data. The reference capacity does not necessarily represent a true “capacity”, rather, it should provide a replicable means to produce a known capacity, and preferably linked to a predetermined deflection criterion. For example, Akbas and Kulhawy (2009) used the failure load interpreted from load tests to represent  $q_{ref}$ , whereas Uzieli and Mayne (2011) used the cone tip resistance to represent  $q_{ref}$ . For this study, both the interpreted capacity,  $q_{ult,i}$ , and slope tangent capacity,  $q_{STC}$  (e.g., Phoon

and Kulhawy 2008), were investigated for potential use as a reference capacity. The slope tangent capacity with a displacement offset equal to  $0.03B'$  was ultimately selected to represent the reference capacity because it significantly reduced the dispersion of the  $q^*-\eta$  curves compared to the interpreted capacity,  $q_{ult,i}$ , it could be readily estimated as a function of  $q_{ult,i}$ , and it is linked to a well-characterized magnitude of displacement. Figure 5.1 shows the bearing pressure-displacement curves for all footings in the load test database (Fig. 5.1a) along with the normalized (i.e.,  $q^*-\eta$ ) curves, where  $q^*$  was established using  $q_{ref} = q_{ult,i}$  (Fig. 5.1b) and  $q_{ref} = q_{STC}$  (Fig. 5.1c). The scatter in the  $q^*-\eta$  curves associated with  $q_{STC}$  (Fig 5.1c) is significantly reduced in comparison to the other bearing pressure-displacement curves, providing a more suitable approach for simulating continuous nonlinear  $q^*-\eta$  behavior in the reliability analyses, described below.

The coefficients  $k_1$ ,  $k_2$ ,  $k_3$  and  $k_4$  in Eqs. 5.2 and 5.3 were determined using linear least squares optimization and allow the simulation of continuous  $q^*-\eta$  curves. The best-fit coefficients for each loading test are summarized in Table 5.3. In nine of the 30 cases where the loading test was not taken to a displacement of at least  $0.03B'$ , the fitting coefficients were determined with a  $q_{STC}$  value estimated by extrapolating the nonlinear bearing pressure-displacement response. Although the results suggest that both the hyperbolic and power law models can be used to accurately predict immediate undrained displacement, goodness-of-fit measures including the sum of the root mean square error (RMSE), coefficient of determination ( $R^2$ ), and mean bias indicate that the hyperbolic model produced a slightly better overall fit to the  $q^*-\eta$  behavior. Therefore, the hyperbolic model (Eq. 5.2) was selected for use in the subsequent reliability calibrations.

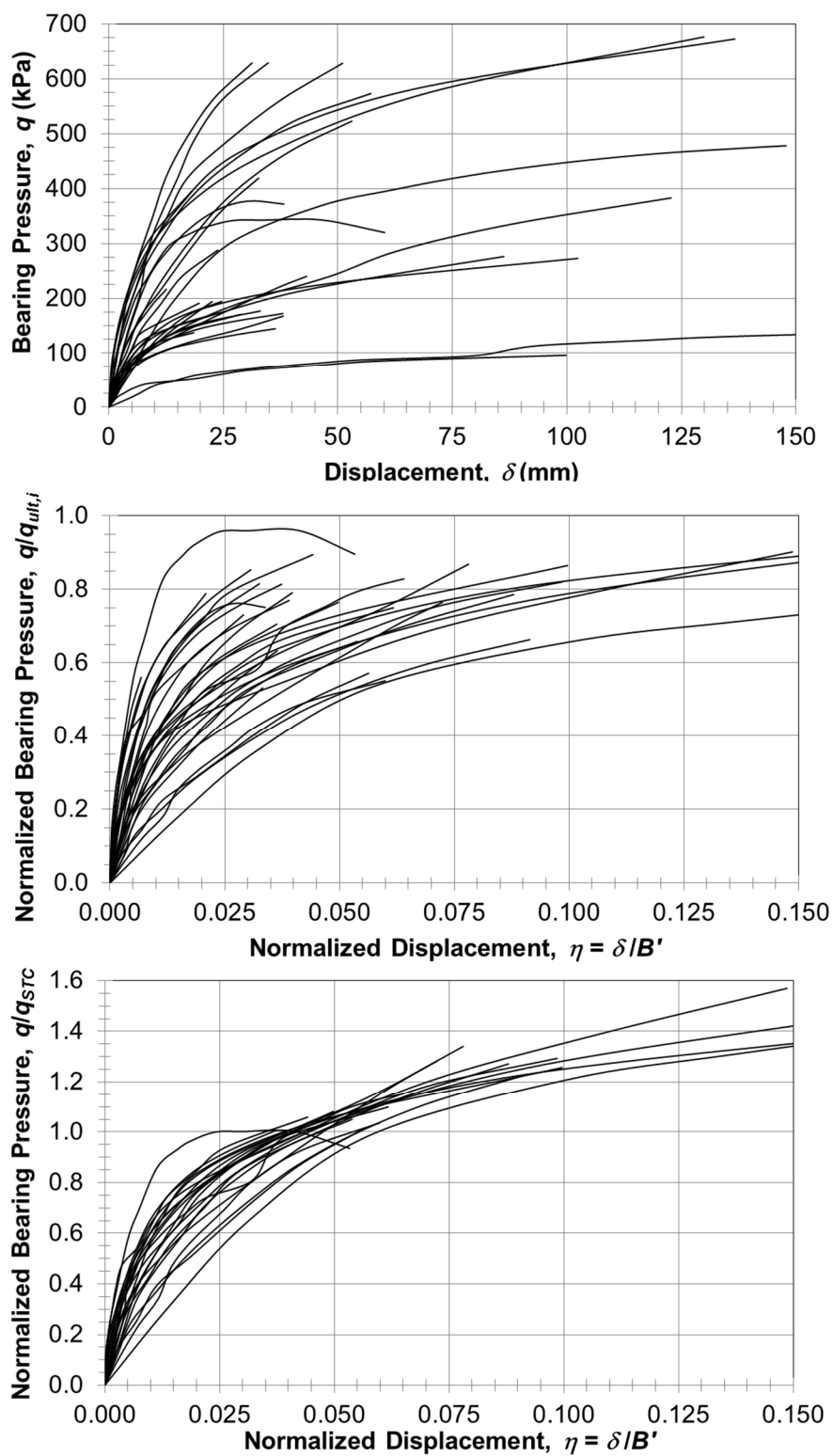


**Figure 5.1** Variation of bearing pressure with displacement for footings in the load test database: (a) observed  $q$ - $\delta$  response, (b) normalized  $q$ - $\delta$  response using  $q_{ult,i}$  and (c) normalized  $q$ - $\delta$  response using  $q_{STC}$ .

**Table 5.3. Summary of bearing pressure-displacement model coefficients and goodness-of-fit parameters.**

Test	Hyperbolic Model					Power Law Model				
	$k_1$	$k_2$	RMSE	$R^2$	Mean Bias	$k_3$	$k_4$	RMSE	$R^2$	Mean Bias
HA-1	0.003	0.958	20.49	0.97	1.00	2.68	0.29	37.68	0.83	0.95
HA-2	0.007	0.763	12.02	0.99	1.00	4.69	0.43	28.17	0.91	0.97
OB-1	0.030	0.544	7.86	1.00	0.99	2.51	0.36	30.91	0.93	0.98
OB-2	0.005	0.851	3.57	1.00	0.93	14.11	0.62	6.78	0.99	0.98
RB-1	0.013	0.682	2.03	1.00	0.98	4.62	0.49	7.88	0.93	0.96
BB-1	0.005	0.855	2.59	1.00	1.04	4.42	0.41	5.97	0.96	0.96
BB-2	0.007	0.808	1.19	1.00	1.01	4.60	0.44	8.48	0.95	0.96
BB-3	0.009	0.771	0.97	1.00	1.00	4.83	0.47	8.28	0.96	0.97
BB-4	0.007	0.822	3.00	1.00	1.01	4.49	0.43	5.78	0.97	0.98
BB-5	0.011	0.730	1.88	1.00	0.98	5.93	0.53	9.58	0.94	0.96
BD-1	0.008	0.783	3.56	1.00	1.01	5.61	0.50	10.26	0.96	0.95
BD-2	0.019	0.614	4.23	0.99	0.99	8.77	0.68	5.05	0.89	0.98
GG-1	0.011	0.688	5.62	1.00	0.98	3.24	0.39	19.38	0.93	0.96
BH-1	0.012	0.721	5.54	0.98	1.02	4.04	0.45	4.00	0.98	0.99
BL-1	0.006	0.845	5.38	0.97	1.10	3.53	0.37	2.81	0.96	0.98
CM-1	0.005	0.852	10.25	0.99	1.01	4.99	0.43	8.65	0.99	0.99
ON-1	0.017	0.596	11.40	0.98	1.11	4.98	0.52	2.69	1.00	1.00
ON-2	0.011	0.647	9.83	0.98	1.39	3.70	0.40	2.53	0.99	1.00
ON-3	0.014	0.652	3.71	1.00	1.04	6.75	0.58	4.95	0.99	0.98
TS-1	0.011	0.658	27.03	0.99	1.07	2.57	0.32	31.01	0.93	0.97
TS-2	0.013	0.614	39.21	0.98	1.27	2.74	0.33	18.94	0.95	0.97
TS-3	0.010	0.792	17.76	0.98	1.17	4.84	0.49	4.16	1.00	0.99
TT-1	0.025	0.540	7.54	1.00	1.04	4.94	0.56	14.30	0.99	0.96
TT-2	0.025	0.565	10.01	0.99	1.06	6.31	0.63	5.26	0.99	0.99
TT-3	0.015	0.634	12.07	1.00	1.05	3.90	0.45	21.88	0.97	0.95
TT-4	0.014	0.574	16.15	0.96	1.05	3.07	0.35	3.73	0.98	1.00
TT-5	0.011	0.707	4.95	0.99	1.01	4.44	0.46	8.76	0.96	0.98
TT-6	0.024	0.532	14.41	0.99	0.98	6.69	0.64	30.25	0.90	0.95
TT-7	0.017	0.627	4.90	1.00	1.00	5.86	0.57	23.54	0.97	0.96
TT-8	0.016	0.618	11.97	1.00	1.03	4.28	0.48	20.45	0.98	0.97
<b>Mean</b>	<b>0.013</b>	<b>0.701</b>	<b>9.37</b>	<b>0.99</b>	<b>1.04</b>	<b>4.94</b>	<b>0.47</b>	<b>13.07</b>	<b>0.96</b>	<b>0.97</b>

The reference capacity,  $q_{STC}$ , used with the bearing pressure-displacement model is specific to a given footing loading test. Thus,  $q_{STC}$  must be estimated for the typical case where a site-specific loading test has not been performed. Figure 5.2 shows that a linear relationship between  $q_{STC}$  and  $q_{ult,i}$  exists, suggesting that  $q_{STC}$  can be readily estimated as a function of the interpreted capacity; a similar correlation was noted in separate SLS simulations reported by Stuedlein and Uzielli (2014). The ratios of  $q_{STC}$  to  $q_{ult,i}$  for the loading tests are summarized in Table 5.2, and exhibit a mean ratio of 0.643. In turn,  $q_{ult,i}$  must also be estimated in the absence of site-specific loading tests, which is accomplished using the bearing capacity equation (Eq. 5.1). The mobilized resistance may be estimated as a function of displacement using the predicted bearing capacity,  $q_{ult,p}$ :

$$q_{mob} = \frac{\eta}{k_1+k_2\eta} q_{STC} = \frac{\eta}{k_1+k_2\eta} M_{STC} q_{ult,p} = M_\eta M_{STC} q_{ult,p} \quad (5.4)$$

where  $q_{ult,p}$  is calculated from Eq. 5.1,  $M_{STC}$  is the model factor used to scale the predicted ultimate resistance to the slope tangent resistance and equals the mean of  $q_{STC}/q_{ult,i}$  (i.e., 0.643, see Fig. 5.2), and  $M_\eta$  is the hyperbolic model factor used to scale to the mobilized resistance based on the allowable normalized undrained footing displacement,  $\eta$ . In order to ensure that the reliability-based SLS calibrations are accurate, the model uncertainty associated with the bearing capacity estimate  $q_{ult,p}$  (Eq. 5.1), as well as the uncertainty associated with the normalized bearing pressure-displacement model (Eq. 5.2), and the parameters  $k_1$  and  $k_2$ , and  $q_{STC}$  must be incorporated in a systematic basis. The framework used to accomplish this is described in the following section.

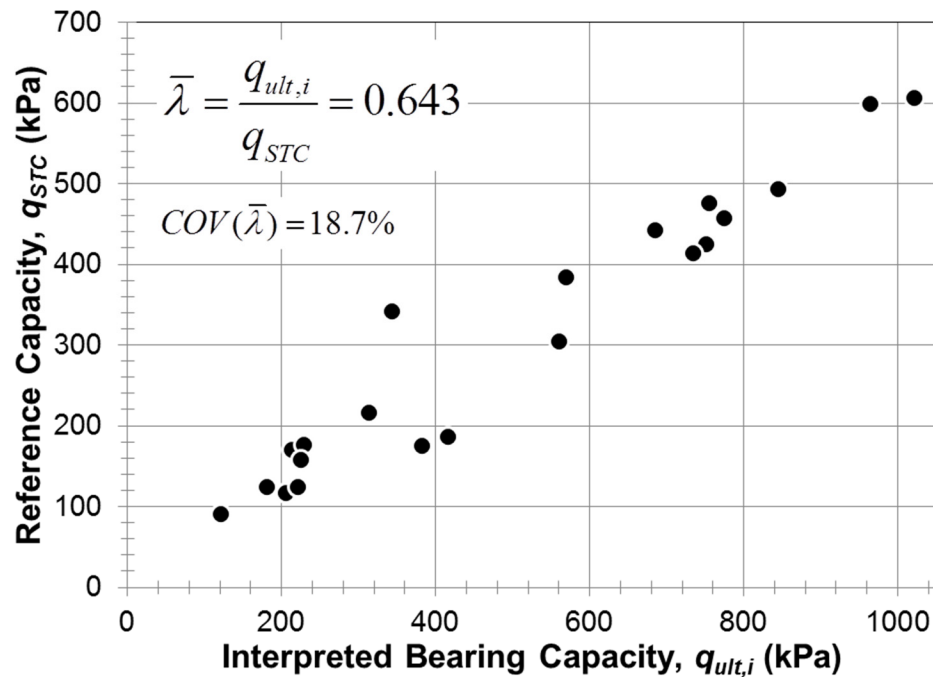


**Figure 5.2** Variation of the reference slope tangent capacity with the interpreted bearing capacity.

## 5.5 APPLICATION OF BEARING PRESSURE-DISPLACEMENT MODEL TO RELIABILITY-BASED DESIGN

Reliability-based limit state design requires calibration of appropriate load and resistance factors that are based on the uncertainty associated with the design input parameters. Input parameters associated with estimating the serviceability-level resistance for spread footings on clay were described previously (i.e.,  $q_{ult,p}$ ,  $M_{STC}$ ,  $k_1$  and  $k_2$ ). Additional sources of uncertainty include the load and structural response parameters, such as the design bearing pressure, the allowable settlement, and footing size.

Incorporating this uncertainty into the limit state design may be efficiently accomplished using probabilistic methods and an appropriate performance function,  $P$ . The margin of safety, defined as the difference between the resistance,  $R$ , and load,  $Q$ , represents an appropriate performance function with a corresponding joint probability



distribution function. In consideration of the various sources of uncertainty contributing to the system reliability, the probability of failure,  $p_f$ , may be defined using the margin of safety and represented by (Baecher and Christian 2003, Allen et al. 2005, Phoon 2008):

$$p_f = \Pr(R - Q < 0) = \Pr(P < 0) \leq p_T \quad (5.5)$$

where  $p_T$  is the acceptable target probability that the load will be greater than the resistance, typically in the range of 1 to 0.1 percent for geotechnical applications. The performance function may be reformulated in terms of the allowable mobilized bearing resistance,  $q_{mob}$ , and an applied bearing pressure,  $q_{app}$ , by incorporating the selected bearing pressure-displacement model (Eq. 5.4):

$$p_f = \Pr(M_{STC}M_\eta q_{ult,p} - q_{app} < 0) = \Pr\left(M_{STC}M_\eta < \frac{q_{app}}{q_{ult,p}}\right) \leq p_T \quad (5.6)$$

The characteristic distributions of each random variable can be incorporated into the performance function by defining the ultimate and applied bearing pressures in terms of a deterministic nominal value (i.e.,  $q_{app,n}$  and  $q_{ult,n}$ ) and the corresponding normalized random variables (i.e.,  $q_{app}^*$  and  $q_{ult}^*$ ), with Eq. 5.6 rewritten as (Uzielli and Mayne 2011):

$$p_f = \Pr\left(M_{STC}M_\eta < \frac{q_{app,n}q_{app}^*}{q_{ult,n}q_{ult}^*}\right) = \Pr\left(M_{STC}M_\eta < \frac{1}{\psi_q} \frac{q_{app}^*}{q_{ult}^*}\right) \leq p_T \quad (5.7)$$

where  $\psi_q$  is the combined (i.e., lumped) load and resistance factor assigned to provide an acceptable probability of failure. The lumped load and resistance factor is preferred to partial factors as current design codes (e.g., AASHTO 2012 or Eurocode 7) recommend partial factors equal to 1.0 for SLS design of spread footings without the consideration of uncertainty.

For this study,  $p_f$ , and the associated reliability index,  $\beta = -\Phi^{-1}(p_f)$ , where  $\Phi^{-1}$  represents the inverse standard normal cumulative function, were estimated based on a prescribed

interval of  $\psi_q$  that ranged from one (i.e., no reduction in applied bearing pressure) to 20, and determined using Monte Carlo simulations (MCS) seeded with distributions for each of the varied parameters. The results of the simulations were used to investigate possible relationships between the parameters in the performance function and to provide a simplified procedure for SLS design.

## 5.6 SIMULATION-BASED SERVICEABILITY LIMIT STATE DESIGN CALIBRATIONS

To calibrate the lumped load and resistance factor using an appropriate performance function distribution, the MCS incorporated uncertainty in the bearing capacity model, the normalized bearing pressure-displacement model, the relationship between slope tangent and ultimate bearing capacities, the allowable displacement, the footing width, and the applied loading. Tables 5.4 and 5.5 summarize the statistical parameters of all of the random variables in the reliability simulations. Selection of the nominal values and model distribution of the load and resistance variables are discussed below.

### 5.6.1 Characterization of Resistance Parameters

The nominal values and characteristic distributions for the resistance variables were estimated from the loading test database and normalized bearing pressure-displacement model as follows:

- The nominal bearing capacity,  $q_{ult}^*$ , was set equal to the mean bias between the calculated and interpreted capacities ( $q_{ult,p}$  and  $q_{ult,i}$ , respectively), from the loading test database, and the distribution estimated by fitting to the sample biases summarized in Table 5.2.

- The nominal slope tangent capacity scaling factor,  $M_{STC}$ , was set equal to the mean ratio of  $q_{ult,i}$  to  $q_{STC}$ , and the distribution estimated by fitting to the sample ratios summarized in Table 5.2.
- The nominal value of the hyperbolic model parameters,  $k_1$  and  $k_2$ , were estimated as the mean  $k_1$  and  $k_2$  values indicated in Table 5.3, and distributions were estimated by fitting to the sample values in Table 5.3.

The selected model distributions resulted from fitting to several possible distributions and evaluated using the Akaike Information Criteria ( $AIC$ ; Akaike 1974) and Bayesian Information Criterion ( $BIC$ ; Schwartz 1978) goodness-of-fit tests. The  $AIC$  and  $BIC$  are defined as:

$$AIC = -2 \sum_{i=1}^N \ln f_{pdf}(x_i) + 2k \quad (5.8)$$

$$BIC = -2 \sum_{i=1}^N \ln f_{pdf}(x_i) + k \ln N \quad (5.9)$$

respectively, where  $f_{pdf}$  is the probability density function ( $pdf$ ) of a selected distribution,  $N$  is the sample size with  $x_i$  representing a sample value from the dataset, and  $k$  is the number of parameters associated with the given  $pdf$ . The best-fit model distributions were selected by choosing the distribution that resulted in the lowest  $AIC$  and  $BIC$  values, shown in Table 5.4. The lognormal, gamma, inverse Gaussian, and beta distributions were assessed for suitability of sampling in the MCS. Normal distributions were not included to avoid the potential for negative values leading to inaccurate and/or inappropriate results in the reliability simulations. Note that because the distributions were fit to data available, their robustness should be investigated as new high-quality data becomes available. The normalized resistance model parameters selected for use in the reliability simulations based on the best-fit distributions is summarized in Table 5.5.

**Table 5.4. Summary of AIC and BIC values for selected distributions fit to normalized resistance model parameters.**

Parameter	Distribution	AIC	BIC
$q_{ult}^*$	Lognormal	42.41	45.69
	<b>Gamma</b>	<b>42.08</b>	<b>45.36</b>
	Inverse Gaussian	42.33	45.61
	Beta (general)	44.11	48.12
$M_{STC}$	<b>Lognormal</b>	<b>-24.94</b>	<b>-23.23</b>
	Gamma	-19.80	-18.07
	Inverse Gaussian	-24.90	-23.18
	Beta (general)	n/a	n/a
$k_1$	Lognormal	-214.54	-211.26
	<b>Gamma</b>	<b>-215.05</b>	<b>-211.77</b>
	Inverse Gaussian	-214.71	-211.43
	Beta (general)	-212.91	-208.91
$k_2$	Lognormal	-41.06	-37.78
	Gamma	-41.26	-37.98
	<b>Inverse Gaussian</b>	<b>-41.85</b>	<b>-38.57</b>
	Beta (general)	n/a	n/a

**Note:** Bold value represent lowest AIC and BIC.

**Table 5.5. Summary of fitted normalized resistance model parameters.**

Parameter	Mean	COV (%)	Model Distribution
$q_{ult}^*$	1.25	37.3	Gamma
$M_{STC}$	0.643	18.7	Lognormal
$k_1$	0.013	53.0	Gamma
$k_2$	0.701	16.1	Inverse Gaussian

### 5.6.2 Resistance Parameter Dependence and Copula Analyses

The potential dependence between random variables must be incorporated in reliability simulations to avoid hidden biases that may skew the resulting calibrations (e.g., Phoon and Kulhawy 2008; Uzielli and Mayne 2011, 2012; Stuedlein et al. 2012; Tang et al. 2013, Huffman and Stuedlein 2014). The  $q^*$ - $\eta$  model parameters ( $M_{STC}$ ,  $k_1$  and  $k_2$ ) showed no apparent correlation to the bearing capacity parameters ( $s_u$ ,  $\gamma'$  and  $D_f$ ), as indicated in Fig. 5.3. However, each of the  $q^*$ - $\eta$  model parameters showed moderate to strong correlation to each other as shown in Fig. 5.4. Kendal's rank tau correlations,  $\rho_\tau$ , of -0.80, -0.59 and 0.62 were calculated for the  $k_1$ - $k_2$ ,  $k_1$ - $M_{STC}$  and  $k_2$ - $M_{STC}$  pairs, respectively. Such correlations are common for bivariate load-displacement models used in geotechnical applications (e.g., Phoon and Kulhawy 2008, Stuedlein and Reddy 2013, Huffman and Stuedlein 2014).

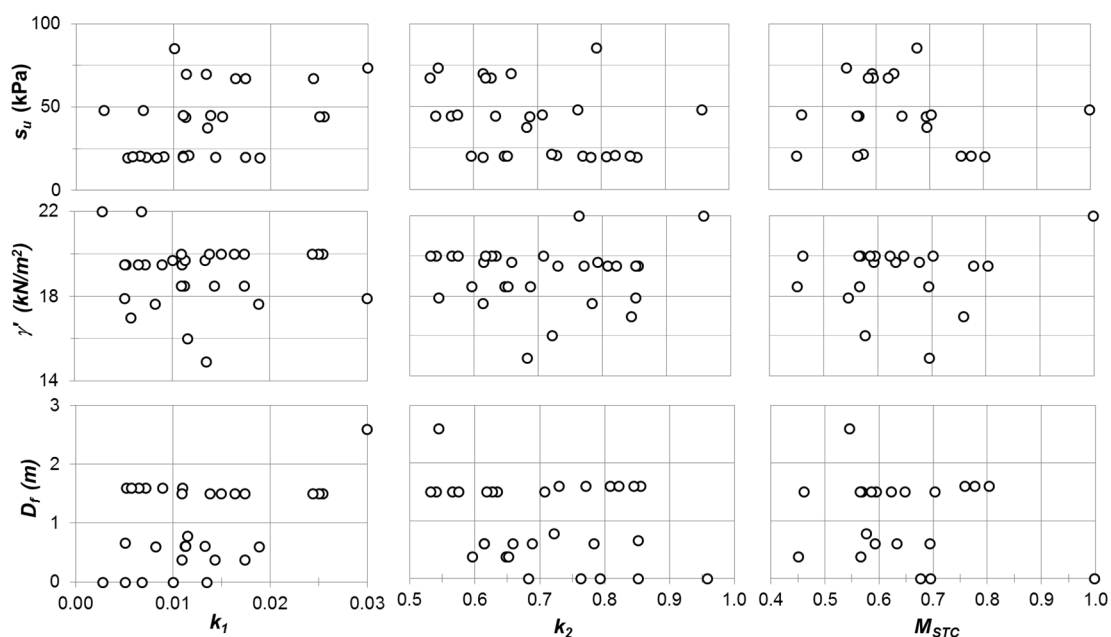


**Figure 5.3** Variation of normalized bearing pressure-displacement model parameters  $k_1$  and  $k_2$ , and model factor  $M_{STC}$  with geometric and soil properties influencing bearing capacity.

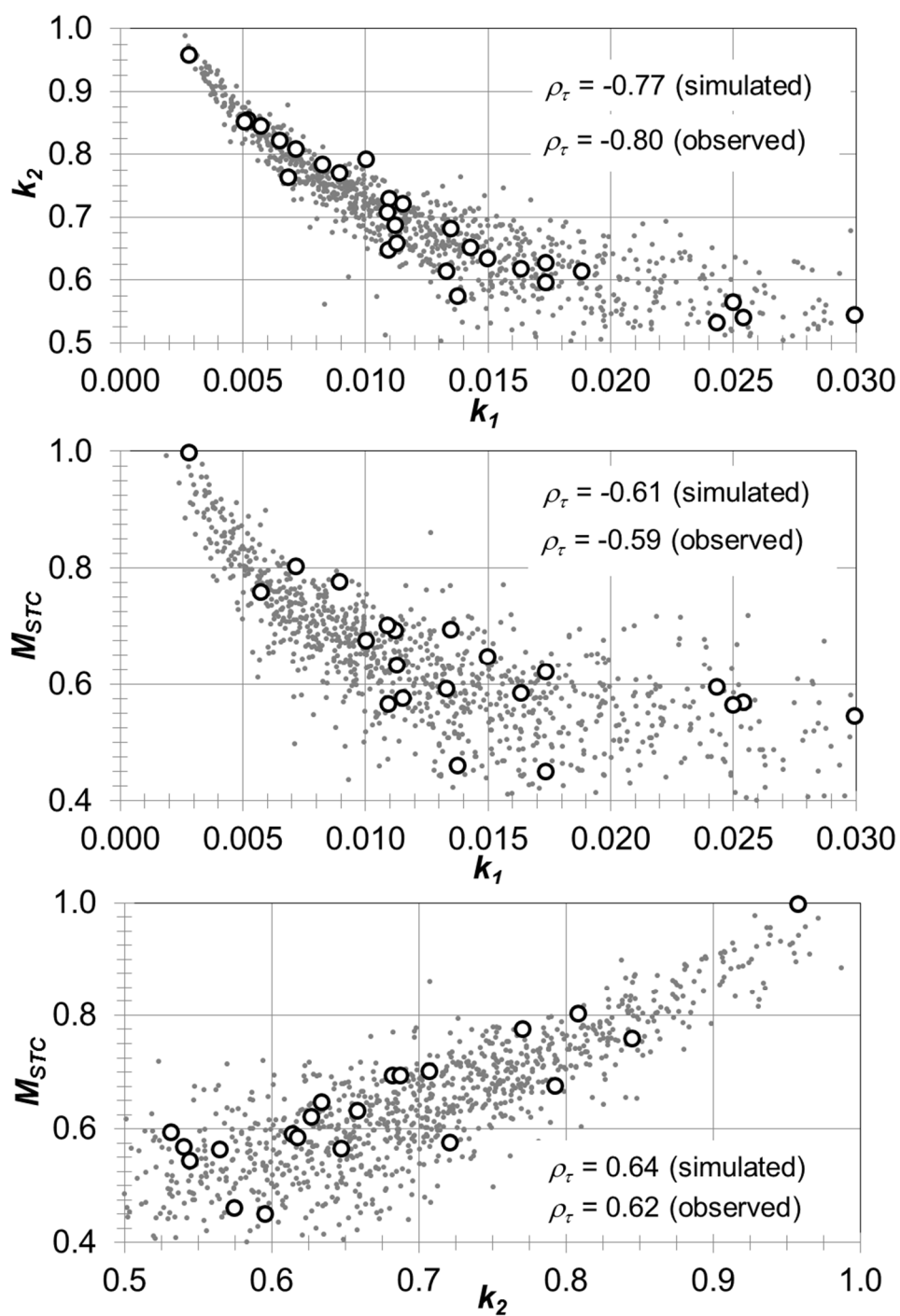


**Figure 5.4** Comparison of observed and simulated ( $n = 1,000$ ) normalized bearing pressure-displacement model parameters  $k_1$  and  $k_2$ , and model factor  $M_{STC}$ .

Copula functions were used to account for the multivariate dependence (i.e., joint distribution) in the reliability simulations. A copula function describes the probability of values in a dataset, similar to the fitted distributions for the individual variables. However, instead of describing the probability distribution of a single variable, the copula function describes the probable values of one variable given the values of the other, correlated variables. These results can then be coupled with the marginal distributions of the individual variables to provide a full description of the probable values (e.g., Nelson 2006). Bivariate copula functions have been used in other recent geotechnical-related studies to account for the dependence between load and displacement model parameters (e.g., Uzielli and Mayne 2011, 2012, Li et al. 2013, Huffman and Stuedlein 2014) and between soil strength parameters (e.g., Tang et al. 2013, Tang et al. 2015, Wu 2013, 2015).

Many copula types are available to account for trends in correlations, including linear or nonlinear correlations, elliptical correlations, and tail-dependent correlations, among others. Most copula functions can be calibrated using a single copula parameter,  $\theta$ , to define the dependence structure between variables. The copula parameter may be calculated based on a relationship to  $\rho_\tau$  that is specific to the copula type.

Copula functions assume uniformly distributed marginal distributions in rank [0,1] space. Therefore, the rank values of the hyperbolic model parameters and model factor ( $k_1$ ,  $k_2$  and  $M_{STC}$ ), referred to herein as  $u_1$ ,  $u_2$  and  $u_{STC}$ , were used with  $\rho_\tau$  to establish  $\theta$  and the copula probability function. A relationship between two variables (e.g.,  $k_1$  and  $k_2$ ) and a two-parameter copula probability function,  $C_{k_1,k_2}$ , is determined by fitting to  $\rho_\tau$  using (e.g., Nelson 2006, Li et al. 2013):

$$\rho_{\tau}(k_1, k_2) = 4 \int_0^1 \int_0^1 C_{k_1, k_2}(u_1, u_2) dC_{k_1, k_2}(u_1, u_2) - 1 \quad (5.10)$$

Dependence between three or more variables can be accounted for using one multivariate copula, or a string of bivariate copulas, known as a vine copula (e.g., Joe 1996, Aas et al. 2009, Brechmann and Schepsmeier 2013). The vine copula approach was selected to represent the dependence between  $k_1$ ,  $k_2$  and  $M_{STC}$  because it is not limited to a single dependence structure and therefore may provide better representation of the correlation between individual variables relative to a single multivariate copula (Brechmann and Schepsmeier 2013). The selection of the bivariate copulas included in the vine, as well as selection of the copula parameters,  $\theta$ , required multiple iterations to determine the best-fit copulas. A canonical (i.e., C-vine) approach (Aas et al. 2009, Brechmann and Schepsmeier 2013) was selected for the simulations herein, which establishes the best-fit bivariate copulas using sequential maximum likelihood estimation (e.g., Lipster and Shiryayev 2001). The order of the variables for this analysis was arbitrarily taken as: (1)  $k_1$ , (2)  $k_2$ , and (3)  $M_{STC}$ , because initial studies showed that the reliability simulations were not sensitive to the order of simulation.

The best-fit copulas were selected from several copula types based on the AIC criteria similar to that used for the marginal distributions (i.e., Eq. 5.8). For each set of dependent variables (i.e.,  $k_1$ - $k_2$ ,  $k_1$ - $M_{STC}$  and  $k_2$ - $M_{STC}$ ), the AIC test was used to estimate the relative likelihood of a two-parameter copula density function,  $c$ . Based on these test criteria, the multi-dimensional vine copula was constructed using the bivariate Clayton copula (rotated 270 degrees) to represent the dependence between  $k_1$ - $k_2$  and  $k_1$ - $M_{STC}$ , and the bivariate Joe copula (rotated 180 degrees) was selected to represent the dependence of  $k_2$ - $M_{STC}$ . A summary of the selected copula types with the respective copula probability functions and



$\theta$  values is shown in Table 5.6. Figure 5.4 shows the fitted  $k_1-k_2$ ,  $k_1-M_{STC}$  and  $k_2-M_{STC}$  pairs from the load test database compared against 1,000 simulated pairs using the distributions indicated in Table 5.5 and variable dependence with vine copula components indicated in Table 5.6. The  $\rho_\tau$  values for the actual and simulated data pairs shown in Fig. 5.4 indicate close agreement between observed and simulated data pairs, and indicate that the simulated values adequately represent the distribution and dependence of the  $q^*-\eta$  model parameters extrapolated from the load test database.

**Table 5.6. Summary of best-fit copula functions representing bivariate dependence in the vine copula.**

Dependent Pair	Best-Fit Copula	Copula Param., $\theta$	Copula Probability Function, $C(u, v)$	General Copula Density Funct., $c(u, v)$
$k_1-k_2$	Clayton (rotated 270°)	-7.054	$u - \left( u^{-\theta} + (1-v)^{-\theta} - u^{-\theta}(1-v)^{-\theta} \right)^{\frac{1}{\theta}}$	
$k_1-M_{STC}$	Clayton (rotated 270°)	-3.143	$u - \left( u^{-\theta} + (1-v)^{-\theta} - u^{-\theta}(1-v)^{-\theta} \right)^{\frac{1}{\theta}}$	$\frac{\partial}{\partial u \partial v} C(u, v)$
$k_2-M_{STC}$	Joe (rotated 180°)	1.398	$u+v-1 - \left( 1 - \left( (1-u)^{-\theta} + (1-v)^{-\theta} - 1 \right)^{\frac{1}{\theta}} \right)$	

**Note:** Coefficients  $u$  and  $v$  represent the rank values of the dependent pairs transposed to  $[0,1]$  space (e.g.,  $u_1$  and  $u_2$  for the  $k_1-k_2$  pairs).

### 5.6.3 Assessment of Lower-Bound Resistance

Najjar and Gilbert (2009) describe the impact of physically meaningful lower-bound soil strength on the reliability of geotechnical performance of driven pile foundations. The lower-bound soil strength is best determined using site-specific soil investigations, with

particular attention to stress history, mineralogy, and secondary soil structure. Najjar (2005) suggests that the lower-bound capacities for foundations on fine-grained soils is limited by the remolded undrained shear strength,  $s_{ur}$ . Therefore, to estimate and characterize the lower-bound capacity reflected in the database considered herein, the bearing capacity was recalculated for each case history using the general bearing capacity equation (Eq. 5.1) with  $s_{ur}$  instead of  $s_u$ . Residual shear strength with depth measurements were report by Bauer (1976), and soil sensitivity ( $s_u/s_{ur}$ ) was either reported or inferred from laboratory test results by Brand et al. (1972), Jardine et al. (1995), and Stuedlein and Holtz (2010). For the remaining portion of the database,  $s_{ur}$  was estimated based on a correlation to the liquidity index,  $LI$ , following Najjar (2005), based on Wroth and Wood (1978):

$$s_{ur} = 170e^{-(4.6LI)} \quad (5.11)$$

where  $s_{ur}$  is in kPa. Najjar (2005) suggests the correlation is appropriate for soils with a sensitivity in the range of 2 to 5. Therefore, where Eq. 5.11 predicted residual soil shear strengths with corresponding sensitivity falling outside of a range of 2 to 5, the assumed residual shear strength was revised to limit the minimum sensitivity value equal to 2 and maximum value equal to 5. Note, application of the reliability-based SLS design procedures described subsequently is not recommended for use with extremely sensitive soils (i.e., soils with sensitivity greater than five), as foundations resting on these soils require careful investigations.

The ratio of bearing capacity calculated using  $s_{ur}$  (i.e., the lower-bound capacity) to those calculated using  $s_u$  was computed and produced a mean lower-bound bearing capacity ratio of 0.47 and standard deviation of 0.18. Therefore, a normalized bearing

capacity,  $q_{ult, min}^*$ , of 0.29, representing the mean ratio minus one standard deviation, was selected to truncate the  $q_{ult}^*$  distribution in the MCS. The inclusion of the lower-bound capacity reduced the number of simulations by approximately 0.1 percent; although not representing a large number of simulations, inclusion of the truncated capacity distribution improves the accuracy of reliability calibrations and removes unnecessary conservatism.

#### 5.6.4 Characterization of Applied Bearing Pressure

The load and resistance factor calibrated herein for SLS design considered uncertainty in the applied bearing pressure in order to maintain consistency with widely-accepted loading scenarios. The loading was modeled using a unit mean normalized applied bearing pressure,  $q_{app}^*$ , equal to 1.00 and  $COV(q_{app}^*)$  equal to 10 and 20 percent for dead and live loads, respectively (Table 5.7). These values suggest that, on average, structure loads can be estimated with relatively close accuracy, but the design accounts for some potential deviation. The unit mean normalized applied bearing pressure was modeled using a lognormal distribution, consistent with national codes (e.g., AASHTO 2012) and reliability analyses performed by others (e.g., Phoon and Kuhawy 2008, Uzielli and Mayne 2011, and Li et al. 2011).

#### 5.6.5 Characterization of Allowable Displacement

Considering the end-user of a calibrated SLS design procedure, an appropriate load and resistance factor should be selected based on a structures' ability to accept deformations arising from foundation movements. This is a function of the structure type and its intended use, and requires close collaboration with the entire design team. To provide a generalized framework, this study explicitly incorporated a continuous range in the allowable

immediate displacements,  $\delta_a$ , in the estimate of the mobilized resistance using the relevant performance function (Eq. 5.7). Table 5.7 summarizes the selected normalized allowable displacements,  $\eta_a$ , which ranged from 0.005 to 0.20, based on an assumed range of mean  $\delta_a$  of 2.5 mm to 600 mm and equivalent footing diameters,  $B'$ , ranging from 0.5 m to 3 m. The dispersion in  $B'$  was modeled using a COV of 2 percent and a normal distribution. It should be noted that the upper values of  $\delta_a$  were included to provide the selected range of  $\eta$ , and  $\delta_a$  may approach unrealistic magnitudes as a result.

**Table 5.7. Summary of assumed normalized bearing pressure and displacement parameters.**

Parameter	Nominal Value	COV (%)	Model Distribution
$q_{app}^*$	1.00	10, 20	Lognormal
$\delta_a$ (mm)	2.5, 5, 7.5, 10, 12.5, 15, 20, 25, 30, 37.5, 50, 75, 100, 112.5, 125, 150, 187.5, 200, 225, 250, 300, 400, 500, 600	0, 20, 40, 60	Lognormal
$B'$ (m)	0.5, 1.0, 1.5, 2.0, 2.5, 3.0	2	Normal
$\eta$	0.005, 0.01, 0.025, 0.05, 0.075, 0.10, 0.20	-	-

Unlike the selection of a representative magnitude of uncertainty in loading, there is not yet a consensus on the suitable design-level dispersion in the allowable immediate or total displacement largely owing to the lack of available data. Phoon and Kulhawy (2008) assumed a COV of 60 percent for  $\delta_a$  based on research by Zhang and Ng (2005) for

structures supported on deep foundations. However, they concede that it is unclear whether available data for allowable displacement typically refers to mean or lower-bound values, which may also affect its dispersion. Uzielli and Mayne (2011) assumed a COV of 60 percent for  $\delta_a$  and lognormal distribution when analyzing the SLS for spread footings on sand. For this study,  $\delta_a$  was modeled using a lognormal distribution and COV of 0, 20, 40 and 60 percent to represent a range of COV, in order to allow professional judgment in the selection of the appropriate lumped load and resistance factor for the corresponding  $COV(\delta_a)$ .

#### 5.6.6 Reliability Simulations and Lumped Factor Calibration

Monte Carlo simulations were used to generate samples from each of the random variable distributions as a means to populate the performance function (Eq. 5.7) and calibrate the lumped load and resistance factor,  $\psi_q$ , to the probability of exceeding the SLS (and corresponding  $\beta$  value). Each random variable (i.e.,  $k_1$ ,  $k_2$ ,  $M_{STC}$ ,  $\delta_a$ ,  $B'$ ,  $q^*_{ult}$  and  $q^*_{app}$ ) was randomly sampled using their source distribution and  $1.5 \times 10^6$  simulations for each  $\psi_q$ , which ranged from 1 to 20. The final number of simulations (i.e., the basis for computing  $p_f$  and  $\beta$ ) was slightly smaller than  $1.5 \times 10^6$ , as simulations associated with  $q^*_{ult, min}$  less than 0.29 were rejected to enforce the truncated bearing capacity distribution as described previously. The reliability calibrations required approximately 2,500 independent simulation scenarios in order to estimate  $\beta$  and  $p_f$  for different combinations of  $\psi_q$ ,  $B'$ ,  $\delta_a$ ,  $COV(\delta_a)$ , and  $COV(q^*_{app})$ , and are associated with a confidence level of 99% or greater for simulations corresponding to  $\beta$  less than or equal to four, sufficiently accurate for reliability levels corresponding to the SLS.

The results of the simulations indicated strong non-linear relationships between  $\psi_q$  and  $\beta$  at any given  $\eta_a$ . Consistent with the service limit displacements of footings on sand reported by Uzielli and Mayne (2011, 2012) and on aggregate pier reinforced clay (Huffman and Stuedlein 2014), the relationships of  $\beta$  and  $\psi_q$  were nearly identical regardless of the  $\delta_a$  and  $B'$  values used to define  $\eta_a$ . Figure 5.5 shows the  $\psi_q$  calibration for  $\text{COV}(q^*_{app})$  of 10 percent, and  $\text{COV}(\delta_a)$  ranging from 0 to 60 percent from the MCS. Figures 5.5a through 5.5d include the results of the entire simulation, whereas Fig. 5.5e through 5.5h include only  $\beta$  values greater than 0, in order to improve the fit of logarithmic trendlines over  $\psi_q$ - $\beta$  pairs that may be suitable for design.

The MCS showed that low reliability indices (i.e., high probability of exceeding the selected magnitude of displacement) logically correspond to low values of  $\psi_q$ . Further, the reliability indices increased sharply with moderate increases in  $\psi_q$ . For example, considering an unfactored loading case (i.e.,  $\psi_q = 1.0$ ) in Figure 5.5a, at a normalized allowable immediate displacement,  $\eta_a$ , of 0.025,  $\beta$  is equal to -0.98, which corresponds to a probability of exceeding  $\eta_a$  of approximately 84 percent. At the same  $\eta_a$ , but considering  $\psi_q$  equal to 3,  $\beta$  rises to 1.26 and a corresponding 10 percent probability of exceeding  $\eta_a$ . As shown in Fig. 5.5, similar trends in the variation of  $\psi_q$  with  $\beta$  were noted for the reliability simulations corresponding to the range in  $\text{COV}(q^*_{app})$  and  $\text{COV}(\delta_a)$  investigated.

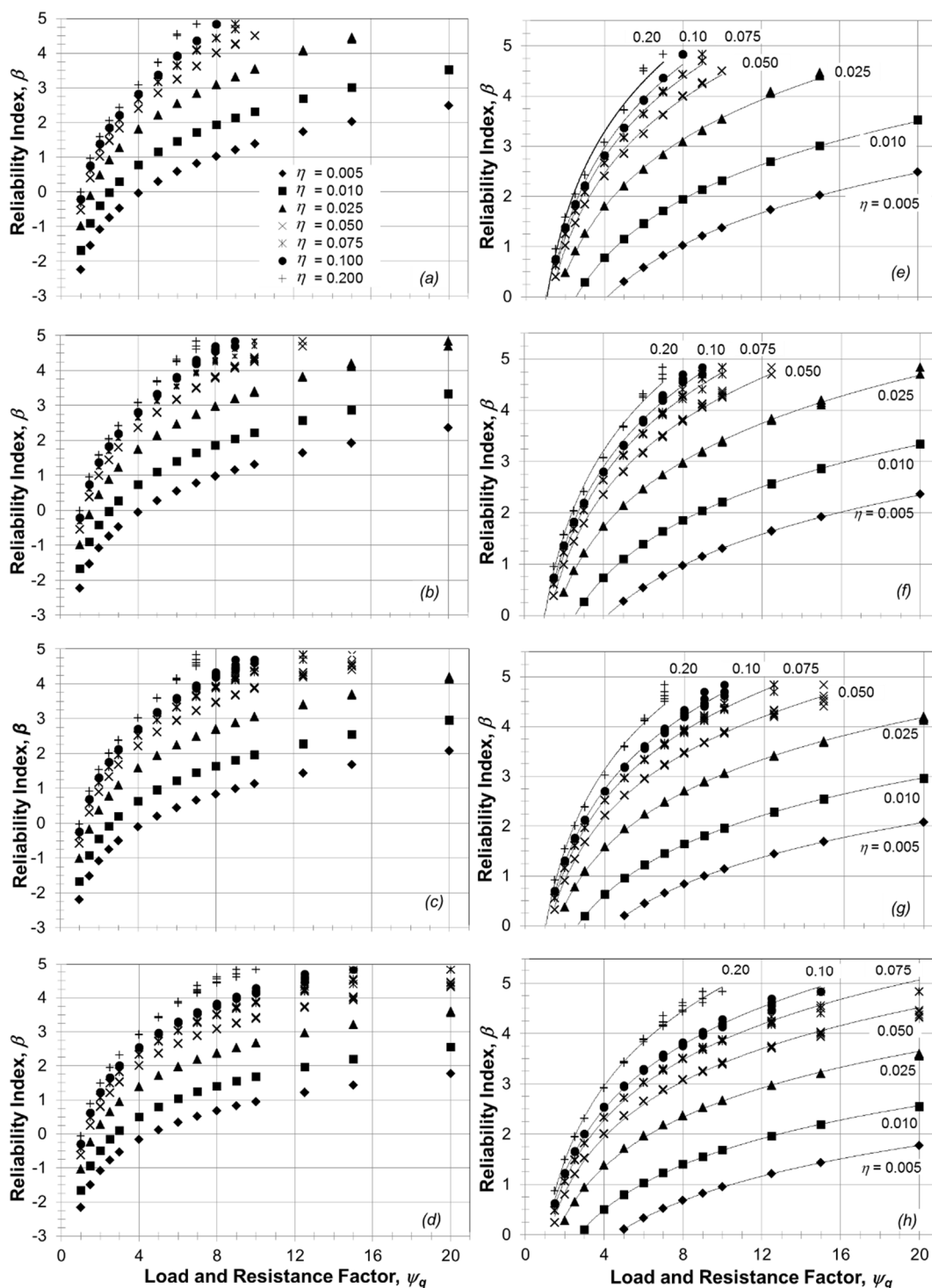


**Figure 5.5** Load and resistance factor,  $\psi_q$ , and reliability index,  $\beta$ , varying with normalized displacement,  $\eta$ , for  $\text{COV}(q_{app}) = 0.10$  and (a and e)  $\text{COV}(\delta_a) = 0$ , (b and f)  $\text{COV}(\delta_a) = 20$  percent, (c and g)  $\text{COV}(\delta_a) = 40$  percent, and (d and h)  $\text{COV}(\delta_a) = 60$  percent. Note, logarithmic-fitted curves shown in (e) through (h) are limited to  $\beta > 0$ .

Uzielli and Mayne (2011) suggested the  $\psi_q$  vs.  $\beta$  relationship could be characterized with the functional form:

$$\beta = p_1 \ln(\psi_q) + p_2 \quad (5.12)$$

for their reliability simulations, where  $p_1$  and  $p_2$  are best fit coefficients. Uzielli and Mayne (2011) also found the coefficient  $p_1$  and constant  $p_2$  varied with the normalized allowable displacement,  $\eta_a$ , in a linear and logarithmic trend, respectively. For this study,  $p_1$  was found to correlate with a three-parameter exponential function of the form:

$$p_1 = a(1 - \exp(-\eta_a/b)) + c \quad (5.13)$$

and  $p_2$  was found to correlate well with a three-parameter log-polynomial function:

$$p_2 = d \ln(\eta) + e \ln(\eta) + f \quad (5.14)$$

where  $a$ ,  $b$  and  $c$  in Eq. 5.13 and  $d$ ,  $e$  and  $f$  in Eq. 5.14 are estimated using least squares optimization. Figure 5.6 shows an example of the regressed, best-fit curves for  $p_1$  and  $p_2$  for the case of  $\text{COV}(q^*_{app}) = 10$  percent and  $\text{COV}(\delta_a) = 0$ . Combining the models used to predict  $p_1$  and  $p_2$  with Eq. 5.12 yields the closed-form model to estimate the reliability index:

$$\beta = \left( a \left( 1 - \exp\left(\frac{-\eta_a}{b}\right) \right) + c \right) \ln(\psi_q) + d \ln(\eta_a)^2 + e \ln(\eta) + f \quad (5.15)$$

which is associated with a confidence level of 99% or better for  $\beta < 4$ . Table 5.8 provides a summary of the best-fit coefficients  $a$ ,  $b$ ,  $c$ ,  $d$ ,  $e$  and  $f$  to estimate the reliability index associated with any  $\eta_a$  and  $\psi_q$  for Eq. 5.15. Note the coefficients will vary depending on the anticipated dispersion of the allowable immediate footing settlement and applied bearing pressure. Alternatively, the load and resistance factor associated with any  $\beta$  and  $\eta_a$  may be computed by inverting Eq. 15:



$$\psi_q = \exp \left[ \frac{\beta - d \ln(\eta_a)^2 - e \ln(\eta_a) - f}{a \left( 1 - \exp\left(\frac{-\eta_a}{b}\right) \right) + c} \right] \quad (5.16)$$

such that the required load and resistance factor can be obtained for a desired level of reliability.

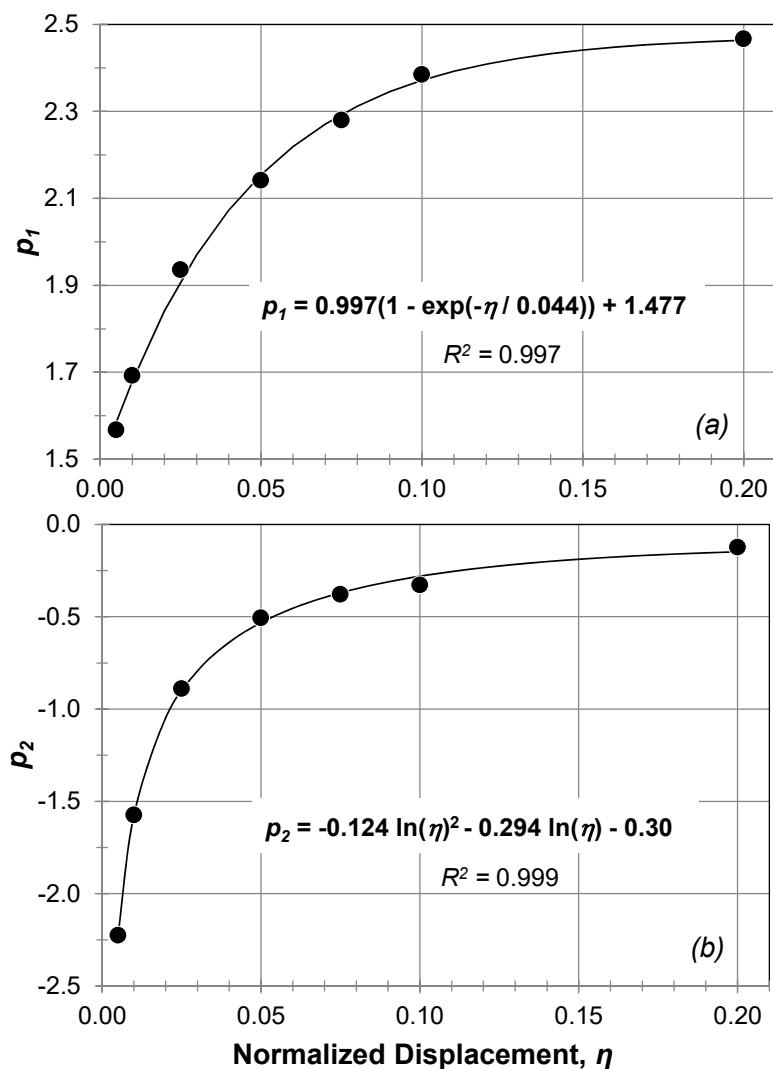


**Figure 5.6** Variation of regressed coefficients (a)  $p_1$  and (b)  $p_2$  with normalized displacement. Curves shown for  $\text{COV}(q_{app}) = 10$  percent and  $\text{COV}(\delta_a) = 0$ .

**Table 5.8. Summary of best-fit coefficient for Eqs. 5.16 and 5.17 and multiplying factor,  $M_{\psi,95}$**

$COV(\delta_a)$ (%)	$COV(q_{app}^*)$ (%)	$a$	$b$	$c$	$d$	$e$	$f$	$M_{\psi,95}$
0	10	0.997	0.044	1.477	-0.124	-0.294	-0.300	1.08
20	10	0.974	0.045	1.412	-0.121	-0.285	-0.245	1.06
40	10	1.099	0.073	1.299	-0.136	-0.429	-0.444	1.05
60	10	1.164	0.114	1.176	-0.103	-0.181	0.096	1.09
0	20	0.733	0.033	1.417	-0.122	-0.277	-0.159	1.05
20	20	0.778	0.037	1.359	-0.116	-0.252	-0.126	1.06
40	20	0.869	0.063	1.273	-0.128	-0.369	-0.278	1.05
60	20	1.049	0.114	1.163	-0.096	-0.135	0.193	1.10

### 5.6.7 Comparison of MCS Results and Closed-Form Model

The closed-form model used to predict the load and resistance factor for the given normalized displacement and reliability index introduces variability owing to the errors associated with the fitting to the reliability simulations (i.e., Eqs. 5.12, 5.13, and 5.14). To quantify the error, the  $\beta$  values produced by the fitting to the MCS were substituted into Eq. 5.16 to calculate  $\psi_q$  and compare to the actual MCS. The results of the comparison are plotted in Fig. 5.7 for the range of  $COV(q_{app}^*)$  and the range of  $COV(\delta_a)$  investigated and for  $\beta$  resulting from the prescribed interval of  $\psi_q$  ranging from 1 to 20. A mean bias of 1.0 was calculated for each combination of  $COV(q_{app}^*)$  and  $COV(\delta_a)$ , with COV in the bias ranging from 2.2 to 5 percent, indicating relatively small error. The error typically becomes greater at the largest values of  $\psi_q$ , which is attributed primarily to the larger dispersion of  $p_f$  and  $\beta$  estimated from the MCS for large  $\psi_q$  values (Fig. 5.5) and error in the hyperbolic  $q^*$ - $\eta$  model at small displacements.

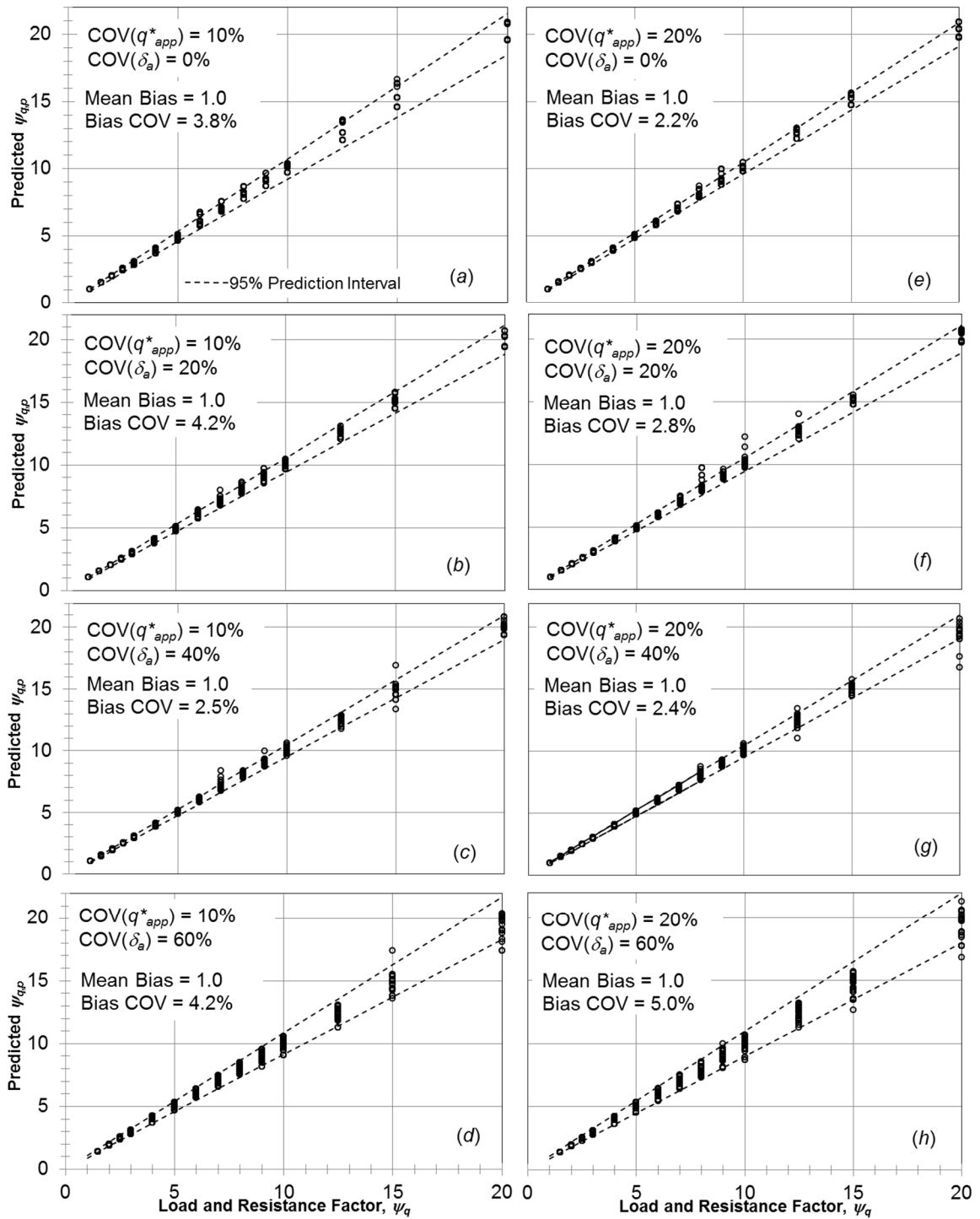


**Figure 5.7** Comparison of MCS-based load and resistance factor,  $\psi_q$  and predicted load and resistance factor,  $\psi_{q,p}$  using Eq. 5.17, along with 95 percent prediction interval. Comparisons in (a) through (d) represent  $COV(q^*_{app}) = 10$  percent, whereas comparisons in (e) through (h) represent  $COV(q^*_{app}) = 20$  percent.

To account for the error in Eq. 5.16 and the increased dispersion at the largest values of  $\psi_q$ , a factor  $M_{\psi,95}$  may be multiplied by  $\psi_q$  such that a lumped load and resistance factor,  $\psi_{q,95} = \psi_q * M_{\psi,95}$  represents the 95 percent confidence level in the simulation-based  $\psi_q$ . Adjustment factors ranging from  $M_{\psi,95} = 1.05$  to 1.10 were computed for the various combinations of  $\text{COV}(q^*_{app})$  and  $\text{COV}(\delta_a)$ , and are provided in Table 5.8.

## 5.7 APPLICATION OF THE RELIABILITY CALIBRATIONS

### 5.7.1 Design Example

Upon loading, a spread footing on clay will experience immediate displacement in addition to consolidation settlement and possibly secondary compression. Therefore, the foundation designer will need to establish the total tolerable displacement, and then perform the required analyses to determine whether one component of displacement or a combination of these components is likely to exceed the target probability associated with exceeding the tolerable displacement. Settlement analysis associated with consolidation is well established and not addressed herein. Instead the focus is on immediate displacement only. The following steps (Fig. 5.8) are required to estimate the corresponding allowable bearing pressure associated with a 1 percent probability of exceedance ( $\beta = 2.33$ ) for a typical equivalent footing diameter of 1 meter and nominal allowable immediate footing displacement of 25 mm:

1. Estimate the bearing capacity of the spread footing using Eq. 5.1. That is, calculate  $q_{ult,p}$ .
2. Establish the mobilized resistance,  $q_{mob}$ , using Eq. 5.4 with the allowable immediate displacement and estimated slope tangent capacity,  $q_{STC}$ . For this example, the

normalized allowable immediate displacement,  $\eta_a$ , is 0.025. The coefficients  $k_1$  and  $k_2$  provided in Table 5.5 are 0.013 and 0.701, respectively, resulting in a hyperbolic model factor,  $M_\eta$ , of 0.819. The slope tangent model factor,  $M_{STC}$ , is 0.643 (Table 5.5). Therefore, the mobilized resistance is  $(0.819)(0.643)q_{ult,p} = 0.527q_{ult,p}$ .

3. The resistance factor,  $\psi_q$ , is applied to  $q_{ult,p}$  based on the selected target probability of exceeding the service level displacement. Estimate  $\psi_q$  using Eq. 5.16 based on the allowable immediate displacement and coefficients  $a$ ,  $b$ ,  $c$ ,  $d$ ,  $e$  and  $f$  (Table 5.8). A  $COV(\delta_a)$  and  $COV(q^*_{app})$  of 0 and 10 percent were assumed, respectively, for this example. For a  $pf$  of 1 percent ( $\beta = 2.33$ ),  $\psi_q$  equals approximately 5.4 using Eq. 5.16. The adjustment factor,  $M_{\psi,95} = 1.08$  (Table 5.8) is recommended for the prescribed  $COV(\delta_a)$  and  $COV(q^*_{app})$  values, resulting in a  $\psi_{q,95}$  value of approximately 5.8.
4. The allowable bearing pressure that limits immediate displacement to 25 mm or less with probability of exceeding the allowable immediate displacement of 1 percent may then be computed by combining the results from steps 1 through 3, resulting in  $(1/\psi_{q,95})(M_\eta)(M_{STC})(q_{ult,p})$ , or  $0.09q_{ult,p}$ .

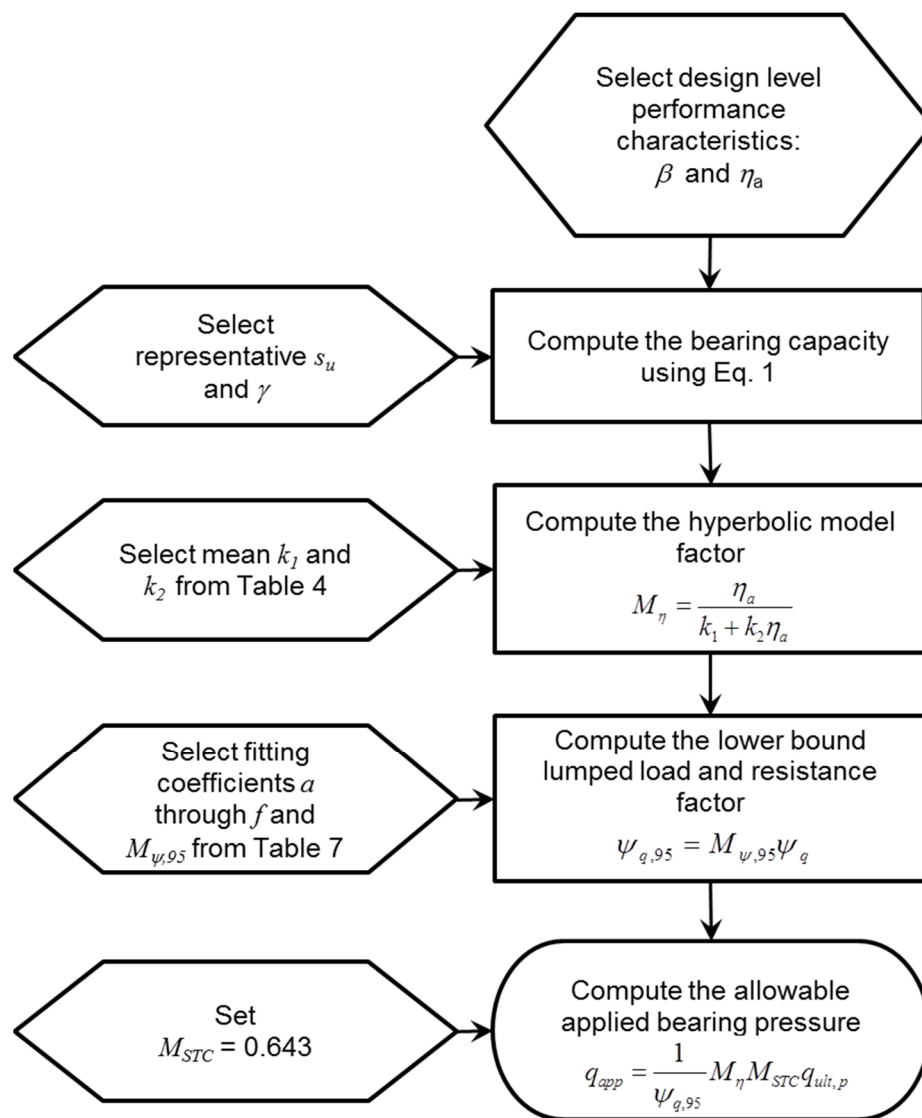


**Figure 5.8** Procedure for implementation of the proposed reliability-based serviceability limit state methodology for immediate settlements of spread footings on plastic, fine-grained soils.

### 5.7.2 Discussion

An interesting result of the example provided above is to note that the selected probability of 1 percent of exceeding the immediate displacement produced a relatively low bearing pressure value (i.e.,  $0.09q_{ult}$ ). Allowable stress design (ASD) factors of safety for spread footings typically range between 3 to 4 (i.e.,  $0.25q_{ult}$  to  $0.33q_{ult}$ ). For the design

example included above, this range of ASD factors of safety results in an equivalent  $\psi_q$  factor ranging from 1.32 to 1.57, and a probability of exceeding the allowable immediate displacement ranging from 50 to 64 percent. This suggests that evaluating a spread footing on clay using traditional formulas to determine bearing capacity (i.e., ULS) and applying a typical ASD factor of safety in the range of 3 to 4 could result in a relatively high probability of exceeding the target immediate displacement. On the other hand, Eurocode 7 (e.g. Orr and Breysse 2008) includes SLS provisions of  $\beta = 1.5$  (or  $p_f = 6.7$  percent) over a 50-year service life. For these less stringent conditions,  $\psi_{q,95} = 3.80$  and  $q = 0.14q_{ult,p}$ , representing an increase in bearing pressure of more than 50 percent. Thus, the designer's judgment can be readily incorporated into the proposed RBD procedure based on the quality of information and the requirements of the structure. Note that for the given examples, where  $\delta_a = 25$  mm, the margin of immediate displacement exceeding the target magnitude could range from an insignificant amount (i.e., on the order of 1 mm) or a significant amount (10 mm). Obviously, efforts to improve the understanding of the spatial variability of pertinent design parameters at a particular site to reduce the overall risk of exceeding a given limit state remain warranted.

Immediate displacement may comprise just a portion of the total settlement under a given foundation and separate analyses must be conducted to estimate consolidation settlements if the possibility for triggering primary consolidation exists. Additionally, the practitioner must estimate the total differential settlement possible, and the procedure proposed herein can be used to help judge the likelihood of exceeding a target immediate differential settlement. This can be useful where staged construction is required, or where footings of significantly different bearing pressures or bearing loads are to be supported.

In practice, when the duration between successive construction loads is long, and where strength gain occurs, the procedure described herein may be updated to reflect the increased capacity and refine the estimate of immediate and differential settlement. Additionally, it is recommended that practitioners perform separate analyses for the assessment of construction, using dead loads and dead load statistics, and for live loading events that may occur over the life of the structure. The gain in strength resulting from possible consolidation should be incorporated into the evaluation of immediate settlement for long-term live loading events. Finally, when justified, the procedure described herein can be used to plan and execute footing loading tests conducted to support design recommendations.

## 5.8 SUMMARY

Immediate or undrained displacement of spread footings on plastic, fine-grained soils should be evaluated as part of serviceability limit state (SLS) design assessments, as it may provide a significant portion of the total settlement. A comprehensive SLS design approach will include analyses to accurately estimate undrained displacement and determine if the expected differential displacement is within acceptable limits. A suitable probabilistic SLS design approach can provide an estimate of the probability of exceeding the allowable immediate displacement and allow various design alternatives to be rapidly evaluated.

This paper describes the development of a reliability-based SLS procedure for the estimation of the allowable bearing pressure at a given immediate displacement and its corresponding probability of exceeding this value for spread footings on plastic, fine-grained soils. The framework developed herein was based on a new loading test database



to characterize and simulate the nonlinear, inelastic bearing pressure-displacement response. First, the normalized bearing pressure-displacement ( $q^*-\eta$ ) response was estimated based on a novel reference slope-tangent capacity and hyperbolic resistance-mobilized displacement model. The probability of exceeding the estimated immediate displacement was then established using a performance function and Monte Carlo simulations in combination with the dispersion of the various controlling loading and resistance parameters. Correlation in the resistance parameters was accounted for using appropriate vine copulas, and truncation of the lower-bound resistance was accomplished using methods proposed by Najjar and Gilbert (2009).

Evaluation of the Monte Carlo simulations indicated a nonlinear relationship between the load and resistance factor,  $\psi_q$ , and the reliability index,  $\beta$ , used to reference a target probability of exceeding the SLS design. A new and convenient set of equations were proposed to provide  $\psi_q$  given a target  $\beta$  value based on an acceptable probability of exceeding the allowable immediate displacement. In order to illustrate the use of the proposed procedure, an example of its application was provided. The results of the example suggested that the probability of exceeding the allowable immediate settlement can be relatively high using traditional factors of safety, although the magnitude of the settlement exceeding SLS may range from insignificant to significant.

The analysis and procedure presented herein is appropriate for estimating immediate undrained settlement of rigid footings on plastic fine-grained soil with undrained shear strengths in the relative range of soft to stiff, and for evaluating the reliability of the settlement calculation. Because the spatial variability and measurement errors were not

explicitly treated in this study, the results of this study should not be extrapolated to foundation or soil conditions that are outside the range included in the database.

## 5.9 REFERENCES

- Aas, K., Czado, C., Frigessi, A., and Bakken, H. (2009). "Pair-Copula Construction of Multiple Dependence," *Insurance: Mathematics and Economics*, Vol. 44, No. 2, pp. 182-198.
- AASHTO (2012) *AASHTO LRFD Bridge Design Specifications, 6<sup>th</sup> Ed.*, Washington, DC.
- Akaike, H. (1974) "A New Look at the Statistical Model Identification," *Transactions on Automatic Control*, IEEE, Vol. 19, No. 6, pp. 716-723.
- Akbas, S.O. and Kulhawy, F.H. (2009). "Axial Compression of Footings in Cohesionless Soils I: Load-Settlement Behavior," *Journal of Geotechnical and Geoenvironmental Engineering*, ASCE, Vol. 135, No. 11, pp. 1562-1574.
- Allen, T.A., Nowak, A.S., and Bathurst, R.J. (2005). "Calibration to Determine Load and Resistance Factors for Geotechnical and Structural Design," *Transportation Research Circular E-C079*, Transportation Research Board of the National Academies, Washington D.C., 93 p.
- Andersen, K.H. and Stenhamar, P. (1982). "Static Plate Loading Test on Overconsolidated Clay," *Journal of the Geotechnical Engineering Division*, ASCE, Vol. 108, No. 7, pp. 918-934.
- Baecher, G.B. and Christian, J.T. (2003) *Reliability and Statistics in Geotechnical Engineering*, John Wiley and Sons, Ltd., London and New York, 605 pp.
- Bauer, G.E., Shields, D.H., and Scott, J.D. (1976). "Predicted and Observed Footing Settlements in a Fissured Clay," Ottawa, Pentech Press, pp.287-302.
- Bergado, D.T., Rantucci, G. and Widodo, S. (1984). "Full Scale Load Tests of Granular Piles and Sand Drains in the Soft Bangkok Clay," Asian Institute of Technology, pp. 111-118.
- Brand, E.W., Muktabhant, C. and Taechathummarak, A. (1972). "Load Tests on Small Foundations in Soft Clay," *Conference Proceedings: Performance of Earth and Earth Supported Structures*, ASCE, pp. 903-928.
- Brechmann, E.C., and Schepsmeier, U. (2013). "Modeling Dependence with C- and D-Vine Copulas: The R Package CDVine," *Journal of Statistical Software*, Vol. 52, No. 3, 27 pg.
- Consoli, N. C., Schnaid, F. and Milititsky, J. (1998). "Interpretation of Plate Load Tests on Residual Soil Site," *Journal of Geotechnical and Geoenvironmental Engineering*, ASCE, 124(9), pp. 857-867.

- D'Appolonia and Lambe, T.W. (1970). "Method for Predicting Initial Settlement," *Journal of the Soil Mechanics and Foundations Division*, ASCE, Vol. 96, No. SM2, pp. 523-544.
- D'Appolonia, D., Poulos, H. and Ladd, C. (1971). "Initial Settlement of Structures on Clay," *Journal of the Soil Mechanics and Foundations Division*, Vol. 97, No. SM10, pp. 1359-1377.
- Deshmukh, A.M. and Ganpule, V.T. (1994). "Influence of Flexible Mat on Settlements of Marine Clay," *Vertical and Horizontal Deformations of Foundations and Embankments*, ASCE, pp. 887-896.
- Fenton, G.A., Griffiths, D.V., and Cavers, W. (2005) "Resistance Factors for Settlement Design," *Canadian Geotechnical Journal*, Vol. 42, No. 5, pp. 1422 – 1436.
- Foye, K.C., Basu, P., and Prezzi, M. (2008). "Immediate Settlement of Shallow Foundations Bearing on Clay," *International Journal of Geomechanics*, ASCE, Vol. 8, No. 5, pp. 300-310.
- Greenwood, D.A. (1975). "Vibroflotation: Rationale for Design and Practice," *Methods of Treatment of Unstable Ground*, F. G. Bell, ed., Newness-Buttersworth, London, UK, pp. 189-209.
- Hansen, J. B. (1970). "A Revised and Extended Formula for Bearing Capacity," *DGI Bulletin*, pp. 5-11.
- Huffman, J.C., and Stuedlein, A.W. (2014). "Reliability-based Serviceability Limit State Design of Spread Footings on Aggregate Pier Reinforced Clay," *Journal of Geotechnical and Geoenvironmental Engineering*, ASCE, Vol. 140, No. 10, 04014055.
- Jardine, R.J., Lehane, B. M., Smith, P.R. and Gildea, P.A. (1995). "Vertical Loading Experiments on Rigid Pad Foundations at Bothkennar," *Geotechnique*, Vol. 45, No. 4, pp. 573-597.
- Jardine, R.J., Potts, D. M., Fourie, A.B. and Burland, J.B. (1986). "Studies of the Influence of Non-linear Stress-Strain Characteristics in Soil-Structure Interaction," *Geotechnique*, Vol. 36, No. 3, pp. 377-396.
- Joe, H. (1996). "Families of m-Variate Distributions with Given Margins and  $m(m-1)/2$  Bivariate Dependence Parameters," *Distributions with Fixed Marginals and Related Topics*, Institute of Mathematical Statistics, pp. 120-141.
- Lambe, T.W., Whitman, R.V. (1969). *Soil Mechanics*, John Wiley and Sons, Inc., New York.
- Lehane, B.M. (2003). "Vertically loaded shallow foundation on soft clayey silt," *ICE - Geotechnical Engineering*, Vol. 156, No. 1, pp. 17-26.
- Li, D.Q., Tang, X.S., Phoon, K.K., Chen, Y.F., Zhou, C.B. (2013). "Bivariate Simulation Using Copula and its Application to Probabilistic Pile Settlement Analysis," *International Journal for Numerical and Analytical Methods in Geomechanics*, Vol. 37, No. 6, pp. 597-617.

- Lipster, R.S. and Shiryaev, A.N. (2001). *Statistics of Random Processes II: Applications, 2<sup>nd</sup> Ed.*, Springer-Verlag, Berlin.
- Marsland, A. and Powell, J.J.M. (1980). "Cyclic loading tests on 865 mm diameter plates of a stiff clay till," Swansea, Balkema Press, pp. 837-847.
- Meyerhof, G.G. (1963). "Some Recent Research on the Bearing Capacity of Foundations," *Canadian Geotechnical Journal*, Vol. 1, No. 1, pp. 16-26.
- Najjar, S.S. (2005). "The Importance of Lower-Bound Capacities in Geotechnical Reliability Assessments," *Ph.D. Thesis*, University of Texas at Austin, 317 pp.
- Najjar, S.S., and Gilbert, R.B. (2009). "Importance of Lower-Bound Capacities in the Design of Deep Foundations," *Journal of Geotechnical and Geoenvironmental Engineering*, ASCE, Vol. 135, No. 7, pp. 890-900.
- Newton, V.C. (1975). "Ultimate Bearing Capacity of Shallow Footings on Plastic Silt," *M.S. Thesis*, Oregon State University, 49 p.
- Orr, T.L. and Breyse, D. (2008). "Eurocode 7 and Reliability-based Design," *Reliability-based Design in Geotechnical Engineering: Computations and Applications*, Chapter 8, Ed. K.K. Phoon, Taylor and Francis, pp. 298-343.
- Phoon, K.K. (2003). "Practical Guidelines for Reliability-Based Design Calibration," *Paper presented at Session TC 23 (1) "Advances in Geotechnical Limit State Design"*, 12th Asian Regional Conference on SMGE, August 7-8, 2003, Singapore.
- Phoon, K.K. (2008). "Numerical Recipes for Reliability Analysis – A Primer," *Reliability-Based Design in Geotechnical Engineering: Computations and Applications*, Taylor and Francis, London, pp. 1-75.
- Phoon, K.K. and Kulhawy, F.H. (2008). "Serviceability Limit State Reliability-Based Design," *Reliability-Based Design in Geotechnical Engineering: Computations and Applications*, Taylor and Francis, London, pp. 344-384.
- Roberts, L.A. and Misra, A. (2010). "LRFD of Shallow Foundations at the Service Limit State," *Georisk: Assessment and Management of Risk for Engineered Systems and Geohazards*, Vol. 4, No. 1, pp. 13-21.
- Strahler, A.W. (2012). "Bearing Capacity and Immediate Settlement of Shallow Foundation on Clay," *M.S. Thesis*, Oregon State University, 214 p.
- Strahler, A.W. and Stuedlein, A.W. (2013). "Characterization of Model Uncertainty in Immediate Settlement Calculations for Spread Footings on Clay," *Proceedings, 18<sup>th</sup> International Conference on Soil Mechanics and Geotechnical Engineering*, Paris, 2014, 4 p.
- Strahler, A.W. and Stuedlein, A.W. (2014). "Accuracy, Uncertainty, and Reliability of the Bearing Capacity Equation for Shallow Foundations on Saturated Clay," *Geo-Characterization and Modeling for Sustainability*, GeoCongress 2014, GSP No. TBD, ASCE, Atlanta, GA, February 23-26, 2014, 12 p.

- Stuedlein, A.W. and Holtz, R.D. (2010). "Undrained Displacement Behavior of Spread Footings in Clay," *The Art of Foundation Engineering Practice*, Honoring Clyde N. Baker, Jr., P.E., S.E., ASCE, pp. 653-669.
- Stuedlein, A.W. and Holtz, R.D. (2012). "Analysis of Footing Load Tests on Aggregate Pier Reinforced Clay," *Journal of Geotechnical and Geoenvironmental Engineering*, ASCE, Vol. 138, No. 9, pp. 1091-1103.
- Stuedlein, A.W. and Reddy, S.C. (2013). "Factors Affecting the Reliability of Augered Cast-In-Place Piles in Granular Soils at the Serviceability Limit State," *Journal of the Deep Foundations Institute*, Vol. 7, No. 2, pp. 46-57.
- Stuedlein, A.W. and Uzielli, M. (2014). "Serviceability Limit State Design for Uplift of Helical Anchors in Clay," *Geomechanics and Geoengineering*, Vol. 9 No. 3 pp. 173-186.
- Stuedlein, A.W., Neely, W. and Gurtowski, T. (2012). "Reliability-Based Design of Augered Cast-in-Place Piles in Granular Soils," *Journal of Geotechnical and Geoenvironmental Engineering*, ASCE, Vol. 138, No. 6, pp. 709-717.
- Schwarz, G. (1978). "Estimating the Dimension of a Model," *The Annals of Statistics*, Vol. 6, No. 2, pp. 461-464.
- Tand, K.E., Funegard, E.G. and Briaud, J.L. (1986). "Bearing Capacity of Footings on Clay CPT Method," *Use of In Situ Tests in Geotechnical Engineering*, ASCE, pp. 1017-1033.
- Tang, X.S., Li, D.Q., Rong, G., Phoon, K.K., Zhou, C.B. (2013). "Impact of Copula Selection on Geotechnical Reliability Under Incomplete Probability Information," *Computers and Geotechnics*, Vol. 49, pp. 264-278.
- Tang, X.S., Li, D.Q., Zhou, C.B., Phoon, K.K., Zhou, C.B. (2015). "Copulas-based Approaches for Evaluating Slope Reliability Under Incomplete Probability Information," *Structural Safety*, Vol. 50, pp. 90-99.
- Terzaghi, K. (1943). *Theoretical Soil Mechanics*, John Wiley and Sons, Inc., New York.
- Terzaghi, K., Peck, R. and Mesri, G. (1996). *Soil Mechanics in Engineering Practice*, 3rd ed., John Wiley and Sons, Inc., New York.
- Uzielli, M. and Mayne, P. (2011). "Serviceability Limit State CPT-based Design for Vertically Loaded Shallow Footings on Sand," *Geomechanics and Geoengineering: An International Journal*, Vol. 6, No. 2, pp. 91-107.
- Uzielli, M. and Mayne, P., (2012). "Load-Displacement Uncertainty of Vertically Loaded Shallow Footings on Sands and Effects on Probabilistic Settlement," *Georisk*, Vol. 6, No. 1, pp. 50-69.
- Wang, Y. (2011). "Reliability-based Design of Spread Foundations by Monte Carlo Simulations," *Geotechnique*, Vol. 61, No. 8, pp. 677-685.

- Wroth, C.P. and Wood, D.M., (1978). "The Correlation of Index Properties with Some Basic Engineering Properties of Soils," *Canadian Geotechnical Journal*, Vol. 15, No. 2, pp. 137-145.
- Wu, X.Z. (2013). "Trivariate Analysis of Soil Ranking-Related Characteristics and its Application to Probabilistic Stability Assessments in Geotechnical Engineering Problems," *Soils and Foundations*, Vol. 53, No. 4, pp. 540-556.
- Wu, X.Z. (2015). "Assessing the Correlation Performance Functions of an Engineering System via Probabilistic Analysis," *Structural Safety*, Vol. 52, pp. 10-19.
- Zhang, L.M. and Ng, A.M.Y (2005). "Probabilistic Limiting Tolerable Displacements for Serviceability Limit State Design of Foundations," *Geotechnique*, Vol. 55, No. 2, pp. 151-161.

**CHAPTER 6:  
CALIBRATION AND ASSESSMENT OF RELIABILITY-BASED  
SERVICEABILITY LIMIT STATE PROCEDURES FOR  
FOUNDATION ENGINEERING**

Authors:

Jonathan C. Huffman, John P. Martin, and Armin W. Stuedlein

Journal:

Georisk: Assessment and Management of Risk for Engineered Systems and Geohazards  
Taylor & Francis Group  
5 Howick Place  
London, United Kingdom

Volume 10, Issue 4 (2016)

## 6.1 ABSTRACT

This paper uses an existing reliability-based serviceability limit state (RBSLS) procedure to illustrate some of the critical elements in the calibration of RBSLS models and to serve as guide for future calibration work. First the impact of copula model selection to simulate the correlation structure of the bearing pressure-displacement model parameters used is described by illustrating its impact on the calibrated, lumped load and resistance factor (i.e., a pseudo-factor of safety). Then, the impact of copula model selection on the allowable bearing pressure at a given magnitude of displacement is demonstrated. Thereafter, the normalization protocol selected for the existing RBSLS procedure is critically examined by comparing it to alternative, newly-developed normalization protocols. A framework for the evaluation and assessment of the normalization protocol and copula model selection is then described. The reliability of the suitably revised RBSLS procedure is then contrasted to the previous effort by comparing the lumped load and resistance factors and accuracy determined by comparing to newly conducted, full-scale loading tests of spread footings on aggregate pier-reinforced ground. It is shown that the new RBSLS procedure produces a more accurate estimate of the actual reliability than the previous effort. The framework proposed here takes a critical assessment of the distinct elements of reliability-based serviceability limit state calibration and application.

**Author Keywords:** Reliability-based Design, Serviceability Limit State, Full-Scale Loading Tests, probability of failure



## 6.2 INTRODUCTION

Among the most critical and distinctive elements in reliability-based foundation engineering applications lies the need to sufficiently capture the propagation of model error and other sources of uncertainty in order to accurately capture the geo-structural risk and reliability. With increased understanding of the response and capacity of foundations at the ultimate limit state (ULS) over the last decade, geotechnical research has now been focused on the improvement in modeling of the deformation-based or serviceability limit state (SLS) design. However, the models now largely adopted for SLS design are implemented with parameters that may be imperfectly correlated. Additionally, conditioning of the load-displacement response to reduce scatter often requires the transformation of a ULS-based capacity to a deformation-based capacity, and this transformation may introduce additional uncertainty as well as exhibit imperfect correlation to the load-displacement model parameters. Therefore there is a need to investigate and address these statistical and real possibilities in a logical, rational, and robust fashion.

This paper uses an existing reliability-based serviceability limit state (RBSLS) procedure to illustrate some of the critical elements in the calibration of RBSLS models and to serve as guide for future calibration work. First the impact of copula model selection to simulate the correlation structure of the bearing pressure-displacement model parameters used is described by illustrating its impact on the calibrated, lumped load and resistance factor (i.e., a pseudo-factor of safety). Then, the impact of copula model selection on the allowable bearing pressure at a given magnitude of displacement is demonstrated. Thereafter, the normalization protocol selected for the existing RBSLS procedure is critically examined by comparing it to alternative, newly-developed normalization

protocols. A framework for the evaluation and assessment of the normalization protocol and copula model selection is then described. The reliability of the suitably revised RBSLS procedure is then contrasted to the previous effort by comparing the lumped load and resistance factors and accuracy determined by comparing to newly conducted, full-scale loading tests of spread footings on aggregate pier-reinforced ground. It is shown that the new RBSLS procedure produces a more accurate estimate of the actual reliability than the previous effort. The framework proposed here takes a critical assessment of the distinct elements of reliability-based serviceability limit state calibration and application.

### 6.3 REVIEW OF RBSLS FRAMEWORK AND SELECTED PROCEDURE

It is useful to review the framework for reliability-based serviceability limit state procedures in order to illustrate those factors that govern its calibration and performance. To illustrate the selected framework in context, this study uses a RBSLS procedure developed by Huffman and Stuedlein (2014) for use with shallow footings supported on aggregate pier-reinforced plastic, fine-grained soil. Although this procedure is referenced throughout the paper, additional insight into relevant governing factors will be demonstrated using a dataset developed by Huffman et al. (2015) for the RBSLS procedure calibration for shallow footings on unreinforced, plastic fine-grained soils. A review of the RBSLS procedure for aggregate pier reinforced ground follows.

#### 6.3.1 Selected Ultimate and Serviceability Limit State Models

Serviceability limit state design of foundations is governed by allowable displacement, which may be predicted relative to the applied bearing pressure and/or a selected reference capacity,  $q_{ref}$ . The RBSLS procedure proposed by Huffman and Stuedlein (2014) for

predicting allowable footing displacements from an applied bearing pressure was based on the bearing pressure-displacement ( $q$ - $\delta$ ) curves derived from thirty full-scale footing loading tests, and the bearing capacity,  $q_{ult,i}$ , interpreted from the tests, as a basis for the determination of a reference capacity,  $q_{ref}$ . The predicted bearing capacity,  $q_{ult,p}$ , corresponding to the ultimate limit state (ULS), was identified as logical reference capacity at the time owing to its ability to be estimated with a high degree of confidence using an empirical procedure proposed by Stuedlein and Holtz (2013), given by (in kilopascals):

$$q_{ult,p} = \exp(b_0 + b_1 \cdot S_r + b_2 \cdot a_r + b_3 \cdot d_f \cdot S_r + b_4 \cdot \tau_{mp}^{-1} + b_5 \cdot \tau_{mp}) \quad (6.1)$$

where  $b_0, \dots, b_5$  represent fitted coefficients,  $S_r$  = slenderness ratio of the aggregate piers (equal to  $L_p/D_p$  = the ratio of pier length to pier diameter),  $a_r$  = area replacement ratio (the area ratio of aggregate pier to native soil beneath the footing),  $d_f$  = the depth of footing embedment,  $\tau_{mp}$  = the shear mass participation factor for the native soil, given by the ratio of the undrained shear strength,  $s_u$ , of the plastic fine-grained soil to the  $a_r$ . The best-fit model coefficients were determined equal to  $b_0 = 4.756$ ,  $b_1 = 0.013$ ,  $b_2 = 1.914$ ,  $b_3 = 0.070$ ,  $b_4 = 13.71$ , and  $b_5 = 0.005$ , and are based on constructed (i.e., known) aggregate pier/footing geometry and soil parameters.

Huffman and Stuedlein (2014) selected Eq. 6.1 to represent  $q_{ref}$  because of its accuracy, as it is characterized with a mean bias (i.e., average ratio of  $q_{ult,i}$  to  $q_{ult,p}$ ) of 1.00 and coefficient of variation ( $COV$ ) in point bias of 13.1% (Stuedlein and Holtz 2013). As described subsequently, the selection of the reference capacity represents a critical task with important implications on the degree of reliability of foundation performance. However, it is also shown herein that the magnitude of uncertainty in the reference capacity may be less influential than the magnitude of variability in the normalized bearing pressure-

displacement curves generated with the reference capacity. With regard to demonstration of the RBLS framework, the selection of Eq. 6.1 for  $q_{ref}$  allowed formulation of a power law model prescribing the mobilized resistance,  $q_{mob}$ , associated with an immediate displacement,  $\delta$ , for footings supported on aggregate pier-reinforced clay (Huffman and Stuedlein 2014):

$$q_{mob} = c_1 \cdot \left( \frac{\delta}{B'} \right)^{c_2} \cdot q_{ult,p} = c_1 \cdot (\eta)^{c_2} \cdot q_{ref} \quad (6.2)$$

where  $B'$  = the equivalent footing diameter,  $c_1$  and  $c_2$  represent the fitted coefficient and exponent, respectively, and  $\eta$  = footing diameter-normalized displacement. For square footings,  $B'$  is defined as the diameter that provides the same area as that of a square footing (Mayne and Poulos 1999).

The key in any reliability-based design approach is the tracking and inclusion of all relevant sources of uncertainty and model error. Equation 6.2, which forms the basis for calibrated load and resistance factors (described subsequently), is impacted by the uncertainty and error in all of parameters describing  $q_{mob}$ , which includes the model error in  $q_{ref}$ ,  $c_1$ , and  $c_2$ . Table 6.1 summarizes the mean values of these parameters and their statistical distributions. Note that in loading tests,  $q_{mob}$  equals the loading applied to the footing,  $q_{app}$ , and is invariant. The reliability simulations in this study incorporates variability in loading appropriate for the modeling of dead loads (with a COV = 10%) and live loads (with a COV = 20%).

**Table 6.1. Summary of statistical distributions describing ULS and SLS model parameters used in the demonstration procedure (modified from Huffman and Stuedlein 2014).**

Parameter	Mean Value	COV (%)	Distribution
$c_1$	3.088	40.7	lognormal
$c_2$	0.454	23.3	lognormal
$q'_{ref}$	0.997	13.1	lognormal
$q'_{app}$	1.000	10, 20	lognormal

### 6.3.2 Monte Carlo Simulation-based Performance Function Simulation

Monte Carlo simulation (MCS) has been widely used in assessment of geotechnical risk (Wang et al. 2010, Li et al. 2013, Wang 2011) and RBD procedure calibration (Wang and Kulhawy 2008, Wang and Cao 2013). The performance function,  $P$ , equal to the margin of safety (i.e., difference between the mobilized resistance and applied load) that limits the probability of failure,  $p_f$ , to a pre-determined magnitude was used to form the probabilistic framework for incorporating the observed or assumed uncertainty in the SLS function (Eq. 6.2). The general framework for the performance function is given by (Baecher and Christian 2003, Phoon 2008):

$$p_f = \Pr(q_{mob} - q_{app} < 0) = \Pr(P < 0) \leq p_T \quad (6.3)$$

where  $p_T$  is a target probability. For the MCS used in the demonstration procedure, the mobilized resistance is estimated from Eq. 6.2 and can be incorporated into the performance function as follows:

$$p_f = \Pr(c_1 \cdot \eta^{c_2} \cdot q_{ref} - q_{app} < 0) = \Pr\left(c_1 \cdot \eta^{c_2} < \frac{q_{app}}{q_{ref}}\right) \quad (6.4)$$

where  $q_{app}$  = the applied bearing pressure, associated with an allowable displacement, and  $q_{ref}$  equals the ultimate resistance predicted using Eq. 6.1. Because it is convenient to calibrate the RBSLS procedure on a generalized basis, the normalized unit mean random variables for  $q_{ult,p}$  and  $q_{app}$ , each associated with an observed or assumed distribution (e.g., Uzielli and Mayne 2011), can be incorporated into Eq. 6.4 for ease of incorporation into the MCS:

$$p_f = \Pr\left(c_1 \cdot \eta^{c_2} < \frac{q_{app,n} \cdot q'_{app}}{q_{ref,n} \cdot q'_{ref}}\right) = \Pr\left(c_1 \cdot \eta^{c_2} < \frac{1}{\psi_Q} \frac{q'_{app}}{q'_{ref}}\right) \quad (6.5)$$

where  $q_{app,n}$  and  $q_{ref,n}$  are equal to the nominal values of the applied bearing pressure and predicted ultimate resistance, respectively, and  $q'_{app}$  and  $q'_{ref}$  represent the normalized random values distributed as shown in Table 6.1. By dividing  $q_{app,n}$  by  $q_{ref,n}$ , Eq. 6.5 becomes unitless and allows the introduction of  $\psi_Q$ , which represents a combined (i.e., “lumped”) load and resistance factor. Thus,  $p_f$  can then be solved in terms of  $\psi_Q$  based on a predetermined allowable displacement and given footing size.

Monte Carlo simulations (MCS) were used to solve  $p_f$  and the associated reliability index,  $\beta$ , using prescribed magnitudes of  $\psi_Q$  ranging from 1 to 20. The reader is referred to Huffman and Stuedlein (2014) for a description of the details of the statistical distributions called by the MCS, including the range in variation of allowable displacement,  $\delta_a$ ,  $B'$ ,  $COV(q'_{app})$ ,  $COV(\delta_a)$ , and  $\psi_Q$ . Once calibrated using the MCS, the allowable bearing pressure,  $q_{all}$ , satisfying the given serviceability limit state of immediate displacement for spread footings supported on aggregate pier reinforced plastic, fine-grained soil may be computed using:

$$q_{all} = \frac{1}{\psi_Q} \cdot c_1 \cdot \eta^{c_2} \cdot q_{ref} \quad (6.6)$$

which is a convenient, deterministic style formulation with all the attendant qualities of a fully-probabilistic procedure. The database of footing loading tests underpinning this RBSLS procedure, and the various modeling decisions invoked during calibration of the procedure, is used herein as vehicle for illustrating the factors governing RBSLS procedure calibration and performance evaluation following calibration.

## 6.4 FACTORS AFFECTING CALIBRATION OF RBSLS MODELS

### 6.4.1 Assessment of Correlation Structure Model and Impact on Reliability

#### 6.4.1.1 *Fitting of Copulas for Monte Carlo Simulation of Bivariate $q$ - $\delta$ Model Parameters*

Bivariate power law model parameters associated with Eqs. 6.2 and 6.6 must be evaluated for dependence, and if any is identified, accounted for so as to avoid biases that can influence the reliability simulations (e.g., Phoon and Kulhawy 2008; Uzielli and Mayne 2011; Tang et al. 2013). Indeed, dependence was observed between the normalized  $q$ - $\delta$  model parameters  $c_1$  and  $c_2$ , as shown in Fig. 6.1. This dependence is associated with an “observed” sample Kendall’s Tau correlation coefficient,  $\rho_{\tau,obs}$ , of 0.43. Dependence between other variables included in the reliability simulations were also investigated, but none were observed (Huffman and Stuedlein 2014).

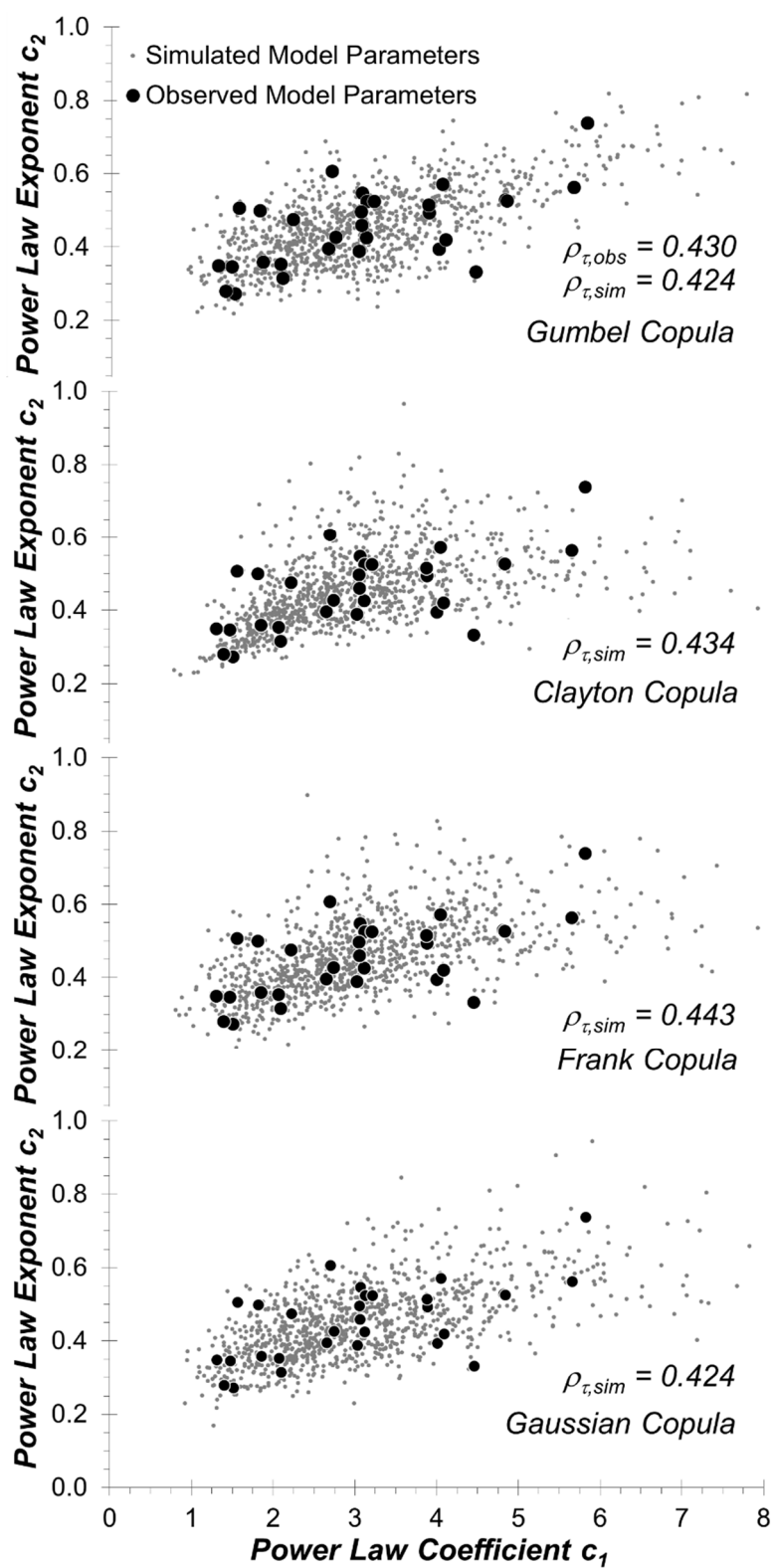


**Figure 6.1**

Comparison of 1,000  $c_1$ - $c_2$  pairs simulated using various copula models fitted to the sample pairs derived from the load test database of footings on aggregate pier-reinforced ground.



Identifying the dependence between relevant model parameters represents the first task in RBSLS calibrations. The second task is to develop an appropriate approach to simulate the model parameters from source distributions in appropriate regard for the observed dependence across the model parameters. Thus, the evaluation and selection of an appropriate model to simulate the observed correlation structure is of great importance (Li et al. 2013). To evaluate the influence of correlation structure model on the reliability calibrations, bivariate Gaussian, Frank, Clayton and Gumbel copula functions were investigated. Copula functions, each with its own formulation for associating ranked variables, allow the description of different correlation structures (see Nelson 2006). The bivariate Gaussian copula models positive or negative elliptical correlation between the two parameters being investigated, whereas the Frank copula models a uniform linear correlation. The Clayton and Gumbel copulas model positive correlation only, with the Clayton copula providing for greater left-tail dependence and the Gumbel copula providing for greater right-tail dependence of the marginal distributions of the simulated parameters. Copulas are calibrated with a copula parameter,  $\theta$ , which is a function of the sample  $\rho_\tau$ , to describe the relative strength of the correlation between dependent parameters.

Copula functions assume uniformly distributed marginal distributions in the rank  $[0,1]$  space. Therefore, standardized rank values  $u_1$  and  $u_2$  of the power law model parameters  $c_1$  and  $c_2$  were calculated by dividing the rank values by the total number of values in the dataset. The  $u_1$  and  $u_2$  values were used with  $\rho_\tau$  to establish the copula parameter,  $\theta$ , and the copula probability functions. The relationship between  $c_1$  and  $c_2$  and a two-parameter copula probability function,  $C_{c_1,c_2}$ , is determined by fitting to  $\rho_\tau$  using (Nelson 2006, Li et al. 2013):

$$\rho_{\tau}(c_1, c_2) = 4 \cdot \int_0^1 \int_0^1 C_{c_1, c_2}(u_1, u_2) \cdot dC_{c_1, c_2}(u_1, u_2) - 1 \quad (6.7)$$

The best-fit copula was evaluated using the Akaike information criteria (AIC; Akaike 1974) and Bayesian information criteria (BIC; Schwarz 1978). The probability functions for the different copulas investigated herein and the best-fit copula parameters determined from Eq. 6.7 are summarized in Table 6.2.

**Table 6.2. Selected copula functions, copula parameters, and goodness-of-fit outcomes (modified from Huffman and Stuedlein 2014).**

Copula	Copula Function, $C(u_1, u_2)$	Copula Parameter, $\theta$	AIC	BIC
Gaussian	$\Phi_{\theta}(\Phi^{-1}(u_1), \Phi^{-1}(u_2))$	0.626	-12.9	-11.5
Frank	$-\frac{1}{\theta} \ln \left[ 1 + \frac{(e^{-\theta u_1} - 1)(e^{-\theta u_2} - 1)}{e^{-\theta} - 1} \right]$	4.593	-12.0	-10.6
Clayton	$(u_1^{-\theta} + u_2^{-\theta} - 1)^{-1/\theta}$	1.510	-11.0	-9.6
Gumbel	$\exp \left\{ - \left[ (-\ln u_1)^{\theta} + (-\ln u_2)^{\theta} \right]^{1/\theta} \right\}$	1.755	-14.4	-13.0

The lowest AIC and BIC values were realized using the Gumbel copula, indicating that it provided the best fit among the selected copula types for modeling the correlation structure between bearing pressure-displacement model parameters. As a result, the Gumbel copula was used in the reliability calibrations reported by Huffman and Stuedlein (2014). The degree of fit between the sample  $c_1$ - $c_2$  and 1,000 simulations for each copula model is shown in Fig. 6.1. The simulated  $c_1$ - $c_2$  pairs appear to closely correspond to the observed values for each copula investigated as shown in Fig. 6.1 and by comparison of

$\rho_\tau$ . However, certain deviations in the trends, associated with the degree of dependence of the marginal distributions along their tails, are noted, and these deviations strongly impact the reliability of the RBSLS procedure and subsequent allowable bearing pressure, as described subsequently.

#### 6.4.1.2 Impact of Correlation Structure Model on Calibrated Load and Resistance Factor

The MCS of the performance function resulted in smooth relationships between the lumped load and resistance factor,  $\psi_Q$ , and the reliability index,  $\beta$ , as a function of the allowable normalized immediate displacement,  $\eta_a$ , equal to the ratio of  $\delta_a$  and  $B'$ . Following MCS, the calibrated  $\psi_Q$  was determined equal to (Huffman and Stuedlein 2014):

$$\psi_Q = \exp\left[\frac{\beta - c \cdot \ln(\eta_a) - d}{a \cdot \ln(\eta_a) + b}\right] \quad (6.8)$$

where  $a$ ,  $b$ ,  $c$ , and  $d$  are fitting parameters that vary with the assumed  $\text{COV}(\delta_a)$  and  $\text{COV}(q'_{app})$ . Table 6.3 provides the fitting parameters associated with Eq. 6.8, and the MCS completed with the correlation structure of the power law coefficients accounted for using the best-fit Gumbel copula.

**Table 6.3. Summary of best-fit coefficients for Eq. 6.8, valid for  $\beta > 0$  and  $\psi_Q \leq 10$ .**

$\text{COV}(\delta_a)$	$\text{COV}(q'_{app})$	$a$	$b$	$c$	$d$
0.0	0.10	0.100	2.549	0.996	2.543
0.2	0.10	0.096	2.478	0.972	2.465
0.4	0.10	0.064	2.212	0.935	2.359
0.6	0.10	0.059	2.041	0.846	2.048
0.0	0.20	0.079	2.365	0.946	2.408
0.2	0.20	0.080	2.319	0.923	2.330
0.4	0.20	0.066	2.153	0.879	2.183
0.6	0.20	0.061	1.994	0.803	1.921

The correlation structure of the  $c_1$ - $c_2$  pairs is critical for reliability simulations as the larger the deviation in the simulated pairs from the sample pairs, the greater the deviation from the sample-based to simulated normalized bearing pressure-displacement response, leading to inaccurate reliability analyses. The effect of copula model selection on the lumped load and resistance factor can be evaluated by comparing  $\psi_Q$  generated from the MCS for a given probability of exceeding the serviceability limit state.

Consider, for example, a typical design scenario for a footing with an equivalent diameter of 1 m. The goal is to identify the appropriate  $\psi_Q$  for a given  $\beta$  or  $p_f$  with Eq. 6.8 and then use Eq. 6.6 to compute the bearing pressure associated with the allowable immediate displacement. For this example, it was assumed that  $\text{COV}(\delta_a) = 0$  and  $\text{COV}(q'_{app}) = 10$  percent, and MCS-based fitting parameters corresponding to this case selected from Table 6.3.

Figure 6.2 presents the variation of the calibrated load and resistance factor simulated using each of the four copulas as well as the case with an assumed zero correlation between model parameters, with the probability of exceeding  $\eta_a$  equal to 0.010, 0.025, and 0.050. This corresponds to allowable immediate displacements of 10, 25, and 50 mm for the 1 m diameter footing. In general, the probability of exceeding the SLS decreases as  $\eta_a$  increases for each correlation structure model, due to the greater deviation in modeled bearing pressure-displacement response at smaller displacements than those at greater displacements (described in greater detail below). Similar observations have been noted in other studies, such as by Uzielli and Mayne (2011) and Stuedlein and Reddy (2014).

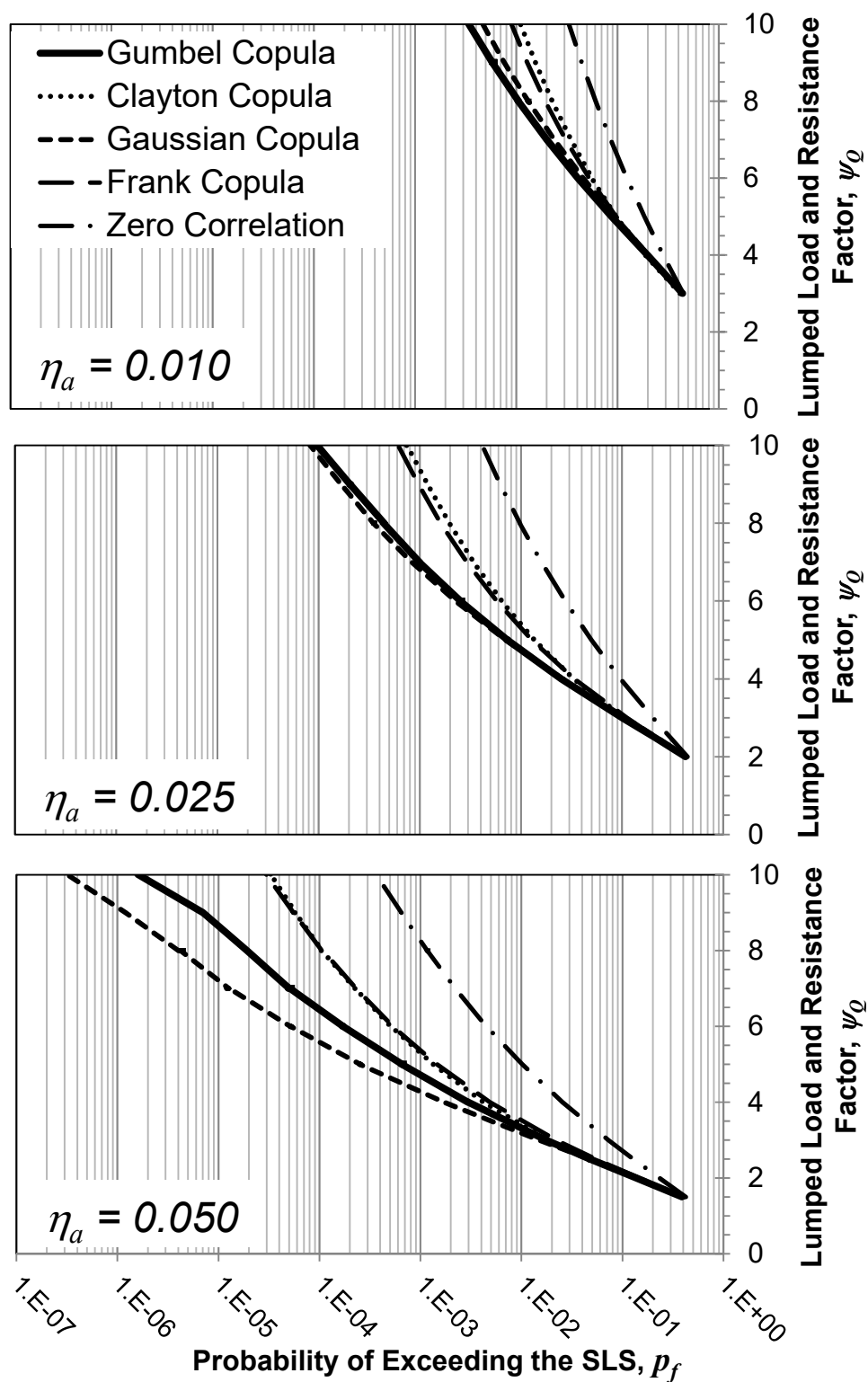


**Figure 6.2** Impact of correlation structure model selection on the lumped load and resistance factor as a function of probability of exceeding the serviceability limit state for  $\text{COV}(\delta_a) = 0$  and  $\text{COV}(q'_{app}) = 10\%$ .

Figure 6.2 shows that the probability of exceeding the SLS at a given  $\psi_Q$  depends strongly on the correlation structure model considered and that ignoring the bivariate dependence of the bearing pressure-displacement models results in the highest (i.e., most conservative) probability. The difference between the  $\psi_Q$  generated from the best-fit Gumbel copula and the less appropriate copulas increases with decreasing  $p_f$ , and, for this study, becomes notable in the range in  $p_f$  of 3 to 5%, corresponding to  $\beta$  in the range of 1.88 to 1.64, respectively. This range in  $\beta$  approaches the upper-bound magnitude of acceptable  $p_f$  for the SLS.

In general, the  $c_1$ - $c_2$  pairs simulated using poorly-fitted copulas result in a greater likelihood that extreme  $c_1$ - $c_2$  pairs will be sampled, and the frequency of softer bearing pressure-displacement curves generated increases correspondingly, and therefore the  $p_f$  is greater using the more poorly-fitted copulas than those simulated using the better-fitting copulas. For example, the Gaussian copula, which was the second best-fitted copula (Table 6.2), generally produced similar  $\psi_Q$  as those using the Gumbel copula, although the difference increases with increasing  $\eta_a$ . Consider for example the 2.5- and 5-fold larger probabilities of exceeding the SLS using the Gumbel copula at  $\psi_Q = 5$  and 10, respectively, as compared to those for the Gaussian copula. On the other hand, the poorest-fitted copula (i.e., the Clayton copula) always returned  $\psi_Q$  larger than those produced using the best-fitted Gumbel copula, which would result in cost-inefficiency for a given level of reliability. These results become more pronounced the better the selected copulas fit the correlation structure of the bivariate model parameters. Thus, decisions regarding the modeling of the correlation structure in the bearing pressure-displacement model

parameters represent a critical task in the calibration of RBLS procedures with significant consequences on reliability.

#### 6.4.1.3 *Impact of Correlation Structure Model on Allowable Bearing Pressure, $q_{all}$*

It is useful to assess the impact of correlation structure model (i.e., the selected copula) on the allowable bearing pressure,  $q_{all}$ , associated with each copula model to highlight the importance of this modeling decision on the predicted serviceability limit state. To this end, the allowable bearing pressure is computed using Eq. 6.6 using the mean (nominal) parameters  $c_1$  and  $c_2$  (Table 6.1) for the normalized allowable bearing displacement at probabilities of exceeding the SLS of 10, 1, and 0.1 percent (i.e.,  $\beta = 1.28, 2.33, 3.09$ , respectively). The resulting  $q_{all}$  is presented in Fig. 6.3 as a percentage of the ultimate resistance,  $q_{ult,p}$ , and corresponds to the case of  $COV(\delta_a) = 0$  and  $COV(q'_{app}) = 10$  percent. Figure 6.3 shows that at high probabilities of exceeding the SLS, there is very little difference in the allowable bearing pressure given that a fitted copula was used to account for the bivariate bearing pressure-displacement model parameters. Ignoring the bivariate relationship between  $c_1$  and  $c_2$  resulted in a reduction of bearing pressure ranging from about 20 to 25 percent. However, as the probability of exceeding the SLS decreases, the selection of correlation structure model becomes increasingly important. For example, at  $p_f = 0.1$  percent, the bearing pressures derived using the best-fitting Gumbel copula are approximately 10 percent greater than those using the less appropriate Frank and Clayton copulas. Again, use of an appropriately-fitted copula to capture the correlation structure of the bivariate bearing pressure-displacement model parameters is critical for the optimization of the allowable bearing pressure and cost-effective foundations. It is noted

here that for SLS design, the target  $\beta$  should lie within the range of 1.5 to 2.0 ( $p_f$  ranging from 6.4% to 2.3%), less than for ULS design, given the differences in consequences of exceeding the limit state. The allowable bearing pressure will generally lie in the range of 15 to 40% of the ULS capacity for the Gumbel copula-based RBSLS procedure described above (Fig. 6.3).

## 6.4.2 Assessment of Normalization Protocol for Bearing Pressure-Displacement Curves and Impact on Computed Reliability

### 6.4.2.1 *Impact of Normalization Protocol on Scatter in $q$ - $\delta$ Curves*

The preceding discussion evaluated the impact of correlation structure model selection for models of  $q$ - $\delta$  curves where the mobilized capacity was normalized by a reference capacity equal to the predicted ultimate resistance. This modeling decision was made by Huffman and Stuedlein (2014) following the assessment of variance reduction as compared to the raw  $q$ - $\delta$  curves. The comparison is shown in Fig. 6.4a and 6.4b; the scatter of data is significantly reduced for the case where  $q_{mob}$  is normalized by  $q_{ult,p}$  (Fig. 6.4b). The implication for reliability analyses is that a target allowable bearing pressure at a given displacement will be associated with a more accurate probability of exceedance.



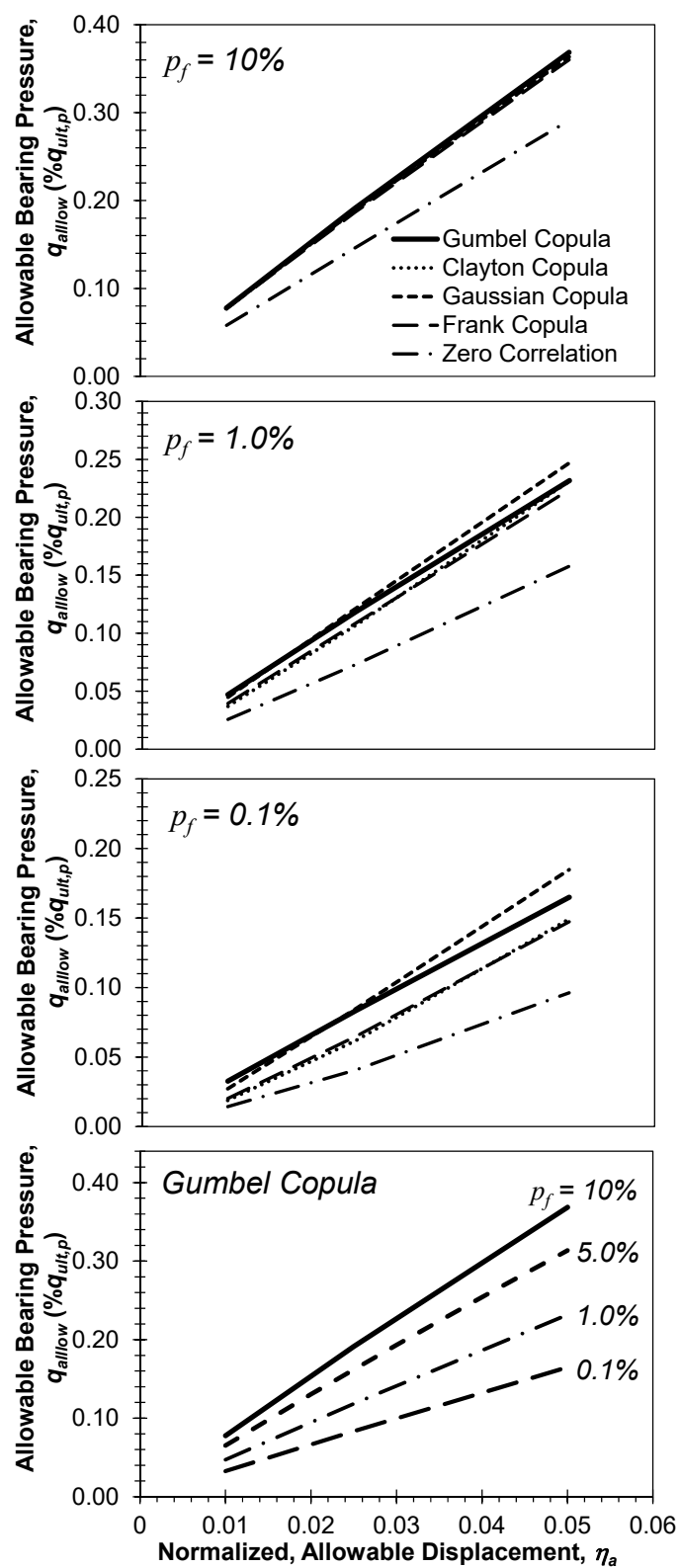


**Figure 6.3** Impact of correlation structure model selection on the allowable bearing pressure considering allowable immediate displacement.

Using a high-quality loading test database of footings on *unreinforced*, plastic, fine-grained soils, Huffman et al. (2015) determined that further reduction in the scatter of  $q$ - $\delta$  curves is possible by normalizing  $q_{mob}$  by a reference capacity other than that associated with the ultimate resistance. They determined that the slope tangent capacity (e.g., Phoon and Kulhawy 2008) with displacement offset of  $0.03B$ ,  $q_{STC,0.03B}$ , resulted in the best normalization of (i.e., least variance in)  $q_{mob}$ . Compare Fig. 6.4b through 6.4d for the footing loading test database assessed in this study; normalization of mobilized capacity by the slope tangent capacity with offsets of  $0.01$  and  $0.02B$ ,  $q_{STC,0.01B}$  and  $q_{STC,0.02B}$ , respectively, produced further decreases in scatter relative to normalization using  $q_{ult,i}$ . Normalization by  $q_{STC,0.01B}$  and  $q_{STC,0.02B}$  resulted in a collapse of the  $q$ - $\delta$  curves in the low-magnitude  $\eta$  range with more or less equal efficacy. However, normalization of  $q_{mob}$  by  $q_{STC,0.02B}$  produced improved reduction in scatter as  $\eta$  increased. In addition, normalization of  $q_{mob}$  by  $q_{STC,0.03B}$  was investigated (i.e., the protocol selected for the RBSLS procedure proposed by Huffman et al. 2015), but this resulted in increasing levels of scatter for the loading test data described herein and will therefore not be considered further in this study. It is recommended that future studies evaluate a number of various normalization protocols, since an approach that is successful for reducing scatter in one database may not be suitable for reducing scatter in another database.

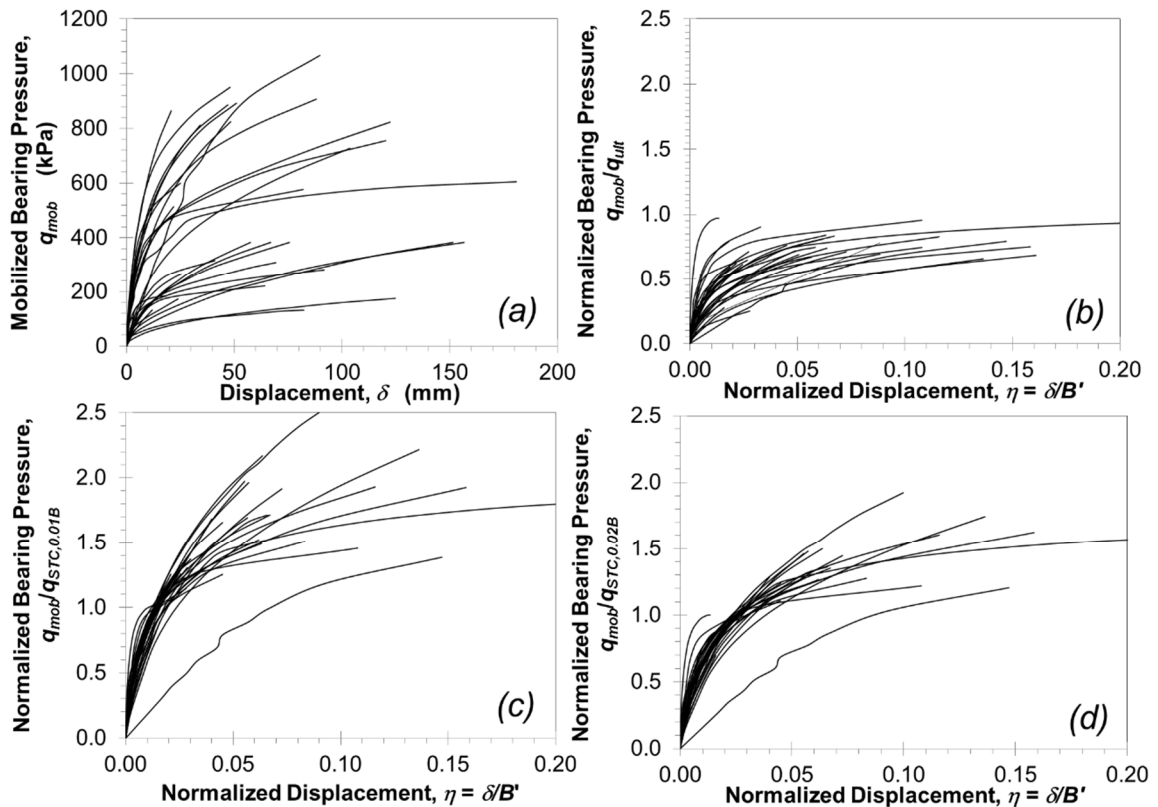


**Figure 6.4** Comparison of raw and normalized bearing pressure-displacement curves in the footing loading test database: (a) raw  $q$ - $d$  curves, (b) bearing pressure normalized by ultimate resistance, (c) bearing pressure normalized by the slope tangent capacity with 0.01B offset, and (d) bearing pressure normalized by the slope tangent capacity with 0.02B offset.

#### 6.4.2.2 Decision Framework for Selection of Appropriate Normalization Protocol

Once the various trial normalization protocols have been developed, a single normalization approach must be selected for use in the MCS-based reliability calibrations. Graphically, it appeared that normalization of  $q_{mob}$  by  $q_{STC,0.02B}$  produced the least scatter (Fig. 4d). However, such initial observations should be quantified and corresponding linkage to, and error propagation in, some capacity that can be computed directly (e.g.,  $q_{ult,p}$ ; see Eq. 6.1) must be established. The decision framework proposed to support

selection of the most appropriate normalization protocol consists of the following five steps:

1. Fit the most appropriate model of the normalized bearing pressure-displacement curves to the observed loading test data; in this case, the power law presented in Eq. 6.2 is used for ease of comparison.
2. Characterize, and fit continuous distributions to, the marginal distributions of the sample  $q$ - $\delta$  model parameters.
3. Establish the correlation between multivariate  $q$ - $\delta$  model parameters.
4. Determine the correlation and model transformation error between the reference capacity (e.g.,  $q_{STC,0.02B}$ ) and the predicted ultimate capacity and fit corresponding continuous distributions.
5. Select the overall best normalization protocol and fitted copula model of the corresponding bivariate model parameters.

Each of these tasks is required for executing the MCS required to generate an appropriate RBSLS procedure. Step 1 is readily accomplished for each of the trial normalization protocols to be investigated using ordinary least squares or other fitting algorithm. Step 2 requires the statistical characterization of the marginal distributions of the model parameters for the fitted  $q$ - $\delta$  curves (i.e.,  $c_1$  and  $c_2$ ). Figures 6.5a and 6.5b compare the lognormal distributions of  $c_1$  and  $c_2$  for the various normalization protocols investigated. In general, the larger the spread in the distribution of the bivariate model parameters, the greater the variability in possible displacement for the foundation types being modeled. As shown in Figure 6.5a, the power law coefficient  $c_1$  has the least spread for  $q_{mob}$  normalized by  $q_{ult}$ , followed by the normalization by  $q_{STC,0.02B}$ , and the largest by

$q_{STC,0.01B}$ . However, the influence of the power law exponent  $c_2$ , which controls the curvature of the normalized  $q$ - $\delta$  curves, as well as the magnitude and sign of the bivariate correlation, cannot be excluded from consideration. Based on Figs. 6.4 and 6.5, the tentative decision for normalization using  $q_{STC,0.02B}$  may be anticipated.

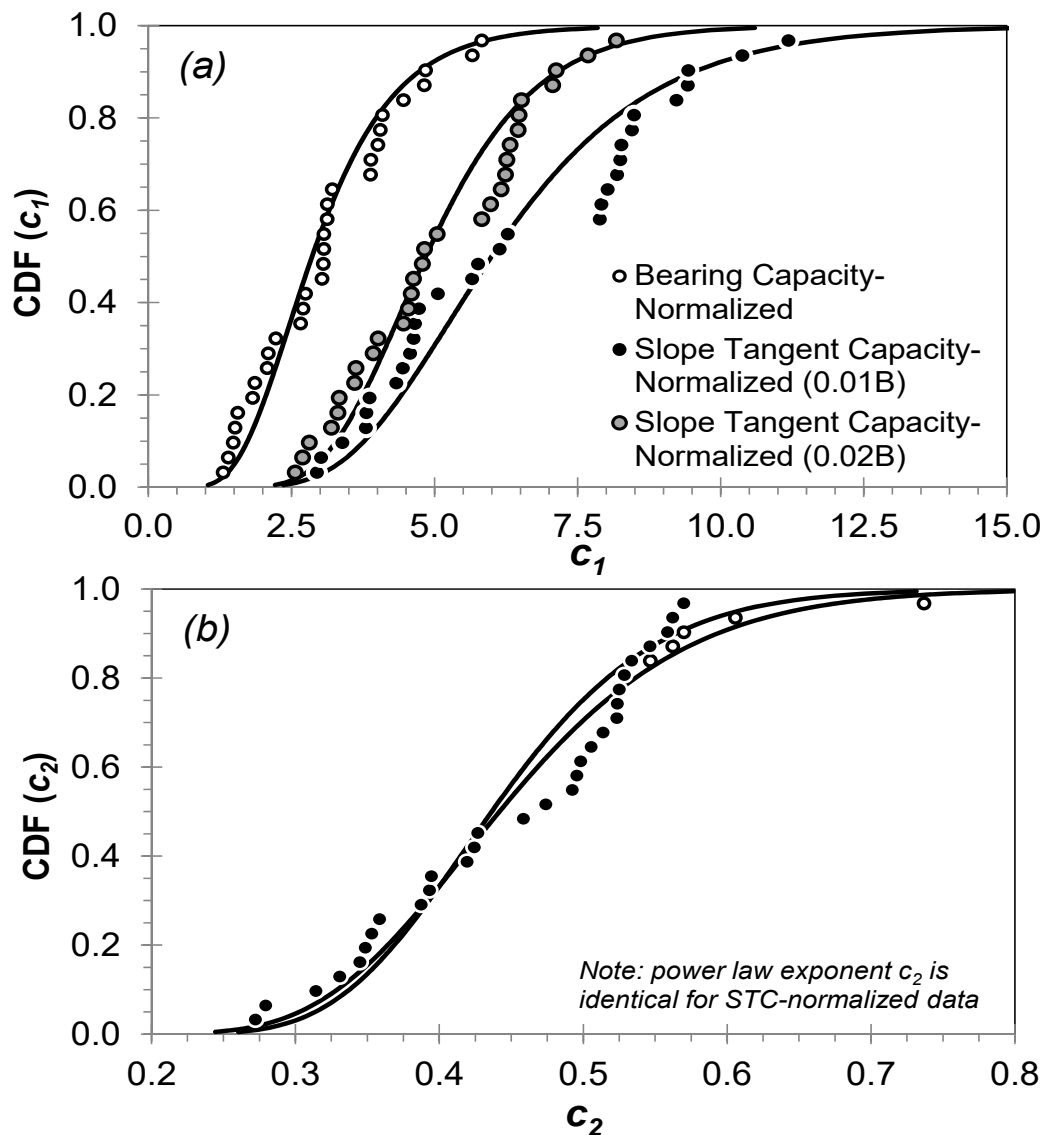


**Figure 6.5** Comparison of sample and fitted continuous lognormal distributions for power law model parameters (a)  $c_1$ , and (b)  $c_2$ .

Step 3 requires that the correlation between bivariate model parameters be established, preferably using a non-parametric correlation metric. Owing to its usefulness in copula model fitting, as well as its relative strength (Li et al. 2013; Li and Tang 2014, Ching and Phoon 2014), the use of the non-parametric Kendall's Tau rank correlation is recommended. Figure 6.6 compares the dependence between  $c_1$  and  $c_2$  using the normalization protocol for  $q_{mob}$  using  $q_{ult,p}$  as described by Huffman and Stuedlein (2014) to that arising from normalization of  $q_{mob}$  using  $q_{STC,0.01B}$  and  $q_{STC,0.02B}$ . Two useful observations from Fig. 6.6 may be readily made: (1) use of  $q_{STC}$  results in much stronger, less variable correlation between  $c_1$  and  $c_2$ , and that (2) the range in  $c_1$  is less for  $q_{STC,0.02B}$  than  $q_{STC,0.01B}$ . In regard to the former observation, the difference in  $\rho_\tau$  between the two  $q_{STC}$  normalization protocols is negligible. Thus, little new decision support information is gained between Steps 2 and 3 for this particular dataset.

Appropriate MCS required for reliability calibrations require that all model errors associated with model transformations be properly incorporated. Step 4 ensures that the reference capacity used to normalize the  $q$ - $\delta$  curves is linked to a capacity that can be computed (with its attendant error, such as Eq. 6.1). Thus, the model factor (equal to the average ratio of  $q_{STC}$  to  $q_{ult,i}$ )  $M_{STC}$ , and coefficient of variation,  $COV(M_{STC})$ , in  $M_{STC}$  for such a transformation must be quantified. As described previously, Huffman et al. (2015) developed a RBLS procedure that used a reference capacity and model factor to relate the computed bearing capacity to the reference factor. This decision was made based on the assessment of capacities shown in Fig. 6.7a. Increasing the slope tangent offset from  $0.01B$  to  $0.03B$  resulted in increasing  $M_{STC}$  and decreasing  $COV(M_{STC})$ . While further increases in the displacement offset may have resulted in further reductions in  $COV(M_{STC})$ , the

number of  $q$ - $\delta$  curves that have displacements to sufficient magnitude to accurately quantify  $M_{STC}$  and  $COV(M_{STC})$  decreases.

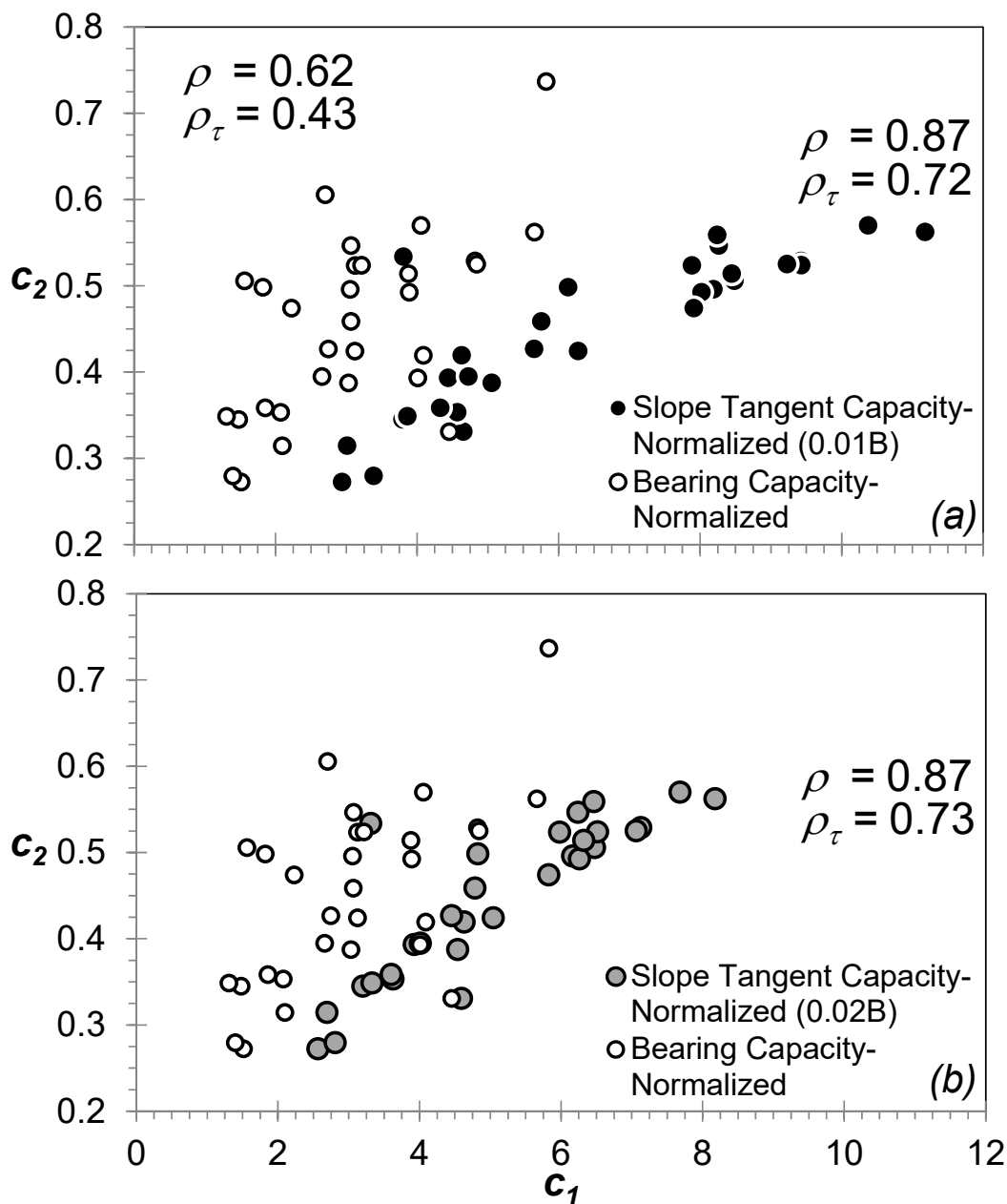


**Figure 6.6** Comparison of correlation between the bivariate power law parameters reported by Huffman and Stuedlein (2014) using  $q_{ult,p}$ -normalized  $q_{mob}$  versus (a)  $q_{STC,0.01B}$ -normalized and (b)  $q_{STC,0.02B}$ -normalized  $q_{mob}$ .

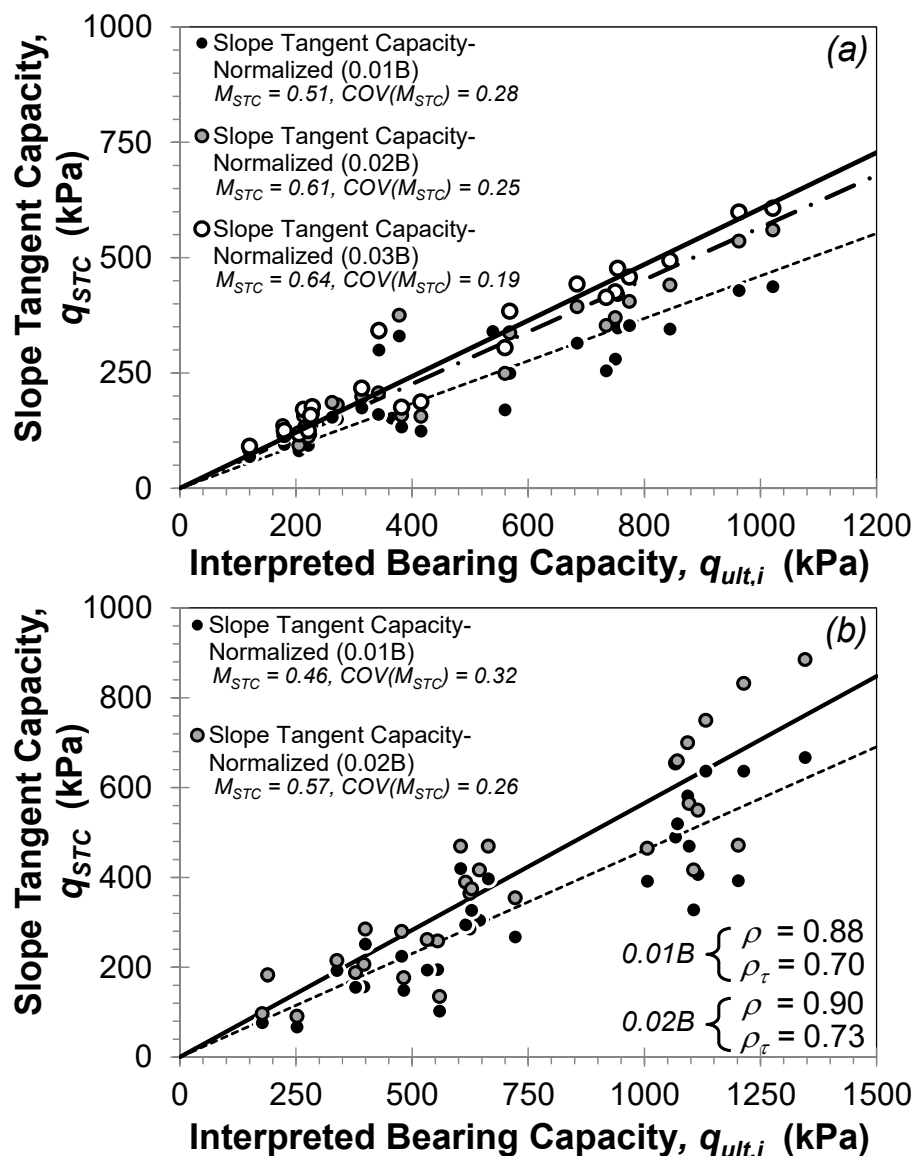


**Figure 6.7** Correlation and variability between bearing capacity and the slope tangent capacities for (a) spread footings resting on unreinforced clayey soils reported by Huffman et al. (2015), and (b) spread footings resting on reinforced clayey soils considered in this study.

Thus, the selection of the final normalization protocol should consider the magnitude of  $COV(M_{STC})$  as well as the *reliability* in the estimate of transformation error, the latter of which requires as much high-quality data as possible. Figure 7b presents the quantification of average  $M_{STC}$  and  $COV(M_{STC})$  for the database of shallow foundations on reinforced, plastic, fine-grained soils considered in this study. Slight, but largely negligible



improvement in correlation was observed for normalization by  $q_{STC,0.02B}$ ; however,  $COV(M_{STC})$  was markedly less for this case, thus providing confirmatory information to that gained in Step 2 for the selection of the suitable normalization protocol. The best-fitting normal distribution ( $\mu_{M_{STC}} = 0.57$ ,  $COV(M_{STC}) = 26\%$ ) allowed sampling of  $M_{STC}$  in the MCS used in the corresponding reliability simulations.

Owing to the comparisons in Steps 2 and 4, normalization of mobilized capacity using the slope tangent capacity with a  $0.02B$  offset was selected (Step 5) for use in revising the Huffman and Stuedlein (2014) RBSLS procedure for shallow foundations on aggregate pier-improved ground. Following the prescription for copula fitting in Section 6.4.1 above, the Gumbel copula model (rotated  $180^\circ$ ) was determined to represent the most appropriate copula for MCS with  $\rho_{t,obs} = 0.733$  and  $\theta = 3.82$ . The accuracy in the revised, fitted copula model relating the  $q_{STC,0.02B}$ -normalized bivariate model parameters may be compared in Fig. 6.8, which indicates satisfactory preservation of the observed correlation. Thus, the ingredients required for revising the RBSLS procedure for aggregate pier-reinforced ground have been finalized.

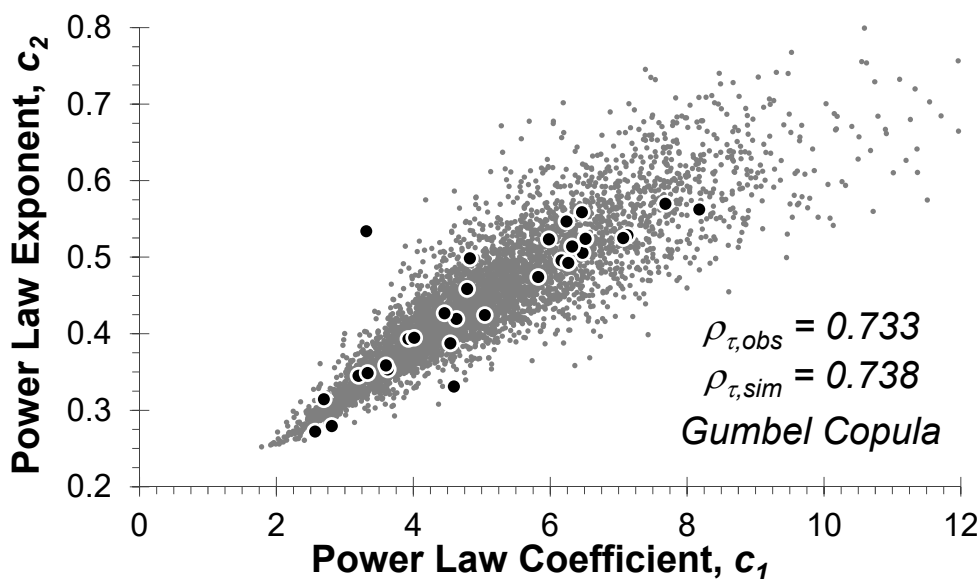


**Figure 6.8** Comparison of 5,000  $c_1$ - $c_2$  pairs simulated using the Gumbel copula model (rotated 180°) fitted to the sample pairs derived from the load test database of footings on aggregate pier-reinforced ground.

#### 6.4.2.3 Comparison of Previous and Updated RBSLS Procedure

With all contributing random variables and their marginal distributions and correlations characterized for reliability calibrations, including bivariate normalized  $q$ - $\delta$  model parameters, the reference capacity transformation model factors, and applied bearing pressures, new MCS may be performed and compared to the previously developed RBSLS procedure. For the purposes of comparison, Fig. 6.9 presents the Huffman and Stuedlein (2014) and updated RBSLS calibrations for the case of  $\text{COV}(\delta_a) = 0$  and  $\text{COV}(q'_{app}) = 10\%$ . In general, the previous and updated reliability indices are fairly similar up to  $\beta$  of approximately 2.25, but deviate at an increasing rate for  $\beta$  greater than 2.25. For allowable, normalized displacements,  $\eta_a$ , equal to 0.005, the updated RBSLS calibrations provide smaller  $\psi_Q$  (and therefore greater allowable bearing pressure), however, this advantage ceases for  $\eta_a$  equal to or greater than 0.01. Normalization of

applied bearing pressures with a reference capacity resulted in a reduction in the scatter of the normalized  $q$ - $\delta$  curves and increased the small-displacement  $q_{all}$ . However, the incorporation of a reference capacity required the use of a model factor to relate  $q_{STC}$  and  $q_{ult,i}$ , resulting in slightly lower  $\beta$  for a given  $\psi_Q$ . It is noted that the use of RBSLS procedures for  $\beta$  greater than about two will be infrequent. While it may be tempting to regard the revised calibration as less advantageous given the slightly smaller  $\beta$  for a given  $\psi_Q$ , such suppositions are not advised in the absence of independent full-scale performance to evaluate the true “accuracy” of revised RBSLS procedure. Such comparisons follow.

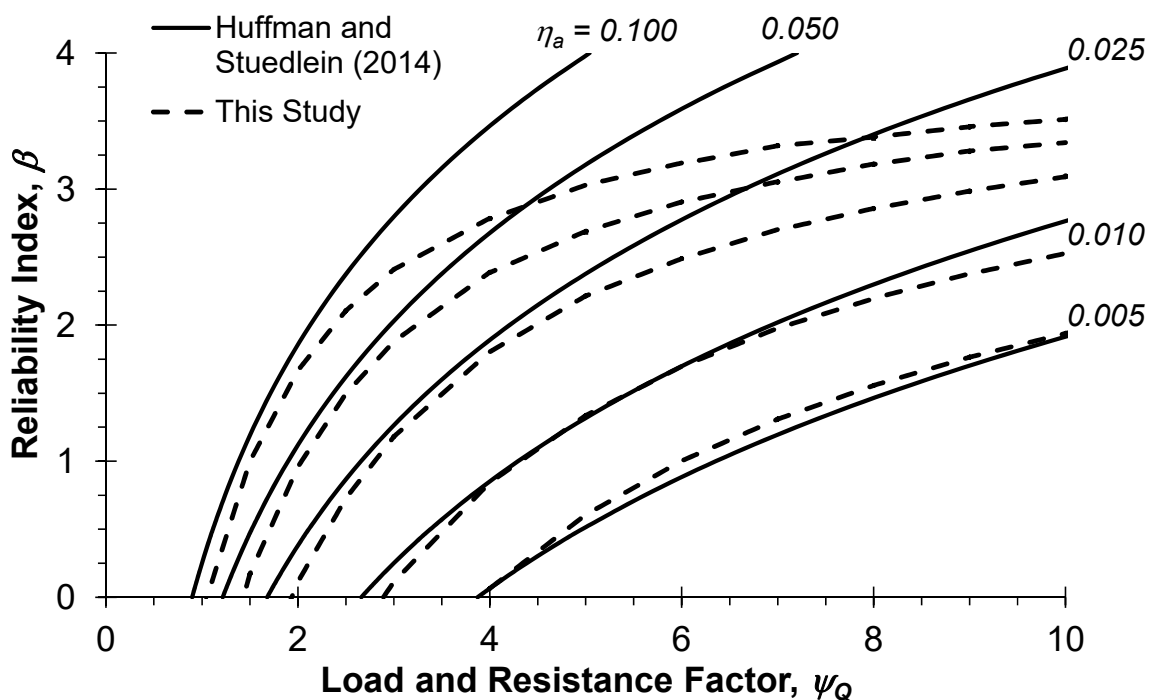


**Figure 6.9** Variation of load and resistance factor,  $\psi_Q$ , and reliability index,  $\beta$ , for various magnitudes of normalized allowable displacement,  $\eta_a$ , for  $COV(q_{app}) = 0.10$  and  $COV(\delta_a) = 0$ .

## 6.5 ASSESSMENT OF RBSLS MODELS

### 6.5.1 Need to Re-visit and Assess RBSLS Models

Calibration of a suitable geotechnical reliability-based limit state model will typically employ a database of full-scale tests, such as those described above, in order to characterize applicable resistance parameters for a given model and to evaluate load and resistance factors. However, the development of a suitable database for the calibration of such models is difficult owing to the expense of large-scale testing and subsequent scarcity of high-quality loading test data. Therefore, the accuracy of the reliability-based model and those procedures used to develop it should be evaluated independently, and improved, as new loading test data becomes available. Without re-evaluation and revision, needless expense associated with material waste, on the conservative side, or provision of design that does not meet the intended reliability, could occur. Such outcomes only serve to impede the implementation of RBD in geotechnical engineering as practitioners rightly question the usefulness of inaccurate approaches.

In the previous sections, a revised RBSLS procedure was developed to attempt to provide a more accurate assessment of the reliability of spread footings on aggregate pier-reinforced ground. However, the “improvement” in reliability could not be quantified in the absence of an independent dataset. New full-scale loading test data are required to assess the improvement, if any, in the new RBSLS procedure.

### 6.5.2 New Full-Scale Loading Test Data: Test Site and Subsurface Conditions

New full-scale loading tests were recently completed at the Oregon State University (OSU) geotechnical field test site on aggregate pier-improved soils. A layout of the site is

shown in Fig. 6.10a. The loading tests were completed during two seasons (Spring and Fall) in order to observe potential differences in the undrained shear response of the foundation soils with seasonal changes in the natural moisture content and groundwater table elevation. Subsurface explorations were completed in conjunction with the loading tests and included three soil borings and eight cone penetration (CPT) tests. The soil profile underlying the site consists of stiff, dilative clayey silt to silty clay extending to a depth of 4 to 4.5 m, followed by loose to medium dense silty to clayey sand to a depth of 5.5 to 6 m. The sand is underlain by stiff clayey silt with some sand extending to at least 10 m. Figure 10b provides a representative cross-section interpolated from the explorations near Section A-A'.

The performance of the footings was controlled by the upper clayey silt to silty clay layer. This soil unit has medium plasticity, with USCS classifications ranging from CL (low plasticity clay) to ML and MH (low and high plasticity silt). The undrained shear strength of this stratum within the depth of influence beneath the footings was estimated from triaxial CU tests and back-calculations with the CPT cone tip resistance,  $q_t$ . During the Spring test series,  $s_u$  was estimated equal to 50 kPa;  $s_u$  was estimated equal to 65 kPa during the Fall test series when the groundwater table was deeper and matric suction stresses increased.

The testing program included eight tests on aggregate pier improved soil (*n.b.*, test G4DS in Fig. 6.10a had not yet been conducted). The test footings consisted of rigid concrete foundations, formed and constructed in place. All but one of the tests consisted of a circular footing with a base diameter of 0.76 m. The remaining test (G4DF) consisted of a 2.44 m wide square footing. The circular footings supported on reinforced soil were

constructed on a single aggregate pier with the same diameter as the footing (i.e.,  $a_r = 100\%$ ). Test G4DF was constructed on four aggregate piers resulting in  $a_r = 31\%$ . A summary of the test designations and pertinent soil parameters and footing and pier dimensions are summarized in Table 6.4; the predicted bearing capacity provided in the table was calculated using Eq. 6.1.

**Table 6.4. Summary of pertinent soil information, ground improvement geometry, and footing dimensions.**

<b>Loading Test</b>	<b><math>s_u</math> (kPa)</b>	<b><math>B'</math> (m)</b>	<b><math>D_f</math> (m)</b>	<b><math>D_p</math> (m)</b>	<b><math>L_p</math> (m)</b>	<b><math>a_r</math> (%)</b>	<b><math>q_{ult,p}</math> (kPa)</b>
T2DS	50	0.76	0.46	0.76	1.52	100	842
T3DS	50	0.76	0.46	0.76	2.28	100	881
T4DS	50	0.76	0.46	0.76	3.04	100	922
T5DS	50	0.76	0.46	0.76	3.80	100	965
T3DF	65	0.76	0.46	0.76	2.28	100	1,013
T4DF	65	0.76	0.46	0.76	3.04	100	1,060
T5DF	65	0.76	0.46	0.76	3.80	100	1,109
G4DF	65	2.75	0.30	0.76	3.04	30.5	652

The aggregate piers supporting the different loading tests extended to varying depths corresponding to pier lengths of 2, 3, 4 and 5  $D_p$ . The bottom of the deepest aggregate piers (i.e., those with a pier length of 5  $D_p$ ) extended into the silty to clayey sand layer. However, the loading test results suggest that this pier exhibited a bulging failure consistent with aggregate piers with large slenderness ratios (Stuedlein and Holtz 2013).

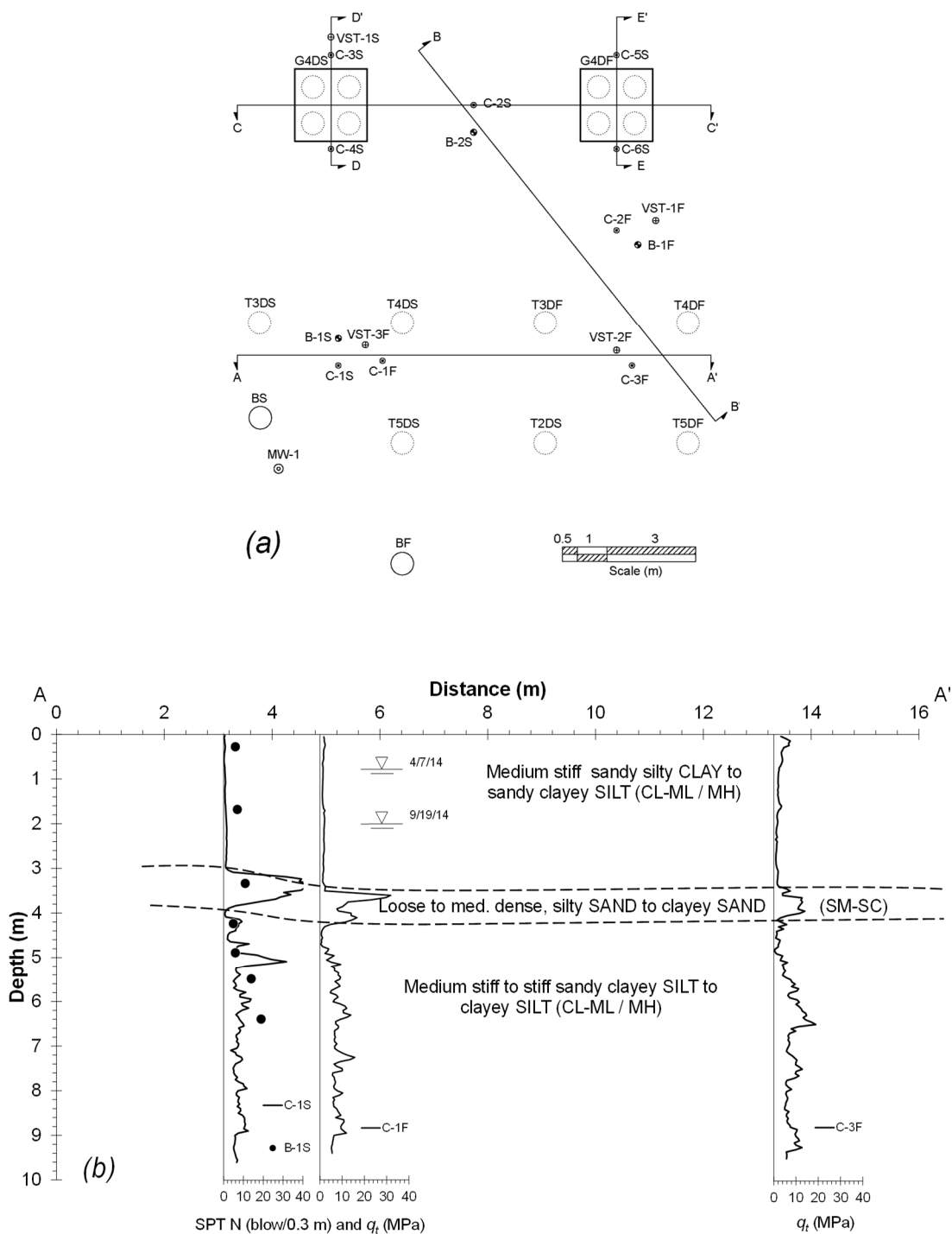


**Figure 6.10** Test site for new footing loading tests: (a) the site and exploration plan, and (b) Section A-A', indicating the results of mud rotary borings with standard penetration tests (SPT) and cone penetration tests (CPTs). Note significant difference in  $q_t$  in upper silty CLAY to clayey SILT layer between the spring (C-1S) and fall (C-1F and C-3F) soundings.

### 6.5.3 Comparison of Original and Revised Models to Footing Performance

Comparison of the original and revised RBSLS procedures to the observed footing performance provides the independent means necessary to evaluate the improvement, if any, in the new reliability calibrations. Figure 6.11 compares the ultimate resistance-normalized bearing pressure-displacement curves with the mean predicted responses (i.e., the expected response,  $\mu$ ) and  $\pm 1$  standard deviation,  $\sigma$ , whereas Fig. 6.12 presents the comparison of empirical cumulative distribution functions (CDFs) of normalized capacity at a given normalized displacement to those dictated by the RBSLS procedures. The  $\mu$  and  $\mu \pm \sigma$  curves were generated from 5,000 new MCS (e.g., corresponding to the  $c_1$ - $c_2$  pairs shown in Fig. 6.8, and new  $M_{STC}$ , for the revised procedure). As shown in Fig. 6.11a, the revised RBSLS model provides a slightly softer (i.e., reduced) mean normalized bearing pressure-displacement response, and the total variability in the response has also reduced as exhibited by the narrower breadth in the  $\mu \pm \sigma$  response. Figure 6.11b compares the revised RBSLS model to the new footing loading test data directly, and shows that much of the test data falls within the expected standard deviation. The expected response is particularly accurate at normalized bearing pressures less than approximately  $0.6q_{ult}$ ; with increased displacements, the SLS model tends to over-predict the bearing resistance. However, typical SLS design requirements target allowable bearing pressures less than  $0.5q_{ult}$  and therefore the loss of accuracy is associated with less frequent service level loading conditions.



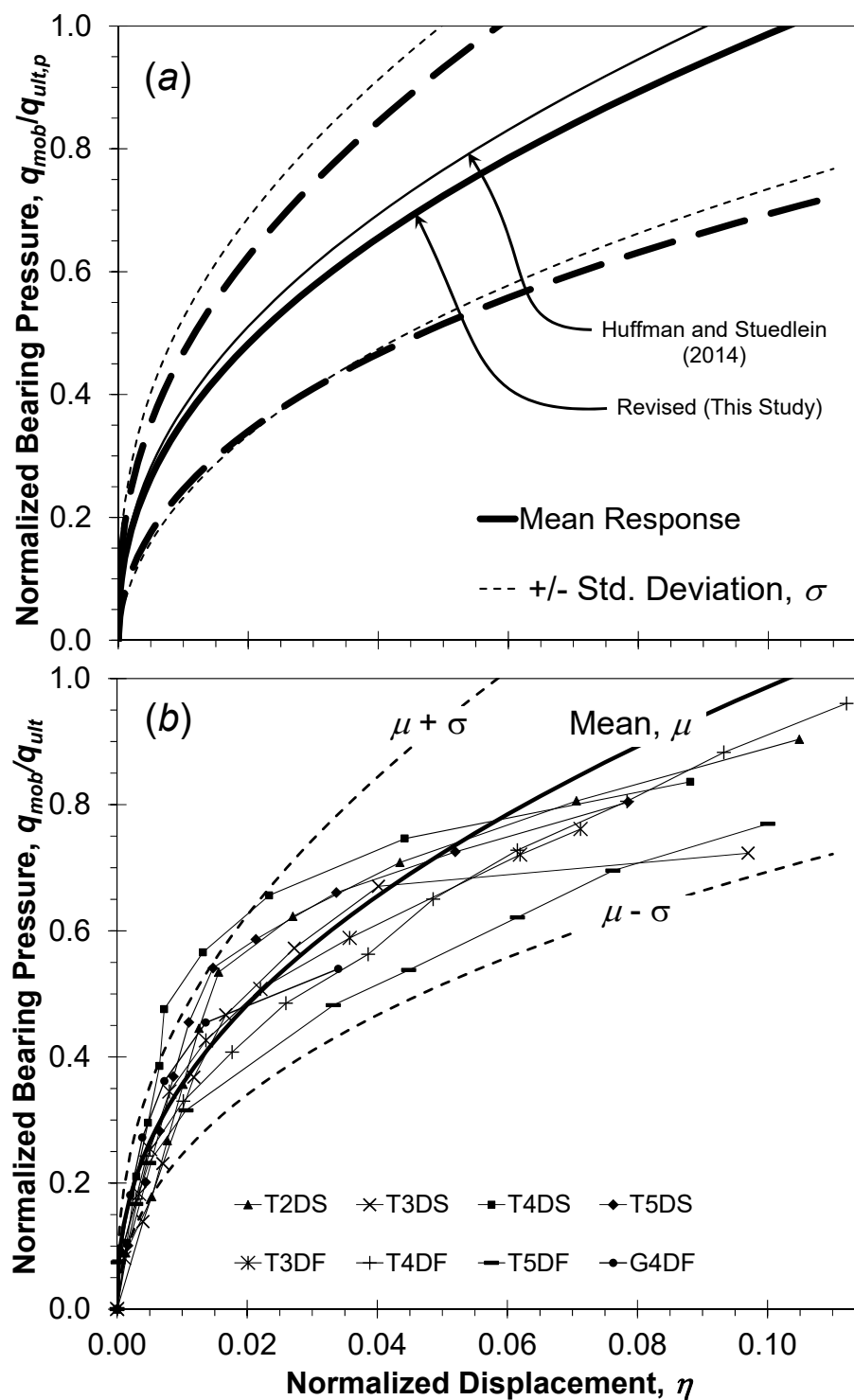


**Figure 6.11** Normalized bearing pressure-displacement curves associated with the RBSLS procedures: (a) comparison of Huffman and Stuedlein (2014) with the revised RBSLS procedure revised in this study, and (b) comparison of new full-scale loading tests to the revised RBSLS procedure.

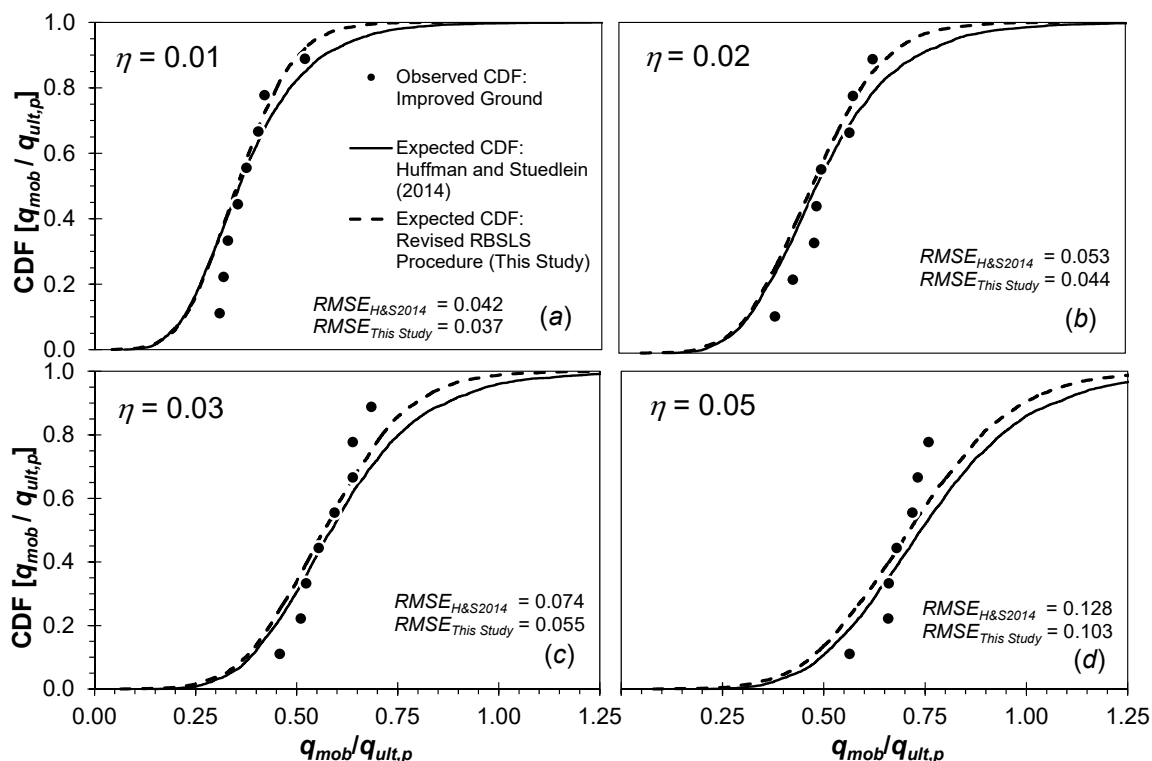


**Figure 6.12** Comparison of the observed and expected cumulative distribution functions (CDFs) of the normalized resistance at  $\eta = \delta/B'$  of (a) 0.01, (b) 0.02, (c) 0.03, and (d) 0.05.

Figure 6.12 compares the empirical CDFs of normalized capacity to those implied by the original and revised RBSLS procedure for aggregate pier-improved plastic, fine-grained soil. In general, the empirical CDF indicates less scatter than either the original or revised RBSLS procedure. This can be explained by the consideration of new full-scale loading test data that has been developed at just one site (i.e., the intra-site variability is less than the inter-site variability). However, in every instance, the root mean squared error (RMSE) is smaller for the revised RBSLS procedure, indicating that the revised procedure is more accurate for the new loading test data. In an alternate comparison of accuracy, Figure 6.13 compares the mean bias (the ratio of measured to estimated normalized capacity) and  $COV$  in bias for the empirical and RBSLS model CDFs for the normalized

displacements investigated. While the mean bias and its trend with  $\eta$  is similar (within 3 to 5%), the *COV* in bias has been largely reduced using the revised RBSLS procedure.

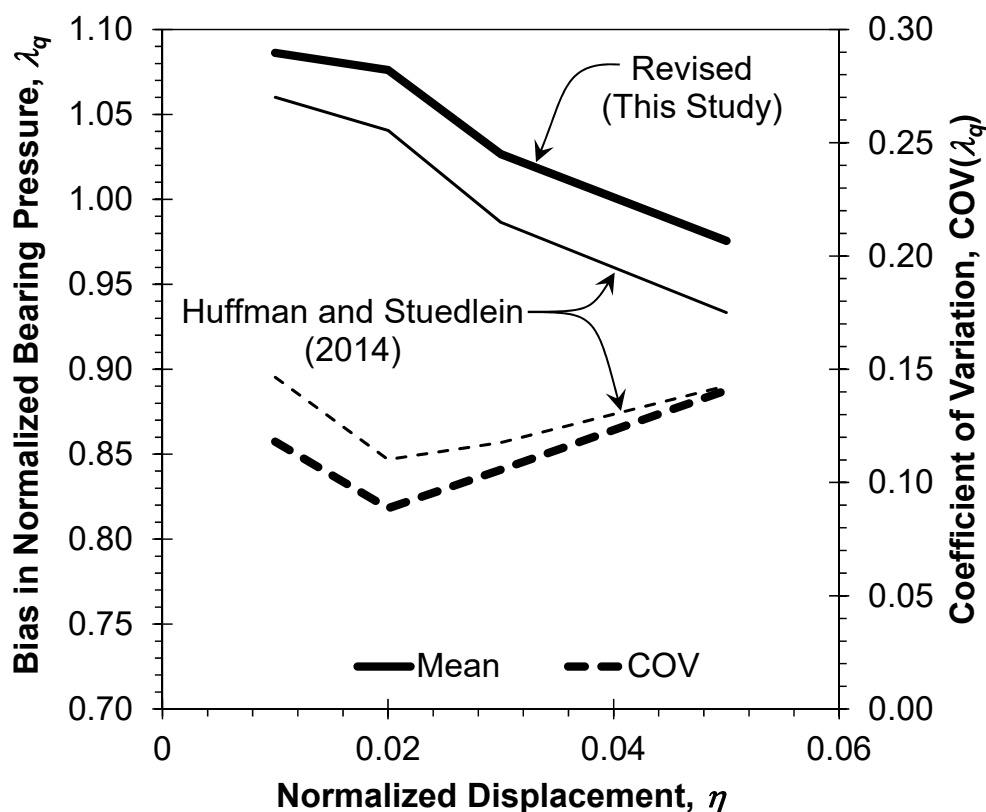


**Figure 6.13** Comparison of bias and COV in bias for calibrated model and sample CDFs for the original and revised RBSLS procedures.

#### 6.5.4 Implications for a Future RBSLS Procedure

It has been independently established with that the use of a reference capacity for the normalization protocol, as opposed to normalizing mobilized capacity with the ultimate resistance as done by Huffman and Stuedlein (2014), resulted in a more accurate reliability-based serviceability limit state procedure for the new spread footings on aggregate pier-reinforced clayey soil investigated herein. With the addition of new loading test data, as well as the soon-to-be completed final test, it will be possible to prepare a revised RBSLS

procedure that reflects all known high-quality loading test data with a view to further improving the accuracy of the procedure. Herein lies the task of geotechnical reliability specialists: to continuously improve reliability-based design procedures for use by practitioners and incorporation into code-based design.

## 6.6 SUMMARY AND CONCLUSIONS

The development of reliability-based serviceability limit state (RBSLS) models requires the careful, deliberate assessment of the various contributors to error and variability. This paper explored the impact of model selection on the propagation of error and its impact on reliability, as well as the independent evaluation of an existing and a newly revised RBSLS models. It was shown that the selection of model used to capture the bivariate distribution of bearing pressure-displacement curves can have a significant effect on the computed reliability (e.g., Figs. 6.1 and 6.2). The impact of copula model on reliability was also illustrated through the effect on allowable bearing pressure at a given footing displacement (Fig. 6.3).

The paper also illustrated a step-by-step procedure for making decisions regarding copula model fitting, scatter reduction through normalization of bearing pressure-displacement curves, and capturing suitable propagation of error through the various components comprising the full RBSLS calibration. It was shown that a slope tangent capacity with an offset equal to two percent of the footing width dramatically reduced scatter in the bearing pressure-displacement curves as compared to a previous effort that used the ultimate bearing pressure, and differences in the associated calibrated load and resistance factor were compared. While future studies may show that other offset

magnitudes produce better scatter reduction, the approach described herein will provide the framework for the evaluation of suitable normalization.

Finally, a new suite of full-scale loading test data was used to make an independent comparison of the accuracy in an existing and newly revised RBSLS procedure. It was shown that the new framework described above and used to revise the RBSLS procedure produced a more accurate estimation of the scatter in the empirical distribution of displacement-dependent allowable bearing pressure, lending confidence to the proposed calibration framework. This paper should serve as a valuable reference for RBSLS calibrations that are sure to be integrated and harmonized into future design codes.

## 6.7 REFERENCES

- Akaike, H. (1974) "A New Look at the Statistical Model Identification," *Transactions on Automatic Control*, IEEE, Vol. 19, No. 6, 716-723.
- Baecher, G.B. and Christian, J.T. (2003) *Reliability and Statistics in Geotechnical Engineering*, John Wiley and Sons, Ltd., London and New York, 605 pp.
- Ching, J. and Phoon, K.K. (2014) "Correlations among some clay parameters — the multivariate distribution," *Canadian Geotechnical Engineering*, 51(6), 686-704.
- Huffman, J.C., Strahler, A.W., and Stuedlein, A.W. (2015) "Reliability-based Serviceability Limit State Design for Immediate Settlement of Spread Footings on Clay," *Soils and Foundations*, Vol. 55, No. 4, 798-812.
- Huffman, J.C. and Stuedlein, A.W. (2014) "Reliability-based Serviceability Limit State Design of Spread Footings on Aggregate Pier Reinforced Clay," *Journal of Geotechnical and Geoenvironmental Engineering*, ASCE, Vol. 140, No. 10, 04014055.
- Li, D.Q., Tang, X.S., Phoon, K.K., Chen, Y.F., Zhou, C.B. (2013) "Bivariate Simulation Using Copula and its Application to Probabilistic Pile Settlement Analysis," *International Journal for Numerical and Analytical Methods in Geomechanics*, John Wiley & Sons, Vol. 37, No. 6, 597-617.
- Li, D.Q. and Tang, X.S. (2014) "Modeling and simulation of bivariate distribution of shear strength parameters using copulas," *Chapter 2, Risk and Reliability in Geotechnical Engineering*, Phoon and Ching, Eds., 624 pp.

- Li, L., Wang, Y., Cao, Z., Chu, X. (2013) "Risk de-aggregation and system reliability analysis of slope stability using representative slip surfaces," *Computers and Geotechnics*, 53, 95-105.
- Mayne, P. and Poulos, H. (1999). "Approximate Displacement Influence Factors for Elastic Shallow Foundations." *J. Geotech. Geoenviron. Eng.*, 125(6), 453-460.
- Nelson, R.B. (2006) *An Introduction to Copulas: Second Ed.*, Springer, New York, 269 p.
- Phoon, K.K. (2008) "Numerical Recipes for Reliability Analysis – A Primer," *Reliability Based Design in Geotechnical Engineering: Computations and Applications*, Taylor and Francis, London, 1-75.
- Phoon, K.K., and Kulhawy, F.H. (2008) "Serviceability Limit State Reliability-Based Design," *Reliability Based Design in Geotechnical Engineering: Computations and Applications*, Taylor and Francis, London, 344-384.
- Schwarz, G. (1978) "Estimating the Dimension of a Model," *The Annals of Statistics*, Vol. 6, No. 2, 461-464.
- Stuedlein, A.W., and Holtz, R.D. (2013) "Bearing Capacity of Spread Footings on Aggregate Pier Reinforced Clay," *Journal of Geotechnical and Geoenvironmental Engineering*, ASCE, Vol. 139, No. 1, 49-58.
- Stuedlein, A.W. and Reddy, S.C. (2014) "Factors Affecting the Reliability of Augered Cast-In-Place Piles in Granular Soils at the Serviceability Limit State" *Journal of the Deep Foundations Institute*, Vol. 7, No. 2, 46-57.
- Tang, X.S., Li, D.Q., Rong, G., Phoon, K.K., Zhou, C.B. (2013) "Impact of Copula Selection on Geotechnical Reliability Under Incomplete Probability Information," *Computers and Geotechnics*, Elsevier, Vol. 49, 264-278.
- Uzielli, M. and Mayne, P., (2011) "Serviceability Limit State CPT-based Design for Vertically Loaded Shallow Footings on Sand," *Geomechanics and Geoengineering: An International Journal*, Taylor and Francis, Vol. 6, No. 2, 91-107.
- Wang, Y. (2011) "Reliability-based design of spread foundations by Monte Carlo simulations," *Geotechnique*, 61 (8), 677-685.
- Wang, Y., and Cao, Z. (2013) "Expanded reliability-based design of piles in spatially variable soil using efficient Monte Carlo simulations," *Soils and Foundations*, 53(6), 820-834.
- Wang, Y., Cao, Z., and Au, S.-K. (2011) "Efficient Monte Carlo simulation of parameter sensitivity in probabilistic slope stability analysis," *Computers and Geotechnics*, 37 (7), 1015-1022.
- Wang, Y., and Kulhawy, F.H. (2008) "Reliability index for serviceability limit state of building foundations," *Journal of Geotechnical and Geoenvironmental Engineering*, 134 (11), 1587-1594.

## **CHAPTER 7: RELIABILITY-BASED ASSESSMENT OF FOUNDATION AND STRUCTURE PERFORMANCE WITH SPATIALLY VARIABLE SOIL**

### 7.1 INTRODUCTION

Inherent soil spatial variability and soil-structure interaction (SSI) are two of the most important aspects when considering geotechnical foundation design and performance of the structure those foundations are supporting. However, fully incorporating soil variability and SSI into a comprehensive reliability-based limit state model remains a challenge for researchers and practitioners of geotechnical and structural engineering. Perhaps one of the greatest challenges lies in the computational limitations for robust reliability analyses that combines realistic soil and structural behavior.

The soil, foundations, and structure form a system that interact and influence the performance of the building components with variable levels of reliability and/or uncertainty. Contributions to system uncertainty is manifested in various mechanisms including inherent soil spatial variability, error in analytical soil-foundation modeling, and variation in soil-structure interaction, as generalized in Fig. 7.1. Inherent soil spatial variability is caused by soil depositional, loading, and weathering history, resulting in heterogeneity of soil engineering properties even in relatively uniform strata (e.g., Phoon and Kulhawy 1999a, Elktab et al. 2002, Uzielli et al. 2007, Stuedlein et al. 2012; Bong and Stuedlein 2017). This phenomenon is typically evaluated using random field theory (RFT) and characterized for a selected soil property using the scale of fluctuation,  $\delta$ , the trend function,  $t(z)$  (often depth,  $z$ , dependent based on stress history), and the coefficient of

variation of inherent soil variability,  $COV_w$ , (Vanmarke 1977, 1983; Phoon and Kulhawy 1999a, 1999b). The error in analytical models used to predict soil response under foundation loads (e.g., bearing capacity or settlement equations) is closely related to inherent soil spatial variability and arises in part from the use of generalized soil properties (e.g., average or best estimate) and potential insufficiency of the assumed theoretical failure mechanism (e.g., Baecher and Christian 2003, Phoon 2008). Variability in the global response to SSI is particularly important when the structure is supported on multiple foundations spread over a large building footprint. When considering SSI, both the stiffness and strength of the structural elements and the inherent soil spatial variability between individual footings influence load distribution and re-distribution within the structure, which in turn affects the soil response, applied bearing pressure, and footing displacement (Noorzaei et al. 1995, Houy et al. 2005). It is the combination of these uncertainties that influence total and differential displacement between individual foundations and across the building footprint, impacting the performance of the structure at the serviceability (SLS) and ultimate limit states (ULS).

A traditional approach to address multiple sources of uncertainty within geotechnical foundation design has been to apply a factor of safety (FS) to the results of the selected analytical model (e.g., bearing capacity), thereby reducing the allowable foundation loads and lowering the risk of unsatisfactory foundation and structure performance. However, the selected FS value is relatively arbitrary and philosophically incorrect because it does not provide a means to characterize or understand the disparate sources of variability or give a sense to the actual risk level or reliability associated the analysis and design (e.g., Gilbert 1997, Duncan 2000, Allen 2005).



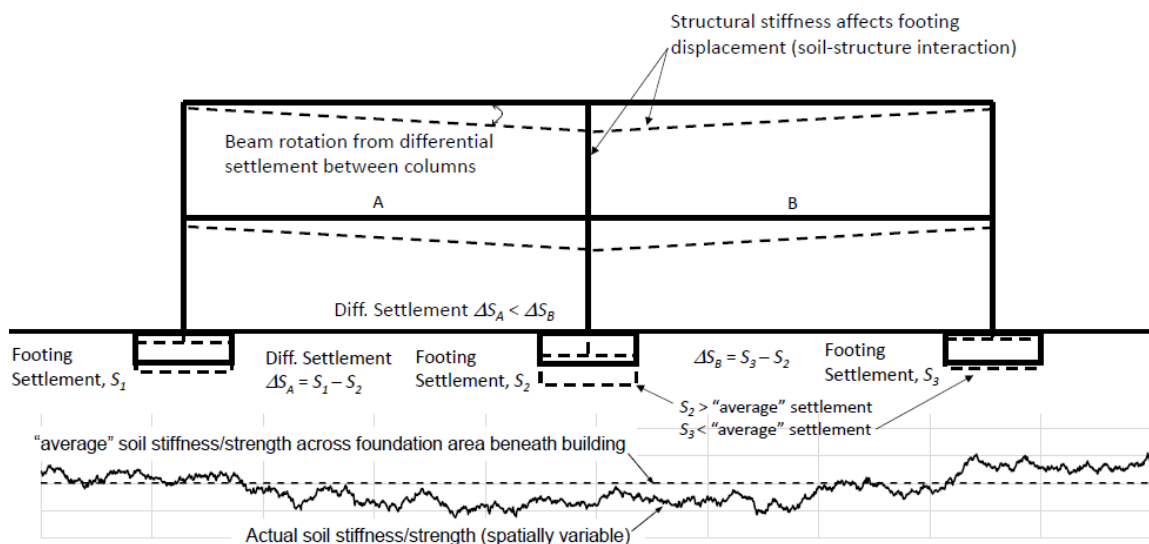


**Figure 7.1** Example of structure and foundation response in spatially variable soil.

More recently, a significant effort has been made by the geotechnical research community to better characterize inherent soil spatial variability and develop reliability-based design (RBD) methods using rigorous statistical analyses to probabilistically evaluate the variability associated with multiple geotechnical design elements and the risk of exceeding a given limit state for bearing resistance, foundation displacement, or other design considerations. Phoon et al. (1995) provided a framework for RBD methods to assess shallow foundations considering both ULS (i.e., bearing capacity) and SLS (i.e., allowable footing displacement) design. Further studies considering RBD limit state design of shallow footings include those by Fenton and Griffiths (2002, 2003a, 2003b, 2005), Phoon et al. (2003), Roberts and Misra (2010), Fenton et al. (2011), Uzielli and Mayne (2011, 2012), Wang (2011), Zhang and Ng (2013), Stuedlein et al. (2014), and Chapters 4, 5, and 6 of this thesis (Huffman and Stuedlein 2014; Huffman et al. 2015, 2016). The above-referenced studies cover a range of RBD design concepts by considering

foundation analyses for varying soil types (e.g., cohesive or cohesionless), unimproved or improved soil (e.g., footings on aggregate piers), different loading conditions, and, in some cases, specifically ULS or SLS design.

One limitation for many recent RBD studies is their focus on single foundations in isolation, which is customary practice for typical foundation analysis, but limits their applicability when considering multi-foundation systems supporting a structure where inherent soil variability and soil-structure interaction are key factors. Another related challenge for RBD studies and analyses, particularly for serviceability design, is the consideration of structural performance (e.g., vertical movement or rotation of structural members) as it relates to the inherent variability of the foundation soil (Stuedlein and Bong 2017, Bong and Stuedlein 2018).

Fenton and Griffiths (2002, 2005) and Ahmed and Soubra (2014) conducted probabilistic analyses for SLS design considering two adjacent foundations and soils modeled with spatial variability in either two or three dimensions using finite element or finite difference analyses. A key outcome of these studies is the relationship shown between the foundation spacing and horizontal autocorrelation distance (or scale of fluctuation,  $\delta_h$ ), wherein the probability of exceeding tolerable differential settlement between adjacent footings is typically greatest when  $\delta_h$  is approximately equal to the center-to-center distance between the footings. The models used by Fenton and Griffiths (2002, 2005) and Ahmed and Soubra (2014) were based on soil characterized with a spatially random Young's modulus,  $E$ , in combination with linear-elastic or elastic-perfectly plastic response. This approach is most suitable for estimating the settlement of footings supported on medium dense to dense granular soils (i.e., sand and gravel) under

serviceability-level foundation loads, but does not reflect the response of plastic, fine-grained soils (i.e., clay or clayey silt), which displace nonlinearly even at relatively small foundation loads (D'Appolonia et al. 1971, Jardine et al. 1986, Foye et al. 2008, Stuedlein and Holtz 2010; Strahler and Stuedlein 2013). In addition, the footings were modeled to act independently from one another (i.e., not connected by a structure), providing a means to evaluate the effect of inherent soil spatial variability, but without consideration of the SSI that includes flexural and shear rigidity of the overall structure and corresponding load distribution relationships between the structure, foundations, and the supporting soil.

The goal of the current study is to further develop RBD for spread footings supported on plastic, fine-grained soils by incorporating suitable SSI for the foundation system with the observed variability of the undrained bearing pressure-displacement response of the foundations and the anticipated range of soil variability in terms of the undrained shear strength across the building footprint. This analysis consists of the evaluation of shear-type “immediate settlement”, typically associated with the process of construction as opposed to long-term consolidation analyses (i.e., appropriate for structures supported on overconsolidated soils and in which primary consolidation is not triggered). Concurrently, this study compares the performance of a selected steel-frame structure with the simulated footing displacements to better characterize serviceability-level displacement and rotation of the building elements relative to the footings and foundation soil. Variability in the structural elements was not considered for the current study because such variability (e.g., strength and stiffness of fabricated steel beams and columns or reinforced concrete foundations) is significantly lower and less complex compared to the variability of

naturally-deposited soils (Phoon and Kulhawy 1999b, Allen 2005, Allen et al. 2005, Fenton and Griffiths 2008). Furthermore, including structural variability may partially obscure the observed role of soil spatial variability on structural performance.

New reliability analyses were completed using Monte Carlo simulations (MCS) with the bearing pressure-displacement model developed in Chapter 5 (Huffman et al. 2015) modified to include a multi-foundation system and variable soil shear strength distributed across the building area. To investigate the effects of soil-structure interaction, the MCS were completed for both a series of footings acting independently and for a series of footings acting as a system supporting a two-dimensional, three-story, steel moment resisting frame (SMRF) building. The building-foundation-soil response was incorporated using a structural model developed as part of the SAC Steel project as documented in FEMA-355C (2000) and Barbosa et al. (2017), and structural element response based on Lignos and Krawinkler (2011) and Ribeiro et al. (2014, 2015). Simulations of rotation and corresponding bending moments for structural beam elements within the building also allowed a comparison of building response to that of the spatially variable foundation soil subject to the applied bearing pressures. Subsequent analyses were then completed with additional MCS and a revised bearing pressure-displacement model using site-specific resistance parameters and correlation relationships to evaluate possible intra-site versus inter-site differences in soil variability and model error, and its effect on the soil-structure-foundation response.

## 7.2 BUILDING AND SOIL MODEL

The model developed for this study includes three components: the building, the footings, and the foundation soil. Model components were constructed and loading simulations were completed using the open-source programs R (version 3.3) and Open System for Earthquake Engineering Simulation (OpenSees; McKenna et al. 2010). OpenSees version 2.5 was used with adaption to include a new material, *HyperbolicQy* (Belejo et al. 2020), that models nonlinear vertical foundation displacement similar to the method developed in Chapter 5 (Huffman et al. 2015). A description of each of component is detailed in the following sections.

### 7.2.1 Building Model and Foundations

#### 7.2.1.1 SAC Building Model

The building model used for this study is a three-story steel moment-resisting frame (SMFR) structure, originally developed as part of the SAC steel project and documented in FEMA-355C (2000) and Barbosa et al. (2017). The SAC steel project studied the response of different multi-story, steel moment-frame structures designed based on UBC 1994 code for locations in Boston, Los Angeles, and Seattle, but subjected to new loading from observations made with building performance after the 1994 Northridge earthquake. The building model used for this study is consistent with the Seattle (SE) three-story building, with structural members and connections based on code requirements for that region. The structure is comprised of multiple sizes of W-sections and includes 4 bays and 5 columns, each spaced at 9.15 m on-center. Each of the building levels has a story height of 3.96 m. A schematic of the two-dimensional model is shown in Fig. 7.2, with

identification of beam and column section members; pertinent section strength parameters for the beams are summarized in Table 7.1.

The structure was designed with an external frame to resist lateral (seismic) loads and internal frame to resist gravity loads. A two-dimensional model using the external frame of the building was developed and evaluated with the program OpenSees consistent with the approach described in Barbosa et al. (2017) assuming strong-column weak-beam ductile behavior without the consideration of brittle mechanisms or fracture at the connections. The columns were modeled as nonlinear force-based fiber-section beam-column elements, and the beams were modeled as finite length plastic-hinge beam-column elements. Floor mass (i.e., gravity load) was applied at the beam-column joints.

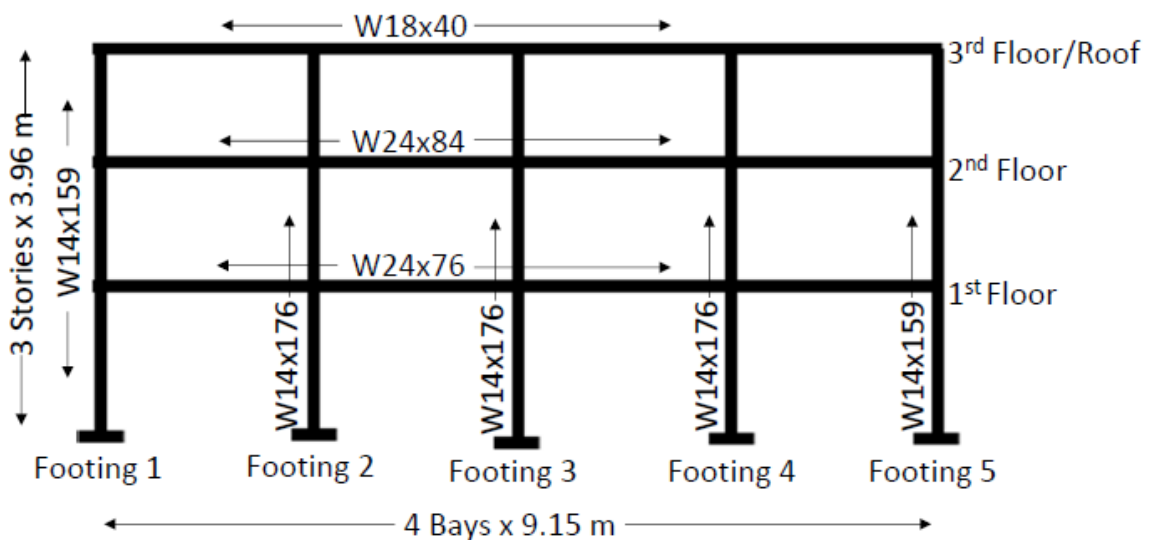


**Figure 7.2** Structural model used with OpenSees analysis for MCS. Based on SE three-story building per FEMA-355C (2000) and Barbosa et al. (2017).

**Table 7.1. Summary of Seattle (SE) three-story building steel beam section members and strength parameters (compare to Fig. 7.3).**

Location	Section	Yield Mom., $M_y$ (kN-m)	Yield Rot., $\theta_y$ (rad.)	Cap. Mom., $M_c$ (kN-m)	Cap. Rot., $\theta_c$ (rad.)	Resid. Mom., $M_r$ (kN-m)	Resid. Rot., $\theta_r$ (rad.)	Ultimate Rot., $\theta_u$ (rad.)
1st floor beams	W24x76	1,128	0.0065	1,241	0.019	451	0.067	0.262
2nd floor beams	W24x84	1,263	0.0064	1,390	0.020	505	0.075	0.262
3rd floor/roof beams	W18x40	442	0.0087	486	0.028	177	0.091	0.262

- Notes:**
1. Section strength parameters are based on ASTM A572 steel with yield strength  $f_y = 344.14$  MPa and elastic modulus  $E_{steel} = 200$  GPa.
  2. Section strength parameters were calculated based on the initial moment-rotation backbone curve in Lignos and Krawinkler (2011).
  3. Residual strength ratio  $\kappa = M_r/M_y$  of 0.4 was used for all section members.
  4. Ultimate rotation,  $\theta_u$ , for all members was set equal to  $0.4L_p$ , where  $L_p$  is the plastic hinge length set equal to  $L/6$  and  $L$  is the total beam length (Ribeiro et al. 2015).

A moment-rotation ( $M-\theta$ ) backbone curve was assumed for the steel structural elements based on the modified Ibarra-Krawinkler (IK) deterioration model as described in Lignos et al. (2011), Lignos and Krawinkler (2011), and Ribeiro et al. (2014, 2015). An example of the generalized  $M-\theta$  backbone curve for the beam sections is shown in Fig. 7.3. The yield moment,  $M_y$ , in the backbone curve is equal to the yield stress,  $F_y$ , multiplied by the plastic section modulus,  $Z$ , of the beam. Therefore,  $M_y$  represents the ultimate limit state for the flexural beam response based on traditional limit state definitions (e.g., LRFD). For this study, evaluation of the steel structure focused on flexural performance of the beam elements.

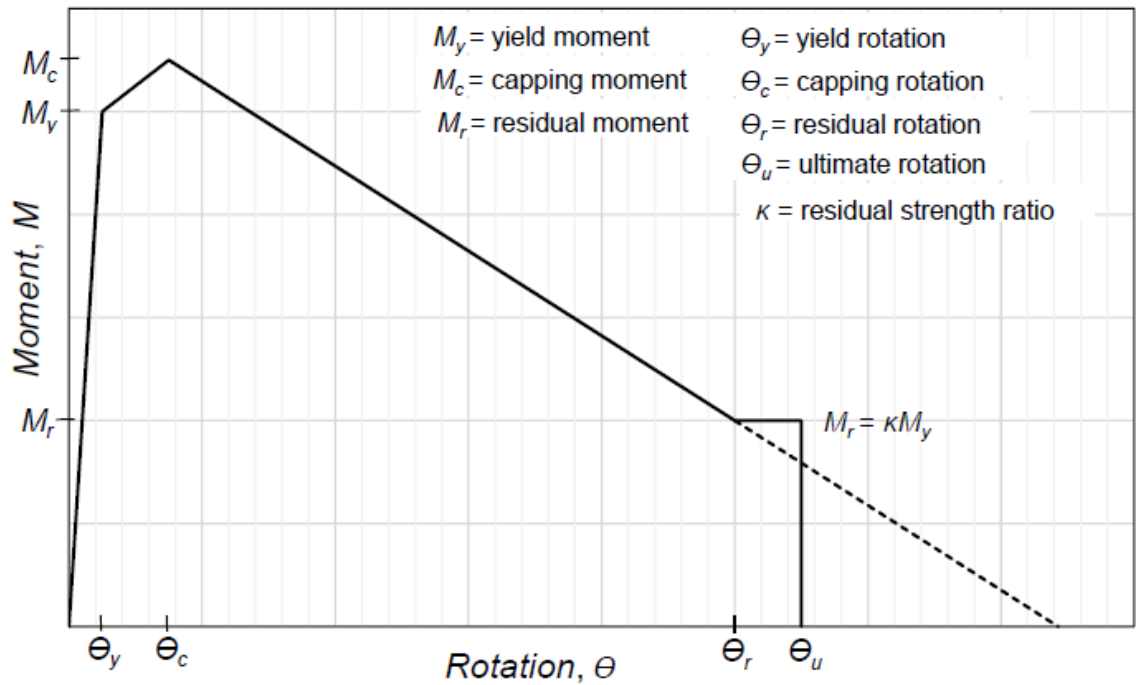


**Figure 7.3** General moment-rotation backbone curve for steel structural members (adapted from Lignos and Krawinkler 2011; Ribeiro et al. 2014, 2015).

### 7.2.1.2 Foundations

Foundations supporting the five columns of the SMRF structure were modeled as square reinforced concrete footings within OpenSees using nonlinear soil-foundation springs detailed in Section 7.2.2. The footings were sized to accommodate the calculated dead (DL) and live (LL) loads for the three-story SE building, equal to approximately 520 kN at the exterior footings (Footings 1 and 5) and 820 kN at the interior footings (Footings 2, 3 and 4). The actual loading at each footing varied and was not symmetric, primarily because of variable soil stiffness and SSI effects, as detailed in subsequent sections below.

The soil bearing capacity was calculated assuming a nominal or “average” undrained shear strength,  $s_u$ , equal to 70 kPa and soil unit weight,  $\gamma$ , equal to 19 kN/m<sup>3</sup> (note that the



term average and nominal are used somewhat interchangeably throughout this chapter and typically meant to represent a best-estimate and/or mean value with some known or unknown characteristic distribution). The assumed shear strength is consistent with a stiff, overconsolidated fine-grained soil loaded in undrained (i.e.,  $\phi = 0$ ) conditions. The footing embedment depth,  $D_f$ , and footing thickness was set equal to 0.6 m. Based on these parameters, exterior footings with width,  $B$ , and length,  $L$ , equal to 1.675 m and interior footings with  $B$  and  $L$  equal to 2.125 m were sized to provide nominal allowable bearing pressures in the range of 181 to 185 kPa with a typical factor of safety (FS) of 2.5 for bearing capacity. A summary of the pertinent foundation parameters used in the design model is provided in Table 7.2.

**Table 7.2. Summary of footing dimensions and nominal loads and resistances.**

Footing	Width $B$ (m)	Length $L$ (m)	Depth $D_f$ (m)	DL+LL Applied Load (kN)	Applied Bearing Press. (kPa)	Bearing Cap., $q_{ult,p}$ (kPa)	Ult. Passive Resist., $P_{ult}$ (kN)
1 (left exterior)	1.675	1.675	0.6	510	182	498	197
2 (left interior)	2.125	2.125	0.6	817	181	486	236
3 (middle interior)	2.125	2.125	0.6	819	181	486	236
4 (right interior)	2.125	2.125	0.6	794	176	486	236
5 (right exterior)	1.675	1.675	0.6	517	184	498	197

- Notes:**
1. Nominal applied loads and resulting bearing pressures are based on the SE three-story building pre-Northridge design per FEMA-355C (2000). Actual loads in the MCS reliability analyses varied based on varying soil-foundation spring resistances and soil-structure interaction as described in this dissertation chapter.
  2. Nominal bearing capacity and passive resistance are based on Eqs. 2 and 5 and assume an undrained shear strength  $s_u = 70$  kPa. Actual resistances in the MCS reliability analyses varied based on varying  $s_u$  values as described in this dissertation chapter.

The foundation loads were assumed to be imparted “instantaneously”, to simulate the load transferred during construction of the building (i.e., dead loads). Thus, the simulation of the footing displacement corresponds to the immediate settlement case where soil strains are primarily deviatoric in nature and analogous to the footing loading tests used to calibrate the bearing pressure-displacement model. No drainage and/or strength gain is assumed to occur during construction. For implementation in OpenSees, loading occurred as a ten-step process (but without consideration of time) to simulate the response across the different building, foundation, and soil elements.

## 7.2.2 Nonlinear Soil-Foundation Springs

### 7.2.2.1 *Vertical and Rotational Resistance*

The vertical and rotational soil resistance to foundation displacement was modeled based on the nonlinear bearing pressure-displacement behavior developed in Chapter 5 (Huffman et al. 2015). The model was developed from a series of high-quality foundation loading tests wherein the soil undrained shear strength was mobilized concurrent with immediate (distortion) foundation displacement. The mobilized soil resistance calculated as:

$$q_{mob} = \frac{\eta}{k_1 + k_2 \eta} M_{STC} q_{ult,p} \quad (7.1)$$

where  $q_{mob}$  is the mobilized resistance at a given vertical displacement (or settlement),  $s$ ,  $\eta = s/B'$  is the normalized displacement, and  $B'$  is the equivalent footing diameter, defined as the diameter that produces the same area as that of a square footing (e.g., Mayne and Poulos 1999). The equivalent footing diameter was selected for normalization in consideration of using various footing shapes for design. The coefficients  $k_1$  and  $k_2$  are

best-fit hyperbolic model parameters based on the loading test results. The model factor,  $M_{STC}$ , is used to scale the bearing capacity to the slope tangent capacity observed in the loading tests with a slope tangent offset set equal to  $0.03B'$ . The  $k_1$ ,  $k_2$ , and  $M_{STC}$  mean values and statistical distributions calculated from the loading test data are summarized in Chapter 5 (Huffman et al. 2015) and in Table 7.3. Normalized bearing pressure-displacement measurements from the loading test database are shown on Fig. 7.4 along with the normalized bearing pressure-displacement curve calculated using Eq. 7.1 and the global coefficient values summarized in Table 7.3. The model is appropriate for a relatively wide range of footing sizes supported on overconsolidated clayey soils and where primarily consolidation will not be triggered under the imposed foundation loads.

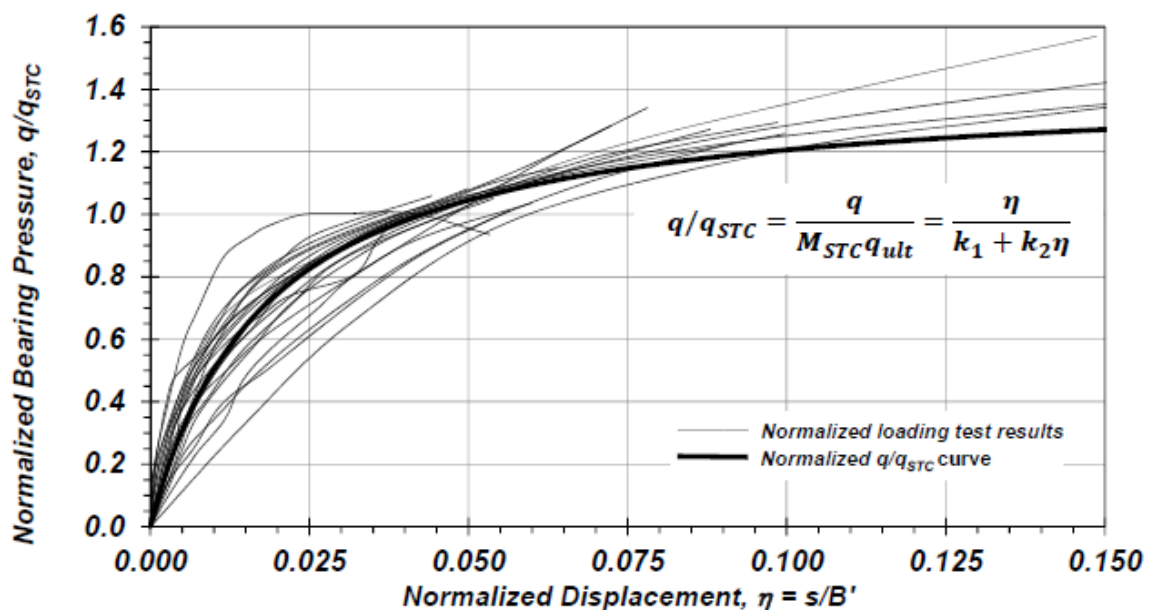


**Figure 7.4** Normalized global dataset footing loading test results and mean bearing pressure-displacement curve based on Eq. 7.1.

**Table 7.3. Summary of assumed or fitted soil resistance parameters for MCS.**

	<b>Parameter</b>	<b>Mean</b>	<b>COV (%)</b>	<b>Model Distribution</b>
	$s_u$	70 kPa	Note 1	Note 1
	$\gamma$	19 kN/m <sup>3</sup>	Note 2	Note 2
	$E_{soil}$	12,260 kPa	Notes 2, 3	Notes 2, 3
	$K_{max}$ (exterior)	129,745 kN/m	Notes 2, 4	Notes 2, 4
	$K_{max}$ (interior)	150,304 kN/m	Notes 2, 4	Notes 2, 4
Global loading test database (Note 5)	$M_{STC}$	0.643	18.7	Lognormal
	$k_1$	0.013	53.0	Gamma
	$k_2$	0.701	16.1	Inverse Gaussian
OSU GEFRS loading tests	$M_{STC}$	0.544	14.6	Uniform (Note 6)
	$k_1$	0.017	11.7	Uniform (Note 6)
	$k_2$	0.589	28.0	Uniform (Note 6)

- Notes:**
1. The undrained shear strength,  $s_u$ , used to calculate  $q_{ult}$  and  $P_{ult}$  for the MCS varied based on the given random field with a range of  $COV_{w,h}$  and  $\delta_h$  as noted below.
  2. The MCS analyses did not include variability for the soil unit weight,  $\gamma$ , initial elastic modulus,  $E_{soil}$ , or initial passive stiffness,  $K_{max}$ .
  3.  $E_{soil}$  was calculated based on Eq. 7.4 assuming an  $OCR$  of 8, as discussed below and in Section 7.2.2.2.
  4.  $K_{max}$  for interior and exterior footing lateral resistance was calculated based on Douglas and Davis (1964), as discussed in Section 7.2.2.2.
  5. See Chapter 5 (Huffman et al. 2015) for further discussion of parameter fitting for the global loading test database.
  6. Distribution of the OSU GEFRS (i.e., intra-site) model parameters for MCS analyses assumed a uniform distribution with limits set equal to +/- one-half standard deviation from the observed maximum and minimum values; described in detail below.

The predicted bearing capacity,  $q_{ult,p}$ , was calculated for each footing using the general bearing capacity equation (e.g., Terzaghi 1943) with Meyerhof (1963) bearing capacity factors, and shape and depth factors from Brinch Hansen (1970) as:

$$q_{ult,p} = s_u N_c \lambda_{cs} \lambda_{cd} + \gamma D_f N_q \lambda_{qs} \lambda_{qd} \quad (7.2)$$

where  $N_c$  and  $N_q$  represent bearing capacity factors (assumed equal to 5.14 and 1.0, respectively, for the  $\phi = 0$  condition), and  $\lambda_{cs}$ ,  $\lambda_{qs}$ ,  $\lambda_{cd}$ , and  $\lambda_{qd}$  are the Brinch Hansen (1970) shape and depth factors, respectively. Equation 7.2 assumes a general shear type failure with mobilization of the undrained shear strength that is volumetrically averaged based on the foundation bearing area and accounts for soil nonlinearity within the depth of influence. The calculated bearing capacity for the different footings with assumed nominal undrained shear strength,  $s_u = 70$  kPa is indicated in Table 7.2. For the MCS analyses, the actual bearing capacity (and mobilized resistance) beneath the footings varied based on the distribution of the spatially-dependent undrained shear strength, as described below.

The nonlinear bearing pressure-displacement relationship estimated using Eq. 7.1 was originally developed to estimate the response from vertical footing loads only. To account for rotational resistance, the footing-bearing pressure response was modified based on a beam-on-nonlinear-Winkler-foundation (BNWF) model. The BNWF approach has been used extensively to model rocking or rotation of shallow foundations under static and seismic loads with either linear or nonlinear soil response (e.g., Houlsby et al. 2005, Harden et al. 2005, Raychowdhury 2008, Harden and Hutchinson 2009, Raychowdhury and Hutchinson 2009). With this approach, the soil resistance is modeled as a series of spring elements with the individual resistance of each spring being proportional to its area of influence. A schematic of the BNWF foundation spring is shown in Fig. 7.5.

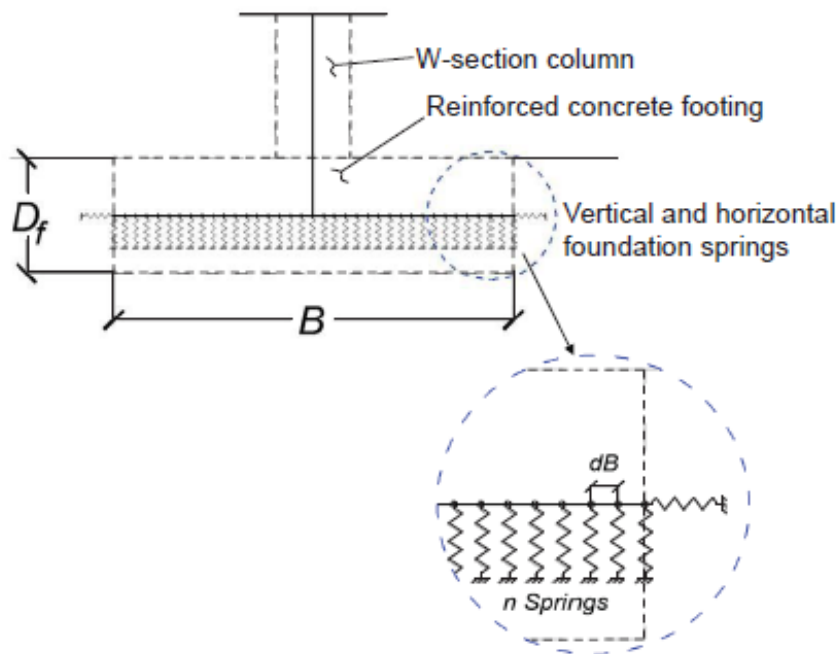


**Figure 7.5** Footing model with vertical and horizontal soil-foundation springs.

Using the nonlinear bearing pressure-displacement model for analysis within OpenSees required implementing a new material model, *HyperbolicQy* (Belejo et al. 2020), to represent the BNFW soil springs. The material model is a compression-only, zero-length spring with tensile gap model, which provides resistance in compression and separation of the interface in tension. Input parameters include coefficients  $k_1$  and  $k_2$ , slope tangent capacity  $q_{stc}$  (for bearing pressure) or  $Q_{stc}$  (for load), and footing width,  $B$ .

The BNWF springs were spaced evenly across the base of the footings and were specified to have equal unit resistance, except for the end springs (located at the footing edges), which had one-half the unit resistance and acted over half the tributary area of the other springs. The approach using evenly-spaced and equally-stiff springs assumes the reinforced concrete footings are very stiff compared to the underlying soil and distribute the bearing pressure relatively evenly under the building loads. This approach is

appropriate for the rigid spread footings consistent with this study. To confirm the relative stiffness of the footings compared to the foundation soil, the foundation flexibility factor,  $K_f$ , was computed using (Brown 1969, Mayne and Poulos 1999):

$$K_f = (E_{fnd}/E_{soil}) \left( \frac{D_f}{B'/2} \right)^3 \quad (7.3)$$

where  $E_{fnd}$  is the elastic modulus of the footing,  $E_{soil}$  is the soil elastic modulus, and  $D_f$  and  $B'$  are footing dimensions as described above. Brown (1969) indicates a  $K_f$  value greater than 10 provides a foundation acting in a “perfectly rigid” manner; in other words, the foundations are suitably stiff to assume an equal distribution of displacement across the bearing area of the footing. To calculate the flexibility factor,  $E_{fnd}$  was assumed to be approximately 27.8 GPa based on a concrete compressive strength,  $f'_c$ , set equal to 35 MPa. The plastic, fine-grained foundation soil generally has nonlinear stress-strain properties. However, an initial elastic modulus at low strains may be calculated as (Strahler and Stuedlein, 2013):

$$E_{soil} = (11 * OCR + 33)P_{ATM} \quad (7.4)$$

where OCR is the overconsolidation ratio (i.e., ratio of maximum past pressure to existing overburden pressure of the foundation soil) and  $P_{ATM}$  is atmospheric pressure (101.3 kPa). An OCR of 8 was assumed for this study, consistent with the stiff soil profile within the relatively shallow depth of influence of the foundations. Based on these conditions, the calculated  $K_f$  factor is significantly greater than 10 for both the exterior and interior foundations.

The total number of vertical foundation springs, set equal to 101, was selected in consideration of a spring discretization study wherein the number of springs within the model was increased until the results for soil resistance and footing displacement

converged to a stable value for a given rotational load (or moment) applied at the midpoint of the footing. Figure 7.6 provides an example of the simulated moment-deflection or rotational stiffness curves for varying numbers of springs beneath the foundation. The deflection was measured at the edge of the footing where deformation into the soil from the applied moment is greatest. Deflection was also checked at the midpoint of the footing. The change in the rotational stiffness with additional vertical footing springs becomes negligible when the number of springs is greater than or equal to 101. The foundations springs were modeled to provide resistance in compression only, with zero tensile (e.g., uplift) resistance. Therefore, uplift resistance could be provided by the weight of the foundations but not from the soil.

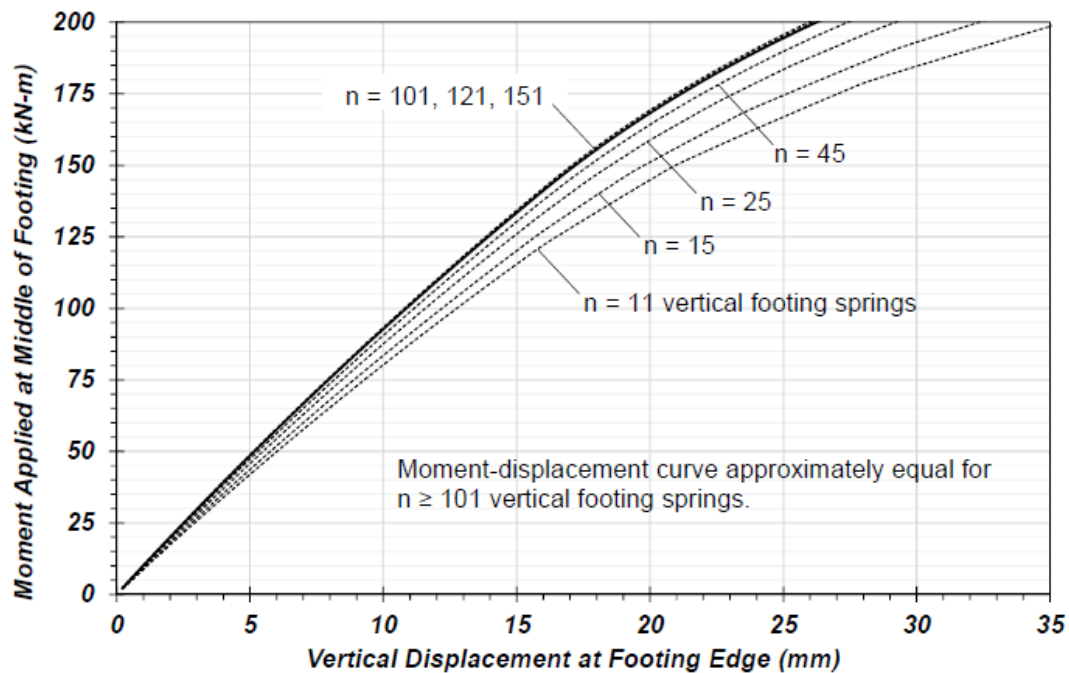


**Figure 7.6** Moment versus displacement for varying number of equally spaced vertical footing springs.



### 7.2.2.2 Horizontal Resistance

Horizontal or lateral resistance on the sides of the footings arising from passive pressure were modeled as a single spring with passive resistance-displacement response using a nonlinear hyperbolic relationship based on Duncan and Mokwa (2001), calculated as:

$$P_{mob} = \frac{\Delta x}{\frac{1}{K_{max}} + R_f \frac{\Delta x}{P_{ult}}} \quad (7.5)$$

where  $P_{mob}$  is the mobilized passive resistance at a given lateral displacement,  $\Delta x$ ,  $K_{max}$  is the initial lateral soil stiffness (i.e., initial slope of the hyperbolic curve),  $P_{ult}$  is the calculated ultimate passive resistance, and  $R_f$  is the ratio of the ultimate passive pressure divided by the asymptote of the hyperbolic curve. Both  $P_{mob}$  and  $P_{ult}$  are in units of force (e.g., kN), displacement is units of length (m), and  $K_{max}$  is in units of force/length (e.g., kN/m). The failure ratio  $R_f$  is unitless and assumed to be equal to 0.85 for this study following discussions in Duncan and Mokwa (2001). Figure 7.7 shows an example of the nonlinear passive resistance-displacement curve. Pertinent soil parameters for calculating passive resistance for this study are summarized in Table 7.3. The spring was implemented in OpenSees using the uniaxial material, *HyperbolicGapMaterial* (Wilson and Elgamal 2006).

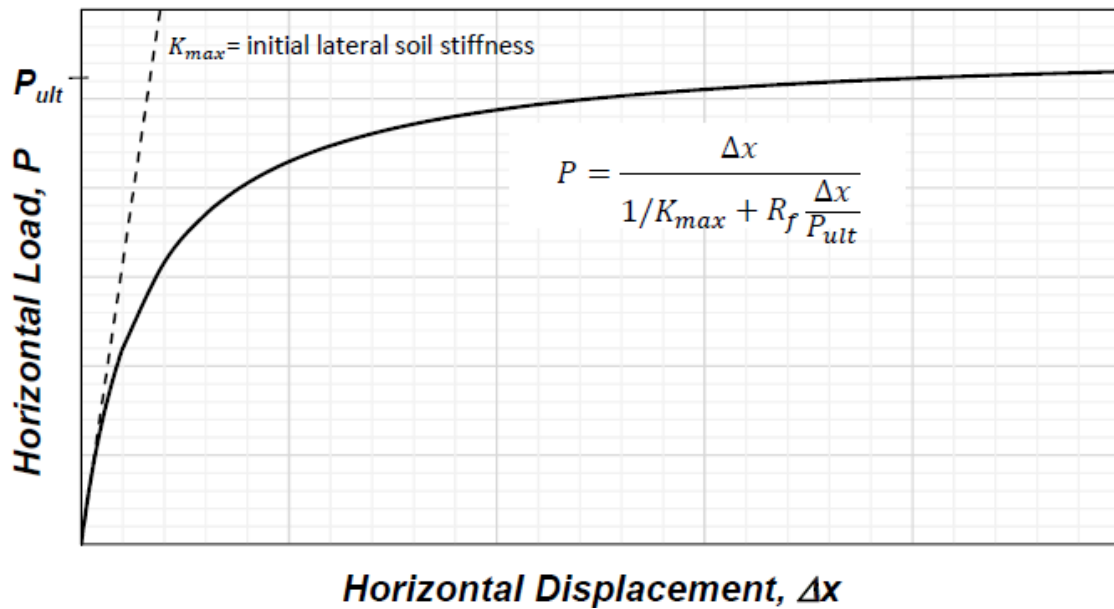


**Figure 7.7** Horizontal load versus deflection curve based on Eq. 7.5 (adapted from Duncan and Mokwa 2001).

Consistent with the recommendations in Duncan and Mokwa (2001), the initial stiffness,  $K_{max}$ , was estimated based on an elastic half-space solution developed by Douglas and Davis (1964), which requires estimates for the initial soil elastic modulus,  $E_{soil}$ , and Poisson's ratio,  $\nu$ . The initial stiffness also depends on the surface area (i.e., footing embedment,  $D_f$  and length,  $L$ ) where the passive resistance develops. The initial soil elastic modulus was calculated as described in Eq. 7.4. A Poisson's ratio,  $\nu = 0.5$  was assumed, consistent with saturated, undrained behavior of the foundation soil. This implies the soil does not compress with loading, but instead deforms in shear. Footing embedment depth and length are noted in Table 7.2.

The ultimate passive resistance acting on the foundations was calculated based on the undrained shear strength and embedment depth, including 3D effects, as (e.g., Terzaghi et al. 1996):

$$P_{ult} = (P_p - P_a)L + 2s_u D_f^2 \quad (7.6)$$

where  $P_p$  and  $P_a$  are the unit passive and active resistances developed in the soil. For this case, no active pressure was assumed (i.e.,  $P_a = 0$ ) because the footing embedment is less than the critical depth of embedment for the stiff foundation soil (Terzaghi et al. 1996). The unit passive resistance was calculated as (e.g., Terzaghi et al. 1996):

$$P_p = \frac{1}{2}\gamma D_f^2 + 2s_u D_f \quad (7.7)$$

Consistent with the vertical foundation springs, the horizontal springs were modeled having no resistance in tension. However, the springs were assumed to act in both horizontal directions because the footings were modeled as being laterally supported (i.e., buried) on all sides. The calculated passive resistance for the different footings with assumed nominal undrained shear strength,  $s_u = 70$  kPa is indicated in Table 7.2. The actual passive resistance mobilized on the sides of the footings varied based on the varying undrained shear strength, as described below.

### 7.2.3 Soil Spatial Variability and Random Field Model

The bearing capacity, ultimate passive resistance, and mobilized resistances for shallow spread footings under total stress ( $\phi = 0$ ) analyses depend primarily on the undrained shear strength,  $s_u$ , of the foundation soil, which exhibits inherent variability with depth and distance. Spread footing analyses typically assume a representative or nominal value of  $s_u$  averaged over the foundation width and depth of influence (e.g., Skempton 1951), providing a reasonable approximation of the individual footing response. However, the variability in  $s_u$  between individual footings must still be accounted for when evaluating the overall foundation system of a structure and the subsequent structural response.

Soil spatial variability for geotechnical analyses is often represented using random field theory (RFT Vanmarke 1977, 1983), considering in-situ soil properties that exhibit location-specific dependence and must be modeled probabilistically. A soil property, for example  $s_u$ , can be conveniently represented over a horizontal distance,  $x$ , as (e.g., Phoon and Kulhawy 1999a):

$$s_u(x) = t(x) + w(x) \quad (7.8)$$

where  $t(x)$  is the trend function and  $w(x)$  is the fluctuation about the trend that represents the inherent soil variability. The magnitude and breadth of the variability about the trend can be described in terms of the coefficient of inherent variability,  $COV_w$ , and the scale of fluctuation,  $\delta$ , termed random field model (RFM) parameters. When  $w$  can be considered statistically homogeneous (i.e., stationary), the coefficient of inherent variability is defined as (e.g., Phoon and Kulhawy 1999a):

$$COV_w(x) = \frac{\sigma_w(x)}{t(x)} \quad (7.9)$$

where  $\sigma_w$  is the standard deviation of  $w$ .

The scale of fluctuation is defined as (Vanmarcke 1977, 1983):

$$\delta = \int_{-\infty}^{+\infty} \rho_{\Delta x} d(\Delta x) = 2 \int_0^{+\infty} \rho_{\Delta x} d(\Delta x) \quad (7.10)$$

where  $\rho_{\Delta x}$  is the autocorrelation between incremental points along  $x$ . Several methods have been developed for estimating  $\delta$  for a given set of data (e.g., a soil layer) as discussed by Vanmarcke (1977, 1983), Jaksa (1995), Jaksa et al. (1999), Phoon et al. (2003), Uzielli et al. (2007), and Stuedlein et al. (2012a), among others. In general, the scale of fluctuation is the distance within which a soil exhibits strong correlation. A small  $\delta$  value indicates

greater frequency in fluctuation above and below the trend value  $t(x)$ , while a large  $\delta$  value indicates a longer distance between the observed property crossing  $t(x)$ .

Phoon et al. (1995) completed an extensive literature review to estimate typical values of the coefficient of inherent variability and the scale of fluctuation for different soil engineering properties (also summarized in Phoon and Kulhawy 1999a). They reported coefficients of inherent variability,  $COV_w$ , for  $s_u$  (hereafter defined as  $COV_w(s_u)$ ) ranging from 6 to 80 percent for various laboratory strength tests, with mean  $COV_w(s_u)$  ranging from 22 to 33 percent. They also reported  $COV_w(s_u)$  ranging from 4 to 44 percent for in-situ vane shear tests, with a mean  $COV_w(s_u)$  of 24 percent. It should be noted that  $COV_w(s_u)$  in the referenced study did not distinguish between measurements in the vertical or horizontal direction, which may be important for anisotropic soils. Therefore, the horizontal coefficient of inherent variability is further defined herein as  $COV_{w,h}$ . For the scale of fluctuation in the horizontal direction,  $\delta_h$ , Phoon et al. (1995) reported  $s_u$  measurements from in-situ vane shear tests for three studies indicating  $\delta_h(s_u)$  values ranging from 46 to 60 m with a mean value of 50.7 m. Despite the effort by Phoon et al. (1995), real world data for  $COV_{w,h}(s_u)$  and  $\delta_h(s_u)$  are limited in both quantity and by large distances that separate the measurements, indicating that the resolution of these RFM parameters is low. Stuedlein and Bong (2017) opine that there is still a need to identify typical values of  $COV_{w,h}(s_u)$  and  $\delta_h(s_u)$ , possibly based on soil type or geologic formation, but acknowledge the limited data stems from the lack of horizontal explorations that could provide better resolution of these RFM parameters.

Owing to the large range of reported  $COV_{w,h}(s_u)$  and  $\delta_h(s_u)$ , but relative lack of data, characteristic values to model soil variability were not selected for this study. Instead, the

variability of  $s_u$  across the width of the building was modeled using RFT assuming  $COV_{w,h}(s_u)$  of 0, 5, 10, 20, 30, 50 and 100 percent, and  $\delta_h(s_u)$  of 0.1, 0.2, 0.5, 1, 2, 5, 10, 20, 30, 50 and 100 m. The intent is to study how the change in each RFM parameter, or combination of RFM parameters, affects the soil response and how it contributes to the resulting foundation and structural performance due to SSI. The selected range in values for  $COV_{w,h}(s_u)$  and  $\delta_h(s_u)$  is meant to encompass the range in expected real-world RFM parameters. Several lower magnitude values of  $\delta_h(s_u)$  were selected because these closer distances were assumed to have greater impact on foundation performance, as discussed in more detail below.

Horizontal  $s_u$  profiles across the building area were generated using the program R with the aid of the package RandomFields (Schlather et al. 2016). A nominal undrained shear strength across the entire building area  $s_u = 70$  kPa was used for all simulations and specific  $s_u$  values were generated at a horizontal interval of  $x = 0.02$  m for each combination of  $COV_{w,h}(s_u)$  and  $\delta_h(s_u)$  noted above. Selected examples of horizontal  $s_u$  profiles with combinations of  $COV_{w,h}(s_u)$  equal to 10 and 30 percent and  $\delta_h(s_u)$  equal to 5, 20 and 50 m are provided in Fig. 7.8.

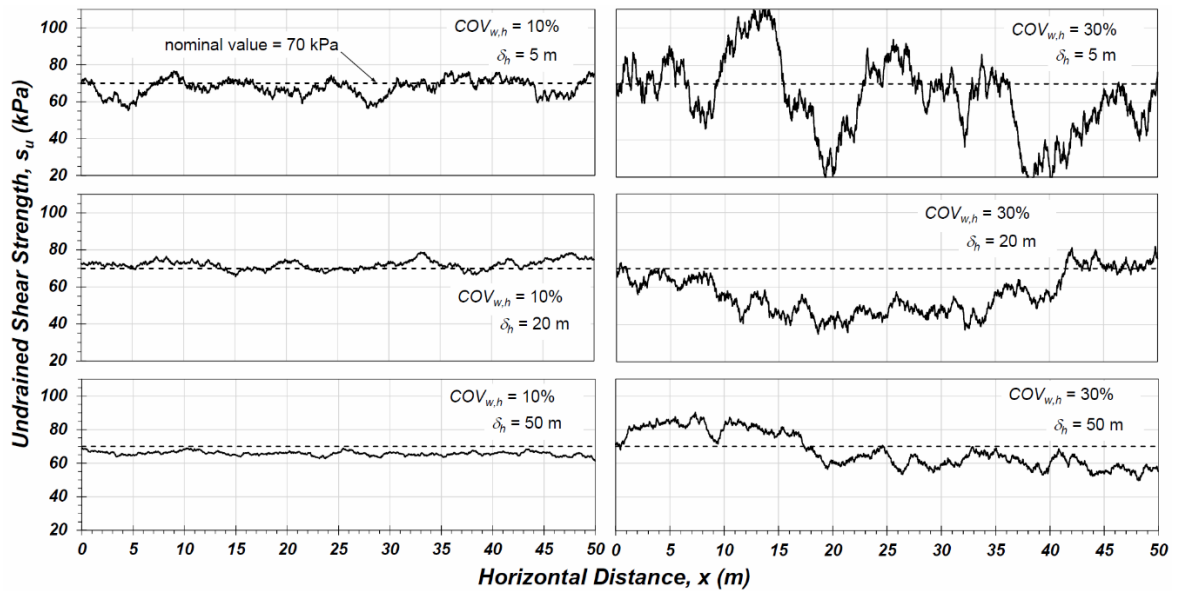


**Figure 7.8** Examples of undrained shear strength across horizontal building footprints with varying  $COV_{w,h}$  and  $\delta_h$  values.

The operative  $s_u$  for each of the five footing locations was computed in consideration of the local horizontal variability. For bearing resistance beneath individual footings,  $s_u$  was calculated as the mean value across the width,  $B$ , of the footing. For passive resistance on each side of the footing,  $s_u$  was calculated as the mean value extending from the edge of the individual footing to a distance  $B$  beyond the footing given the anticipated lack of full passive failure during construction of the SE building.

#### 7.2.4 Inter-site versus Intra-site Bearing Pressure-Displacement Response

The nonlinear bearing pressure-displacement response (Eq. 7.1) developed in Chapter 5 (Huffman et al. 2015) includes normalized parameters  $k_1$ ,  $k_2$ , and  $M_{STC}$ , which were calibrated from full-scale footing loading tests using a global (i.e., inter-site) database. These parameters were treated as random variables in the reliability analyses with noted

characteristic distributions summarized in Table 7.3 and correlation structure as summarized in Chapter 5 (Huffman et al. 2015) and in Table 7.4. Figures 7.9 and 7.10 provide plots of the model parameters. A global database was used in Chapter 5 (Huffman et al. 2015) for two related reasons: (1) the intent of the study was to provide a general (i.e., global) means to evaluate SLS design of spread footings on plastic, fine-grained soil subject to immediate displacement; and (2) the larger dataset allows for a more robust statistical characterization of the SLS parameters compared to a small dataset that may be obtained from a single site.

Geotechnical design parameters often exhibit strong site-specific characteristics and correlation structure based on the governing geologic unit. Therefore, it is reasonable that the bearing pressure-displacement model parameters, even when normalized, will have site-specific (i.e., intra-site) characteristics that influence the bearing pressure-displacement response. To investigate the potential for intra-site-specific characteristics influencing the foundation bearing pressure-displacement response, separate MCS were completed using model parameters generated based on either the global dataset or a subset from a single test location. The intra-site model parameters were developed based on loading tests completed at the Oregon State University (OSU) Geotechnical Engineering Field Research Site (GEFRS). These include loading tests performed by Newton (1975), which were included in the original global dataset, and newer tests performed by Martin (2018). When compared to the global dataset, the OSU GEFRS dataset model parameters ( $k_1$ ,  $k_2$  and  $M_{STC}$ ) exhibit a notably smaller range of values, as observed in Figures 7.9 and 7.10.



**Table 7.4. Summary of copula functions representing bivariate dependence in the vine copula used for MCS.**

	Dependent Pair	Best-Fit Copula	Copula Param., $\theta$	Copula Probability Function, $C(u, v)$
Global loading test database (Note 1)	$k_1-k_2$	Clayton (rotated 270°)	-7.054	$u - [u^{-\theta} + (1-v)^{-\theta} - u^{-\theta}(1-v)^{-\theta}]^{-\frac{1}{\theta}}$
	$k_1-M_{STC}$	Clayton (rotated 270°)	-3.143	$u - [u^{-\theta} + (1-v)^{-\theta} - u^{-\theta}(1-v)^{-\theta}]^{-\frac{1}{\theta}}$
	$k_2-M_{STC}$	Joe (rotated 180°)	1.398	$u + v - 1 - \left[ \left( 1 - ((1-u)^{-\theta} + (1-v)^{-\theta} - 1) \right)^{\frac{1}{\theta}} \right]$
OSU GEFRS loading tests (Note 2)	$k_1-k_2$	Frank	-16.124	$-\frac{1}{\theta} \log \left[ 1 + \frac{(\exp(-\theta u) - 1)(\exp(-\theta v) - 1)}{\exp(-\theta) - 1} \right]$
	$k_1-M_{STC}$	Frank	-2.590	$-\frac{1}{\theta} \log \left[ 1 + \frac{(\exp(-\theta u) - 1)(\exp(-\theta v) - 1)}{\exp(-\theta) - 1} \right]$
	$k_2-M_{STC}$	Frank	4.425	$-\frac{1}{\theta} \log \left[ 1 + \frac{(\exp(-\theta u) - 1)(\exp(-\theta v) - 1)}{\exp(-\theta) - 1} \right]$

- Notes:**
1. See Chapter 5 (Huffman et al. 2015) for further discussion of vine copula fitting for the global loading test database soil-foundation spring parameters.
  2. The Frank copula fitting for each of the OSU GEFRS (i.e., intra-site) model parameters was selected to provide a uniform linear correlation structure for the rank values.
  3. Coefficients  $u$  and  $v$  for copula density functions represent the rank values of the dependent variable pairs transposed to  $[0,1]$  space (e.g.,  $u_1$  and  $u_2$  for the  $k_1-k_2$  pairs).

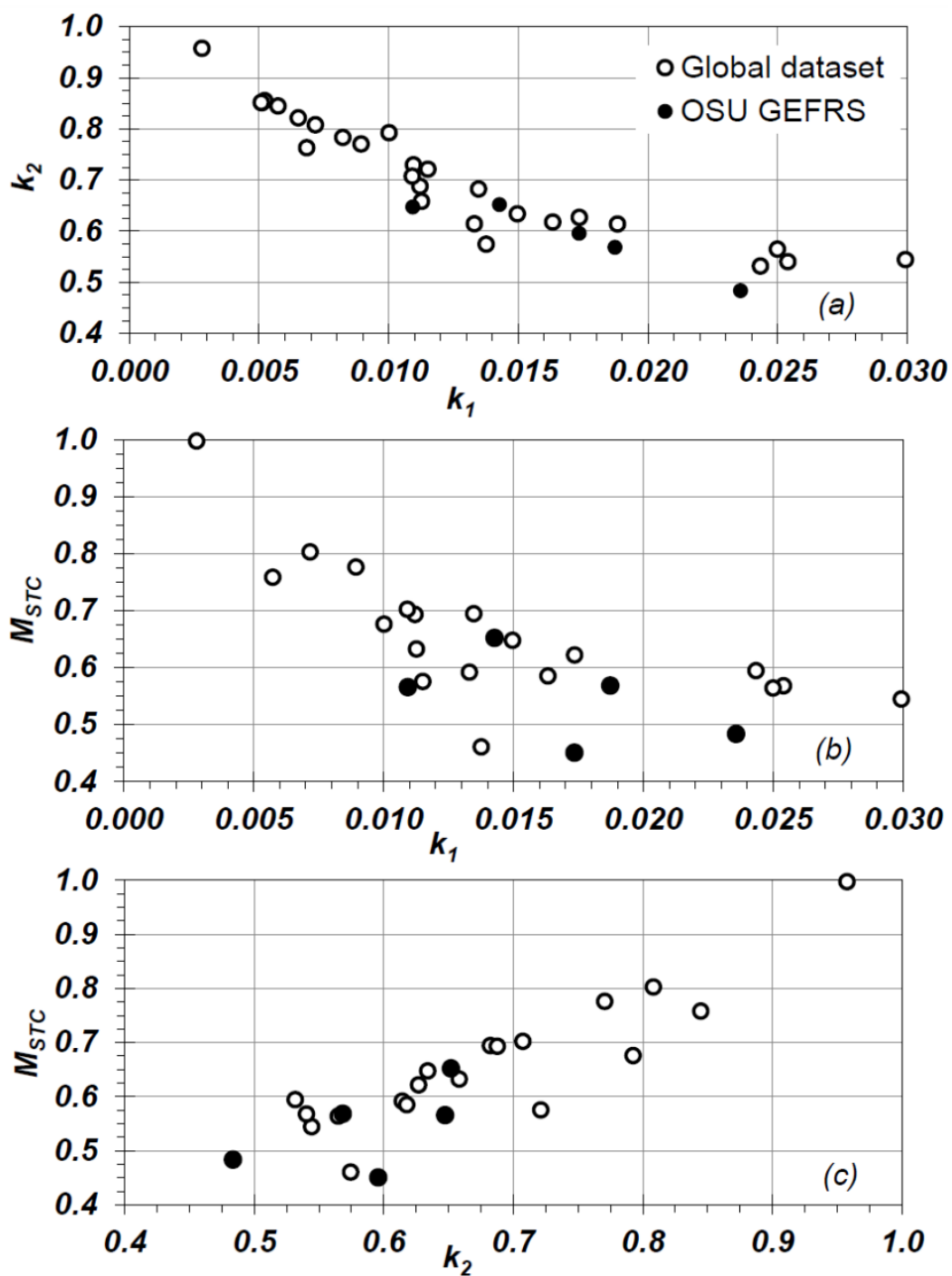


**Figure 7.9** Normalized bearing pressure-displacement factors from the global and OSU GEFRS datasets plotted versus each other for a)  $k_1$ - $k_2$ , b)  $k_1$ - $M_{STC}$ , and c)  $k_2$ - $M_{STC}$ .

Because the intra-site  $k_1$ ,  $k_2$  and  $M_{STC}$  parameters were fit based on only five loading tests, the distribution and dependence structure of each parameter cannot be characterized using the same robust fitting procedure described in Chapter 5 (Huffman et al. 2015) for the global dataset. Instead the MCS analyses for the intra-site study described below sampled each parameter by assuming a uniform distribution with a range extending plus/minus one-half standard deviation beyond the maximum and minimum values fit from the five OSU GEFRS loading tests. Parameter dependence was modeled using multi-dimensional vine copula analyses, consistent with Chapter 5 (Huffman et al. 2015). However, bivariate Frank copulas were used to describe the dependence structure between each of the parameters (i.e.,  $k_1$ - $k_2$ ,  $k_1$ - $M_{STC}$ , and  $k_2$ - $M_{STC}$  dependence), instead of the combination of best-fit Clayton (rotated 270°) and Joe (rotated 180°) copulas as summarized in Chapter 5 (Huffman et al. 2015) and Table 7.4. The Frank copula was selected because it generally describes a linear rank dependence structure without stronger or weaker tail dependence, suitable for the limited dataset. Samples of simulated  $k_1$ - $k_2$ ,  $k_1$ - $M_{STC}$  and  $k_2$ - $M_{STC}$  pairs are plotted with the OSU GEFRS dataset and the global dataset in Fig. 7.10. It should be recognized that the parameter distribution and dependence structure selected herein may not truly represent the specific characteristics of GEFRS because of the small sample size and selected fitting and sampling procedure. However, these parameters may be assumed to represent the intra-site model parameters for a general location similar in geotechnical characterization as the GEFRS and suitable for the investigation conducted in this study.

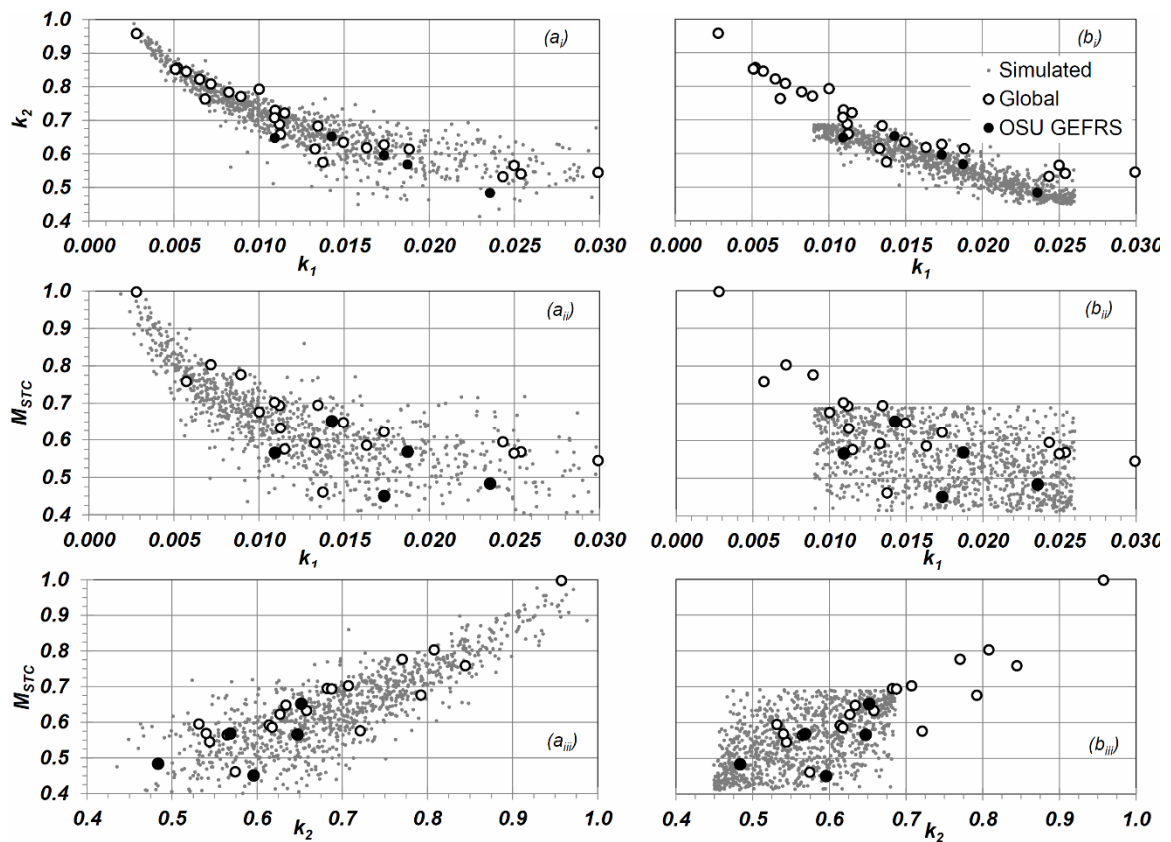


**Figure 7.10** Normalized bearing pressure-displacement factors from the global and OSU GEFRS datasets with  $n = 1,000$  simulated values based on a) global dataset characteristics distributions and dependencies and b) OSU GEFRS characteristics distributions and dependencies.

### 7.3 RELIABILITY ANALYSIS AND MONTE CARLO SIMULATIONS

Reliability analyses were completed with MCS using R and OpenSees and the building-foundation-soil models described above. Four separate cases with multiple sets of MCS were completed to evaluate the effects of inherent soil spatial variability, soil-foundation model variability, and soil-structure interaction on the foundation and building performance. These cases include:

- **Case 1.** Footings were modeled to act “independently” without the effects soil-structure interaction that results from structural stiffness and re-distribution of

building and foundation loads. To do so, the MCS was completed using R, wherein the simulated foundation loads were applied as a uniform bearing pressure acting over the footing area. The model included the five footings with center-to-center spacing equal to 9.15 m, consistent with the layout of the structure. The loads were applied as a vertical bearing pressure only. Therefore, rotational and lateral resistance springs were not required. The vertical soil-foundation resistance parameters ( $k_1$ ,  $k_2$  and  $M_{STC}$ ) were generated by seeding the MCS with characteristic distributions and dependence structure based on the global (inter-site) database consistent with Chapter 5 (Huffman et al. 2015). The MCS was not programmed to analyze bearing capacity failure. Therefore, when necessary for extreme footing displacements (i.e., footings on soft soil where the sampled  $s_u$  is very low), the total vertical displacement for the individual footings was limited to a depth equal to the footing width,  $B$ . It is assumed that any additional foundation movement would likely result in rotational failure and/or horizontal displacement of the footing with little or no additional vertical displacement, consistent with typical bearing capacity models (e.g., Terzaghi 1943).

- **Case 2.** This case is similar to Case 1, with the exception that the soil-foundation parameters for vertical springs were generated by seeding the MCS with characteristic distributions and dependence structure based on the site-specific (intra-site) parameters developed from the OSU GEFRS loading test results.
- **Case 3.** The effects of soil-structure interaction between the foundations and the SMRF building model are captured. The building and foundation models were developed in OpenSees as described above, with soil-foundation spring parameters

and variable  $s_u$  values sampled from profiles generated in R. The soil-foundation parameters for vertical and rotational springs ( $k_1$ ,  $k_2$  and  $M_{STC}$ ) were generated by seeding the MCS with characteristic distributions and dependence structure based on the global database consistent with Chapter 5 (Huffman et al. 2015). Within OpenSees, recorders were used to “measure” simulated footing displacement and rotation from soil movement (i.e., mobilization of the soil-springs). Recorders were also used to measure simulated displacement and rotation at the ends of individual beam.

- **Case 4.** This case is similar to Case 3, with the exception that the soil-foundation parameters for vertical and rotational springs were generated by seeding the MCS with characteristic distributions and dependence structure based on the site-specific (intra-site) parameters developed from the OSU GEFRS loading test results.

The MCS analyses were completed for the range of  $COV_{w,h}(s_u)$  and  $\delta_h(s_u)$  values indicated above to vary  $s_u$  across the building footprint. Fifty-thousand realizations were simulated for each MCS run associated with different combinations of  $COV_{w,h}(s_u)$  and  $\delta_h(s_u)$ . The minimum number of realizations for each MCS run must be enough to provide confidence in the results. Broding et al. (1964) describes a concise relationship between the number of MCS realizations,  $N$ , target probability of failure,  $p_f$ , desired confidence level,  $\alpha$ , and number of variables,  $X$ , as:

$$N \geq -\frac{\ln(1-\alpha)}{p_f} \cdot X \quad (7.11)$$

The number of variables,  $X$ , is 16 when considering the three foundation-soil spring parameters ( $k_1$ ,  $k_2$  and  $M_{STC}$ ) for each of the five footings, plus the undrained shear strength,

$s_u$ . The target probability of failure (or probability of exceeding a selected limit state value) must be selected *a-priori*. For the typical target value for exceeding the footing serviceability limit state to be on the order of 0.01 to 0.001 (e.g., Fenton and Griffiths 2008), and a confidence level,  $\alpha = 99$  percent, then the required number of realizations,  $N$ , is in the range of approximately 7,000 to 70,000. For a confidence level,  $\alpha = 95$  percent,  $N$  is in the range of approximately 5,000 to 50,000. Therefore, the selected number of realizations, 50,000, is reasonable for a confidence interval of at least 95%.

The number of realizations was also selected in part based on utility and computational limits. Whereas Case 1 and 2 MCS runs were each completed within minutes, the Case 3 and 4 MCS runs using data from R in combinations with OpenSees took significantly longer. The exact timing of each MCS run completed with OpenSees cannot be reported accurately because the simulations stopped or paused several times due to different circumstances that included non-convergence of individual simulations, lag time from queuing of multiple data requests from multiple users, and similar issues using remote computing and different host servers. However, it can be reported that both Case 3 and 4 MCS took several months to greater than one year to generate the full number of intended runs.

Generation and sampling of model parameters and development of the nonlinear soil-foundation springs were completed as described in Chapter 5 (Huffman et al. 2015), with the following exceptions. The mobilized vertical and rotational resistance is a function of the predicted bearing capacity,  $q_{ult,p}$ . Chapter 5 (Huffman et al. 2015) included variability in  $q_{ult,p}$  based on the interpreted-versus-predicted bearing capacity from the global loading test database, identified in Chapter 5 (Huffman et al. 2015) as the  $q_{ult,i}/q_{ult,p}$

bias. For this study,  $q_{ult,p}$  was considered to be a deterministic value and variability in the bearing resistance was modeled based on the inherent variability of  $s_u$ . This change was considered necessary because most of the variability observed between the measured and predicted bearing capacities in the loading tests is believed to be from variation in the actual, rather than assumed or generalized,  $s_u$  values. Therefore, including variability in both the sampled  $q_{ult,p}$  and  $s_u$  values would result in an overestimate of variability in the overall soil-foundation spring model that is not reflective of actual conditions. Chapter 5 (Huffman et al. 2015) also included a lower-bound truncation for the distribution of bearing resistance, identified as  $q^{*}_{ult,min}$ . The lower-bound resistance was based on calculating  $q_{ult,p}$  using remolded undrained shear strength,  $s_{ur}$ , estimated from the global loading test database following recommendations by Najjar (2005) and Najjar and Gilbert (2009). Since  $q_{ult,p}$  was considered a deterministic value, the lower-bound truncation within the current MCS was provided by limiting the lower-bound  $s_u$  values based on the characteristic  $s_{ur}$  value, as estimated from loading tests. Following similar procedures as outlined in Chapter 5 (Huffman et al. 2015), a lower-bound  $s_{ur}$ -to- $s_u$  ratio of 0.24 was selected, which is equal to the mean  $s_{ur}$ -to- $s_u$  ratio of 0.44 from the database minus one standard deviation equal to 0.20. In this case, for a selected mean value of  $s_u$  equal to 70 kPa for the foundation soil, the minimum  $s_u$  value was set equal to 16.4 kPa (i.e., 70 kPa multiplied by 0.24). The following sections describe the results of the four cases of MCS reliability analyses.



### 7.3.1 Case 1: Soil-Foundation Response (Inter-site Soil Parameters)

This case focused on evaluating the soil-foundation response for the five building footings acting independently. As an initial benchmark for comparison apart from the Case 1 MCS results, vertical foundation displacements were estimated using Eq. 7.1 in combination with the mean resistance parameters ( $k_1$ ,  $k_2$ , and  $M_{STC}$ ) for the global dataset summarized in Table 7.3, and ultimate bearing resistance using Eq. 7.2 assuming  $s_u$  equal to 70 kPa and  $\gamma$  equal to 19 kN/m<sup>3</sup>. Table 7.5 provides a summary of the calculated vertical displacements,  $s$ , which range from approximately 23.2 to 29.3 mm. Because these initial calculations assumed no variation in the soil strength or soil-foundation resistance parameters, the difference in vertical displacements for the individual footings is solely due to the variation in footing size and modest variation in applied bearing pressure noted in Table 7.2. The calculated displacements reported in Table 7.5 serve to provide a reference for comparison to the median displacements returned from the MCS analyses. The calculated values summarized in Table 7.5 are typically lower than the mean displacements returned from the MCS, particularly for simulations that include greater variability in soil strength (i.e., larger  $COV_{w,h}(s_u)$  values), because the largest displacements from individual simulations tend to skew the mean values higher, as discussed in more detail below.

The corresponding differential displacement and angular distortion are also summarized in Table 7.5. The differential displacement,  $\Delta s$ , was calculated as the absolute difference in total vertical displacement between adjacent footings. Angular distortion,  $\Delta s/l$ , was calculated as the differential displacement divided by the bay width or center-to-center distance between the footings ( $l = 9.15$  m). The calculated differential displacements and corresponding angular distortions between footings summarized in

Table 7.5 would only be accurate if the soil were truly uniform without any variability in the shear strength or the soil-spring parameters across the building footprint. Therefore,  $\Delta s$  and  $\Delta s/l$  values in Table 7.5 should not be considered benchmark values or physically meaningful. Instead, these values are only noted to introduce the concepts of differential displacement and angular distortion for discussion later in this study.

**Table 7.5. Calculated vertical footing displacements and corresponding differential displacement and distortion across each bay based on mean resistance parameters.**

		Bay 1		Bay 2	Bay 3	Bay 4	
		Footing 1	Footing 2	Footing 3	Footing 4	Footing 5	
Global loading test database (Case 1 and 3)	Vertical displacement, $s$ (mm)	23.2	29.2	29.3	27.9	23.8	
	Differential displacement, $\Delta s$ (mm)		6.0	0.1	1.5	4.1	
	Angular distortion, $\Delta s/l$		1/1,523	1/76,459	1/6,232	1/2,221	
OSU GEFRS loading tests (Case 2 and 4)	Vertical displacement, $s$ (mm)	36.3	45.7	45.9	43.6	37.2	
	Differential displacement, $\Delta s$ (mm)		9.4	0.2	2.3	6.5	
	Angular distortion, $\Delta s/l$		1/973	1/49,078	1/4,000	1/1,416	

- Notes:**
1. Vertical displacements were calculated based on Eqs. 7.1 and 7.2 and the mean resistance parameters for the global loading test database summarized in Table 7.3.
  2. Differential displacement across each bay was calculated as the difference in vertical displacements between adjacent footings.
  3. Angular distortion across each bay was calculated as the differential displacement divided over the center-to-center footing distance of 9.15 m. Values are provided in fraction format for ease of comparison between values.

Table 7.6 provides a summary of selected results of simulated footing displacements for the Case 1 MCS. Because of the large amount of data analyzed, and for the sake of brevity, only MCS results for  $COV_{w,h}(s_u)$  equal to 10 and 30 percent are reported in Table 7.6 (additional MCS data is presented in Appendix C of this dissertation). The selected  $COV_{w,h}(s_u)$  values represented in Table 7.6 are within the range of mean values reported by Phoon et al. (1995) for field and lab-measured  $s_u$  data and provide a basis for comparison. Table 7.6 reports the mean and median vertical footing displacements, the standard deviation of vertical displacement, the coefficient of variation,  $COV(s)$ , defined as the standard deviation divided by the mean vertical displacement, and the failure rate, defined herein as the percent of simulations where the vertical displacement,  $s$ , was equal to footing width,  $B$ , for each of the five footings (see description at the beginning of Section 7.3 for Case 1 summary). For the case with  $COV_{w,h}(s_u)$  equal to 10 percent, there is little change in the simulated mean or median footing displacement with changes in the horizontal scale of fluctuation,  $\delta_h(s_u)$ . Furthermore, no simulations with  $COV_{w,h}(s_u)$  equal to 10 percent reached displacements equal to  $B$  (i.e., bearing failure). However, for  $COV_{w,h}(s_u)$  equal to 30 percent, the median displacement remains approximately constant but a significant increase in mean footing displacement are noted for  $\delta_h(s_u)$  increasing from 0.1 m to 10 m. The increase in mean displacement then stabilizes for  $\delta_h(s_u)$  greater than 10 m. In addition, the footing failure rate increases from 0 to greater than 2 percent as  $\delta_h(s_u)$  increases for  $COV_{w,h}(s_u)$  equal to 30 percent.

**Table 7.6. Summary of vertical footing displacement for selected Case 1 MCS results with  $COV_{w,h}(s_u)$  values of 10 and 30 percent.**

Footing:	$COV_{w,h}(s_u) = 10\%$					$COV_{w,h}(s_u) = 30\%$				
	1	2	3	4	5	1	2	3	4	5
<b><math>\delta_h(s_u) = 0.1 \text{ m}</math></b>										
Mean $s$ (mm)	25.2	26.1	26.5	25.0	25.9	26.0	26.8	26.9	25.3	26.4
Median $s$ (mm)	21.4	22.1	22.4	21.2	21.9	21.5	22.3	22.4	21.1	22.0
Std. dev. $s$ (mm)	17.1	17.8	18.1	17.0	19.1	18.7	19.2	19.2	18.0	18.9
COV( $s$ )	0.68	0.68	0.68	0.68	0.74	0.72	0.71	0.71	0.71	0.71
Failure rate (%)	0.00	0.00	0.00	0.00	0.00	0.00	0.00	0.00	0.00	0.00
<b><math>\delta_h(s_u) = 0.2 \text{ m}</math></b>										
Mean $s$ (mm)	25.5	26.3	26.5	25.1	26.0	26.9	27.4	27.8	26.2	27.5
Median $s$ (mm)	21.6	22.2	22.3	21.2	21.9	21.7	22.4	22.6	21.5	22.2
Std. dev. $s$ (mm)	17.4	18.0	18.1	17.1	17.8	22.5	20.8	21.0	19.7	24.0
COV( $s$ )	0.68	0.68	0.69	0.68	0.69	0.84	0.76	0.76	0.75	0.87
Failure rate (%)	0.00	0.00	0.00	0.00	0.00	0.00	0.00	0.00	0.00	0.00
<b><math>\delta_h(s_u) = 0.5 \text{ m}</math></b>										
Mean $s$ (mm)	25.6	26.5	26.6	25.2	26.1	30.9	31.1	30.6	29.2	31.5
Median $s$ (mm)	21.5	22.2	22.3	21.2	21.8	22.1	22.8	22.8	21.8	22.5
Std. dev. $s$ (mm)	17.9	18.4	18.4	17.4	18.3	57.9	59.9	47.8	50.8	58.1
COV( $s$ )	0.70	0.69	0.69	0.69	0.70	1.87	1.93	1.56	1.74	1.84
Failure rate (%)	0.00	0.00	0.00	0.00	0.00	0.07	0.05	0.03	0.04	0.08
<b><math>\delta_h(s_u) = 1 \text{ m}</math></b>										
Mean $s$ (mm)	25.6	26.6	26.5	25.3	26.2	39.6	40.0	40.7	37.0	42.3
Median $s$ (mm)	21.4	22.2	22.2	21.2	21.8	22.2	22.9	23.2	22.1	22.8
Std. dev. $s$ (mm)	17.8	18.6	18.5	17.7	18.4	116.8	131.3	131.6	117.1	128.8
COV( $s$ )	0.70	0.70	0.70	0.70	0.70	2.95	3.28	3.23	3.16	3.05
Failure rate (%)	0.00	0.00	0.00	0.00	0.00	0.41	0.33	0.33	0.26	0.50
<b><math>\delta_h(s_u) = 2 \text{ m}</math></b>										
Mean $s$ (mm)	25.9	27.0	26.7	25.5	26.2	50.1	54.8	55.9	51.5	54.6
Median $s$ (mm)	21.6	22.4	22.3	21.2	21.9	22.4	23.3	23.4	22.2	23.0
Std. dev. $s$ (mm)	18.2	21.3	19.0	20.2	18.5	168.6	204.0	212.0	197.4	183.2
COV( $s$ )	0.70	0.79	0.71	0.79	0.70	3.36	3.73	3.79	3.84	3.35
Failure rate (%)	0.00	0.00	0.00	0.00	0.00	0.94	0.84	0.94	0.79	1.11
<b><math>\delta_h(s_u) = 5 \text{ m}</math></b>										
Mean $s$ (mm)	26.0	26.9	26.9	25.6	26.5	64.9	73.9	74.3	67.9	68.4
Median $s$ (mm)	21.6	22.4	22.5	21.3	22.0	22.5	23.4	23.5	22.2	23.2
Std. dev. $s$ (mm)	18.5	19.3	19.2	18.1	18.8	224.1	279.8	279.3	264.7	232.1
COV( $s$ )	0.71	0.72	0.71	0.71	0.71	3.45	3.79	3.76	3.90	3.40
Failure rate (%)	0.00	0.00	0.00	0.00	0.00	1.72	1.69	1.67	1.50	1.86

**Notes:** 1. Results based on MCS with  $n = 50,000$  realizations.

2. Coefficient of variation,  $COV = \text{standard deviation}/\text{mean}$ .

3. Failure rate is defined herein as the percentage of MCS realizations with vertical displacement,  $s$ , is equal to the footing width,  $B$ .

**Table 7.6. Summary of vertical footing displacement for selected Case 1 MCS results with  $COV_{w,h}(s_u)$  values of 10 and 30 percent (continued).**

Footing:	$COV_{w,h}(s_u) = 10\%$					$COV_{w,h}(s_u) = 30\%$				
	1	2	3	4	5	1	2	3	4	5
<b><math>\delta_h(s_u) = 10 \text{ m}</math></b>										
Mean $s$ (mm)	25.9	27.0	27.1	25.6	26.6	71.1	82.2	81.6	75.9	74.4
Median $s$ (mm)	21.5	22.4	22.5	21.2	22.1	22.6	23.5	23.7	22.5	23.1
Std. dev. $s$ (mm)	18.4	19.3	19.4	18.3	19.2	242.8	305.8	302.7	291.9	250.8
COV( $s$ )	0.71	0.72	0.72	0.72	0.72	3.41	3.72	3.71	3.84	3.37
Failure rate (%)	0.00	0.00	0.00	0.00	0.00	2.04	2.05	1.98	1.86	2.19
<b><math>\delta_h(s_u) = 20 \text{ m}</math></b>										
Mean $s$ (mm)	25.9	26.9	27.2	25.8	26.6	72.4	85.2	86.8	78.5	72.9
Median $s$ (mm)	21.5	22.3	22.6	21.4	22.1	22.7	23.4	23.6	22.0	22.9
Std. dev. $s$ (mm)	18.6	19.3	19.7	18.4	19.1	245.2	315.4	319.5	301.8	246.6
COV( $s$ )	0.72	0.72	0.72	0.72	0.72	3.39	3.70	3.68	3.84	3.38
Failure rate (%)	0.00	0.00	0.00	0.00	0.00	2.09	2.17	2.25	1.99	2.11
<b><math>\delta_h(s_u) = 30 \text{ m}</math></b>										
Mean $s$ (mm)	25.8	27.0	27.0	25.6	26.6	72.6	88.2	90.5	83.3	78.1
Median $s$ (mm)	21.6	22.4	22.3	21.3	22.1	22.9	23.4	23.7	22.5	23.2
Std. dev. $s$ (mm)	18.3	19.5	19.5	18.4	19.3	247.3	325.0	329.8	313.3	261.4
COV( $s$ )	0.71	0.72	0.72	0.72	0.72	3.41	3.68	3.65	3.76	3.35
Failure rate (%)	0.00	0.00	0.00	0.00	0.00	2.14	2.33	2.40	2.16	2.40
<b><math>\delta_h(s_u) = 50 \text{ m}</math></b>										
Mean $s$ (mm)	26.0	27.1	27.1	25.8	26.8	72.8	86.6	86.4	80.9	76.1
Median $s$ (mm)	21.6	22.5	22.4	21.5	22.2	22.5	23.4	23.6	22.3	23.3
Std. dev. $s$ (mm)	18.7	19.5	19.5	21.2	19.3	248.6	320.0	317.8	307.4	254.6
COV( $s$ )	0.72	0.72	0.72	0.82	0.72	3.42	3.70	3.68	3.80	3.34
Failure rate (%)	0.00	0.00	0.00	0.00	0.00	2.15	2.26	2.21	2.07	2.26
<b><math>\delta_h(s_u) = 100 \text{ m}</math></b>										
Mean $s$ (mm)	26.1	27.0	27.1	25.7	26.7	73.6	90.3	91.5	83.1	77.6
Median $s$ (mm)	21.6	22.4	22.4	21.4	22.1	22.5	23.8	23.7	22.3	23.1
Std. dev. $s$ (mm)	18.8	19.6	19.7	18.4	19.3	251.2	329.9	333.3	314.5	259.5
COV( $s$ )	0.72	0.72	0.73	0.72	0.72	3.41	3.66	3.64	3.78	3.34
Failure rate (%)	0.00	0.00	0.00	0.00	0.00	2.23	2.39	2.45	2.17	2.35

**Notes:** 1. Results based on MCS with  $n = 50,000$  realizations.

2. Coefficient of variation,  $COV = \text{standard deviation}/\text{mean}$ .

3. Failure rate is defined herein as the percentage of MCS realizations with vertical displacement,  $s$ , equal to the footing width,  $B$ .

Some of these trends noted in Table 7.6 can also be observed by comparing the cumulative distributions shown in Fig. 7.11, which includes the example for Footing 2 (Fig. 7.2) with  $\delta_h(s_u)$  equal to 50 m and the full range of  $COV_{w,h}(s_u)$  values included in this study. Results for the other footing locations (i.e., Footings 1, 3, 4 and 5) are generally consistent with those shown for Footing 2. While the median vertical footing displacement for each of the  $COV_{w,h}(s_u)$  values is in the range of  $s = 20$  to 25 mm, the mean footing displacement for larger values of  $COV_{w,h}(s_u)$  becomes significantly greater (e.g., mean  $s = 86.6$  mm for  $COV_{w,h}(s_u) = 30$  percent and  $\delta_h(s_u) = 50$  m; Table 7.6) owing to the frequency at which large vertical displacements occur for larger values of  $COV_{w,h}(s_u)$ .

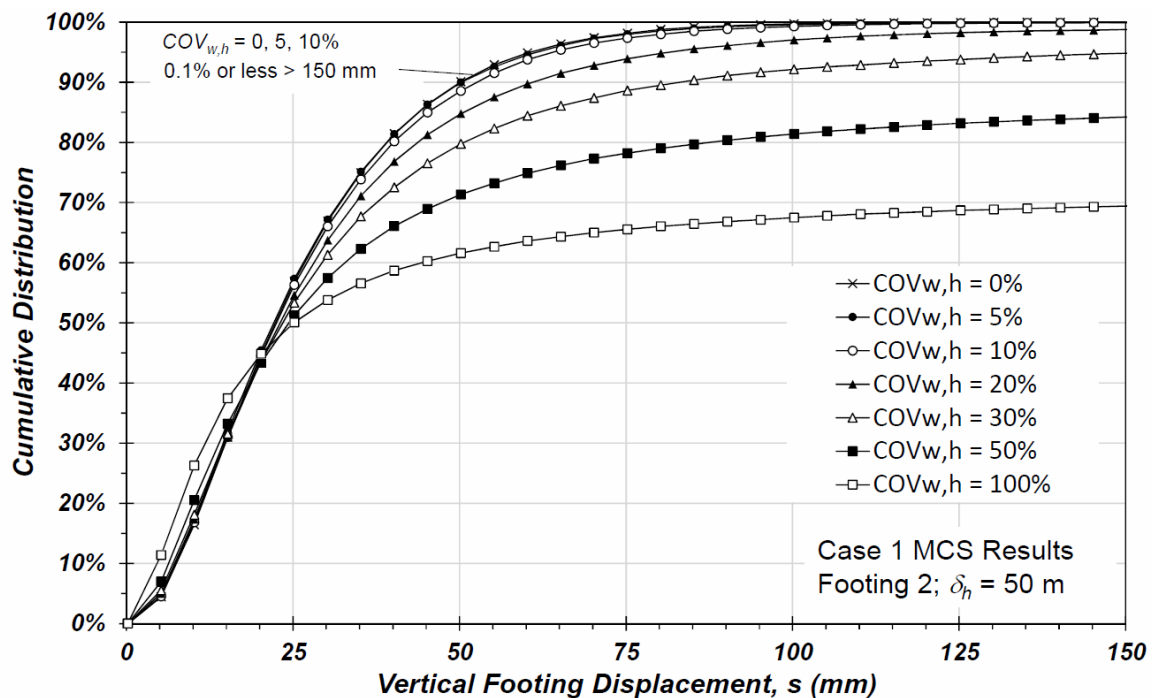


**Figure 7.11** Distribution of vertical footing displacement for selected Case 1 MCS results for Footing 2.

While total settlement of individual footings is an important aspect of geotechnical and structural performance, typically the greater concern for structures supported on multiple foundations is differential displacement,  $\Delta s$ , or angular distortion,  $\Delta s/l$ , across the multiple foundations. Skempton and MacDonald (1956) and Polshkin and Tokar (1957) initially proposed guidelines based on observed foundation settlements (total and differential) and corresponding building performance. Those studies were reprised by Grant et al. (1974), Burland and Wroth (1974), and Wahls (1981) to help establish guidelines for allowable or tolerable building foundation settlements and angular distortion. Building performance with relation to foundation movement from deep excavations or tunneling was studied by Clough and O'Rourke (1990), Boscardin and Cording (1989), and Son and Cording (2005, 2011). Stuedlein and Bong (2017) studied the role of soil spatial variability on static and liquefaction-induced differential foundation settlements and building performance. Despite the variation between structure types (e.g., load-bearing brick walls versus steel frames), the general recommendations provided by Skempton and MacDonald (1956) remain widely accepted as the basis for the comparison of structural performance. For example,  $\Delta s/l$  exceeding 1/150 has been shown to cause structural damage associated with the ultimate limit state (ULS) in many structural elements, while  $\Delta s/l$  greater than 1/300 will often cause cracking or distortion exceeding the serviceability limit state (SLS). Relatively minor or cosmetic damage is often observed when  $\Delta s/l$  exceeds 1/500. Therefore, this level of angular distortion may be considered an "allowable" limit for typical design (Skempton and MacDonald 1956). For the structure evaluated in this study with center-to-center footing distance (or bay width)  $l = 9.15$  m, the corresponding

differential displacements are  $\Delta s = 61$  mm for  $\Delta s/l = 1/150$ ,  $\Delta s = 30.5$  mm for  $\Delta s/l = 1/300$ , and  $\Delta s = 18.3$  mm for  $\Delta s/l = 1/500$ .

Table 7.7 provides a summary of mean and median differential displacements and angular distortions at selected bay locations for the Case 1 MCS for each of the corresponding values of  $COV_{w,h}(s_u)$  and  $\delta_h(s_u)$  included in this study. Similar to the individual footing settlements documented in Table 7.6, the simulated differential displacements and angular distortions were observed to be relatively consistent between each of the four building bays. Therefore, only the maximum value of the mean and median  $\Delta s$  and  $\Delta s/l$  are reported for the respective building bay for the different combinations of  $COV_{w,h}(s_u)$  and  $\delta_h(s_u)$ . Also consistent with the individual footing settlement, it is observed that the mean and median values of  $\Delta s$  and  $\Delta s/l$  remain relatively consistent for  $COV_{w,h}(s_u) = 0, 5$  and  $10$  percent for all values of  $\delta_h(s_u)$ . For  $COV_{w,h}(s_u) = 20$  percent and greater, the median  $\Delta s$  and  $\Delta s/l$  values increase modestly with larger  $COV_{w,h}(s_u)$  values, while the mean values increase significantly. These trends can also be observed by comparing the cumulative distribution of  $\Delta s$ , shown in Fig. 7.12, which includes the example for Bay 1 (i.e., Footings 1 and 2) with  $\delta_h(s_u)$  equal to  $50$  m and the range of  $COV_{w,h}(s_u)$  values. Noted performance benchmarks with  $\Delta s/l = 1/500, 1/300$  and  $1/150$  are also identified in Fig. 7.12. The median differential displacements between adjacent footings were typically on the order of two-thirds of the median vertical displacements at the individual footings.



**Table 7.7. Summary of differential displacement and angular distortion at selected building bay for Case 1 MCS.**

$COV_{w,h}(s_u) =$	0	5%	10%	20%	30%	50%	100%
<b><math>\delta_n(s_u) = 0.1 \text{ m}</math></b>							
Mean $\Delta s$ (mm)	18.9	19.0	19.1	19.4	19.9	21.3	22.8
Median $\Delta s$ (mm)	14.5	14.5	14.7	14.7	15.0	15.4	14.0
COV( $\Delta s$ )	0.88	0.88	0.96	0.90	0.92	1.32	2.43
Mean $\Delta s/l$	1/484	1/481	1/479	1/473	1/459	1/429	1/401
Median $\Delta s/l$	1/633	1/630	1/624	1/622	1/611	1/594	1/655
<b><math>\delta_n(s_u) = 0.2 \text{ m}</math></b>							
Mean $\Delta s$ (mm)	19.0	18.9	19.1	19.7	21.0	27.1	47.9
Median $\Delta s$ (mm)	14.5	14.6	14.7	14.9	15.4	16.2	15.8
COV( $\Delta s$ )	0.88	0.88	0.88	1.04	1.08	2.54	4.11
Mean $\Delta s/l$	1/483	1/483	1/480	1/464	1/435	1/337	1/191
Median $\Delta s/l$	1/629	1/628	1/623	1/614	1/595	1/564	1/580
<b><math>\delta_n(s_u) = 0.5 \text{ m}</math></b>							
Mean $\Delta s$ (mm)	19.0	19.1	19.4	21.1	27.9	76.9	207.3
Median $\Delta s$ (mm)	14.6	14.6	14.8	15.4	16.5	19.4	22.3
COV( $\Delta s$ )	0.88	1.01	0.90	1.07	2.82	3.80	2.73
Mean $\Delta s/l$	1/483	1/479	1/472	1/433	1/328	1/119	1/44
Median $\Delta s/l$	1/625	1/625	1/620	1/594	1/554	1/472	1/411
<b><math>\delta_n(s_u) = 1 \text{ m}</math></b>							
Mean $\Delta s$ (mm)	19.0	19.2	19.6	22.9	45.3	175.5	411.9
Median $\Delta s$ (mm)	14.7	14.7	14.8	16.0	17.6	22.7	31.3
COV( $\Delta s$ )	1.01	0.89	0.90	1.61	3.99	2.92	1.91
Mean $\Delta s/l$	1/482	1/476	1/467	1/400	1/202	1/52	1/22
Median $\Delta s/l$	1/625	1/622	1/617	1/573	1/519	1/403	1/293
<b><math>\delta_n(s_u) = 2 \text{ m}</math></b>							
Mean $\Delta s$ (mm)	18.8	19.0	19.9	26.3	73.8	290.1	602.3
Median $\Delta s$ (mm)	14.5	14.7	14.9	16.3	18.7	25.3	46.7
COV( $\Delta s$ )	0.96	0.89	1.03	2.72	3.92	2.29	1.52
Mean $\Delta s/l$	1/487	1/481	1/459	1/348	1/124	1/32	1/15
Median $\Delta s/l$	1/631	1/622	1/613	1/562	1/490	1/362	1/196
<b><math>\delta_n(s_u) = 5 \text{ m}</math></b>							
Mean $\Delta s$ (mm)	18.9	19.3	20.0	30.0	106.2	367.4	673.2
Median $\Delta s$ (mm)	14.5	14.7	15.1	16.3	19.0	25.9	63.8
COV( $\Delta s$ )	0.88	1.01	0.92	3.43	3.58	2.04	1.40
Mean $\Delta s/l$	1/485	1/475	1/458	1/305	1/86	1/25	1/14
Median $\Delta s/l$	1/629	1/624	1/607	1/560	1/483	1/353	1/143

**Notes:** 1. Results based on MCS with  $n = 50,000$  realizations.

2. Selected values reported for each  $COV_{w,h}$  represent the largest mean or median value observed for Bay 1, 2, 3 or 4. Results were typically similar for the other bays not reported in this table.
3. Differential displacement coefficient of variation,  $COV = \text{standard deviation}/\text{mean}$ .
4. Angular distortion across the selected bay,  $\Delta s/l$ , was calculated as the differential displacement divided over the center-to-center footing distance of 9.15 m. Values are provided in fraction format for ease of comparison between values.

**Table 7.7. Summary of differential displacement and angular distortion at selected building bay for Case 1 MCS (continued).**

$COV_{w,h}(s_u) =$	0	5%	10%	20%	30%	50%	100%
<b><math>\delta_h(s_u) = 10 \text{ m}</math></b>							
Mean $\Delta s$ (mm)	18.9	19.1	19.9	30.5	109.8	346.6	601.0
Median $\Delta s$ (mm)	14.6	14.7	14.9	15.9	18.1	24.0	53.8
COV( $\Delta s$ )	0.88	0.89	0.92	3.59	3.55	2.10	1.51
Mean $\Delta s/l$	1/484	1/480	1/460	1/300	1/83	1/26	1/15
Median $\Delta s/l$	1/627	1/624	1/613	1/575	1/504	1/380	1/170
<b><math>\delta_h(s_u) = 20 \text{ m}</math></b>							
Mean $\Delta s$ (mm)	19.0	19.1	19.9	31.3	101.7	290.1	491.6
Median $\Delta s$ (mm)	14.6	14.7	15.0	15.9	17.1	21.3	37.8
COV( $\Delta s$ )	1.01	0.89	0.92	3.77	3.67	2.32	1.77
Mean $\Delta s/l$	1/483	1/479	1/459	1/292	1/90	1/32	1/18
Median $\Delta s/l$	1/628	1/624	1/611	1/576	1/536	1/430	1/242
<b><math>\delta_h(s_u) = 30 \text{ m}</math></b>							
Mean $\Delta s$ (mm)	19.0	19.2	19.6	30.7	96.6	251.9	446.5
Median $\Delta s$ (mm)	14.7	14.7	14.7	15.6	16.7	19.7	32.9
COV( $\Delta s$ )	0.88	0.89	0.93	3.76	3.73	2.48	1.94
Mean $\Delta s/l$	1/482	1/476	1/466	1/298	1/95	1/36	1/20
Median $\Delta s/l$	1/623	1/624	1/624	1/588	1/549	1/466	1/278
<b><math>\delta_h(s_u) = 50 \text{ m}</math></b>							
Mean $\Delta s$ (mm)	18.8	19.2	19.7	30.0	79.7	217.5	378.5
Median $\Delta s$ (mm)	14.5	14.7	14.8	15.6	16.0	18.8	26.8
COV( $\Delta s$ )	0.88	0.97	1.07	3.76	3.92	2.72	2.21
Mean $\Delta s/l$	1/485	1/478	1/463	1/298	1/115	1/42	1/24
Median $\Delta s/l$	1/631	1/622	1/617	1/588	1/572	1/488	1/342
<b><math>\delta_h(s_u) = 100 \text{ m}</math></b>							
Mean $\Delta s$ (mm)	19.0	19.1	19.7	28.8	70.6	179.7	312.4
Median $\Delta s$ (mm)	14.7	14.7	14.8	15.3	15.7	17.8	22.5
COV( $\Delta s$ )	0.88	0.89	0.93	3.65	4.04	3.07	2.61
Mean $\Delta s/l$	1/482	1/478	1/465	1/318	1/130	1/51	1/22
Median $\Delta s/l$	1/622	1/623	1/620	1/598	1/581	1/515	1/407

**Notes:** 1. Results based on MCS with  $n = 50,000$  realizations.

2. Selected values reported for each  $COV_{w,h}$  represent the largest mean or median value observed for Bay 1, 2, 3 or 4. Results were typically similar for the other bays not reported in this table.
3. Differential displacement coefficient of variation,  $COV = \text{standard deviation}/\text{mean}$ .
4. Angular distortion across the selected bay,  $\Delta s/l$ , was calculated as the differential displacement divided over the center-to-center footing distance of 9.15 m. Values are provided in fraction format for ease of comparison between values.

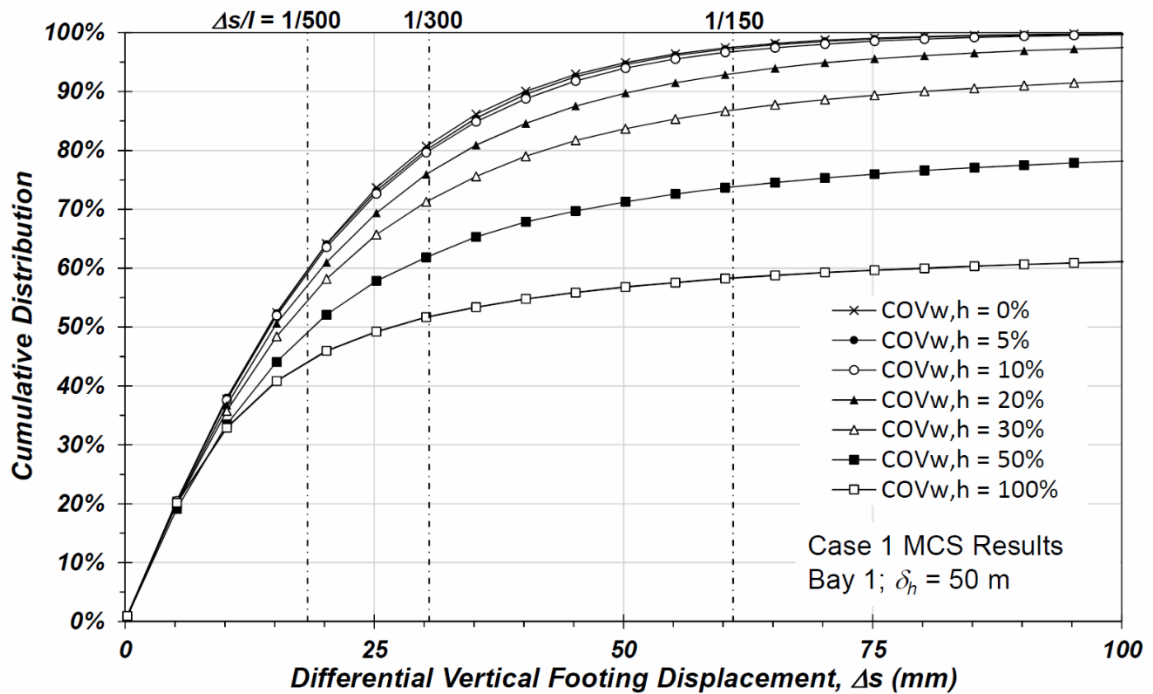


**Figure 7.12** Distribution of differential footing displacement for selected Case 1 MCS results for Bay 1.

Another trend that becomes apparent when inspecting the results summarized in Table 7.7 is that for larger  $COV_{w,h}(s_u)$  values (i.e., greater than 20 percent), the mean and median  $\Delta s$  and  $\Delta s/l$  values reach a maximum magnitude when  $\delta_h(s_u)$  is in the range of 5 to 10 m. This can also be observed by plotting the probability of exceeding selected  $\Delta s/l$  values for varying  $\delta_h(s_u)$ . Figure 7.13 presents the probability of exceedance of selected limit state  $\Delta s/l$  equal to 1/500, 1/300 and 1/150 with varying  $\delta_h(s_u)$  for Bay 1; it is apparent that the change in  $\delta_h(s_u)$  does not affect the probability of exceeding a selected  $\Delta s/l$  value for low  $COV_{w,h}(s_u)$  (i.e., less than approximately 10 percent). For  $COV_{w,h}(s_u)$  equal to 0 (not shown), 5 percent (Fig. 7.13a), and 10 percent (Fig. 7.13b), the probability of exceeding  $\Delta s/l$  equal to 1/150, 1/300 and 1/500 is approximately 0.03, 0.20, and 0.40, respectively, regardless of  $\delta_h(s_u)$ .

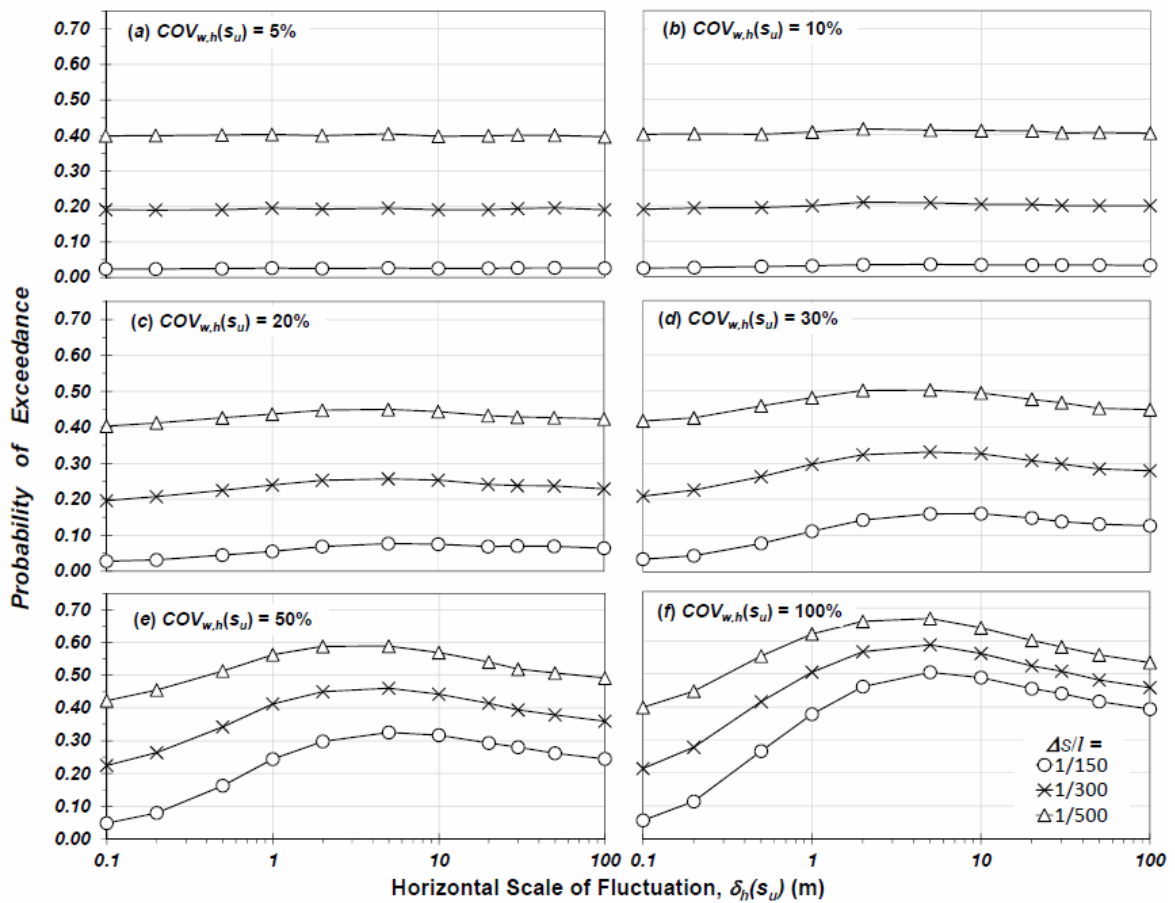


**Figure 7.13** Case 1 MCS results for Bay1. Probability of exceedance of selected limit state angular distortion for varying horizontal scale of fluctuation.

For  $COV_{w,h}(s_u)$  greater than 20 percent (Figs. 7.13c through 7.13f), there is a pronounced sensitivity of the probability of exceeding a given limit state as  $COV_{w,h}(s_u)$  increases. Furthermore, the maximum probability of exceedance of the selected limit state angular distortions is observed when  $\delta_h(s_u)$  is approximately 5 m, or approximately one-half of the bay width (i.e.,  $l/2$ ). This finding is on the same order of magnitude as that reported by Fenton and Griffiths (2002) and Ahmed and Soubra (2014), which predicted a peak probability of exceedance (defined herein as the critical scale of fluctuation or  $\delta_h(s_u)_{crit}$ ) at  $\delta_h/l$  equal to approximately 1.0. Ahmed and Soubra (2014) suggest  $\delta_h(s_u)_{crit}$

occurs at  $\delta_h/l = 1.0$  because this represents the greatest possibility of each individual footing being supported on disparate soils, resulting in differential movement between footings. For smaller horizontal scales of fluctuation when the soil strength or stiffness is fluctuating more erratically about the mean (e.g., Fig. 7.8d), the footings, which are very stiff relative to the foundation soil will span softer soil zones. Soil acts more homogeneously under footing loads for larger horizontal scales of fluctuation, thus, the footings are less susceptible to large differential displacements. The difference in maximum probability of exceedance for Case 1 MCS occurring for approximately  $\delta_h/l = 0.5$  instead of  $\delta_h/l = 1.0$  is not readily apparent, but may be due in part to the non-linear soil response assumed for this study compared to linear response assumed in other studies.

Fenton and Griffiths (2002) and Ahmed and Soubra (2014) computed footing displacement based on a randomly-distributed elastic modulus,  $E$ , and various scales of fluctuation,  $\delta_h$ . Their analyses indicated that differential footing displacement (and corresponding angular distortion) will go to zero as the horizontal scale of fluctuation,  $\delta_h(E)$ , reaches either zero or infinity. Herein, the estimated footing displacement and angular distortion with soil variability represents the use of variable undrained shear strength ( $COV_{w,h}(s_u)$  and  $\delta_h(s_u)$ ), and variable foundation spring parameters ( $k_1$ ,  $k_2$  and  $M_{STC}$ ) estimated from full-scale loading tests. Because the current study used multiple parameters to estimate foundation resistance and displacement under the building loads, the results do not indicate zero differential displacement and/or angular distortion for very large or small values of  $\delta_h(s_u)$ . Instead, Figure 7.13 suggests that for  $COV_{w,h}(s_u)$  greater than approximately 10 percent, the probability of exceeding a selected limit state angular distortion will increase rapidly as  $\delta_h(s_u)$  approaches approximately  $l/2$ , then decrease

slightly to moderately until reaching a relative plateau or steady-state value. The steady-state probability at very large  $\delta_h(s_u)$  values is greater than the initial probability of exceedance when  $\delta_h(s_u)$  is very small. For example, Figure 7.13 indicates that with  $COV_{w,h}(s_u) = 50$  percent (Fig. 7.13e) the probability of exceeding  $\Delta s/l = 1/150$  is approximately 0.05 for small values of  $\delta_h(s_u)$ , reaching a plateau of approximately 0.25 as  $\delta_h(s_u)$  increases. The probability of exceeding  $\Delta s/l = 1/500$  is approximately 0.40 for small  $\delta_h(s_u)$ , reaching a plateau value of approximately 0.50 as  $\delta_h(s_u)$  increases. While the results presented in Fenton and Griffiths (2002) and Ahmed and Soubra (2014) are most relevant for soils that remain relatively elastic with loading (e.g., medium dense to dense granular soils), the results presented in this study are expected to be more accurate for modeling foundations supported on plastic fine-grained soils under undrained loading conditions as previously described herein.

### 7.3.2 Case 2: Soil-Foundation Response (Intra-site Soil Parameters)

Case 2 evaluated the soil-foundation response considering independent responses of the five footings, similar to Case 1, but used the selected intra-site soil-foundation spring parameters to identify differences in the global performance stemming from the use of site-specific parameters. The mean spring parameters (i.e.,  $k_1$ ,  $k_2$  and  $M_{STC}$ ) are summarized in Table 7.3 and example parameter distributions for Case 2 MCS are plotted in Figure 7.10b (i through iii). Figure 7.14 provides a comparison of the calculated bearing pressure-displacement curves using the mean inter- (Case 1) and intra-site (Case 2) parameters. The normalized bearing pressure-displacement curves (Figure 7.14a) generated from these two sets of parameters are similar. However, the lower mean intra-site  $M_{STC}$  value of 0.544

compared to the mean inter-site value of 0.643 results in the intra-site curve having an overall softer response and experiencing greater vertical displacement for the exterior and interior building footings at all levels of applied bearing pressure (Figure 7.14b and 7.14c). For example, at the mean applied bearing pressure of approximately 180 kPa for the footings in this study, the predicted displacement is approximately 24 to 28 mm for the exterior and interior footings using the inter-site parameters, but approximately 37 to 44 mm for the exterior and interior footings using the intra-site parameters.

Table 7.8 provides a summary of Case 2 MCS results for vertical footing displacements where  $COV_{w,h}(s_u)$  equals 10 and 30 percent, respectively. As expected from the calculated displacements noted above, these results suggest greater mean and median footing displacements for Case 2 MCS compared to the Case 1 results summarized in Table 7.6. The trends are generally the same between the Case 1 and Case 2 MCS, with increasing mean displacements for increasing  $COV_{w,h}(s_u)$  and  $\delta_h(s_u)$ . However, the standard deviation and corresponding  $COV(s)$  for the Case 2 results are modestly lower. The reason for this becomes more apparent when comparing the results for differential displacements and angular distortions, as discussed below.

Table 7.9 provides a summary of the mean and median differential displacements and angular distortions at selected bay locations for the Case 2 MCS for each of the corresponding  $COV_{w,h}(s_u)$  and  $\delta_h(s_u)$ . Like the Case 1 results summarized in Table 7.7, the Case 2 MCS results indicated relatively consistent values for each of the four building bays and only the maximum values are reported in Table 7.9. The Case 2 MCS results indicated median differential displacements between footings,  $\Delta s$ , typically on the order 40 percent of the magnitude of the total displacement at individual footings,  $s$ . This is significantly

less compared to the Case 1 MCS results indicated above, where  $\Delta s$  was typically two-thirds of  $s$ , a result of the smaller overall uncertainty in the footing spring model parameters associated with a specific site.

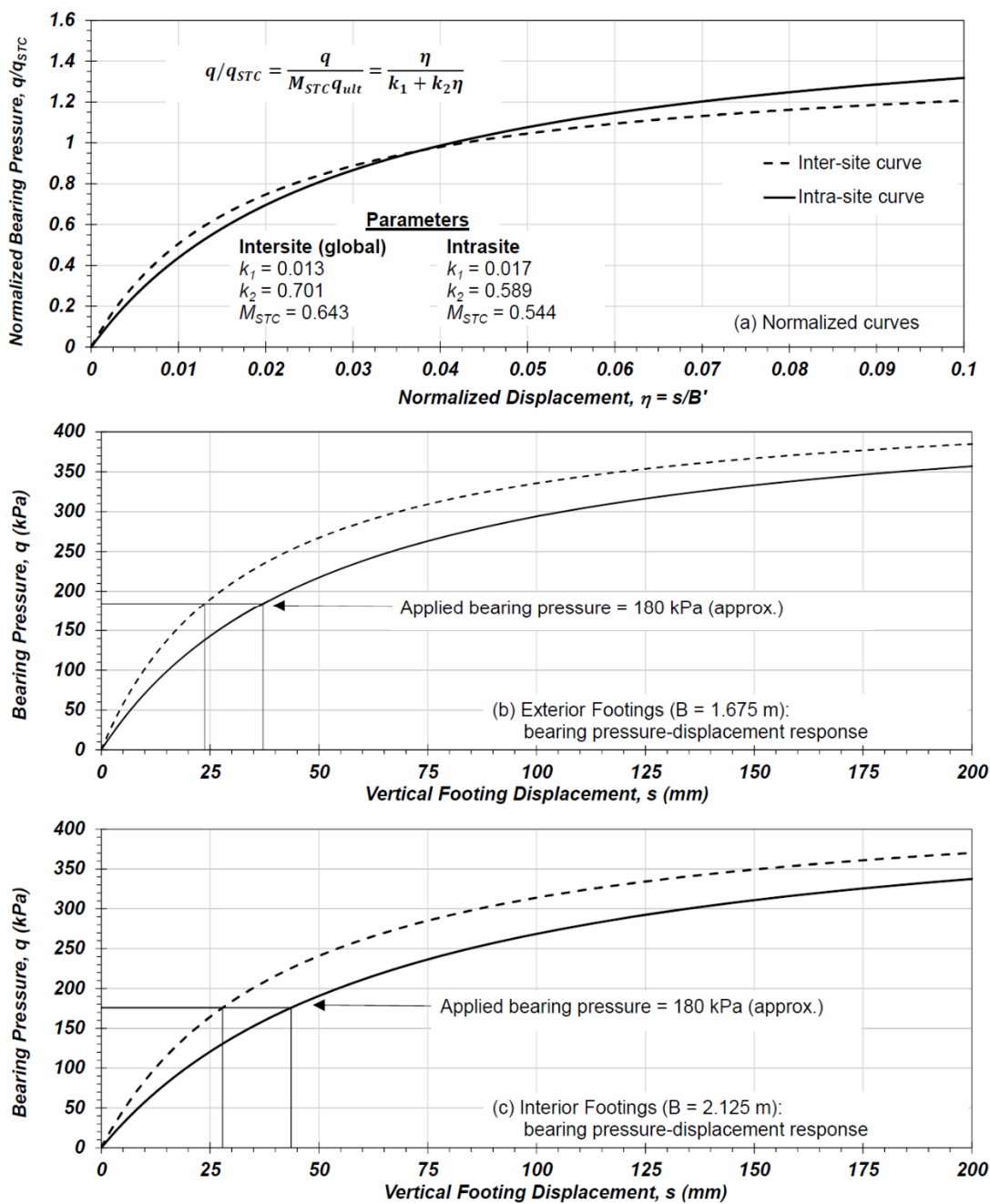


**Figure 7.14** Calculated bearing pressure-displacement response for footings using mean values for inter- and intra-site parameters.



**Table 7.8. Summary of vertical footing displacement for selected Case 2 MCS results with  $COV_{w,h}(s_u)$  values of 10 and 30 percent.**

Footing	$COV_{w,h}(s_u) = 10\%$					$COV_{w,h}(s_u) = 30\%$				
	1	2	3	4	5	1	2	3	4	5
<b><math>\delta_h(s_u) = 0.1 \text{ m}</math></b>										
Mean $s$ (mm)	36.1	37.5	37.7	35.7	36.9	37.1	38.2	38.4	36.5	38.0
Median $s$ (mm)	34.3	35.5	35.7	33.8	34.9	34.6	35.8	35.9	34.2	35.4
Std. dev. $s$ (mm)	13.6	14.1	14.2	13.4	13.9	15.4	15.7	15.7	14.9	15.8
COV( $s$ )	0.38	0.38	0.38	0.38	0.38	0.42	0.41	0.41	0.41	0.42
Failure rate (%)	0.00	0.00	0.00	0.00	0.00	0.00	0.00	0.00	0.00	0.00
<b><math>\delta_h(s_u) = 0.2 \text{ m}</math></b>										
Mean $s$ (mm)	36.3	37.4	37.7	35.8	37.1	38.1	39.0	39.2	37.2	39.1
Median $s$ (mm)	34.4	35.4	35.7	33.9	35.1	34.7	36.0	36.1	34.4	35.6
Std. dev. $s$ (mm)	13.8	14.2	14.3	13.5	14.1	17.9	17.9	17.7	16.6	18.9
COV( $s$ )	0.38	0.38	0.38	0.38	0.38	0.47	0.46	0.45	0.45	0.48
Failure rate (%)	0.00	0.00	0.00	0.00	0.00	0.00	0.00	0.00	0.00	0.00
<b><math>\delta_h(s_u) = 0.5 \text{ m}</math></b>										
Mean $s$ (mm)	36.4	37.8	38.0	35.9	37.2	42.4	42.5	42.6	40.0	43.3
Median $s$ (mm)	34.3	35.7	35.9	33.9	35.1	35.1	36.2	36.2	34.6	35.7
Std. dev. $s$ (mm)	14.2	14.6	14.7	13.8	14.6	51.6	49.4	48.2	38.3	53.7
COV( $s$ )	0.39	0.39	0.39	0.39	0.39	1.22	1.16	1.13	0.96	1.24
Failure rate (%)	0.00	0.00	0.00	0.00	0.00	0.06	0.04	0.03	0.02	0.06
<b><math>\delta_h(s_u) = 1 \text{ m}</math></b>										
Mean $s$ (mm)	36.7	37.9	38.2	36.2	37.5	51.1	50.8	51.4	47.7	52.9
Median $s$ (mm)	34.5	35.6	35.9	34.1	35.3	35.3	36.3	36.5	34.6	36.3
Std. dev. $s$ (mm)	14.6	15.1	15.1	14.3	15.0	110.0	112.6	115.9	107.3	114.6
COV( $s$ )	0.40	0.40	0.40	0.39	0.40	2.15	2.21	2.25	2.25	2.16
Failure rate (%)	0.00	0.00	0.00	0.00	0.00	0.36	0.22	0.24	0.21	0.39
<b><math>\delta_h(s_u) = 2 \text{ m}</math></b>										
Mean $s$ (mm)	36.9	38.1	38.4	36.5	37.6	62.4	65.8	65.8	60.1	64.3
Median $s$ (mm)	34.6	35.6	35.9	34.2	35.2	35.4	36.7	36.8	35.1	36.1
Std. dev. $s$ (mm)	15.0	15.4	15.6	14.8	15.3	162.9	193.9	191.0	174.3	166.6
COV( $s$ )	0.41	0.40	0.41	0.40	0.41	2.61	2.95	2.90	2.90	2.59
Failure rate (%)	0.00	0.00	0.00	0.00	0.00	0.85	0.76	0.73	0.60	0.88
<b><math>\delta_h(s_u) = 5 \text{ m}</math></b>										
Mean $s$ (mm)	36.9	38.3	38.4	36.6	37.9	73.8	83.3	83.2	77.8	76.2
Median $s$ (mm)	34.5	35.7	35.9	34.1	35.4	35.6	36.8	36.7	35.2	36.2
Std. dev. $s$ (mm)	15.2	15.8	15.9	15.1	15.6	204.8	260.6	262.1	249.9	211.3
COV( $s$ )	0.41	0.41	0.41	0.41	0.41	2.77	3.13	3.15	3.21	2.77
Failure rate (%)	0.00	0.00	0.00	0.00	0.00	1.39	1.42	1.45	1.32	1.48

**Notes:** 1. Results based on MCS with  $n = 50,000$  realizations.

2. Coefficient of variation,  $COV = \text{standard deviation}/\text{mean}$ .

3. Failure rate is defined herein as the percentage of MCS realizations with vertical displacement,  $s$ , equal to the footing width,  $B$ .

**Table 7.8. Summary of vertical footing displacement for selected Case 2 MCS results with  $COV_{w,h}(s_u)$  values of 10 and 30 percent (continued).**

Footing	$COV_{w,h}(s_u) = 10\%$					$COV_{w,h}(s_u) = 30\%$				
	1	2	3	4	5	1	2	3	4	5
<b><math>\delta_h(s_u) = 10 \text{ m}</math></b>										
Mean $s$ (mm)	37.0	38.4	38.5	36.6	37.9	78.1	88.5	90.8	84.3	82.2
Median $s$ (mm)	34.6	35.8	35.9	34.2	35.3	35.4	36.8	36.9	35.0	36.2
Std. dev. $s$ (mm)	15.4	15.9	15.9	15.2	15.7	219.7	278.7	285.4	271.0	229.7
COV( $s$ )	0.42	0.42	0.41	0.41	0.42	2.81	3.15	3.14	3.22	2.79
Failure rate (%)	0.00	0.00	0.00	0.00	0.00	1.63	1.64	1.75	1.56	1.79
<b><math>\delta_h(s_u) = 20 \text{ m}</math></b>										
Mean $s$ (mm)	37.1	38.4	38.5	36.6	37.8	81.3	91.7	93.2	86.0	83.8
Median $s$ (mm)	34.6	35.9	35.9	34.2	35.2	35.3	36.5	36.9	35.1	36.4
Std. dev. $s$ (mm)	15.4	16.0	16.2	15.1	15.8	230.6	290.3	292.8	277.9	235.9
COV( $s$ )	0.41	0.42	0.42	0.41	0.42	2.84	3.17	3.14	3.23	2.81
Failure rate (%)	0.00	0.00	0.00	0.00	0.00	1.81	1.83	1.83	1.66	1.93
<b><math>\delta_h(s_u) = 30 \text{ m}</math></b>										
Mean $s$ (mm)	37.2	38.4	38.6	36.7	38.0	82.5	95.5	95.7	87.1	84.2
Median $s$ (mm)	34.7	35.8	36.0	34.2	35.3	35.4	36.7	36.7	34.9	36.1
Std. dev. $s$ (mm)	15.6	15.9	16.1	15.1	16.0	234.5	300.3	302.6	281.5	236.7
COV( $s$ )	0.42	0.42	0.42	0.41	0.42	2.84	3.15	3.16	3.23	2.81
Failure rate (%)	0.00	0.00	0.00	0.00	0.00	1.87	1.94	1.99	1.71	1.93
<b><math>\delta_h(s_u) = 50 \text{ m}</math></b>										
Mean $s$ (mm)	37.0	38.4	38.6	36.5	37.8	85.6	97.5	98.9	90.9	86.2
Median $s$ (mm)	34.5	35.8	36.0	34.0	35.2	35.6	36.8	36.8	35.0	36.3
Std. dev. $s$ (mm)	15.4	16.2	16.1	15.3	16.0	243.3	307.9	311.0	293.6	242.8
COV( $s$ )	0.42	0.42	0.42	0.42	0.42	2.84	3.16	3.14	3.23	2.82
Failure rate (%)	0.00	0.00	0.00	0.00	0.00	2.06	2.06	2.12	1.86	2.05
<b><math>\delta_h(s_u) = 100 \text{ m}</math></b>										
Mean $s$ (mm)	37.0	38.5	38.7	36.7	37.9	83.3	96.7	97.6	90.9	86.7
Median $s$ (mm)	34.6	35.9	36.0	34.2	35.3	35.5	36.6	36.7	35.2	36.2
Std. dev. $s$ (mm)	15.4	16.1	16.2	15.3	15.9	236.6	304.5	308.0	294.6	243.6
COV( $s$ )	0.42	0.42	0.42	0.42	0.42	2.84	3.15	3.16	3.24	2.81
Failure rate (%)	0.00	0.00	0.00	0.00	0.00	1.92	2.01	2.07	1.89	2.02

**Notes:** 1. Results based on MCS with  $n = 50,000$  realizations.

2. Coefficient of variation,  $COV = \text{standard deviation}/\text{mean}$ .

3. Failure rate is defined herein as the percentage of MCS realizations with vertical displacement,  $s$ , equal to the footing width,  $B$ .

**Table 7.9. Summary of differential displacement and angular distortion at selected building bay for Case 2 MCS.**

$COV_{w,h}(s_u) =$	0	5%	10%	20%	30%	50%	100%
<b><math>\delta_n(s_u) = 0.1 \text{ m}</math></b>							
Mean $\Delta s$ (mm)	15.8	15.9	16.1	16.9	17.6	19.6	22.1
Median $\Delta s$ (mm)	13.5	13.5	13.7	14.1	14.6	15.3	14.8
COV( $\Delta s$ )	0.74	0.74	0.75	0.75	0.78	1.02	1.97
Mean $\Delta s/l$	1/578	1/577	1/567	1/555	1/521	1/466	1/415
Median $\Delta s/l$	1/677	1/680	1/667	1/656	1/628	1/597	1/617
<b><math>\delta_n(s_u) = 0.2 \text{ m}</math></b>							
Mean $\Delta s$ (mm)	15.9	16.0	16.2	17.2	19.1	26.2	49.3
Median $\Delta s$ (mm)	13.6	13.6	13.8	14.4	15.3	17.1	18.3
COV( $\Delta s$ )	0.74	0.74	0.75	0.78	0.88	2.23	3.69
Mean $\Delta s/l$	1/574	1/573	1/565	1/532	1/480	1/349	1/186
Median $\Delta s/l$	1/673	1/672	1/664	1/637	1/598	1/534	1/499
<b><math>\delta_n(s_u) = 0.5 \text{ m}</math></b>							
Mean $\Delta s$ (mm)	15.9	16.0	16.6	18.9	26.5	73.1	193.5
Median $\Delta s$ (mm)	13.7	13.7	13.9	15.1	17.1	21.8	27.6
COV( $\Delta s$ )	0.74	0.74	0.75	0.87	2.49	3.61	2.72
Mean $\Delta s/l$	1/575	1/570	1/553	1/485	1/345	1/125	1/47
Median $\Delta s/l$	1/670	1/669	1/656	1/605	1/535	1/421	1/331
<b><math>\delta_n(s_u) = 1 \text{ m}</math></b>							
Mean $\Delta s$ (mm)	15.9	16.2	16.9	21.2	43.2	160.2	394.1
Median $\Delta s$ (mm)	13.5	13.9	14.2	16.0	18.8	26.3	40.7
COV( $\Delta s$ )	0.74	0.75	0.77	1.52	3.74	2.87	1.90
Mean $\Delta s/l$	1/575	1/564	1/541	1/431	1/212	1/57	1/23
Median $\Delta s/l$	1/676	1/660	1/646	1/572	1/487	1/348	1/225
<b><math>\delta_n(s_u) = 2 \text{ m}</math></b>							
Mean $\Delta s$ (mm)	15.9	16.2	17.3	25.2	70.4	270.8	569.1
Median $\Delta s$ (mm)	13.6	13.8	14.4	16.8	20.6	30.6	59.9
COV( $\Delta s$ )	0.73	0.75	0.78	2.63	3.77	2.31	1.52
Mean $\Delta s/l$	1/574	1/564	1/529	1/363	1/130	1/34	1/16
Median $\Delta s/l$	1/671	1/664	1/636	1/543	1/445	1/299	1/153
<b><math>\delta_n(s_u) = 5 \text{ m}</math></b>							
Mean $\Delta s$ (mm)	15.9	16.3	17.4	28.5	99.7	354.0	657.3
Median $\Delta s$ (mm)	13.6	13.8	14.4	16.9	20.6	31.0	80.0
COV( $\Delta s$ )	0.74	0.75	0.79	3.26	3.54	2.04	1.39
Mean $\Delta s/l$	1/574	1/562	1/525	1/321	1/92	1/26	1/14
Median $\Delta s/l$	1/671	1/663	1/635	1/543	1/444	1/295	1/114

**Notes:** 1. Results based on MCS with  $n = 50,000$  realizations.

2. Selected values reported for each  $COV_{w,h}$  represent the largest mean or median value observed for Bay 1, 2, 3 or 4. Results were typically similar for the other bays not reported in this table.
3. Differential displacement coefficient of variation,  $COV = \text{standard deviation}/\text{mean}$ .
4. Angular distortion across the selected bay,  $\Delta s/l$ , was calculated as the differential displacement divided over the center-to-center footing distance of 9.15 m. Values are provided in fraction format for ease of comparison between values.

**Table 7.9. Summary of differential displacement and angular distortion at selected building bay for Case 2 MCS (continued).**

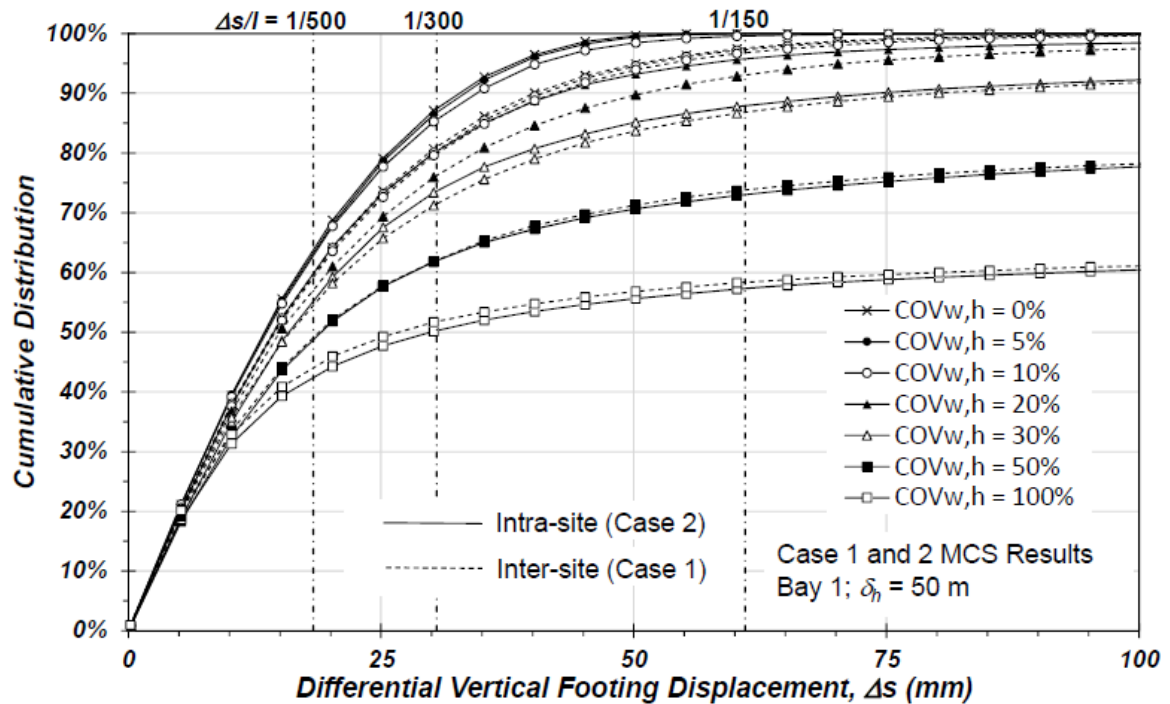
$COV_{w,h}(s_u) =$	0	5%	10%	20%	30%	50%	100%
<b><math>\delta_h(s_u) = 10 \text{ m}</math></b>							
Mean $\Delta s$ (mm)	16.0	16.0	17.1	29.5	101.7	332.8	588.4
Median $\Delta s$ (mm)	13.8	13.7	14.1	16.3	19.3	26.9	63.6
COV( $\Delta s$ )	0.74	0.75	0.79	3.65	3.53	2.10	1.52
Mean $\Delta s/l$	1/572	1/565	1/534	1/310	1/90	1/27	1/16
Median $\Delta s/l$	1/665	1/668	1/647	1/560	1/474	1/340	1/144
<b><math>\delta_h(s_u) = 20 \text{ m}</math></b>							
Mean $\Delta s$ (mm)	15.9	16.1	16.9	26.6	90.8	280.2	488.9
Median $\Delta s$ (mm)	13.6	13.6	14.1	15.3	17.3	22.8	46.9
COV( $\Delta s$ )	0.74	0.75	0.78	3.57	3.69	2.30	1.75
Mean $\Delta s/l$	1/575	1/570	1/542	1/344	1/101	1/33	1/19
Median $\Delta s/l$	1/674	1/674	1/650	1/598	1/529	1/401	1/195
<b><math>\delta_h(s_u) = 30 \text{ m}</math></b>							
Mean $\Delta s$ (mm)	15.9	16.1	16.7	26.9	83.8	239.2	432.8
Median $\Delta s$ (mm)	13.6	13.7	13.7	15.0	16.4	20.7	37.3
COV( $\Delta s$ )	0.74	0.75	0.78	3.80	3.83	2.47	1.93
Mean $\Delta s/l$	1/575	1/568	1/549	1/341	1/109	1/38	1/21
Median $\Delta s/l$	1/672	1/668	1/666	1/611	1/557	1/442	1/245
<b><math>\delta_h(s_u) = 50 \text{ m}</math></b>							
Mean $\Delta s$ (mm)	16.0	16.1	16.7	24.9	76.5	210.9	372.7
Median $\Delta s$ (mm)	13.8	13.7	13.8	14.6	15.8	18.9	29.9
COV( $\Delta s$ )	0.74	0.74	0.79	3.58	3.94	2.71	2.17
Mean $\Delta s/l$	1/571	1/569	1/549	1/367	1/120	1/43	1/25
Median $\Delta s/l$	1/664	1/668	1/662	1/628	1/580	1/484	1/306
<b><math>\delta_h(s_u) = 100 \text{ m}</math></b>							
Mean $\Delta s$ (mm)	15.9	16.1	16.5	24.9	62.5	169.7	307.7
Median $\Delta s$ (mm)	13.5	13.7	13.7	14.6	15.1	17.3	23.4
COV( $\Delta s$ )	0.74	0.74	0.78	3.58	4.12	3.03	2.55
Mean $\Delta s/l$	1/577	1/570	1/554	1/367	1/146	1/55	1/30
Median $\Delta s/l$	1/677	1/669	1/669	1/628	1/607	1/530	1/391

**Notes:** 1. Results based on MCS with  $n = 50,000$  realizations.

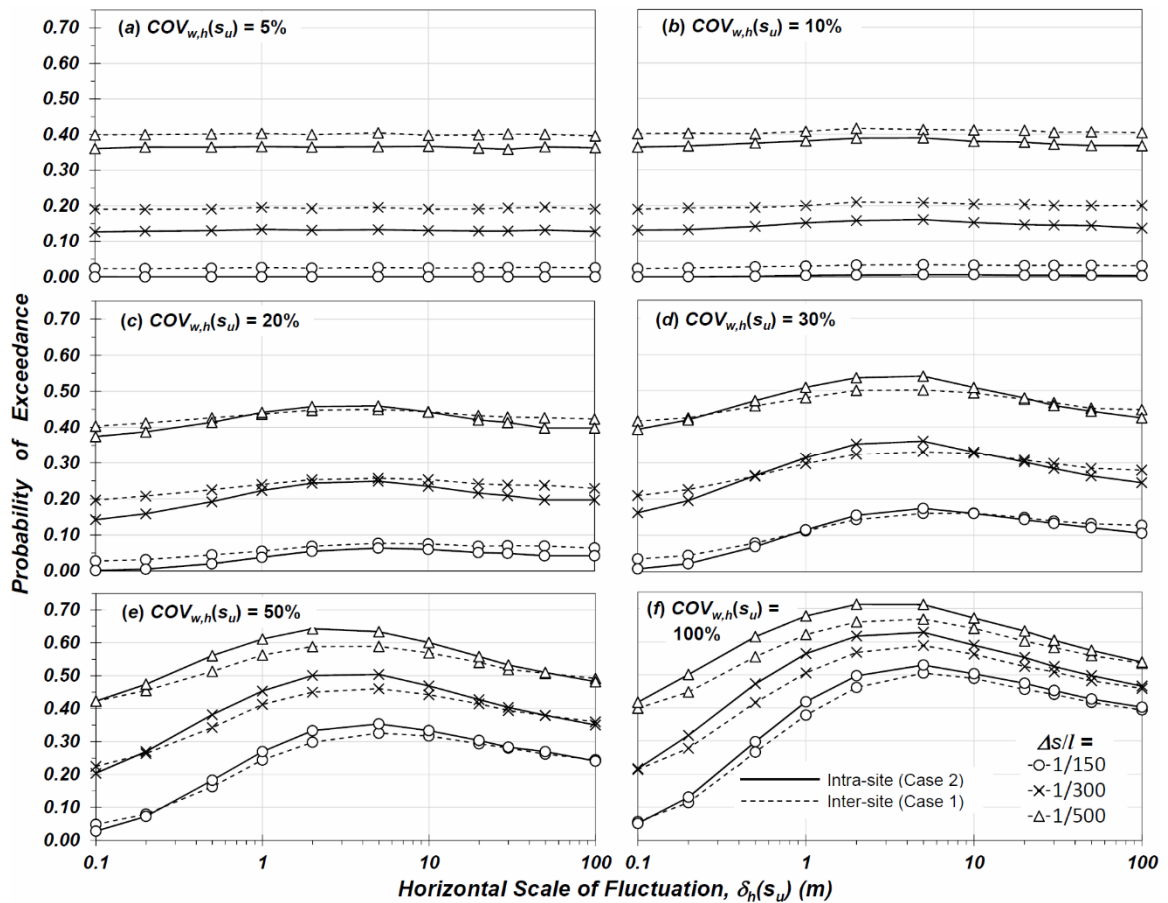
2. Selected values reported for each  $COV_{w,h}$  represent the largest mean or median value observed for Bay 1, 2, 3 or 4. Results were typically similar for the other bays not reported in this table.
3. Differential displacement coefficient of variation,  $COV = \text{standard deviation}/\text{mean}$ .
4. Angular distortion across the selected bay,  $\Delta s/l$ , was calculated as the differential displacement divided over the center-to-center footing distance of 9.15 m. Values are provided in fraction format for ease of comparison between values.

Figure 7.15 compares the cumulative distribution of differential displacements across Bay 1 for  $\delta_h(s_u)$  equal to 50 m and the range of  $COV_{w,h}(s_u)$  for Cases 1 and 2. Figure 7.16 compares the Case 1 and 2 MCS results for probability of exceedance of selected limit state  $\Delta s/l$  values equal to 1/500, 1/300 and 1/150 for varying  $\delta_h(s_u)$  values at Bay 1. Figures 7.15 and 7.16 indicate the Case 2 MCS results are similar to Case 1 with respect to the trends noted above. However, when comparing Case 1 and Case 2 results, it is noted that while the total vertical displacement at the individual footings is modestly greater for Case 2 MCS using the intra-site parameters (compare Tables 7.6 and 7.8), the differential displacements and corresponding angular distortions are similar between the two cases, and lower for Case 2 in some instances. For example, in Figure 7.15 it can be observed that the percent of realizations exceeding the limit state angular distortion values of  $\Delta s/l = 1/500$ ,  $1/300$  and  $1/150$  are lower for Case 2 when  $COV_{w,h}(s_u)$  is less than or equal to 20 percent. As  $COV_{w,h}(s_u)$  increases, the Case 1 and Case 2 results are in closer agreement, with the probability of exceedance typically being slightly lower for the Case 1 MCS. The same general results are observed in Figure 7.16 for the range of  $\delta_h(s_u)$  considered. These observations stem from the use of the footing spring model parameters that exhibit a smaller range in variability to represent the intra-site or site-specific scenario (i.e., Case 2) versus the inter-site or global scenario (Case 1; Fig. 7.10) As a result, the relative difference in soil-foundation spring resistance between individual footings is comparable for the Case 1 and Case 2 MCS even though the intra-site parameters typically provide a softer spring resistance compared to the inter-site parameters. It is only the larger values of  $COV_{w,h}(s_u)$  and when soil strength is most variable that the softer intra-site

foundation springs (Case 2) result in slightly greater differential foundation displacements and angular distortions.



**Figure 7.15** Distribution of differential footing displacement for selected Case 1 and 2 MCS results for Bay 1.



**Figure 7.16** Case 1 (inter-site) and Case 2 (intra-site) MCS results for Bay 1. Probability of exceedance of selected limit state angular distortion for varying horizontal scale of fluctuation.

The comparison of the Case 1 and Case 2 MCS provides two observations. First, when possible, site-specific spring parameters calibrated from foundation loading tests should be used to more accurately predict displacements of individual footings supported on a given soil stratum. Even when the foundation spring parameters are normalized based on foundation size and relative bearing resistance, the soil-foundation spring parameters will have site-specific characteristics due to regional depositional history of the soil and therefore similar mechanical responses. The range in normalized bearing pressure-displacement response from the loading tests compiled in Chapter 5 (Huffman et al. 2015)

is in part why the resistance parameters proposed in that study resulted in relatively low “allowable” bearing pressures compared to the calculated resistance for selected service-level displacements. A second, related observation then arises when comparing the Case 1 and Case 2 MCS results. When site-specific loading tests are not available to calibrate the soil-foundation spring parameters, using the global (inter-site) parameters should generally provide a close, and potentially conservative, approximation of differential displacements even when the site-specific soil conditions generally result in a softer soil-foundation spring. This is because the characteristic distributions of the soil-foundation spring parameters estimated from the global (inter-site) database will generally exhibit greater variability compared to the characteristic distributions of the spring parameters calibrated for a specific site or region. Whether the inter-site spring parameters are slightly over- or under-conservative relative to the intra-site springs depends in part on the soil variability (i.e., the combination of  $\delta_h(s_u)$  and  $COV_{w,h}(s_u)$  values), as exemplified in Figs. 7.15 and 7.16.

### 7.3.3 Case 3: Soil-Foundation-Structure Response (Inter-site Soil Parameters)

The Case 3 MCS used the same global soil-foundation spring parameters as Case 1, but also incorporated the SMRF building model via OpenSees to consider the effect of soil-structure interaction. Unlike Cases 1 and 2 with footings acting independently under the predetermined foundation loads, the interaction between the soil, the footings, and the steel-frame building serve to redistribute foundation loads and corresponding footing displacements that depended on the stiffness of the structure and the variable stiffness of the foundation soil within the building footprint. The performance of the footings and the



steel structure were monitored during the OpenSees simulations. The MCS results are presented for the foundation response first, followed by a discussion of the building response.

### 7.3.3.1 *Soil-Foundation Performance*

Tables 7.10 and 7.11 provide a summary of total and differential vertical footing displacements, and the corresponding angular distortions for the Case 3 MCS consistent with the assessments provided in Tables 7.6 and 7.7 for the Case 1 MCS. The results for Case 3 MCS can be directly compared to the Case 1 results to quantify the influence of SSI on the footing performance.

Comparing total vertical foundation displacements in Table 7.10 and Table 7.6, the median displacements recorded for both cases are typically close in magnitude but slightly greater for the Case 3 MCS. Median footing displacements generally range from approximately 21 to 24 mm for the for Case 1 footings, and from approximately 22 to 30 mm for Case 3. However, as the coefficient of inherent soil variability increases (e.g.,  $COV_{w,h}(s_u) = 30$  percent in Table 7.6 and Table 7.10), the magnitude of the mean footing displacements becomes much greater for the footings acting independently (Case 1) compared to the footings that are working as a system within the overall structure (Case 3). The failure rate is also much greater for Case 1 (approximately 2 percent for  $\delta_h(s_u) \geq 10$  m) compared to Case 3 (typically less than 0.1 percent for all  $\delta_h(s_u)$  values). This indicates the Case 1 footings have a much greater tendency to exhibit extreme displacements for the cases when softer and more variable soils are present, while the Case 3 footings tend to

distribute (and/or redistribute) load more evenly between each of the footings within the foundation system.

The structural influence on footing load distribution and resulting footing displacement incorporated in Case 3 MCS becomes more apparent when comparing the differential displacements,  $\Delta s$ , and angular distortions,  $\Delta s/l$ , between Cases 1 and 3. Comparison of Tables 7.7 and 7.11 indicate the median differential displacement between footings (and/or across the building bays) for Case 3 MCS is typically about two-thirds of the Case 1 MCS results for most combinations of  $COV_{w,h}(s_u)$  and  $\delta_h(s_u)$ . Furthermore, the mean  $\Delta s$  values are significantly smaller for Case 3 as compared to Case 1, particularly for  $COV_{w,h}(s_u)$  greater than 30 percent, indicating a lower occurrence of extremely large  $\Delta s$  and  $\Delta s/l$  values when SSI is considered. When comparing total and differential vertical displacements, the Case 3 MCS results indicated median differential displacement,  $\Delta s$ , typically on the order of 35 to 40 percent of the magnitude of the total displacement,  $s$ , for individual footings, which significantly less compared to the Case 1 MCS (and for reference is closer in magnitude to the Case 2 MCS results).

**Table 7.10. Summary of vertical footing displacement for selected Case 3 MCS results with  $COV_{w,h}(s_u)$  values of 10 and 30 percent.**

Footing	$COV_{w,h}(s_u) = 10\%$					$COV_{w,h}(s_u) = 30\%$				
	1	2	3	4	5	1	2	3	4	5
<b><math>\delta_h(s_u) = 0.1 \text{ m}</math></b>										
Mean $s$ (mm)	24.7	28.4	28.8	28.2	24.3	25.2	28.9	29.1	28.4	24.6
Median $s$ (mm)	22.3	27.2	27.7	27.1	22.1	22.5	27.4	27.9	27.0	22.2
Std. dev. $s$ (mm)	14.2	13.4	13.1	13.2	13.9	15.0	13.9	13.5	13.7	14.4
COV( $s$ )	0.57	0.47	0.46	0.47	0.57	0.59	0.48	0.47	0.48	0.59
Failure rate (%)	0.00	0.00	0.00	0.00	0.00	0.00	0.00	0.00	0.00	0.00
<b><math>\delta_h(s_u) = 0.2 \text{ m}</math></b>										
Mean $s$ (mm)	24.9	28.6	28.8	28.3	24.4	25.6	29.2	29.5	29.0	25.2
Median $s$ (mm)	22.6	27.3	27.8	27.0	22.0	22.7	27.6	28.2	27.5	22.4
Std. dev. $s$ (mm)	14.3	13.5	13.2	13.3	14.0	15.7	14.3	13.9	14.1	15.4
COV( $s$ )	0.57	0.47	0.46	0.47	0.58	0.61	0.49	0.47	0.49	0.61
Failure rate (%)	0.00	0.00	0.00	0.00	0.00	0.00	0.00	0.00	0.00	0.00
<b><math>\delta_h(s_u) = 0.5 \text{ m}</math></b>										
Mean $s$ (mm)	24.9	28.7	28.9	28.3	24.4	26.8	30.2	30.3	29.9	26.2
Median $s$ (mm)	22.4	27.3	27.8	27.1	22.0	23.0	28.3	28.6	27.9	22.6
Std. dev. $s$ (mm)	14.6	13.6	13.3	13.3	14.1	17.8	15.6	15.0	15.4	17.5
COV( $s$ )	0.59	0.47	0.46	0.47	0.58	0.66	0.52	0.49	0.52	0.67
Failure rate (%)	0.00	0.00	0.00	0.00	0.00	0.00	0.00	0.00	0.00	0.00
<b><math>\delta_h(s_u) = 1 \text{ m}</math></b>										
Mean $s$ (mm)	24.9	28.7	28.9	28.4	24.5	28.0	31.2	31.3	30.9	27.6
Median $s$ (mm)	22.4	27.3	27.7	27.1	22.0	23.2	28.5	29.2	28.5	22.9
Std. dev. $s$ (mm)	14.5	13.7	13.3	13.5	14.3	20.7	17.2	16.2	17.1	20.3
COV( $s$ )	0.58	0.48	0.46	0.47	0.58	0.74	0.55	0.52	0.55	0.73
Failure rate (%)	0.00	0.00	0.00	0.00	0.00	0.00	0.00	0.00	0.00	0.00
<b><math>\delta_h(s_u) = 2 \text{ m}</math></b>										
Mean $s$ (mm)	25.2	28.9	29.0	28.4	24.5	29.2	32.4	32.3	32.0	28.9
Median $s$ (mm)	22.6	27.6	27.8	27.0	22.0	23.4	29.1	29.6	28.7	23.2
Std. dev. $s$ (mm)	14.8	13.9	13.4	13.6	14.4	23.8	19.4	17.9	19.2	23.3
COV( $s$ )	0.59	0.48	0.46	0.48	0.59	0.81	0.60	0.56	0.60	0.81
Failure rate (%)	0.00	0.00	0.00	0.00	0.00	0.00	0.00	0.00	0.00	0.00
<b><math>\delta_h(s_u) = 5 \text{ m}</math></b>										
Mean $s$ (mm)	25.2	28.9	29.1	28.6	24.7	32.0	34.7	34.4	34.2	31.4
Median $s$ (mm)	22.5	27.5	27.9	27.2	22.1	23.6	29.4	30.0	28.9	23.2
Std. dev. $s$ (mm)	15.0	14.0	13.6	13.7	14.6	38.2	29.2	24.3	26.5	33.6
COV( $s$ )	0.59	0.48	0.47	0.48	0.59	1.20	0.84	0.71	0.78	1.07
Failure rate (%)	0.00	0.00	0.00	0.00	0.00	0.00	0.00	0.00	0.00	0.00

**Notes:** 1. Results based on MCS with  $n = 50,000$  realizations.

2. Coefficient of variation,  $COV = \text{standard deviation}/\text{mean}$ .

3. Failure rate is defined herein as the percentage of MCS realizations with vertical displacement,  $s$ , greater than or equal to the footing width,  $B$ .

**Table 7.10. Summary of vertical footing displacement for selected Case 3 MCS results with  $COV_{w,h}(s_u)$  values of 10 and 30 percent (continued).**

Footing	$COV_{w,h}(s_u) = 10\%$					$COV_{w,h}(s_u) = 30\%$				
	1	2	3	4	5	1	2	3	4	5
<b><math>\delta_h(s_u) = 10 \text{ m}</math></b>										
Mean $s$ (mm)	25.3	29.1	29.2	28.6	24.9	36.3	38.6	38.0	38.0	35.4
Median $s$ (mm)	22.6	27.6	27.9	27.2	22.2	23.4	29.6	30.1	29.2	23.0
Std. dev. $s$ (mm)	15.1	14.2	13.9	13.9	14.8	67.6	51.5	42.8	48.6	62.7
COV( $s$ )	0.60	0.49	0.47	0.49	0.59	1.86	1.34	1.13	1.28	1.77
Failure rate (%)	0.00	0.00	0.00	0.00	0.00	0.01	0.00	0.00	0.00	0.01
<b><math>\delta_h(s_u) = 20 \text{ m}</math></b>										
Mean $s$ (mm)	25.3	29.1	29.4	28.9	25.0	42.2	43.8	43.1	42.7	40.2
Median $s$ (mm)	22.5	27.5	28.1	27.4	22.2	23.3	29.2	29.7	28.6	22.6
Std. dev. $s$ (mm)	15.2	14.3	14.0	14.1	15.0	107.0	85.2	73.9	80.1	98.0
COV( $s$ )	0.60	0.49	0.48	0.49	0.60	2.54	1.94	1.72	1.88	2.44
Failure rate (%)	0.00	0.00	0.00	0.00	0.00	0.06	0.01	0.01	0.01	0.04
<b><math>\delta_h(s_u) = 30 \text{ m}</math></b>										
Mean $s$ (mm)	25.3	29.2	29.3	28.8	25.0	44.2	46.4	46.1	46.5	44.2
Median $s$ (mm)	22.5	27.5	27.9	27.2	22.1	23.4	29.1	29.8	28.9	22.8
Std. dev. $s$ (mm)	15.3	14.4	14.1	14.2	15.2	122.6	101.8	93.6	103.1	123.8
COV( $s$ )	0.60	0.49	0.48	0.49	0.61	2.77	2.19	2.03	2.22	2.80
Failure rate (%)	0.00	0.00	0.00	0.00	0.00	0.06	0.02	0.02	0.02	0.07
<b><math>\delta_h(s_u) = 50 \text{ m}</math></b>										
Mean $s$ (mm)	25.5	29.3	29.4	29.0	25.1	46.1	48.3	47.9	47.8	45.3
Median $s$ (mm)	22.6	27.6	27.9	27.3	22.3	22.9	28.9	29.5	28.6	22.9
Std. dev. $s$ (mm)	15.5	14.6	14.2	14.3	15.3	159.0	128.4	112.6	118.8	142.3
COV( $s$ )	0.61	0.50	0.48	0.49	0.61	3.45	2.66	2.35	2.49	3.14
Failure rate (%)	0.00	0.00	0.00	0.00	0.00	0.08	0.03	0.03	0.03	0.08
<b><math>\delta_h(s_u) = 100 \text{ m}</math></b>										
Mean $s$ (mm)	25.5	29.3	29.4	28.9	25.1	48.7	51.5	51.3	51.0	48.1
Median $s$ (mm)	22.6	27.6	28.0	27.3	22.2	23.1	29.1	29.4	28.3	22.8
Std. dev. $s$ (mm)	15.6	14.5	14.3	14.4	15.3	195.4	177.3	174.9	189.2	214.5
COV( $s$ )	0.61	0.50	0.48	0.50	0.61	4.02	3.44	3.41	3.71	4.46
Failure rate (%)	0.00	0.00	0.00	0.00	0.00	0.12	0.06	0.07	0.06	0.13

**Notes:** 1. Results based on MCS with  $n = 50,000$  realizations.

2. Coefficient of variation,  $COV = \text{standard deviation}/\text{mean}$ .

3. Failure rate is defined herein as the percentage of MCS realizations with vertical displacement,  $s$ , greater than or equal to the footing width,  $B$ .

**Table 7.11. Summary of differential displacement and angular distortion at selected building bay for Case 3 MCS.**

$COV_{w,h}(s_u) =$	0	5%	10%	20%	30%	50%	100%
<b><math>\delta_n(s_u) = 0.1 \text{ m}</math></b>							
Mean $\Delta s$ (mm)	11.5	11.5	11.6	11.6	11.9	12.2	12.2
Median $\Delta s$ (mm)	9.7	9.7	9.8	9.8	10.0	10.2	10.1
COV( $\Delta s$ )	0.75	0.75	0.75	0.76	0.76	0.77	0.78
Mean $\Delta s/l$	1/795	1/797	1/792	1/789	1/771	1/752	1/749
Median $\Delta s/l$	1/943	1/942	1/933	1/935	1/911	1/899	1/905
<b><math>\delta_n(s_u) = 0.2 \text{ m}</math></b>							
Mean $\Delta s$ (mm)	11.6	11.5	11.5	11.8	12.1	13.0	13.9
Median $\Delta s$ (mm)	9.8	9.8	9.8	10.0	10.3	10.8	11.1
COV( $\Delta s$ )	0.75	0.75	0.75	0.75	0.76	0.78	0.83
Mean $\Delta s/l$	1/791	1/793	1/793	1/775	1/754	1/702	1/660
Median $\Delta s/l$	1/936	1/935	1/935	1/916	1/892	1/847	1/825
<b><math>\delta_n(s_u) = 0.5 \text{ m}</math></b>							
Mean $\Delta s$ (mm)	11.5	11.5	11.6	12.2	13.0	15.4	19.6
Median $\Delta s$ (mm)	9.7	9.7	9.8	10.4	10.8	12.3	14.2
COV( $\Delta s$ )	0.75	0.75	0.76	0.77	0.78	0.84	1.07
Mean $\Delta s/l$	1/795	1/794	1/790	1/750	1/702	1/595	1/466
Median $\Delta s/l$	1/944	1/939	1/937	1/889	1/846	1/746	1/644
<b><math>\delta_n(s_u) = 1 \text{ m}</math></b>							
Mean $\Delta s$ (mm)	11.5	11.6	11.7	12.5	13.9	18.6	26.9
Median $\Delta s$ (mm)	9.7	9.8	9.9	10.4	11.4	14.1	17.9
COV( $\Delta s$ )	0.75	0.75	0.75	0.77	0.80	0.98	1.33
Mean $\Delta s/l$	1/797	1/790	1/784	1/735	1/657	1/491	1/340
Median $\Delta s/l$	1/943	1/930	1/926	1/876	1/802	1/648	1/511
<b><math>\delta_n(s_u) = 2 \text{ m}</math></b>							
Mean $\Delta s$ (mm)	11.4	11.5	11.8	12.8	14.9	21.9	35.8
Median $\Delta s$ (mm)	9.7	9.8	10.0	10.7	11.9	15.4	22.1
COV( $\Delta s$ )	0.75	0.75	0.76	0.77	0.83	1.18	1.43
Mean $\Delta s/l$	1/802	1/797	1/784	1/716	1/615	1/419	1/256
Median $\Delta s/l$	1/939	1/933	1/926	1/858	1/767	1/593	1/415
<b><math>\delta_n(s_u) = 5 \text{ m}</math></b>							
Mean $\Delta s$ (mm)	11.5	11.6	11.8	12.9	15.8	27.8	50.5
Median $\Delta s$ (mm)	9.7	9.9	10.0	10.7	12.1	16.2	26.7
COV( $\Delta s$ )	0.75	0.76	0.76	0.79	1.02	2.89	1.54
Mean $\Delta s/l$	1/795	1/786	1/775	1/710	1/578	1/329	1/181
Median $\Delta s/l$	1/941	1/926	1/917	1/857	1/757	1/563	1/343

**Notes:** 1. Results based on MCS with  $n = 50,000$  realizations.

2. Selected values reported for each  $COV_{w,h}$  represent the largest mean or median value observed for Bay 1, 2, 3 or 4. Results were typically similar for the other bays not reported in this table.
3. Differential displacement coefficient of variation,  $COV = \text{standard deviation}/\text{mean}$ .
4. Angular distortion across the selected bay,  $\Delta s/l$ , was calculated as the differential displacement divided over the center-to-center footing distance of 9.15 m. Values are provided in fraction format for ease of comparison between values.

**Table 7.11. Summary of differential displacement and angular distortion at selected building bay for Case 3 MCS (continued).**

$COV_{w,h}(s_u) =$	0	5%	10%	20%	30%	50%	100%
<b><math>\delta_h(s_u) = 10 \text{ m}</math></b>							
Mean $\Delta s$ (mm)	11.5	11.5	11.8	12.9	17.5	34.8	61.2
Median $\Delta s$ (mm)	9.8	9.7	10.0	10.6	12.0	16.1	26.9
COV( $\Delta s$ )	0.75	0.76	0.75	0.83	1.46	1.73	1.53
Mean $\Delta s/l$	1/793	1/794	1/774	1/711	1/524	1/263	1/150
Median $\Delta s/l$	1/936	1/941	1/912	1/863	1/761	1/567	1/340
<b><math>\delta_h(s_u) = 20 \text{ m}</math></b>							
Mean $\Delta s$ (mm)	11.5	11.5	11.7	12.9	19.2	40.9	67.1
Median $\Delta s$ (mm)	9.7	9.7	10.0	10.4	11.6	15.1	23.6
COV( $\Delta s$ )	0.75	0.76	0.76	0.95	1.84	2.01	1.86
Mean $\Delta s/l$	1/795	1/795	1/775	1/709	1/477	1/224	1/136
Median $\Delta s/l$	1/942	1/939	1/918	1/876	1/789	1/604	1/387
<b><math>\delta_h(s_u) = 30 \text{ m}</math></b>							
Mean $\Delta s$ (mm)	11.5	11.6	11.7	13.0	19.9	41.4	67.9
Median $\Delta s$ (mm)	9.7	9.8	9.9	10.3	11.3	14.2	21.9
COV( $\Delta s$ )	0.75	0.75	0.76	1.16	1.96	2.02	1.88
Mean $\Delta s/l$	1/797	1/791	1/780	1/705	1/460	1/221	1/135
Median $\Delta s/l$	1/945	1/937	1/919	1/891	1/807	1/643	1/418
<b><math>\delta_h(s_u) = 50 \text{ m}</math></b>							
Mean $\Delta s$ (mm)	11.5	11.5	11.6	12.9	20.0	41.9	68.6
Median $\Delta s$ (mm)	9.8	9.8	9.8	10.2	11.0	13.5	18.3
COV( $\Delta s$ )	0.75	0.76	0.76	1.12	2.47	2.27	2.23
Mean $\Delta s/l$	1/795	1/793	1/782	1/710	1/458	1/218	1/133
Median $\Delta s/l$	1/933	1/936	1/929	1/896	1/832	1/680	1/500
<b><math>\delta_h(s_u) = 100 \text{ m}</math></b>							
Mean $\Delta s$ (mm)	11.5	11.5	11.6	12.8	19.6	39.7	64.4
Median $\Delta s$ (mm)	9.8	9.7	9.8	10.0	10.7	12.5	15.5
COV( $\Delta s$ )	0.75	0.75	0.76	1.21	2.92	2.63	2.44
Mean $\Delta s/l$	1/795	1/796	1/786	1/721	1/468	1/230	1/142
Median $\Delta s/l$	1/933	1/939	1/934	1/915	1/852	1/730	1/589

**Notes:** 1. Results based on MCS with  $n = 50,000$  realizations.

2. Selected values reported for each  $COV_{w,h}$  represent the largest mean or median value observed for Bay 1, 2, 3 or 4. Results were typically similar for the other bays not reported in this table.
3. Differential displacement coefficient of variation,  $COV = \text{standard deviation}/\text{mean}$ .
4. Angular distortion across the selected bay,  $\Delta s/l$ , was calculated as the differential displacement divided over the center-to-center footing distance of 9.15 m. Values are provided in fraction format for ease of comparison between values.

Figure 7.17 compares the MCS results for Cases 1 and 3 for the cumulative distribution of differential displacements across Bay 1 for  $\delta_h(s_u) = 50$  m and the range of  $COV_{w,h}(s_u)$  considered. Figure 7.18 compares the probability of exceedance of selected limit state  $\Delta s/l$  values equal to 1/500, 1/300 and 1/150 for varying  $\delta_h(s_u)$  values at Bay 1 derived from the Case 1 and 3 MCS. Figure 7.18 demonstrates the role of SSI influencing the critical scale of fluctuation,  $\delta_h(s_u)_{crit}$  as the  $\Delta s/l$  limit state varies. Recall the  $\delta_h(s_u)_{crit}$  was typically equal to 5 m or approximately  $l/2$  for each of the limit state  $\Delta s/l$  values for the Case 1 MCS and where  $COV_{w,h}(s_u) \geq 30$  percent (Figs. 7.13 and 7.18). However, for the Case 3 MCS,  $\delta_h(s_u)_{crit}$  tends to increase as the limit state progresses from the “allowable” ( $\Delta s/l = 1/500$ ) to the “ultimate” ( $\Delta s/l = 1/150$ ) criterions. This is most pronounced for large  $COV_{w,h}(s_u)$ . For example, in Figure 7.18(f) ( $COV_{w,h}(s_u) = 100$  percent) Case 3 MCS,  $\delta_h(s_u)_{crit} = 5$  m for  $\Delta s/l = 1/500$ , 10 m for  $\Delta s/l = 1/300$ , and approximately 20 m to 30 m for  $\Delta s/l = 1/150$ . This suggests that the probability of exceeding smaller and/or “allowable” differential displacements or angular distortions is influenced more by the local footing-to-footing distance, while the probability of exceeding larger distortions is influenced more at the scale of the entire structure footprint and across multiple footings.

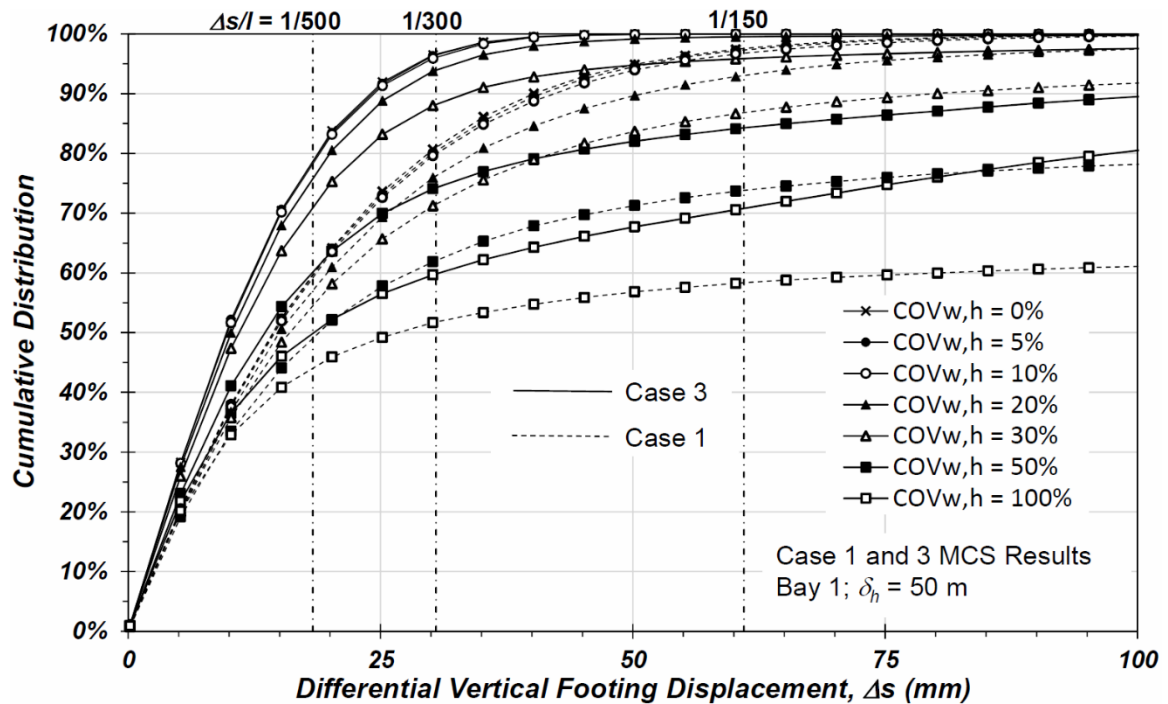


**Figure 7.17** Distribution of differential footing displacement for selected Case 1 and 3 MCS results for Bay 1.

The response to larger angular distortions (e.g.,  $\Delta s/l \geq 1/150$ ) observed for Case 3 MCS appears analogous to Case 1 MCS observations wherein, at smaller  $\delta_h(s_u)$  values, the stiff structure redistributes load accordingly when a single footing is underlain by softer soil. However, in cases with soft soil over a larger area, the distance  $\delta_h(s_u)_{crit}$  coincides with multiple footing widths and, by observation of the MCS results, may be approximately equal to one-half the building width.



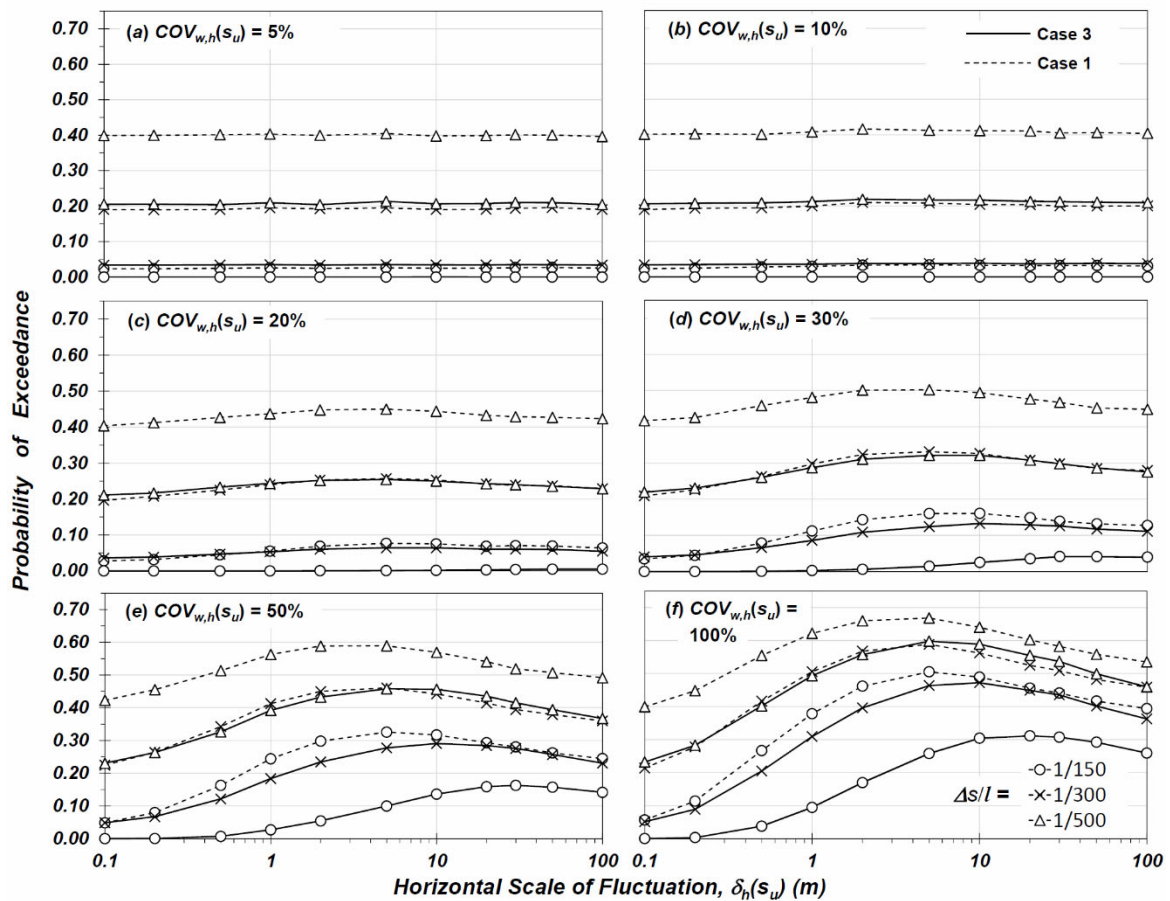


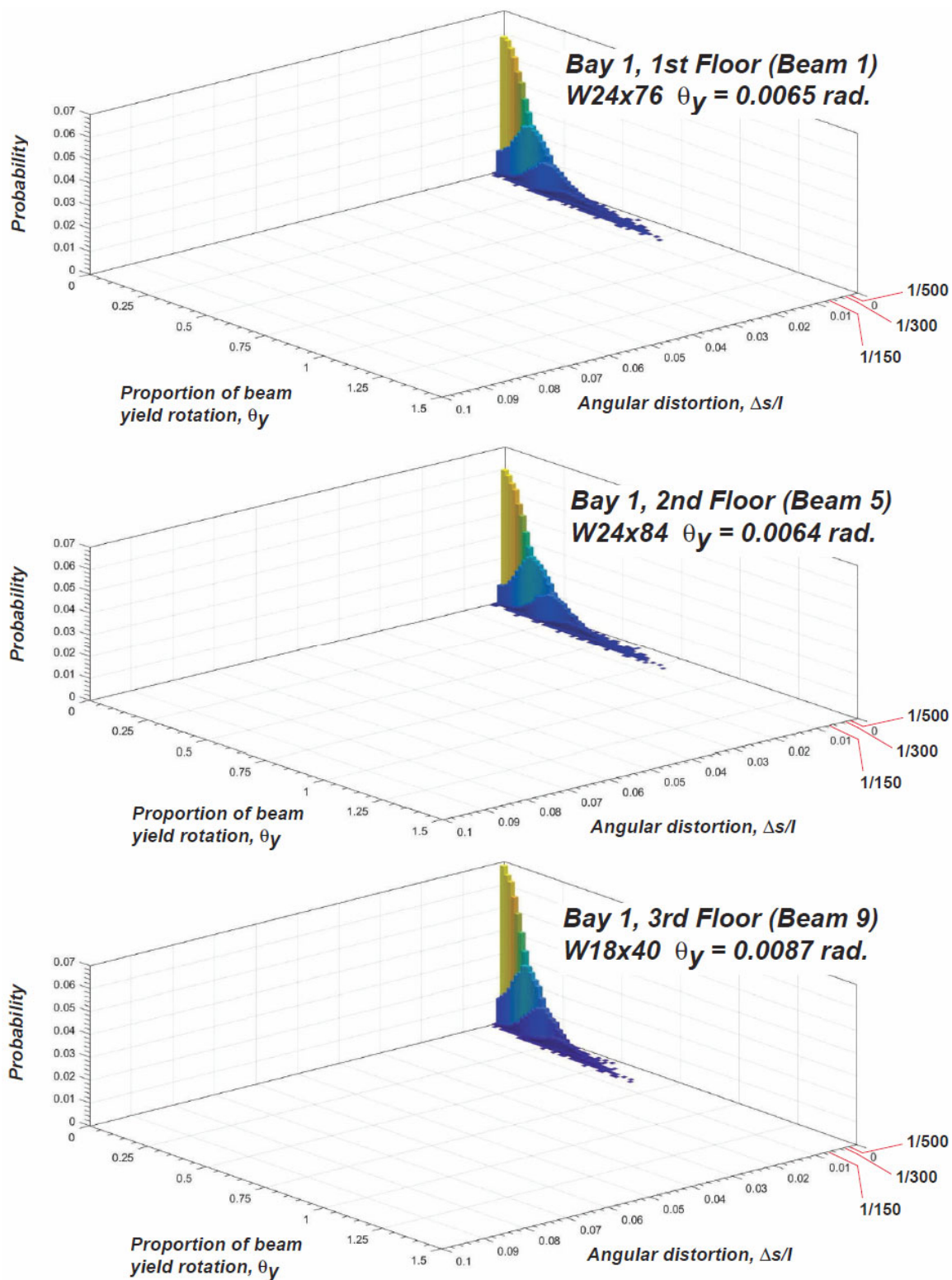
**Figure 7.18** Case 1 and Case 3 MCS results for Bay 1. Probability of exceedance of selected limit state angular distortion for varying horizontal scale of fluctuation.

### 7.3.3.2 Structural Performance

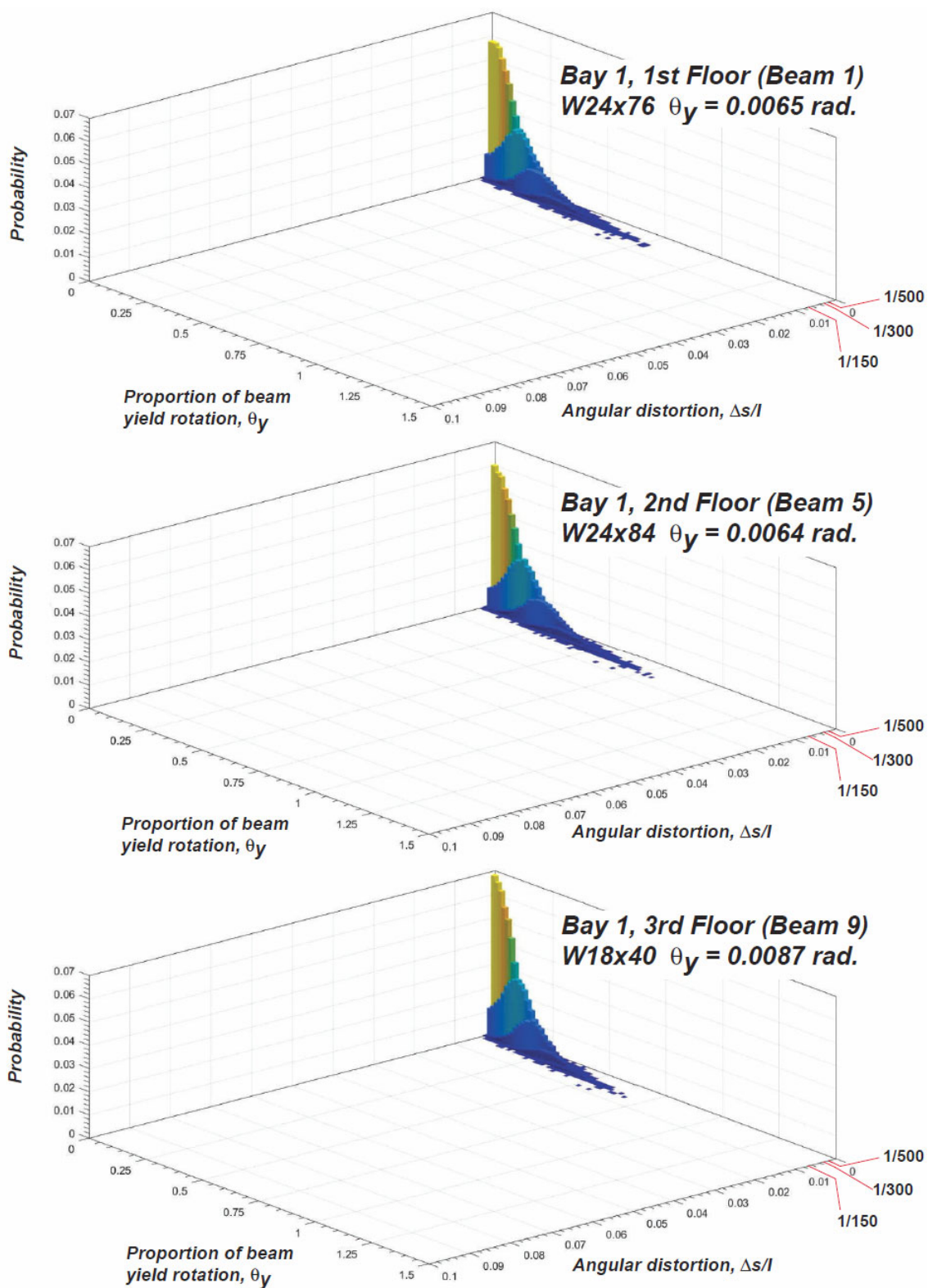
The performance of the three-story SMRF structure was evaluated using the beam rotations and corresponding bending moments. The relationship between rotation and bending moment was included within OpenSees using the  $M-\theta$  backbone curves developed using the modified Ibarra-Krawinkler (IK) deterioration model shown in Fig. 7.3. Pertinent strength parameters for each beam are summarized in Table 7.1. The beams were modeled with rigid connections to the columns and with uniform loads (DL plus LL) acting over the

length of the beams. Therefore, the maximum moment and corresponding rotation is expected to occur at the ends of the beams. Recorders measured the maximum moment and rotation at the ends of the beam (i.e., 24 connections for the 12 beams comprising the 2D structure) to capture the simulated beam responses.

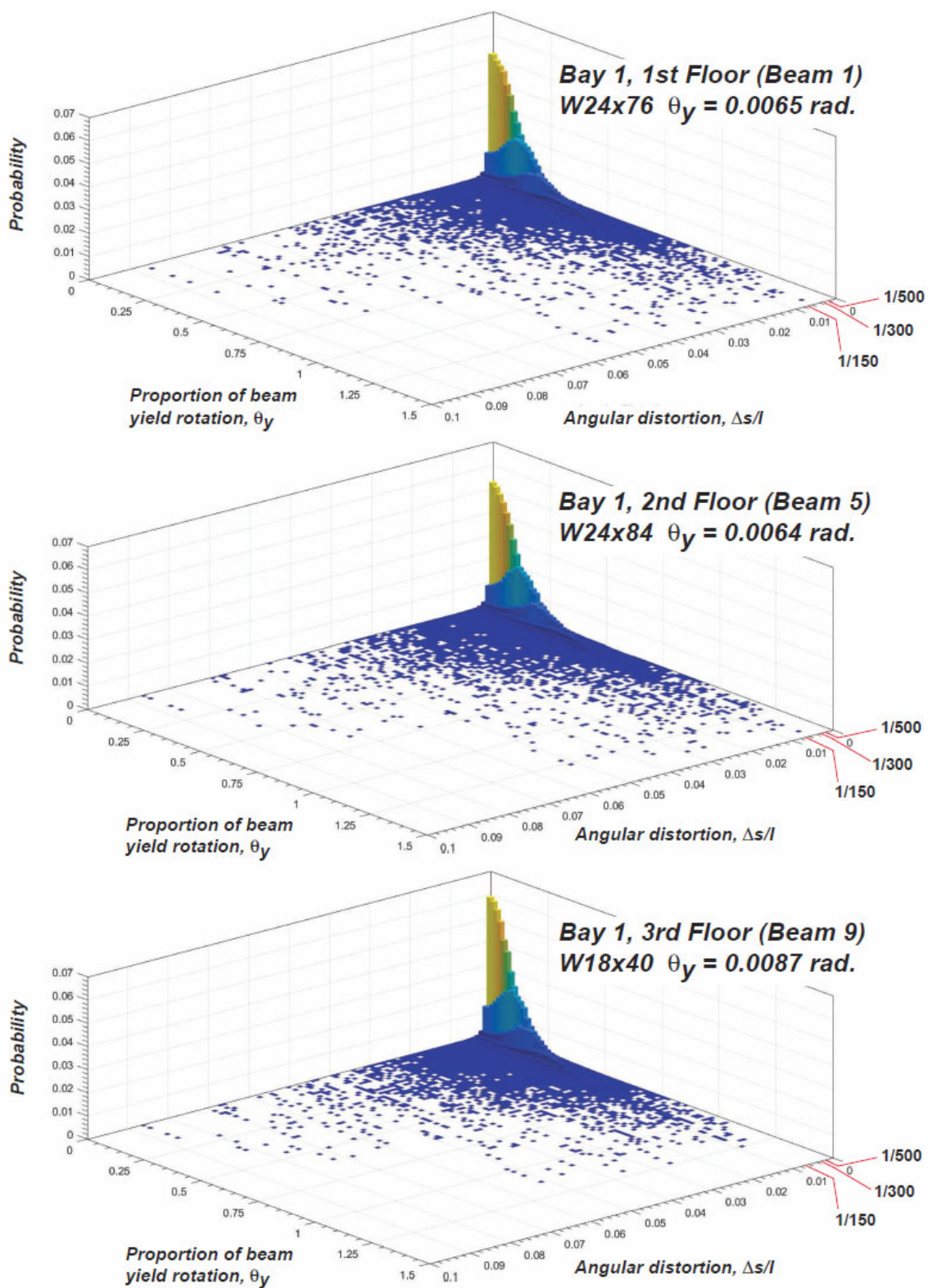
A main goal of this study is to compare the structural performance to the foundation response in consideration of soil spatial variability. Figures 7.19 through 7.23 provide probability density scatter plots of beam end rotation,  $\theta$ , versus angular distortion,  $\Delta s/l$ , for selected combinations  $COV_{w,h}(s_u)$  and  $\delta_h(s_u)$  for Bay 1 (similar results were observed for the other bays). The beams on each of the three floors were plotted separately to observe potential differences between each floor, and because the beam sections differ from floor to floor. Beam rotation is plotted in terms of the yield rotation,  $\theta_y$ , which coincides with the yield moment,  $M_y$ , and is comparable to the LRFD ultimate limit state for flexure. Soil spatial variability is represented in the figures with selected combinations of  $COV_{w,h}(s_u)$  and  $\delta_h(s_u)$  equal to 5 percent and 5 m, 5 percent and 50 m, 30 percent and 50 m, 50 percent and 5 m, and 50 percent and 50 m, respectively. The combination of  $COV_{w,h}(s_u) = 30$  percent and  $\delta_h(s_u) = 50$  m (Figure 7.21) was selected to represent a typical condition since these values fall within the range of mean values reported by Phoon et al. (1995). The other  $COV_{w,h}(s_u)$  and  $\delta_h(s_u)$  combinations were selected to provide a range above and below the assumed typical condition. The results suggest that there is no obvious correlation between the angular distortion between footings and the beam rotation. However, it is readily observed that as soil spatial variability increases there is more variability in both  $\theta$  and  $\Delta s/l$  and greater probability of larger  $\theta$  and  $\Delta s/l$  values.



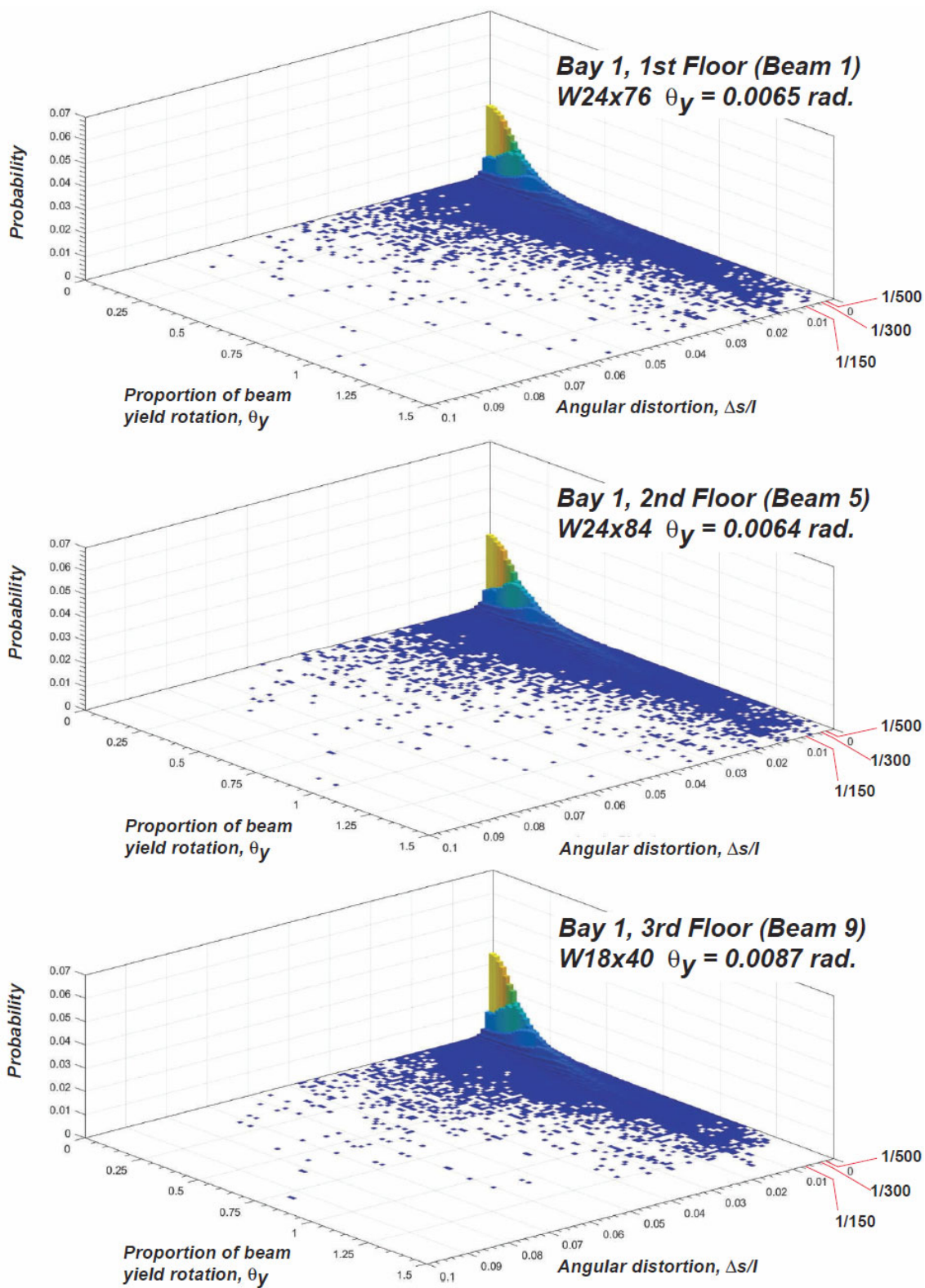
**Figure 7.19** Case 3 MCS. Probability density of angular distortion versus beam yield rotation at Bay 1 for  $COV_{w,h}(S_u) = 5$  percent and  $\delta_h(S_u) = 5$  m.



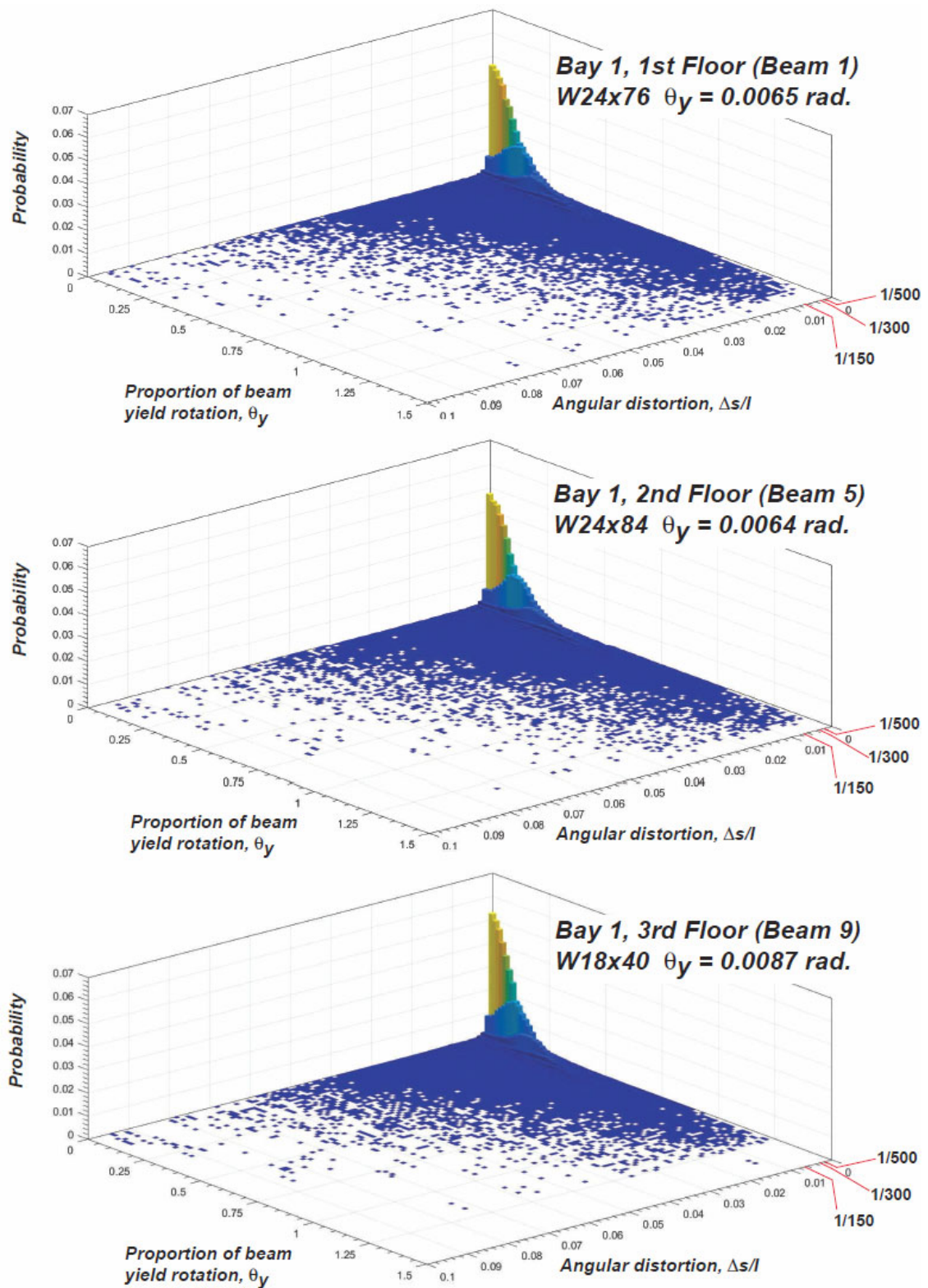
**Figure 7.20** Case 3 MCS. Probability density of angular distortion versus beam yield rotation at Bay 1 for  $COV_{w,h}(S_u) = 5$  percent and  $\delta_h(S_u) = 50$  m.



**Figure 7.21** Case 3 MCS. Probability density of angular distortion versus beam yield rotation at Bay 1 for  $COV_{w,h}(S_u) = 30$  percent and  $\delta_h(S_u) = 50$  m.



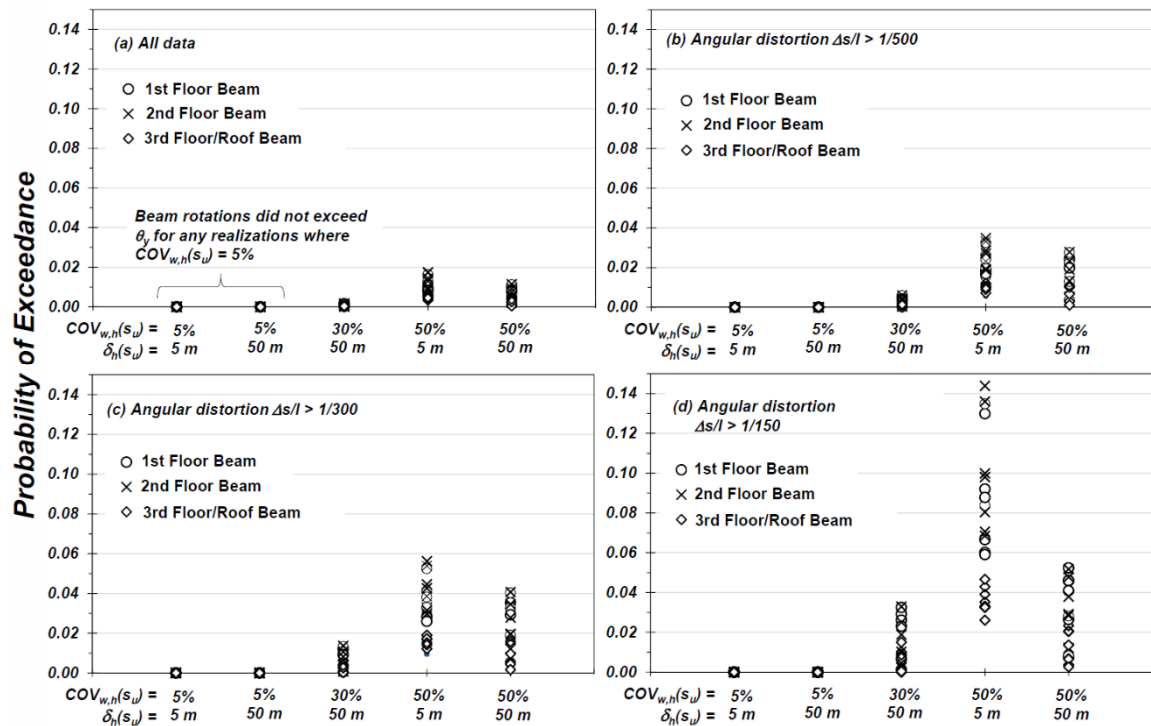
**Figure 7.22** Case 3 MCS. Probability density of angular distortion versus beam yield rotation at Bay 1 for  $COV_{w,h}(s_u) = 50$  percent and  $\delta_h(s_u) = 5$  m.



**Figure 7.23** Case 3 MCS. Probability density of angular distortion versus beam yield rotation at Bay 1 for  $COV_{w,h}(S_u) = 50$  percent and  $\delta_h(S_u) = 50$  m.

Limit state angular distortion values for  $\Delta s/l = 1/500$ ,  $1/300$  and  $1/150$  are shown on the plots in Figures 7.19 through 7.23 but are difficult to interpret because of the large scale for  $\Delta s/l$  that extends well beyond  $1/150$ , implemented to represent all of the simulation results. To provide additional detail for comparison of  $\theta_y$  at the selected limit state  $\Delta s/l$ , Figure 7.24 compares the probability of exceedance of  $\theta_y$  for each beam for the selected combinations of  $COV_{w,h}(s_u)$  and  $\delta_h(s_u)$  at individual beam-column connections. Figure 7.24 indicates that there are relatively few occurrences where  $\theta_y$  is exceeded. For example, in Fig. 7.24a, which includes results from all data for the selected combinations of  $COV_{w,h}(s_u)$  and  $\delta_h(s_u)$ , the maximum probability of occurrence for exceeding  $\theta_y$  occurs for the combination of  $COV_{w,h}(s_u) = 50$  percent and  $\delta_h(s_u) = 5$  m, with probability in the range of approximately 0 to 2 percent, depending on the selected beam location. The beam yield rotation was not exceeded for the case with  $COV_{w,h}(s_u) = 5$  percent. However, as limit state  $\Delta s/l$  increases from  $1/500$  to  $1/150$ , the probability of exceeding  $\theta_y$  increases with increases in  $COV_{w,h}(s_u)$ , and the combination of  $COV_{w,h}(s_u) = 50$  percent and  $\delta_h(s_u) = 5$  m consistently provided the highest probability of exceeding  $\theta_y$  for the selected limit state angular distortions and combinations of soil spatial variability (see Fig. 7.24b, 7.24c and 7.24d).

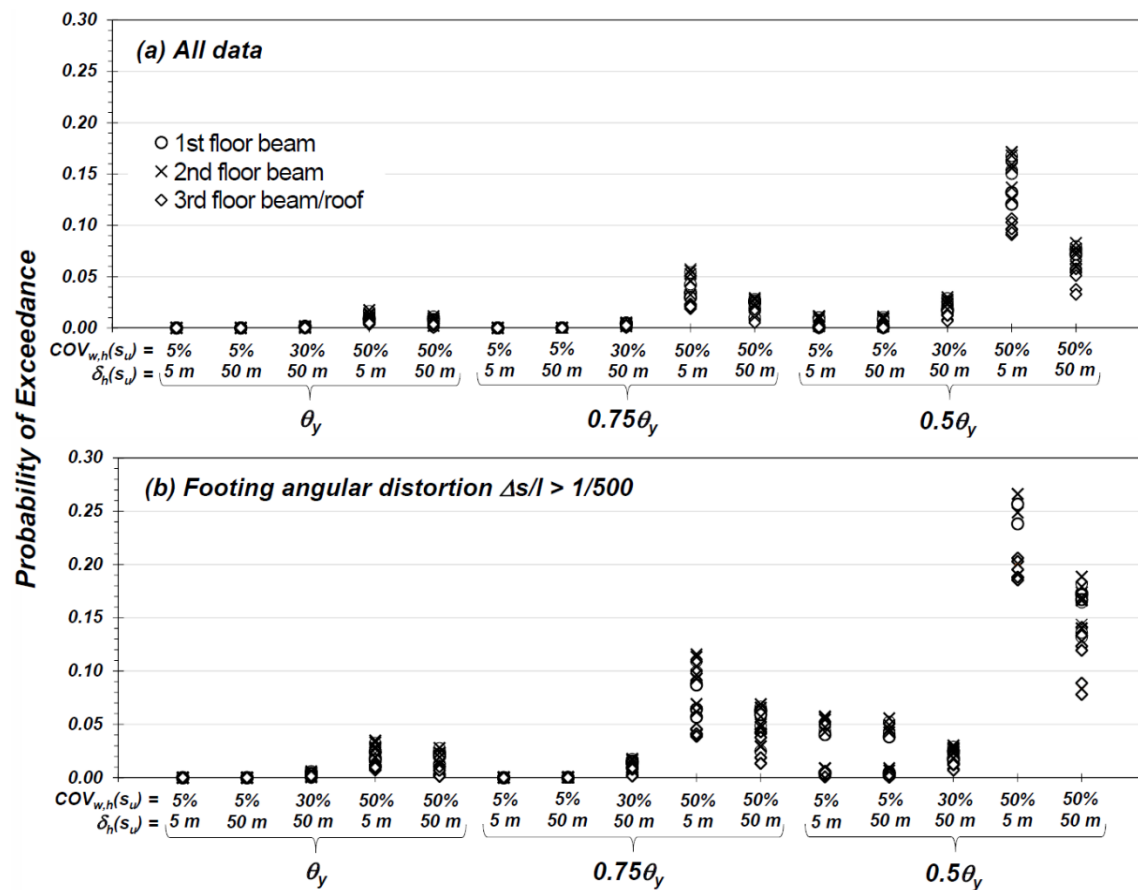




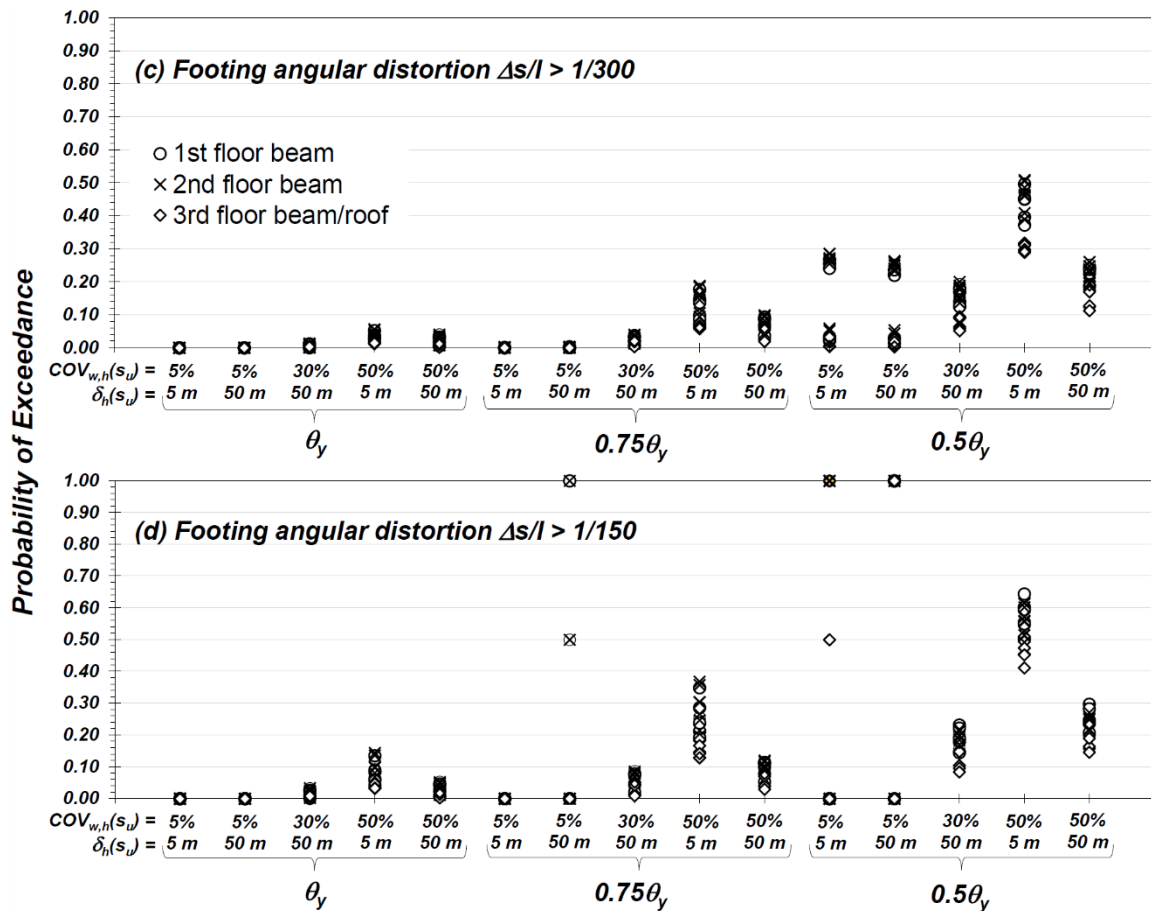
**Figure 7.24** Case 3 MCS. Probability of beam end rotation exceeding  $\theta_y$  for selected values of angular distortion and combinations of  $COV_{w,h}(s_u)$  and  $\delta_h(s_u)$ , and conditioned with a) all data is included, b) data is limited to instances where  $\Delta s/l > 1/500$ , c) data is limited to instances where  $\Delta s/l > 1/300$ , and d) data is limited to instances where  $\Delta s/l > 1/150$ .

Figure 7.25 provides a similar comparison to Figure 7.24 but also includes the probability of exceeding beam rotations equal to  $0.5\theta_y$  and  $0.75\theta_y$  (note: for easier interpretation, Fig. 7.25a and 7.25b are plotted separately and at different scales relative to Fig. 7.25c and 7.25d). The selected beam rotations equal to  $0.5\theta_y$  and  $0.75\theta_y$  do not explicitly represent a given performance criterion, but instead give insight for beam response approaching the serviceability limit state. From Figure 7.25, it is observed that as  $\Delta s/l$  increases, the probability of exceeding any  $\theta$  also increases. Furthermore, and consistent with data shown on Figure 7.24, the combination of  $COV_{w,h}(s_u) = 50$  percent and  $\delta_h(s_u) = 5$  m provides the highest probability of exceeding the selected  $\theta$  values. The

reason for this combination of  $COV_{w,h}(s_u)$  and  $\delta_h(s_u)$  providing a more critical case for beam response becomes more apparent when exploring other combinations of  $COV_{w,h}(s_u)$  and  $\delta_h(s_u)$ , as described below.



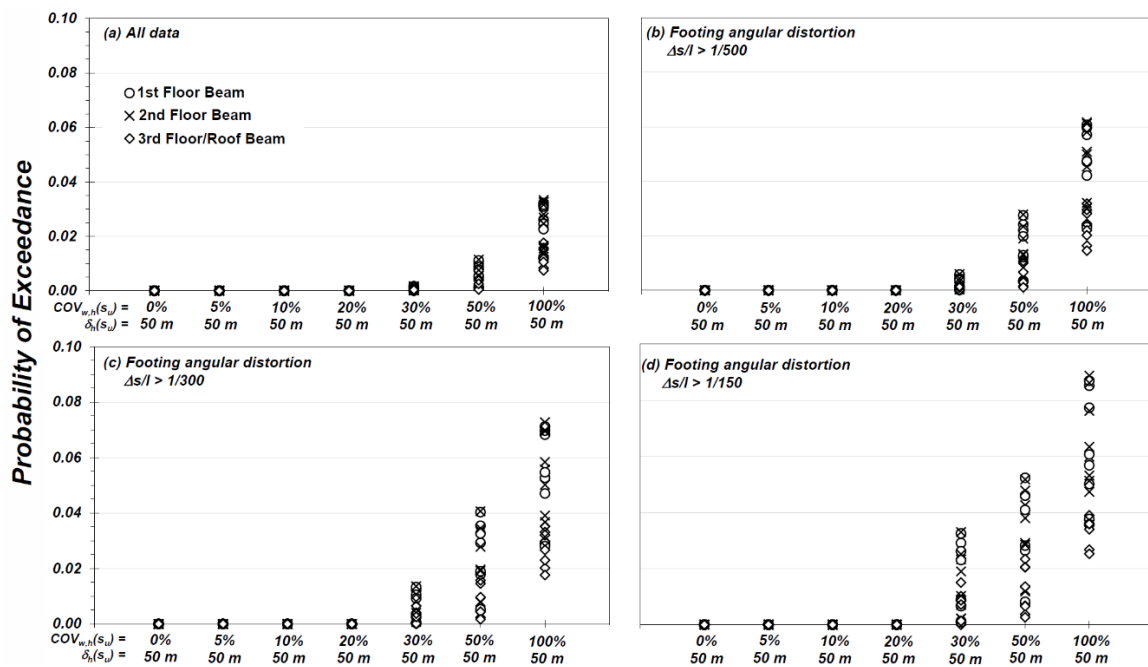
**Figure 7.25** Case 3 MCS results. Probability of beam end rotation exceeding  $\theta_y$  or portion of  $\theta_y$  for selected values of angular distortion and combinations of  $COV_{w,h}(s_u)$  and  $\delta_h(s_u)$ , and conditioned with a) all data is included, b) data is limited to instances where  $\Delta s/l > 1/500$ , c) data is limited to instances where  $\Delta s/l > 1/300$ , and d) data is limited to instances where  $\Delta s/l > 1/150$ . Continued next page.



**Figure 7.25 (cont.)** Case 3 MCS results. Probability of beam end rotation exceeding  $\theta_y$  or portion of  $\theta_y$  for selected values of angular distortion and combinations of  $COV_{w,h}(s_u)$  and  $\delta_h(s_u)$ , and conditioned with a) all data is included, b) data is limited to instances where  $\Delta s/l > 1/500$ , c) data is limited to instances where  $\Delta s/l > 1/300$ , and d) data is limited to instances where  $\Delta s/l > 1/150$ .

Figure 7.25d includes notably large probabilities of exceeding  $0.5\theta_y$  and  $0.75\theta_y$  for  $COV_{w,h}(s_u) = 5$  percent. The reason for the higher probabilities of exceeding  $0.5\theta_y$  or  $0.75\theta_y$  is because there were very few MCS realizations (typically 0 to 2 for MCS with  $n = 50,000$  realizations) for  $COV_{w,h}(s_u) = 5$  percent where  $\Delta s/l$  exceeded  $1/150$ . As a result, probability of exceeding the selected beam rotation value is either 0, 0.50 or 1.0.

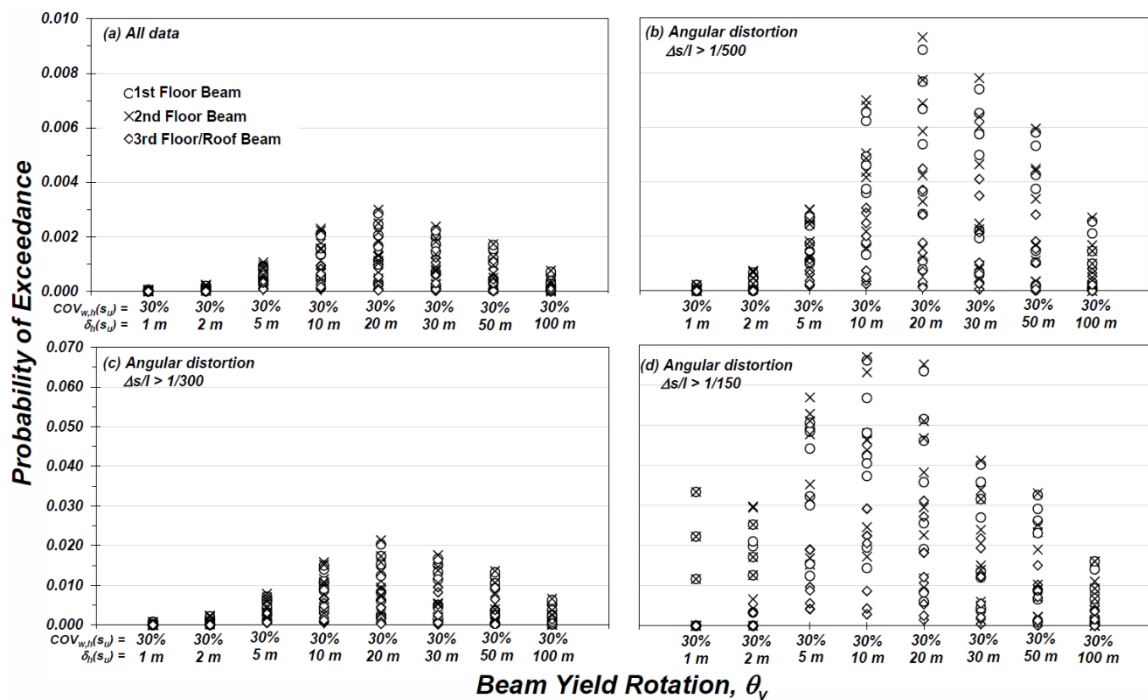
The data summarized in Figures 7.24 and 7.25 show that as  $COV_{w,h}(s_u)$  increases, the probability of beam rotation exceeding  $\theta_y$  also increases. This is intuitive because cases with larger  $COV_{w,h}(s_u)$  generally provide additional occurrences of soft soil conditions, leading to greater risk of large footing displacements affecting building performance. The trend of increased probability of exceedance of  $\theta_y$  with increase in  $COV_{w,h}(s_u)$  is readily observed in Figure 7.26, which restricts the probability of exceeding a given limit state for a single scale of fluctuation equal to 50 m.



**Figure 7.26** Case 3 MCS. Probability of beam end rotation exceeding  $\theta_y$  for selected values of angular distortion and where  $COV_{w,h}(s_u) = 0$  to  $100\%$  and  $\delta_h(s_u) = 50$  m.

The relationship of beam rotation to  $\delta_h(s_u)$  is not readily apparent from Figs. 7.24 and 7.25. Accordingly, Figures 7.27 and 7.28 present the probability of beam rotation exceeding  $\theta_y$  for constant  $COV_{w,h}(s_u)$  equal to 30 percent (i.e., the assumed “average”

value) and range of  $\delta_h(s_u)$  values between 1 m and 100 m. Consistent with Fig. 7.24, Fig. 7.27 compares the probability of exceeding  $\theta_y$  at each beam end (note: Fig. 7.27a and 7.27b are plotted with probability of exceedance ranging from 0 to 0.01 while Fig. 7.27c and 7.27d are plotted with probability of exceedance ranging from 0 to 0.07). It is apparent that for constant  $COV_{w,h}(s_u)$ , the maximum probability of exceeding  $\theta_y$  for a given beam generally coincides with  $\delta_h(s_u) = 20$  m (i.e., approximately  $2l$ ). This scale of fluctuation coincides with  $\delta_h(s_u)_{crit}$  associated with the ultimate limit state criteria for angular distortion ( $\Delta s/l = 1/150$ ) identified in Figure 7.18.



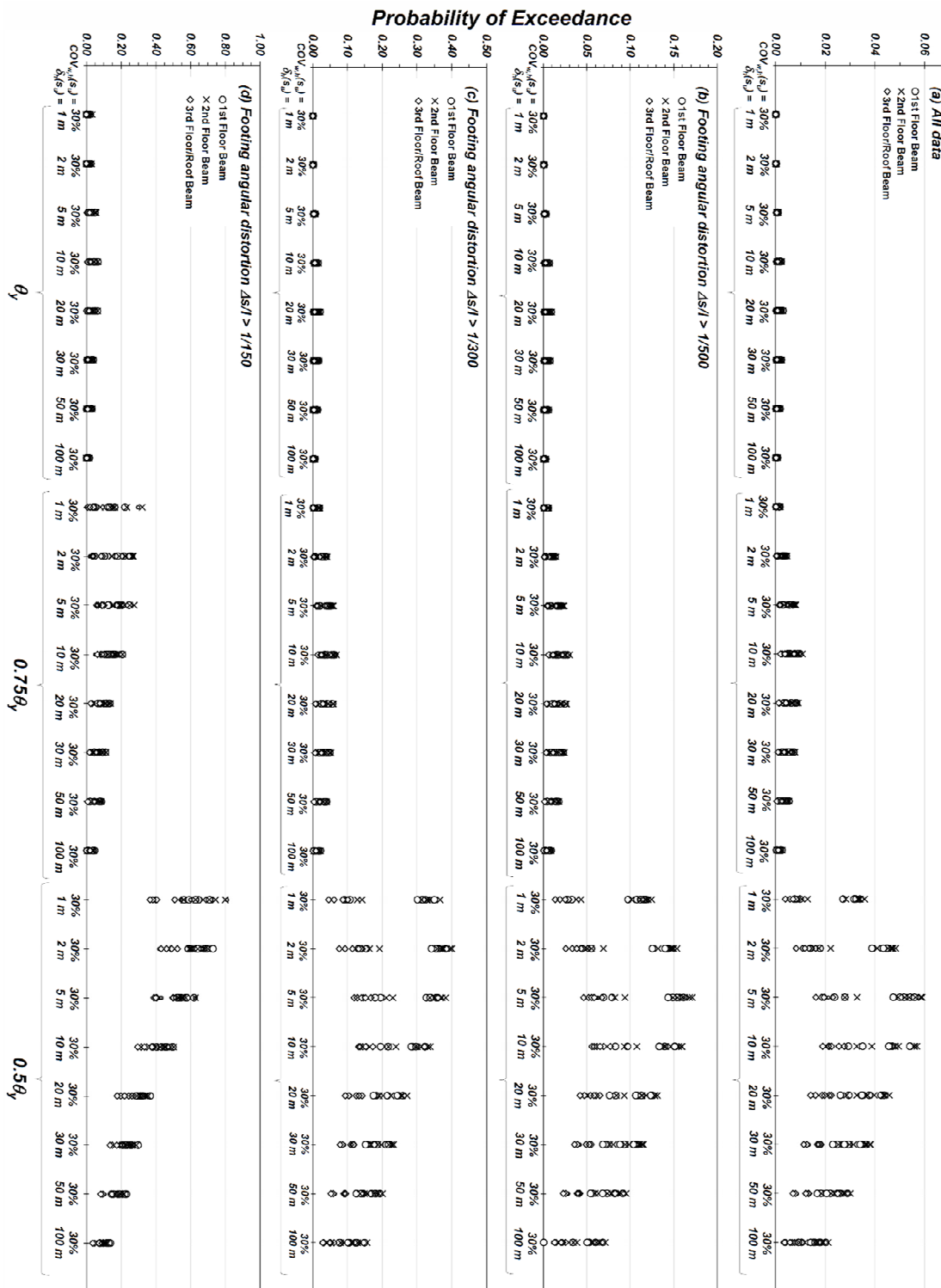
**Figure 7.27** Case 3 MCS. Probability of beam end rotation exceeding  $\theta_y$  for selected values of angular distortion and where  $COV_{w,h}(s_u) = 30\%$  and  $\delta_h(s_u) = 1$  to 100 m (Note (a) and (b) are plotted at different scales relative to (c) and (d) to provide better clarity to interpret probabilities).

Figure 7.28 is similar to Figure 7.25 and includes probability of exceeding beam end rotations equal  $\theta_y$ ,  $0.75\theta_y$ , and  $0.5\theta_y$ . A notable comparison between beam end rotation and footing response is most apparent when observing rotation equal to  $0.5\theta_y$ , which is analogous to the service or allowable limit state performance for the beams. When including all MCS data (Fig. 7.28a), the peak probability of exceeding  $0.5\theta_y$  occurs at  $\delta_h(s_u) = 5$  m (i.e., approximately  $l/2$ ), which coincides with  $\delta_h(s_u)_{crit}$  for the “allowable” ( $\Delta s/l = 1/500$ ) angular distortion indicated in Fig. 7.18. As the observed simulations are narrowed to only include more extreme angular distortions (e.g., Fig. 7.28d where  $\Delta s/l > 1/150$ ), the probability of exceeding  $0.5\theta_y$  becomes greatest for the smaller values of  $\delta_h(s_u)$  that were investigated herein.

When comparing the probabilities of exceedance in Figures 7.24 through 7.28, it is apparent that the 3<sup>rd</sup> floor beams generally exhibit lower probabilities of exceeding  $\theta_y$  (or proportion of  $\theta_y$ ) compared to the 1<sup>st</sup> and 2<sup>nd</sup> floor beams. This is due to the 3<sup>rd</sup> floor beam section (W18x40) having a higher yield rotation compared to the 1<sup>st</sup> floor (W24x76) and 2<sup>nd</sup> floor (W24x84) beams, and not because the beams that comprise each floor experience larger or smaller rotations, on average, at the beam-to-column connections. Table 7.12 provides a summary of  $\theta$  recorded at each of the connections for the MCS with  $COV_{w,h}(s_u) = 30$  percent and  $\delta_h(s_u) = 50$  m. Metrics for beam rotation are presented for all data and for the occurrences where angular distortion exceeded the selected limited state values of  $\Delta s/l = 1/500$ ,  $1/300$  and  $1/150$ . For the selected MCS scenario, the simulated beam end rotations, on average, are similar for all beams with mean  $\theta$  in the range of 0.0009 to 0.0012 radians and median  $\theta$  in the range of 0.0007 to 0.0010 radians. Larger mean and

median  $\theta$  values were observed when  $\Delta s/l$  exceeds the selected limit state values, but these larger  $\theta$  values are relatively consistent between each of the floors and corresponding beams. It should be noted that the yield moment,  $M_y$ , for the W18x40 section is equal to approximately one-third of the yield moment for the W24x76 and W24x84 sections. Therefore, the load imparted on the 3<sup>rd</sup> floor beams is correspondingly less compared to the 1<sup>st</sup> and 2<sup>nd</sup> floors. This suggests, in general, the structure is efficiently transferring loads according to foundation response and the stiffness of each beam section.

To provide further perspective of the beam rotations relative to foundation performance with variable soils, Figures 7.29 and 7.30 present the probability of exceeding  $\theta_y$  for beams in Bay 1 with varying  $\delta_h(s_u)$  and  $COV_{w,h}(s_u) = 30$  or 50 percent. For these cases, maximum probabilities of exceeding  $\theta_y$  occur when  $\delta_h(s_u)$  is in the range of 10 to 20 m (i.e., approximately  $l$  to  $2l$ ). Similar trends were observed in Figures 7.18, 7.27, and 7.28, where the probability of exceeding  $\Delta s/l$  at beam end rotations exceeding  $\theta_y$  increases as  $\delta_h(s_u)$  approaches  $\delta_h(s_u)_{crit}$  equal to approximately 20 m, then reduces at larger magnitudes of  $\delta_h(s_u)$ . However, while Figure 7.18 shows the probability of exceeding  $\Delta s/l$  plateauing as  $\delta_h(s_u)$  approaches and exceeds  $\delta_h(s_u)_{crit}$ , Figures 7.29 and 7.30 show that the probability of exceeding  $\theta_y$  dissipates more quickly for  $\delta_h(s_u)$  greater than  $\delta_h(s_u)_{crit}$ . The causes for the reduction in the probability of exceedance of  $\theta_y$  are described below.



**Figure 7.28** Case 3 MCS results. Probability of beam end rotation exceeding  $\theta_y$  or portion of  $\theta_y$  for selected values of angular distortion and where  $COV_{w,h}(s_u) = 30\%$  and  $\delta_h(s_u) = 1$  to 100 m. (Note different scales used in (a) through (d) to provide better clarity to interpret probabilities).



**Table 7.12. Case 3 MCS for  $COV_{w,h}(s_u) = 30$  percent and  $\delta_h(s_u) = 50$  m. Summary of beam rotation at each beam end for varying footing angular distortion limits.**

Beam connection =	All results		$\Delta s/l > 1/500$		$\Delta s/l > 1/300$		$\Delta s/l > 1/150$	
	Left, i	Right, j	Left, i	Right, j	Left, i	Right, j	Left, i	Right, j
<b>Beam 1 (1<sup>st</sup> floor)</b>								
Mean $\theta$ (rad.)	0.0009	0.0011	0.0016	0.0019	0.0020	0.0022	0.0022	0.0021
Median $\theta$ (rad.)	0.0007	0.0009	0.0015	0.0018	0.0020	0.0021	0.0019	0.0017
St. dev. $\theta$ (rad.)	0.0008	0.0009	0.0010	0.0011	0.0013	0.0014	0.0017	0.0017
COV ( $\theta$ )	0.90	0.85	0.63	0.59	0.64	0.65	0.77	0.83
Prob. of exceeding $\theta_s$	0.0015	0.0017	0.0053	0.0058	0.0123	0.0133	0.0291	0.0325
<b>Beam 2 (1<sup>st</sup> floor)</b>								
Mean $\theta$ (rad.)	0.0011	0.0011	0.0018	0.0019	0.0020	0.0021	0.0018	0.0019
Median $\theta$ (rad.)	0.0009	0.0009	0.0018	0.0019	0.0020	0.0021	0.0016	0.0016
St. dev. $\theta$ (rad.)	0.0008	0.0009	0.0010	0.0010	0.0012	0.0013	0.0013	0.0015
COV ( $\theta$ )	0.78	0.80	0.53	0.54	0.59	0.60	0.71	0.76
Prob. of exceeding $\theta_s$	0.0001	0.0003	0.0002	0.0010	0.0005	0.0025	0.0013	0.0066
<b>Beam 3 (1<sup>st</sup> floor)</b>								
Mean $\theta$ (rad.)	0.0011	0.0011	0.0019	0.0018	0.0021	0.0020	0.0019	0.0018
Median $\theta$ (rad.)	0.0009	0.0009	0.0018	0.0018	0.0020	0.0019	0.0016	0.0015
St. dev. $\theta$ (rad.)	0.0009	0.0008	0.0010	0.0010	0.0012	0.0012	0.0015	0.0013
COV ( $\theta$ )	0.79	0.77	0.54	0.53	0.61	0.59	0.77	0.71
Prob. of exceeding $\theta_s$	0.0004	0.0000	0.0015	0.0001	0.0035	0.0003	0.0089	0.0009
<b>Beam 4 (1<sup>st</sup> floor)</b>								
Mean $\theta$ (rad.)	0.0011	0.0009	0.0018	0.0016	0.0021	0.0020	0.0020	0.0021
Median $\theta$ (rad.)	0.0009	0.0007	0.0018	0.0015	0.0020	0.0019	0.0015	0.0017
St. dev. $\theta$ (rad.)	0.0009	0.0008	0.0011	0.0010	0.0014	0.0013	0.0017	0.0016
COV ( $\theta$ )	0.83	0.89	0.59	0.61	0.66	0.64	0.85	0.78
Prob. of exceeding $\theta_s$	0.0012	0.0011	0.0043	0.0037	0.0105	0.0092	0.0262	0.0231
<b>Beam 5 (2<sup>nd</sup> floor)</b>								
Mean $\theta$ (rad.)	0.0009	0.0011	0.0017	0.0019	0.0020	0.0022	0.0021	0.0021
Median $\theta$ (rad.)	0.0007	0.0009	0.0016	0.0018	0.0020	0.0021	0.0018	0.0017
St. dev. $\theta$ (rad.)	0.0008	0.0009	0.0010	0.0011	0.0013	0.0014	0.0016	0.0017
COV ( $\theta$ )	0.90	0.85	0.60	0.59	0.63	0.64	0.76	0.82
Prob. of exceeding $\theta_s$	0.0013	0.0017	0.0045	0.0059	0.0102	0.0136	0.0233	0.0330
<b>Beam 6 (2<sup>nd</sup> floor)</b>								
Mean $\theta$ (rad.)	0.0011	0.0011	0.0018	0.0019	0.0020	0.0021	0.0019	0.0020
Median $\theta$ (rad.)	0.0009	0.0009	0.0018	0.0019	0.0020	0.0021	0.0017	0.0016
St. dev. $\theta$ (rad.)	0.0009	0.0009	0.0010	0.0010	0.0012	0.0013	0.0013	0.0015
COV ( $\theta$ )	0.78	0.80	0.53	0.54	0.59	0.60	0.71	0.75
Prob. of exceeding $\theta_s$	0.0001	0.0003	0.0003	0.0011	0.0008	0.0026	0.0022	0.0070

**Notes:** 1. “All results” based on MCS with  $n = 50,000$  realizations.

2.  $\Delta s/l > 1/500$  results based on subset of MCS with  $n$  realizations ranging from 13,639 to 14,341.

3.  $\Delta s/l > 1/300$  results based on subset of MCS with  $n$  realizations ranging from 5,515 to 6,086.

4.  $\Delta s/l > 1/150$  results based on subset of MCS with  $n$  realizations ranging from 1,950 to 2,279.

**Table 7.12. Case 3 MCS for  $COV_{w,h}(s_u) = 30$  percent and  $\delta_h(s_u) = 50$  m. Summary of beam rotation at each beam end for varying footing angular distortion limits (continued).**

Beam connection =	All results		$\Delta s/l > 1/500$		$\Delta s/l > 1/300$		$\Delta s/l > 1/150$	
	Left, i	Right, j	Left, i	Right, j	Left, i	Right, j	Left, i	Right, j
<b>Beam 7 (2<sup>nd</sup> floor)</b>								
Mean $\theta$ (rad.)	0.0011	0.0011	0.0019	0.0018	0.0021	0.0020	0.0019	0.0018
Median $\theta$ (rad.)	0.0009	0.0009	0.0018	0.0018	0.0020	0.0020	0.0016	0.0016
St. dev. $\theta$ (rad.)	0.0009	0.0008	0.0010	0.0010	0.0012	0.0012	0.0015	0.0013
COV ( $\theta$ )	0.79	0.78	0.54	0.53	0.60	0.59	0.77	0.71
Prob. of exceeding $\theta_s$	0.0005	0.0001	0.0017	0.0004	0.0040	0.0008	0.0102	0.0022
<b>Beam 8 (2<sup>nd</sup> floor)</b>								
Mean $\theta$ (rad.)	0.0011	0.0009	0.0018	0.0016	0.0021	0.0020	0.0020	0.0020
Median $\theta$ (rad.)	0.0009	0.0007	0.0018	0.0015	0.0020	0.0019	0.0016	0.0017
St. dev. $\theta$ (rad.)	0.0009	0.0008	0.0011	0.0010	0.0014	0.0013	0.0017	0.0016
COV ( $\theta$ )	0.83	0.88	0.58	0.59	0.65	0.63	0.84	0.78
Prob. of exceeding $\theta_s$	0.0013	0.0010	0.0044	0.0034	0.0107	0.0082	0.0251	0.0190
<b>Beam 9 (3<sup>rd</sup> floor)</b>								
Mean $\theta$ (rad.)	0.0011	0.0012	0.0020	0.0021	0.0025	0.0025	0.0027	0.0025
Median $\theta$ (rad.)	0.0009	0.0009	0.0018	0.0020	0.0024	0.0024	0.0023	0.0021
St. dev. $\theta$ (rad.)	0.0010	0.0010	0.0012	0.0012	0.0016	0.0016	0.0020	0.0019
COV ( $\theta$ )	0.88	0.87	0.62	0.59	0.63	0.63	0.76	0.78
Prob. of exceeding $\theta_s$	0.0008	0.00005	0.0028	0.0018	0.0065	0.0041	0.0150	0.0102
<b>Beam 10 (3<sup>rd</sup> floor)</b>								
Mean $\theta$ (rad.)	0.0012	0.0012	0.0020	0.0021	0.0022	0.0023	0.0021	0.0022
Median $\theta$ (rad.)	0.0010	0.0010	0.0020	0.0020	0.0022	0.0023	0.0018	0.0018
St. dev. $\theta$ (rad.)	0.0009	0.0010	0.0011	0.0011	0.0013	0.0014	0.0015	0.0016
COV ( $\theta$ )	0.79	0.80	0.53	0.53	0.59	0.59	0.72	0.74
Prob. of exceeding $\theta_s$	0.0000	0.0001	0.0000	0.0002	0.0000	0.0005	0.0000	0.0013
<b>Beam 11 (3<sup>rd</sup> floor)</b>								
Mean $\theta$ (rad.)	0.0012	0.0012	0.0020	0.0020	0.0023	0.0022	0.0021	0.0021
Median $\theta$ (rad.)	0.0010	0.0010	0.0020	0.0020	0.0022	0.0022	0.0018	0.0018
St. dev. $\theta$ (rad.)	0.0010	0.0009	0.0011	0.0011	0.0013	0.0013	0.0016	0.0015
COV ( $\theta$ )	0.79	0.79	0.53	0.53	0.59	0.59	0.75	0.73
Prob. of exceeding $\theta_s$	0.0001	0.0000	0.0002	0.0001	0.0005	0.0002	0.0013	0.0004
<b>Beam 12 (3<sup>rd</sup> floor)</b>								
Mean $\theta$ (rad.)	0.0012	0.0011	0.0021	0.0020	0.0024	0.0024	0.0024	0.0026
Median $\theta$ (rad.)	0.0009	0.0009	0.0020	0.0018	0.0023	0.0023	0.0019	0.0021
St. dev. $\theta$ (rad.)	0.0010	0.0010	0.0012	0.0012	0.0015	0.0015	0.0019	0.0020
COV ( $\theta$ )	0.86	0.87	0.58	0.61	0.64	0.63	0.81	0.77
Prob. of exceeding $\theta_s$	0.0003	0.0004	0.0010	0.0015	0.0025	0.0038	0.0072	0.0087

**Notes:** 1. “All results” based on MCS with  $n = 50,000$  realizations.

2.  $\Delta s/l > 1/500$  results based on subset of MCS with  $n$  realizations ranging from 13,639 to 14,341.

3.  $\Delta s/l > 1/300$  results based on subset of MCS with  $n$  realizations ranging from 5,515 to 6,086.

4.  $\Delta s/l > 1/150$  results based on subset of MCS with  $n$  realizations ranging from 1,950 to 2,279.

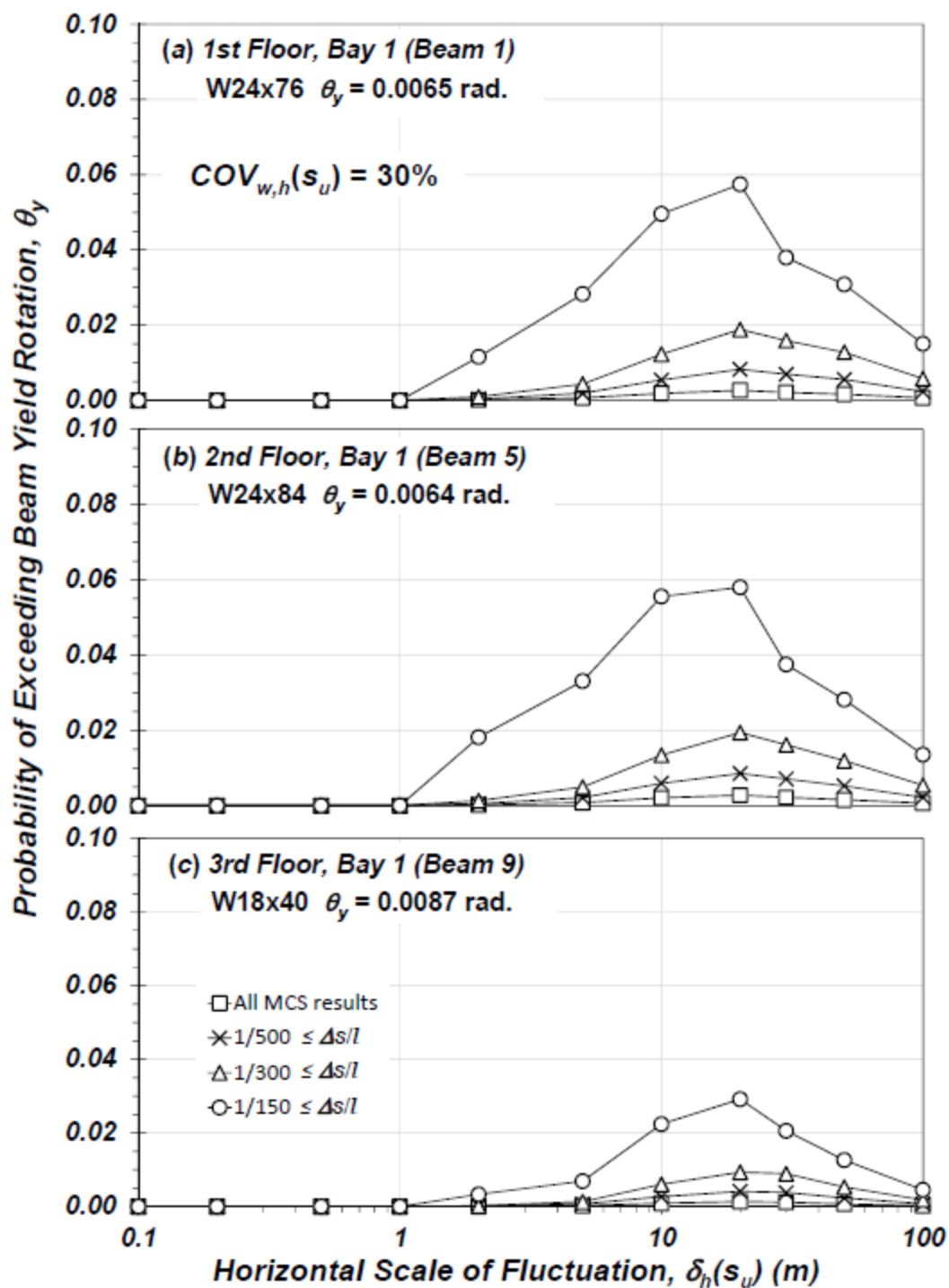


Figure 7.29 Case 3 MCS results for Bay 1. Probability of exceedance of beam yield rotation for  $COV_{w,h}(s_u) = 30\%$  with varying horizontal scale of fluctuation.

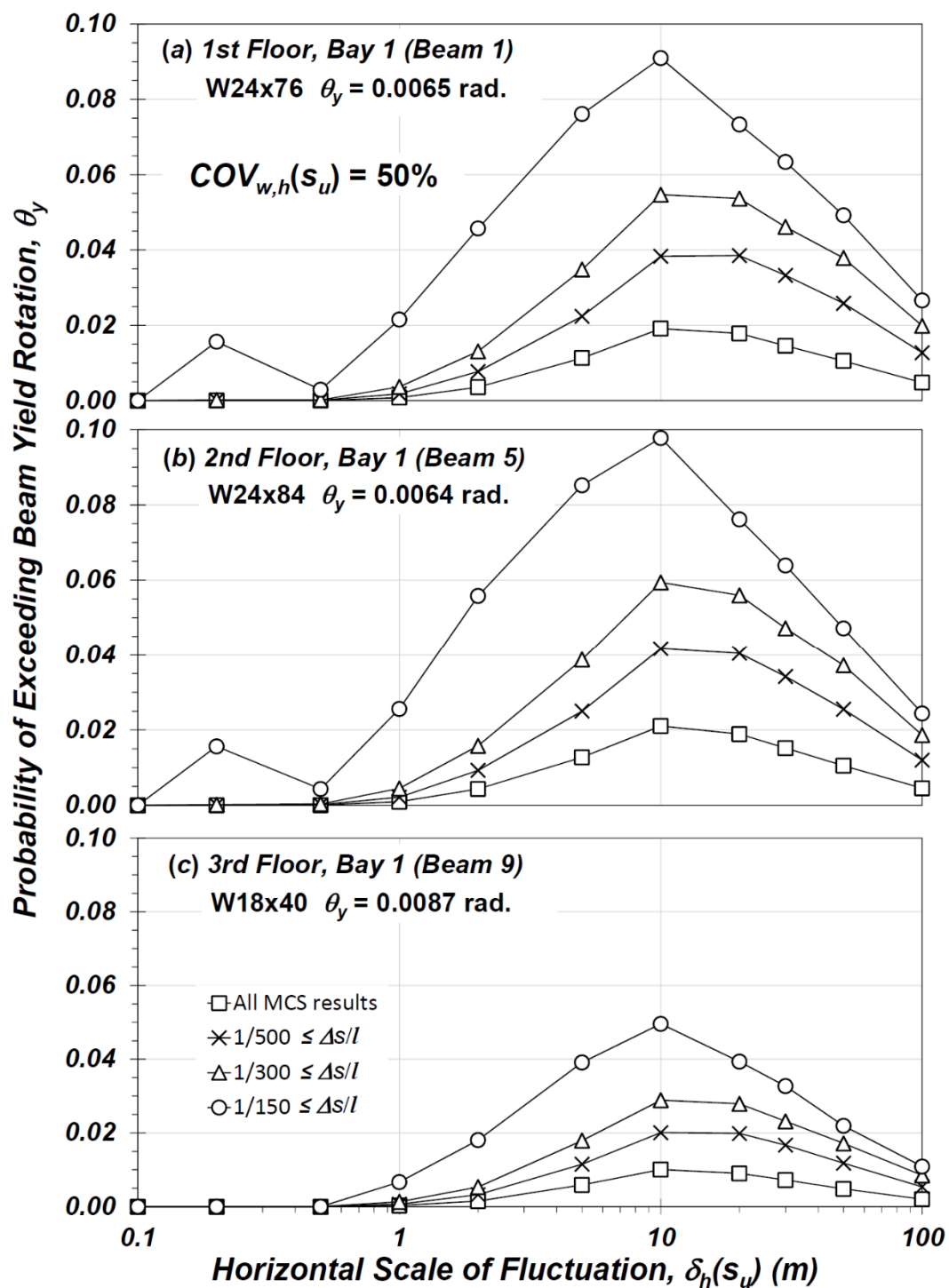
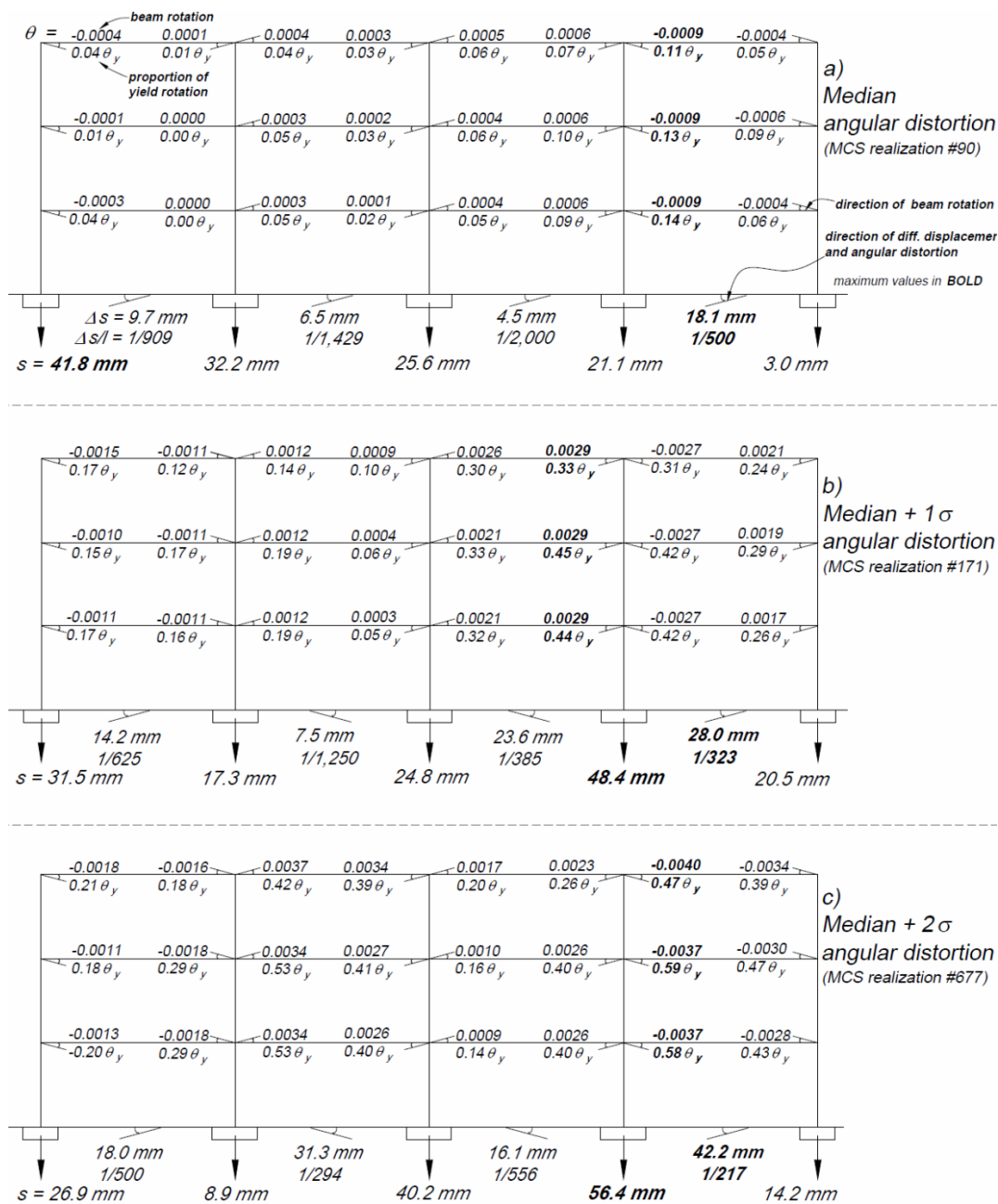


Figure 7.30 Case 3 MCS results for Bay 1. Probability of exceedance of beam yield rotation for  $COV_{w,h}(s_u) = 50\%$  with varying horizontal scale of fluctuation.

Figures 7.31 through 7.35 and Table 7.13 summarize the beam rotations, foundation settlements, and angular distortions for selected MCS realizations to provide a comprehensive presentation of the individual beam responses relative to footing displacements. The combinations of  $COV_{w,h}(s_u)$  and  $\delta_h(s_u)$  used in Figures 7.19 through 7.25 are used in Figures 7.31 through 7.35 to represent a range of soil spatial variability simulated. Each figure includes three realizations where the mean of the four differential displacements measured between each footing (and corresponding angular distortion across each bay) for a given realization is equal to (a) the median value from the MCS results, (b) the median plus one standard deviation, and (c) the median plus two standard deviations. The largest values of  $s$ ,  $\Delta s$  and  $\Delta s/l$  from the selected examples are documented in Fig. 7.35c for the scenario that includes  $COV_{w,h}(s_u) = 50$  percent and  $\delta_h(s_u) = 50$  m and where the average  $\Delta s/l$  is equal to the median plus two standard deviations relative to the MCS results. For the Fig. 7.35c realization,  $\Delta s$  ranges from 152 mm to 218 mm and  $\Delta s/l$  ranges from 1/60 to 1/42. The maximum beam rotations on each floor recorded at the beam-to-column connections range from  $0.47\theta_y$  to  $0.58\theta_y$ . Of interest to note is that the  $\Delta s/l$  values are well above the assumed ultimate limit state value of 1/150 while the corresponding structural response at the beam-to-column connections is well below the ultimate limit state rotation threshold. The largest beam rotations were recorded for the realization summarized in Fig. 7.34b, which includes the scenario for  $COV_{w,h}(s_u) = 50$  percent and  $\delta_h(s_u) = 5$  m with average  $\Delta s/l$  equal to the median plus one standard deviation. In Fig 7.34b, the maximum beam rotations on each floor, observed for Bay 1 beam-to-column connections, ranged from  $0.72\theta_y$  to  $0.93\theta_y$ . The angular distortion

associated with Bay 1 was low, with  $\Delta s/l = 1/1,250$ . However, at the adjacent Bay 2,  $\Delta s/l = 1/87$ . This suggests that  $\theta$  values are not necessarily greatest where  $\Delta s/l$  is largest, but where the change in  $\Delta s/l$  between adjacent bays is largest.



**Figure 7.31** Selected Case 3 MCS realizations for  $COV_{w,h}(s_u) = 5\%$  and  $\delta_h(s_u) = 5 \text{ m}$  where mean  $\Delta s/l$  between footings is equal to a) median value, b) median plus 1 standard deviation, c) median plus 2 standard deviations.

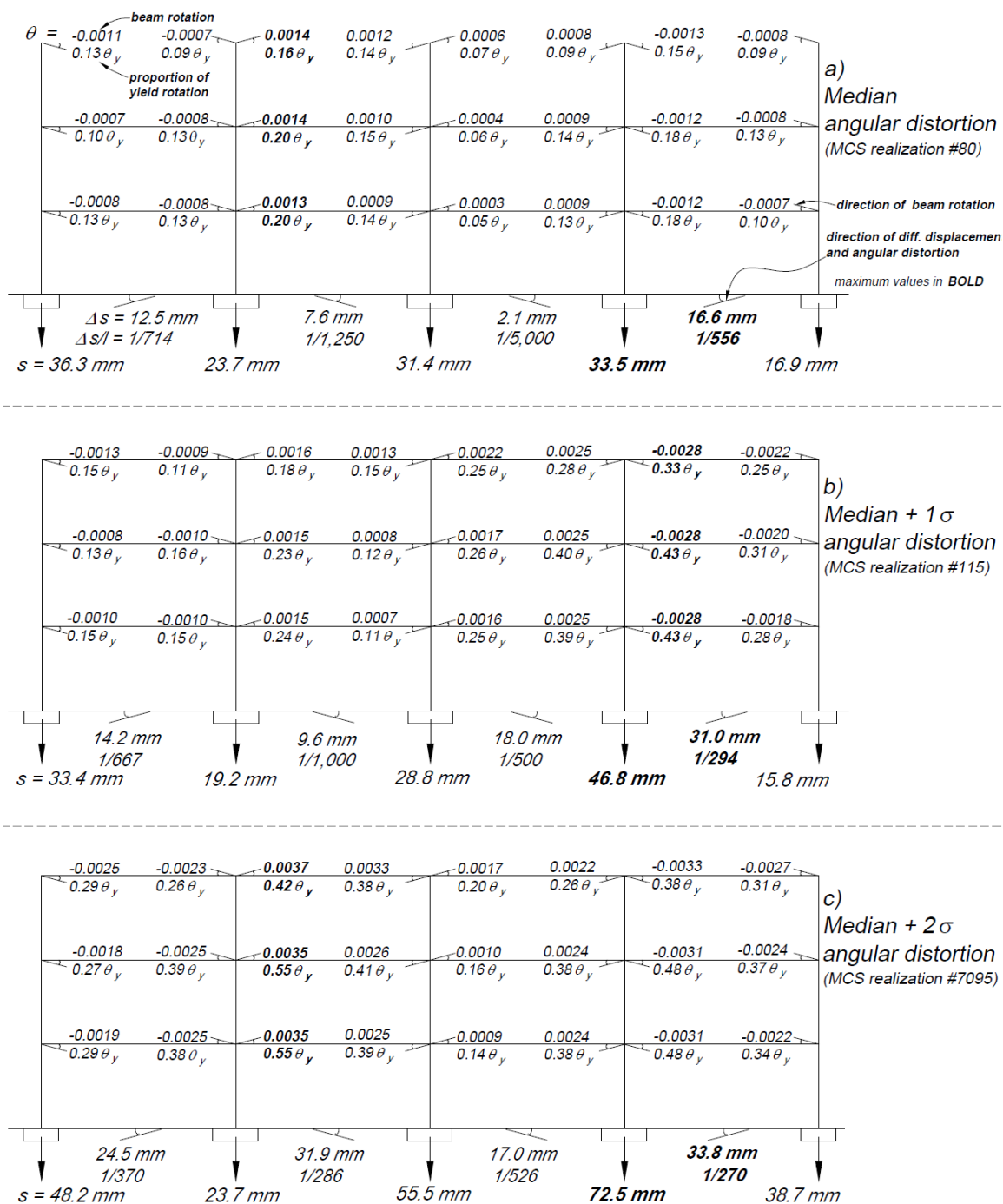


**Figure 7.32** Selected Case 3 MCS realizations for  $COV_{w,h}(s_u) = 5\%$  and  $\delta_h(s_u) = 50 \text{ mm}$  where mean  $\Delta s/l$  between footings is equal to a) median value, b) median plus 1 standard deviation, c) median plus 2 standard deviations.

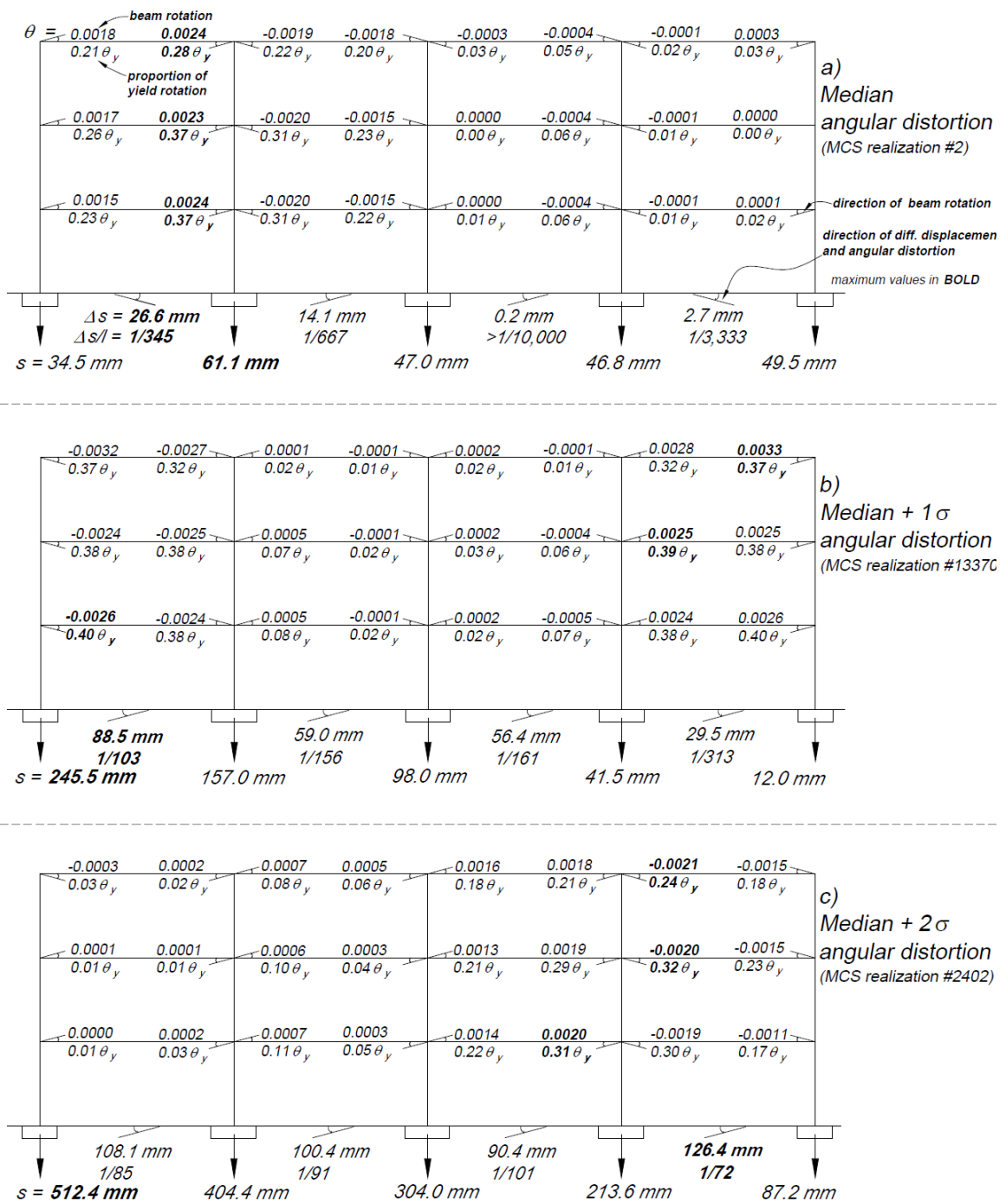


**Figure 7.33** Selected Case 3 MCS realizations for  $COV_{w,h}(s_u) = 30\%$  and  $\delta_h(s_u) = 50 \text{ m}$  where mean  $\Delta s/l$  between footings is equal to a) median value, b) median plus 1 standard deviation, c) median plus 2 standard deviations.



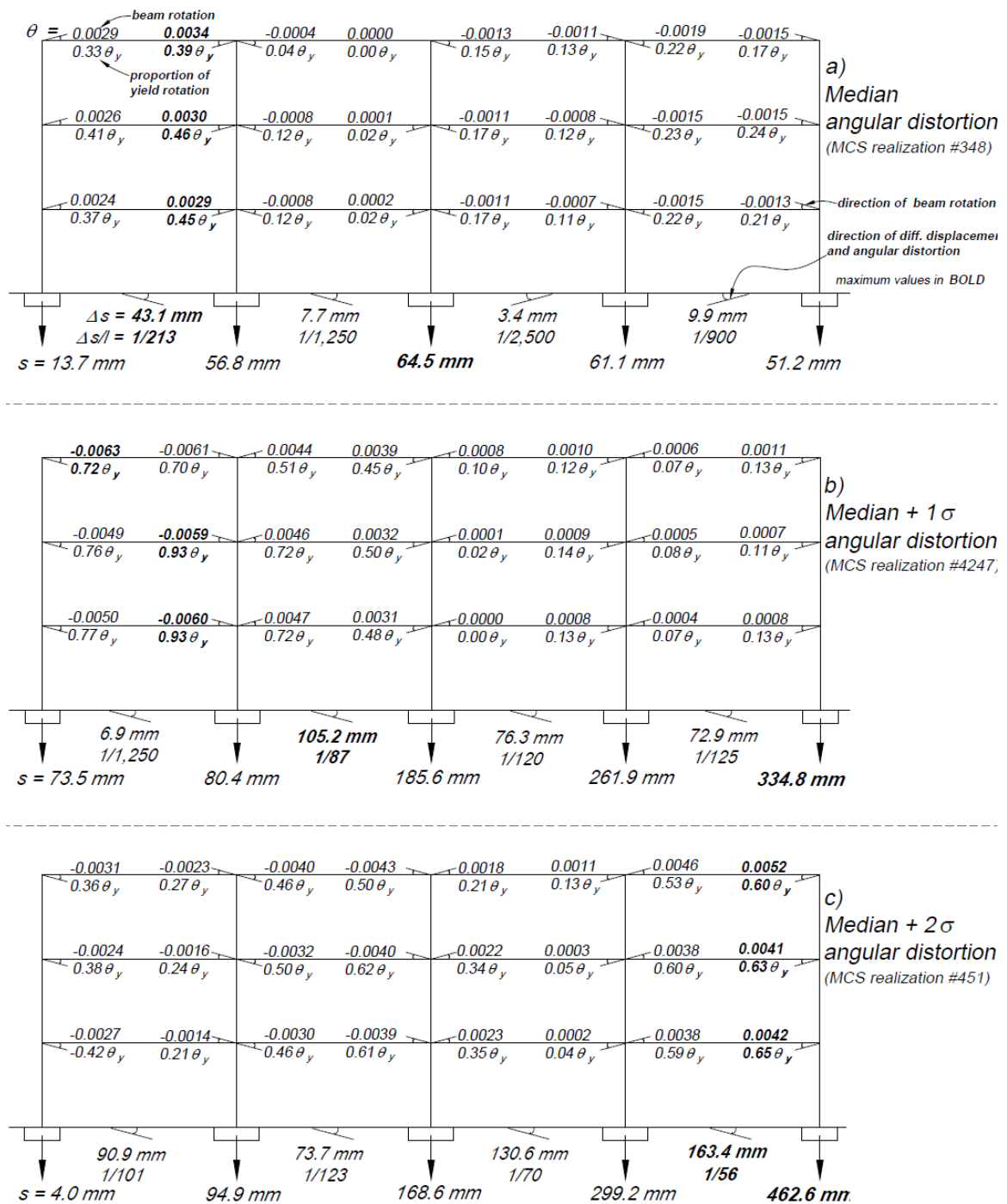


**Figure 7.34** Selected Case 3 MCS realizations for  $COV_{w,h}(s_u) = 50\%$  and  $\delta_h(s_u) = 5 \text{ m}$  where mean  $\Delta s/l$  between footings is equal to a) median value, b) median plus 1 standard deviation, c) median plus 2 standard deviations.

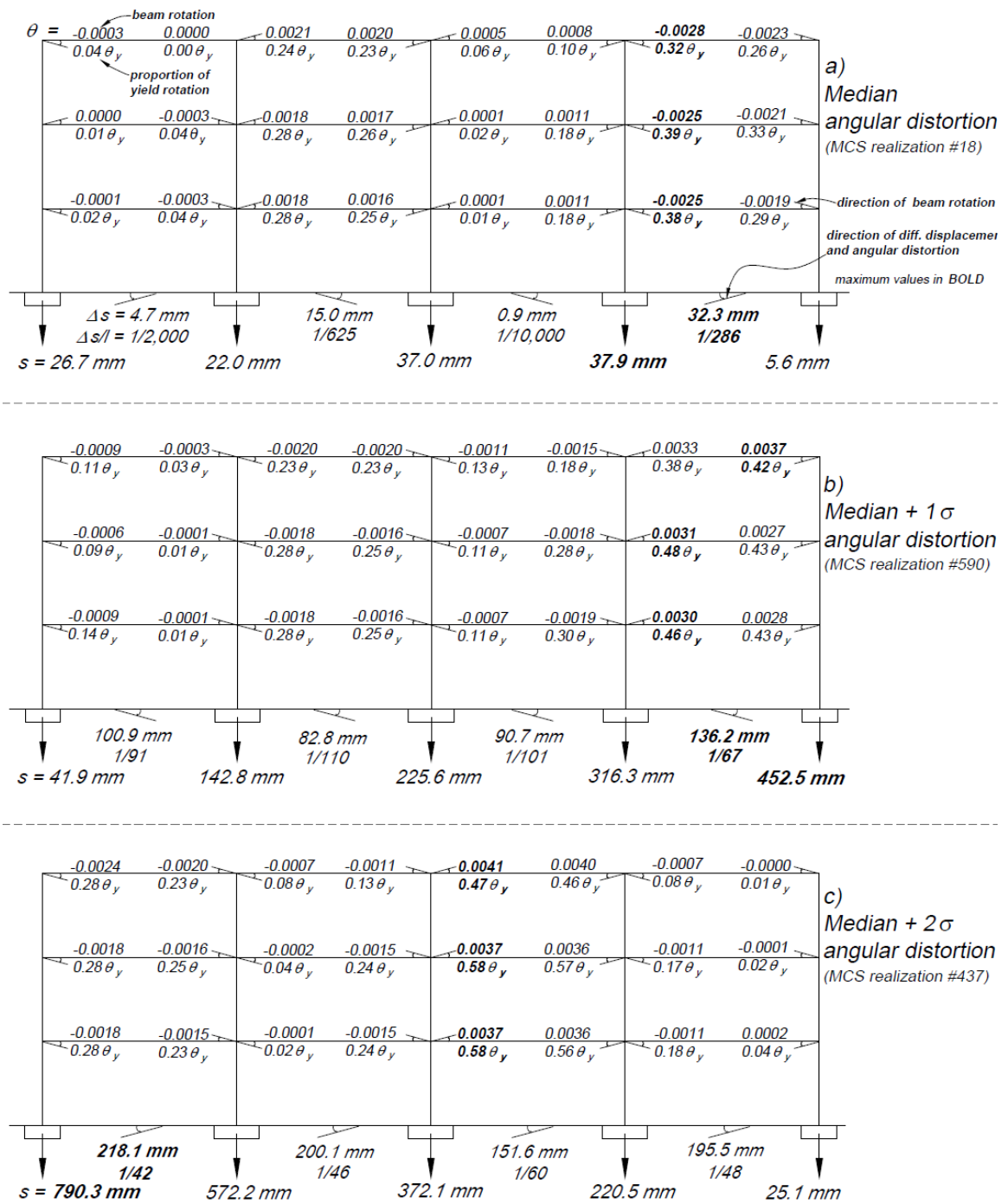


**Figure 7.35** Selected Case 3 MCS realizations for  $COV_{w,h}(s_u) = 50\%$  and  $\delta_h(s_u) = 50 \text{ m}$  where mean  $\Delta s/l$  between footings is equal to a) median value, b) median plus 1 standard deviation, c) median plus 2 standard deviations.

To investigate further, the occurrence of beam end rotations that exceeded the yield rotation,  $\theta_y$ , were tabulated for the selected combinations of  $COV_{w,h}(S_u)$  and  $\delta_h(S_u)$  equal to 30 percent and 50 m, 50 percent and 5 m, and 50 percent and 50 m (note:  $COV_{w,h}(S_u) = 5$  percent are not included in the tabulation since no exceedance of  $\theta_y$  occurred). The exceedance of  $\theta_y$  for each beam within the structure was compared to the angular distortion,  $\Delta s/l$ , between each bay and the median  $\Delta s/l$  values are summarized in Table 7.13. Locations in Table 7.13 where the beam yielding coincides with the bay where median angular distortion is reported are noted in **bold** (e.g., Beams 1, 5 and 9 coinciding with Bay 1). For the two scenarios of  $COV_{w,h}(S_u) = 30$  percent and  $\delta_h(S_u) = 50$  m and  $COV_{w,h}(S_u) = 50$  percent and  $\delta_h(S_u) = 50$  m, when the beam and bay locations in Table 7.13 coincide, the median  $\Delta s/l$  values ranged from 1/33 to 1/95, depending on location. However, for the scenario of  $COV_{w,h}(S_u) = 50$  percent and  $\delta_h(S_u) = 5$  m, the median  $\Delta s/l$  values are typically one-half to two-thirds lower at the same locations, ranging from 1/47 to 1/119. This suggests that when beam yield rotation occurred, it generally coincided with a smaller angular distortion when  $\delta_h(S_u)$  was smaller. This is further observed in Fig. 7.36, which presents the median  $\Delta s/l$  with varying  $\delta_h(S_u)$  and constant  $COV_{w,h}(S_u) = 30$  percent for each beam for cases where beam yield rotation,  $\theta_y$ , was exceeded. A trend of larger angular distortions required to cause beam yield rotation when  $\delta_h(S_u)$  is large, and smaller angular distortions required to cause beam yield rotation when  $\delta_h(S_u)$  is small, is apparent. Table 7.14 accompanies the data provided in Figure 7.36 and includes a summary  $\Delta s/l$  across each of the bays and the median  $\Delta s/l$  when  $\theta_y$  was exceeded for the scenario with constant  $COV_{w,h}(S_u) = 30$  percent and  $\delta_h(S_u)$  varying between 1 m and 100 m.

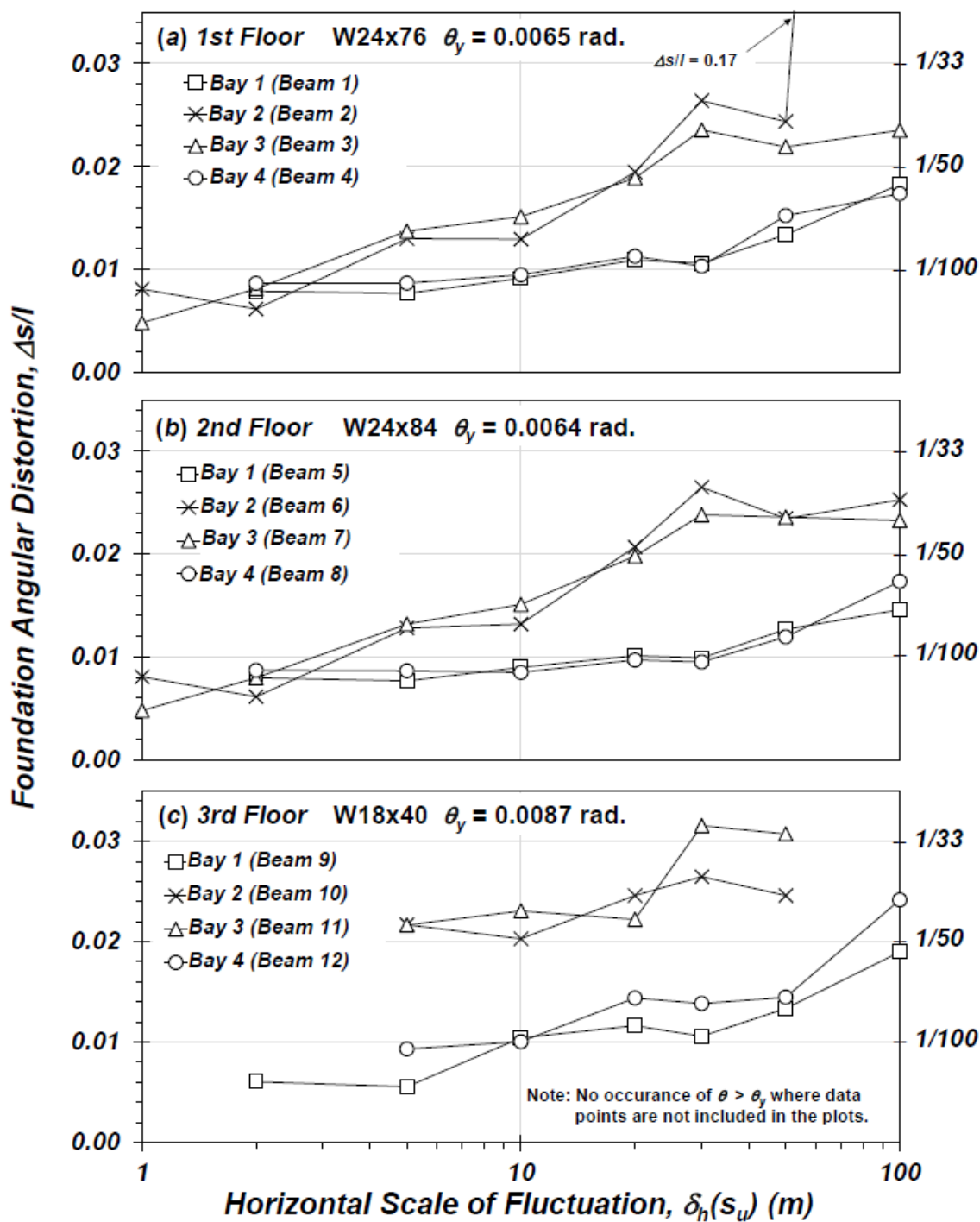


**Figure 7.36** Case 3 MCS. Median angular distortion across each bay at occurrences when beam rotation,  $\theta > \theta_y$ .  $COV_{w,h}(s_u) = 30$  m.

**Table 7.13. Case 3 MCS for selected combinations of  $COV_{w,h}(s_u)$  and  $\delta_h(s_u)$ . Yield rotation occurrences for each beam at the beam ends and summary of median footing angular distortion across each bay when beam yield rotation occurs.**

	Frequency of $\theta > \theta_y$	Median $\Delta s/l$ when $\theta > \theta_y$ occurs			
		Bay 1	Bay 2	Bay 3	Bay 4
<b><math>COV_{w,h}(s_u) = 30\%</math> <math>\delta_h(s_u) = 50</math> m</b>					
Beam 1 (Bay 1, 1 <sup>st</sup> Floor)	93	<b>1/75</b>	1/43	1/36	1/41
Beam 2 (Bay 2, 1 <sup>st</sup> Floor)	17	1/49	<b>1/41</b>	1/96	1/127
Beam 3 (Bay 3, 1 <sup>st</sup> Floor)	23	1/133	1/87	<b>1/46</b>	1/55
Beam 4 (Bay 4, 1 <sup>st</sup> Floor)	73	1/36	1/34	1/40	<b>1/66</b>
Beam 5 (Bay 1, 2 <sup>nd</sup> Floor)	91	<b>1/79</b>	1/48	1/38	1/43
Beam 6 (Bay 2, 2 <sup>nd</sup> Floor)	19	1/51	<b>1/43</b>	1/99	1/176
Beam 7 (Bay 3, 2 <sup>nd</sup> Floor)	27	1/108	1/63	<b>1/42</b>	1/49
Beam 8 (Bay 4, 2 <sup>nd</sup> Floor)	69	1/40	1/39	1/48	<b>1/84</b>
Beam 9 (Bay 1, 3 <sup>rd</sup> Floor)	41	<b>1/75</b>	1/40	1/33	1/37
Beam 10 (Bay 2, 3 <sup>rd</sup> Floor)	3	1/47	<b>1/41</b>	1/99	1/127
Beam 11 (Bay 3, 3 <sup>rd</sup> Floor)	3	1/91	1/60	<b>1/33</b>	1/39
Beam 12 (Bay 4, 3 <sup>rd</sup> Floor)	23	1/37	1/34	1/43	<b>1/69</b>
<b><math>COV_{w,h}(s_u) = 50\%</math> <math>\delta_h(s_u) = 5</math> m</b>					
Beam 1 (Bay 1, 1 <sup>st</sup> Floor)	732	<b>1/115</b>	1/126	1/63	1/76
Beam 2 (Bay 2, 1 <sup>st</sup> Floor)	912	1/145	<b>1/79</b>	1/196	1/165
Beam 3 (Bay 3, 1 <sup>st</sup> Floor)	939	1/175	1/192	<b>1/74</b>	1/140
Beam 4 (Bay 4, 1 <sup>st</sup> Floor)	639	1/64	1/56	1/91	<b>1/114</b>
Beam 5 (Bay 1, 2 <sup>nd</sup> Floor)	784	<b>1/119</b>	1/153	1/71	1/82
Beam 6 (Bay 2, 2 <sup>nd</sup> Floor)	946	1/152	<b>1/80</b>	1/191	1/160
Beam 7 (Bay 3, 2 <sup>nd</sup> Floor)	990	1/164	1/194	<b>1/76</b>	1/146
Beam 8 (Bay 4, 2 <sup>nd</sup> Floor)	712	1/71	1/62	1/114	<b>1/118</b>
Beam 9 (Bay 1, 3 <sup>rd</sup> Floor)	341	<b>1/106</b>	1/92	1/48	1/60
Beam 10 (Bay 2, 3 <sup>rd</sup> Floor)	228	1/67	<b>1/50</b>	1/178	1/161
Beam 11 (Bay 3, 3 <sup>rd</sup> Floor)	259	1/203	1/150	<b>1/47</b>	1/68
Beam 12 (Bay 4, 3 <sup>rd</sup> Floor)	270	1/55	1/46	1/86	<b>1/107</b>
<b><math>COV_{w,h}(s_u) = 50\%</math> <math>\delta_h(s_u) = 50</math> m</b>					
Beam 1 (Bay 1, 1 <sup>st</sup> Floor)	607	<b>1/86</b>	1/50	1/37	1/43
Beam 2 (Bay 2, 1 <sup>st</sup> Floor)	275	1/54	<b>1/42</b>	1/77	1/105
Beam 3 (Bay 3, 1 <sup>st</sup> Floor)	294	1/109	1/77	<b>1/44</b>	1/57
Beam 4 (Bay 4, 1 <sup>st</sup> Floor)	509	1/38	1/35	1/46	<b>1/75</b>
Beam 5 (Bay 1, 2 <sup>nd</sup> Floor)	604	<b>1/95</b>	1/52	1/39	1/45
Beam 6 (Bay 2, 2 <sup>nd</sup> Floor)	295	1/54	<b>1/42</b>	1/76	1/105
Beam 7 (Bay 3, 2 <sup>nd</sup> Floor)	301	1/107	1/76	<b>1/43</b>	1/56
Beam 8 (Bay 4, 2 <sup>nd</sup> Floor)	521	1/40	1/36	1/49	<b>1/80</b>
Beam 9 (Bay 1, 3 <sup>rd</sup> Floor)	272	<b>1/95</b>	1/51	1/36	1/43
Beam 10 (Bay 2, 3 <sup>rd</sup> Floor)	58	1/42	<b>1/34</b>	1/90	1/136
Beam 11 (Bay 3, 3 <sup>rd</sup> Floor)	62	1/145	1/85	<b>1/39</b>	1/50
Beam 12 (Bay 4, 3 <sup>rd</sup> Floor)	198	1/35	1/32	1/45	<b>1/72</b>

**Note:** Number of occurrences of  $\theta_y$  for each beam may include either left or right side beam end, or both sides. Footing angular rotation noted in **bold** where the bay location coincides with the selected beam.

**Table 7.14. Case 3 MCS for  $COV_{w,h}(s_u) = 30$  percent and  $\delta_h(s_u) = 1$  to 100 m. Yield rotation occurrences for each beam at the beam ends and summary of median footing angular distortion across each bay when beam yield rotation occurs.**

	Frequency of $\theta > \theta_y$	Median $\Delta s/l$ when $\theta > \theta_y$ occurs			
		Bay 1	Bay 2	Bay 3	Bay 4
<b><math>COV_{w,h}(s_u) = 30\%</math> <math>\delta_h(s_u) = 1</math> m</b>					
Beam 1 (Bay 1, 1 <sup>st</sup> Floor)	0	N/A	N/A	N/A	N/A
Beam 2 (Bay 2, 1 <sup>st</sup> Floor)	4	1/473	<b>1/124</b>	1/599	1/331
Beam 3 (Bay 3, 1 <sup>st</sup> Floor)	2	1/184	1/125	<b>1/209</b>	1/436
Beam 4 (Bay 4, 1 <sup>st</sup> Floor)	0	N/A	N/A	N/A	<b>N/A</b>
Beam 5 (Bay 1, 2 <sup>nd</sup> Floor)	0	<b>N/A</b>	N/A	N/A	N/A
Beam 6 (Bay 2, 2 <sup>nd</sup> Floor)	4	1/473	<b>1/124</b>	1/599	1/331
Beam 7 (Bay 3, 2 <sup>nd</sup> Floor)	2	1/184	1/125	<b>1/209</b>	1/436
Beam 8 (Bay 4, 2 <sup>nd</sup> Floor)	0	N/A	N/A	N/A	<b>N/A</b>
Beam 9 (Bay 1, 3 <sup>rd</sup> Floor)	0	<b>N/A</b>	N/A	N/A	N/A
Beam 10 (Bay 2, 3 <sup>rd</sup> Floor)	0	N/A	<b>N/A</b>	N/A	N/A
Beam 11 (Bay 3, 3 <sup>rd</sup> Floor)	0	N/A	N/A	<b>N/A</b>	N/A
Beam 12 (Bay 4, 3 <sup>rd</sup> Floor)	0	N/A	N/A	N/A	<b>N/A</b>
<b><math>COV_{w,h}(s_u) = 30\%</math> <math>\delta_h(s_u) = 2</math> m</b>					
Beam 1 (Bay 1, 1 <sup>st</sup> Floor)	9	<b>1/127</b>	1/320	1/132	1/197
Beam 2 (Bay 2, 1 <sup>st</sup> Floor)	8	1/282	<b>1/163</b>	1/282	1/216
Beam 3 (Bay 3, 1 <sup>st</sup> Floor)	14	1/189	1/692	<b>1/123</b>	1/230
Beam 4 (Bay 4, 1 <sup>st</sup> Floor)	4	1/361	1/189	1/1628	<b>1/116</b>
Beam 5 (Bay 1, 2 <sup>nd</sup> Floor)	12	<b>1/126</b>	1/346	1/158	1/350
Beam 6 (Bay 2, 2 <sup>nd</sup> Floor)	8	1/282	<b>1/163</b>	1/282	1/216
Beam 7 (Bay 3, 2 <sup>nd</sup> Floor)	15	1/202	1/680	<b>1/126</b>	1/230
Beam 8 (Bay 4, 2 <sup>nd</sup> Floor)	4	1/234	1/177	1/1373	<b>1/115</b>
Beam 9 (Bay 1, 3 <sup>rd</sup> Floor)	2	<b>1/165</b>	1/154	1/74	1/81
Beam 10 (Bay 2, 3 <sup>rd</sup> Floor)	0	N/A	<b>N/A</b>	N/A	N/A
Beam 11 (Bay 3, 3 <sup>rd</sup> Floor)	0	N/A	N/A	<b>N/A</b>	N/A
Beam 12 (Bay 4, 3 <sup>rd</sup> Floor)	0	N/A	N/A	N/A	<b>N/A</b>
<b><math>COV_{w,h}(s_u) = 30\%</math> <math>\delta_h(s_u) = 5</math> m</b>					
Beam 1 (Bay 1, 1 <sup>st</sup> Floor)	50	<b>1/131</b>	1/146	1/89	1/99
Beam 2 (Bay 2, 1 <sup>st</sup> Floor)	48	1/139	<b>1/77</b>	1/174	1/273
Beam 3 (Bay 3, 1 <sup>st</sup> Floor)	49	1/228	1/228	<b>1/73</b>	1/179
Beam 4 (Bay 4, 1 <sup>st</sup> Floor)	47	1/57	1/50	1/72	<b>1/116</b>
Beam 5 (Bay 1, 2 <sup>nd</sup> Floor)	54	<b>1/130</b>	1/211	1/137	1/161
Beam 6 (Bay 2, 2 <sup>nd</sup> Floor)	50	1/142	<b>1/78</b>	1/178	1/267
Beam 7 (Bay 3, 2 <sup>nd</sup> Floor)	53	1/190	1/240	<b>1/76</b>	1/212
Beam 8 (Bay 4, 2 <sup>nd</sup> Floor)	52	1/62	1/58	1/109	<b>1/116</b>
Beam 9 (Bay 1, 3 <sup>rd</sup> Floor)	15	<b>1/180</b>	1/70	1/49	1/59
Beam 10 (Bay 2, 3 <sup>rd</sup> Floor)	5	1/59	<b>1/46</b>	1/130	1/207
Beam 11 (Bay 3, 3 <sup>rd</sup> Floor)	6	1/255	1/478	<b>1/46</b>	1/67
Beam 12 (Bay 4, 3 <sup>rd</sup> Floor)	22	1/51	1/41	1/52	<b>1/107</b>

**Note:** Number of occurrences of  $\theta_y$  for each beam may include either left or right side beam end, or both sides. Footing angular rotation noted in **bold** where the bay location coincides with the selected beam.

**Table 7.14. Case 3 MCS for  $COV_{w,h}(S_u) = 30$  percent and  $\delta_h(S_u) = 1$  to 100 m. Yield rotation occurrences for each beam at the beam ends and summary of median footing angular distortion across each bay when beam yield rotation occurs (continued).**

	Frequency of $\theta > \theta_y$	Median $\Delta s/l$ when $\theta > \theta_y$ occurs			
		Bay 1	Bay 2	Bay 3	Bay 4
<b><math>COV_{w,h}(S_u) = 30\%</math> <math>\delta_h(S_u) = 10</math> m</b>					
Beam 1 (Bay 1, 1 <sup>st</sup> Floor)	113	<b>1/110</b>	1/70	1/47	1/56
Beam 2 (Bay 2, 1 <sup>st</sup> Floor)	78	1/141	<b>1/77</b>	1/169	1/229
Beam 3 (Bay 3, 1 <sup>st</sup> Floor)	80	1/176	1/176	<b>1/66</b>	1/117
Beam 4 (Bay 4, 1 <sup>st</sup> Floor)	111	1/51	1/44	1/58	<b>1/106</b>
Beam 5 (Bay 1, 2 <sup>nd</sup> Floor)	121	<b>1/111</b>	1/74	1/50	1/61
Beam 6 (Bay 2, 2 <sup>nd</sup> Floor)	84	1/139	<b>1/76</b>	1/143	1/201
Beam 7 (Bay 3, 2 <sup>nd</sup> Floor)	88	1/176	1/176	<b>1/66</b>	1/122
Beam 8 (Bay 4, 2 <sup>nd</sup> Floor)	117	1/53	1/47	1/61	<b>1/118</b>
Beam 9 (Bay 1, 3 <sup>rd</sup> Floor)	50	<b>1/96</b>	1/67	1/43	1/50
Beam 10 (Bay 2, 3 <sup>rd</sup> Floor)	6	1/60	<b>1/49</b>	1/703	1/295
Beam 11 (Bay 3, 3 <sup>rd</sup> Floor)	15	1/177	1/119	<b>1/43</b>	1/62
Beam 12 (Bay 4, 3 <sup>rd</sup> Floor)	48	1/49	1/42	1/56	<b>1/100</b>
<b><math>COV_{w,h}(S_u) = 30\%</math> <math>\delta_h(S_u) = 20</math> m</b>					
Beam 1 (Bay 1, 1 <sup>st</sup> Floor)	152	<b>1/92</b>	1/51	1/42	1/48
Beam 2 (Bay 2, 1 <sup>st</sup> Floor)	63	1/70	<b>1/51</b>	1/119	1/219
Beam 3 (Bay 3, 1 <sup>st</sup> Floor)	54	1/121	1/87	<b>1/53</b>	1/80
Beam 4 (Bay 4, 1 <sup>st</sup> Floor)	113	1/44	1/38	1/50	<b>1/89</b>
Beam 5 (Bay 1, 2 <sup>nd</sup> Floor)	160	<b>1/99</b>	1/53	1/42	1/50
Beam 6 (Bay 2, 2 <sup>nd</sup> Floor)	73	1/69	<b>1/48</b>	1/103	1/208
Beam 7 (Bay 3, 2 <sup>nd</sup> Floor)	61	1/114	1/75	<b>1/51</b>	1/72
Beam 8 (Bay 4, 2 <sup>nd</sup> Floor)	121	1/47	1/42	1/55	<b>1/103</b>
Beam 9 (Bay 1, 3 <sup>rd</sup> Floor)	76	<b>1/86</b>	1/48	1/37	1/44
Beam 10 (Bay 2, 3 <sup>rd</sup> Floor)	11	1/49	<b>1/41</b>	1/82	1/217
Beam 11 (Bay 3, 3 <sup>rd</sup> Floor)	5	1/172	1/166	<b>1/45</b>	1/56
Beam 12 (Bay 4, 3 <sup>rd</sup> Floor)	43	1/35	1/31	1/43	<b>1/69</b>
<b><math>COV_{w,h}(S_u) = 30\%</math> <math>\delta_h(S_u) = 30</math> m</b>					
Beam 1 (Bay 1, 1 <sup>st</sup> Floor)	123	<b>1/95</b>	1/50	1/40	1/46
Beam 2 (Bay 2, 1 <sup>st</sup> Floor)	41	1/47	<b>1/38</b>	1/74	1/105
Beam 3 (Bay 3, 1 <sup>st</sup> Floor)	36	1/114	1/69	<b>1/42</b>	1/55
Beam 4 (Bay 4, 1 <sup>st</sup> Floor)	96	1/44	1/39	1/53	<b>1/97</b>
Beam 5 (Bay 1, 2 <sup>nd</sup> Floor)	125	<b>1/101</b>	1/52	1/41	1/48
Beam 6 (Bay 2, 2 <sup>nd</sup> Floor)	41	1/47	<b>1/38</b>	1/63	1/83
Beam 7 (Bay 3, 2 <sup>nd</sup> Floor)	44	1/117	1/69	<b>1/42</b>	1/55
Beam 8 (Bay 4, 2 <sup>nd</sup> Floor)	97	1/46	1/42	1/53	<b>1/105</b>
Beam 9 (Bay 1, 3 <sup>rd</sup> Floor)	67	<b>1/95</b>	1/47	1/38	1/44
Beam 10 (Bay 2, 3 <sup>rd</sup> Floor)	4	1/45	<b>1/38</b>	1/83	1/164
Beam 11 (Bay 3, 3 <sup>rd</sup> Floor)	5	1/106	1/65	<b>1/32</b>	1/38
Beam 12 (Bay 4, 3 <sup>rd</sup> Floor)	31	1/35	1/33	1/44	<b>1/72</b>

**Note:** Number of occurrences of  $\theta_y$  for each beam may include either left or right side beam end, or both sides. Footing angular rotation noted in **bold** where the bay location coincides with the selected beam.

**Table 7.14. Case 3 MCS for  $COV_{w,h}(s_u) = 30$  percent and  $\delta_h(s_u) = 1$  to 100 m. Yield rotation occurrences for each beam at the beam ends and summary of median footing angular distortion across each bay when beam yield rotation occurs (continued).**

	Frequency of $\theta > \theta_y$	Median $\Delta s/l$ when $\theta > \theta_y$ occurs			
		Bay 1	Bay 2	Bay 3	Bay 4
<b><math>COV_{w,h}(s_u) = 30\%</math> <math>\delta_h(s_u) = 50</math> m</b>					
Beam 1 (Bay 1, 1 <sup>st</sup> Floor)	93	<b>1/75</b>	1/43	1/36	1/41
Beam 2 (Bay 2, 1 <sup>st</sup> Floor)	17	1/49	<b>1/41</b>	1/96	1/127
Beam 3 (Bay 3, 1 <sup>st</sup> Floor)	23	1/133	1/87	<b>1/46</b>	1/55
Beam 4 (Bay 4, 1 <sup>st</sup> Floor)	73	1/36	1/34	1/40	<b>1/66</b>
Beam 5 (Bay 1, 2 <sup>nd</sup> Floor)	91	<b>1/79</b>	1/48	1/38	1/43
Beam 6 (Bay 2, 2 <sup>nd</sup> Floor)	19	1/51	<b>1/43</b>	1/99	1/176
Beam 7 (Bay 3, 2 <sup>nd</sup> Floor)	27	1/108	1/63	<b>1/42</b>	1/49
Beam 8 (Bay 4, 2 <sup>nd</sup> Floor)	69	1/40	1/39	1/48	<b>1/84</b>
Beam 9 (Bay 1, 3 <sup>rd</sup> Floor)	41	<b>1/75</b>	1/40	1/33	1/37
Beam 10 (Bay 2, 3 <sup>rd</sup> Floor)	3	1/47	<b>1/41</b>	1/99	1/127
Beam 11 (Bay 3, 3 <sup>rd</sup> Floor)	3	1/91	1/60	<b>1/33</b>	1/39
Beam 12 (Bay 4, 3 <sup>rd</sup> Floor)	23	1/37	1/34	1/43	<b>1/69</b>
<b><math>COV_{w,h}(s_u) = 30\%</math> <math>\delta_h(s_u) = 100</math> m</b>					
Beam 1 (Bay 1, 1 <sup>st</sup> Floor)	38	<b>1/55</b>	1/36	1/29	1/32
Beam 2 (Bay 2, 1 <sup>st</sup> Floor)	5	1/6	<b>1/6</b>	1/6	1/6
Beam 3 (Bay 3, 1 <sup>st</sup> Floor)	3	1/132	1/83	<b>1/43</b>	1/45
Beam 4 (Bay 4, 1 <sup>st</sup> Floor)	21	1/34	1/31	1/38	<b>1/58</b>
Beam 5 (Bay 1, 2 <sup>nd</sup> Floor)	39	<b>1/69</b>	1/39	1/37	1/40
Beam 6 (Bay 2, 2 <sup>nd</sup> Floor)	4	1/44	<b>1/40</b>	1/59	1/70
Beam 7 (Bay 3, 2 <sup>nd</sup> Floor)	2	1/145	1/91	<b>1/43</b>	1/46
Beam 8 (Bay 4, 2 <sup>nd</sup> Floor)	21	1/34	1/31	1/38	<b>1/58</b>
Beam 9 (Bay 1, 3 <sup>rd</sup> Floor)	11	<b>1/53</b>	1/35	1/29	1/31
Beam 10 (Bay 2, 3 <sup>rd</sup> Floor)	0	N/A	N/A	N/A	N/A
Beam 11 (Bay 3, 3 <sup>rd</sup> Floor)	0	N/A	N/A	<b>N/A</b>	N/A
Beam 12 (Bay 4, 3 <sup>rd</sup> Floor)	7	1/26	1/25	1/31	<b>1/41</b>

**Note:** Number of occurrences of  $\theta_y$  for each beam may include either left or right side beam end, or both sides. Footing angular rotation noted in **bold** where the bay location coincides with the selected beam.



A study of individual MCS realizations where beam rotation exceeds  $\theta_y$  helps further explain the relationship of  $\theta_y$  with varying soil  $\delta_h(s_u)$  values. Figures 7.37 through 7.39 present graphical summaries of selected MCS realizations, each with three scenarios of soil variability that include combinations of  $COV_{w,h}(s_u)$  and  $\delta_h(s_u)$  equal to 30 percent and 50 m, 50 percent and 5 m, and 50 percent and 50 m and in which beam yield rotation was exceeded for more than one beam at the beam-to-column connections. The locations of beam yield rotation (i.e.,  $\theta \geq 1.0\theta_y$ ) are noted in **bold** in each scenario. Each of the realizations in Figures 7.37 through 7.39 include footing locations where very large total and differential displacement (and corresponding angular distortion) occurred. However, instances of exceeding  $\theta_y$  do not necessarily occur at the location where  $\Delta s/l$  is largest. Instead, there are instances where  $\Delta s/l$  is relatively small across a given bay, but significant beam yield rotation occurs because the adjacent bay has experienced a significant angular distortion. Noted examples are shown in Fig. 7.31a Bay 1, Fig. 7.32a Bay 1, Fig. 7.32b Bay 3, Fig. 7.32c Bay 4, and Fig. 7.33b Bay 1.

The scenarios with  $COV_{w,h}(s_u) = 50$  percent and  $\delta_h(s_u) = 5$  m (Fig. 7.38) show occurrences of adjacent bays supported on footings with smaller  $\Delta s/l$  next to larger  $\Delta s/l$ , causing larger beam stress and rotation. This appears due to greater fluctuation in soil strength over short distances compared to the examples with large  $\delta_h(s_u)$ . Conversely, when  $\delta_h(s_u)$  is larger (e.g., 50 m in Figs. 7.37 and 7.39), there is potential for larger total and differential footing displacements (depending on  $COV_{w,h}(s_u)$ ), but the displacements across the building and between footings tend to increase in one direction, resulting in an overall tilting of the structure, which does not necessarily impart greater stresses on the

structural components. In other words, a structure subject to large differential displacement and angular distortion may not exceed the yield capacity of individual elements if  $\Delta s$  and  $\Delta s/l$  are relatively consistent across the entire structure. Large magnitude  $\Delta s/l$  values coupled with large magnitude  $\delta_h(s_u)$  do not necessarily translate to greater instances of exceeding  $\theta_y$  because the structure may be tilting monolithically in one direction. This observation agrees with the relationships shown in Figs. 7.28 and 7.29 versus Fig. 7.18, where the probability of exceeding  $\theta_y$  for building members dissipates quickly for  $\delta_h(s_u)$  greater than  $\delta_h(s_u)_{crit}$ , while the probability of exceeding limit state values of  $\Delta s/l$  at the foundation level plateau near peak levels when  $\delta_h(s_u)$  approaches and exceeds  $\delta_h(s_u)_{crit}$ . It also explains the relationship shown in Fig. 7.36 where smaller magnitude angular distortions accompany beam rotations exceeding  $\theta_y$  when  $\delta_h(s_u)$  is smaller.

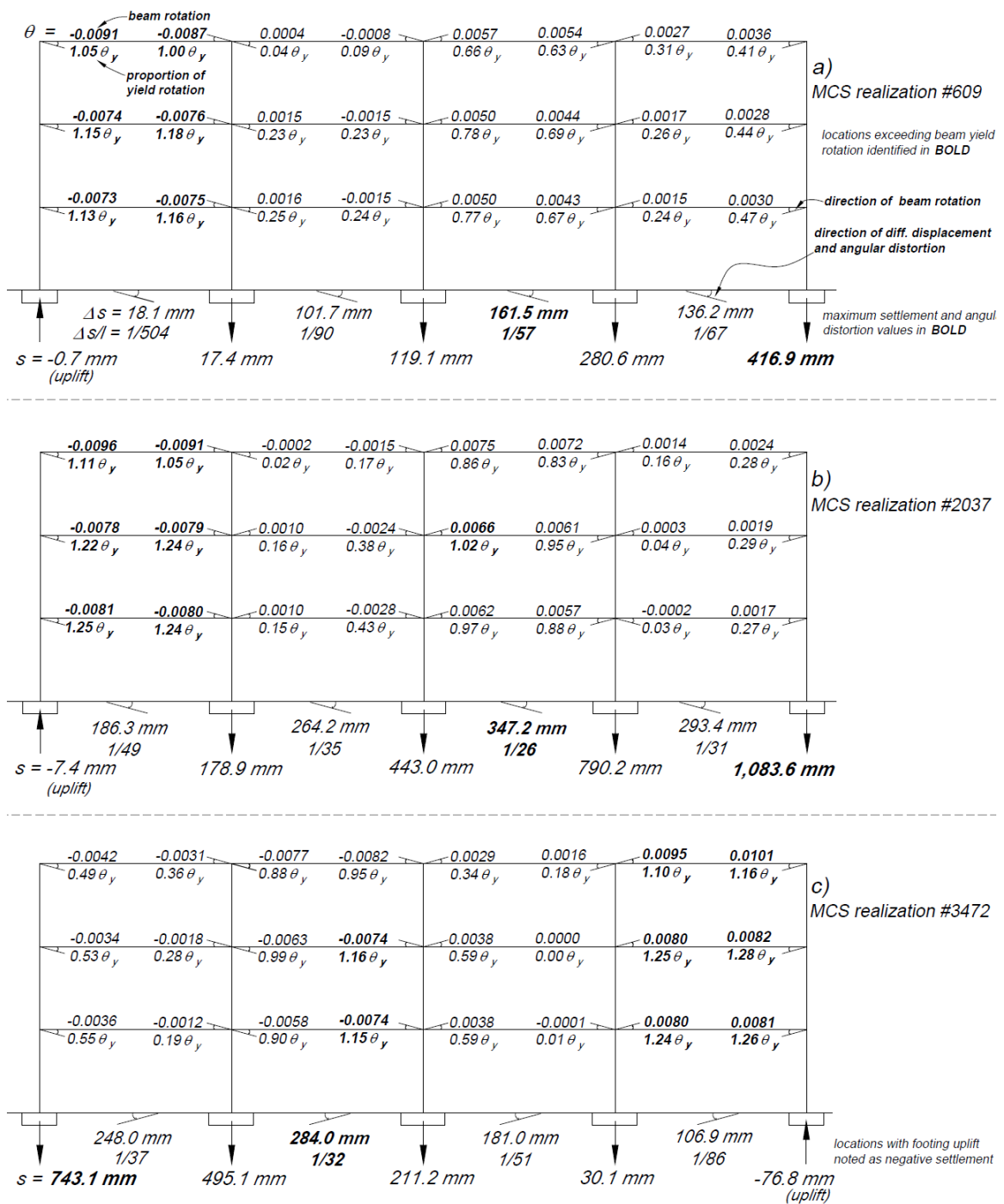


**Figure 7.37** Selected Case 3 MCS realizations for  $COV_{w,h}(S_u) = 30\%$  and  $\delta_h(S_u) = 50$  m where beam rotation exceeded  $\theta_y$  at multiple beam ends.

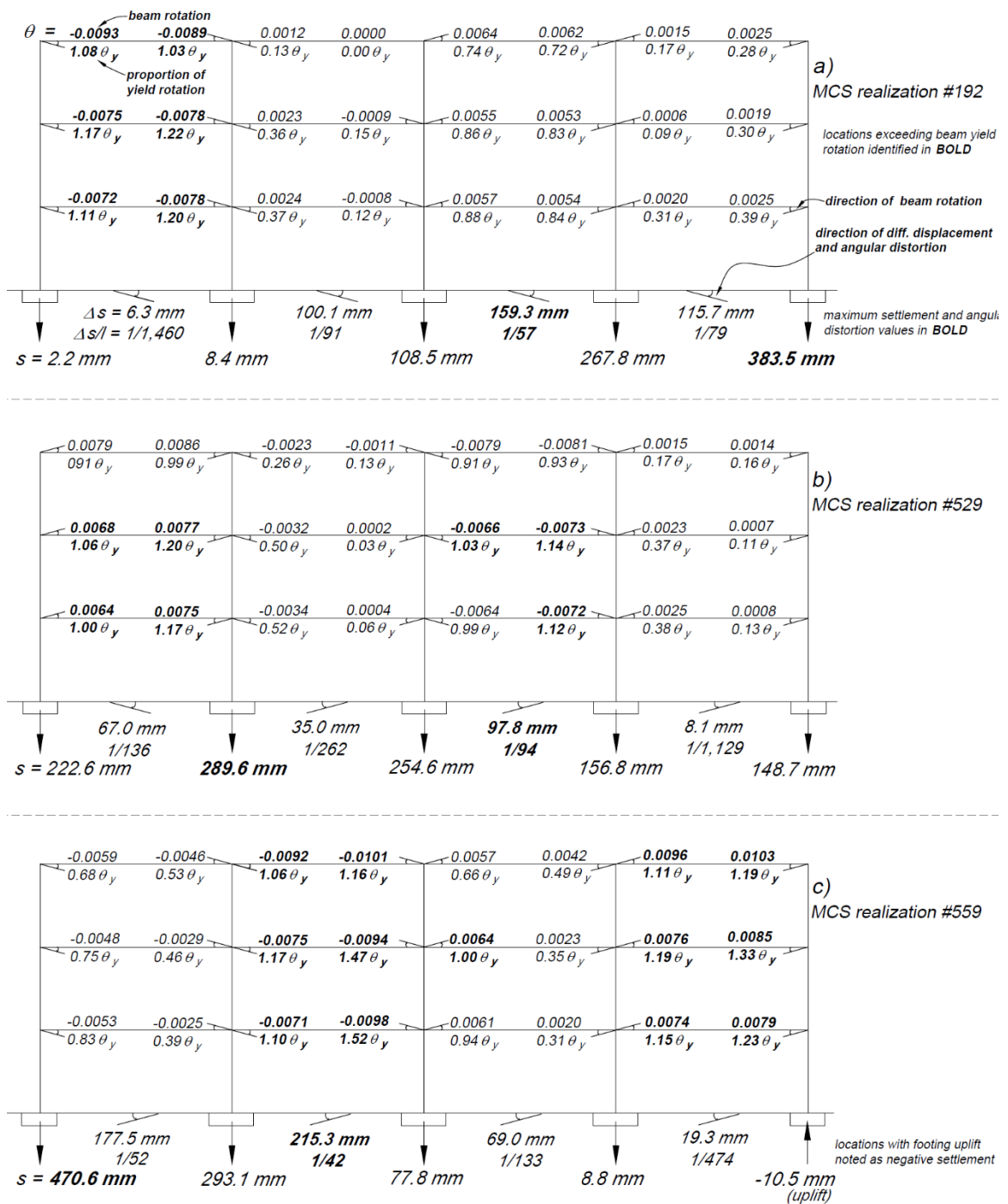


**Figure 7.38** Selected Case 3 MCS realizations for  $COV_{w,h}(s_u) = 50\%$  and  $\delta_h(s_u) = 5 \text{ m}$  where beam rotation exceeded  $\theta_y$  at multiple beam ends.

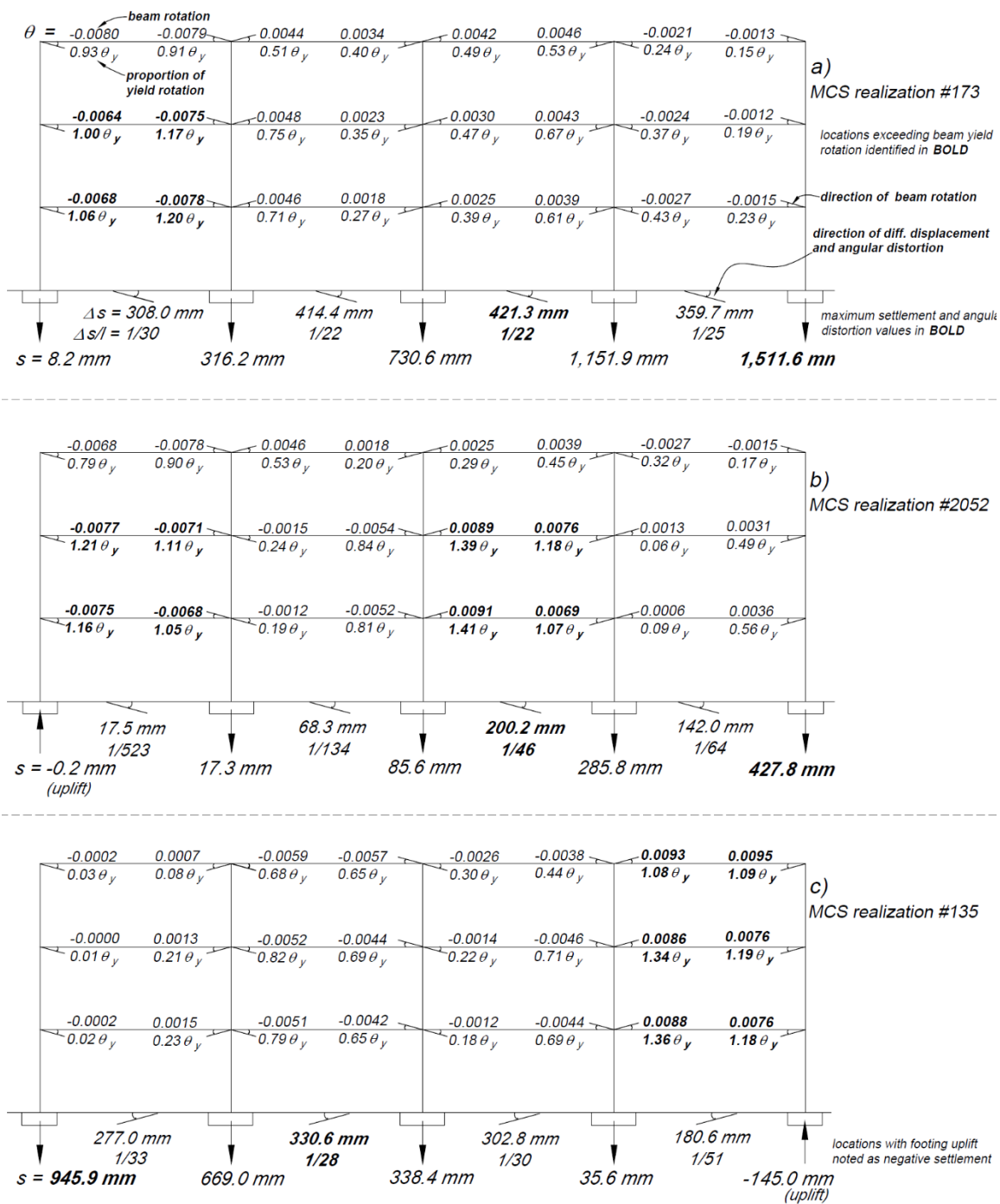


**Figure 7.39** Selected Case 3 MCS realizations for  $COV_{w,h}(s_u) = 50\%$  and  $\delta_h(s_u) = 50 \text{ m}$  where beam rotation exceeded  $\theta_y$  at multiple beam ends.

### 7.3.4 Case 4: Soil-Foundation-Structure Response (Intra-site Soil Parameters)

The Case 4 MCS used the same intra-site (OSU GEFRS) soil-foundation spring parameters as Case 2 and incorporated the SMRF building model via OpenSees to consider SSI effects on the foundation and building response. Consistent with the Case 3 discussion, the MCS results are presented for the foundation response first, followed by the building response.

#### 7.3.4.1 Soil-Foundation Performance

Tables 7.15 and 7.16 provide a summary of the mean and median total and differential vertical footing displacements and angular distortions for the Case 4 MCS analogous to the assessments provided in Tables 7.6 through 7.11 for the Cases 1 through 3 MCS. Figure 7.40 plots the cumulative distribution of differential displacement across Bay 1 for the scenario with  $\delta_h(s_u) = 50$  m and  $COV_{w,h}(s_u) = 30$  percent for all four MCS cases. Figures 7.41 and 7.42 compare the probability of exceedance of selected limit state angular distortion,  $\Delta s/l$ , values equal to 1/500, 1/300 and 1/150 for varying  $\delta_h(s_u)$  values at Bay 1 derived from the Case 2 and 4 MCS (Figure 7.41) or the Case 3 and 4 MCS (Figure 7.42). The results for Case 4 MCS can be directly compared to Case 3 results to evaluate inter-versus intra-site soil spring parameters; and the Case 4 MCS can be compared to Case 2 to quantify the SSI influence on the footing performance. The tables and figure show that the results for the Case 4 MCS generally agree with the trends identified in previous sections of this chapter when comparing the Cases 1, 2 and 3 MCS, with some differences as discussed herein.

**Table 7.15. Summary of vertical footing displacement for selected Case 4 MCS results with  $COV_{w,h}(s_u)$  values of 10 and 30 percent.**

Footing	$COV_{w,h}(s_u) = 10\%$					$COV_{w,h}(s_u) = 30\%$				
	1	2	3	4	5	1	2	3	4	5
<b><math>\delta_h(s_u) = 0.1 \text{ m}</math></b>										
Mean $s$ (mm)	37.7	43.4	44.1	43.1	37.3	38.4	43.9	44.6	43.4	37.8
Median $s$ (mm)	36.5	42.8	43.7	42.7	36.2	36.9	43.3	44.1	42.8	36.3
Std. dev. $s$ (mm)	12.1	11.0	10.6	10.8	12.0	13.3	11.7	11.3	11.6	13.1
COV( $s$ )	0.32	0.25	0.24	0.25	0.32	0.35	0.27	0.25	0.27	0.35
Failure rate (%)	0.00	0.00	0.00	0.00	0.00	0.00	0.00	0.00	0.00	0.00
<b><math>\delta_h(s_u) = 0.2 \text{ m}</math></b>										
Mean $s$ (mm)	37.9	43.5	44.2	43.0	37.3	39.0	44.3	44.9	43.8	38.4
Median $s$ (mm)	36.7	43.1	43.9	42.5	36.1	37.0	43.4	44.1	42.9	36.5
Std. dev. $s$ (mm)	12.3	11.0	10.7	10.9	12.1	14.6	12.6	12.0	12.4	14.4
COV( $s$ )	0.32	0.25	0.24	0.25	0.32	0.37	0.28	0.27	0.28	0.37
Failure rate (%)	0.00	0.00	0.00	0.00	0.00	0.00	0.00	0.00	0.00	0.00
<b><math>\delta_h(s_u) = 0.5 \text{ m}</math></b>										
Mean $s$ (mm)	38.0	43.6	44.3	43.3	37.6	40.5	45.5	46.1	45.1	39.9
Median $s$ (mm)	36.7	43.0	43.9	42.7	36.3	37.4	43.9	45.1	43.6	36.9
Std. dev. $s$ (mm)	12.5	11.2	10.9	11.1	12.4	18.0	14.7	13.9	14.5	17.6
COV( $s$ )	0.33	0.26	0.25	0.26	0.33	0.45	0.32	0.30	0.32	0.44
Failure rate (%)	0.00	0.00	0.00	0.00	0.00	0.00	0.00	0.00	0.00	0.00
<b><math>\delta_h(s_u) = 1 \text{ m}</math></b>										
Mean $s$ (mm)	38.1	43.7	44.4	43.3	37.6	42.2	46.9	47.2	46.4	41.5
Median $s$ (mm)	36.8	43.1	43.9	42.7	36.2	37.6	44.5	45.3	44.0	37.1
Std. dev. $s$ (mm)	12.8	11.4	11.0	11.3	12.6	22.0	17.4	16.0	17.1	21.6
COV( $s$ )	0.34	0.26	0.25	0.26	0.33	0.52	0.37	0.34	0.37	0.52
Failure rate (%)	0.00	0.00	0.00	0.00	0.00	0.00	0.00	0.00	0.00	0.00
<b><math>\delta_h(s_u) = 2 \text{ m}</math></b>										
Mean $s$ (mm)	38.2	43.8	44.4	43.3	37.7	43.8	48.3	48.6	47.9	43.2
Median $s$ (mm)	36.7	43.1	44.0	42.7	36.3	37.8	44.9	46.0	44.5	37.2
Std. dev. $s$ (mm)	13.1	11.6	11.2	11.5	12.9	26.3	20.2	18.4	20.4	26.3
COV( $s$ )	0.34	0.27	0.25	0.26	0.34	0.60	0.42	0.38	0.42	0.61
Failure rate (%)	0.00	0.00	0.00	0.00	0.00	0.00	0.00	0.00	0.00	0.00
<b><math>\delta_h(s_u) = 5 \text{ m}</math></b>										
Mean $s$ (mm)	38.4	44.0	44.7	43.5	37.9	46.8	51.2	51.3	50.8	46.2
Median $s$ (mm)	36.8	43.2	44.1	42.7	36.4	37.7	45.3	46.5	45.0	37.3
Std. dev. $s$ (mm)	13.5	12.1	11.6	11.9	13.2	39.5	30.2	26.2	30.2	39.4
COV( $s$ )	0.35	0.27	0.26	0.27	0.35	0.84	0.59	0.51	0.59	0.85
Failure rate (%)	0.00	0.00	0.00	0.00	0.00	0.00	0.00	0.00	0.00	0.00

**Notes:** 1. Results based on MCS with  $n = 50,000$  realizations.

2. Coefficient of variation,  $COV = \text{standard deviation}/\text{mean}$ .

3. Failure rate is defined herein as the percentage of MCS realizations with vertical displacement,  $s$ , greater than or equal to the footing width,  $B$ .

**Table 7.15. Summary of vertical footing displacement for selected Case 4 MCS results with  $COV_{w,h}(s_u)$  values of 10 and 30 percent (continued).**

Footing	$COV_{w,h}(s_u) = 10\%$					$COV_{w,h}(s_u) = 30\%$				
	1	2	3	4	5	1	2	3	4	5
<b><math>\delta_h(s_u) = 10 \text{ m}</math></b>										
Mean $s$ (mm)	38.5	44.1	44.9	43.7	38.1	51.8	55.7	55.7	55.2	51.2
Median $s$ (mm)	36.8	43.3	44.1	42.9	36.4	37.6	45.1	46.4	44.8	36.9
Std. dev. $s$ (mm)	13.8	12.4	12.0	12.2	13.6	69.9	53.4	46.0	53.4	69.3
COV( $s$ )	0.36	0.28	0.27	0.28	0.36	1.35	0.96	0.83	0.97	1.36
Failure rate (%)	0.00	0.00	0.00	0.00	0.00	0.02	0.00	0.00	0.00	0.02
<b><math>\delta_h(s_u) = 20 \text{ m}</math></b>										
Mean $s$ (mm)	38.7	44.3	45.0	43.8	38.1	59.4	62.9	62.6	62.0	58.2
Median $s$ (mm)	36.8	43.3	44.2	42.8	36.4	37.1	44.9	46.0	44.5	36.6
Std. dev. $s$ (mm)	14.1	12.8	12.4	12.6	13.9	117.7	93.2	81.7	90.7	112.7
COV( $s$ )	0.36	0.29	0.28	0.29	0.36	1.98	1.48	1.31	1.46	1.94
Failure rate (%)	0.00	0.00	0.00	0.00	0.00	0.07	0.01	0.01	0.01	0.07
<b><math>\delta_h(s_u) = 30 \text{ m}</math></b>										
Mean $s$ (mm)	38.9	44.5	45.2	44.0	38.2	59.0	62.7	62.7	62.3	58.3
Median $s$ (mm)	37.0	43.3	44.3	42.9	36.3	37.1	44.7	45.7	44.2	36.4
Std. dev. $s$ (mm)	14.3	12.9	12.6	12.8	14.0	123.6	98.8	87.2	95.7	117.7
COV( $s$ )	0.37	0.29	0.28	0.29	0.37	2.10	1.58	1.39	1.54	2.02
Failure rate (%)	0.00	0.00	0.00	0.00	0.00	0.08	0.02	0.01	0.01	0.09
<b><math>\delta_h(s_u) = 50 \text{ m}</math></b>										
Mean $s$ (mm)	38.7	44.4	45.2	44.0	38.3	48.2	53.2	53.7	53.1	48.3
Median $s$ (mm)	36.8	43.1	44.1	42.9	36.4	36.9	44.1	45.1	43.6	36.5
Std. dev. $s$ (mm)	14.3	13.1	12.7	12.9	14.0	45.5	39.5	38.0	40.7	47.5
COV( $s$ )	0.37	0.30	0.28	0.29	0.37	0.94	0.74	0.71	0.77	0.98
Failure rate (%)	0.00	0.00	0.00	0.00	0.00	0.00	0.00	0.00	0.00	0.00
<b><math>\delta_h(s_u) = 100 \text{ m}</math></b>										
Mean $s$ (mm)	38.8	44.4	45.2	44.0	38.3	43.7	49.2	49.9	49.2	44.1
Median $s$ (mm)	36.9	43.3	44.2	42.7	36.4	37.2	43.7	44.7	43.3	36.6
Std. dev. $s$ (mm)	14.4	13.3	13.0	13.1	14.2	46.1	43.8	43.2	44.1	46.7
COV( $s$ )	0.37	0.30	0.29	0.30	0.37	1.05	0.89	0.87	0.90	1.06
Failure rate (%)	0.00	0.00	0.00	0.00	0.00	0.00	0.00	0.00	0.00	0.00

**Notes:** 1. Results based on MCS with  $n = 50,000$  realizations.

2. Coefficient of variation,  $COV = \text{standard deviation}/\text{mean}$ .

3. Failure rate is defined herein as the percentage of MCS realizations with vertical displacement,  $s$ , greater than or equal to the footing width,  $B$ .



**Table 7.16. Summary of differential displacement and angular distortion at selected building bay for Case 4 MCS.**

$COV_{w,h}(s_u) =$	0	5%	10%	20%	30%	50%	100%
<b><math>\delta_n(s_u) = 0.1</math> m</b>							
Mean $\Delta s$ (mm)	9.6	9.7	9.7	9.8	10.2	10.9	11.6
Median $\Delta s$ (mm)	8.2	8.4	8.3	8.5	8.8	9.4	9.8
COV( $\Delta s$ )	0.73	0.73	0.73	0.73	0.73	0.74	0.76
Mean $\Delta s/l$	1/954	1/946	1/946	1/931	1/898	1/838	1/788
Median $\Delta s/l$	1/1,114	1/1,094	1/1,103	1/1,077	1/1,046	1/974	1/931
<b><math>\delta_n(s_u) = 0.2</math> m</b>							
Mean $\Delta s$ (mm)	9.7	9.6	9.7	10.1	10.8	12.4	14.3
Median $\Delta s$ (mm)	8.3	8.3	8.3	8.7	9.2	10.5	11.7
COV( $\Delta s$ )	0.73	0.73	0.73	0.73	0.73	0.75	0.80
Mean $\Delta s/l$	1/948	1/952	1/941	1/907	1/849	1/740	1/640
Median $\Delta s/l$	1/1,097	1/1,104	1/1,097	1/1,046	1/990	1/874	1/782
<b><math>\delta_n(s_u) = 0.5</math> m</b>							
Mean $\Delta s$ (mm)	9.6	9.7	9.8	10.7	12.1	15.8	20.5
Median $\Delta s$ (mm)	8.2	8.3	8.5	9.2	10.3	12.9	1/15.9
COV( $\Delta s$ )	0.73	0.73	0.73	0.73	0.75	0.81	0.86
Mean $\Delta s/l$	1/956	1/948	1/931	1/856	1/753	1/578	1/446
Median $\Delta s/l$	1/1,112	1/1,098	1/1,083	1/997	1/888	1/710	1/577
<b><math>\delta_n(s_u) = 1</math> m</b>							
Mean $\Delta s$ (mm)	9.5	9.6	9.8	11.2	13.6	19.0	26.0
Median $\Delta s$ (mm)	8.2	8.3	8.5	9.6	11.3	15.0	19.8
COV( $\Delta s$ )	0.73	0.73	0.73	0.74	0.79	0.85	0.86
Mean $\Delta s/l$	1/964	1/952	1/929	1/816	1/674	1/481	1/352
Median $\Delta s/l$	1/1,121	1/1,109	1/1,083	1/952	1/812	1/609	1/462
<b><math>\delta_n(s_u) = 2</math> m</b>							
Mean $\Delta s$ (mm)	9.6	9.7	10.1	11.8	14.9	22.0	30.5
Median $\Delta s$ (mm)	8.3	8.4	8.7	10.0	12.0	16.8	23.0
COV( $\Delta s$ )	0.73	0.73	0.73	0.75	0.84	0.87	0.87
Mean $\Delta s/l$	1/954	1/940	1/909	1/778	1/615	1/416	1/300
Median $\Delta s/l$	1/1,102	1/1,093	1/1,050	1/914	1/760	1/554	1/397
<b><math>\delta_n(s_u) = 5</math> m</b>							
Mean $\Delta s$ (mm)	9.6	9.7	10.1	12.0	16.1	23.9	33.5
Median $\Delta s$ (mm)	8.3	8.4	8.7	10.1	12.4	16.9	23.9
COV( $\Delta s$ )	0.73	0.73	0.73	0.77	0.98	0.97	0.96
Mean $\Delta s/l$	1/954	1/944	1/903	1/764	1/567	1/383	1/273
Median $\Delta s/l$	1/1,108	1/1,095	1/1,049	1/909	1/736	1/541	1/384

**Notes:** 1. Results based on MCS with  $n = 50,000$  realizations.

2. Selected values reported for each  $COV_{w,h}$  represent the largest mean or median value observed for Bay 1, 2, 3 or 4. Results were typically similar for the other bays not reported in this table.
3. Differential displacement coefficient of variation,  $COV = \text{standard deviation}/\text{mean}$ .
4. Angular distortion across the selected bay,  $\Delta s/l$ , was calculated as the differential displacement divided over the center-to-center footing distance of 9.15 m. Values are provided in fraction format for ease of comparison between values.

**Table 7.16. Summary of differential displacement and angular distortion at selected building bay for Case 4 MCS (continued).**

$COV_{w,h}(s_u) =$	0	5%	10%	20%	30%	50%	100%
<b><math>\delta_h(s_u) = 10 \text{ m}</math></b>							
Mean $\Delta s$ (mm)	9.6	9.7	10.1	11.9	17.2	23.9	33.2
Median $\Delta s$ (mm)	8.2	8.4	8.6	9.9	12.0	15.9	21.1
COV( $\Delta s$ )	0.73	0.73	0.73	0.81	1.39	1.07	1.11
Mean $\Delta s/l$	1/955	1/945	1/910	1/768	1/531	1/383	1/276
Median $\Delta s/l$	1/1,113	1/1,094	1/1,059	1/923	1/765	1/574	1/434
<b><math>\delta_h(s_u) = 20 \text{ m}</math></b>							
Mean $\Delta s$ (mm)	9.6	9.7	9.9	11.7	19.6	23.7	32.4
Median $\Delta s$ (mm)	8.2	8.3	8.5	9.6	10.7	14.7	17.7
COV( $\Delta s$ )	0.73	0.73	0.74	0.98	2.01	1.23	1.37
Mean $\Delta s/l$	1/955	1/944	1/922	1/779	1/466	1/386	1/282
Median $\Delta s/l$	1/1,109	1/1,098	1/1,074	1/958	1/855	1/622	1/517
<b><math>\delta_h(s_u) = 30 \text{ m}</math></b>							
Mean $\Delta s$ (mm)	9.6	9.7	9.9	11.5	18.7	23.0	32.5
Median $\Delta s$ (mm)	8.2	8.4	8.5	9.3	10.2	13.7	16.8
COV( $\Delta s$ )	0.73	0.73	0.73	1.07	2.15	1.26	1.47
Mean $\Delta s/l$	1/955	1/945	1/925	1/793	1/488	1/398	1/281
Median $\Delta s/l$	1/1,115	1/1,093	1/1,078	1/986	1/898	1/668	1/545
<b><math>\delta_h(s_u) = 50 \text{ m}</math></b>							
Mean $\Delta s$ (mm)	9.6	9.6	9.8	11.4	13.4	21.2	31.4
Median $\Delta s$ (mm)	8.3	8.3	8.4	9.0	10.0	12.5	15.7
COV( $\Delta s$ )	0.73	0.73	0.73	1.23	1.05	1.35	1.54
Mean $\Delta s/l$	1/954	1/948	1/935	1/802	1/683	1/431	1/291
Median $\Delta s/l$	1/1,105	1/1,101	1/1,085	1/1,011	1/911	1/735	1/582
<b><math>\delta_h(s_u) = 100 \text{ m}</math></b>							
Mean $\Delta s$ (mm)	9.6	9.6	9.7	11.2	11.4	17.0	28.7
Median $\Delta s$ (mm)	8.2	8.2	8.3	8.8	9.2	10.5	14.6
COV( $\Delta s$ )	0.73	0.73	0.73	1.39	0.88	1.29	1.58
Mean $\Delta s/l$	1/956	1/952	1/944	1/814	1/802	1/537	1/319
Median $\Delta s/l$	1/1,110	1/1,110	1/1,101	1/1,041	1/991	1/868	1/629

**Notes:** 1. Results based on MCS with  $n = 50,000$  realizations.

2. Selected values reported for each  $COV_{w,h}$  represent the largest mean or median value observed for Bay 1, 2, 3 or 4. Results were typically similar for the other bays not reported in this table.
3. Differential displacement coefficient of variation,  $COV = \text{standard deviation}/\text{mean}$ .
4. Angular distortion across the selected bay,  $\Delta s/l$ , was calculated as the differential displacement divided over the center-to-center footing distance of 9.15 m. Values are provided in fraction format for ease of comparison between values.

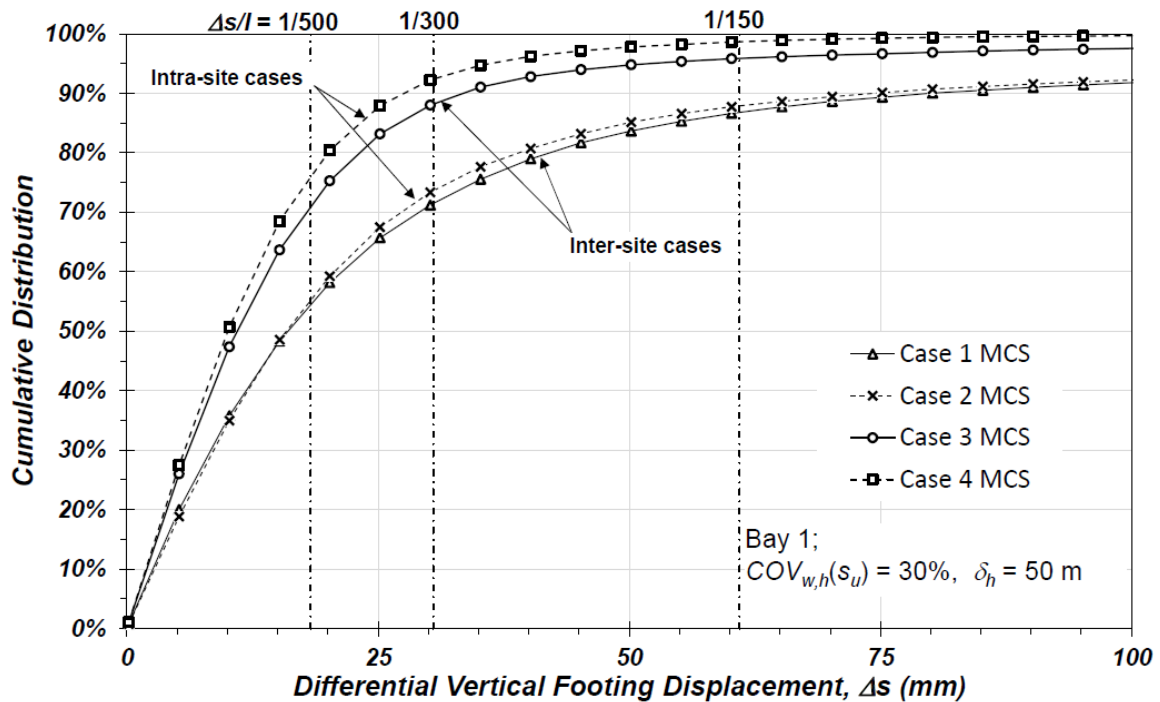


**Figure 7.40** Distribution of differential footing displacement for each MCS case. Results for Bay 1 where  $COV_{w,h}(s_u) = 30$  percent and  $\delta_h = 50$  m.

The intra-site soil-spring parameters (i.e.,  $k_1$ ,  $k_2$  and  $M_{STC}$ ) used in Cases 4 and 2 MCS result in larger individual footing displacements relative to the inter-site parameters in the Cases 1 and 3 MCS because the soil-foundation spring of the former are generally softer owing to the larger mean  $M_{STC}$  value in intra-site model. However, the differential displacements between footings and corresponding angular distortions are typically less for footings modeled with the intra-site soil-foundation springs (Cases 2 and 4) because the intra-site parameters have lower dispersion relative to the inter-site parameters (Cases 1 and 3). Comparing Case 4 (Table 7.16) to Case 3 (Table 7.11) indicates lower differential displacements for Case 4 for the selected range of  $COV_{w,h}(s_u)$  and  $\delta_h(s_u)$ . This improvement in differential displacements for Case 4 is relatively modest at  $COV_{w,h}(s_u) \leq 20$  percent, with the mean and median differential displacements,  $\Delta s$ , typically 5 to 15 percent less for

Case 4 compared to Case 3. However, at greater  $COV_{w,h}(s_u)$  the improvement becomes more significant; for example at  $COV_{w,h}(s_u) = 100$  percent and  $\delta_h(s_u) = 100$  m, the median  $\Delta s$  is approximately 35 percent less for Case 4 versus Case 3 (15.5 mm versus 23.9 mm) and the mean  $\Delta s$  is nearly one-half for Case 4 versus Case 3 (33.5 mm versus 64.4 mm).

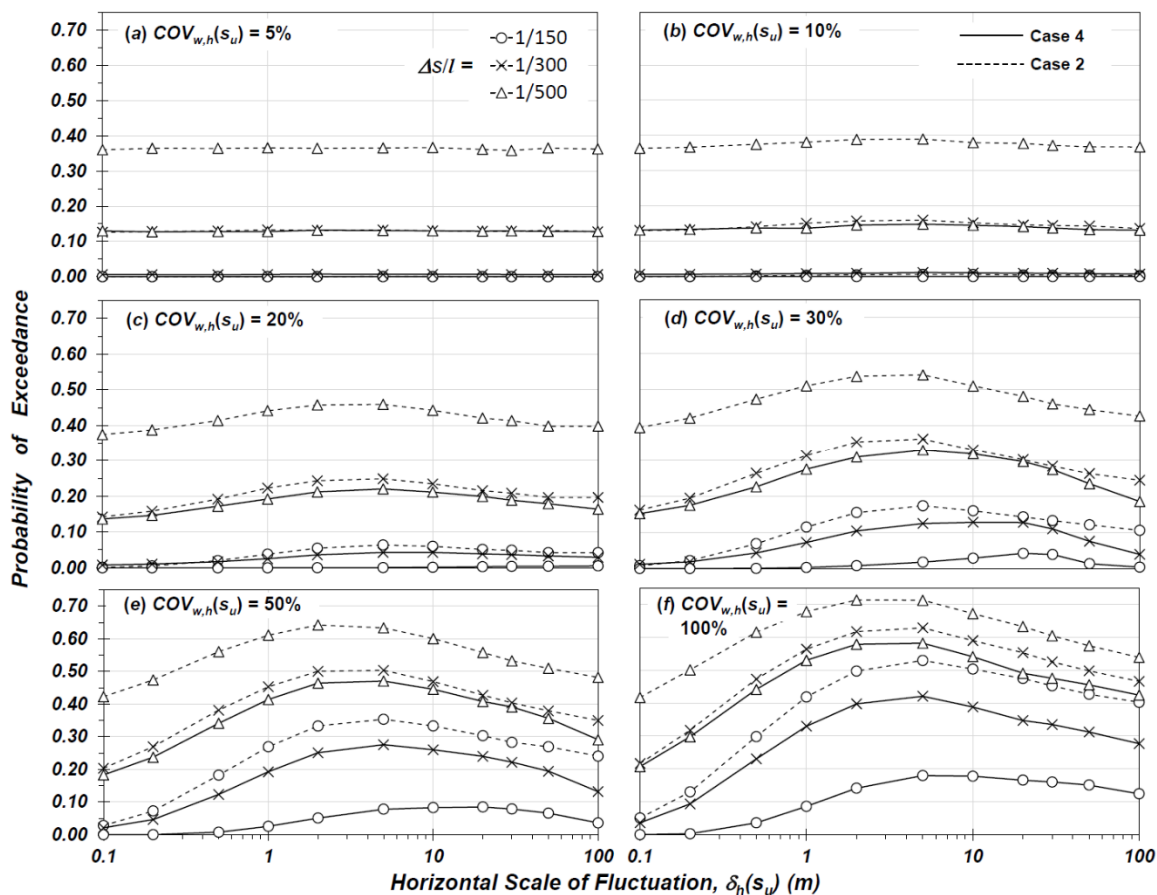


**Figure 7.41** Case 2 and Case 4 MCS results for Bay 1. Probability of exceedance of selected limit state angular distortion for varying horizontal scale of fluctuation.

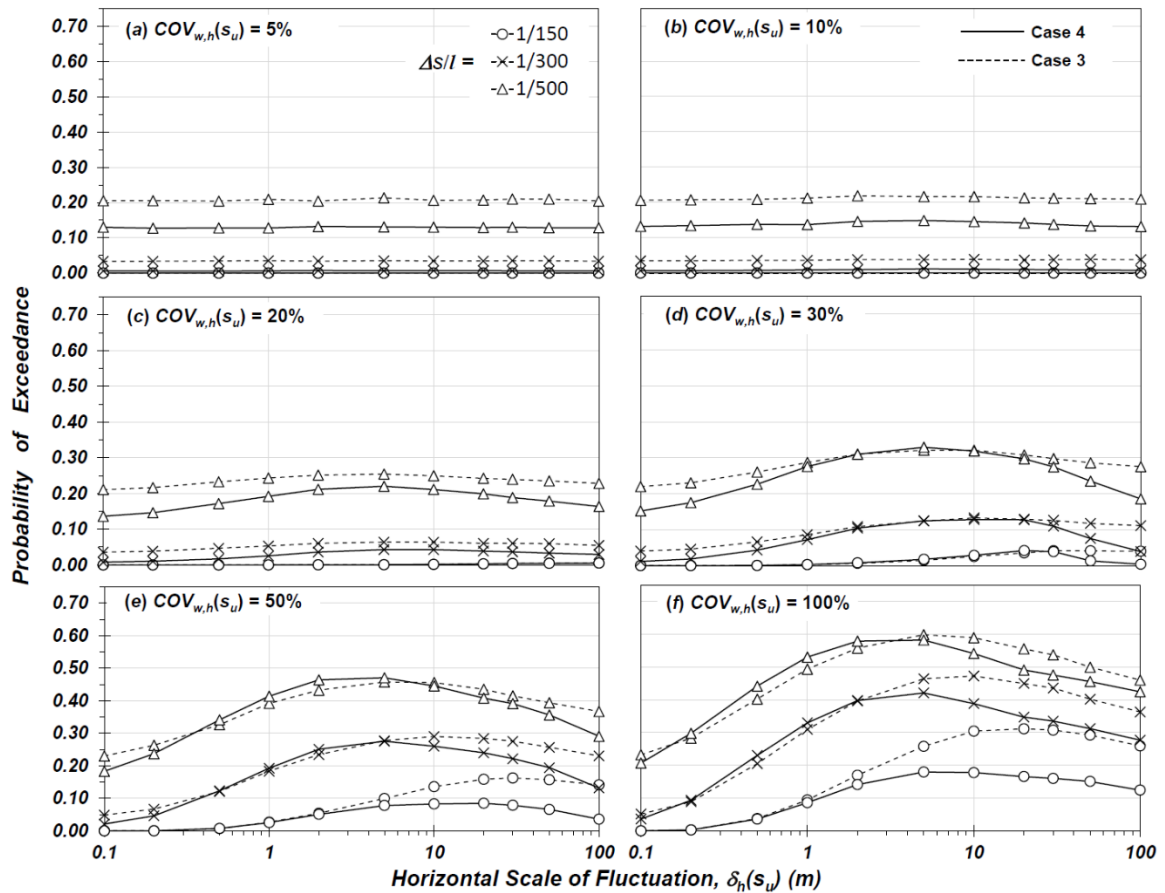


**Figure 7.42** Case 3 and Case 4 MCS results for Bay 1. Probability of exceedance of selected limit state angular distortion for varying horizontal scale of fluctuation.

The intra-site soil-spring parameters (i.e.,  $k_1$ ,  $k_2$  and  $M_{STC}$ ) used in Cases 4 and 2 MCS result in larger individual footing displacements relative to the inter-site parameters in the Cases 1 and 3 MCS because the soil-foundation spring of the former are generally softer owing to the larger mean  $M_{STC}$  value in intra-site model. However, the differential displacements between footings and corresponding angular distortions are typically less for footings modeled with the intra-site soil-foundation springs (Cases 2 and 4) because the intra-site parameters have lower dispersion relative to the inter-site parameters (Cases 1 and 3). Comparing Case 4 (Table 7.16) to Case 3 (Table 7.11) indicates lower differential

displacements for Case 4 for the selected range of  $COV_{w,h}(s_u)$  and  $\delta_h(s_u)$ . This improvement in differential displacements for Case 4 is relatively modest at  $COV_{w,h}(s_u) \leq 20$  percent, with the mean and median differential displacements,  $\Delta s$ , typically 5 to 15 percent less for Case 4 compared to Case 3. However, at greater  $COV_{w,h}(s_u)$  the improvement becomes more significant; for example at  $COV_{w,h}(s_u) = 100$  percent and  $\delta_h(s_u) = 100$  m, the median  $\Delta s$  is approximately 35 percent less for Case 4 versus Case 3 (15.5 mm versus 23.9 mm) and the mean  $\Delta s$  is nearly one-half for Case 4 versus Case 3 (33.5 mm versus 64.4 mm).

The reduction in differential displacement and angular distortion is more pronounced for intra- versus inter-site soil-spring parameters where SSI is included (i.e., Case 4 versus Case 3) compared to when the footings are modeled independently (i.e., Case 2 versus Case 1). As discussed in Section 7.3.2 when comparing Case 2 (intra-site) versus Case 1 (inter-site), the differential displacement and angular distortion for the Case 2 MCS is typically less than Case 1 MCS, except at the largest values of  $COV_{w,h}(s_u)$  when soil strength is most variable, then differential displacements and angular distortions were slightly lower for Case 1 MCS. However, when including the steel structure in Cases 3 and 4 MCS, the differential displacement and angular distortion for Case 4 (intra-site) is less than Case 3 (inter-site) for the range of  $COV_{w,h}(s_u)$  and  $\delta_h(s_u)$  combinations. This indicates the structure connecting the footings serves to improve redistribution of load (or moment) to and from the footings as the variability of the soil strength increases, and this improvement in foundation performance is amplified when the soil-foundation spring parameters ( $k_1$ ,  $k_2$  and  $M_{STC}$ ) have lower dispersion. The improvement in foundation performance demonstrated with the Case 3 and 4 MCS comparison is observed in the response of the structural members, as discussed below.

### 7.3.4.2 Structural Performance

The performance of the three-story SMRF structure was evaluated for Case 4 MCS in the same manner as described in Section 7.3.3.2 for the Case 3 MCS, focusing on the beam rotation,  $\theta$ , at the ends of each beam where rotation and corresponding moment are expected to be greatest. The beam performance was evaluated with changes in spatial variability for the foundation soil by comparing  $\theta$  for varying magnitudes of  $COV_{w,h}(S_u)$  and  $\delta_h(S_u)$ , and the resulting angular distortions across the structure bays.

Figure 7.43 compares the probability of exceeding beam end yield rotation,  $\theta_y$ , for each beam where  $COV_{w,h}(S_u) = 30$  percent and  $\delta_h(S_u)$  ranges from 1 m to 100 m. The results are plotted for all MCS data (Fig. 7.43a) and for the data encompassing only selected limit state angular distortions,  $\Delta s/l$ , equal to 1/500, 1/300, and 1/150 (Fig. 7.43b, c, and d). Figure 7.44 provides similar information as Fig. 7.43 with beam rotation at various levels of soil strength variability, but also includes fractions of beam yield rotation equal to  $0.75\theta_y$  and  $0.5\theta_y$ . Consistent with the Case 3 MCS (e.g., Figs. 7.27a and 7.28a), when including all simulations (Figs. 7.43a and 7.44a) the Case 4 MCS resulted in few instances of beam rotation reaching yield conditions; with peak probability of exceedance equal to approximately 0.25 percent for Beam 1 (1<sup>st</sup> floor) and Beam 5 (2<sup>nd</sup> floor) and other beams having lower probability of exceeding  $\theta_y$  in the range of 0.01 to 0.22 percent. Also consistent with Case 3 MCS, the probability of exceeding  $\theta_y$  or portion of  $\theta_y$  increases when considering instances where limit state  $\Delta s/l$  are exceeded (Figs. 7.43b through d and 7.44b through d). The probability of exceeding  $\theta_y$  is typically maximum for a given beam when the soil shear strength scale of fluctuation,  $\delta_h(S_u)$ , is 10 m to 20 m (i.e., approximately

1 to 2 times bay width,  $l$ ). These values of  $\delta_h(s_u)$  are slightly greater in magnitude compared to the  $\delta_h(s_u)_{crit}$  values indicated by Figs. 7.41 and 7.42, which typically indicate  $\delta_h(s_u)_{crit}$  ranging from 5 m to 10 m (i.e., approximately  $0.5l$  to  $1.0l$ ). Thus, the critical autocorrelation length depends on which metric is used (i.e., angular distortion or yield rotation) due to their definition and the role of the performance (e.g., deformation) of neighboring bays on the induced moments at the beam ends.

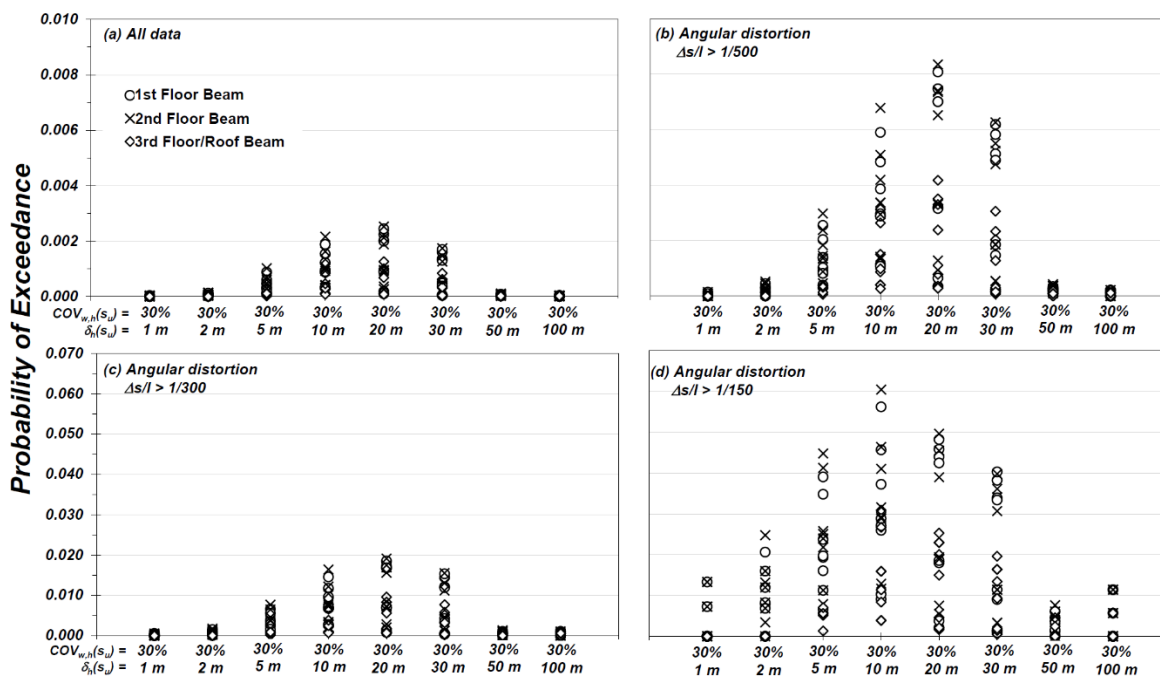


**Figure 7.43** Case 4 MCS. Probability of beam end rotation exceeding  $\theta_y$  for selected values of angular distortion and where  $COV_{w,h}(s_u) = 30\%$  and  $\delta_h(s_u) = 1$  to 100 m (Note (a) and (b) are plotted at different scales relative to (c) and (d) to provide better clarity to interpret probabilities).



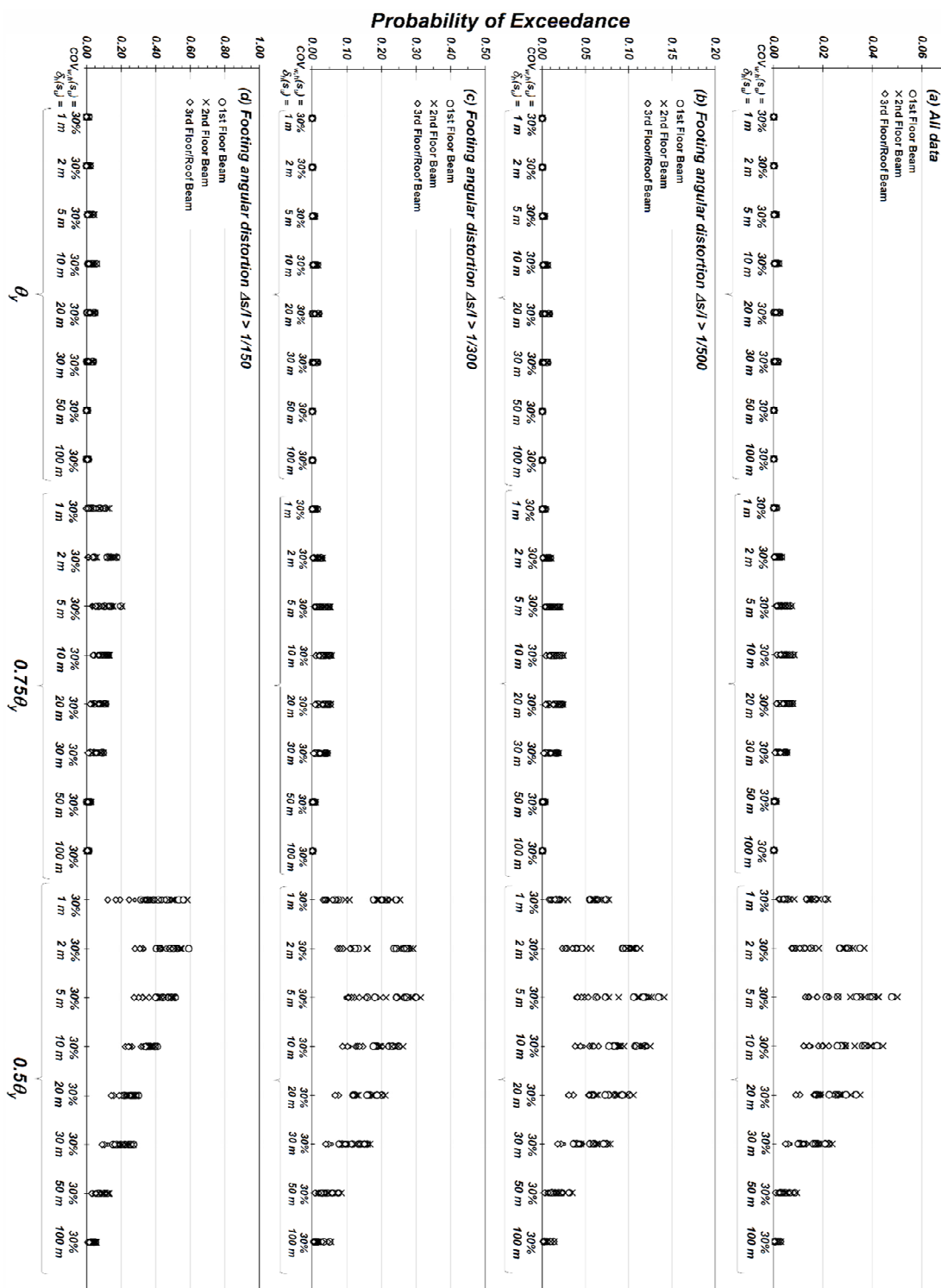


**Figure 7.44** Case 4 MCS results. Probability of beam end rotation exceeding  $\theta_y$  or portion of  $\theta_y$  for selected values of angular distortion and where  $COV_{w,h}(s_u) = 30\%$  and  $\delta_h(s_u) = 1$  to 100 m. (Note different scales used in (a) through (d) to provide better clarity to interpret probabilities).

The data provided in Fig. 7.44 for probability of exceeding  $\theta_y$  or portion of  $\theta_y$  across the range of  $\delta_h(s_u)$  values indicates the same general trends for the Case 4 MCS intra-site soil-foundation springs when compared to the data in Fig. 7.28 for the Case 3 MCS inter-site soil-foundation springs. The observations for Case 3 are detailed in Section 7.3.3.2. However, a noteworthy comparison of Case 4 and Case 3 MCS is that the probability of exceeding  $\theta_y$  or portion of  $\theta_y$  is reduced approximately 15 to 30 percent for the Case 4 intra-site spring model. For example, when comparing the probability of exceeding beam rotation equal to  $0.5\theta_y$  for all MCS data (Figs. 7.44a and 7.28a), the probability is greatest for both Case 4 and Case 3 MCS when  $\delta_h(s_u)$  is in the range of 5 m to 10 m, but the peak probability for Case 3 (occurring for a 2<sup>nd</sup> floor beam) is equal to approximately 6 percent, while for Case 4 it is approximately 5 percent. This demonstrates how improvement in the foundation performance for the intra-site soil-foundation springs with lower dispersion of spring parameters ( $k_1$ ,  $k_2$ , and  $M_{STC}$ ) relative to the inter-site springs influences the performance of structural members. Again, this is despite the intra-site (Case 4) vertical foundation spring being relatively softer with greater total foundation settlement, on average, relative to the inter-site (Case 3) foundation spring.

Figures 7.45 and 7.46 provide further perspective of the beam rotations relative to foundation performance with variable soils and intra- versus inter-site soil foundation spring parameters. The figures present the probability of exceeding  $\theta_y$  for beams in Bay 1 with varying  $\delta_h(s_u)$  and  $COV_{w,h}(s_u) = 30$  (Fig. 7.45) or 50 percent (Fig. 7.46). Data for Case 3 MCS that was plotted in Figs. 7.29 and 7.30 is included along with data for the Case 4 MCS. The Case 3 MCS indicated maximum probabilities of exceeding  $\theta_y$  occurring when

$\delta_h(s_u)$  is in the range of 10 to 20 m (i.e., approximately  $1l$  to  $2l$ ). The Case 4 MCS indicated maximum probabilities of exceeding  $\theta_y$  occurring when  $\delta_h(s_u)$  equal to 10 m (i.e., approximately  $1l$ ), and for most combinations of  $\delta_h(s_u)$  and  $COV_{w,h}(s_u)$  plotted in Figs. 7.45 and 7.46 the probability of exceeding  $\theta_y$  is typically less for the Case 4 MCS relative to the Case 3 MCS. This agrees with the results presented in Figs. 7.44 and 7.28 and further demonstrates the improved performance of the structure supported on foundations with intra-site soil-foundation springs relative to inter-site soil foundation springs.

When investigating structure performance with the Case 3 MCS, it was observed that when beam yield rotation occurred, it generally coincided with a smaller  $\Delta s/l$  when  $\delta_h(s_u)$  was smaller and larger  $\Delta s/l$  when  $\delta_h(s_u)$  was larger. This trend is consistent for the Case 4 MCS as well. Figure 7.47 presents the median  $\Delta s/l$  with varying  $\delta_h(s_u)$  and constant  $COV_{w,h}(s_u) = 30$  percent for each beam for Case 4 MCS where beam yield rotation,  $\theta_y$ , was exceeded. The results presented in Fig. 7.47 are generally consistent with those presented in Fig. 7.36 for Case 3 MCS which indicate beam yield occurring at larger  $\Delta s/l$  as  $\delta_h(s_u)$  increases (note: results are not included in Fig. 7.47 for some instances of very large and small  $\delta_h(s_u)$  because the number of realizations where beam yield rotation occurred was equal to 4 or less for 50,000 simulations and not statistically representative). Consistent with the Case 3 MCS, instances of exceeding  $\theta_y$  do not necessarily occur at the location where  $\Delta s/l$  is largest, but instead occur most frequently where adjacent bays have significant disparity in angular distortion between bays. Therefore, a structure subject to large differential displacement and angular distortion may not exceed the yield capacity of

individual elements if  $\Delta s$  and  $\Delta s/l$  are relatively consistent across the entire structure and the structure is tilting monolithically.

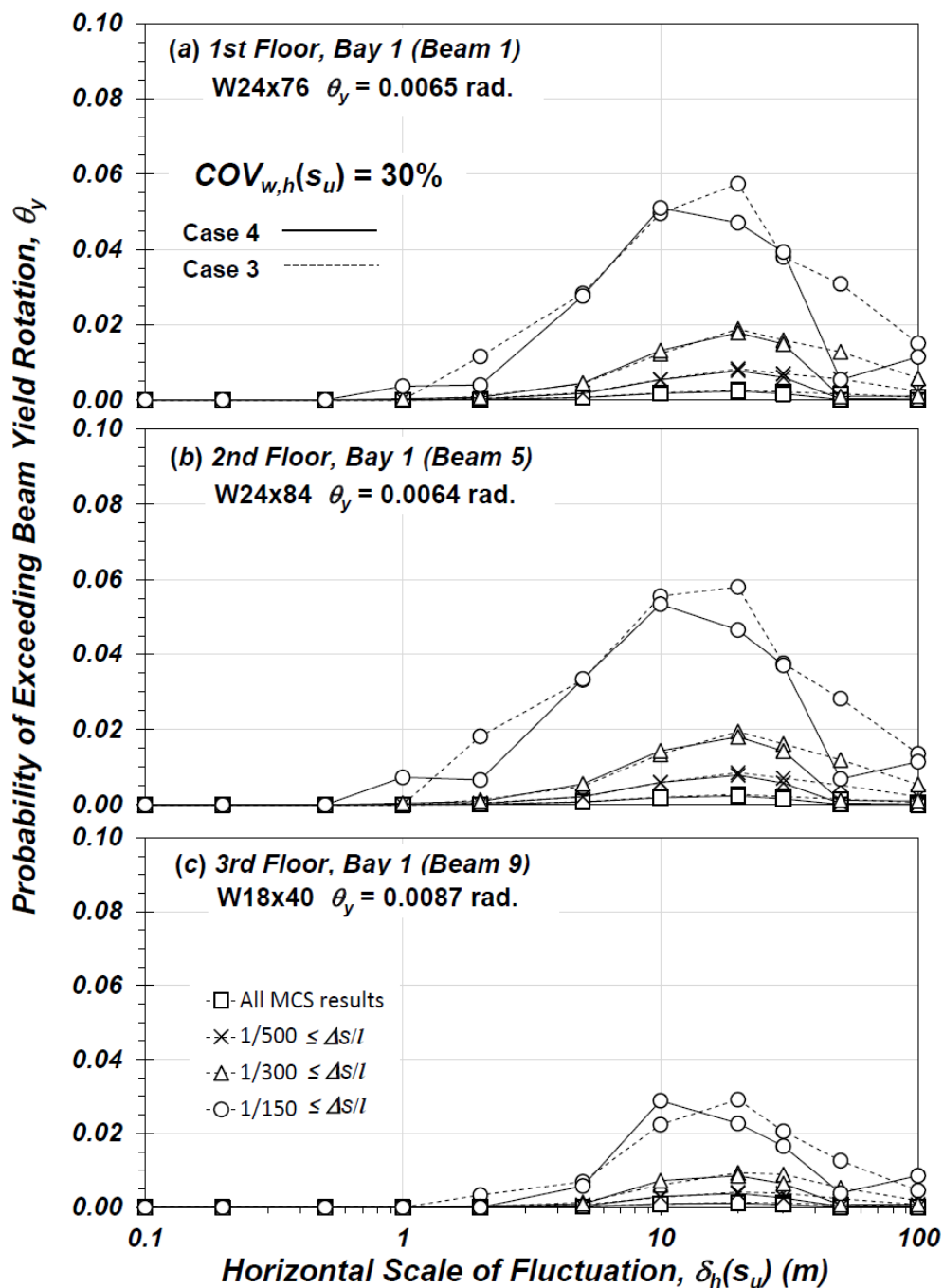


**Figure 7.45** Case 3 and Case 4 MCS results for Bay 1. Probability of exceedance of beam yield rotation for  $COV_{w,h}(s_u) = 30\%$  with varying horizontal scale of fluctuation.

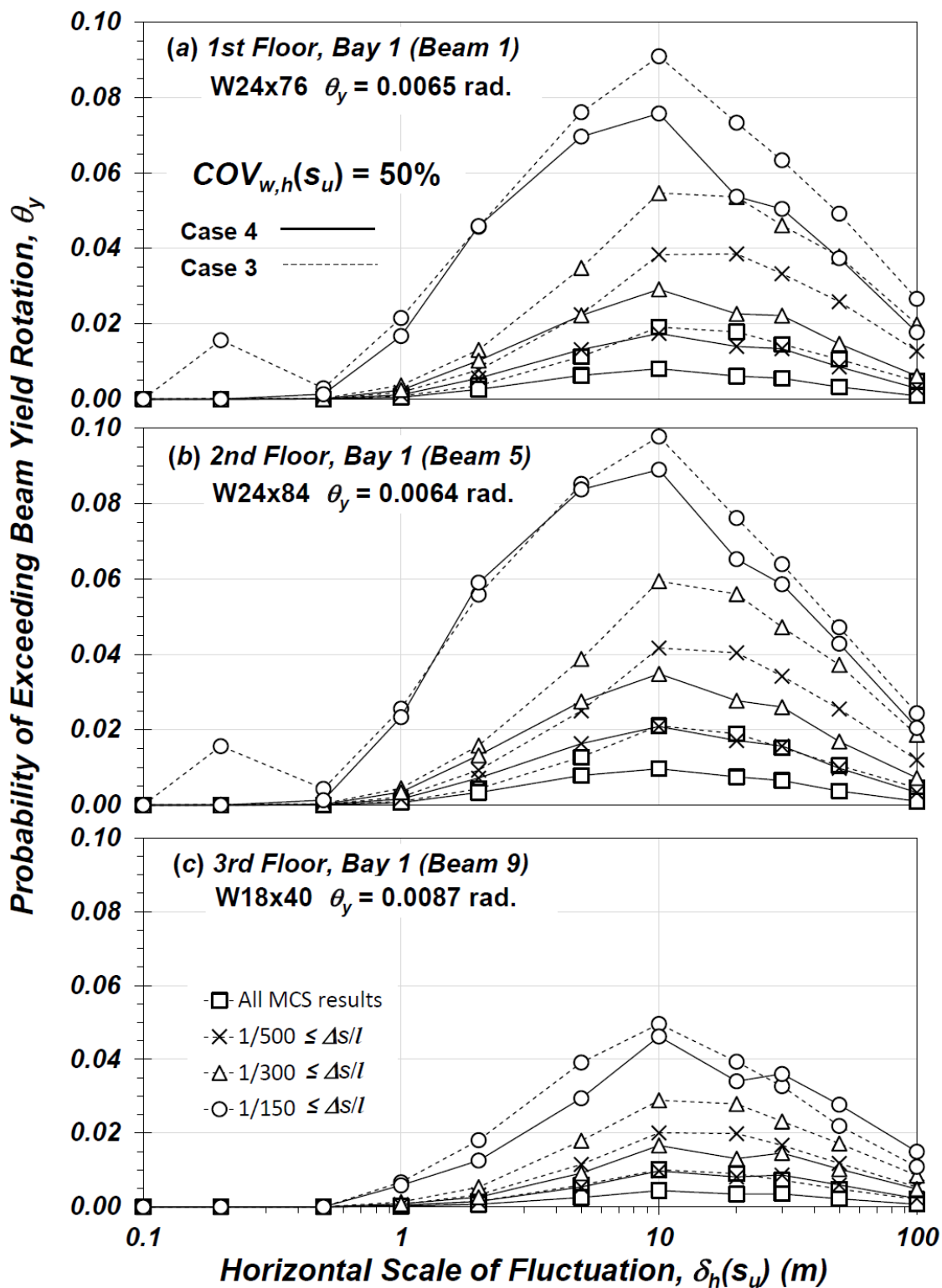


**Figure 7.46** Case 3 and Case 4 MCS results for Bay 1. Probability of exceedance of beam yield rotation for  $COV_{w,h}(s_u) = 50\%$  with varying horizontal scale of fluctuation.

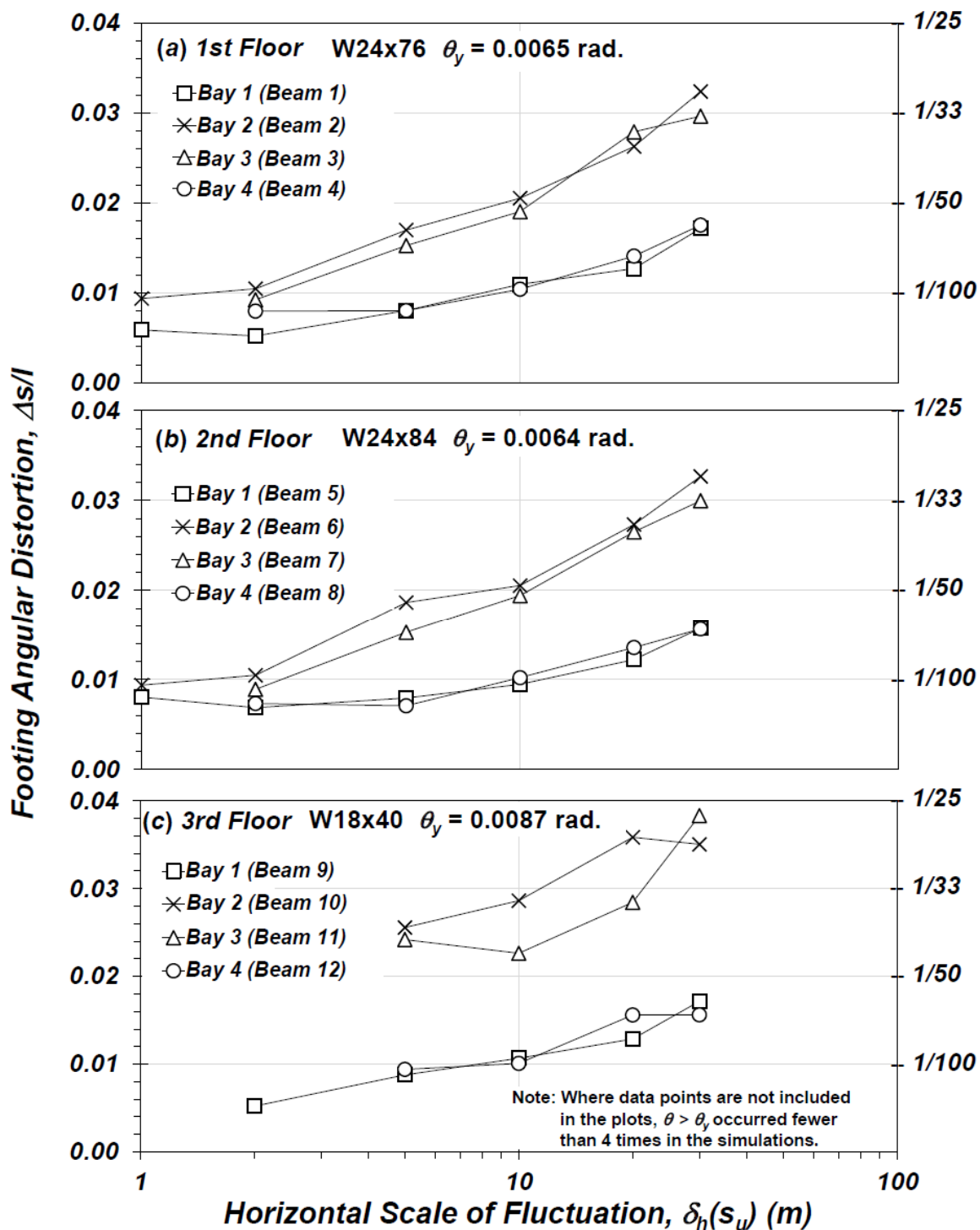


Figure 7.47 Case 4 MCS. Median angular distortion across each bay at occurrences when beam rotation,  $\theta > \theta_y$ .  $COV_{w,h}(s_u) = 30$  m.

## 7.4 SUMMARY AND CONCLUSIONS

The inherent spatial variability of soil and soil-structure interaction are two critically important aspects when considering geotechnical foundation design and performance of the supported structure. However, fully incorporating soil variability and SSI into a comprehensive limit state (e.g., SLS or ULS) model remains a challenge for geotechnical and structural engineering researchers and practitioners. This chapter explored foundation and structure performance using reliability analyses with Monte Carlo simulations (MCS). The soil-foundation model developed in Chapter 5 (Huffman et al. 2015) for plastic, fine-grained soil with undrained conditions was incorporated into the reliability analyses and modified to include a multi-foundation system and variable soil shear strength in combination with loading from a two-dimensional, three-story, SMRF building as documented in FEMA-355C (2000) and Barbosa et al. (2017). Furthermore, this chapter investigated differences between inter-site and intra-site soil variability by comparing soil-foundation springs based on parameters using the global foundation loading test database (i.e., inter-site parameters) from Chapter 5 (Huffman et al. 2015) or a subset developed from foundation loading tests for a single site documented in Newton (1975) and Martin (2018) (i.e., intra-site parameters). The intent of this study is to further the understanding of foundation and structure performance with respect to soil variability and SSI that can be incorporated into reliability-based design models. Several important observations from the analyses were documented herein and summarized below.

The effect of soil spatial variability on foundation and building performance was investigated by selecting a nominal or “average” soil undrained shear strength,  $s_u$ , with variability defined using random field theory (Vanmarke 1977, 1983). The soil variability

was simulated using a range in horizontal scale of fluctuation,  $\delta_h(s_u)$ , and coefficient of inherent variability,  $COV_{w,h}(s_u)$ , and considered MCS cases that included inter-site or intra-site soil-spring parameters acting independent of the structure (i.e., Cases 1 and 2 with no SSI) and inter-site or intra-site soil-spring parameters with structure influence (i.e., Cases 3 and 4). For all cases, the influence of  $\delta_h(s_u)$  on differential footing displacement and angular distortion was observed to increase concurrently with increasing  $COV_{w,h}(s_u)$  (e.g., see Figs 7.13, 7.16, 7.18, and 7.41). Additionally, the influence of  $\delta_h(s_u)$  on  $\Delta s$  or  $\Delta s/l$  only becomes significant at  $COV_{w,h}(s_u)$  greater than approximately 20 percent.

The soil-foundation response was first modeled with the five footings subject to the building load but acting independent of the structure (Cases 1 and 2) to provide a baseline for comparison of foundation performance when the structure and SSI effects are included. The soil-foundation model without the structure is also comparable to previous studies (e.g., Fenton and Griffiths, 2002, and Ahmed and Soubra, 2014) that evaluated foundation performance in the presence of spatially variable soil. The current study identified similarities with the previous research; for example, the probability of exceeding a given magnitude  $\Delta s$  between adjacent footings typically varies relative to the horizontal scale of fluctuation,  $\delta_h$ , for a selected soil-foundation displacement parameter. Furthermore, the critical scale of fluctuation,  $\delta_{h,crit}$  (defined herein as  $\delta_h$  corresponding to the largest probability of exceeding a given magnitude of  $\Delta s$ ) typically occurs when  $\delta_h$  is on the order of  $0.5l$  to  $1.0l$ , where  $l$  is the center-to-center distance between adjacent footings. While previous studies used soil elastic modulus,  $E$ , as the selected soil-foundation displacement parameter, this study used a spatially variable undrained shear strength,  $s_u$ , in combination



with nonlinear soil-foundation spring parameters calibrated from either inter- or intra-site loading tests. When the footing displacement is calculated based on  $E$ , the displacement goes to zero as the horizontal scale of fluctuation,  $\delta_h(E)$ , reaches either zero or infinity. Because the current study used multiple parameters to estimate foundation resistance and displacement under the building loads, the results do not indicate zero differential displacement (or corresponding angular distortion) for very large or small values of  $\delta_h(s_u)$ , which is more accurate for modeling foundations supported on plastic fine-grained soils under undrained loading conditions. This is an important design consideration for developing future limit state foundation design methods that include the effects of spatially variable soil and the relationship with foundation spacing.

When the SMRF building was included in the model (Cases 3 and 4) the steel structure provided increased rigidity between footings compared to Cases 1 and 2, and corresponding redistribution of foundation loads based on soil stiffness. As a result, for Cases 3 and 4 MCS there was a lower number of instances of extreme individual vertical footing displacements and the magnitude of differential footing displacements was lower compared to Cases 1 and 2 MCS with consistent soil variability parameters. Soil-structure interaction with the inclusion of the building also typically increased the magnitude of  $\delta_h(s_u)_{crit}$  to be on the order of  $1l$  to  $2l$ , suggesting the critical scale of fluctuation is influenced by the span sizes and the scale of the entire building footprint (e.g., the distance between multiple footings) instead of only the distance between adjacent footings.

The results documented in this study can be used to help develop new models or improve existing models for estimating foundation settlements, for example the reliability-based SLS procedure developed in Chapter 5 (Huffman et al. 2015). However, additional

studies should be completed to provide a more robust model that evaluates the influence of foundation spacing, structure type (e.g., steel frame versus reinforced concrete, masonry, or other), building height (or number of stories), and potential 3-dimensional effects. A comprehensive study may be hampered to some degree by available computing resources, as encountered during this work.

The intra-site soil-foundation spring parameters ( $k_1$ ,  $k_2$  and  $M_{STC}$ ) used with the Cases 2 and 4 MCS exhibited larger mean and median vertical displacements for individual footings relative to Cases 1 and 3 MCS that used inter-site soil-foundation spring parameters. The disparity in foundation displacement between intra-site and inter-site cases occurred because the nominal  $M_{STC}$  parameter used for intra-site cases ( $M_{STC} = 0.544$ ) is less than that used for inter-site cases ( $M_{STC} = 0.643$ ), which directly affects the average spring stiffness (e.g., see Eq. 7.1). However, the overall dispersion in the intra-site spring parameters is lower compared to the inter-site parameters, which leads to less variable stiffness between footings. As a result, the differential foundation displacement and angular distortion is typically less for the intra-site cases, which is consistent with the expectation that local practitioners with significant experience in a given geological region anticipate good building performance when applying personally-developed “rules of thumb”. Furthermore, greater reduction in  $\Delta s$  and  $\Delta s/l$  was observed for Case 4 which included the influence of the building relative to Case 2 that modeled independent footings. The results confirm that when possible, site-specific spring parameters calibrated from foundation loading tests should be used to more accurately predict displacements of individual footings supported on a given soil stratum. When site-specific loading tests are not available to calibrate the soil-foundation spring parameters and site-specific spring

parameters cannot be calibrated by other means (e.g., correlation to other in-situ testing), the global (inter-site) parameters should provide a generally conservative approximation of differential displacements even when the site-specific soil conditions result in a softer soil-foundation spring.

Structural performance in Cases 3 and 4 MCS were evaluated by measuring beam end rotation adjacent to the beam-to-column connection, where the bending moments were greatest. The beam rotations were also assessed relative to angular distortion under the conditions of spatially variable foundation soils. Intuitively, as the variability in soil shear strength increased, represented by an increase in  $COV_{w,h}(s_u)$ , the likelihood for beams reaching the point of yield rotation,  $\theta_y$ , also increased (e.g., see Fig.7.26). The likelihood for individual beams reaching  $\theta_y$  also peaked with  $\delta_h(s_u)$  in the range of 10 to 20 m (i.e., approximately  $1l$  to  $2l$ ), which corresponds to the same magnitude of horizontal scale of fluctuation where angular distortion,  $\Delta s/l$ , is most likely to exceed  $1/150$  (often considered an ultimate limit state value for  $\Delta s/l$ ). When considering smaller magnitudes of beam rotation corresponding closer to a serviceability limit state, the critical scale of fluctuation reduced to approximately 5 m (approximately  $0.5l$ ), suggesting the performance of the beams at the serviceability level may be controlled more at the local footing-to-footing distance or across a single bay.

Overall, the structure performed well with relatively few occurrences of individual beams exceeding  $\theta_y$ . When considering all data, the probability of exceeding  $\theta_y$  peaks at approximately 4 to 5 percent for the most variable soil conditions when  $COV_{w,h}(s_u) = 100$  percent and  $\delta_h(s_u) = \delta_h(s_u)_{crit}$  (i.e., approximately  $1l$  to  $2l$ ). When considering only cases where  $\Delta s/l$  exceeds  $1/150$ , the peak probability of exceeding  $\theta_y$  increases to

approximately 15 percent. There is no obvious correlation between  $\theta$  and  $\Delta s/l$  across individual bays (e.g., see probability distribution in Figs. 7.19 through 7.23). However, by inspecting individual realizations where beam yield rotation occurred, the results indicate that  $\theta$  values are not necessarily largest where  $\Delta s/l$  is largest, but where the change in  $\Delta s/l$  between adjacent bays is largest. Furthermore, a relationship was observed wherein larger angular distortion is generally required to cause beam yield rotation when  $\delta_h(s_u)$  is large, and smaller angular distortion is generally required to cause beam yield rotation when  $\delta_h(s_u)$  is small (e.g., see trend in Figs. 7.36 and 7.47). These observations indicate that large magnitude  $\Delta s/l$  values coupled with large magnitude  $\delta_h(s_u)$  do not necessarily translate to greater instances of exceeding  $\theta_y$  because the structure is likely tilting monolithically in one direction, causing less stress on the beams. Conversely, large magnitude  $\Delta s/l$  values coupled with smaller magnitude  $\delta_h(s_u)$  provides greater probability of adjacent bays experiencing disparate angular distortions and greater beam stresses.

As noted above, the results documented herein can be used to develop or improve reliability-based limit state foundation design models. The analyses presented in Chapter 5 (Huffman et al. 2015) developed a nonlinear soil-foundation displacement spring for plastic, fine-grained soils with undrained loading (Eq. 7.1) and lumped load and resistance factor,  $\psi_q$ , that Eq. 7.1 is divided by to provide foundation bearing resistance at the serviceability level. The load and resistance factor was calibrated based on the observed dispersion and correlation of the spring parameters, the estimated variability of the applied load and allowable displacement, and accepted target probability of exceeding the calculated displacement. The results presented herein may be used to help further calibrate

$\psi_q$  to incorporate the effects of spatially variable soil (i.e., varying  $COV_{w,h}(s_u)$  and  $\delta_h(s_u)$ ) and the observed structural performance. For example,  $\psi_q$  should increase for larger  $COV_{w,h}(s_u)$  and for  $\delta_h(s_u)$  approaching  $\delta_h(s_u)_{crit}$ , and the allowable displacement can be calibrated based on anticipated beam rotation. However, the magnitude for which each variable affects the calibrated  $\psi_q$  can vary based on foundation spacing, building type and height, and similar variables. Construction considerations such as the inspection of footing excavations to confirm soil properties, or construction sequencing and load application also affect long- and short-term building and foundation performance. Additional reliability analysis will be required to fully understand the impact of each variable. The work presented herein may be used as a framework for carrying out such analyses.

## 7.5 REFERENCES

- Ahmed, A. and Soubra A.-H. (2014). "Probabilistic analysis at the serviceability limit state of two neighboring strip footings resting on a spatially random soil," *Struct. Safety*, 49, 2–9.
- Allen, T.A. (2005) "Development of Geotechnical Resistance Factors and Downdrag Load Factors for LRFD Foundation Strength Limit State Design," *Report No. FHWA-NHI-05-052*, Federal Highway Administration, Washington D.C.
- Allen, T.A., Nowak, A.S., and Bathurst, R.J. (2005). "Calibration to Determine Load and Resistance Factors for Geotechnical and Structural Design," *Transportation Research Circular E-C079*, Transportation Research Board of the National Academies, Washington D.C.
- Baecher, G.B. and Christian, J.T. (2003). *Reliability and Statistics in Geotechnical Engineering*, John Wiley and Sons, Inc., London.
- Barbosa, A.R, Ribeiro, F.L.A. and Neves, L.A.C. (2017). "Influence of earthquake ground-motion on damage estimation: application to steel moment resisting frames," *Earthquake Engng Struct. Dyn.*, 46(1), 27-49.
- Belejo, A.F.V., Barbosa, A.R., Huffman, J.C., and Stuedlein, A.W. (2020) "Influence of ground-motion duration on damage estimation of steel moment resisting frames accounting for soil-structure interaction effects," *J. Struct. Eng.*, In Review.
- Bong, T. and Stuedlein, A.W. (2017). "Spatial variability of CPT parameters and silty fines in liquefiable beach sands," *J. Geotech. Geoenviron. Eng.*, 143(12), 04017093.

- Bong, T. and Stuedlein, A.W. (2018). "Effect of cone penetration conditioning on random field model parameters and impact of spatial variability in liquefaction-induced differential settlements," *J. Geotech. Geoenviron. Eng.*, 144(5), 04018018.
- Boscardin, M.D. and Cording, E.J. (1989). "Building response to excavation-induced settlement," *J. Geot. Eng.*, 115(1), 1-21.
- Brinch Hansen, J. (1970). "A revised and extended formula for bearing capacity," *Bulletin No. 28*, Danish Geotechnical Institute, Copenhagen, Denmark, 5–11.
- Broding, W.C., Diederich, F.W. and Parker, P.S. (1964) "Structural optimization and design based on a reliability design criterion," *J. Spacecraft*, 1(1), 56-61.
- Burland, J.B. and Wroth, C.P. (1974). "Settlement behavior of buildings and associated damage," *Proc., Conf. on Settlement of Structures*, Cambridge Univ., Instn. of Civil Engrs., London, 611-654.
- Clough, G.W. and O'Rourke, T.D. (1990). "Construction induced movements of in situ walls," *Design and Performance of Earth Retaining Structures*, GSP No. 25, ASCE, New York, NY, 439-470.
- D'Appolonia, D., Poulos, H. and Ladd, C. (1971). "Initial settlement of structures on clay," *J. Soil Mech. Found. Div.* 97 (SM10), 1359–1377.
- Douglas, D.J. and Davis, E.H. (1964). "The movements of buried footings due to moment and horizontal load and the movement of anchor plates," *Géotechnique*, 14(2), 115–132.
- Duncan, J.M. (2000). "Factors of safety and reliability in geotechnical engineering," *J. Geotech. Geoenviron. Eng.*, 126(4), 307-316.
- Duncan, J.M. and Mokwa, R.L. (2001). "Passive earth pressures: theories and tests," *J. Geotech. Geoenviron. Eng.*, 127(3), 248-257.
- Elktab, T., Chalaturnyk, R. and Robertson, P.K. (2003). "An overview of soil heterogeneity: quantification and implications on geotechnical field problems," *Can. Geotech. J.* 40(1), 1-15. doi:10.1139/t02-090.
- FEMA (2000). "State of the art report on systems performance of steel moment frames subject to earthquake ground shaking," *FEMA-355C*, Washington, DC.
- Fenton, G.A. and Griffiths, D.V. (2002). "Probabilistic foundation settlement on spatially random soil," *J. Geotech. Geoenviron. Eng.*, 128(5), 381-390.
- Fenton G.A. and Griffiths, D.V. (2003). "Bearing capacity prediction of spatially random  $c-\phi$  soils," *Can. Geotech. J.* 40(1), 54–65.
- Fenton, G.A. and Griffiths, D.V. (2005). "Three-dimensional probabilistic foundation settlement," *J. Geotech. Geoenviron. Eng.*, 131(2), 232-239.
- Fenton, G.A. and Griffiths, D.V. (2008). *Risk Assessment in Geotechnical Engineering*, John Wiley and Sons, Inc., New Jersey.

- Fenton, G.A., Griffiths, D.V. and Cavers, W. (2005). "Resistance factors for settlement design," *Can. Geotech. J.* 42(5), 1422–1436.
- Fenton, G.A., Griffiths, D.V. and Ojomo, O.O. (2011). "Consequence factors in the ultimate limit state design of shallow foundations", *Can. Geotech. J.* 48(2), 265-279.
- Foye, K.C., Basu, P. and Prezzi, M. (2008). "Immediate settlement of shallow foundations bearing on clay," *Int. J. Geomech.*, 8(5), 300–310.
- Gilbert, R.B. (1997). "Basic random variables," In G.A. Fenton (ed.), *Probabilistic Methods in Geotechnical Engineering*, ASCE GeoLogan '97 Conference, Logan, Utah.
- Grant, R., Christian, J.T., and Vanmarcke, E.H. (1974), "Differential settlement of buildings," *J. Geotech. Engrg. Div.*, 100(9), 973-991.
- Griffiths, D.V. and Fenton, G.A. (2001). Bearing capacity of spatially random soil: the undrained clay Prandtl problem revisited," *Géotechnique*, 51(4), 351–359.
- Griffiths, D.V., Fenton, G.A. and Manoharan, N. (2002). "Bearing capacity of a rough rigid strip footing on cohesive soil: A probabilistic study," *J. Geotech. Geoenviron. Eng.*, 128(9), 743-755.
- Harden, C.W., Hutchinson, T.C., Martin, G.R., and Kutter, B.L. (2005). (Numerical modeling of the nonlinear cyclic response of shallow foundations," *PEER Report 2005/04*, Pacific Earthquake Engineering Research Center, University of California, Berkeley.
- Harden, C.W. and Hutchinson, T.C. (2009). "Beam-on-nonlinear-Winkler-foundation modeling of shallow, rocking-dominated footings," *Earthquake Spectra*, 25(2), 277-300.
- Honjo, Y. and Otake, Y. (2013). "A simple method to assess the effects of soil spatial variability on the performance of a shallow foundation," *Foundation Engineering in the Face of Uncertainty*, ASCE Geo-Congress 2013, San Diego, California.
- Huffman, J.C., Martin, J.P. and Stuedlein, A.W. (2016). "Calibration and assessment of reliability-based serviceability limit state procedures for foundation engineering," *Georisk*, 10(4), 208-293.
- Huffman, J.C., Strahler, A.W. and Stuedlein, A.W. (2015). "Reliability-based serviceability limit state design for immediate settlement of spread footings on clay," *Soils and Foundations*, 55(4), 798-812.
- Huffman, J.C. and Stuedlein, A.W. (2014). "Reliability-based serviceability limit state design of spread footings on aggregate pier reinforced clay," *J. Geotech. Geoenviron. Eng.*, 140(10), 04014055.
- Houlsby, G.T., Cassidy, M.J., and Einav, I. (2005). "A generalised Winkler model for the behaviour of shallow foundations," *Géotechnique*, 55(6), 449-460.
- Houy, L., Breysse, D. and Denis, A. (2005). "Influence of soil heterogeneity on load redistribution and settlement of a hyperstatic three-support frame," *Géotechnique*, 55(2), 163-170.

- Jaksa, M.B. (1995). "The influence of spatial variability on the geotechnical design properties of a stiff overconsolidated clay," *Ph.D. thesis*, Faculty of Engineering, Univ. of Adelaide, Australia.
- Jaksa, M.B., Brooker, P.I. and Kaggwa, W.S. (1997). "Experimental evaluation of the scale of influence of a stiff clay," *Proc., 8<sup>th</sup> Int. Conf. on Application of Statistics and Probability*, Belkema, Rotterdam, Netherlands, 415-422.
- Jardine, R.J., Potts, D.M., Fourie, A.B. and Burland, J.B. (1986). "Studies of the influence of non-linear stress-strain characteristics in soil-structure interaction," *Géotechnique*, 36(3), 377-396.
- Lignos, D.G. and Krawinkler, H. (2011). "Deterioration modeling of steel components in support of collapse prediction of steel moment frames under earthquake loading," *J. Struct. Eng.*, 137(11), 1291-1302.
- Lignos, D.G., Krawinkler, H. and Whittaker, A.S. (2011). "Prediction and validation of sidesway collapse of two scale models of a 4-story steel moment frame." *Earthquake Eng. Struct. Dyn.*, 40(7), 807-825.
- McKenna, F., Scott, M.H., and Fenves, G.L. (2010). "Nonlinear finite-element analysis software using objective composition," *Journal of Computing in Civil Engineering*, 24(1), 95-107.
- Martin, J.P. (2018). "A full-scale experimental investigation of the bearing performance of aggregate pier-supported shallow foundations", *M.S. thesis*, Oregon State University.
- Meyerhof, G.G. (1963). "Some recent research on the bearing capacity of foundations," *Can. Geotech. J.*, 1(1), 16-26.
- Najjar, S.S. (2005). "The importance of lower-bound capacities in geotechnical reliability assessments," *Ph.D. thesis*, University of Texas at Austin.
- Najjar, S.S., and Gilbert, R.B. (2009). "Importance of lower-bound capacities in the design of deep foundations," *J. Geotech. Geoenviron. Eng.*, 135(7), 890-900.
- Newton, V.C. (1975). "Ultimate bearing capacity of shallow footings on plastic silt," *M.S. thesis*, Oregon State University.
- Noorzaei, J., Viladkar, M.N. and Godbole, P.N. (1995). "Influence of strain hardening on soil-structure interaction of framed structures," *Comput. Struct.* 55(3), 789-z
- OpenSees*, Version 2.5.0 [Computer software], Berkeley, CA, Pacific Earthquake Engineering Research Center (PEER).
- Phoon, K.K. (2008). "Numerical Recipes for Reliability Analysis – A Primer." In *Reliability Based Design in Geotechnical Engineering: Computations and Applications*, edited by K. K. Phoon, 1-75, Taylor and Francis, London.
- Phoon, K.K. and Kulhawy, F.H. (1999a). "Characterization of geotechnical variability," *Can. Geotech. J.* 36(4), 612-624.
- Phoon, K.K. and Kulhawy, F.H. (1999b). "Evaluation of geotechnical property variability," *Can. Geotech. J.* 36(4), 625-639.



- Phoon, K.K., Kulhawy, F.H. and Grigoriu, M.D. (1995). "Reliability-based design of foundations for transmission line structures," *Electric Power Research Institute*, Palo Alto, Report TR-1005000.
- Phoon, K.K., Kulhawy, F.H. and Grigoriu, M.D. (2003). "Multiple resistance factor design for shallow transmission line structure foundations," *J. Geotech. Geoenviron. Eng.*, 129(9), 807-818.
- Phoon, K.K., Quek, S.T. and An, P. (2003). "Identification of statistically homogeneous soil layers using modified Bartlett statistics," *J. Geotech. Geoenviron. Eng.*, 129(7), 649-659.
- R Code Team, R: A language and environment for statistical computing, [Computer software, Version 3.3], R Foundation for Statistical Computing, Vienna, Austria, URL: <http://R-project.org/>.
- Raychowdhury, P. (2008). "Nonlinear Winkler-based shallow foundation model for performance assessment of seismically loaded structures," Ph.D. thesis, Univ. of California, San Diego.
- Raychowdhury, P. and Hutchinson, T.C. (2009). "Performance evaluation of a nonlinear Winkler-based shallow foundation model using centrifuge test results," *Earthquake Engng. Struct. Dyn.*, 38(5), 679-698.
- Ribeiro, F.L., Barbosa, A.R., and Neves, L.C. (2014). "Applications of reliability-based robustness assessment of steel moment resisting frames structures under post-mainshock cascading events," *J. Struct. Eng.* 140, Special Issue: Computational Simulation in Structural Engineering, A4014008, DOI: 10.1061/(ASCE)ST.1943-541X.0000939.
- Ribeiro, F.L., Barbosa, A.R., Scott, M.H., and Neves, L.C. (2015). "Deterioration modeling of steel moment resisting frames using finite-length plastic hinge force-based beam-column elements," *J. Struct. Eng.*, 141(2), 04014112.
- Roberts, L.A. and Misra, A. (2010). "LRFD of shallow foundations at the service limit state: Assessment and management of risk for engineered systems and geohazards," *Georisk*, 4(1), 13-21.
- Schlather, M., Malinowski, A., Oesting, M., Boecker, D., Strokorb, K., Engelke, S., Martini, J., Ballani, F., Moreva, O., Berreth, C., Menck, P., Gross, S., Ober, U., Burmeister, K., Manitz, J., Ribeiro, P., Singleton, R., Pfaff, B., and R Core Team (2016). "RandomFields," R Package [Computer software], URL: <http://ms.math.uni-mannheim.de/de/publications/software>.
- Sivakumar Babu, G.L., Srivastava, A. and Murthy, D.S.N. (2006). "Reliability analysis of the bearing capacity of a shallow foundation resting on cohesive soil," *Can. Geotech. J.* 40(1), 1-15. doi:10.1139/t02-090.
- Skempton, A.W. (1951). "The bearing capacity of clays," *Proc. Building Research Congress*, Vol. 1, 180-189.

- Skempton, A.W. and MacDonald, D.H. (1956). "Allowable Settlement of Buildings," *Ins. Civ. Eng.*, III, Vol. 5, 727-768.
- Son, M. and Cording, E. (2005). "Estimation of building damage due to excavation-induced ground movements." *J. Geotech. Geoenviron. Eng.*, 131(2), 162-177.
- Son, M. and Cording, E. (2011). "Responses of buildings with different structural types to excavation-induced ground settlements," *J. Geotech. Geoenviron. Eng.*, 137(4), 323-333.
- Strahler, A.W. and Stuedlein, A.W. (2013). "Characterization of Model Uncertainty in Immediate Settlement Calculations for Spread Footings on Clay," *Proceedings, 18<sup>th</sup> International Conference on Soil Mechanics and Geotechnical Engineering*, Paris, 2014, 4 p.
- Stuedlein, A.W. and Bong, T. (2017). "Effect of spatial variability on static and liquefaction-induced differential settlements," *Geo-Risk 2017: Keynote Lectures*, GSP No. 282, 31–51.
- Stuedlein, A.W. and Holtz, R.D. (2010). "Undrained displacement behavior of spread footings in clay," In: Honoring Clyde, N., Baker Jr., P.E., S.E. (Eds.), *The Art of Foundation Engineering Practice*, ASCE, 653–669.
- Stuedlein, A.W., Huffman, J.C. and Reddy, S.C. (2014) "Ultimate limit state reliability-based design of spread footings on aggregate pier-reinforced clay," *Proceedings of the Institution of Civil Engineers - Ground Improvement*, 167(4), 291-300.
- Stuedlein, A.W., Kramer, S.L., Arduino, P. and Holtz, R.D. (2012a). "Geotechnical characterization and random field modeling of desiccated clay," *J. Geotech. Geoenviron. Eng.*, 138(11), 1301-1313.
- Stuedlein, A.W., Kramer, S.L., Arduino, P. and Holtz, R.D. (2012b) "Reliability of spread footing performance in desiccated clay," *J. Geotech. Geoenviron. Eng.*, 138(11), 1314-1325.
- Terzaghi, K. (1943). *Theoretical Soil Mechanics*, John Wiley and Sons, Inc., New York.
- Terzaghi, K., Peck, R.B., and Mesri, G. (1996). *Soil Mechanics in Engineering Practice*, 3<sup>rd</sup> ed., John Wiley and Sons, Inc., New York.
- UBC (1994). "Structural Engineering Design Provisions," *Uniform Building Code*, Vol. 2, International Conference of Building Officials.
- Uzielli, M., Lacasse, S., Nadim, F. and Phoon, K.K. (2007). "Soil variability analysis for geotechnical practice," In T.S. Tan, K.K. Phoon, D.W. Hight and S. Leroueil (eds.), *Proceedings of the 2<sup>nd</sup> Int. Workshop on Characterization and Engineering Properties of Natural Soils, Vol. 3*, (IS-Singapore), Taylor and Francis Group, London, 1653 – 1752, ISBN 978-0-415-42691-6.
- Uzielli, M. and Mayne, P. (2011). "Serviceability limit state CPT-based design for vertically loaded shallow footings on sand," *An International Journal. Geomech. Geoenviron. Eng.*, 6(2), 91–107.

- Uzielli, M. and Mayne, P. (2012). "Load–displacement uncertainty of vertically loaded shallow footings on sands and effects on probabilistic settlement," *Georisk*, 6(1), 50–69.
- Vanmarcke, E. H. (1977). "Probabilistic modeling of soil profiles," *J. Geotech. Engrg. Div.*, 103(11), 1227–1246.
- Vanmarcke, E. H. (1983). *Random fields: Analysis and synthesis*, MIT, Cambridge, MA.
- Wahls, H. E. (1981). "Tolerable settlement of buildings," *J. Geotech. Engrg. Div.*, 107(11), 1489-1504.
- Wang, Y. (2011). "Reliability-based design of spread foundations by Monte Carlo simulations," *Géotechnique*, 61(8), 677-685.
- Wilson, P. and Elgamal, A. (2006). "Large scale measurement of lateral earth pressure on bridge abutment back-wall subjected to static and dynamic loading," *Proceedings of the New Zealand Workshop on Geotechnical Earthquake Engineering*, University of Canterbury, Christchurch, New Zealand: 307-315.
- Zhang, L.M. and Ng, A.M.Y. (2005). "Probabilistic limiting tolerable displacements for serviceability limit state design of foundations," *Géotechnique*, 55(2), 151–161.

## CHAPTER 8: SUMMARY AND CONCLUSIONS

Recent efforts have been made by the engineering community to adopt reliability-based design (RBD) methods for geotechnical applications to better quantify the multiple uncertainties and provide cost-effective design for an accepted level of risk based on probabilistic analysis. However, improvements to current RBD methods for foundation design remain necessary. The research presented in this dissertation improves upon current methods associated with geotechnical design of spread footings supported on plastic, fine-grained soil (i.e., clay or clayey silt) and on aggregate pier-improved fine-grained soil. Particularly, this research focused on improving our understanding of soil and foundation performance at the serviceability limit state (SLS), and how it relates to the structure that is being supported on shallow foundations; the proposed, general framework is termed reliability-based serviceability limit state (RBSLS) design. This chapter summarizes the work conducted and conclusions drawn from the research contained in this dissertation, followed by recommendations for additional research.

### 8.1 SUMMARY OF WORK COMPLETED

#### 8.1.1 Reliability-based SLS Design of Spread Footings on Aggregate Pier Reinforced Clay

Chapter 4 developed a new RBSLS procedure for the design of spread footings supported on aggregate pier-improved clay. The model includes a normalized, bivariate bearing pressure-displacement equation calibrated based on the results of several full-scale foundation loading tests for footings supported on one or multiple aggregate piers. The

loading test database was compiled from the literature and previously vetted by Stuedlein and Holtz (2013). The proposed method also includes a lumped load and resistance factor,  $\psi_q$ , calculated based on a relationship to the reliability index,  $\beta$ , associated with the probability of exceeding a selected design vertical foundation displacement. The lumped load and resistance factor was calibrated using Monte Carlo simulations (MCS) seeded with statistical distributions representing the dispersion in the normalized bearing pressure-displacement behavior, the bias between the calculated and observed reference capacity, uncertainty in the allowable footing displacement and applied bearing pressure, and the dependence structure observed between the model parameters. Further analysis was completed to demonstrate the importance of including suitable dependence structure (e.g., copula selection) within the reliability simulations and the consequence of overly conservative or unconservative (i.e., uneconomical) design when proper correlation structure is not included.

The SLS method developed in Chapter 4 provides an improvement over existing methods currently used to predict the load-displacement response of footings on aggregate pier reinforced clay that assume a unit cell concept and/or linear (elastic) soil-pier spring. Such methods do not accurately model the nonlinear bearing pressure-soil response that is observed in full-scale loading tests. Furthermore, the proposed SLS method incorporates probabilistic RBD procedures that heretofore have been absent in most settlement analyses methods for footings on aggregate pier reinforced clay.

### 8.1.2 Reliability-based SLS Design for Immediate Settlement of Spread Footings on Clay

Code-based SLS design for spread footings on clay typically focuses solely on consolidation settlement using deterministic analysis. That approach neglects the potentially large, immediate (i.e., distortion) settlement associated with construction. It also neglects to include inherent uncertainties such as soil variability or model (transformation) uncertainty that are addressed by comprehensive probabilistic reliability-based design. Chapter 5 developed a new RBSLS design method that improves upon current code-based design by addressing the shortcomings identified above.

The new RBSLS design procedure outlined in chapter 5 for estimating immediate settlement of a footing supported on clay was developed using much of the same framework outlined above for Chapter 4. The model includes a normalized, bivariate bearing pressure-displacement equation calibrated based on the results of full-scale foundation loading tests initially vetted by Strahler and Stuedlein (2014). A lumped load and resistance factor,  $\psi_q$ , linked to a target  $\beta$  value was calibrated using MCS seeded with statistical distributions representing the dispersion in the normalized bearing pressure-displacement behavior, the bias between the calculated and observed reference capacity, uncertainty in the allowable footing displacement and applied bearing pressure, and the dependence structure observed between the model parameters.

The reference capacity was set equal to a slope-tangent capacity,  $q_{STC}$ , that is linked to the calculated bearing capacity (i.e., ultimate resistance) and estimated from the loading tests. This step was taken to reduce dispersion in the normalized bearing pressure-displacement model. The slope-tangent factor,  $M_{STC}$ , used to scale the estimated bearing

capacity to slope-tangent capacity exhibited correlation to the bivariate model parameters and, therefore, required vine copula functions seeded in the MCS to properly account for this dependence.

### 8.1.3 Calibration and Assessment of Reliability-based SLS Procedures for Foundation Engineering

The state-of-practice for serviceability limit state geotechnical foundation design is evolving as new and existing tools are being implemented to better incorporate reliability-based design elements. Among the most critical elements in RBD foundation analysis is the need to limit the dispersion associated with selected design models to the extent practical, while also sufficiently capturing the propagation and model error, dependence structure, and other sources of uncertainty. Chapter 6 explored the impact of model selection on the propagation of error and its impact on reliability, as well as the independent evaluation of an existing and a newly revised RBSLS model based on the work previously documented in Chapter 4 for a spread footing supported on aggregate pier reinforced clay. The independent evaluation relied on data from several new, high-quality loading tests conducted at the Oregon State University Geotechnical Engineering Field Research Site (OSU GEFRS) with various-sized footings supported on one or multiple aggregated piers. New research showed that the selection of model used to capture the bivariate distribution of bearing pressure–displacement curves can have a significant effect on the computed reliability. The impact of copula model on reliability was also illustrated through the effect on allowable bearing pressure at a given footing displacement.

Chapter 6 further contributed to improving the state of RBSLS foundation design by providing a step-by-step procedure for making decisions regarding copula model fitting,

scatter reduction through normalizations of bearing pressure-displacement curves, and capturing suitable propagation of error through the various components comprising the full reliability-based SLS calibration.

#### 8.1.4 Reliability-based Assessment of Foundation and Structure Performance with Spatially Variable Soil

The inherent spatial variability of soil and soil-structure interaction (SSI) are two critically important aspects when considering geotechnical foundation design and performance of the supported structure. However, fully incorporating soil variability and SSI into a comprehensive limit state model remains a challenge for geotechnical and structural engineering researchers and practitioners. Chapter 7 explored foundation and structure performance with reliability analyses using MCS that incorporated the soil-foundation model developed in Chapter 5, modified to include a multi-foundation system and variable soil shear strength in combination with loading from a two-dimensional, three-story, steel moment-resisting frame (SMRF) building as documented in FEMA-355C (2000) and Barbosa et al. (2017). The effect of variable soil shear strength was evaluated by considering a range in of values for the coefficient of variation of inherent soil variability for undrained shear strength,  $COV_w(s_u)$ , and horizontal scale of fluctuation in undrained shear strength,  $\delta_h(s_u)$ , within the MCS analysis. Chapter 7 also investigated differences between inter-site and intra-site soil variability by comparing soil-foundation springs based on parameters using the global foundation loading test database from Chapter 5 or a subset developed from foundation loading tests for a single site documented in Newton (1975) and Martin (2018). The intent of the research was to further the



understanding of foundation and structure performance with respect to soil variability and SSI that can be incorporated into reliability-based design models.

The MCS analyses was implemented in four separate cases. The soil-foundation response was first modeled in MCS Cases 1 and 2 with the five footings subject to the building load but acting independent of the structure to provide a baseline for comparison of foundation performance when the structure and SSI effects are included. Case 1 assumed soil-spring parameters based on the intra-site (global) dataset and Case 2 assumed soil-spring parameters based on the local intra-site dataset. Following that, the structure model was applied in MCS Cases 3 and 4 using the program OpenSees. Recorders implemented in OpenSees tabulated foundation displacement and maximum beam rotations. Case 3 assumed soil-spring parameters based on the intra-site dataset and Case 4 assumed soil-spring parameters based on the intra-site dataset.

## 8.2 CONCLUSIONS DRAWN FROM THIS WORK

### 8.2.1 Reliability-based SLS Design of Spread Footings on Aggregate Pier Reinforced Clay

Chapter 4 proposed RBLS design procedures for shallow foundations on aggregate pier-reinforced clay, in which the following conclusions were drawn:

- In a first effort, the use of an existing ultimate bearing resistance model proposed by others served to reduce the scatter in normalized bearing pressure-displacement responses of shallow foundations on aggregate pier reinforced clay;

- The hyperbolic and power law models evaluated for capturing the bearing pressure-displacement relationship of shallow foundations on aggregate pier reinforced clay were deemed suitable for the purpose;
- The power law model was determined most accurate over the range in bearing pressures and displacements present within the selected database of full-scale loading tests and appropriate for the purposes of calibrating a RBSLS procedure;
- The bivariate bearing pressure-displacement model parameters were successfully simulated using calibrated copulas; the Gumbel copula was determined most suitable for use in Monte Carlo simulations;
- Lower-bound shear strengths served to effectively limit the variability of possible undrained shear strengths to reasonable and expected values, thus providing an accurate basis for RBSLS calibrations; and,
- A lumped load and resistance factor calibrated using Monte Carlo simulations of six random variables, including correlated variables, conveniently captured the reliability of footing displacements and eliminated the need for cumbersome calculations necessary for implementation in every-day engineering practice.

### 8.2.2 Reliability-based SLS Design for Immediate Settlement of Spread Footings on Clay

Chapter 5 proposed RBSLS design procedures for the immediate settlement of shallow foundations on clay, in which the following conclusions were drawn:

- Traditional bearing capacity estimates for shallow foundations on clayey soils were determined biased, with the capacity under-predicted by 25% and a coefficient of variation of 37%;
- The novel use of a slope-tangent capacity for shallow foundations, determined using the bearing pressure-displacement responses derived from full-scale loading test data, was determined superior to the ultimate bearing resistance as a reference capacity to reduce the scatter in normalized bearing pressure-displacement responses;
- Similar to the findings in Chapter 4, the parameters describing the best-fitting hyperbolic model used to simulate the normalized bearing pressure-displacement responses exhibited correlation. However, a vine copula using a combination of Clayton and Joe copula functions was established to capture the trivariate dependence structure necessary for use in sampling during the Monte Carlo simulations due to the correlation of the slope-tangent capacity and the hyperbolic model parameters; and,
- A lumped load and resistance factor calibrated using Monte Carlo simulations of seven random variables, including three mutually-dependent variables, readily captured the reliability of immediate settlements associated with shallow foundations on clay and provided an accessible RBSLS procedure for practicing engineers.

### 8.2.3 Calibration and Assessment of Reliability-based SLS Procedures for Foundation Engineering

Chapter 6 proposed revised RBSLS design procedures for shallow foundations on aggregate pier-reinforced clay and a general framework for calibrating RBSLS foundation design, in which the following conclusions were drawn:

- Use of a slope-tangent capacity with offset equal to 2% of the footing width was shown to significantly reduce scatter in the normalized bearing pressure-displacement ( $q$ - $\delta$ ) curves as compared to the previous reference capacity (i.e., the ultimate bearing resistance) used in Chapter 4;
- Future efforts to generate a RBSLS design procedure should follow the recommended framework for exploring the suitability of possible reference capacities;
- A revised lumped load and resistance factor ( $\psi_q$ ) calibrated using Monte Carlo simulations of seven random variables, including correlated variables, captured the reliability of footing displacements for use in a convenient RBSLS procedure;
- Investigating various correlation structures using different copula functions for the multivariate  $q$ - $\delta$  model showed that the probability of exceeding the SLS at a given  $\psi_q$  value depends strongly on the correlation structure model considered, and that ignoring the dependence of the  $q$ - $\delta$  model (i.e., no copula function) results in the highest and/or most conservative probability; and,
- A power law model with recalibrated coefficients and new slope-tangent capacity factor was determined to provide the best-fit to existing full-scale

loading tests, and was used to evaluate an independent check on the goodness-of-fit to the bearing pressure-displacement response derived from new full-scale loading tests.

#### 8.2.4 Reliability-based Assessment of Foundation and Structure Performance with Spatially Variable Soil

The research documented in Chapter 7 resulted in many novel conclusions drawn from the evaluation of four specific MCS cases. The following provides a summary of the most important conclusions:

- Use of spatially variable undrained shear strengths,  $s_u$ , in combination with calibrated nonlinear soil-foundation spring parameters, provides a more accurate displacement estimate for foundations supported on plastic fine-grained soils under undrained loading conditions compared to models using an elastic soil modulus,  $E$ , to establish the soil-foundation response;
- For footings modeled independent of the structure (Cases 1 and 2), the critical scale of fluctuation,  $\delta_{h,crit}$  (defined as  $\delta_h$  corresponding to the largest probability of exceeding a given magnitude of  $\Delta s$ ) typically occurred with  $\delta_h$  on the order of  $0.5l$  to  $1.0l$ , where  $l$  is the center-to-center distance between adjacent footings;
- When including a realistic building model and associated soil-structure interaction (Cases 3 and 4), the magnitude of  $\delta_{h(s_u)crit}$  typically increased to  $1l$  to  $2l$ , suggesting that the critical scale of fluctuation is influenced by the scale of the entire building rather than just the distance between adjacent footings.

- The soil-foundation spring parameters for the intra-site model (Cases 2 and 4) exhibited larger mean and median vertical displacements for individual footings because the nominal slope-tangent model coefficient used for intra-site cases is less than that used for inter-site cases (Cases 1 and 3), directly affecting the average spring stiffness.
- Even though the inter-site soil-foundation stiffness is greater for individual footings, the overall dispersion in the intra-site spring parameters is lower compared to the inter-site parameters, leading to less variable stiffness between footings. As a result, the differential foundation displacement and angular distortion is typically less for the intra-site cases.
- When a realistic building model and associated SSI was included (Cases 3 and 4), the steel structure provided increased rigidity between footings and corresponding redistribution of foundation loads based on soil stiffness. As a result, there is lower instances of extreme individual vertical footing displacements and the magnitude of differential footing displacements is lower.
- Overall, the steel, moment restrained frame structure modeled in Cases 3 and 4 MCS performed well with relatively few occurrences of individual beams exceeding the beam yield rotation,  $\theta_y$ .
- Considering all of the results derived from Cases 3 and 4, the probability of exceeding  $\theta_y$  achieved a maximum of approximately 4 to 5 percent for the most variable soil conditions (i.e.,  $COV_{w,h}(S_u) = 100$  percent and  $\delta_h(S_u) = \delta_h(S_u)_{crit} =$  approximately  $1l$  to  $2l$ ). When considering only instances

where angular distortion between footings,  $\Delta s/l$ , exceeds 1/150, the maximum probability of exceeding  $\theta_y$  increased to approximately 15 percent.

- The greatest probability for individual beams exceeding  $\theta_y$  occurred for  $\delta_h(s_u)$  in the range of 10 to 20 m (i.e., approximately  $1l$  to  $2l$ ), and corresponds to the same magnitude of horizontal scale of fluctuation where angular distortion,  $\Delta s/l$ , is most likely to exceed 1/150.
- When considering smaller magnitudes of beam rotation approximately corresponding to a serviceability limit state (e.g.,  $0.5\theta_y$ ), the critical scale of fluctuation reduced to approximately 5 m (approximately  $0.5l$ ), suggesting the performance of the beams at the serviceability level may be controlled by local footing conditions.
- There was no obvious correlation between beam rotation,  $\theta$ , and  $\Delta s/l$  across individual bays; further,  $\theta$  was not necessarily largest where  $\Delta s/l$  was largest, but where the *change* in  $\Delta s/l$  between adjacent bays was largest.
- For occurrences where individual beams exceeded their yield rotation, larger magnitude angular distortion,  $\Delta s/l$ , generally accompanied the yield rotation when  $\delta_h(s_u)$  was large, and smaller magnitude  $\Delta s/l$  generally accompanied the yield rotation when  $\delta_h(s_u)$  was small. Furthermore, large magnitude  $\Delta s/l$  values coupled with large magnitude  $\delta_h(s_u)$  did not necessarily translate to greater instances of exceeding  $\theta_y$  because the modeled structure was likely tilting monolithically in one direction, causing less stress on the beams. Conversely, large magnitude  $\Delta s/l$  values coupled with smaller magnitude

$\delta_h(s_u)$  provided greater probability of adjacent bays experiencing disparate angular distortions and greater beam stresses.

### 8.3 SUGGESTIONS FOR FUTURE RESEARCH

Suitable RBSLS calibration of design procedures for foundations requires an accurate characterization of the dispersion and/or characteristic distributions of individual model parameters, model error (e.g., bias between measured and calculated results), and correlation structure of the relevant variables. The analyses presented herein depended in part on the compiled databases of high-quality foundation loading tests, which provided the backbone for probabilistic analysis. The following suggestions for future research could be followed to expand and extend the research conducted as part of this dissertation and presented in Chapters 4 through 6:

- The execution of new full-scale loading tests of foundations supported on clay, aggregate pier-reinforced clay, or other ground improvements that include detailed documentation of the foundation soils, the loading test set-up, and bearing pressure-displacement response. Here, loading tests taken as close as practical to the ultimate bearing resistance would be critical in order to establish the ultimate limit state and associated uncertainty;
- The independent evaluation of the SLS soil-foundation models proposed herein based on the results of new loading tests, with recalibration of the RBSLS models that incorporate the new data; and,
- Improved identification of those characteristics of bearing pressure-displacement performance for specific regions to improve the understanding of



variability associated with specific geological regions and determination of improved recommendations for development of intra-site model dependencies.

The research documented in Chapter 7 was in part a culmination of the research in previous chapters of this dissertation and collaboration with structural engineering researchers. The overall goal was to develop or improve upon limit state foundation design and provide a better understanding of the role of soil-structure interaction in overall infrastructure system performance by combining an RBLS model with spatially varying soil that interacted with a calibrated numerical model of a building frame. The following suggestions are provided to expand and extend the work in Chapter 7:

- Additional analysis using building models with different numbers of foundations and foundation spacing to further evaluate relationships between foundation distance and the scale of fluctuation of critical soil strength properties;
- Analysis using structure models with different building heights (or number of stories) to evaluate the effect on building performance and footing performance with larger foundation loads. For example, the role of additional floors on propagation of bending stresses and/or structural details specified to mitigate differential settlements could be explored to reduce the frequency of poor structure performance;
- Additional analysis using buildings constructed using reinforced concrete, masonry, or other construction materials would provide insight into the role of construction materials on the overall system performance;

- Expanding analysis from two- to three-dimensional to better understand structural response; and,
- Calibration of a lumped load and resistance factor,  $\psi_q$ , to incorporate the effects of spatially variable soil (i.e., varying  $COV_{w,h}(s_u)$  and  $\delta_h(s_u)$ ) and soil-structure interaction to eliminate the need for conducting time-consuming numerical simulations and make the effects of spatial variability and soil-structure interaction accessible to every-day practitioners.

## COMPLETE LIST OF REFERENCES

- Aas, K., Czado, C., Frigessi, A., and Bakken, H. (2009). "Pair-Copula Construction of Multiple Dependence," *Insurance: Mathematics and Economics*, 44(2), 182-198.
- AASHTO (2012) *AASHTO LRFD Bridge Design Specifications*, 6<sup>th</sup> Ed., American Association of State Highway and Transportation Officials, Washington, DC.
- AASHTO (2017) *AASHTO LRFD Bridge Design Specifications*, 8<sup>th</sup> Ed., American Association of State Highway and Transportation Officials, Washington, DC.
- ASTM (1994) ASTM D1194-94: *Standard test method for bearing capacity of soil for static load and spread footings* (withdrawn 2003), ASTM International, West Conshohocken, PA.
- Aboshi, H., Ichimoto, E., Enoki, M., and Harada, K. (1979) "The Composer – A Method to Improve Characteristics of Soft Clays by Inclusion of Large Diameter Sand Columns," *Proceedings, Reinforced Earth and Other Techniques*, Vol. 1, Paris, France.
- Ahmed, A. and Soubra A.-H. (2014). "Probabilistic analysis at the serviceability limit state of two neighboring strip footings resting on a spatially random soil," *Struct. Safety*, 49, 2–9.
- Akaike, H. (1974) "A New Look at the Statistical Model Identification," *Transactions on Automatic Control*, IEEE, 19(6), 716-723.
- Akbas, S.O. and Kulhawy, F.H. (2009). "Axial Compression of Footings in Cohesionless Soils I: Load-Settlement Behavior," *Journal of Geotechnical and Geoenvironmental Engineering*, ASCE, 135(11), 1562-1574.
- Alamgir, M., Miura, N., Poorooshasb, H. B., and Madhav, M. R. (1996). "Deformation Analysis of Soft Ground Reinforced by Columnar Inclusions." *Computers and Geotechnics*, 18(4), 267–290.
- Allen, T.A. (2005) "Development of Geotechnical Resistance Factors and Downdrag Load Factors for LRFD Foundation Strength Limit State Design," *Report No. FHWA-NHI-05-052*, Federal Highway Administration, Washington D.C.
- Allen, T.A., Nowak, A.S., and Bathurst, R.J. (2005). "Calibration to Determine Load and Resistance Factors for Geotechnical and Structural Design," *Transportation Research Circular E-C079*, Transportation Research Board of the National Academies, Washington D.C.
- Allotey, N. and El Naggar, M.H. (2008). "Generalized dynamic Winkler model for nonlinear soil-structure interaction analysis," *Can. Geotech. J.*, 45, 560-573.
- Andersen, K.H. and Stenhamar, P. (1982). "Static Plate Loading Test on Overconsolidated Clay," *Journal of the Geotechnical Engineering Division*, ASCE, 108(7), 918-934.

- Anderson, T.W., Darling, D.A. (1952) "Asymptotic theory of certain 'goodness-of-fit' criteria based on stochastic processes," *Annals of Mathematical Statistics*, 23(2), 193-212.
- Baecher, G.B. and Christian, J.T. (2003). *Reliability and Statistics in Geotechnical Engineering*, John Wiley and Sons, Ltd., London and New York, 605 pp.
- Balaam, N.P. and Booker, J.R. (1981). "Analysis of Rigid Rafts Supported by Granular Piles," *International Journal of Numerical and Analytical Methods in Geomechanics*, 5(4), 379-404.
- Balaam, N.P., Brown, P.T., and Poulos, H.G. (1977) "Settlement Analysis of Soft Clays Reinforced with Granular Piles," *Proceedings, 5th Southeast Asian Conference on Soil Engineering*, July 2-4, Bangkok, Thailand.
- Barbosa, A.R, Ribeiro, F.L.A. and Neves, L.A.C. (2017). "Influence of earthquake ground-motion on damage estimation: application to steel moment resisting frames," *Earthquake Engng Struct. Dyn.*, 46(1), 27-49.
- Barker, R., Duncan, J., Rojiani, K., Ooi, P., Tan, C., and Kim, S. (1991) *NCHRP Report 343: Manuals for the Design of Bridge Foundations*. TRB, National Research Council, Washington, DC.
- Barksdale, R. D., and Bachus, R. C. (1983). "Design and Construction of Stone Columns," *Report No. FHWA/RD 83/026*, Federal Highway Administration.
- Bathurst, R.J. and Javankhoshdel, S. (2017). "Influence of model type, bias and input parameter variability on reliability analysis for simple limit states in soil-structure interaction problems," *Georisk*, 11(1), 42-54.
- Bauer, G.E., Shields, D.H., and Scott, J.D. (1976). "Predicted and Observed Footing Settlements in a Fissured Clay," Ottawa, Pentech Press, 287-302.
- Baumann, V., and Bauer, G.E.A. (1974) "The Performance of Foundation on Various Soils Stabilized by Vibrocompaction Method," *Canadian Geotechnical Journal*, Vol. 11, 509-530.
- Belejo, A.F.V., Barbosa, A.R., Huffman, J.C., and Stuedlein, A.W. (2020) "Influence of ground-motion duration on damage estimation of steel moment resisting frames accounting for soil-structure interaction effects," *J. Struct. Eng.*, In Review.
- Bergado, D.T., and Lam, F.L. (1987) "Full Scale Load Test of Granular Piles with Different Densities and Different Proportions of Gravel and Sand in the Soft Bangkok Clay," *Soils and Foundations Journal*, 27(1), Japan, 86-93.
- Bergado, D.T., Rantucci, G. and Widodo, S. (1984). "Full Scale Load Tests of Granular Piles and Sand Drains in the Soft Bangkok Clay," *Asian Institute of Technology*, 111-118.
- Bhat, C.R. and Eluru, N. (2009) "A copula-based approach to accommodating residential self-selection effects in travel behavior modeling," *Transportation Research Part B: Methodological*, 43(7), 749-765.

- Bong, T. and Stuedlein, A.W. (2018). "Effect of cone penetration conditioning on random field model parameters and impact of spatial variability in liquefaction-induced differential settlements," *J. Geotech. Geoenviron. Eng.*, 144(5), 04018018.
- Boscardin, M.D. and Cording, E.J. (1989). "Building response to excavation-induced settlement," *J. Geot. Eng.*, 115(1), 1-21.
- Bowles, J.E. (1988) *Foundation Analysis and Design*, 4<sup>th</sup> ed. McGraw-Hill, Inc. New York, NY.
- Brand, E.W., Muktabhant, C. and Taechathummarak, A. (1972). "Load Tests on Small Foundations in Soft Clay," *Conference Proceedings: Performance of Earth and Earth Supported Structures*, ASCE, 903-928.
- Brechmann, E.C. and Schepsmeier, U. (2013). "Modeling Dependence with C- and D-Vine Copulas: The R Package CDVine," *Journal of Statistical Software*, 52(3), 27 pg.
- Breysse, D, Niandou, H., Elachachi, S., and Houy, L. (2004). "A generic approach to soil-structure interaction considering the effects of soil heterogeneity," *Géotechnique*, 54(2), 143–150.
- Brinch Hansen, J. (1970). "A revised and extended formula for bearing capacity," *Bulletin No. 28*, Danish Geotechnical Institute, Copenhagen, Denmark, 5–11.
- Broding, W.C., Diederich, F.W. and Parker, P.S. (1964) "Structural optimization and design based on a reliability design criterion," *J. Spacecraft*, 1(1), 56-61.
- Buckle, I., Friedland, I., Mander, J., Martin, G., Nutt, R., and Power, M. (2006). *Seismic Retrofitting Manual for Highway Structures: Part 1 – Bridges*, Federal Highway Administration, Report No. FHWA-HRT-06-032.
- Burland, J.B. and Wroth, C.P. (1974). "Settlement behavior of buildings and associated damage," *Proc., Conf. on Settlement of Structures*, Cambridge Univ., Instn. of Civil Engrs., London, 611-654.
- Chin, F. (1971). *Estimation of the Ultimate Load of Piles from Tests not Carried to Failure*. Singapore, University of Singapore, pp. 81-90.
- Christian, J.T. and Carrier, W.D. (1978). "Janbu, Bjerrum and Kjaernsli's chart reinterpreted," *Can. Geotech. J.*, 15, 123-128.
- Clough, G.W. and O'Rourke, T.D. (1990). "Construction induced movements of in situ walls," *Design and Performance of Earth Retaining Structures*, GSP No. 25, ASCE, New York, NY, 439-470.
- Coduto, D. (2001). *Foundation Design: Principals and Practices*. 2<sup>nd</sup> ed. Prentice-Hall Inc, New Jersey.
- Consoli, N. C., Schnaid, F. and Milititsky, J. (1998). "Interpretation of Plate Load Tests on Residual Soil Site," *Journal of Geotechnical and Geoenvironmental Engineering*, 124(9), 857-867.
- D'Appolonia and Lambe, T.W. (1970). "Method for Predicting Initial Settlement," *Journal of the Soil Mechanics and Foundations Division*, 96(SM2), 523-544.

- D'Appolonia, D., Poulos, H. and Ladd, C. (1971). "Initial Settlement of Structures on Clay," *Journal of the Soil Mechanics and Foundations Division*, 97(SM10), 1359-1377.
- Datye, K.R., (1982). "Note on Design Approach and Calculations for Stone Columns," *Indian Geotechnical Journal*, 1982.
- Datye, K.R. and Nagaraju, S.S. (1981). "Design approach and field control for stone columns," *Proceedings*, 10<sup>th</sup> International Conference on Soil Mechanics and Foundation Engineering, Stockholm.
- Das, B.M. (1984) *Principles of Foundation Engineering*, Brooks/Cole Engineering Division, Monterey, CA.
- Das, B.M. (2007) *Principles of Foundation Engineering*, 7<sup>th</sup> ed., Cengage Learning, Stamford, CT.
- Das, B.M. and Larbi-Cherif, S. (1983) "Bearing capacity of two closely spaced shallow foundations on sand," *Soils and Foundations*, 23(1), 1-7.
- Deshmukh, A.M. and Ganpule, V.T. (1994). "Influence of Flexible Mat on Settlements of Marine Clay," *Vertical and Horizontal Deformations of Foundations and Embankments*, ASCE, 887-896.
- Dithinde, M., Phoon, K.K., De Wet, M., and Retief, J.V. (2011) "Characterization of Model Uncertainty in the Static Pile Design Formula," *Journal of Geotechnical and Geoenvironmental Engineering*, 137(1), 70-85.
- Douglas, D.J. and Davis, E.H. (1964). "The movements of buried footings due to moment and horizontal load and the movement of anchor plates," *Géotechnique*, 14(2), 115–132.
- Duncan, J.M. (2000). "Factors of safety and reliability in geotechnical engineering," *J. Geotech. Geoenviron. Eng.*, 126(4), 307-316.
- Duncan, J. M., Byrne, P., Wong, K. S., and Mabry, P. (1980). "Strength, stress-strain and bulk modulus parameters for finite element analysis of stress and movements in soil masses." *UCB/GT/80-01*, University of California, Berkeley, Calif.
- Duncan, J. M., and Chang, C. Y. (1970). "Nonlinear analysis of stress and strain in soils." *J. Soil Mech. and Found. Div.*, 96(5), 1629–1653.
- Duncan, J.M. and Mokwa, R.L. (2001). "Passive earth pressures: theories and tests," *J. Geotech. Geoenviron. Eng.*, 127(3), 248-257.
- Elktab, T., Chalaturnyk, R. and Robertson, P.K. (2003). "An overview of soil heterogeneity: quantification and implications on geotechnical field problems," *Can. Geotech. J.* 40(1), 1-15. doi:10.1139/t02-090.
- FEMA (2000). "State of the art report on systems performance of steel moment frames subject to earthquake ground shaking," *FEMA-355C*, Washington, DC.

- Fellenius, B.H. and Rahman, M.M. (2019). "Load-movement response by t-z and q-z functions," *Geotechnical Engineering Journal of the SEAGS & AGSSEA*, 50(3), ISSN 0046-5828.
- Fenton, G.A. and Griffiths, D.V. (2002). "Probabilistic foundation settlement on spatially random soil," *J. Geotech. Geoenviron. Eng.*, 128(5), 381-390.
- Fenton G.A. and Griffiths, D.V. (2003). "Bearing capacity prediction of spatially random  $c$ - $\phi$  soils," *Can. Geotech. J.* 40(1), 54–65.
- Fenton, G.A. and Griffiths, D.V. (2005). "Three-dimensional probabilistic foundation settlement," *J. Geotech. Geoenviron. Eng.*, 131(2), 232-239.
- Fenton, G.A. and Griffiths, D.V. (2008). *Risk Assessment in Geotechnical Engineering*, John Wiley and Sons, Inc., New Jersey.
- Fenton, G.A., Griffiths, D.V. and Cavers, W. (2005). "Resistance factors for settlement design," *Can. Geotech. J.* 42(5), 1422–1436.
- Fenton, G.A., Griffiths, D.V. and Ojomo, O.O. (2011). "Consequence factors in the ultimate limit state design of shallow foundations," *Can. Geotech. J.* 48(2), 265-279.
- Foye, K.C., Basu, P., and Prezzi, M. (2008). "Immediate Settlement of Shallow Foundations Bearing on Clay," *International Journal of Geomechanics*, 8(5), 300-310.
- Fox, N.S., and Cowell, M.J. (1998). "Geopier Foundation and Soil Reinforcement Manual," Geopier Foundation Company.
- French, S.E. (1999). *Design of Shallow Foundations*, ASCE Press, Reston VA, ISBN 0-7844-0371-6, 374 p.
- Georigadis, M. (1983). Development of  $p$ - $y$  curves for layered soils," *Proceedings: Geotechnical Practices in Offshore Engineering*, ASCE, 536-545.
- Gilbert, R.B. (1997). "Basic random variables," In G.A. Fenton (ed.), *Probabilistic Methods in Geotechnical Engineering*, ASCE GeoLogan '97 Conference, Logan, Utah.
- Goughnour, R.R. and Bayuk, A.A. (1979). "Analysis of stone column – soil matrix interaction under vertical load," *Proceedings - International Conference on Soil Reinforcement: Reinforced Earth and other Techniques*, Paris, 271-278.
- Grant, R., Christian, J.T., and Vanmarcke, E.H. (1974). "Differential settlement of buildings," *J. Geotech. Engrg. Div.*, 100(9), 973-991.
- Greenwood, D.A. (1975). "Vibroflotation: Rationale for Design and Practice," *Methods of Treatment of Unstable Ground*, F. G. Bell, ed., Newness-Buttersworth, London, UK, 189-209.
- Griffiths, D.V. and Fenton, G.A. (2001). Bearing capacity of spatially random soil: the undrained clay Prandtl problem revisited," *Géotechnique*, 51(4), 351–359.
- Griffiths, D.V., Fenton, G.A. and Manoharan, N. (2002). "Bearing capacity of a rough rigid strip footing on cohesive soil: A probabilistic study," *J. Geotech. Geoenviron. Eng.*, 128(9), 743-755.

- Griffiths, D.V., Huang, J.S. and Fenton, G.A. (2009). "Influence of spatial variability on slope reliability using 2-D random fields," *J. Geotech. Geoenviron. Eng.*, 135 (10): 1367–1378.
- Han, J. and Ye, S. (1991). "Field Tests of Soft Clay Stabilized by Stone Columns in Coastal Areas of China," *Proceedings, 4th International Deep Foundations Institute Conference*, Vol. 1, Balkema Press, Rotterdam, The Netherlands.
- Hansen, J. B. (1970). "A Revised and Extended Formula for Bearing Capacity," *DGI Bulletin*, 5-11.
- Harden, C.W., Hutchinson, T.C., Martin, G.R., and Kutter, B.L. (2005). (Numerical modeling of the nonlinear cyclic response of shallow foundations," *PEER Report 2005/04*, Pacific Earthquake Engineering Research Center, University of California, Berkeley.
- Harden, C.W. and Hutchinson, T.C. (2009). "Beam-on-nonlinear-Winkler-foundation modeling of shallow, rocking-dominated footings," *Earthquake Spectra*, 25(2), 277-300.
- Hirany, A. and Kulhawy, F. (1988) *Conduct and Interpretation of Load Tests on Drilled Shaft Foundations*, New York: EPRI.
- Honjo, Y. and Otake, Y. (2013). "A simple method to assess the effects of soil spatial variability on the performance of a shallow foundation," *Foundation Engineering in the Face of Uncertainty*, ASCE Geo-Congress 2013, San Diego, California.
- Horvath, J.S. (1993). "Beam-column-analogy model for soil-structure interaction analysis," *J. Geotech. Geoenviron. Eng.*, 119(2), 358-364.
- Horvath, J.S. and Colasanti, R.J. (2011). "Practical subgrade model for improved soil-structure interaction analysis: Model development," *Int. J. Geomech.*, 11(1), 59-64.
- Houlsby, G.T., Cassidy, M.J., and Einav, I. (2005). "A generalised Winkler model for the behaviour of shallow foundations," *Géotechnique*, 55(6), 449-460.
- Houy, L., Breysse, D. and Denis, A. (2005). "Influence of soil heterogeneity on load redistribution and settlement of a hyperstatic three-support frame," *Géotechnique*, 55(2), 163-170.
- Huffman, J.C., Martin, J.P. and Stuedlein, A.W. (2016). "Calibration and assessment of reliability-based serviceability limit state procedures for foundation engineering," *Georisk*, 10(4), 208-293.
- Huffman, J.C., Strahler, A.W. and Stuedlein, A.W. (2015). "Reliability-based serviceability limit state design for immediate settlement of spread footings on clay," *Soils and Foundations*, 55(4), 798-812.
- Huffman, J.C. and Stuedlein, A.W. (2014). "Reliability-based serviceability limit state design of spread footings on aggregate pier reinforced clay," *J. Geotech. Geoenviron. Eng.*, 140(10), 04014055.



- Hughes, J.M.O. and Withers, N.J. (1974) "Reinforcing of soft cohesive soils with stone columns," *Ground Engineering*, 7(3), 42-49.
- Hughes, J.M.O., Withers, N.J., and Greenwood, D.A. (1975) "A Field Trial of the Reinforcing Effect of a Stone Column in Soil," *Geotechnique*, 25(1), Thomas Telford Ltd., London, UK.
- Jaksa, M.B. (1995). "The influence of spatial variability on the geotechnical design properties of a stiff overconsolidated clay," *Ph.D. thesis*, Faculty of Engineering, Univ. of Adelaide, Australia.
- Jaksa, M.B., Brooker, P.I. and Kaggwa, W.S. (1997). "Experimental evaluation of the scale of influence of a stiff clay," *Proc., 8<sup>th</sup> Int. Conf. on Application of Statistics and Probability*, Belkema, Rotterdam, Netherlands, 415-422.
- Janbu, N., Bjerrum, L. and Kjaernsli, B. (1956). "Veiledning ved losning av fundamentering – soppgaver," *Publication No. 16*, 30-32, Norwegian Geotechnical Institute.
- Jardine, R.J., Lehane, B. M., Smith, P.R. and Gildea, P.A. (1995). "Vertical Loading Experiments on Rigid Pad Foundations at Bothkennar," *Geotechnique*, 45(4), 573-597.
- Jardine, R.J., Potts, D. M., Fourie, A.B. and Burland, J.B. (1986). "Studies of the Influence of Non-linear Stress-Strain Characteristics in Soil-Structure Interaction," *Geotechnique*, 36(3), 377-396.
- Javankhoshdel, S. and Bathurst, R.J. (2014) "Simplified probabilistic slope stability design charts for cohesive and c- $\phi$  soils," *Canadian Geotechnical Journal*, 51(9), 1033-1045.
- Javankhoshdel, S. and Bathurst, R.J. (2016) "Influence of cross-correlation between soil parameters on probability of failure of simple cohesive and c- $\phi$  slopes" *Canadian Geotechnical Journal*, 53(5), 839-853.
- Jeon, S. and Kulhawy, F. (2001) *Evaluation of Axial Compression Behavior of Micropiles*. Blacksburg, Virginia, ASCE, pp. 460-471.
- Joe, H. (1996). "Families of m-Variate Distributions with Given Margins and  $m(m-1)/2$  Bivariate Dependence Parameters," *Distributions with Fixed Marginals and Related Topics*, Institute of Mathematical Statistics, pp. 120-141.
- Juran, I. and Guermazi, A. (1988) "Settlement Response of Soft Soils Reinforced by Compacted Sand Columns," *Journal of Geotechnical Engineering*, Vol. 114. No. 8, ASCE, Reston, VA, 930-943.
- Kavazanjian, E., Wang, J-N.J., Martin, G.R., Shamsabadi, A., Lam, I., and Dickenson, S.E. (2011) *LRFD Seismic Analysis and Design of Transportation Geotechnical Features and Structural Foundations*, National Highway Institute, FHWA-NHI-11-032, 588 p.
- Kulhawy, F.H. and Phoon, K.K. (2002). "Observations on geotechnical reliability-based design development in North America," *Proc., GeoCongress 2006: Geotechnical Engineering in the Information Technology Age*, ASCE, Atlanta, USA.

- Kulhawy, F.H. and Phoon, K.K. (2006). "Some Critical Issues in Geo-RBD Calibrations for Foundations," *Proc., International Workshop on Foundation Design Codes and Soil Investigation in view of International Harmonization and Performance Based Design*, Tokyo, Japan, pp. 31-48.
- Kumar, J. and Ghosh, P. (2007) "Ultimate bearing capacity of two interfering rough strip footings," *Int'l Journal of Geomechanics*, 7(1), 53-62.
- Lambe, T.W., Whitman, R.V. (1969). *Soil Mechanics*, John Wiley and Sons, Inc., New York.
- Lavasan, A.A. and Ghazavi, M. (2012) "Behavior of closely spaced square and circular footings on reinforced sand," *Soils and Foundations*, 52(1), 160-167.
- Lawton, E.C., Fox, N.S., Handy, R.L. (1994) "Control of Settlement and Uplift of Structures Using Short Aggregate Piers," *In-Situ Deep Soil Improvement*, GSP No. 45, Rollins, K.M., ed., ASCE, New York, New York.
- Lawton, E.C. and Warner, B.J. (2004). "Performance of a Group of GeoPier Elements Loaded in Compression Compared to Single Geopier Elements and Unreinforced Soil," *Report No. UUCVEEN 04-12*, University of Utah, Salt Lake City, UT. pp 257.
- Le, T.M.H. (2014) "Reliability of heterogeneous slopes with cross-correlated shear strength parameters," *Georisk*, 8(4), 250-257.
- Lehane, B.M. (2003). "Vertically loaded shallow foundation on soft clayey silt," *ICE - Geotechnical Engineering*, 156(1), 17-26.
- Li, D.Q., Tang, X.S., Phoon, K.K., Chen, Y.F., Zhou, C.B. (2013). "Bivariate Simulation Using Copula and its Application to Probabilistic Pile Settlement Analysis," *International Journal for Numerical and Analytical Methods in Geomechanics*, 37(6), 597-617.
- Lignos, D.G. and Krawinkler, H. (2011). "Deterioration modeling of steel components in support of collapse prediction of steel moment frames under earthquake loading," *J. Struct. Eng.*, 137(11), 1291-1302.
- Lignos, D.G., Krawinkler, H. and Whittaker, A.S. (2011). "Prediction and validation of sidesway collapse of two scale models of a 4-story steel moment frame." *Earthquake Eng. Struct. Dyn.*, 40(7), 807-825.
- Lillis, C., Lutnegger, A. J., Adams, M. (2004) "Performance of a Group of GeoPier Elements Loaded in Compression Compared to Single GeoPier Elements and Unreinforced Soil," *Report No. UUCVEEN 04-12*, University of Utah, Salt Lake City, UT, pp. 257.
- Lipster, R.S. and Shiryaev, A.N. (2001). *Statistics of Random Processes II: Applications*, 2<sup>nd</sup> Ed., Springer-Verlag, Berlin.
- McConville, F.X. (2008). "Functions for Easier Curve Fitting," *Chemical Engineering*, Access Intelligence, LLC, 48-51.

- McKenna, F., Scott, M.H., and Fenves, G.L. (2010). "Nonlinear finite-element analysis software using objective composition," *Journal of Computing in Civil Engineering*, 24(1), 95-107.
- Marsland, A. and Powell, J.J.M. (1980). "Cyclic loading tests on 865 mm diameter plates of a stiff clay till," Swansea, Balkema Press, 837-847.
- Mabrouki, A., Benmeddour, D., Frank, R. and Mellas, M. (2010) "Numerical study of the bearing capacity for two interfering strip footings on sands," *Computers and Geotechnics*, 37(2010), 431-439.
- Martin, J.P. (2018). "A full-scale experimental investigation of the bearing performance of aggregate pier-supported shallow foundations", *M.S. thesis*, Oregon State University.
- Mayne, P.W., Poulos, H.G. (1999) "Approximate Displacement Influence Factors for Elastic Shallow Foundations," *Journal of Geotechnical and Geoenvironmental Engineering*, 125(6), 453-460.
- Meyerhof, G.G. (1951) "The Ultimate bearing Capacity of Foundations," *Geotechnique*, 2(4), 301-331.
- Meyerhof, G.G. (1963). "Some Recent Research on the Bearing Capacity of Foundations," *Canadian Geotechnical Journal*, 1(1), 16-26.
- Mitchell, J.K. (1981). "Soil Improvement--State-of-the-Art Report," Session 12, Proceedings of the Tenth International Conference on Soil Mechanics and Foundation Engineering, Stockholm, Vol. 4, 506-565.
- Najjar, S.S. (2005) "The Importance of Lower-Bound Capacities in Geotechnical Reliability Assessments," *Ph.D. Thesis*, University of Texas at Austin, 317 pp.
- Najjar, S.S., and Gilbert, R.B. (2009) "Importance of Lower-Bound Capacities in the Design of Deep Foundations," *Journal of Geotechnical and Geoenvironmental Engineering*, ASCE, 135(7), 890-900.
- NEHRP Consultants Joint Venture (2012) *Soil-Structure Interaction for Building Structures*, U.S. Dept. of Commerce, NIST GCR 12-917-21, 292 p.
- Nelson, R.B. (2006) *An Introduction to Copulas*, 2<sup>nd</sup> ed., Springer, New York, 269 p.
- Newton, V.C. (1975) "Ultimate Bearing Capacity of Shallow Footings on Plastic Silt," *M.S. Thesis*, Oregon State University, 49 p.
- Noorzaei, J., Viladkar, M.N. and Godbole, P.N. (1995). "Influence of strain hardening on soil-structure interaction of framed structures," *Comput. Struct.* 55(3), 789-795.
- OpenSees*, Version 2.5.0 [Computer software], Pacific Earthquake Engineering Research Center (PEER), Berkeley, CA.
- Orr, T.L. and Breysse, D. (2008). "Eurocode 7 and Reliability-based Design," *Reliability-based Design in Geotechnical Engineering: Computations and Applications* (Chapter 8), ed. K.K. Phoon, Taylor and Francis, 298-343.

- Paikowsky, S. G., Birgisson, B., McVay, M., Nguyen, T., Kuo, C., Baecher, G., Ayyub, B., Stenersen, K., O'Malley, K., Chernauskas, L., and O'Neill, M. (2004) "Load and Resistance Factor Design (LRFD) for Deep Foundations," *NCHRP Report 507*, Transportation Research Board of the National Academies, Washington, D.C., 126 pp.
- Paikowsky, S. and Tolosko, T. (1999) *Extrapolation of Pile Capacity from Non-Failed Load Tests*, McLean: FHWA.
- Peck, R.B., Hanson, W.E. and Thornburn, T.H. (1974). *Foundation Engineering*, 2<sup>nd</sup> ed., John Wiley & Sons, New York, NY.
- Phoon, K.K. (2003). "Practical Guidelines for Reliability-Based Design Calibration," *Paper presented at Session TC 23 (1) "Advances in Geotechnical Limit State Design"*, 12th Asian Regional Conference on SMGE, August 7-8, 2003, Singapore.
- Phoon, K.K. (2008) "Numerical Recipes for Reliability Analysis – A Primer," *Reliability-Based Design in Geotechnical Engineering: Computations and Applications*, Taylor and Francis, London, 1-75.
- Phoon, K.K. and Kulhawy, F.H. (1999a). "Characterization of geotechnical variability," *Can. Geotech. J.* 36(4), 612-624.
- Phoon, K.K. and Kulhawy, F.H. (1999b). "Evaluation of geotechnical property variability," *Can. Geotech. J.* 36(4), 625-639.
- Phoon, K.K., and Kulhawy, F.H. (2008) "Serviceability Limit State Reliability-Based Design," *Reliability-Based Design in Geotechnical Engineering: Computations and Applications*, Taylor and Francis, London, 344-384.
- Phoon, K.K., Kulhawy, F.H. and Grigoriu, M.D. (1995). "Reliability-based design of foundations for transmission line structures," *Electric Power Research Institute*, Palo Alto, Report TR-1005000.
- Phoon, K.K., Kulhawy, F.H. and Grigoriu, M.D. (2003). "Multiple resistance factor design for shallow transmission line structure foundations," *J. Geotech. Geoenviron. Eng.*, 129(9), 807-818.
- Phoon, K.K., Quek, S.T. and An, P. (2003). "Identification of statistically homogeneous soil layers using modified Bartlett statistics," *J. Geotech. Geoenviron. Eng.*, 129(7), 649-659.
- Prandtl, L. (1920) "On the penetrating strengths (hardness) of plastic construction materials and the strength of cutting edges" (translated), *Zeit. angew. Math Mech.*, 1(1), 15-20.
- Priebe, H.J. (1976) "Abschätzung des Setzungsverhaltens eins durch Stopfuerdichtung verbesserten Baugrundes," *Die Bautechnik*, Vol. 53, H.5, Germany.
- R Code Team, R: A language and environment for statistical computing, [Computer software, Version 3.3], R Foundation for Statistical Computing, Vienna, Austria, URL: <http://R-project.org/>.

- Raychowdhury, P. (2008). "Nonlinear Winkler-based shallow foundation model for performance assessment of seismically loaded structures," Ph.D. thesis, Univ. of California, San Diego.
- Raychowdhury, P. and Hutchinson, T.C. (2009). "Performance evaluation of a nonlinear Winkler-based shallow foundation model using centrifuge test results," *Earthquake Engng. Struct. Dyn.*, 38(5), 679-698.
- Reece, L.C. (1984). *Handbook on Design of Piles and Drilled Shafts Under Lateral Load*, Federal Highway Administration, Report No. FHWA-IF-99-025.
- Ribeiro, F.L., Barbosa, A.R., and Neves, L.C. (2014). "Applications of reliability-based robustness assessment of steel moment resisting frames structures under post-mainshock cascading events," *J. Struct. Eng.* 140, Special Issue: Computational Simulation in Structural Engineering, A4014008, DOI: 10.1061/(ASCE)ST.1943-541X.0000939.
- Ribeiro, F.L., Barbosa, A.R., Scott, M.H., and Neves, L.C. (2015). "Deterioration modeling of steel moment resisting frames using finite-length plastic hinge force-based beam-column elements," *J. Struct. Eng.*, 141(2), 04014112.
- Roberts, L.A. and Misra, A. (2010). "LRFD of shallow foundations at the service limit state: Assessment and management of risk for engineered systems and geohazards," *Georisk*, 4(1), 13–21.
- Schlather, M., Malinowski, A., Oesting, M., Boecker, D., Strokorb, K., Engelke, S., Martini, J., Ballani, F., Moreva, O., Berreth, C., Menck, P., Gross, S., Ober, U., Burmeister, K., Manitz, J., Ribeiro, P., Singleton, R., Pfaff, B., and R Core Team (2016). "RandomFields," R Package [Computer software], URL: <http://ms.math.uni-mannheim.de/de/publications/software>.
- Scott, B., Kim, B. J., and Salgado, R. (2003). "Assessment of Current Load Factors for Use in Geotechnical Load and Resistance Factor Design," *Journal of Geotechnical and Geoenvironmental Engineering*, ASCE, Vol. 129, No. 4, pp. 287-295.
- Sehn, A.L., and Blackburn, J.T. (2008). "Predicting Performance of Aggregate Piers," *23<sup>rd</sup> Central Pennsylvania Geotechnical Conference*, Hershey, Pennsylvania, May 28-30, 2008.
- Sivakumar Babu, G.L., Srivastava, A. and Murthy, D.S.N. (2006). "Reliability analysis of the bearing capacity of a shallow foundation resting on cohesive soil," *Can. Geotech. J.* 40(1), 1-15. doi:10.1139/t02-090.
- Skempton, A.W. (1951). "The bearing capacity of clays," *Proc. Building Research Congress*, Vol. 1, 180-189.
- Skempton, A.W. and MacDonald, D.H. (1956). "Allowable Settlement of Buildings," *Ins. Civ. Eng.*, III, Vol. 5, 727-768.
- Son, M. and Cording, E. (2005). "Estimation of building damage due to excavation-induced ground movements." *J. Geotech. Geoenviron. Eng.*, 131(2), 162-177.

- Son, M. and Cording, E. (2011). "Responses of buildings with different structural types to excavation-induced ground settlements," *J. Geotech. Geoenviron. Eng.*, 137(4), 323-333.
- Stavridis, L.T. (2002). "Simplified analysis of layered soil-structure interaction," *J. Struct. Eng.*, 128(2), 224-230.
- Stewart, J.P., Fenves, G.L., and Seed, R.B. (1999). "Seismic soil-structure interaction in buildings I: Analytical methods," *J. Geotech. Geoenviron. Eng.*, 125(1), 26-37.
- Strahler, A.W. (2012). "Bearing Capacity and Immediate Settlement of Shallow Foundation on Clay," *M.S. Thesis*, Oregon State University, 214 p.
- Strahler, A.W. and Stuedlein, A.W. (2013). "Characterization of Model Uncertainty in Immediate Settlement Calculations for Spread Footings on Clay," *Proceedings, 18<sup>th</sup> International Conference on Soil Mechanics and Geotechnical Engineering*, Paris, 2014, 4 p.
- Strahler, A.W. and Stuedlein, A.W. (2014). "Accuracy, Uncertainty, and Reliability of the Bearing Capacity Equation for Shallow Foundations on Saturated Clay," *Geo-Characterization and Modeling for Sustainability*, GeoCongress 2014, GSP No. TBD, ASCE, Atlanta, GA, February 23-26, 2014, 12 p.
- Stuart, J.G. (1967) "Interference between foundations with special reference to surface footings in sand," *Geotechnique*, 12(1), 15-23.
- Stuedlein, A.W. (2008) "Bearing Capacity and Displacement of Spread Footings on Aggregate Pier Reinforced Clay," *Ph.D. Thesis*, University of Washington, 585 p.
- Stuedlein, A.W. and Bong, T. (2017). "Effect of spatial variability on static and liquefaction-induced differential settlements," *Geo-Risk 2017: Keynote Lectures*, GSP No. 282, 31–51.
- Stuedlein, A.W. and Holtz, R.D. (2010). "Undrained Displacement Behavior of Spread Footings in Clay," *The Art of Foundation Engineering Practice*, Honoring Clyde N. Baker, Jr., P.E., S.E., ASCE, 653-669.
- Stuedlein, A.W., and Holtz, R.D. (2012) "Analysis of Footing Load Tests on Aggregate Pier Reinforced Clay," *Journal of Geotechnical and Geoenvironmental Engineering*, ASCE, 138(9), 1091-1103.
- Stuedlein, A.W. and Holtz, R.D. (2013) "Bearing Capacity of Spread Footings on Aggregate Pier Reinforced Clay," *Journal of Geotechnical and Geoenvironmental Engineering*, ASCE, 139(1), 49-58.
- Stuedlein, A.W. and Holtz, R.D. (2014) "Displacement of Spread Footings on Aggregate Pier Reinforced Clay," *Journal of Geotechnical and Geoenvironmental Engineering*, ASCE, 140(1), 36-45.
- Stuedlein, A.W., Huffman, J.C. and Reddy, S.C. (2014) "Ultimate limit state reliability-based design of spread footings on aggregate pier-reinforced clay," *Proceedings of the Institution of Civil Engineers - Ground Improvement*, 167(4), 291-300.

- Stuedlein, A.W., Kramer, S.L., Arduino, P. and Holtz, R.D. (2012). "Geotechnical characterization and random field modeling of desiccated clay," *J. Geotech. Geoenviron. Eng.*, 138(11), 1301-1313.
- Stuedlein, A.W. and Reddy, S.C. (2013). "Factors Affecting the Reliability of Augered Cast-In-Place Piles in Granular Soils at the Serviceability Limit State," *Journal of the Deep Foundations Institute*, 7(2), 46-57.
- Stuedlein, A.W. and Uzielli, M. (2014). "Serviceability Limit State Design for Uplift of Helical Anchors in Clay," *Geomechanics and Geoengineering*, 9(3), 173-186.
- Stuedlein, A.W., Neely, W. and Gurtowski, T. (2012). "Reliability-Based Design of Augered Cast-in-Place Piles in Granular Soils," *J. Geotech. Geoenviron. Eng.*, 138(6), 709-717.
- Schwarz, G. (1978). "Estimating the Dimension of a Model," *The Annals of Statistics*, 6(2), 461-464.
- Tand, K.E., Funegard, E.G. and Briaud, J.L. (1986). "Bearing Capacity of Footings on Clay CPT Method," *Use of In Situ Tests in Geotechnical Engineering*, ASCE, 1017-1033.
- Tang, X.S., Li, D.Q., Rong, G., Phoon, K.K., Zhou, C.B. (2013). "Impact of Copula Selection on Geotechnical Reliability Under Incomplete Probability Information," *Computers and Geotechnics*, 49, 264-278.
- Tang, X.S., Li, D.Q., Zhou, C.B., Phoon, K.K., Zhou, C.B. (2015). "Copulas-based Approaches for Evaluating Slope Reliability Under Incomplete Probability Information," *Structural Safety*, 50, 90-99.
- Terzaghi, K. (1943). *Theoretical Soil Mechanics*, John Wiley and Sons, Inc., New York.
- Terzaghi, K., Peck, R. and Mesri, G. (1996). *Soil Mechanics in Engineering Practice*, 3<sup>rd</sup> ed., John Wiley and Sons, Inc., New York.
- UBC (1994). "Structural Engineering Design Provisions," *Uniform Building Code*, Vol. 2, International Conference of Building Officials.
- U.S. Army Corps of Engineers (1997). "Engineering and Design, Introduction to probability and reliability methods for use in geotechnical engineering," *Engr. Tech. Letter No. 1110-2-547*, Dept. of the Army, Washington.
- Uzielli, M., Lacasse, S., Nadim, F. and Phoon, K.K. (2007). "Soil variability analysis for geotechnical practice," In T.S. Tan, K.K. Phoon, D.W. Hight and S. Leroueil (eds.), *Proceedings of the 2<sup>nd</sup> Int. Workshop on Characterization and Engineering Properties of Natural Soils, Vol. 3*, (IS-Singapore), Taylor and Francis Group, London, 1653 – 1752, ISBN 978-0-415-42691-6.
- Uzielli, M. and Mayne, P., (2011) "Serviceability Limit State CPT-based Design for Vertically Loaded Shallow Footings on Sand," *Geomechanics and Geoengineering: An International Journal*, Taylor and Francis, 6(2), 91-107.

- Uzielli, M. and Mayne, P., (2012) “Load–Displacement Uncertainty of Vertically Loaded Shallow Footings on Sands and Effects on Probabilistic Settlement,” *Georisk*, Vol. 6, No. 1, pp. 50–69.
- Van Impe, W., and De Beer, E. (1983) “Improvement of Settlement Behavior of Soft Layers by Means of Stone Columns,” *Improvement of Ground*, Proceedings of The Eighth European Conference on Soil Mechanics and Foundations Engineering, Rathmayer, H.G., and Saari, K.H.O., eds., Balkema, Rotterdam, The Netherlands, 309-312.
- Vanmarcke, E. H. (1977). “Probabilistic modeling of soil profiles,” *J. Geotech. Engrg. Div.*, 103(11), 1227–1246.
- Vanmarcke, E. H. (1983). *Random fields: Analysis and synthesis*, MIT, Cambridge, MA.
- Vesić, A.S. (1972) “Expansion of cavities in infinite soil mass,” *Journal of the Soil Mechanics and Foundation Division*, 98(SM3), 265-290.
- Vesić, A.S. (1973) “Analysis of ultimate loads of shallow foundations,” *Journal of the Soil Mechanics and Foundation Division*, 99(SM1), 45-73.
- Vesić, A.S. (1974) “Bearing capacity of shallow foundations (Ch. 3)”, *Foundation Engineering Handbook*, 1<sup>st</sup> ed., 121-147, Wingkerton, H.F. and Fang, H.-Y. (ed.), Van Nostrand Reinhold, New York.
- Wallays, M. (1981). Personal communication with R.D. Barksdale, as documented in Barksdale, R. D., and Bachus, R. C. (1983).
- Wahls, H. E. (1981). "Tolerable settlement of buildings," *J. Geotech. Engrg. Div.*, 107(11), 1489-1504.
- Wang, M.C. and Jao, M. (2002) “Behavior of interacting parallel strip footing,” *Electronic Journal of Geotechnical Engineering*, 7(A).
- Wang, Y. (2011). “Reliability-based Design of Spread Foundations by Monte Carlo Simulations,” *Geotechnique*, 61(8), 677-685.
- White, D.J., Pham, H.T., and Hoevelkamp, K.K., (2007) “Support Mechanisms of Rammed Aggregate Piers. I - Experimental Results,” *J. Geotech. Geoenviron. Eng.*, 133(12), 1503-1511.
- Wong, H.Y. (1975). “Vibroflotation – Its effect on weak cohesive soils,” *Civil Engineering* (London), No. 824, 44-67.
- Wroth, C.P. and Wood, D.M., (1978). “The Correlation of Index Properties with Some Basic Engineering Properties of Soils,” *Canadian Geotechnical Journal*, 15(2), 137-145.
- Wu, X.Z. (2013). “Trivariate Analysis of Soil Ranking-Related Characteristics and its Application to Probabilistic Stability Assessments in Geotechnical Engineering Problems,” *Soils and Foundations*, 53(4), 540-556.
- Wu, X.Z. (2015). “Assessing the Correlation Performance Functions of an Engineering System via Probabilistic Analysis,” *Structural Safety*, 52, 10-19.
- Zhang, L.M., Ng, A.M.Y., (2005) “Probabilistic Limiting Tolerable Displacements for Serviceability Limit State Design of Foundations,” *Geotechnique*, 55(2), 151-161.



## APPENDIX A: CHAPTER 4 SUPPLEMENTAL DATA

**Note:** The supplemental data contained herein is also provided as Appendix S1 accompanying the journal publication, and is available online in the ASCE library ([www.ascelibrary.com](http://www.ascelibrary.com)).

### Simulation of $k_3$ - $k_4$ Pairs using the Gumbel Copula and Comparison to Observed Pairs

*EXCEL spreadsheet calculations (only) adapted from:*

Aas, K. (2004) "Modelling the dependence structure of financial assets: A survey of four copulas," Note No. SAMBA/22/04, Norwegian Computing Center, Oslo, Norway, 22 pp.

*Actual reliability simulations used Matlab or R computer programs.  
Provided for illustration purposes only.*

#### Procedure:

1. Determine correlation between parameters in the sample set (a Kendall's tau rank correlation of 0.43 was estimated for the  $k_3$ - $k_4$  pairs for the dataset).
2. Estimate the copula coefficient for the given copula based on Kendall's tau (the copula coefficient is 'Gumbel\_Delta' in this spreadsheet).
3. Calculate/simulate values of the positive stable variate based on the parameters indicated below (a Gumbel Copula-specific calculation).
4. Simulate uniformly distributed correlated ranked pairs,  $u_3$  and  $u_4$ , based on the copula selected.
5. Calculate the simulated  $k_3$ - $k_4$  pairs using the  $u_3$ - $u_4$  pairs and the known marginal distributions of  $k_3$  and  $k_4$ .

#### Variables and Calculations for Excel (Note: variable X coded in Visual Basic)

<b>Kendall's Tau =</b>	calculated outside of Excel
<b>Gumbel_Delta =</b>	$1/(1-\text{Kendall's\_Tau})$
<b>Gumbel_Gamma =</b>	$(\text{COS}(\text{PI}()/2*\text{Gumbel\_Delta}))^{\text{Gumbel\_Delta}}$

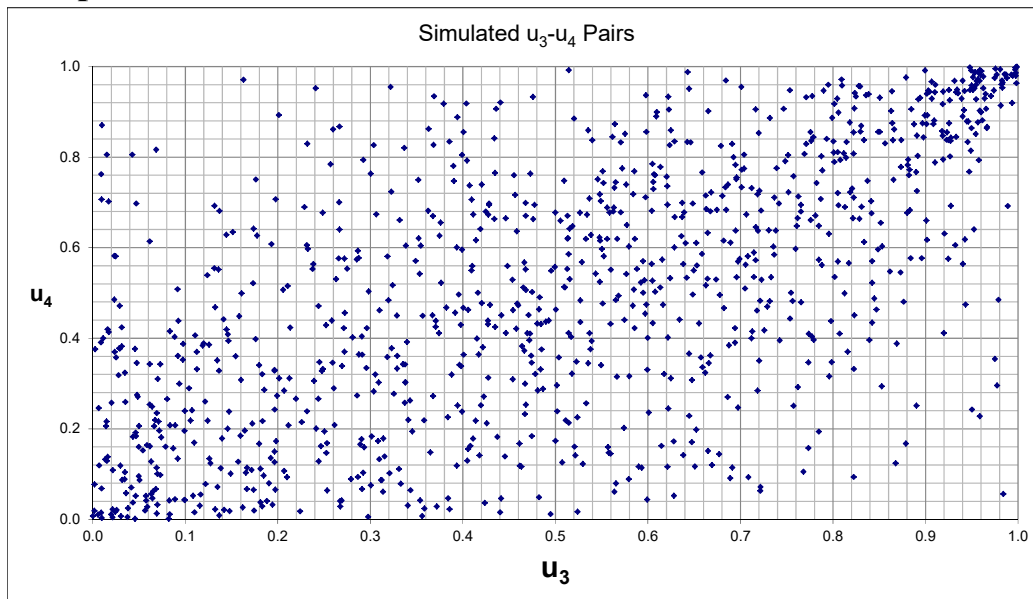
```

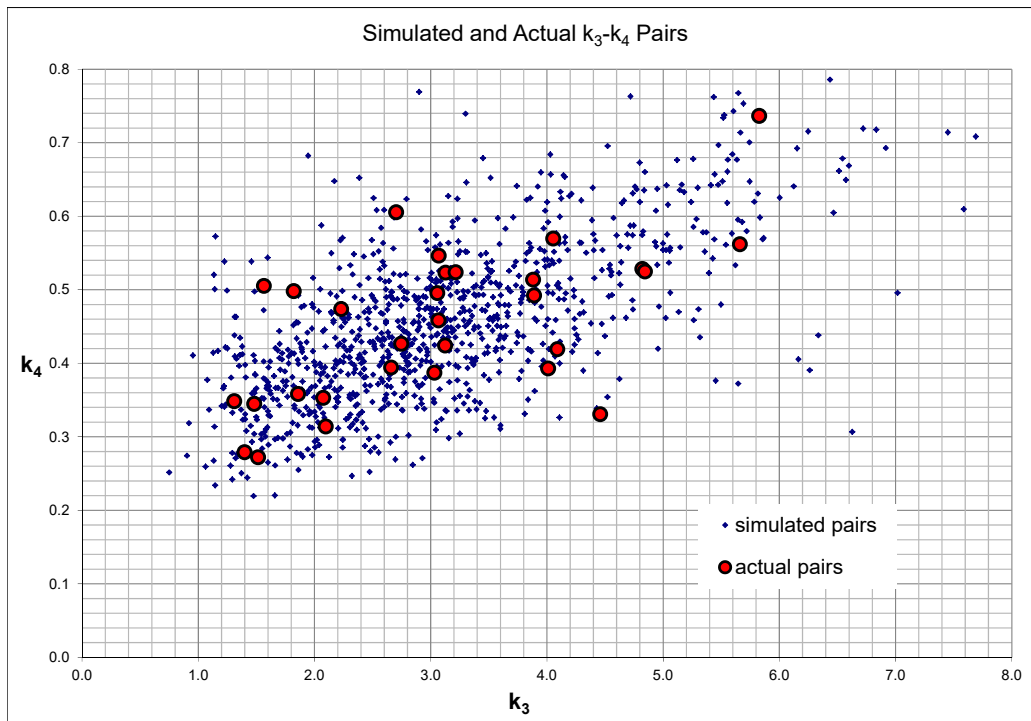
X = StableRV(Alpha,Beta,Gumbel_Gamma,0)
Alpha = 1/Gumbel_Gamma
Beta = 1.0
Big_Theta = (Rnd() - 0.5) * Pi_Const
W = -Log(1 - Rnd())
Theta_0 = Atn(Beta * Tan(Pi_Const * Alpha / 2)) / Alpha
If Alpha <> 1 Then
Z = (Sin(Alpha * (Theta_0 + Big_Theta))) / (Cos(Alpha * Theta_0) * Cos(Big_Theta)) ^ (1 / Alpha)
Z = Z * (Cos(Alpha * Theta_0 + (Alpha - 1) * Big_Theta) / W) ^ ((1 - Alpha) / Alpha)
X = Gamma * Z + Delta
Else
Z = (2 / Pi_Const) * ((Pi_Const / 2 + Beta * Big_Theta) * Tan(Big_Theta) - Beta * Log((Pi_Const / 2 + Beta * Big_Theta) * Cos(Big_Theta))) / (Pi_Const / 2 + Beta * Big_Theta)
X = Gamma * Z + (Delta + Beta * (2 / Pi_Const) * Gamma * Log(Gamma))
End If
StableRV = X

u3 = EXP(-((-LN(RAND()/X))^(1/Gumbel_Delta)))
u4 = EXP(-((-LN(RAND()/X))^(1/Gumbel_Delta)))
Simulated k3 = LOGNORM.INV(u3,k3_Lognorm.Mean,k3_Lognorm.St.dev)
Simulated k4 = LOGNORM.INV(u4,k4_Lognorm.Mean,k4_Lognorm.St.dev)
Correlation Coeff. = CORREL(u3:u4)

```

### Sample Results (Spreadsheet Print-out Follows)





	A	B	C	D	E	F	G	H	I	J
1	<b>Gumbel Copula: Simulation of Correlated Parameters and Comparison to <math>k_3</math>-<math>k_4</math> Pairs.</b>									
2	<b>Spreadsheet adapted from:</b>									
3	Aas, K. (2004) "Modelling the dependence structure of financial assets: A survey of four copulas,"									
4	Note No. SAMBA/22/04, Norwegian Computing Center, Oslo, Norway, 22 pp.									
5	<b>For illustration purposes only.</b>									
6										
7						$k_3$	$k_4$			
8	<b>Gumbel_Delta</b>	1.755		Lognorm. Mean =		1.05	-0.82			
9	<b>Gumbel_Gamma</b>	0.4389		Lognorm. St. Dev. =		0.39	0.23			
10										
11										
12				<b>Kendall's Tau</b>		<b>Gumbel_Delta</b>			<b>Correlation Coeff</b>	
13				0.4302		1.755			0.62	
14										
15										
16										
17		Gumbel-specific Positive Stable Variate		Simulated Ranked Pairs			Simulated		Actual	
18	<b>Index</b>	<b>X</b>	$u_3$	$u_4$		$k_3$	$k_4$		$k_3$	$k_4$
19	1	0.1542	0.1090	0.0014		1.7654	0.2222		3.0672	0.5466
20	2	2.0654	0.5784	0.5664		3.0906	0.4591		3.1264	0.5234
21	3	8.0527	0.8059	0.6224		4.0105	0.4747		1.5635	0.5056
22	4	1.9601	0.3244	0.6934		2.3928	0.4962		5.8254	0.7368
23	5	3.3174	0.7341	0.8590		3.6539	0.5658		4.4569	0.3309
24	6	0.2428	0.0165	0.0068		1.2406	0.2506		3.0553	0.4958
25	7	2.9151	0.6254	0.6835		3.2417	0.4931		4.0536	0.5699
26	8	0.8152	0.1528	0.2906		1.9146	0.3892		5.6592	0.5623
27	9	0.7952	0.5915	0.1915		3.1315	0.3615		3.8883	0.4924
28	10	2.1119	0.2721	0.7694		2.2552	0.5233		4.8196	0.5286
29	11	0.2434	0.1563	0.8036		1.9258	0.5377		4.0101	0.3933
30	12	24.4140	0.7762	0.8917		3.8510	0.5870		1.5125	0.2723
31	13	5.1103	0.9296	0.9665		5.0934	0.6731		2.0741	0.3532
32	14	5.9299	0.6766	0.6961		3.4226	0.4971		2.2280	0.4741
33	15	1.5411	0.1992	0.4634		2.0546	0.4326		1.3975	0.2794
34	16	2.3292	0.7133	0.7101		3.5659	0.5018		2.7017	0.6057
35	17	2.6900	0.4196	0.6535		2.6417	0.4838		3.0315	0.3874
36	18	4.6789	0.7540	0.7813		3.7438	0.5281		3.1232	0.4243
37	19	11.9425	0.6839	0.9085		3.4502	0.6000		2.0959	0.3144
38	20	0.4353	0.3990	0.2163		2.5874	0.3689		4.0887	0.4194
39	21	2.3256	0.4713	0.8351		2.7806	0.5527		1.8567	0.3586
40	22	0.6677	0.2266	0.7378		2.1320	0.5114		1.4791	0.3449
41	23	0.6930	0.0590	0.4006		1.5503	0.4170		2.6588	0.3946
42	24	3.5526	0.4562	0.4232		2.7395	0.4226		1.3086	0.3487
43	25	1.8169	0.8259	0.6978		4.1304	0.4977		3.2141	0.5239
44	26	1.0294	0.3961	0.6862		2.5798	0.4939		3.0652	0.4585
45	27	1.0685	0.4180	0.5033		2.6375	0.4427		3.8798	0.5139
46	28	0.5712	0.0987	0.2337		1.7262	0.3738		4.8417	0.5251
47	29	0.2195	0.0082	0.1130		1.1169	0.3345		2.7458	0.4268
48	30	10.1439	0.8042	0.8845		4.0005	0.5819		1.8199	0.4984
49	31	6.8844	0.7395	0.6498		3.6777	0.4827			
50	32	1.3645	0.4979	0.8362		2.8543	0.5533			
51	33	48.0360	0.8989	0.9628		4.7140	0.6658			
52	34	17.2683	0.8215	0.9491		4.1029	0.6436			
53	35	47.5496	0.8928	0.8459		4.6516	0.5584			
54	36	0.1694	0.0911	0.0263		1.6963	0.2830			

	A	B	C	D	E	F	G	H	I	J
55	37	0.5015	0.0356	0.3529		1.4110	0.4051			
56	38	49.4971	0.8278	0.8290		4.1425	0.5497			
57	39	1.8820	0.3765	0.7234		2.5284	0.5063			
58	40	8.8366	0.8787	0.8300		4.5203	0.5502			
59	41	39.8824	0.8306	0.8838		4.1602	0.5813			
60	42	0.1599	0.0512	0.0633		1.5087	0.3110			
61	43	2.7033	0.4188	0.4921		2.6395	0.4398			
62	44	2.6980	0.8746	0.4101		4.4853	0.4193			
63	45	0.1665	0.4178	0.3349		2.6368	0.4006			
64	46	0.8998	0.7600	0.4668		3.7717	0.4334			
65	47	0.5582	0.1533	0.5100		1.9163	0.4444			
66	48	0.9874	0.2507	0.4291		2.1981	0.4240			
67	49	0.1724	0.0766	0.1718		1.6344	0.3554			
68	50	0.7764	0.6654	0.7701		3.3814	0.5236			
69	51	1.9521	0.6468	0.7022		3.3151	0.4991			
70	52	0.4805	0.0899	0.5694		1.6912	0.4599			
71	53	1.1693	0.8345	0.7212		4.1856	0.5056			
72	54	5.0519	0.6151	0.6304		3.2076	0.4769			
73	55	0.1966	0.5722	0.6718		3.0716	0.4894			
74	56	0.2598	0.0417	0.0780		1.4515	0.3189			
75	57	0.9973	0.0974	0.4551		1.7213	0.4305			
76	58	0.2703	0.2696	0.0847		2.2487	0.3221			
77	59	0.1839	0.4297	0.8129		2.6685	0.5419			
78	60	0.2008	0.6278	0.0370		3.2498	0.2931			
79	61	0.2518	0.0484	0.4756		1.4924	0.4356			
80	62	15.8704	0.7984	0.6720		3.9684	0.4895			
81	63	0.2647	0.6264	0.1882		3.2450	0.3605			
82	64	1.1042	0.4741	0.6099		2.7883	0.4711			
83	65	0.3934	0.0763	0.1989		1.6331	0.3638			
84	66	29.7281	0.8962	0.9435		4.6861	0.6359			
85	67	1.1442	0.2773	0.4289		2.2691	0.4240			
86	68	0.3025	0.1481	0.0527		1.8996	0.3045			
87	69	0.5824	0.5620	0.3077		3.0406	0.3936			
88	70	0.4564	0.1241	0.6772		1.8194	0.4911			
89	71	1.5966	0.8050	0.4397		4.0051	0.4267			
90	72	3.4439	0.8636	0.5409		4.3949	0.4524			
91	73	238.0483	0.9502	0.9371		5.4511	0.6281			
92	74	1.9682	0.5849	0.6150		3.1107	0.4725			
93	75	0.3058	0.2940	0.6978		2.3133	0.4977			
94	76	13.3872	0.9227	0.8581		4.9950	0.5653			
95	77	2.5352	0.5987	0.7127		3.1546	0.5026			
96	78	0.5060	0.1844	0.5283		2.0114	0.4491			
97	79	0.6065	0.3131	0.1649		2.3634	0.3532			
98	80	0.2119	0.5752	0.2378		3.0807	0.3750			
99	81	0.6046	0.3687	0.2774		2.5081	0.3857			
100	82	12.8055	0.6898	0.7772		3.4728	0.5265			
101	83	0.1345	0.0544	0.1392		1.5262	0.3444			
102	84	3.7041	0.7505	0.6604		3.7274	0.4859			
103	85	0.2194	0.6446	0.4445		3.3074	0.4279			
104	86	0.5784	0.1141	0.1192		1.7841	0.3369			
105	87	0.9775	0.4124	0.4324		2.6226	0.4249			
106	88	0.5394	0.4443	0.3116		2.7074	0.3946			
107	89	6.2733	0.5937	0.8274		3.1384	0.5489			
108	90	0.5017	0.3299	0.2570		2.4071	0.3803			
109	91	1.9487	0.3972	0.2339		2.5826	0.3739			

	A	B	C	D	E	F	G	H	I	J
110	92	0.5394	0.3034	0.3524		2.3379	0.4050			
111	93	0.3109	0.2513	0.0597		2.1995	0.3089			
112	94	0.2826	0.0385	0.2955		1.4308	0.3905			
113	95	0.4149	0.2851	0.1294		2.2899	0.3408			
114	96	13.6261	0.6838	0.8089		3.4495	0.5401			
115	97	0.2405	0.0696	0.3190		1.6026	0.3965			
116	98	2.7447	0.7803	0.4024		3.8720	0.4174			
117	99	0.6670	0.4485	0.2846		2.7187	0.3876			
118	100	0.9184	0.8057	0.7233		4.0094	0.5063			
119	101	1.7105	0.4097	0.7660		2.6154	0.5220			
120	102	4.8345	0.5399	0.7659		2.9748	0.5220			
121	103	0.2796	0.2612	0.3965		2.2263	0.4160			
122	104	14.6183	0.7345	0.8142		3.6557	0.5425			
123	105	2.4336	0.6130	0.4555		3.2008	0.4306			
124	106	1.0235	0.2807	0.3303		2.2783	0.3994			
125	107	0.6167	0.0698	0.1712		1.6037	0.3552			
126	108	5.5795	0.3236	0.7488		2.3908	0.5155			
127	109	0.2460	0.5530	0.1569		3.0133	0.3505			
128	110	0.6120	0.4998	0.1939		2.8596	0.3623			
129	111	4.7780	0.6421	0.6796		3.2987	0.4918			
130	112	0.2919	0.0196	0.1442		1.2755	0.3461			
131	113	7.0198	0.7735	0.9094		3.8377	0.6008			
132	114	0.1774	0.3269	0.1226		2.3994	0.3382			
133	115	4.2168	0.8602	0.5337		4.3685	0.4505			
134	116	0.5751	0.3890	0.6223		2.5610	0.4746			
135	117	2.5583	0.3614	0.7019		2.4891	0.4990			
136	118	7.9217	0.5617	0.7966		3.0395	0.5346			
137	119	0.4686	0.2903	0.1143		2.3036	0.3350			
138	120	0.6562	0.3112	0.3986		2.3584	0.4165			
139	121	2.2567	0.5452	0.6509		2.9904	0.4830			
140	122	1.0909	0.5217	0.8318		2.9218	0.5510			
141	123	12.4730	0.7773	0.8078		3.8569	0.5396			
142	124	4.0289	0.7027	0.6641		3.5233	0.4870			
143	125	0.5784	0.4756	0.0902		2.7923	0.3247			
144	126	13.1242	0.6800	0.9359		3.4354	0.6268			
145	127	0.8401	0.7427	0.2880		3.6919	0.3885			
146	128	3.6786	0.6757	0.6840		3.4193	0.4932			
147	129	1.8106	0.2611	0.6060		2.2260	0.4700			
148	130	0.3775	0.2972	0.1624		2.3218	0.3523			
149	131	1.1901	0.5503	0.8725		3.0053	0.5740			
150	132	0.2995	0.0859	0.1098		1.6745	0.3332			
151	133	0.9242	0.1281	0.2651		1.8333	0.3825			
152	134	1.5972	0.7947	0.7033		3.9480	0.4995			
153	135	0.5845	0.4925	0.4878		2.8392	0.4387			
154	136	1.0115	0.3933	0.3608		2.5724	0.4071			
155	137	1.3243	0.5780	0.5377		3.0894	0.4515			
156	138	1.4954	0.3926	0.4049		2.5705	0.4180			
157	139	0.7885	0.4485	0.2560		2.7187	0.3800			
158	140	8.4808	0.8137	0.7462		4.0561	0.5145			
159	141	0.2974	0.2385	0.0754		2.1649	0.3175			
160	142	3.1249	0.7686	0.8104		3.8134	0.5408			
161	143	1.7929	0.8544	0.5326		4.3246	0.4502			
162	144	0.8381	0.6668	0.4723		3.3863	0.4348			
163	145	0.5082	0.2985	0.3926		2.3252	0.4150			
164	146	180.2991	0.9491	0.9721		5.4295	0.6857			

	A	B	C	D	E	F	G	H	I	J
165	147	372.3695	0.9424	0.9822		5.3013	0.7160			
166	148	7.0554	0.6560	0.7170		3.3474	0.5041			
167	149	2.1234	0.4787	0.7157		2.8010	0.5037			
168	150	0.2907	0.3657	0.2835		2.5004	0.3873			
169	151	2.5453	0.4534	0.5141		2.7320	0.4454			
170	152	36.1430	0.9376	0.8707		5.2178	0.5728			
171	153	1.8117	0.7528	0.6980		3.7382	0.4978			
172	154	75.9925	0.9210	0.8983		4.9722	0.5919			
173	155	7.2398	0.9818	0.8746		6.4911	0.5753			
174	156	0.2653	0.1861	0.3134		2.0165	0.3951			
175	157	0.3085	0.2074	0.1413		2.0780	0.3451			
176	158	0.2147	0.0843	0.1940		1.6680	0.3623			
177	159	0.3152	0.2153	0.0420		2.1005	0.2970			
178	160	2.1165	0.5674	0.7295		3.0568	0.5085			
179	161	1.1239	0.7103	0.3008		3.5539	0.3919			
180	162	8.6359	0.7627	0.5884		3.7849	0.4651			
181	163	1.9890	0.5313	0.7198		2.9496	0.5051			
182	164	0.7557	0.2480	0.5419		2.1907	0.4526			
183	165	5.8254	0.9228	0.7848		4.9970	0.5296			
184	166	1.3846	0.3076	0.3005		2.3489	0.3918			
185	167	0.2132	0.0071	0.0246		1.0939	0.2811			
186	168	0.3239	0.0434	0.1443		1.4623	0.3462			
187	169	0.5154	0.7742	0.2417		3.8410	0.3761			
188	170	4.9377	0.6819	0.8841		3.4423	0.5816			
189	171	17.5054	0.9301	0.7605		5.1009	0.5199			
190	172	0.5284	0.7267	0.1453		3.6219	0.3465			
191	173	0.2738	0.2535	0.3297		2.2054	0.3992			
192	174	7.7738	0.9519	0.8745		5.4876	0.5752			
193	175	3.8713	0.7970	0.7004		3.9608	0.4985			
194	176	1.0656	0.6079	0.1921		3.1840	0.3617			
195	177	55.8743	0.9823	0.9683		6.5211	0.6769			
196	178	0.5373	0.6310	0.3775		3.2608	0.4112			
197	179	0.1298	0.0145	0.0508		1.2157	0.3033			
198	180	0.1946	0.4464	0.0299		2.7132	0.2866			
199	181	0.7061	0.1540	0.3466		1.9185	0.4035			
200	182	0.1464	0.0024	0.0198		0.9451	0.2753			
201	183	10.0122	0.6252	0.9202		3.2411	0.6104			
202	184	3.8131	0.7692	0.7857		3.8163	0.5300			
203	185	0.3250	0.1945	0.0417		2.0411	0.2967			
204	186	2.8576	0.5246	0.6372		2.9302	0.4789			
205	187	1.6070	0.6378	0.5492		3.2838	0.4545			
206	188	0.3953	0.2046	0.2207		2.0701	0.3702			
207	189	445.8153	0.9985	0.9679		9.1757	0.6761			
208	190	3.0463	0.8769	0.8018		4.5053	0.5369			
209	191	0.2795	0.0869	0.4151		1.6787	0.4206			
210	192	0.4505	0.6951	0.4497		3.4932	0.4292			
211	193	1.8696	0.4222	0.4187		2.6484	0.4215			
212	194	0.3536	0.1914	0.0789		2.0319	0.3193			
213	195	0.1497	0.0486	0.0025		1.4933	0.2319			
214	196	19.4638	0.8034	0.9322		3.9963	0.6226			
215	197	0.4094	0.0946	0.2857		1.7103	0.3879			
216	198	0.9964	0.1170	0.4695		1.7944	0.4341			
217	199	1001.4591	0.9789	0.9908		6.3412	0.7598			
218	200	2.2596	0.7935	0.4170		3.9417	0.4210			
219	201	9.8128	0.6309	0.8746		3.2603	0.5753			

	A	B	C	D	E	F	G	H	I	J
220	202	9.1874	0.6645	0.9432		3.3780	0.6356			
221	203	1.5351	0.2564	0.3601		2.2132	0.4069			
222	204	30.7178	0.7952	0.7045		3.9508	0.4999			
223	205	1.8257	0.3303	0.4829		2.4082	0.4375			
224	206	6.0114	0.7987	0.8007		3.9698	0.5364			
225	207	2.6165	0.8608	0.6549		4.3735	0.4842			
226	208	0.8394	0.5360	0.8605		2.9634	0.5666			
227	209	0.4083	0.4659	0.3750		2.7659	0.4106			
228	210	4.8876	0.8086	0.7117		4.0259	0.5023			
229	211	62.0986	0.9406	0.9879		5.2696	0.7415			
230	212	81.7323	0.9057	0.8531		4.7876	0.5624			
231	213	2.0011	0.3592	0.6501		2.4834	0.4828			
232	214	0.7284	0.2551	0.9694		2.2099	0.6795			
233	215	1.0698	0.0818	0.3819		1.6574	0.4123			
234	216	3.3435	0.8652	0.6623		4.4076	0.4864			
235	217	0.7088	0.3155	0.3487		2.3697	0.4040			
236	218	0.2953	0.0497	0.1495		1.5001	0.3480			
237	219	1.6522	0.6733	0.1653		3.4104	0.3533			
238	220	0.6823	0.4383	0.4037		2.6913	0.4177			
239	221	12.6049	0.8651	0.8718		4.4068	0.5735			
240	222	0.6953	0.4379	0.1728		2.6905	0.3557			
241	223	4.3190	0.8854	0.8892		4.5806	0.5852			
242	224	2.2309	0.5750	0.8601		3.0800	0.5664			
243	225	0.5074	0.0713	0.2972		1.6105	0.3909			
244	226	76.0838	0.8379	0.9633		4.2081	0.6667			
245	227	0.3268	0.2235	0.4500		2.1235	0.4292			
246	228	0.3554	0.1123	0.0819		1.7773	0.3208			
247	229	1.6623	0.8875	0.6599		4.6007	0.4857			
248	230	1.7340	0.3628	0.3106		2.4929	0.3944			
249	231	2.3368	0.5143	0.4265		2.9007	0.4234			
250	232	7.0632	0.7800	0.5507		3.8706	0.4549			
251	233	11.3295	0.8143	0.8577		4.0592	0.5650			
252	234	0.5526	0.3154	0.2785		2.3694	0.3860			
253	235	0.1778	0.2428	0.6397		2.1766	0.4797			
254	236	0.2640	0.2820	0.1076		2.2815	0.3323			
255	237	0.6891	0.3010	0.4812		2.3316	0.4370			
256	238	0.2063	0.2030	0.3564		2.0656	0.4060			
257	239	94.5768	0.9605	0.9610		5.6918	0.6625			
258	240	0.7113	0.2770	0.0388		2.2685	0.2945			
259	241	1.0643	0.3621	0.7265		2.4910	0.5074			
260	242	7.9763	0.8781	0.7348		4.5157	0.5104			
261	243	5.6619	0.8657	0.6694		4.4115	0.4886			
262	244	3.5314	0.7031	0.5731		3.5247	0.4609			
263	245	0.2068	0.6932	0.0240		3.4857	0.2804			
264	246	0.1980	0.3360	0.3151		2.4229	0.3955			
265	247	6.8912	0.7026	0.6324		3.5229	0.4775			
266	248	0.1725	0.0013	0.1427		0.8794	0.3456			
267	249	0.3196	0.0740	0.4150		1.6229	0.4205			
268	250	2.8380	0.7647	0.4790		3.7946	0.4365			
269	251	0.7240	0.2528	0.2967		2.2035	0.3908			
270	252	1.9780	0.7394	0.6325		3.6775	0.4776			
271	253	1.6771	0.4817	0.4997		2.8092	0.4417			
272	254	0.6238	0.4408	0.4476		2.6980	0.4286			
273	255	0.5073	0.2439	0.4180		2.1796	0.4213			
274	256	0.8051	0.2713	0.3863		2.2533	0.4134			



	A	B	C	D	E	F	G	H	I	J
275	257	6.3880	0.5953	0.5667		3.1437	0.4592			
276	258	0.2480	0.5292	0.2081		2.9434	0.3665			
277	259	1.0893	0.5590	0.8780		3.0313	0.5775			
278	260	2.3682	0.6127	0.8179		3.1999	0.5443			
279	261	4.0960	0.8658	0.8066		4.4128	0.5391			
280	262	0.5430	0.1131	0.2718		1.7805	0.3843			
281	263	1.4441	0.3079	0.6659		2.3498	0.4875			
282	264	2.5270	0.4950	0.5830		2.8462	0.4636			
283	265	218.9346	0.9563	0.9516		5.5881	0.6471			
284	266	31.0390	0.7997	0.9188		3.9754	0.6091			
285	267	1.3517	0.6972	0.2932		3.5014	0.3899			
286	268	0.7400	0.8024	0.4865		3.9908	0.4384			
287	269	0.2719	0.6925	0.0344		3.4831	0.2908			
288	270	1.5769	0.3948	0.5354		2.5763	0.4509			
289	271	1.0755	0.2325	0.4195		2.1483	0.4216			
290	272	36.5756	0.8843	0.8231		4.5713	0.5468			
291	273	1.3318	0.4692	0.4635		2.7750	0.4326			
292	274	61.8268	0.9683	0.9238		5.9177	0.6139			
293	275	19.3189	0.9083	0.8543		4.8160	0.5630			
294	276	2.7842	0.4542	0.4387		2.7341	0.4264			
295	277	1.0662	0.2984	0.1417		2.3249	0.3453			
296	278	0.9912	0.4815	0.4585		2.8086	0.4314			
297	279	4.2632	0.8686	0.7632		4.4350	0.5209			
298	280	1.1243	0.2530	0.6512		2.2041	0.4831			
299	281	21.5697	0.9632	0.9568		5.7641	0.6552			
300	282	37.9756	0.9296	0.9552		5.0926	0.6527			
301	283	0.1668	0.3210	0.4030		2.3839	0.4176			
302	284	0.2804	0.2668	0.1640		2.2414	0.3529			
303	285	1.0741	0.2516	0.3437		2.2003	0.4028			
304	286	2.4651	0.5002	0.7427		2.8608	0.5132			
305	287	0.3866	0.4734	0.4648		2.7864	0.4329			
306	288	0.4829	0.2146	0.5468		2.0985	0.4539			
307	289	0.1315	0.0001	0.2180		0.6554	0.3694			
308	290	30.0941	0.8177	0.8970		4.0797	0.5909			
309	291	0.3906	0.1273	0.3840		1.8305	0.4128			
310	292	0.1371	0.5956	0.5602		3.1445	0.4575			
311	293	1.4271	0.3587	0.2957		2.4822	0.3905			
312	294	51.2788	0.8585	0.9735		4.3559	0.6892			
313	295	0.4922	0.5668	0.1267		3.0550	0.3398			
314	296	0.3628	0.1584	0.1227		1.9324	0.3383			
315	297	457.4214	0.9767	0.9364		6.2384	0.6273			
316	298	0.2542	0.0130	0.4257		1.1965	0.4232			
317	299	0.1185	0.0845	0.1672		1.6688	0.3539			
318	300	0.4328	0.4656	0.1574		2.7650	0.3507			
319	301	1.4526	0.4491	0.9558		2.7204	0.6537			
320	302	0.2653	0.2984	0.5381		2.3248	0.4516			
321	303	2.0877	0.4635	0.1884		2.7594	0.3606			
322	304	2.4602	0.8173	0.6418		4.0773	0.4803			
323	305	0.4974	0.1864	0.0753		2.0174	0.3175			
324	306	15.2011	0.7022	0.8019		3.5212	0.5369			
325	307	0.2902	0.2444	0.1343		2.1809	0.3426			
326	308	65.7010	0.9262	0.9505		5.0440	0.6455			
327	309	1.7877	0.7429	0.8561		3.6931	0.5641			
328	310	0.1490	0.0983	0.1304		1.7248	0.3412			
329	311	7.0789	0.7044	0.7344		3.5300	0.5102			

	A	B	C	D	E	F	G	H	I	J
330	312	0.2607	0.0809	0.0705		1.6533	0.3150			
331	313	1.6190	0.1586	0.3850		1.9329	0.4131			
332	314	98835.2070	0.9974	0.9985		8.5464	0.8729			
333	315	23.5316	0.7879	0.9222		3.9113	0.6123			
334	316	0.2556	0.1008	0.4448		1.7345	0.4279			
335	317	1.7352	0.5625	0.9073		3.0420	0.5990			
336	318	0.9998	0.6520	0.5582		3.3333	0.4569			
337	319	8.0528	0.7868	0.8123		3.9059	0.5417			
338	320	1.0002	0.2436	0.4766		2.1788	0.4359			
339	321	0.9034	0.4562	0.4133		2.7395	0.4201			
340	322	310.9108	0.9281	0.9730		5.0710	0.6880			
341	323	0.1588	0.0013	0.2665		0.8771	0.3828			
342	324	0.8044	0.3386	0.3790		2.4297	0.4116			
343	325	0.9105	0.3827	0.2297		2.5448	0.3727			
344	326	0.0829	0.0014	0.0012		0.8886	0.2195			
345	327	1.1814	0.5685	0.5343		3.0603	0.4506			
346	328	0.2322	0.3877	0.7234		2.5576	0.5063			
347	329	131.6888	0.8720	0.9238		4.4633	0.6139			
348	330	1.6185	0.2438	0.9111		2.1792	0.6022			
349	331	1.2836	0.4092	0.6787		2.6141	0.4915			
350	332	0.4608	0.1579	0.2632		1.9307	0.3819			
351	333	3.7788	0.5855	0.6645		3.1127	0.4871			
352	334	3.6657	0.8244	0.7290		4.1207	0.5083			
353	335	3.3975	0.7953	0.6849		3.9513	0.4935			
354	336	1.3651	0.4870	0.8455		2.8239	0.5582			
355	337	1.0777	0.1436	0.3445		1.8852	0.4030			
356	338	3.7176	0.4705	0.4523		2.7783	0.4298			
357	339	1.9145	0.3600	0.4630		2.4855	0.4325			
358	340	0.7164	0.7035	0.5172		3.5265	0.4462			
359	341	0.5333	0.4461	0.9618		2.7122	0.6640			
360	342	0.6257	0.3708	0.1212		2.5137	0.3377			
361	343	0.4614	0.2887	0.1366		2.2993	0.3434			
362	344	0.1863	0.2098	0.0238		2.0848	0.2802			
363	345	4.2384	0.6760	0.7301		3.4204	0.5087			
364	346	0.4549	0.3736	0.4026		2.5209	0.4175			
365	347	1.9353	0.6327	0.9147		3.2663	0.6053			
366	348	17.3139	0.8384	0.7129		4.2117	0.5027			
367	349	9.2516	0.7279	0.8977		3.6272	0.5914			
368	350	1.8360	0.8453	0.7793		4.2590	0.5273			
369	351	2.0877	0.8115	0.8735		4.0431	0.5746			
370	352	0.1504	0.0251	0.2520		1.3277	0.3789			
371	353	0.1378	0.0031	0.2239		0.9786	0.3711			
372	354	6.3676	0.8567	0.7645		4.3419	0.5214			
373	355	5.5988	0.8223	0.5634		4.1079	0.4583			
374	356	1.0329	0.3816	0.2692		2.5419	0.3836			
375	357	108.2206	0.9086	0.9304		4.8199	0.6206			
376	358	0.2656	0.0564	0.5370		1.5370	0.4513			
377	359	16.8090	0.9438	0.7784		5.3272	0.5270			
378	360	1.0561	0.1402	0.2791		1.8740	0.3862			
379	361	0.5078	0.1181	0.3012		1.7982	0.3920			
380	362	0.4354	0.6976	0.6371		3.5029	0.4789			
381	363	5.8694	0.8871	0.5306		4.5966	0.4497			
382	364	0.3706	0.3052	0.4322		2.3428	0.4248			
383	365	1.5320	0.4520	0.4276		2.7282	0.4237			
384	366	3.8912	0.8902	0.9554		4.6262	0.6530			

	A	B	C	D	E	F	G	H	I	J
385	367	813.3087	0.9924	0.9912		7.4088	0.7627			
386	368	0.6977	0.2916	0.2505		2.3070	0.3785			
387	369	1.4095	0.7214	0.7137		3.5996	0.5030			
388	370	7.3987	0.9489	0.7096		5.4248	0.5016			
389	371	2.3525	0.5456	0.7224		2.9916	0.5060			
390	372	1.5571	0.3966	0.5053		2.5811	0.4432			
391	373	0.2003	0.0784	0.9496		1.6426	0.6443			
392	374	0.7865	0.0847	0.8626		1.6695	0.5679			
393	375	1.1682	0.5697	0.4416		3.0640	0.4272			
394	376	0.7199	0.1315	0.6473		1.8449	0.4819			
395	377	1.4778	0.6858	0.7053		3.4575	0.5002			
396	378	0.5185	0.0646	0.0911		1.5788	0.3252			
397	379	0.1793	0.0970	0.0318		1.7195	0.2884			
398	380	27.4326	0.8243	0.9051		4.1200	0.5972			
399	381	0.2637	0.0033	0.1137		0.9859	0.3348			
400	382	0.2294	0.3815	0.0695		2.5416	0.3145			
401	383	3.3860	0.4165	0.8230		2.6335	0.5467			
402	384	8.0105	0.7020	0.7371		3.5204	0.5112			
403	385	1.5632	0.5097	0.5816		2.8875	0.4632			
404	386	1.8633	0.8766	0.5991		4.5020	0.4681			
405	387	4.7545	0.8283	0.5524		4.1456	0.4554			
406	388	59.3468	0.9746	0.9023		6.1483	0.5949			
407	389	0.2100	0.3493	0.1266		2.4575	0.3398			
408	390	5.7190	0.6918	0.5778		3.4802	0.4622			
409	391	0.3135	0.0706	0.4838		1.6074	0.4377			
410	392	0.5869	0.0838	0.1356		1.6657	0.3431			
411	393	1.1558	0.2781	0.7362		2.2714	0.5108			
412	394	1.1477	0.2456	0.5349		2.1842	0.4508			
413	395	30.9322	0.9107	0.7745		4.8437	0.5254			
414	396	0.7726	0.4317	0.2633		2.6737	0.3820			
415	397	0.9855	0.4621	0.3322		2.7555	0.3999			
416	398	1.4364	0.3178	0.5376		2.3755	0.4515			
417	399	0.4108	0.3383	0.2055		2.4290	0.3657			
418	400	0.4157	0.4199	0.2257		2.6425	0.3716			
419	401	0.4050	0.1670	0.2118		1.9589	0.3676			
420	402	354.4439	0.9838	0.9405		6.6154	0.6322			
421	403	0.5905	0.2524	0.5002		2.2025	0.4419			
422	404	0.1919	0.0338	0.3662		1.3978	0.4084			
423	405	0.6827	0.4758	0.5449		2.7931	0.4534			
424	406	0.3269	0.2094	0.4304		2.0838	0.4244			
425	407	0.3268	0.0807	0.1662		1.6525	0.3536			
426	408	0.8527	0.4137	0.5300		2.6260	0.4495			
427	409	0.1292	0.0635	0.0460		1.5732	0.2999			
428	410	2.1390	0.6483	0.6402		3.3201	0.4798			
429	411	0.7163	0.5116	0.3730		2.8929	0.4101			
430	412	1.0430	0.1152	0.5933		1.7879	0.4665			
431	413	0.8502	0.5127	0.1481		2.8960	0.3475			
432	414	0.4082	0.1138	0.7289		1.7829	0.5083			
433	415	1.5440	0.3429	0.6653		2.4409	0.4874			
434	416	20.8223	0.8111	0.9225		4.0408	0.6127			
435	417	3.7736	0.9275	0.8894		5.0615	0.5853			
436	418	4.6359	0.6694	0.5840		3.3960	0.4639			
437	419	0.4920	0.2389	0.2112		2.1657	0.3674			
438	420	239.5047	0.9440	0.9739		5.3300	0.6903			
439	421	1.0758	0.3915	0.7618		2.5676	0.5204			

	A	B	C	D	E	F	G	H	I	J
440	422	5.5867	0.9429	0.7904		5.3106	0.5320			
441	423	6.1709	0.5064	0.7714		2.8782	0.5241			
442	424	0.2925	0.1439	0.2528		1.8862	0.3791			
443	425	0.2270	0.3728	0.1664		2.5188	0.3537			
444	426	1.1360	0.2905	0.3869		2.3042	0.4136			
445	427	12.8478	0.5980	0.9034		3.1522	0.5959			
446	428	0.8934	0.6823	0.1694		3.4438	0.3546			
447	429	1.3800	0.7476	0.6550		3.7141	0.4842			
448	430	0.6905	0.6376	0.4525		3.2832	0.4299			
449	431	0.5148	0.1076	0.1785		1.7602	0.3575			
450	432	52.7286	0.9470	0.8277		5.3879	0.5490			
451	433	133.6411	0.9446	0.9436		5.3424	0.6361			
452	434	1.1325	0.6468	0.3759		3.3150	0.4108			
453	435	0.3210	0.5384	0.5091		2.9704	0.4441			
454	436	23.3042	0.8914	0.9206		4.6381	0.6108			
455	437	0.9248	0.7468	0.5475		3.7106	0.4541			
456	438	1.6516	0.1883	0.4630		2.0229	0.4325			
457	439	0.4952	0.6246	0.4465		3.2392	0.4284			
458	440	1.8821	0.9186	0.3591		4.9412	0.4066			
459	441	0.4032	0.0750	0.0224		1.6276	0.2785			
460	442	0.4788	0.2384	0.2404		2.1644	0.3757			
461	443	0.2907	0.4055	0.3619		2.6046	0.4073			
462	444	0.2364	0.0114	0.0199		1.1720	0.2754			
463	445	13.7893	0.7926	0.7295		3.9369	0.5085			
464	446	10.6546	0.8697	0.9112		4.4440	0.6023			
465	447	0.3685	0.1695	0.0792		1.9665	0.3195			
466	448	2174.0481	0.9972	0.9940		8.4565	0.7875			
467	449	60.5775	0.9906	0.9604		7.1774	0.6614			
468	450	0.2653	0.0324	0.0524		1.3872	0.3043			
469	451	0.4533	0.4669	0.5090		2.7685	0.4441			
470	452	0.3801	0.5094	0.4236		2.8867	0.4227			
471	453	0.2728	0.4422	0.1514		2.7020	0.3486			
472	454	1.8686	0.7871	0.7980		3.9075	0.5352			
473	455	23.6595	0.8842	0.7943		4.5703	0.5336			
474	456	0.1510	0.1675	0.2000		1.9607	0.3641			
475	457	3.9295	0.4244	0.9173		2.6543	0.6077			
476	458	0.4562	0.3329	0.2477		2.4151	0.3777			
477	459	0.5605	0.0683	0.1818		1.5966	0.3585			
478	460	1.6877	0.3508	0.7120		2.4615	0.5024			
479	461	0.7986	0.5970	0.4619		3.1490	0.4322			
480	462	0.9849	0.4579	0.2333		2.7441	0.3737			
481	463	48.7484	0.9030	0.9545		4.7573	0.6515			
482	464	0.7632	0.8457	0.4283		4.2622	0.4238			
483	465	1.0816	0.2680	0.2348		2.2444	0.3742			
484	466	8.8924	0.7153	0.6549		3.5741	0.4842			
485	467	1.7119	0.2780	0.8240		2.2710	0.5472			
486	468	250.2178	0.9329	0.9184		5.1435	0.6087			
487	469	0.1786	0.3462	0.0155		2.4496	0.2691			
488	470	596.8898	0.9813	0.9860		6.4645	0.7324			
489	471	0.5896	0.7665	0.0846		3.8029	0.3221			
490	472	0.1553	0.0326	0.3347		1.3888	0.4005			
491	473	0.3091	0.2716	0.3585		2.2540	0.4065			
492	474	0.6458	0.3111	0.1570		2.3582	0.3505			
493	475	1.3527	0.3567	0.5667		2.4770	0.4592			
494	476	0.7147	0.2568	0.5858		2.2145	0.4644			

	A	B	C	D	E	F	G	H	I	J
495	477	0.6291	0.2802	0.5202		2.2769	0.4470			
496	478	19.0168	0.8303	0.8213		4.1581	0.5459			
497	479	6.7073	0.8939	0.7205		4.6631	0.5053			
498	480	26.7451	0.6676	0.7954		3.3894	0.5341			
499	481	0.5934	0.4151	0.7623		2.6297	0.5206			
500	482	1.2522	0.3605	0.3371		2.4869	0.4011			
501	483	0.6916	0.2180	0.3691		2.1080	0.4092			
502	484	2.8024	0.4854	0.2314		2.8196	0.3732			
503	485	23.5448	0.8793	0.9307		4.5262	0.6210			
504	486	1.6571	0.5491	0.4927		3.0017	0.4399			
505	487	5.3379	0.7351	0.7126		3.6584	0.5026			
506	488	7.7291	0.8000	0.8033		3.9775	0.5376			
507	489	0.5005	0.6580	0.4239		3.3544	0.4227			
508	490	0.1890	0.1942	0.3834		2.0400	0.4127			
509	491	752.3881	0.9816	0.9742		6.4782	0.6912			
510	492	2.7644	0.1114	0.6887		1.7742	0.4947			
511	493	1.6025	0.1776	0.4127		1.9911	0.4200			
512	494	0.1560	0.2151	0.0454		2.0998	0.2995			
513	495	0.3819	0.3317	0.5121		2.4119	0.4449			
514	496	0.5617	0.8299	0.1381		4.1556	0.3440			
515	497	14.4880	0.7781	0.9339		3.8606	0.6245			
516	498	0.9004	0.8296	0.5170		4.1537	0.4462			
517	499	1.1205	0.2146	0.4112		2.0983	0.4196			
518	500	1.9584	0.2618	0.7516		2.2278	0.5165			
519	501	11.7395	0.7134	0.9675		3.5663	0.6751			
520	502	2.5425	0.6144	0.4825		3.2054	0.4374			
521	503	32.2847	0.9023	0.8672		4.7492	0.5707			
522	504	0.9648	0.5662	0.6104		3.0531	0.4712			
523	505	0.6000	0.6234	0.4346		3.2350	0.4254			
524	506	0.1117	0.5010	0.8667		2.8631	0.5703			
525	507	2.2477	0.7876	0.5281		3.9102	0.4490			
526	508	2.9030	0.5159	0.8788		2.9052	0.5780			
527	509	45.7004	0.8805	0.9727		4.5367	0.6872			
528	510	1.0412	0.8538	0.4326		4.3203	0.4249			
529	511	2.8186	0.6650	0.7787		3.3799	0.5271			
530	512	2.8071	0.7015	0.8605		3.5182	0.5666			
531	513	0.8820	0.4531	0.2431		2.7313	0.3765			
532	514	1.7990	0.4837	0.9070		2.8146	0.5988			
533	515	6.7742	0.7081	0.5871		3.5450	0.4647			
534	516	468.1910	0.9795	0.9420		6.3664	0.6341			
535	517	4.9609	0.8151	0.9168		4.0643	0.6073			
536	518	3.0466	0.4495	0.8360		2.7214	0.5532			
537	519	1.2783	0.7181	0.2789		3.5860	0.3861			
538	520	21.7037	0.8792	0.8078		4.5253	0.5396			
539	521	0.5405	0.8345	0.2520		4.1857	0.3789			
540	522	0.3041	0.0090	0.2932		1.1318	0.3899			
541	523	0.4346	0.5284	0.6795		2.9413	0.4918			
542	524	312.5934	0.9688	0.9762		5.9350	0.6966			
543	525	0.3242	0.2022	0.0540		2.0633	0.3054			
544	526	0.2178	0.1924	0.0094		2.0348	0.2575			
545	527	0.2133	0.0218	0.2574		1.2970	0.3804			
546	528	1.2365	0.2761	0.5968		2.2660	0.4674			
547	529	3.8870	0.9478	0.6207		5.4038	0.4741			
548	530	17.2220	0.8663	0.9085		4.4167	0.6000			
549	531	0.1073	0.1228	0.0782		1.8148	0.3190			

	A	B	C	D	E	F	G	H	I	J
550	532	1.6976	0.5214	0.3085		2.9210	0.3938			
551	533	13.0109	0.9326	0.8495		5.1383	0.5604			
552	534	0.6407	0.5286	0.2232		2.9417	0.3709			
553	535	4.0448	0.7438	0.4821		3.6971	0.4373			
554	536	0.3459	0.0780	0.1800		1.6408	0.3580			
555	537	1.7587	0.6219	0.7086		3.2302	0.5013			
556	538	13.6516	0.8125	0.8628		4.0486	0.5680			
557	539	6424.7516	0.9967	0.9871		8.2746	0.7376			
558	540	7.3241	0.6773	0.9331		3.4253	0.6236			
559	541	0.3926	0.1541	0.1785		1.9188	0.3575			
560	542	1042.1127	0.9852	0.9730		6.7081	0.6881			
561	543	0.5600	0.1821	0.1093		2.0046	0.3330			
562	544	4.0917	0.7964	0.6124		3.9574	0.4718			
563	545	0.6074	0.5554	0.6419		3.0207	0.4803			
564	546	1.9764	0.3518	0.8110		2.4643	0.5411			
565	547	0.2810	0.4372	0.0051		2.6884	0.2449			
566	548	0.7598	0.2326	0.6843		2.1487	0.4933			
567	549	0.3723	0.1272	0.0564		1.8303	0.3069			
568	550	0.4248	0.2244	0.1049		2.1260	0.3311			
569	551	1.2644	0.6773	0.1120		3.4253	0.3341			
570	552	0.2469	0.2765	0.2791		2.2672	0.3862			
571	553	1.8414	0.7693	0.4958		3.8169	0.4407			
572	554	0.3532	0.0507	0.2758		1.5053	0.3853			
573	555	0.2474	0.1001	0.3244		1.7317	0.3979			
574	556	0.7191	0.4337	0.4413		2.6790	0.4271			
575	557	0.5100	0.6278	0.1811		3.2498	0.3583			
576	558	0.2449	0.0353	0.0079		1.4086	0.2537			
577	559	0.2276	0.1410	0.6568		1.8767	0.4848			
578	560	1.0824	0.3229	0.1771		2.3889	0.3571			
579	561	0.1769	0.1909	0.1415		2.0306	0.3452			
580	562	2.6127	0.4562	0.5599		2.7396	0.4574			
581	563	0.3186	0.7748	0.3279		3.8442	0.3988			
582	564	5.5549	0.6365	0.7186		3.2793	0.5047			
583	565	1.4749	0.4288	0.6926		2.6660	0.4960			
584	566	0.9423	0.6550	0.2800		3.3437	0.3864			
585	567	0.2986	0.0780	0.4483		1.6408	0.4288			
586	568	94.4617	0.8907	0.8842		4.6309	0.5817			
587	569	14.4806	0.9585	0.7641		5.6417	0.5213			
588	570	0.3122	0.3584	0.7159		2.4814	0.5037			
589	571	1.5169	0.7970	0.1985		3.9605	0.3636			
590	572	1.2296	0.4762	0.3412		2.7940	0.4022			
591	573	2.8243	0.7608	0.6471		3.7756	0.4819			
592	574	0.3566	0.4221	0.2167		2.6483	0.3690			
593	575	0.4273	0.4224	0.0855		2.6490	0.3225			
594	576	0.6675	0.3463	0.1753		2.4500	0.3565			
595	577	0.7288	0.1930	0.3459		2.0367	0.4033			
596	578	3.6332	0.5233	0.7334		2.9263	0.5098			
597	579	1.9088	0.7990	0.1957		3.9714	0.3628			
598	580	0.7858	0.2739	0.1632		2.2602	0.3526			
599	581	0.4909	0.3125	0.0198		2.3617	0.2753			
600	582	0.5367	0.8137	0.2054		4.0557	0.3657			
601	583	0.2667	0.5249	0.1125		2.9311	0.3343			
602	584	727.8663	0.9780	0.9683		6.2965	0.6769			
603	585	0.4795	0.3824	0.8615		2.5439	0.5672			
604	586	0.4065	0.1821	0.2620		2.0046	0.3816			

	A	B	C	D	E	F	G	H	I	J
605	587	1.8778	0.6443	0.6338		3.3064	0.4779			
606	588	0.1727	0.0298	0.2811		1.3673	0.3867			
607	589	1.1824	0.2809	0.3445		2.2788	0.4030			
608	590	52.9191	0.9121	0.8715		4.8610	0.5733			
609	591	0.2610	0.1806	0.3491		2.0002	0.4041			
610	592	4.3253	0.6872	0.8277		3.4626	0.5490			
611	593	7.1190	0.5679	0.6565		3.0584	0.4847			
612	594	0.2467	0.1807	0.0833		2.0005	0.3215			
613	595	0.1346	0.3136	0.1426		2.3647	0.3456			
614	596	2.1439	0.6048	0.5288		3.1741	0.4492			
615	597	5.2177	0.8605	0.7135		4.3708	0.5029			
616	598	65.9381	0.9429	0.9519		5.3111	0.6476			
617	599	0.2841	0.3559	0.4048		2.4748	0.4180			
618	600	0.6408	0.3315	0.2747		2.4113	0.3850			
619	601	55.2923	0.9627	0.9277		5.7504	0.6178			
620	602	0.7934	0.4890	0.3868		2.8296	0.4135			
621	603	0.9984	0.3053	0.9109		2.3428	0.6021			
622	604	15.8821	0.8773	0.9485		4.5079	0.6426			
623	605	0.8738	0.2116	0.4481		2.0901	0.4288			
624	606	59.5625	0.8521	0.8774		4.3078	0.5771			
625	607	0.4150	0.1483	0.5216		1.9003	0.4473			
626	608	1.7844	0.8709	0.3576		4.4541	0.4063			
627	609	1.3269	0.4572	0.9382		2.7422	0.6294			
628	610	1.4899	0.4619	0.4121		2.7549	0.4198			
629	611	0.3453	0.2392	0.1586		2.1668	0.3511			
630	612	1.8624	0.4797	0.8875		2.8037	0.5839			
631	613	20.2137	0.8477	0.9515		4.2763	0.6470			
632	614	0.4896	0.3785	0.0850		2.5336	0.3223			
633	615	0.8723	0.3883	0.6367		2.5593	0.4788			
634	616	1.2737	0.6101	0.1580		3.1914	0.3509			
635	617	0.9219	0.7216	0.7909		3.6007	0.5322			
636	618	1.4830	0.9752	0.5120		6.1712	0.4449			
637	619	0.5956	0.2603	0.7298		2.2238	0.5086			
638	620	1.5400	0.7576	0.3812		3.7605	0.4122			
639	621	0.1551	0.0893	0.2595		1.6889	0.3809			
640	622	1.5786	0.5085	0.4780		2.8843	0.4362			
641	623	5.5477	0.8688	0.7387		4.4364	0.5117			
642	624	1.1235	0.2513	0.5188		2.1995	0.4466			
643	625	0.5709	0.2721	0.4319		2.2554	0.4247			
644	626	1.5430	0.3387	0.2551		2.4302	0.3797			
645	627	0.5822	0.2444	0.7656		2.1808	0.5219			
646	628	0.4594	0.3259	0.2867		2.3968	0.3882			
647	629	1.4301	0.1742	0.4929		1.9808	0.4400			
648	630	6.0435	0.7938	0.8717		3.9430	0.5734			
649	631	0.4501	0.0129	0.0463		1.1939	0.3002			
650	632	0.2174	0.1324	0.0205		1.8480	0.2762			
651	633	0.1006	0.0033	0.2347		0.9882	0.3741			
652	634	1.8977	0.5831	0.6623		3.1051	0.4864			
653	635	0.2550	0.0102	0.0956		1.1526	0.3272			
654	636	0.7325	0.6178	0.3222		3.2164	0.3973			
655	637	2.5526	0.7552	0.4755		3.7494	0.4356			
656	638	0.1667	0.0678	0.6773		1.5939	0.4911			
657	639	7.4370	0.9225	0.6819		4.9930	0.4925			
658	640	1.9455	0.5261	0.8118		2.9346	0.5414			
659	641	0.7497	0.4909	0.5766		2.8348	0.4619			

	A	B	C	D	E	F	G	H	I	J
660	642	0.1951	0.8752	0.2675		4.4903	0.3831			
661	643	1.9244	0.5577	0.4176		3.0276	0.4212			
662	644	6.3778	0.6983	0.4341		3.5056	0.4253			
663	645	0.4160	0.2810	0.0669		2.2789	0.3130			
664	646	212.8540	0.9506	0.9771		5.4598	0.6992			
665	647	7.7291	0.7617	0.8227		3.7802	0.5466			
666	648	1.9107	0.6425	0.5616		3.2999	0.4578			
667	649	0.1273	0.0048	0.3687		1.0362	0.4090			
668	650	4.4331	0.6897	0.6795		3.4721	0.4918			
669	651	0.1887	0.0976	0.0403		1.7220	0.2957			
670	652	16.6199	0.9397	0.8543		5.2531	0.5631			
671	653	14.3513	0.7643	0.9637		3.7925	0.6676			
672	654	1.0383	0.5003	0.2806		2.8610	0.3866			
673	655	0.2614	0.1075	0.0739		1.7596	0.3168			
674	656	15.9755	0.5172	0.8629		2.9089	0.5681			
675	657	0.6824	0.2628	0.2461		2.2305	0.3773			
676	658	0.4104	0.1114	0.2956		1.7741	0.3905			
677	659	1.0863	0.5864	0.2694		3.1155	0.3836			
678	660	11.5829	0.7333	0.6914		3.6507	0.4956			
679	661	2.6069	0.7549	0.3351		3.7481	0.4006			
680	662	0.2598	0.1174	0.0768		1.7960	0.3183			
681	663	0.7645	0.2945	0.1606		2.3146	0.3517			
682	664	1.4852	0.2954	0.5927		2.3169	0.4663			
683	665	4.1891	0.8136	0.9532		4.0552	0.6495			
684	666	0.5922	0.1087	0.4118		1.7642	0.4197			
685	667	347.0663	0.9581	0.9779		5.6316	0.7016			
686	668	0.3231	0.7320	0.1175		3.6447	0.3363			
687	669	0.6025	0.6776	0.1938		3.4262	0.3622			
688	670	0.7676	0.1728	0.7275		1.9766	0.5078			
689	671	0.1534	0.0293	0.2641		1.3637	0.3822			
690	672	0.2608	0.6217	0.1424		3.2295	0.3455			
691	673	0.8331	0.5815	0.4956		3.1001	0.4407			
692	674	106.3968	0.9733	0.9273		6.0957	0.6174			
693	675	15.8649	0.7556	0.8577		3.7512	0.5650			
694	676	1.4739	0.3727	0.7279		2.5186	0.5079			
695	677	204.3616	0.9627	0.9754		5.7500	0.6942			
696	678	0.4776	0.6738	0.2842		3.4120	0.3875			
697	679	2.2771	0.6789	0.4364		3.4310	0.4258			
698	680	1.2435	0.5689	0.2324		3.0613	0.3735			
699	681	0.8150	0.3607	0.5346		2.4873	0.4507			
700	682	301.3612	0.9583	0.9270		5.6356	0.6171			
701	683	0.4258	0.6422	0.1126		3.2991	0.3343			
702	684	0.2023	0.0156	0.1651		1.2303	0.3532			
703	685	0.3932	0.3196	0.1231		2.3803	0.3384			
704	686	9.9982	0.8551	0.8782		4.3297	0.5776			
705	687	0.2674	0.8725	0.4764		4.4674	0.4358			
706	688	0.6339	0.5819	0.6040		3.1015	0.4694			
707	689	0.2945	0.1250	0.5598		1.8228	0.4574			
708	690	0.2406	0.0320	0.3866		1.3848	0.4135			
709	691	9.0619	0.7549	0.7978		3.7477	0.5351			
710	692	11.2716	0.9096	0.6783		4.8314	0.4914			
711	693	0.5206	0.2171	0.4217		2.1055	0.4222			
712	694	1.1029	0.3827	0.4912		2.5447	0.4396			
713	695	0.1546	0.0303	0.9272		1.3710	0.6174			
714	696	8.5983	0.6051	0.6644		3.1750	0.4871			



	A	B	C	D	E	F	G	H	I	J
715	697	3.2028	0.5109	0.7289		2.8910	0.5083			
716	698	21.4617	0.9516	0.7867		5.4809	0.5304			
717	699	146.9537	0.9484	0.9436		5.4156	0.6361			
718	700	0.9041	0.2082	0.7286		2.0803	0.5081			
719	701	0.2874	0.5834	0.2115		3.1063	0.3675			
720	702	1.4392	0.5612	0.3535		3.0382	0.4052			
721	703	0.8189	0.1674	0.2665		1.9603	0.3828			
722	704	0.6051	0.3218	0.4165		2.3861	0.4209			
723	705	0.2819	0.1155	0.1767		1.7892	0.3569			
724	706	1.5425	0.5757	0.8100		3.0824	0.5406			
725	707	0.4083	0.0767	0.3768		1.6349	0.4110			
726	708	0.6730	0.6891	0.0743		3.4700	0.3170			
727	709	0.4789	0.5948	0.1465		3.1419	0.3469			
728	710	0.5273	0.5905	0.0329		3.1283	0.2895			
729	711	12.9680	0.8712	0.7616		4.4566	0.5203			
730	712	0.4183	0.3642	0.2689		2.4964	0.3835			
731	713	0.6853	0.3703	0.5052		2.5123	0.4431			
732	714	1.4727	0.3966	0.5474		2.5809	0.4541			
733	715	4.1885	0.8314	0.8718		4.1656	0.5735			
734	716	0.6997	0.4458	0.4603		2.7114	0.4318			
735	717	0.2923	0.3509	0.0604		2.4618	0.3093			
736	718	0.3261	0.5964	0.3105		3.1472	0.3943			
737	719	11.4009	0.8998	0.8157		4.7228	0.5432			
738	720	0.3122	0.4092	0.6761		2.6140	0.4907			
739	721	0.1386	0.5942	0.1618		3.1401	0.3521			
740	722	0.8701	0.3941	0.4102		2.5744	0.4194			
741	723	10.5451	0.6010	0.6913		3.1619	0.4956			
742	724	1.1284	0.3603	0.4897		2.4862	0.4392			
743	725	2.3123	0.7191	0.9459		3.5900	0.6392			
744	726	1.9168	0.5770	0.6984		3.0862	0.4979			
745	727	3.4656	0.4132	0.8610		2.6246	0.5670			
746	728	0.7658	0.3978	0.5443		2.5841	0.4533			
747	729	1.7147	0.2611	0.3172		2.2261	0.3961			
748	730	0.2980	0.0139	0.2677		1.2080	0.3832			
749	731	0.4488	0.1688	0.2235		1.9644	0.3710			
750	732	0.5255	0.2509	0.1420		2.1986	0.3454			
751	733	0.3032	0.1840	0.0546		2.0103	0.3057			
752	734	0.3824	0.6115	0.0550		3.1959	0.3060			
753	735	0.1975	0.2866	0.0787		2.2939	0.3192			
754	736	0.5461	0.1354	0.4847		1.8580	0.4379			
755	737	0.5958	0.1214	0.2424		1.8099	0.3763			
756	738	2.8847	0.8345	0.6863		4.1858	0.4940			
757	739	2.3687	0.7122	0.6446		3.5617	0.4811			
758	740	0.1284	0.2509	0.7225		2.1985	0.5060			
759	741	0.4242	0.4690	0.5561		2.7743	0.4564			
760	742	0.3239	0.7967	0.2944		3.9592	0.3902			
761	743	1.8151	0.3032	0.5841		2.3373	0.4639			
762	744	2.3389	0.6322	0.7897		3.2648	0.5317			
763	745	4.9208	0.7499	0.7176		3.7249	0.5043			
764	746	0.4714	0.1409	0.5623		1.8763	0.4580			
765	747	1.0228	0.3898	0.8057		2.5632	0.5387			
766	748	6.2205	0.9769	0.8005		6.2465	0.5363			
767	749	4.7098	0.5921	0.3817		3.1336	0.4123			
768	750	0.4628	0.3568	0.1401		2.4773	0.3447			
769	751	0.3932	0.0728	0.1800		1.6172	0.3580			

	A	B	C	D	E	F	G	H	I	J
770	752	2.7773	0.6982	0.4300		3.5052	0.4243			
771	753	0.4597	0.1665	0.1981		1.9573	0.3635			
772	754	0.1467	0.1210	0.1578		1.8085	0.3508			
773	755	0.4469	0.6997	0.2832		3.5112	0.3873			
774	756	56.3052	0.9884	0.9179		6.9630	0.6083			
775	757	0.7382	0.5086	0.1157		2.8846	0.3355			
776	758	3.1945	0.7433	0.4180		3.6945	0.4213			
777	759	0.3971	0.3952	0.7409		2.5774	0.5125			
778	760	0.3217	0.2116	0.2768		2.0899	0.3856			
779	761	15.9687	0.7842	0.9471		3.8919	0.6407			
780	762	0.3789	0.1479	0.1679		1.8990	0.3541			
781	763	2.5828	0.7930	0.4695		3.9388	0.4341			
782	764	0.7363	0.0935	0.3099		1.7057	0.3942			
783	765	0.4953	0.0990	0.4588		1.7272	0.4314			
784	766	1.2476	0.8293	0.4950		4.1522	0.4405			
785	767	3.9192	0.8661	0.8454		4.4146	0.5581			
786	768	0.1753	0.1386	0.7703		1.8685	0.5237			
787	769	2.3879	0.4160	0.7578		2.6322	0.5189			
788	770	27.1645	0.8832	0.8828		4.5606	0.5807			
789	771	1.5805	0.5798	0.6481		3.0951	0.4822			
790	772	51.9061	0.9506	0.8436		5.4602	0.5572			
791	773	0.2648	0.6350	0.1996		3.2741	0.3640			
792	774	2.0359	0.7300	0.4439		3.6360	0.4277			
793	775	0.2506	0.0765	0.2059		1.6339	0.3658			
794	776	0.7184	0.1290	0.4082		1.8363	0.4189			
795	777	0.3745	0.1429	0.4654		1.8829	0.4331			
796	778	0.6522	0.3421	0.4852		2.4390	0.4381			
797	779	0.3157	0.1023	0.0868		1.7403	0.3231			
798	780	1.3206	0.7148	0.2866		3.5721	0.3882			
799	781	0.1419	0.0057	0.0096		1.0618	0.2579			
800	782	2.7023	0.5932	0.8701		3.1369	0.5724			
801	783	3.1535	0.8484	0.5784		4.2808	0.4624			
802	784	2.6894	0.5056	0.8057		2.8758	0.5386			
803	785	0.4901	0.3021	0.3912		2.3347	0.4146			
804	786	22.3748	0.8635	0.9015		4.3940	0.5943			
805	787	1.8754	0.4341	0.3526		2.6803	0.4050			
806	788	0.2766	0.3611	0.1906		2.4884	0.3613			
807	789	684.8472	0.9986	0.9529		9.2065	0.6491			
808	790	0.6914	0.3071	0.2613		2.3477	0.3814			
809	791	0.1713	0.3798	0.2770		2.5372	0.3856			
810	792	0.3922	0.4034	0.4504		2.5988	0.4293			
811	793	469.8675	0.9775	0.9861		6.2723	0.7325			
812	794	1.2878	0.4217	0.2886		2.6472	0.3887			
813	795	3.9850	0.5937	0.6384		3.1387	0.4793			
814	796	3.4831	0.4562	0.7231		2.7396	0.5062			
815	797	14.9596	0.8002	0.7588		3.9786	0.5192			
816	798	4.3131	0.9037	0.7144		4.7651	0.5032			
817	799	11.5544	0.9788	0.7560		6.3318	0.5182			
818	800	3.8603	0.4456	0.7171		2.7109	0.5042			
819	801	19.3035	0.8570	0.7784		4.3442	0.5270			
820	802	17.5101	0.8592	0.8265		4.3607	0.5484			
821	803	0.5835	0.5665	0.4673		3.0540	0.4335			
822	804	57.1400	0.9309	0.8915		5.1122	0.5868			
823	805	0.2386	0.0228	0.1144		1.3075	0.3350			
824	806	0.5400	0.6375	0.1066		3.2828	0.3319			

	A	B	C	D	E	F	G	H	I	J
825	807	10.4471	0.7944	0.8627		3.9465	0.5680			
826	808	2.2255	0.8199	0.8288		4.0934	0.5495			
827	809	17.3489	0.8000	0.6962		3.9772	0.4972			
828	810	0.3141	0.0969	0.0541		1.7191	0.3054			
829	811	7.3381	0.7294	0.7094		3.6336	0.5015			
830	812	122.7681	0.9046	0.9751		4.7751	0.6935			
831	813	0.4204	0.0112	0.1104		1.1690	0.3334			
832	814	7.4593	0.7638	0.8830		3.7902	0.5808			
833	815	0.5277	0.5021	0.2266		2.8662	0.3718			
834	816	0.2816	0.5292	0.0692		2.9434	0.3143			
835	817	0.3241	0.1186	0.0563		1.8001	0.3068			
836	818	0.1400	0.4885	0.0009		2.8280	0.2161			
837	819	52585.0481	0.9969	0.9984		8.3401	0.8687			
838	820	3.2696	0.5214	0.5914		2.9209	0.4659			
839	821	0.2929	0.8971	0.1250		4.6945	0.3392			
840	822	0.7460	0.5507	0.4010		3.0065	0.4171			
841	823	2.8897	0.8445	0.4341		4.2538	0.4253			
842	824	0.3133	0.0283	0.2749		1.3555	0.3851			
843	825	0.5303	0.4927	0.1398		2.8398	0.3446			
844	826	6.4400	0.9607	0.7409		5.6968	0.5125			
845	827	0.1888	0.1608	0.2520		1.9399	0.3789			
846	828	0.7637	0.4755	0.5267		2.7923	0.4487			
847	829	3.9843	0.5597	0.6529		3.0335	0.4836			
848	830	0.1065	0.3948	0.3387		2.5763	0.4015			
849	831	0.6799	0.3642	0.1102		2.4965	0.3333			
850	832	1.4271	0.9211	0.1643		4.9736	0.3530			
851	833	2.4680	0.5715	0.5704		3.0693	0.4602			
852	834	0.6508	0.7198	0.4659		3.5930	0.4332			
853	835	0.3344	0.2649	0.7293		2.2362	0.5084			
854	836	2.1002	0.6048	0.8156		3.1742	0.5432			
855	837	3.5321	0.5347	0.7884		2.9594	0.5311			
856	838	23.8598	0.7677	0.7902		3.8088	0.5319			
857	839	1.1495	0.4539	0.2550		2.7333	0.3797			
858	840	0.7281	0.1803	0.5177		1.9991	0.4463			
859	841	1.8613	0.5601	0.3863		3.0346	0.4134			
860	842	6.6255	0.9596	0.6317		5.6693	0.4773			
861	843	0.7858	0.4585	0.5369		2.7459	0.4513			
862	844	0.8219	0.7951	0.2532		3.9501	0.3792			
863	845	2.9534	0.8130	0.7417		4.0515	0.5129			
864	846	2.9063	0.4403	0.4883		2.6966	0.4388			
865	847	0.1924	0.0348	0.0631		1.4053	0.3109			
866	848	0.1864	0.2379	0.4064		2.1632	0.4184			
867	849	3.4747	0.5433	0.7079		2.9846	0.5010			
868	850	0.6888	0.1525	0.5477		1.9139	0.4542			
869	851	65.5733	0.8843	0.8672		4.5705	0.5706			
870	852	1446.5257	0.9971	0.9764		8.4472	0.6972			
871	853	1.2952	0.4241	0.2863		2.6536	0.3881			
872	854	0.5477	0.4498	0.6235		2.7222	0.4750			
873	855	0.3010	0.3615	0.1521		2.4893	0.3489			
874	856	1.6399	0.6511	0.8977		3.3300	0.5914			
875	857	74.1972	0.9008	0.8710		4.7332	0.5730			
876	858	6.7260	0.8375	0.8809		4.2056	0.5794			
877	859	0.7870	0.2115	0.1767		2.0898	0.3570			
878	860	1.9147	0.5608	0.4564		3.0368	0.4308			
879	861	0.3018	0.0580	0.1024		1.5450	0.3301			

	A	B	C	D	E	F	G	H	I	J
880	862	133.1059	0.9335	0.8955		5.1521	0.5897			
881	863	1.7587	0.5898	0.8661		3.1262	0.5699			
882	864	1.7330	0.7864	0.7690		3.9038	0.5232			
883	865	179.9930	0.9702	0.9812		5.9813	0.7125			
884	866	0.1993	0.0066	0.0254		1.0835	0.2820			
885	867	0.9055	0.2739	0.5643		2.2602	0.4586			
886	868	19.8539	0.9555	0.8586		5.5685	0.5655			
887	869	9.5468	0.8183	0.9371		4.0834	0.6281			
888	870	0.2416	0.0453	0.3731		1.4741	0.4101			
889	871	0.4598	0.2351	0.6336		2.1556	0.4779			
890	872	0.5170	0.7196	0.3020		3.5919	0.3922			
891	873	0.4420	0.2590	0.4858		2.2202	0.4382			
892	874	0.3951	0.5893	0.4456		3.1247	0.4281			
893	875	0.3971	0.2244	0.2886		2.1258	0.3887			
894	876	102.2661	0.8856	0.9549		4.5833	0.6522			
895	877	0.5725	0.1368	0.3337		1.8627	0.4003			
896	878	0.2263	0.0610	0.1789		1.5605	0.3576			
897	879	0.4887	0.2016	0.1028		2.0616	0.3303			
898	880	3871.7080	0.9991	0.9870		9.6753	0.7368			
899	881	0.2513	0.2249	0.6068		2.1272	0.4702			
900	882	0.2242	0.0345	0.1248		1.4032	0.3391			
901	883	0.6925	0.1115	0.5128		1.7744	0.4451			
902	884	0.2557	0.3806	0.6296		2.5393	0.4767			
903	885	0.3012	0.7414	0.7062		3.6862	0.5005			
904	886	0.5466	0.6988	0.1697		3.5079	0.3547			
905	887	1.0690	0.4053	0.4289		2.6040	0.4240			
906	888	2.7818	0.7338	0.6219		3.6527	0.4745			
907	889	0.2715	0.0041	0.0400		1.0161	0.2955			
908	890	0.4951	0.2264	0.2205		2.1315	0.3701			
909	891	90.5924	0.9486	0.9314		5.4197	0.6217			
910	892	0.2092	0.0860	0.2866		1.6749	0.3881			
911	893	2.7622	0.6351	0.4921		3.2744	0.4398			
912	894	0.4995	0.2319	0.3239		2.1467	0.3978			
913	895	0.1410	0.4394	0.0081		2.6942	0.2543			
914	896	2.7784	0.6201	0.3103		3.2243	0.3943			
915	897	0.4824	0.7245	0.1813		3.6129	0.3584			
916	898	1.3287	0.6347	0.3197		3.2731	0.3967			
917	899	0.4659	0.2367	0.0336		2.1600	0.2901			
918	900	11.7477	0.8959	0.8541		4.6825	0.5630			
919	901	2.0116	0.4742	0.3940		2.7887	0.4153			
920	902	55.7149	0.9087	0.9691		4.8216	0.6786			
921	903	4.0540	0.8733	0.6353		4.4743	0.4784			
922	904	0.6516	0.2718	0.4827		2.2546	0.4374			
923	905	4.1368	0.7858	0.8060		3.9007	0.5388			
924	906	0.4231	0.3155	0.2609		2.3697	0.3813			
925	907	1.1632	0.5604	0.6005		3.0358	0.4684			
926	908	2.8295	0.5307	0.6554		2.9478	0.4844			
927	909	1.0323	0.7680	0.7444		3.8106	0.5138			
928	910	15.1189	0.7690	0.8053		3.8155	0.5385			
929	911	0.6309	0.9366	0.3682		5.2024	0.4089			
930	912	0.1608	0.5639	0.0196		3.0462	0.2750			
931	913	0.3772	0.1001	0.7554		1.7317	0.5179			
932	914	0.8823	0.5856	0.3397		3.1130	0.4018			
933	915	0.6643	0.2791	0.3687		2.2741	0.4090			
934	916	6.1311	0.6334	0.7299		3.2687	0.5086			

	A	B	C	D	E	F	G	H	I	J
935	917	0.2912	0.3978	0.6587		2.5842	0.4854			
936	918	0.1444	0.0261	0.0568		1.3369	0.3071			
937	919	0.1080	0.3910	0.2036		2.5663	0.3652			
938	920	2.7200	0.8827	0.6524		4.5558	0.4834			
939	921	8.1019	0.7828	0.7751		3.8850	0.5256			
940	922	0.2111	0.1208	0.4719		1.8080	0.4347			
941	923	1.6077	0.9078	0.7902		4.8106	0.5319			
942	924	4.4005	0.6803	0.4912		3.4363	0.4396			
943	925	0.1523	0.1822	0.0197		2.0050	0.2752			
944	926	0.3946	0.0375	0.7267		1.4240	0.5075			
945	927	1.4471	0.6943	0.7149		3.4902	0.5034			
946	928	3.8665	0.4953	0.7942		2.8470	0.5336			
947	929	4.5126	0.8462	0.5970		4.2652	0.4675			
948	930	12.3700	0.8117	0.8147		4.0441	0.5428			
949	931	2.6935	0.6495	0.5344		3.3243	0.4507			
950	932	0.3770	0.1602	0.1190		1.9379	0.3369			
951	933	0.4037	0.1152	0.2417		1.7879	0.3761			
952	934	0.4972	0.5376	0.3155		2.9680	0.3956			
953	935	2.5601	0.8563	0.9244		4.3391	0.6145			
954	936	0.4504	0.1620	0.0523		1.9437	0.3042			
955	937	0.2798	0.1139	0.1038		1.7833	0.3307			
956	938	0.6632	0.7390	0.2804		3.6756	0.3865			
957	939	0.9458	0.3239	0.4513		2.3916	0.4296			
958	940	6.0260	0.8481	0.7153		4.2792	0.5035			
959	941	1.9793	0.5011	0.5324		2.8632	0.4502			
960	942	0.8927	0.3214	0.4092		2.3851	0.4191			
961	943	0.3508	0.0971	0.0851		1.7202	0.3223			
962	944	1.4476	0.9214	0.9047		4.9781	0.5969			
963	945	0.3757	0.8777	0.5497		4.5120	0.4547			
964	946	2.2729	0.4662	0.5728		2.7667	0.4608			
965	947	0.2767	0.0986	0.0866		1.7259	0.3230			
966	948	0.4287	0.2181	0.0754		2.1083	0.3176			
967	949	1.7342	0.7725	0.3957		3.8327	0.4158			
968	950	0.6089	0.2102	0.0904		2.0860	0.3248			
969	951	0.1916	0.2680	0.0490		2.2444	0.3021			
970	952	1.4410	0.7638	0.2397		3.7900	0.3755			
971	953	0.3119	0.5978	0.1788		3.1517	0.3576			
972	954	1.4134	0.5787	0.8379		3.0914	0.5542			
973	955	0.4484	0.0154	0.9818		1.2277	0.7147			
974	956	0.5799	0.7218	0.3639		3.6013	0.4078			
975	957	0.3686	0.0669	0.2721		1.5896	0.3843			
976	958	0.5276	0.1816	0.3182		2.0032	0.3963			
977	959	0.8800	0.8552	0.9239		4.3307	0.6140			
978	960	354.1055	0.9651	0.9871		5.8188	0.7374			
979	961	2.9206	0.4679	0.4759		2.7714	0.4357			
980	962	0.8605	0.4246	0.7592		2.6549	0.5194			
981	963	3.4748	0.5978	0.7518		3.1515	0.5166			
982	964	1.2068	0.4616	0.5263		2.7543	0.4486			
983	965	2.9865	0.6319	0.7122		3.2636	0.5025			
984	966	1.0356	0.2486	0.7906		2.1924	0.5320			
985	967	0.3079	0.6381	0.2506		3.2850	0.3785			
986	968	1.7716	0.9209	0.3608		4.9719	0.4071			
987	969	1.2368	0.4838	0.4667		2.8151	0.4334			
988	970	18.4495	0.8704	0.7823		4.4501	0.5285			
989	971	10.2841	0.9495	0.9357		5.4384	0.6265			

	A	B	C	D	E	F	G	H	I	J
990	972	0.4376	0.6088	0.1224		3.1871	0.3382			
991	973	25.5376	0.7156	0.8965		3.5754	0.5904			
992	974	1.2191	0.7274	0.7961		3.6250	0.5344			
993	975	0.7567	0.2472	0.8290		2.1884	0.5497			
994	976	9.1563	0.7688	0.8116		3.8143	0.5413			
995	977	0.2082	0.1093	0.2681		1.7664	0.3833			
996	978	0.5106	0.0528	0.1477		1.5175	0.3474			
997	979	70.6575	0.9057	0.9811		4.7870	0.7121			
998	980	0.2497	0.0806	0.2510		1.6523	0.3786			
999	981	2.4019	0.6893	0.4205		3.4707	0.4219			
1000	982	476.3237	0.9772	0.9781		6.2575	0.7024			
1001	983	1.1091	0.2105	0.6383		2.0870	0.4792			
1002	984	2.3370	0.3059	0.7231		2.3445	0.5062			
1003	985	3.7600	0.2502	0.6491		2.1967	0.4825			
1004	986	0.3886	0.5126	0.2419		2.8958	0.3761			
1005	987	0.2031	0.4339	0.0080		2.6798	0.2541			
1006	988	1.5556	0.8413	0.3814		4.2317	0.4122			
1007	989	0.6026	0.7338	0.1899		3.6527	0.3611			
1008	990	0.4527	0.2279	0.1048		2.1356	0.3311			
1009	991	10.1954	0.8800	0.8292		4.5322	0.5498			
1010	992	0.7218	0.2557	0.4201		2.2115	0.4218			
1011	993	0.3244	0.1990	0.9036		2.0539	0.5960			
1012	994	20.7809	0.8370	0.9165		4.2023	0.6070			
1013	995	2.4134	0.6670	0.4228		3.3871	0.4225			
1014	996	0.2586	0.0428	0.3898		1.4585	0.4143			
1015	997	1.2421	0.2809	0.9077		2.2787	0.5994			
1016	998	1.2991	0.4739	0.6378		2.7878	0.4791			
1017	999	5.6080	0.8957	0.7604		4.6809	0.5198			
1018	1000	5.0793	0.7908	0.4365		3.9268	0.4259			

## APPENDIX B: EXAMPLE CODE

### B.1 EXAMPLE R CODE WRITTEN FOR CHAPTER 5 TO DETERMINE COPULA FITTING FOR HYPERBOLIC MODEL BEARING PRESSURE-DISPLACEMENT EQUATION

```

#read in k1, k2, and mstc values from file
k1k2m<-read.csv("C:\\Users\\Jonny\\Desktop\\R\\k1k2m.csv", header = T)
attach(k1k2m)

#transform k1, k2 and m to uniform variables using rank
u1=rank(k1)/(length(k1)+1)
u2=rank(k2)/(length(k2)+1)
um=rank(m)/(length(m)+1)

#create 'x' matrix with values of u1, u2 and um
x<-matrix(1,length(u1),3)
x[,1]=u1
x[,2]=u2
x[,3]=um

#Find best-fit bivariate vine copulas and copula parameters
#assumes C-vine (type 1) and AIC selection criteria. BIC results are same.
#make sure CDVine package is loaded
CDVineCopSelect(data=x, familyset=NA, type=1, selectioncrit="AIC")

#RESULTS:
#$family = 33 33 16
#which represents k1-k2, k1-m, k2-m (where k2-m is best-fit after fitting the
others)
#33 is rotated Clayton (270 deg.) and 16 is rotated Joe (180 deg.)
#par = -7.053976 -3.142653 1.397515
#par2 = 0 0 0 (i.e., there is no second parameter for these copulas)

```

```

#to simulate ranked parameters using copula data (assume n=5,000 sims)
n=5000
family=c(33,33,16)
par=c(-7.053976, -3.142653, 1.397515)
u_sims=CDVineSim(N=n, family=family, par=par, type=1)
u1_sim=u_sims[,1]
u2_sim=u_sims[,2]
um_sim=u_sims[,3]

#Transform u1, u2 and um into k1, k2 and mstc sims using known marginal
distributions
#The u simulations represent the cumulative distribution, so we need inverse CDF
or quantile (q) dist.

#k1 is best fit to gamma distribution
k1_shape=3.71590850943956
k1_rate=1/0.003433101851711
k1=qgamma(u1_sim,shape=k1_shape,rate=k1_rate)

#k2 is best fit to inv. gaussian distribution (need to make sure statmod package is
loaded)
k2_nu = 0.701447
k2_lambda = 27.91919
k2=qinvGauss(u2_sim,nu=k2_nu,lambda=k2_lambda,lower.tail=TRUE,log.p=FA
LSE)

#mstc is best fit to lognormal distribution
mstc_mean = 0.643048649204319
mstc_stdev = 0.123128154098121
mstc_LN_stdev = sqrt(log(1+(mstc_stdev^2/mstc_mean^2)))
mstc_LN_mean = log(mstc_mean)-0.5*(mstc_LN_stdev)^2
mstc = qlnorm(um_sim,meanlog=mstc_LN_mean,sdlog=mstc_LN_stdev)

#Creat a matrix and write to .csv (Excel) file
k1k2mstc<-matrix(1,length(k1),3)
k1k2mstc[,1]=k1

```



```
k1k2mstc[,2]=k2  
k1k2mstc[,3]=mstc
```

```
write.csv(k1k2mstc,file="H:\\Research (1-4-15)\\Stat Analysis - Load Test  
DB\\Footings on Clay (unimproved)\\MC Sim for  
R\\k1k2mstc_sims.csv",row.names=FALSE,col.names=TRUE)
```

## B.2 EXAMPLE R CODE WRITTEN FOR CHAPTER 5 MONTE CARLO SIMULATIONS

```
#Required R Packages: CDVine, SuppDists
rm(list = ls())
```

```
#Set initial number of simulations
n = 250000
```

```
#Generate random values for normalized bearing capacity
#This step is done first to establish the number of revised simulations
```

```
    #The unit mean bearing capacity, qult, has parameters of the bias calculated from
the dataset
```

```
    #with unit mean=1.25 and COV=0.37
```

```
    #The bias is closest to a gamma distribution - define parameters and generate n
random values
```

```
    qult_shape = 7.52698348510156
```

```
    qult_rate = 1/0.166593308846615
```

```
    qult = matrix(rgamma(n, shape=qult_shape, rate=qult_rate),n,1)
```

```
    #set minimum value of qult based on lower-bound value determined by remolded
undrained shear strength
```

```
    #Average su(remolded) minus 1 standard dev.
```

```
    qult_min = 0.29
```

```
    #revise the number of simulated values, eliminating those less than qult_min
```

```
    qult_rev = matrix(1,n,1)
```

```
    qult_rev[,] <- qult[,] > qult_min
```

```
    for ( i in 1:length(qult_rev[,1])) { if (qult_rev[i,1]==1) qult_rev[i,1]=qult[i,1] }
```

```
    qult_rev<-qult_rev[apply(qult_rev!=0,1,any),,drop=FALSE]
```

```
#check revised number of simulations
```

```
n_prime = length(qult_rev[,1])
```

#Generate uniformly distributed ranked values that will be transformed to the k1, k2 and mstc parameters

```
#to simulate ranked parameters using copula data
#(make sure CDVine package is loaded)
family=c(33,33,16)
par=c(-7.053976, -3.142653, 1.397515)
u_sims = CDVineSim(N=n_prime, family=family, par=par, type=1)
u1_sim = u_sims[,1]
u2_sim = u_sims[,2]
um_sim = u_sims[,3]
```

#Transform u1, u2 and um into k1, k2 and mstc sims using known marginal distributions

#The u simulations represent the cumulative distribution, so we need inverse CDF or quantile (q) dist.

```
#k1 is best fit to gamma distribution
k1_shape=3.71590850943956
k1_rate=1/0.003433101851711
k1= matrix(qgamma(u1_sim, shape=k1_shape, rate=k1_rate), n_prime, 1)
```

```
#k2 is best fit to inv. gaussian distribution
k2_nu = 0.701447
k2_lambda = 27.91919
k2= matrix(qinvGauss(u2_sim, nu=k2_nu, lambda=k2_lambda), n_prime, 1)
```

```
#mstc is best fit to lognormal distribution
mstc_mean = 0.643048649204319
mstc_stdev = 0.123128154098121
mstc_LN_stdev = sqrt(log(1+(mstc_stdev^2/mstc_mean^2)))
mstc_LN_mean = log(mstc_mean)-0.5*(mstc_LN_stdev)^2
mstc = matrix(qlnorm(um_sim, meanlog=mstc_LN_mean,
sdlog=mstc_LN_stdev), n_prime, 1)
```

#Load test data fitting is based on slope tangent capacity, qstc, which is correlated to qult

```

#based on linear relationship mstc=qstc/qult
#Generate values of qstc
    qstc = mstc*qult_rev

#Generate random values for parameters to simulate values of normalized mobilized
resistance

    #Allowable displacement, y_allow, is assumed to have lognorm distribution and
COV=0 to 0.6 (just 0 here)
    #Nominal value of y_allow = y_mean.
    y_mean = c(2.5, 5, 7.5, 10, 12.5, 15, 20, 25, 30, 37.5, 50, 62.5, 75, 100, 112.5,
125, 150, 187.5, 200, 225, 250, 300, 400, 500, 600)
    y_COV = c(0)

    y_allow = matrix(NA, n_prime, length(y_mean))
    k=0
    for (i in 1:length(y_mean)) {
        k=k+1
        y_stdev = y_mean[i]*y_COV
        #Find equivalent lognormal values
        y_LN_stdev = sqrt(log(1+(y_stdev^2/y_mean[i]^2)))
        y_LN_mean = log(y_mean[i])-0.5*(y_LN_stdev)^2
        y_allow[,k] = rlnorm(n_prime, meanlog=y_LN_mean,
sdlog=y_LN_stdev)
    }

    #Bf is the equivalent footing diameter, assumed to range from 0.5m to 3m, and
COV=0.02
    #set COV=0 for this analysis to compare to OpenSees sims
    #Nominal value of Bf is Bf_mean. Generate n random values
    Bf_mean = c(0.5, 1, 1.5, 2, 2.5, 3)
    Bf_COV = 0.00

    Bf = matrix(NA, n_prime, length(Bf_mean))
    k=0
    for (i in 1:length(Bf_mean)) {

```

```

    k=k+1
    Bf_stdev = Bf_mean[i]*Bf_COV
    Bf[,k] = rnorm(n_prime, mean=Bf_mean[i], sd=Bf_stdev)
  }

#Normalize the displacement by footing diam... eta=y_allow/Bf
eta = matrix(NA, n_prime, length(y_allow[1,])*length(Bf[1,]))
k=0
for (i in 1:length(y_allow[1,])) {
  for (j in 1:length(Bf[1,])) {
    k=k+1
    eta[,k] = y_allow[,i]/(Bf[,j]*1000)
  }}

#Reduce eta matrix to include only desired values. We generated 150 columns
#Only want eta at 0.005, 0.01, 0.025, 0.05, 0.075, 0.10, 0.20
#Also want to put in order that is easier to get values from
eta_prime = matrix(NA, n_prime, 42)
eta_prime = eta[,c(
  1, 8, 15, 22, 29, 36,
  7, 20, 33, 40, 47, 54,
  25, 44, 57, 64, 71, 78,
  43, 62, 75, 82, 95, 102,
  55, 74, 87, 100, 107, 120,
  61, 80, 99, 112, 125, 132,
  79, 110, 129, 136, 143, 150)]

eta = eta_prime

#Find the normalized, mobilized resistance assuming hyperbolic function
#Resit_Norm is the normalized resistance
Resist_Norm = matrix(NA, n_prime, length(eta[1,]))
k=0
for (i in 1:length(eta[1,])) {
  k=k+1

```

```

    Resist_Norm[,k] = (eta[,i]/(k1+k2*eta[,i]))*qstc
  }
#Expand normalized resistance matrix for different load/resistance factors
#FS is the load/resistance factor (i.e., Factor of Safety)

FS = matrix(c(1,1.5,2,2.5,3,4,5,6,7,8,9,10,12.5,15,20),1,15)

Resist_Norm_FS = matrix(NA, n_prime,
length(Resist_Norm[1,])*length(FS[1,]))
k=0
for (i in 1:length(FS[1,])) {
  for (j in 1:length(Resist_Norm[1,])) {
    k=k+1
    Resist_Norm_FS[k] = FS[,i]*Resist_Norm[,j]
  }
}

#Generate random values for the normalized loads (bearing pressure)

#Unit mean bearing pressure, q, is assumed to have lognorm dist. with COV=0.1
#Set COV=0 for this analysis to compare with OpenSees sims
#Nominal value of q is q_mean
q_mean = 1
q_COV = 0.00
q_stdev = q_mean*q_COV
#find equivalent lognormal values
q_LN_stdev = sqrt(log(1+(q_stdev^2/q_mean^2)))
q_LN_mean = log(q_mean)-0.5*(q_LN_stdev)^2
#simulate random values and put in 1xn matrix
q = matrix(rlnorm(n_prime, meanlog=q_LN_mean,
sdlog=q_LN_stdev),n_prime,1)

#Compare Resist_Norm_FS to q.

#Performance Function P = R-Q (i.e., P = Resist_Norm_FS - q)
P = matrix(NA, n_prime, length(Resist_Norm_FS[1,]))

```

```

k=0
for (i in 1:length(P[1,])) {
  k=k+1
  P[,k] = Resist_Norm_FS[,i]-q
}
#Find probability of failure,
#Estimated as the number times P is less than 0, divided by the number of
simulations
#Results1 sets values to either 0 or 1 depending if P is less than 0
#Results2 adds the number of "1's" (i.e., number of failures)
#The probability of failure, pf, is the number of failures divided by simulations

Results1 = matrix(NA, n_prime, length(P[1,]))
k=0
for (i in 1:length(Results1[1,])) {
  k=k+1
  Results1[,k] = ifelse(P[,i]<0,1,0)
}

Results2 = matrix(NA, 1, length(Results1[1,]))
k=0
for (i in 1:length(Results2[1,])) {
  k=k+1
  Results2[,k] = sum(Results1[,i])
}
Results2T = t(Results2)

pf = Results2T/n_prime

#write.csv(pf, file = "Z:\\Research\\Stat Analysis - Load Test DB\\Footings on Clay
(unimproved)\\MC Sim for R\\pf_COV=xx.csv")
write.csv(pf, file = "C:\\users\\jhuffman\\Desktop\\pf_COV=0.csv", row.names=FALSE)

```

### B.3 EXAMPLE R CODE WRITTEN FOR CHAPTER 7 MONTE CARLO SIMULATIONS WITH 5 FOOTINGS IN SPATIALLY VARIABLE SOIL

#This file is written for R to complete Monte Carlo simulations for bearing pressure vs. displacement response of multiple footings at a predetermined footing layout (i.e., horizontal spacing) in 2-D space. This assumes 5 footings spaced at 9.15 m on-center.

#The outside footings (Footings 1 and 5) are sized for a maximum load of 517 kN (DL and LL). The interior footings (2 through 4) are

#sized for a maximum load of 819 kN. The footings are sized to include a FS of 2.5 for bearing.

#The initial steps construct a variable soil profile (horizontal) based on assumed mean, COV, and scale of fluctuation (SOF) of  $s_u$ .

#Then bearing capacity is calculated for the given soil parameters ( $s_u$  and  $\gamma$ ) and footing dimensions.

#This generates random values for the reference capacity,  $q_{stc}$ , based on the bearing capacity and linear correlation factor,  $m_{stc}$

#as well as the normalized bearing pressure-displacement coefficients  $k_1$  and  $k_2$ , taking into account the correlation structure between  $m_{stc}$ ,  $k_1$  and  $k_2$

#The random values for  $q_{ult}$ ,  $q_{stc}$ ,  $k_1$  and  $k_2$  are compiled as a matrix and written to a .csv file.

#This file now also generates values for the Hyperbolic Gap Material to input into OpenSees (based on Duncan & Mokwa (2001))

#After developing the soil profile, deterministic footing loads are applied, equal to either (517 kN/(1.675m x 1.675m)=195.8 kPa) or (819 kN/(2.125m x 2.125m)=181.4 kPa).

#Vertical displacement (i.e., settlement) is calculated for each footing.

#UPDATE FROM PREVIOUS ANALYSIS --  $q_{ult}$  is assumed to be DETERMINISTIC. Therefore  $q_{ult\_rnd}$  (random) =  $q_{ult}$

#Required R Packages: RandomFields, CDVine, SuppDists

```
rm(list = ls())
```

#Set initial number of simulations

```
n = 50000
```

#Create matrix [called OpenSees] that will be populated with all pertinent information for import into OpenSees

#For each footing, the matrix includes:



#su\_bearing - undrained shear strength (kPa) for bearing. Average over footing width. Not required for OpenSees, but good to check

#su\_L - undrained shear strength (kPa), left side of footing. Averaged to distance equal to embedment depth (45 deg failure angle)

#su\_R - undrained shear strength (kPa), right side of footing.

#Df - Footing Depth (m)

#B - Footing width (m). Assumed to be the same for L

#No. of Springs (vertical direction)

#k1 - vertical spring parameter

#k2 - vertical spring parameter

#Q\_stc - Slope tangent capacity (kN). qstc over bearing footing bearing area

#Gap\_V - "gap" for vertical spring model. Equal to zero

#Kmax - initial stiffness for hyp. gap model (horizontal spring)

#Kur - rebound curve (equal to Kmax)

#Rf - "Failure ratio" in hyp. gap model (horizontal spring)

#P\_ult\_L - Ultimate passive resistance (kN) for horizontal spring, left side of footing

#P\_ult\_R - Ultimate passive resistance (kN) for horizontal spring, right side of footing

#Gap\_H - "gap" for horizontal spring model. Set very close to zero

```

OpenSees = matrix(NA, n, 5*16)
colnames(OpenSees, do.NULL=TRUE, prefix="col")
colnames(OpenSees) =
  c("su_1", "su_1L", "su_1R", "Df_1", "B_1", "SpringNo.1", "k1_1", "k2_1",
    "q_stc_1", "Gap_V_1", "Kmax_1", "Kur_1", "Rf_1", "P_ult_1L", "P_ult_1R",
    "Gap_H_1",
    "su_2", "su_2L", "su_2R", "Df_2", "B_2", "SpringNo.2", "k1_2", "k2_2",
    "q_stc_2", "Gap_V_2", "Kmax_2", "Kur_2", "Rf_2", "P_ult_2L", "P_ult_2R",
    "Gap_H_2",
    "su_3", "su_3L", "su_3R", "Df_3", "B_3", "SpringNo.3", "k1_3", "k2_3",
    "q_stc_3", "Gap_V_3", "Kmax_3", "Kur_3", "Rf_3", "P_ult_3L", "P_ult_3R",
    "Gap_H_3",
    "su_4", "su_4L", "su_4R", "Df_4", "B_4", "SpringNo.4", "k1_4", "k2_4",
    "q_stc_4", "Gap_V_4", "Kmax_4", "Kur_4", "Rf_4", "P_ult_4L", "P_ult_4R",
    "Gap_H_4",
    "su_5", "su_5L", "su_5R", "Df_5", "B_5", "SpringNo.5", "k1_5", "k2_5",
    "q_stc_5", "Gap_V_5", "Kmax_5", "Kur_5", "Rf_5", "P_ult_5L", "P_ult_5R",
    "Gap_H_5")

```

```

OpenSees_trunc = matrix(NA, n, 5*5)
colnames(OpenSees_trunc, do.NULL=TRUE, prefix="col")
colnames(OpenSees_trunc) =
  c("k1_1", "k2_1", "q_stc_1", "P_ult_1L", "P_ult_1R",
    "k1_2", "k2_2", "q_stc_2", "P_ult_2L", "P_ult_2R",
    "k1_3", "k2_3", "q_stc_3", "P_ult_3L", "P_ult_3R",
    "k1_4", "k2_4", "q_stc_4", "P_ult_4L", "P_ult_4R",
    "k1_5", "k2_5", "q_stc_5", "P_ult_5L", "P_ult_5R")

#Create matrix [called Footing_Settlement] that will be populated with nonlinear
displacement from applied bearing pressure on each footing

Footing_Settlement = matrix(NA, n, 5)
colnames(Footing_Settlement, do.NULL=TRUE, prefix="col")
colnames(Footing_Settlement) =
  c("Footing1_Settlement", "Footing2_Settlement", "Footing3_Settlement",
    "Footing4_Settlement", "Footing5_Settlement")

#Create matrix [called Footing_Loads] that will be be populated with the applied bearing
pressure on each footing

Footing_Loads = matrix(NA, n, 5)
colnames(Footing_Loads, do.NULL=TRUE, prefix="col")
colnames(Footing_Loads) =
  c("Footing1_Load", "Footing2_Load", "Footing3_Load", "Footing4_Load",
    "Footing5_Load")

#Generate horizontal profile of undrained shear strength over distance, x.

  #Define the horizontal length, x_width, in meters.
  #Create a single column matrix, x, currently set to 0.02m so that we can have
footings at a distance of 9.15m
  #make sure x is large enough to accomodate building width

  #define length and sample intervals for x(meters)
  x_width = 50
  interval = 0.02
  seq = seq(0,x_width,by=interval)

```

```

x = matrix(seq, 1, length(seq))

pi = 3.14159265

#set mean value and COV for undrained shear strength, su(kPa)
#Assume COV(su) = [0,0.05,0.10,0.20,0.30,0.50,1.00] - Only one value given
here

su_mean = 70.0

su_COV = 1.00

su_stdev = su_mean*su_COV

su_var = su_stdev^2

#define Scale of Fluctuation for su
#assume SOF = [0.1, 0.2, 0.5, 1.0, 2.0, 5.0, 10, 20, 30, 50, 100] meters - Only one
value given here

SOF = 100.0

#simulate su(kPa) random field along distance x(m)
#simulation is based on mean and COV above, and exponential variogram model
(requires RandomFields package). No nugget included here.
RFoptions(spConform=FALSE)
model = RMexp(var=su_var,scale=SOF)+RMtrend(mean=su_mean)
su_x_sim = RFsimulate(model=model, x=seq, n=n)

#create matrix to compile su(kPa) at defined values along interval of x(m)
su_x <- matrix(unlist(su_x_sim), ncol = length(x), byrow = TRUE)

#Set minimum value of su based on lower-bound value determined by remolded
undrained shear strength
#Average su(remolded) minus 1 standard dev. See Huffman et al. (2015)
su_min = 0.24*su_mean
#Revise su_x to have a minimum value of su_min

```

```

su_x_min = matrix(NA, n, length(seq))
k=0
for (i in 1:length(seq)) {
  k=k+1
  su_x_min[,k] = ifelse(su_x[,i]<su_min,su_min,su_x[,i])
}
rm(su_x)
su_x = su_x_min

```

#Create matrix for x and su\_x; write to a .csv file

```

xsu_x = matrix(NA, n+1, length(seq))
xsu_x[1,] = x
xsu_x[1:n+1,] = su_x

```

#write.csv(xsu\_x, file = "E:\\Building Model --- OpenSees\\OpenSees - imported soil model\\xsu\_x.csv", row.names=FALSE)

#Sample x for average su at selected footing locations

#This example includes 5 footings, with a width of 1.675 or 2.125 m and a center-to-center distance of 9.15 meters

#It is assumed su\_L and su\_R for passive resistance extends to a distance of Df from the footing.

#The range sampled from xsu\_x depends on the footing width, x-location, and x-interval (e.g., 0.02m)

#and needs to be updated accordingly for any change in these parameters

#The building is situated such that the left side of Footing 1 is arbitrarily set at x=5m, so there is space for a left horiz. spring.

#Footing Widths (meters)

B\_outside = 1.675

B\_inside = 2.125

B\_outside\_prime = (B\_outside^2/0.785)^0.5

B\_inside\_prime = (B\_inside^2/0.785)^0.5

#Footing 1 extends from x = 5 to 6.675

Footing\_1 = matrix(NA, n+1, 85)

Footing\_1[,1:85] = xsu\_x[,251:335]

Footing\_1su = matrix(NA, n, 85)

Footing\_1su = Footing\_1[-1,]

```

su_1 = matrix(NA,n,1)
k=0
for (i in 1:n) {
  k=k+1
  su_1[k,] = mean(Footing_1su[k,])
}
#Footing 1L (left of footing) extends from x = 3.325 to 5
Footing_1L = matrix(NA, n+1, 85)
Footing_1L[,1:85] = xsu_x[,167:251]
Footing_1suL = matrix(NA, n, 85)
Footing_1suL = Footing_1L[-1,]
su_1L = matrix(NA,n,1)
k=0
for (i in 1:n) {
  k=k+1
  su_1L[k,] = mean(Footing_1suL[k,])
}

#Footing 1R (right of footing) extends from x = 6.675 to 8.35
Footing_1R = matrix(NA, n+1, 85)
Footing_1R[,1:85] = xsu_x[,335:419]
Footing_1suR = matrix(NA, n, 85)
Footing_1suR = Footing_1R[-1,]
su_1R = matrix(NA,n,1)
k=0
for (i in 1:n) {
  k=k+1
  su_1R[k,] = mean(Footing_1suR[k,])
}

#Footing 2 extends from x = 13.925 to 16.05

Footing_2 = matrix(NA, n+1, 107)
Footing_2[,1:107] = xsu_x[,697:803]
Footing_2su = matrix(NA, n, 107)
Footing_2su = Footing_2[-1,]
su_2 = matrix(NA,n,1)

```

```

k=0
for (i in 1:n) {
  k=k+1
  su_2[k,] = mean(Footing_2su[k,])
}

#Footing 2L (left of footing) extends from x = 11.8 to 13.925
Footing_2L = matrix(NA, n+1, 107)
Footing_2L[,1:107] = xsu_x[,591:697]
Footing_2suL = matrix(NA, n, 107)
Footing_2suL = Footing_2L[-1,]
su_2L = matrix(NA,n,1)
k=0
for (i in 1:n) {
  k=k+1
  su_2L[k,] = mean(Footing_2suL[k,])
}

#Footing 2R (right of footing) extends from x = 16.05 to 18.175
Footing_2R = matrix(NA, n+1, 107)
Footing_2R[,1:107] = xsu_x[,803:909]
Footing_2suR = matrix(NA, n, 107)
Footing_2suR = Footing_2R[-1,]
su_2R = matrix(NA,n,1)
k=0
for (i in 1:n) {
  k=k+1
  su_2R[k,] = mean(Footing_2suR[k,])
}

#Footing 3 extends from x = 23.075 to 25.2

Footing_3 = matrix(NA, n+1, 107)
Footing_3[,1:107] = xsu_x[,1154:1260]
Footing_3su = matrix(NA, n, 107)
Footing_3su = Footing_3[-1,]
su_3 = matrix(NA,n,1)

```

```

k=0
for (i in 1:n) {
  k=k+1
  su_3[k,] = mean(Footing_3su[k,])
}

#Footing 3L (left of footing) extends from x = 20.95 to 23.075
Footing_3L = matrix(NA, n+1, 107)
Footing_3L[,1:107] = xsu_x[,1048:1154]
Footing_3suL = matrix(NA, n, 107)
Footing_3suL = Footing_3L[-1,]
su_3L = matrix(NA,n,1)
k=0
for (i in 1:n) {
  k=k+1
  su_3L[k,] = mean(Footing_3suL[k,])
}

#Footing 3R (right of footing) extends from x = 25.2 to 27.325
Footing_3R = matrix(NA, n+1, 107)
Footing_3R[,1:107] = xsu_x[,1260:1366]
Footing_3suR = matrix(NA, n, 107)
Footing_3suR = Footing_3R[-1,]
su_3R = matrix(NA,n,1)
k=0
for (i in 1:n) {
  k=k+1
  su_3R[k,] = mean(Footing_3suR[k,])
}

#Footing 4 extends from x = 32.225 to 34.35

Footing_4 = matrix(NA, n+1, 107)
Footing_4[,1:107] = xsu_x[,1612:1718]
Footing_4su = matrix(NA, n, 107)
Footing_4su = Footing_4[-1,]

```

```

su_4 = matrix(NA,n,1)
k=0
for (i in 1:n) {
  k=k+1
  su_4[k,] = mean(Footing_4su[k,])
}

#Footing 4L (left of footing) extends from x = 30.1 to 32.225
Footing_4L = matrix(NA, n+1, 107)
Footing_4L[,1:107] = xsu_x[,1506:1612]
Footing_4suL = matrix(NA, n, 107)
Footing_4suL = Footing_4L[-1,]
su_4L = matrix(NA,n,1)
k=0
for (i in 1:n) {
  k=k+1
  su_4L[k,] = mean(Footing_4suL[k,])
}

#Footing 4R (right of footing) extends from x = 34.34 to 36.475
Footing_4R = matrix(NA, n+1, 107)
Footing_4R[,1:107] = xsu_x[,1718:1824]
Footing_4suR = matrix(NA, n, 107)
Footing_4suR = Footing_4R[-1,]
su_4R = matrix(NA,n,1)
k=0
for (i in 1:n) {
  k=k+1
  su_4R[k,] = mean(Footing_4suR[k,])
}

#Footing 5 extends from x = 41.6 to 43.275

Footing_5 = matrix(NA, n+1, 85)
Footing_5[,1:85] = xsu_x[,2081:2165]
Footing_5su = matrix(NA, n, 85)
Footing_5su = Footing_5[-1,]

```



```

su_5 = matrix(NA,n,1)
k=0
for (i in 1:n) {
  k=k+1
  su_5[k,] = mean(Footing_5su[k,])
}

#Footing 5L (left of footing) extends from x = 39.925 to 41.6
Footing_5L = matrix(NA, n+1, 85)
Footing_5L[,1:85] = xsu_x[,1997:2081]
Footing_5suL = matrix(NA, n, 85)
Footing_5suL = Footing_5L[-1,]
su_5L = matrix(NA,n,1)
k=0
for (i in 1:n) {
  k=k+1
  su_5L[k,] = mean(Footing_5suL[k,])
}

#Footing 5R (right of footing) extends from x = 43.275 to 44.95
Footing_5R = matrix(NA, n+1, 85)
Footing_5R[,1:85] = xsu_x[,2165:2249]
Footing_5suR = matrix(NA, n, 85)
Footing_5suR = Footing_5R[-1,]
su_5R = matrix(NA,n,1)
k=0
for (i in 1:n) {
  k=k+1
  su_5R[k,] = mean(Footing_5suR[k,])
}

#Populate OpenSees matrix with footing su values
OpenSees[,"su_1"]=c(su_1)
OpenSees[,"su_1L"]=c(su_1L)
OpenSees[,"su_1R"]=c(su_1R)

OpenSees[,"su_2"]=c(su_2)

```

```
OpenSees[,"su_2L"]=c(su_2L)
OpenSees[,"su_2R"]=c(su_2R)
```

```
OpenSees[,"su_3"]=c(su_3)
OpenSees[,"su_3L"]=c(su_3L)
OpenSees[,"su_3R"]=c(su_3R)
```

```
OpenSees[,"su_4"]=c(su_4)
OpenSees[,"su_4L"]=c(su_4L)
OpenSees[,"su_4R"]=c(su_4R)
```

```
OpenSees[,"su_5"]=c(su_5)
OpenSees[,"su_5L"]=c(su_5L)
OpenSees[,"su_5R"]=c(su_5R)
```

#### #FOOTING 1

```
#Calculate bearing capacity for a given footing and undrained cohesive soil conditions
#set footing parameters (in units of meters) - width B, length L, depth Df, water
depth Dw
```

```
B_1 = B_outside
B_1_prime = B_outside_prime
L_1 = B_outside
Df_1 = 0.6
Dw_1 = 2.4
```

```
#Spring and gap parameters for vertical and horizontal spring models
```

```
SpringNo.1 = 101
Gap_V_1 = 0
Gap_H_1 = 0.000000000001
```

```
OpenSees[,"B_1"]=c(B_1)
OpenSees[,"Df_1"]=c(Df_1)
OpenSees[,"SpringNo.1"]=c(SpringNo.1)
OpenSees[,"Gap_V_1"]=c(Gap_V_1)
OpenSees[,"Gap_H_1"]=c(Gap_H_1)
```

```
#set soil parameters - undrained shear strength su (kPa), unit weight gamma
(kN/m^3), water unit weight gamma_water (kN/m^3)
```

```

#su for bearing is defined as su_1 from above
gamma = 19.0
gamma_water = 9.81

#set initial elastic modulus, Ei (kPa), and poissons ratio, nu. Nu assumes
undrained loading
#Ei is based on Strahler & Stuedlein (2013) fitting: Ei/ATM = 11(OCR)+33.
Assme OCR = 8
ATM = 101.325
OCR = 8
Ei = ATM*(11*OCR+33)
nu = 0.50

#set bearing capacity parameters
Nc = 5.14
sc_1 = 1.+0.2*B_1/L_1
if(Df_1<B_1) {
dc_1 = 1.+0.4*Df_1/B_1
} else {
dc_1 = 1.+0.4*atan(Df_1/B_1)*pi/180
}
Nq = 1.
sq = 1.
dq = 1.

#Calculate bearing capacity, q_ult (kPa)
q_ult_1 = matrix(NA, n, 1)
k=0
for (i in 1:n) {
k=k+1
if(Dw_1<Df_1) {
q_ult_1[k,] = su_1[k,]*Nc*sc_1*dc_1+((gamma*Df_1)-(Df_1-
Dw_1)*(gamma-gamma_water))*Nq*sq*sc_1
} else {
q_ult_1[k,] = su_1[k,]*Nc*sc_1*dc_1+gamma*Df_1*Nq*sq*dq
}
}
}

```

```

Q_ult_1 = matrix(NA, n, 1)
  k=0
  for (i in 1:n) {
    k=k+1
    Q_ult_1[k,] = q_ult_1[k,]*B_1*L_1
  }

```

```

#Generate random values for normalized bearing capacity - i.e., "actual" bearing
#This step is done first to establish the number of revised simulations (##not revising
simulations)

```

```

#THIS IS THE UPDATE - NO RANDOM q_ult

```

```

#The unit mean bearing capacity, qult, has parameters of the bias calculated from
the dataset

```

```

#with unit mean=1.25 and COV=0.37

```

```

#The bias is closest to a gamma distribution - define parameters and generate n
random values

```

```

#qult_shape_1 = 7.52698348510156

```

```

#qult_rate_1 = 1/0.166593308846615

```

```

#qult_1 = matrix(rgamma(n, shape=qult_shape_1, rate=qult_rate_1),n,1)

```

```

#Generate random values of q_ult based on the calculated value and noted distribution

```

```

#q_ult_rnd_1 = matrix(c(q_ult_1*qult_1), n, 1)

```

```

q_ult_rnd_1 = q_ult_1

```

```

Q_ult_rnd_1 = matrix(NA, n, 1)

```

```

  k=0

```

```

  for (i in 1:n) {

```

```

    k=k+1

```

```

    Q_ult_rnd_1[k,] = q_ult_rnd_1[k,]*B_1*L_1

```

```

  }

```

```

#Generate uniformly distributed ranked values that will be transformed to the k1, k2 and
mstc parameters

```

```

#to simulate ranked parameters using copula data

```

```

#(make sure CDVine package is loaded)

```

```

family=c(33,33,16)
par=c(-7.053976, -3.142653, 1.397515)
u_sims_1 = CDVineSim(N=n, family=family, par=par, type=1)
u1_sim_1 = u_sims_1[,1]
u2_sim_1 = u_sims_1[,2]
um_sim_1 = u_sims_1[,3]

#Transform u1, u2 and um into k1, k2 and mstc sims using known marginal
distributions
#The u simulations represent the cumulative distribution, so we need inverse CDF
or quantile (q) dist.

#k1 is best fit to gamma distribution
k1_shape_1 = 3.71590850943956
k1_rate_1 = 1/0.003433101851711
k1_1 = matrix(qgamma(u1_sim_1, shape=k1_shape_1, rate=k1_rate_1), n, 1)

#k2 is best fit to inv. gaussian distribution (need to make sure SuppDists package
is loaded)
k2_nu_1 = 0.701447
k2_lambda_1 = 27.91919
k2_1 = matrix(qinvGauss(u2_sim_1, nu=k2_nu_1, lambda=k2_lambda_1), n, 1)

#mstc is best fit to lognormal distribution
mstc_mean_1 = 0.643048649204319
mstc_stdev_1 = 0.123128154098121
mstc_LN_stdev_1 = sqrt(log(1+(mstc_stdev_1^2/mstc_mean_1^2)))
mstc_LN_mean_1 = log(mstc_mean_1)-0.5*(mstc_LN_stdev_1)^2
mstc_1 = matrix(qlnorm(um_sim_1, meanlog=mstc_LN_mean_1,
sdlog=mstc_LN_stdev_1), n, 1)

OpenSees[,"k1_1"]=c(k1_1)
OpenSees[,"k2_1"]=c(k2_1)
OpenSees_trunc[,"k1_1"]=c(k1_1)
OpenSees_trunc[,"k2_1"]=c(k2_1)

#Calculate the reference capacity, q_stc = mstc*q_ult

```



$$F2 = 2 * \log_{10} \left( \frac{2 * (J1 + \sqrt{1 + J1^2})}{(J1 + J2) + \sqrt{4 + (J1 + J2)^2}} \right) + (J1 - J2) * \log_{10} \left( \frac{2 + \sqrt{4 + (J1 + J2)^2}}{(J1 + J2)} \right) - (J1^2 * (\sqrt{4 + (J1 + J2)^2} / (J1 + J2)) - (\sqrt{1 + J1^2} / J1))$$

$$F3 = - 2 * J1 * \log_{10} \left( \frac{J1}{(1 + \sqrt{1 + J1^2})} \right) + (J1 + J2) * \log_{10} \left( \frac{(J1 + J2)}{(2 + \sqrt{4 + (J1 + J2)^2})} \right) - \log_{10} \left( \frac{((J1 + J2) + \sqrt{4 + (J1 + J2)^2})}{(2 * (J1 + \sqrt{1 + J1^2}))} \right) + ((J1 + J2) / 4) * (\sqrt{4 + (J1 + J2)^2} - (J1 + J2)) - J1 * (\sqrt{1 + J1^2} - J1)$$

$$F4 = - 2 * \log_{10} \left( \frac{2 * (J2 + \sqrt{1 + J2^2})}{(J1 + J2) + \sqrt{4 + (J1 + J2)^2}} \right) + (J1 - J2) * \log_{10} \left( \frac{2 + \sqrt{4 + (J1 + J2)^2}}{(J1 + J2)} \right) + (J2^2 * (\sqrt{4 + (J1 + J2)^2} / (J1 + J2)) - \sqrt{1 + J2^2} / J2)$$

$$F5 = 2 * J2 * \log_{10} \left( \frac{J2}{(1 + \sqrt{1 + J2^2})} \right) - (J1 + J2) * \log_{10} \left( \frac{(J1 + J2)}{(2 + \sqrt{4 + (J1 + J2)^2})} \right) + \log_{10} \left( \frac{((J1 + J2) + \sqrt{4 + (J1 + J2)^2})}{(2 * (J2 + \sqrt{1 + J2^2}))} \right) - ((J1 + J2) / 4) * (\sqrt{4 + (J1 + J2)^2} - (J1 + J2)) - J2 * (J2 - \sqrt{1 + J2^2})$$

#Calculate K\_max(bottom corner) and K\_max(top corner), then average to get K\_max

$$K\_maxb\_1 = (32.0 * \pi * E_i * (1 - \nu) * Df\_1) / ((1 + \nu) * ((3.0 - 4.0 * \nu) * F1 + F2 + 4.0 * (1.0 - 2.0 * \nu) * (1.0 - \nu) * F3))$$

$$K\_max\_1 = (32.0 * \pi * E_i * (1 - \nu) * Df\_1) / ((1 + \nu) * ((3.0 - 4.0 * \nu) * F1 + F4 + 4.0 * (1.0 - 2.0 * \nu) * (1.0 - \nu) * F5))$$

$$K\_max\_1 = (K\_maxb\_1 + K\_max\_1) / 2.0$$

OpenSees[,"Kmax\_1"]=c(K\_max\_1)

OpenSees[,"Kur\_1"]=c(K\_max\_1)

#Input "failure ratio" Rf. Duncan & Mokwa indicate a range from 0.75 to 0.95 and use average Rf= 0.85

$$Rf\_1 = 0.85$$

OpenSees[,"Rf\_1"]=c(Rf\_1)

#Estimate the ultimate passive resistance, P\_ult (or F\_ult in OpenSees model)

#P\_ult\_L is calculated for the passive resistance on the left side of the footing

#P\_ult\_R is calculated for the passive resistance on the right side of the footing

#Calculate unit active force, Pa (kN/unit width). Assume it is zero if Df < Hc (critical height)

#Left of footing

$$Hc\_1L = \text{matrix}(NA, n, 1)$$

$$k=0$$

```

    for (i in 1:n) {
      k=k+1
      Hc_1L[k,] = 4*su_1L[k,]/gamma
    }

Pa_1L = matrix(NA, n, 1)
  k=0
  for (i in 1:n) {
    k=k+1
    if(Hc_1L[k,]<Df_1) {
      Pa_1L[k,] = 0.5*gamma*Df_1^2+2*su_1L[k,]*Df_1
    } else {
      Pa_1L[k,] = 0
    }
  }

#Calculate unit passive force, Pp (kN/unit width)

Pp_1L = matrix(NA, n, 1)
  k=0
  for (i in 1:n) {
    k=k+1
    Pp_1L[k,] = 0.5*gamma*Df_1^2+2*su_1L[k,]*Df_1
  }

#Calculate ultimate passive force, P_ult (kN), including 3D effects

P_ult_1L = matrix(NA, n, 1)
  k=0
  for (i in 1:n) {
    k=k+1
    P_ult_1L[k,] = L_1*(Pp_1L[k,]-Pa_1L[k,])+2*su_1L[k,]*Df_1^2
  }

OpenSees[,"P_ult_1L"]=c(P_ult_1L)
OpenSees_trunc[,"P_ult_1L"]=c(P_ult_1L)

```



```

#Right of footing
Hc_1R = matrix(NA, n, 1)
  k=0
  for (i in 1:n) {
    k=k+1
    Hc_1R[k,] = 4*su_1R[k,]/gamma
  }

Pa_1R = matrix(NA, n, 1)
  k=0
  for (i in 1:n) {
    k=k+1
    if(Hc_1R[k,]<Df_1) {
      Pa_1R[k,] = 0.5*gamma*Df_1^2+2*su_1R[k,]*Df_1
    } else {
      Pa_1R[k,] = 0
    }
  }

#Calculate unit passive force, Pp (kN/unit width)

Pp_1R = matrix(NA, n, 1)
  k=0
  for (i in 1:n) {
    k=k+1
    Pp_1R[k,] = 0.5*gamma*Df_1^2+2*su_1R[k,]*Df_1
  }

#Calculate ultimate passive force, P_ult (kN), including 3D effects

P_ult_1R = matrix(NA, n, 1)
  k=0
  for (i in 1:n) {
    k=k+1
    P_ult_1R[k,] = L_1*(Pp_1R[k,]-Pa_1R[k,])+2*su_1R[k,]*Df_1^2
  }

```

```

OpenSees[,"P_ult_1R"]=c(P_ult_1R)
OpenSees_trunc[,"P_ult_1R"]=c(P_ult_1R)

#FOOTING 2
#Calculate bearing capacity for a given footing and undrained cohesive soil conditions
  #set footing parameters (in units of meters) - width B, length L, depth Df, water
depth Dw
  B_2 = B_inside
  B_2_prime = B_outside_prime
  L_2 = B_inside
  Df_2 = 0.6
  Dw_2 = 2.4

  #Spring and gap parameters for vertical and horizontal spring models
  SpringNo.2 = 101
  Gap_V_2 = 0
  Gap_H_2 = 0.000000000001

  OpenSees[,"B_2"]=c(B_2)
  OpenSees[,"Df_2"]=c(Df_2)
  OpenSees[,"SpringNo.2"]=c(SpringNo.2)
  OpenSees[,"Gap_V_2"]=c(Gap_V_2)
  OpenSees[,"Gap_H_2"]=c(Gap_H_2)

  #set soil parameters - undrained shear strength su (kPa), unit weight gamma
(kN/m^3), water unit weight gamma_water (kN/m^3)
  #su is defined as su_2 from above
  gamma = 19.0
  gamma_water = 9.81

  #set initial elastic modulus, Ei (kPa), and poissons ratio, nu. Nu assumes
undrained loading
  #Ei is based on Strahler & Stuedlein (2013) fitting: Ei/ATM = 11(OCR)+33.
Assme OCR = 8
  ATM = 101.325
  OCR = 8
  Ei = ATM*(11*OCR+33)
  nu = 0.50

```

```

#set bearing capacity parameters
Nc = 5.14
sc_2 = 1.+0.2*B_2/L_2
if(Df_2<B_2) {
dc_2 = 1.+0.4*Df_2/B_2
  } else {
  dc_2 = 1.+0.4*atan(Df_2/B_2)*pi/180
  }
Nq = 1.
sq = 1.
dq = 1.

#Calculate bearing capacity, q_ult (kPa)
q_ult_2 = matrix(NA, n, 1)
  k=0
  for (i in 1:n) {
    k=k+1
    if(Dw_2<Df_2) {
      q_ult_2[k,] = su_2[k,]*Nc*sc_2*dc_2+((gamma*Df_2)-(Df_2-
Dw_2)*(gamma-gamma_water))*Nq*sq*sc_2
    } else {
      q_ult_2[k,] = su_2[k,]*Nc*sc_2*dc_2+gamma*Df_2*Nq*sq*dq
    }
  }

Q_ult_2 = matrix(NA, n, 1)
  k=0
  for (i in 1:n) {
    k=k+1
    Q_ult_2[k,] = q_ult_2[k,]*B_2*L_2
  }

#Generate random values for normalized bearing capacity - i.e., "actual" bearing
#This step is done first to establish the number of revised simulations (##not revising
simulations)
#THIS IS THE UPDATE

```

```

#The unit mean bearing capacity, qult, has parameters of the bias calculated from
the dataset
#with unit mean=1.25 and COV=0.37
#The bias is closest to a gamma distribution - define parameters and generate n
random values
#qult_shape_2 = 7.52698348510156
#qult_rate_2 = 1/0.166593308846615
#qult_2 = matrix(rgamma(n, shape=qult_shape_2, rate=qult_rate_2),n,1)

#Generate random values of q_ult based on the calculated value and noted distribution
#NOT RANDOM NOW

#q_ult_rnd_2 = matrix(c(q_ult_2*qult_2), n, 1)
q_ult_rnd_2 = q_ult_2

Q_ult_rnd_2 = matrix(NA, n, 1)
  k=0
  for (i in 1:n) {
    k=k+1
    Q_ult_rnd_2[k,] = q_ult_rnd_2[k,]*B_2*L_2
  }

#Generate uniformly distributed ranked values that will be transformed to the k1, k2 and
mstc parameters

#to simulate ranked parameters using copula data
#(make sure CDVine package is loaded)
family=c(33,33,16)
par=c(-7.053976, -3.142653, 1.397515)
u_sims_2 = CDVineSim(N=n, family=family, par=par, type=1)
u1_sim_2 = u_sims_2[,1]
u2_sim_2 = u_sims_2[,2]
um_sim_2 = u_sims_2[,3]

#Transform u1, u2 and um into k1, k2 and mstc sims using known marginal
distributions
#The u simulations represent the cumulative distribution, so we need inverse CDF
or quantile (q) dist.

```

```

#k1 is best fit to gamma distribution
k1_shape_2 = 3.71590850943956
k1_rate_2 = 1/0.003433101851711
k1_2 = matrix(qgamma(u1_sim_2, shape=k1_shape_2, rate=k1_rate_2), n, 1)

#k2 is best fit to inv. gaussian distribution (need to make sure SuppDists package
is loaded)
k2_nu_2 = 0.701447
k2_lambda_2 = 27.91919
k2_2 = matrix(qinvGauss(u2_sim_2, nu=k2_nu_2, lambda=k2_lambda_2), n, 1)

#mstc is best fit to lognormal distribution
mstc_mean_2 = 0.643048649204319
mstc_stdev_2 = 0.123128154098121
mstc_LN_stdev_2 = sqrt(log(1+(mstc_stdev_2^2/mstc_mean_2^2)))
mstc_LN_mean_2 = log(mstc_mean_2)-0.5*(mstc_LN_stdev_2)^2
mstc_2 = matrix(qlnorm(um_sim_2, meanlog=mstc_LN_mean_2,
sdlog=mstc_LN_stdev_2), n, 1)

OpenSees[,"k1_2"]=c(k1_2)
OpenSees[,"k2_2"]=c(k2_2)
OpenSees_trunc[,"k1_2"]=c(k1_2)
OpenSees_trunc[,"k2_2"]=c(k2_2)

#Calculate the reference capacity, q_stc = mstc*q_ult

q_stc_2 = matrix(NA, n, 1)
  k=0
  for (i in 1:n) {
    k=k+1
    q_stc_2[k,] = mstc_2[k,]*q_ult_rnd_2[k,]
  }

Q_stc_2 = matrix(NA, n, 1)
  k=0
  for (i in 1:n) {
    k=k+1

```



```

#Calculate K_max(bottom corner) and K_max(top corner), then average to get
K_max
K_maxb_2 = (32.0*pi*Ei*(1-nu)*Df_2)/((1+nu)*((3.0-4.0*nu)*F1+F2+4.0*(1.0-
2.0*nu)*(1.0-nu)*F3))
K_maxt_2 = (32.0*pi*Ei*(1-nu)*Df_2)/((1+nu)*((3.0-4.0*nu)*F1+F4+4.0*(1.0-
2.0*nu)*(1.0-nu)*F5))
K_max_2 = (K_maxb_2+K_maxt_2)/2.0

OpenSees[,"Kmax_2"]=c(K_max_2)
OpenSees[,"Kur_2"]=c(K_max_2)

#Input "failure ratio" Rf. Duncan & Mokwa indicate a range from 0.75 to 0.95
and use average Rf= 0.85
Rf_2 = 0.85

OpenSees[,"Rf_2"]=c(Rf_2)

#Estimate the ultimate passive resistance, P_ult (or F_ult in OpenSees model)
#P_ult_L is calculated for the passive resistance on the left side of the footing
#P_ult_R is calculated for the passive resistance on the right side of the footing
#Calculate unit active force, Pa (kN/unit width). Assume it is zero if Df<Hc
(critical height)

#Left of footing
Hc_2L = matrix(NA, n, 1)
k=0
for (i in 1:n) {
k=k+1
Hc_2L[k,] = 4*su_2L[k,]/gamma
}

Pa_2L = matrix(NA, n, 1)
k=0
for (i in 1:n) {
k=k+1
if(Hc_2L[k,]<Df_2) {
Pa_2L[k,] = 0.5*gamma*Df_2^2+2*su_2L[k,]*Df_2
} else {

```

```

Pa_2L[k,] = 0
}
}

```

#Calculate unit passive force, Pp (kN/unit width)

```

Pp_2L = matrix(NA, n, 1)
k=0
for (i in 1:n) {
k=k+1
Pp_2L[k,] = 0.5*gamma*Df_2^2+2*su_2L[k,]*Df_2
}

```

#Calculate ultimate passive force, P\_ult (kN), including 3D effects

```

P_ult_2L = matrix(NA, n, 1)
k=0
for (i in 1:n) {
k=k+1
P_ult_2L[k,] = L_2*(Pp_2L[k,]-Pa_2L[k,])+2*su_2L[k,]*Df_2^2
}

```

```

OpenSees[,"P_ult_2L"]=c(P_ult_2L)
OpenSees_trunc[,"P_ult_2L"]=c(P_ult_2L)

```

#Right of footing

```

Hc_2R = matrix(NA, n, 1)
k=0
for (i in 1:n) {
k=k+1
Hc_2R[k,] = 4*su_2R[k,]/gamma
}

```

```

Pa_2R = matrix(NA, n, 1)
k=0
for (i in 1:n) {
k=k+1

```



```

        if(Hc_2R[k,]<Df_2) {
            Pa_2R[k,] = 0.5*gamma*Df_2^2+2*su_2R[k,]*Df_2
        } else {
            Pa_2R[k,] = 0
        }
    }
}

```

#Calculate unit passive force, Pp (kN/unit width)

```

Pp_2R = matrix(NA, n, 1)
k=0
for (i in 1:n) {
    k=k+1
    Pp_2R[k,] = 0.5*gamma*Df_2^2+2*su_2R[k,]*Df_2
}

```

#Calculate ultimate passive force, P\_ult (kN), including 3D effects

```

P_ult_2R = matrix(NA, n, 1)
k=0
for (i in 1:n) {
    k=k+1
    P_ult_2R[k,] = L_2*(Pp_2R[k,]-Pa_2R[k,])+2*su_2R[k,]*Df_2^2
}

```

```

OpenSees["P_ult_2R"]=c(P_ult_2R)
OpenSees_trunc["P_ult_2R"]=c(P_ult_2R)

```

#FOOTING 3

#Calculate bearing capacity for a given footing and undrained cohesive soil conditions

#set footing parameters (in units of meters) - width B, length L, depth Df, water depth Dw

```

B_3 = B_inside
B_3_prime = B_outside_prime
L_3 = B_inside
Df_3 = 0.6
Dw_3 = 2.4

```

```

#Spring and gap parameters for vertical and horizontal spring models
SpringNo.3 = 101
Gap_V_3 = 0
Gap_H_3 = 0.000000000001

OpenSees[,"B_3"]=c(B_3)
OpenSees[,"Df_3"]=c(Df_3)
OpenSees[,"SpringNo.3"]=c(SpringNo.3)
OpenSees[,"Gap_V_3"]=c(Gap_V_3)
OpenSees[,"Gap_H_3"]=c(Gap_H_3)

#set soil parameters - undrained shear strength su (kPa), unit weight gamma
(kN/m^3), water unit weight gamma_water (kN/m^3)
#su is defined as su_3 from above
gamma = 19.0
gamma_water = 9.81

#set initial elastic modulus, Ei (kPa), and poissons ratio, nu. Nu assumes
undrained loading
#Ei is based on Strahler & Stuedlein (2013) fitting: Ei/ATM = 11(OCR)+33.
Assme OCR = 8
ATM = 101.325
OCR = 8
Ei = ATM*(11*OCR+33)
nu = 0.50

#set bearing capacity parameters
Nc = 5.14
sc_3 = 1.+0.2*B_3/L_3
if(Df_3<B_3) {
dc_3 = 1.+0.4*Df_3/B_3
} else {
dc_3 = 1.+0.4*atan(Df_3/B_3)*pi/180
}
Nq = 1.
sq = 1.
dq = 1.

```

```

#Calculate bearing capacity, q_ult (kPa)
q_ult_3 = matrix(NA, n, 1)
  k=0
  for (i in 1:n) {
    k=k+1
    if(Dw_3<Df_3) {
      q_ult_3[k,] = su_3[k,]*Nc*sc_3*dc_3+((gamma*Df_3)-(Df_3-
Dw_3)*(gamma-gamma_water))*Nq*sq*sc_3
    } else {
      q_ult_3[k,] = su_3[k,]*Nc*sc_3*dc_3+gamma*Df_3*Nq*sq*dq
    }
  }

Q_ult_3 = matrix(NA, n, 1)
  k=0
  for (i in 1:n) {
    k=k+1
    Q_ult_3[k,] = q_ult_3[k,]*B_3*L_3
  }

#Generate random values for normalized bearing capacity - i.e., "actual" bearing
#This step is done first to establish the number of revised simulations (##not revising
simulations)
#THIS IS THE UPDATE FOR FOOTING 3

  #The unit mean bearing capacity, qult, has parameters of the bias calculated from
the dataset
  #with unit mean=1.25 and COV=0.37
  #The bias is closest to a gamma distribution - define parameters and generate n
random values
  #qult_shape_3 = 7.52698348510156
  #qult_rate_3 = 1/0.166593308846615
  #qult_3 = matrix(rgamma(n, shape=qult_shape_3, rate=qult_rate_3),n,1)

#Generate random values of q_ult based on the calculated value and noted distribution

  #q_ult_rnd_3 = matrix(c(q_ult_3*qult_3), n, 1)
  q_ult_rnd_3 = q_ult_3

```

```

Q_ult_rnd_3 = matrix(NA, n, 1)
  k=0
  for (i in 1:n) {
    k=k+1
    Q_ult_rnd_3[k,] = q_ult_rnd_3[k,]*B_3*L_3
  }

```

#Generate uniformly distributed ranked values that will be transformed to the k1, k2 and mstc parameters

```

#to simulate ranked parameters using copula data
#(make sure CDVine package is loaded)
family=c(33,33,16)
par=c(-7.053976, -3.142653, 1.397515)
u_sims_3 = CDVineSim(N=n, family=family, par=par, type=1)
u1_sim_3 = u_sims_3[,1]
u2_sim_3 = u_sims_3[,2]
um_sim_3 = u_sims_3[,3]

```

#Transform u1, u2 and um into k1, k2 and mstc sims using known marginal distributions

#The u simulations represent the cumulative distribution, so we need inverse CDF or quantile (q) dist.

```

#k1 is best fit to gamma distribution
k1_shape_3 = 3.71590850943956
k1_rate_3 = 1/0.003433101851711
k1_3 = matrix(qgamma(u1_sim_3, shape=k1_shape_3, rate=k1_rate_3), n, 1)

```

#k2 is best fit to inv. gaussian distribution (need to make sure SuppDists package is loaded)

```

k2_nu_3 = 0.701447
k2_lambda_3 = 27.91919
k2_3 = matrix(qinvGauss(u2_sim_3, nu=k2_nu_3, lambda=k2_lambda_3), n, 1)

```

#mstc is best fit to lognormal distribution

```

mstc_mean_3 = 0.643048649204319

```

```

mstc_stdev_3 = 0.123128154098121
mstc_LN_stdev_3 = sqrt(log(1+(mstc_stdev_3^2/mstc_mean_3^2)))
mstc_LN_mean_3 = log(mstc_mean_3)-0.5*(mstc_LN_stdev_3)^2
mstc_3 = matrix(qlnorm(um_sim_3, meanlog=mstc_LN_mean_3,
sdlog=mstc_LN_stdev_3), n, 1)

OpenSees[,"k1_3"]=c(k1_3)
OpenSees[,"k2_3"]=c(k2_3)
OpenSees_trunc[,"k1_3"]=c(k1_3)
OpenSees_trunc[,"k2_3"]=c(k2_3)

#Calculate the reference capacity, q_stc = mstc*q_ult

q_stc_3 = matrix(NA, n, 1)
  k=0
  for (i in 1:n) {
    k=k+1
    q_stc_3[k,] = mstc_3[k,]*q_ult_rnd_3[k,]
  }

Q_stc_3 = matrix(NA, n, 1)
  k=0
  for (i in 1:n) {
    k=k+1
    Q_stc_3[k,] = q_stc_3[k,]*B_3*L_3
  }

OpenSees[,"q_stc_3"]=c(q_stc_3)
OpenSees_trunc[,"q_stc_3"]=c(q_stc_3)

#Generate values for Hyperbolic Gap (i.e., horizontal spring) - Duncan & Mokwa (2001)
Eq.4

#Initial stiffness, K_max, is generated based on Douglas & Davis (1964) Eq. 8
#See spreadsheet - "Duncan Mokwa Horizontal Displacement Calculation" to
check values

```



```

OpenSees[,"Rf_3"]=c(Rf_3)

#Estimate the ultimate passive resistance, P_ult (or F_ult in OpenSees model)
#P_ult_L is calculated for the passive resistance on the left side of the footing
#P_ult_R is calculated for the passive resistance on the right side of the footing
#Calculate unit active force, Pa (kN/unit width). Assume it is zero if Df<Hc
(critical height)

#Left of footing
Hc_3L = matrix(NA, n, 1)
  k=0
  for (i in 1:n) {
    k=k+1
    Hc_3L[k,] = 4*su_3L[k,]/gamma
  }

Pa_3L = matrix(NA, n, 1)
  k=0
  for (i in 1:n) {
    k=k+1
    if(Hc_3L[k,]<Df_3) {
      Pa_3L[k,] = 0.5*gamma*Df_3^2+2*su_3L[k,]*Df_3
    } else {
      Pa_3L[k,] = 0
    }
  }

#Calculate unit passive force, Pp (kN/unit width)

Pp_3L = matrix(NA, n, 1)
  k=0
  for (i in 1:n) {
    k=k+1
    Pp_3L[k,] = 0.5*gamma*Df_3^2+2*su_3L[k,]*Df_3
  }

#Calculate ultimate passive force, P_ult (kN), including 3D effects

```

```

P_ult_3L = matrix(NA, n, 1)
  k=0
  for (i in 1:n) {
    k=k+1
    P_ult_3L[k,] = L_3*(Pp_3L[k,]-Pa_3L[k,])+2*su_3L[k,]*Df_3^2
  }

OpenSees[,"P_ult_3L"]=c(P_ult_3L)
OpenSees_trunc[,"P_ult_3L"]=c(P_ult_3L)

#Right of footing
Hc_3R = matrix(NA, n, 1)
  k=0
  for (i in 1:n) {
    k=k+1
    Hc_3R[k,] = 4*su_3R[k,]/gamma
  }

Pa_3R = matrix(NA, n, 1)
  k=0
  for (i in 1:n) {
    k=k+1
    if(Hc_3R[k,]<Df_3) {
      Pa_3R[k,] = 0.5*gamma*Df_3^2+2*su_3R[k,]*Df_3
    } else {
      Pa_3R[k,] = 0
    }
  }

#Calculate unit passive force, Pp (kN/unit width)

Pp_3R = matrix(NA, n, 1)
  k=0
  for (i in 1:n) {
    k=k+1
    Pp_3R[k,] = 0.5*gamma*Df_3^2+2*su_3R[k,]*Df_3
  }

```



```

    }

#Calculate ultimate passive force, P_ult (kN), including 3D effects

P_ult_3R = matrix(NA, n, 1)
  k=0
  for (i in 1:n) {
    k=k+1
    P_ult_3R[k,] = L_3*(Pp_3R[k,]-Pa_3R[k,])+2*su_3R[k,]*Df_3^2
  }

OpenSees[,"P_ult_3R"]=c(P_ult_3R)
OpenSees_trunc[,"P_ult_3R"]=c(P_ult_3R)

#FOOTING 4
#Calculate bearing capacity for a given footing and undrained cohesive soil conditions
  #set footing parameters (in units of meters) - width B, length L, depth Df, water
depth Dw
  B_4 = B_inside
  B_4_prime = B_outside_prime
  L_4 = B_inside
  Df_4 = 0.6
  Dw_4 = 2.4

#Spring and gap parameters for vertical and horizontal spring models
SpringNo.4 = 101
Gap_V_4 = 0
Gap_H_4 = 0.000000000001

OpenSees[,"B_4"]=c(B_4)
OpenSees[,"Df_4"]=c(Df_4)
OpenSees[,"SpringNo.4"]=c(SpringNo.4)
OpenSees[,"Gap_V_4"]=c(Gap_V_4)
OpenSees[,"Gap_H_4"]=c(Gap_H_4)

  #set soil parameters - undrained shear strength su (kPa), unit weight gamma
(kN/m^3), water unit weight gamma_water (kN/m^3)
  #su is defined as su_4 from above

```

```

gamma = 19.0
gamma_water = 9.81

#set initial elastic modulus, Ei (kPa), and poissons ratio, nu. Nu assumes
undrained loading
#Ei is based on Strahler & Stuedlein (2013) fitting: Ei/ATM = 11(OCR)+33.
Assme OCR = 8
ATM = 101.325
OCR = 8
Ei = ATM*(11*OCR+33)
nu = 0.50

#set bearing capacity parameters
Nc = 5.14
sc_4 = 1.+0.2*B_4/L_4
if(Df_4<B_4) {
dc_4 = 1.+0.4*Df_4/B_4
} else {
dc_4 = 1.+0.4*atan(Df_4/B_4)*pi/180
}
Nq = 1.
sq = 1.
dq = 1.

#Calculate bearing capacity, q_ult (kPa)
q_ult_4 = matrix(NA, n, 1)
k=0
for (i in 1:n) {
k=k+1
if(Dw_4<Df_4) {
q_ult_4[k,] = su_4[k,]*Nc*sc_4*dc_4+((gamma*Df_4)-(Df_4-
Dw_4)*(gamma-gamma_water))*Nq*sq*sc_4
} else {
q_ult_4[k,] = su_4[k,]*Nc*sc_4*dc_4+gamma*Df_4*Nq*sq*dq
}
}

Q_ult_4 = matrix(NA, n, 1)

```

```

k=0
for (i in 1:n) {
k=k+1
Q_ult_4[k,] = q_ult_4[k,]*B_4*L_4
}

```

#Generate random values for normalized bearing capacity - i.e., "actual" bearing  
 #This step is done first to establish the number of revised simulations (##not revising  
 simulations)

#THIS IS THE UPDATE FOR FOOTING 4

#The unit mean bearing capacity, qult, has parameters of the bias calculated from  
 the dataset

#with unit mean=1.25 and COV=0.37

#The bias is closest to a gamma distribution - define parameters and generate n  
 random values

#qult\_shape\_4 = 7.52698348510156

#qult\_rate\_4 = 1/0.166593308846615

#qult\_4 = matrix(rgamma(n, shape=qult\_shape\_4, rate=qult\_rate\_4),n,1)

#Generate random values of q\_ult based on the calculated value and noted distribution

#q\_ult\_rnd\_4 = matrix(c(q\_ult\_4\*qult\_4), n, 1)

q\_ult\_rnd\_4 = q\_ult\_4

Q\_ult\_rnd\_4 = matrix(NA, n, 1)

k=0

for (i in 1:n) {

k=k+1

Q\_ult\_rnd\_4[k,] = q\_ult\_rnd\_4[k,]\*B\_4\*L\_4

}

#Generate uniformly distributed ranked values that will be transformed to the k1, k2 and  
 mstc parameters

#to simulate ranked parameters using copula data

##(make sure CDVine package is loaded)

family=c(33,33,16)

```

par=c(-7.053976, -3.142653, 1.397515)
u_sims_4 = CDVineSim(N=n, family=family, par=par, type=1)
u1_sim_4 = u_sims_4[,1]
u2_sim_4 = u_sims_4[,2]
um_sim_4 = u_sims_4[,3]

#Transform u1, u2 and um into k1, k2 and mstc sims using known marginal
distributions
#The u simulations represent the cumulative distribution, so we need inverse CDF
or quantile (q) dist.

#k1 is best fit to gamma distribution
k1_shape_4 = 3.71590850943956
k1_rate_4 = 1/0.003433101851711
k1_4 = matrix(qgamma(u1_sim_4, shape=k1_shape_4, rate=k1_rate_4), n, 1)

#k2 is best fit to inv. guassian distribution (need to make sure SuppDists package
is loaded)
k2_nu_4 = 0.701447
k2_lambda_4 = 27.91919
k2_4 = matrix(qinvGauss(u2_sim_4, nu=k2_nu_4, lambda=k2_lambda_4), n, 1)

#mstc is best fit to lognormal distribution
mstc_mean_4 = 0.643048649204319
mstc_stdev_4 = 0.123128154098121
mstc_LN_stdev_4 = sqrt(log(1+(mstc_stdev_4^2/mstc_mean_4^2)))
mstc_LN_mean_4 = log(mstc_mean_4)-0.5*(mstc_LN_stdev_4)^2
mstc_4 = matrix(qlnorm(um_sim_4, meanlog=mstc_LN_mean_4,
sdlog=mstc_LN_stdev_4), n, 1)

OpenSees[,"k1_4"]=c(k1_4)
OpenSees[,"k2_4"]=c(k2_4)
OpenSees_trunc[,"k1_4"]=c(k1_4)
OpenSees_trunc[,"k2_4"]=c(k2_4)

#Calculate the reference capacity, q_stc = mstc*q_ult

q_stc_4 = matrix(NA, n, 1)

```

```

k=0
for (i in 1:n) {
k=k+1
q_stc_4[k,] = mstc_4[k,]*q_ult_rnd_4[k,]
}

```

```

Q_stc_4 = matrix(NA, n, 1)
k=0
for (i in 1:n) {
k=k+1
Q_stc_4[k,] = q_stc_4[k,]*B_4*L_4
}

```

```

OpenSees[, "q_stc_4"] = c(q_stc_4)
OpenSees_trunc[, "q_stc_4"] = c(q_stc_4)

```

#Generate values for Hyperbolic Gap (i.e., horizontal spring) - Duncan & Mokwa (2001) Eq.4

#Initial stiffness, K\_max, is generated based on Douglas & Davis (1964) Eq. 8  
 #See spreadsheet - "Duncan Mokwa Horizontal Displacement Calculation" to check values

#c1 and c2 are the bottom depth and top of the footing. This assumes c1=Df and c2=0 (no embedment). However, c2 has to be slightly greater than 0 or F4 and F5 don't compute

```

c1 = Df_4
c2 = 0.000000000000000000000001

```

#b, J1 and J2 are used to calculate constants F1 through F5

```

b = 0.5*L_4
J1 = 2.0*c1/b
J2 = 2.0*c2/b

```

#Calculate constants F1, F2, F3, F4, F5 for D&D Eq. 8 input

```

F1 = -(J1-J2)*log10((J1-J2)/(2+sqrt(4+(J1+J2)^2)))-2*log10(2/((J1-J2)+sqrt(4+(J1-J2)^2)))

```

```

F2 = 2*log10((2*(J1+sqrt(1+J1^2)))/((J1+J2)+sqrt(4+(J1+J2)^2)))+(J1-J2)*log10(2+sqrt(4+(J1+J2)^2)/(J1+J2))-(J1^2)*((sqrt(4+(J1+J2)^2)/(J1+J2))-(sqrt(1+J1^2)/J1))

```

```

F3 = -
2*J1*log10(J1/(1+sqrt(1+J1^2)))+(J1+J2)*log10((J1+J2)/(2+sqrt(4+(J1+J2)^2)))-
log10(((J1+J2)+sqrt(4+(J1+J2)^2))/(2*(J1+sqrt(1+J1^2))))+((J1+J2)/4)*(sqrt(4+(J1+J2)^
2)-(J1+J2))-J1*(sqrt(1+J1^2)-J1)
F4 = -2*log10((2*(J2+sqrt(1+J2^2)))/((J1+J2)+sqrt(4+(J1+J2)^2)))+(J1-
J2)*log10((2+sqrt(4+(J1+J2)^2))/(J1+J2))+(J2^2)*((sqrt(4+(J1+J2)^2)/(J1+J2))-
sqrt(1+J2^2)/J2)
F5 = 2*J2*log10(J2/(1+sqrt(1+J2^2)))-
(J1+J2)*log10((J1+J2)/(2+sqrt(4+(J1+J2)^2)))+log10(((J1+J2)+sqrt(4+(J1+J2)^2))/(2*(J
2+sqrt(1+J2^2))))-((J1+J2)/4)*(sqrt(4+(J1+J2)^2)-(J1+J2))-J2*(J2-sqrt(1+J2^2))

#Calculate K_max(bottom corner) and K_max(top corner), then average to get
K_max
K_maxb_4 = (32.0*pi*Ei*(1-nu)*Df_4)/((1+nu)*((3.0-4.0*nu)*F1+F2+4.0*(1.0-
2.0*nu)*(1.0-nu)*F3))
K_maxt_4 = (32.0*pi*Ei*(1-nu)*Df_4)/((1+nu)*((3.0-4.0*nu)*F1+F4+4.0*(1.0-
2.0*nu)*(1.0-nu)*F5))
K_max_4 = (K_maxb_4+K_maxt_4)/2.0

OpenSees[,"Kmax_4"]=c(K_max_4)
OpenSees[,"Kur_4"]=c(K_max_4)

#Input "failure ratio" Rf. Duncan & Mokwa indicate a range from 0.75 to 0.95
and use average Rf= 0.85
Rf_4 = 0.85

OpenSees[,"Rf_4"]=c(Rf_4)

#Estimate the ultimate passive resistance, P_ult (or F_ult in OpenSees model)
#P_ult_L is calculated for the passive resistance on the left side of the footing
#P_ult_R is calculated for the passive resistance on the right side of the footing
#Calculate unit active force, Pa (kN/unit width). Assume it is zero if Df<Hc
(critical height)

#Left of footing
Hc_4L = matrix(NA, n, 1)
k=0
for (i in 1:n) {
k=k+1
Hc_4L[k,] = 4*su_4L[k,]/gamma

```

```

    }

Pa_4L = matrix(NA, n, 1)
  k=0
  for (i in 1:n) {
    k=k+1
    if(Hc_4L[k,]<Df_4) {
      Pa_4L[k,] = 0.5*gamma*Df_4^2+2*su_4L[k,]*Df_4
    } else {
      Pa_4L[k,] = 0
    }
  }

#Calculate unit passive force, Pp (kN/unit width)

Pp_4L = matrix(NA, n, 1)
  k=0
  for (i in 1:n) {
    k=k+1
    Pp_4L[k,] = 0.5*gamma*Df_4^2+2*su_4L[k,]*Df_4
  }

#Calculate ultimate passive force, P_ult (kN), including 3D effects

P_ult_4L = matrix(NA, n, 1)
  k=0
  for (i in 1:n) {
    k=k+1
    P_ult_4L[k,] = L_4*(Pp_4L[k,]-Pa_4L[k,])+2*su_4L[k,]*Df_4^2
  }

OpenSees[,"P_ult_4L"]=c(P_ult_4L)
OpenSees_trunc[,"P_ult_4L"]=c(P_ult_4L)

#Right of footing
Hc_4R = matrix(NA, n, 1)
  k=0

```

```

    for (i in 1:n) {
      k=k+1
      Hc_4R[k,] = 4*su_4R[k,]/gamma
    }

Pa_4R = matrix(NA, n, 1)
  k=0
  for (i in 1:n) {
    k=k+1
    if(Hc_4R[k,]<Df_4) {
      Pa_4R[k,] = 0.5*gamma*Df_4^2+2*su_4R[k,]*Df_4
    } else {
      Pa_4R[k,] = 0
    }
  }

#Calculate unit passive force, Pp (kN/unit width)

Pp_4R = matrix(NA, n, 1)
  k=0
  for (i in 1:n) {
    k=k+1
    Pp_4R[k,] = 0.5*gamma*Df_4^2+2*su_4R[k,]*Df_4
  }

#Calculate ultimate passive force, P_ult (kN), including 3D effects

P_ult_4R = matrix(NA, n, 1)
  k=0
  for (i in 1:n) {
    k=k+1
    P_ult_4R[k,] = L_4*(Pp_4R[k,]-Pa_4R[k,])+2*su_4R[k,]*Df_4^2
  }

OpenSees[,"P_ult_4R"]=c(P_ult_4R)
OpenSees_trunc[,"P_ult_4R"]=c(P_ult_4R)

```



## #FOOTING 5

#Calculate bearing capacity for a given footing and undrained cohesive soil conditions

#set footing parameters (in units of meters) - width B, length L, depth Df, water depth Dw

$$B\_5 = B\_outside$$

$$B\_5\_prime = B\_outside\_prime$$

$$L\_5 = B\_outside$$

$$Df\_5 = 0.6$$

$$Dw\_5 = 2.4$$

#Spring and gap parameters for vertical and horizontal spring models

$$SpringNo.5 = 101$$

$$Gap\_V\_5 = 0$$

$$Gap\_H\_5 = 0.000000000001$$

$$OpenSees[,"B\_5"]=c(B\_5)$$

$$OpenSees[,"Df\_5"]=c(Df\_5)$$

$$OpenSees[,"SpringNo.5"]=c(SpringNo.5)$$

$$OpenSees[,"Gap\_V\_5"]=c(Gap\_V\_5)$$

$$OpenSees[,"Gap\_H\_5"]=c(Gap\_H\_5)$$

#set soil parameters - undrained shear strength  $s_u$  (kPa), unit weight  $\gamma$  (kN/m<sup>3</sup>), water unit weight  $\gamma_{water}$  (kN/m<sup>3</sup>)# $s_u$  is defined as  $s_{u\_5}$  from above

$$\gamma = 19.0$$

$$\gamma_{water} = 9.81$$

#set initial elastic modulus,  $E_i$  (kPa), and poissons ratio,  $\nu$ .  $\nu$  assumes undrained loading# $E_i$  is based on Strahler & Stuedlein (2013) fitting:  $E_i/ATM = 11(OCR)+33$ .

Assme OCR = 8

$$ATM = 101.325$$

$$OCR = 8$$

$$E_i = ATM*(11*OCR+33)$$

$$\nu = 0.50$$

#set bearing capacity parameters

$$N_c = 5.14$$

```

sc_5 = 1.+0.2*B_5/L_5
if(Df_5<B_5) {
dc_5 = 1.+0.4*Df_5/B_5
  } else {
  dc_5 = 1.+0.4*atan(Df_5/B_5)*pi/180
  }
Nq = 1.
sq = 1.
dq = 1.

#Calculate bearing capacity, q_ult (kPa)
q_ult_5 = matrix(NA, n, 1)
  k=0
  for (i in 1:n) {
  k=k+1
  if(Dw_5<Df_5) {
    q_ult_5[k,] = su_5[k,]*Nc*sc_5*dc_5+((gamma*Df_5)-(Df_5-
Dw_5)*(gamma-gamma_water))*Nq*sq*sc_5
  } else {
    q_ult_5[k,] = su_5[k,]*Nc*sc_5*dc_5+gamma*Df_5*Nq*sq*dq
  }
  }

Q_ult_5 = matrix(NA, n, 1)
  k=0
  for (i in 1:n) {
  k=k+1
  Q_ult_5[k,] = q_ult_5[k,]*B_5*L_5
  }

#Generate random values for normalized bearing capacity - i.e., "actual" bearing
#This step is done first to establish the number of revised simulations (##not revising
simulations)
#THIS IS THE UPDATE FOR FOOTING 5

#The unit mean bearing capacity, qult, has parameters of the bias calculated from
the dataset
#with unit mean=1.25 and COV=0.37

```

#The bias is closest to a gamma distribution - define parameters and generate n random values

```
#qult_shape_5 = 7.52698348510156
```

```
#qult_rate_5 = 1/0.166593308846615
```

```
#qult_5 = matrix(rgamma(n, shape=qult_shape_5, rate=qult_rate_5),n,1)
```

#Generate random values of q\_ult based on the calculated value and noted distribution

```
#q_ult_rnd_5 = matrix(c(q_ult_5*qult_5), n, 1)
```

```
q_ult_rnd_5 = q_ult_5
```

```
Q_ult_rnd_5 = matrix(NA, n, 1)
```

```
  k=0
```

```
  for (i in 1:n) {
```

```
    k=k+1
```

```
    Q_ult_rnd_5[k,] = q_ult_rnd_5[k,]*B_5*L_5
```

```
  }
```

#Generate uniformly distributed ranked values that will be transformed to the k1, k2 and mstc parameters

```
#to simulate ranked parameters using copula data
```

```
 #(make sure CDVine package is loaded)
```

```
 family=c(33,33,16)
```

```
 par=c(-7.053976, -3.142653, 1.397515)
```

```
 u_sims_5 = CDVineSim(N=n, family=family, par=par, type=1)
```

```
 u1_sim_5 = u_sims_5[,1]
```

```
 u2_sim_5 = u_sims_5[,2]
```

```
 um_sim_5 = u_sims_5[,3]
```

#Transform u1, u2 and um into k1, k2 and mstc sims using known marginal distributions

#The u simulations represent the cumulative distribution, so we need inverse CDF or quantile (q) dist.

```
#k1 is best fit to gamma distribution
```

```
k1_shape_5 = 3.71590850943956
```

```
k1_rate_5 = 1/0.003433101851711
```

```

k1_5 = matrix(qgamma(u1_sim_5, shape=k1_shape_5, rate=k1_rate_5), n, 1)

#k2 is best fit to inv. gaussian distribution (need to make sure SuppDists package
is loaded)
k2_nu_5 = 0.701447
k2_lambda_5 = 27.91919
k2_5 = matrix(qinvGauss(u2_sim_5, nu=k2_nu_5, lambda=k2_lambda_5), n, 1)

#mstc is best fit to lognormal distribution
mstc_mean_5 = 0.643048649204319
mstc_stdev_5 = 0.123128154098121
mstc_LN_stdev_5 = sqrt(log(1+(mstc_stdev_5^2/mstc_mean_5^2)))
mstc_LN_mean_5 = log(mstc_mean_5)-0.5*(mstc_LN_stdev_5)^2
mstc_5 = matrix(qlnorm(um_sim_5, meanlog=mstc_LN_mean_5,
sdlog=mstc_LN_stdev_5), n, 1)

OpenSees["k1_5"]=c(k1_5)
OpenSees["k2_5"]=c(k2_5)
OpenSees_trunc["k1_5"]=c(k1_5)
OpenSees_trunc["k2_5"]=c(k2_5)

#Calculate the reference capacity, q_stc = mstc*q_ult

q_stc_5 = matrix(NA, n, 1)
  k=0
  for (i in 1:n) {
    k=k+1
    q_stc_5[k,] = mstc_5[k,]*q_ult_rnd_5[k,]
  }

Q_stc_5 = matrix(NA, n, 1)
  k=0
  for (i in 1:n) {
    k=k+1
    Q_stc_5[k,] = q_stc_5[k,]*B_5*L_5
  }

OpenSees["q_stc_5"]=c(q_stc_5)

```



$$K_{\text{maxt}_5} = (32.0 * \pi * E_i * (1 - \nu) * Df_5) / ((1 + \nu) * ((3.0 - 4.0 * \nu) * F1 + F4 + 4.0 * (1.0 - 2.0 * \nu) * (1.0 - \nu) * F5))$$

$$K_{\text{max}_5} = (K_{\text{maxb}_5} + K_{\text{maxt}_5}) / 2.0$$

OpenSees[,"Kmax\_5"]=c(K\_max\_5)

OpenSees[,"Kur\_5"]=c(K\_max\_5)

#Input "failure ratio" Rf. Duncan & Mokwa indicate a range from 0.75 to 0.95 and use average Rf= 0.85

$$Rf_5 = 0.85$$

OpenSees[,"Rf\_5"]=c(Rf\_5)

#Estimate the ultimate passive resistance, P\_ult (or F\_ult in OpenSees model)

#P\_ult\_L is calculated for the passive resistance on the left side of the footing

#P\_ult\_R is calculated for the passive resistance on the right side of the footing

#Calculate unit active force, Pa (kN/unit width). Assume it is zero if Df<Hc (critical height)

#Left of footing

Hc\_5L = matrix(NA, n, 1)

k=0

for (i in 1:n) {

k=k+1

Hc\_5L[k,] = 4\*su\_5L[k,]/gamma

}

Pa\_5L = matrix(NA, n, 1)

k=0

for (i in 1:n) {

k=k+1

if(Hc\_5L[k,]<Df\_5) {

Pa\_5L[k,] = 0.5\*gamma\*Df\_5^2+2\*su\_5L[k,]\*Df\_5

} else {

Pa\_5L[k,] = 0

}

}

```
#Calculate unit passive force, Pp (kN/unit width)
```

```
Pp_5L = matrix(NA, n, 1)
  k=0
  for (i in 1:n) {
    k=k+1
    Pp_5L[k,] = 0.5*gamma*Df_5^2+2*su_5L[k,]*Df_5
  }
```

```
#Calculate ultimate passive force, P_ult (kN), including 3D effects
```

```
P_ult_5L = matrix(NA, n, 1)
  k=0
  for (i in 1:n) {
    k=k+1
    P_ult_5L[k,] = L_5*(Pp_5L[k,]-Pa_5L[k,])+2*su_5L[k,]*Df_5^2
  }
```

```
OpenSees[,"P_ult_5L"]=c(P_ult_5L)
```

```
OpenSees_trunc[,"P_ult_5L"]=c(P_ult_5L)
```

```
#Right of footing
```

```
Hc_5R = matrix(NA, n, 1)
  k=0
  for (i in 1:n) {
    k=k+1
    Hc_5R[k,] = 4*su_5R[k,]/gamma
  }
```

```
Pa_5R = matrix(NA, n, 1)
```

```
  k=0
  for (i in 1:n) {
    k=k+1
    if(Hc_5R[k,]<Df_5) {
      Pa_5R[k,] = 0.5*gamma*Df_5^2+2*su_5R[k,]*Df_5
    } else {
      Pa_5R[k,] = 0
    }
  }
```

```

}
}

```

```
#Calculate unit passive force, Pp (kN/unit width)
```

```

Pp_5R = matrix(NA, n, 1)
  k=0
  for (i in 1:n) {
    k=k+1
    Pp_5R[k,] = 0.5*gamma*Df_5^2+2*su_5R[k,]*Df_5
  }

```

```
#Calculate ultimate passive force, P_ult (kN), including 3D effects
```

```

P_ult_5R = matrix(NA, n, 1)
  k=0
  for (i in 1:n) {
    k=k+1
    P_ult_5R[k,] = L_5*(Pp_5R[k,]-Pa_5R[k,])+2*su_5R[k,]*Df_5^2
  }

```

```

OpenSees[,"P_ult_5R"]=c(P_ult_5R)
OpenSees_trunc[,"P_ult_5R"]=c(P_ult_5R)

```

```
#GENERATE LOADS AND CALCULATE VERTICAL DISPLACEMENT FOR EACH FOOTING
```

```
#Calculate bearing pressure at each footing location. Column loads (in kN) at each footing are as follows:
```

```

Column_1 = 510
Column_2 = 817
Column_3 = 819
Column_4 = 794
Column_5 = 517

```

```
#Calculate applied bearing pressure for each footing (in kPa) as follows:
```



```

Footing1_Load = Column_1/(B_1*L_1)
Footing2_Load = Column_2/(B_2*L_2)
Footing3_Load = Column_3/(B_3*L_3)
Footing4_Load = Column_4/(B_4*L_4)
Footing5_Load = Column_5/(B_5*L_5)

```

```
#Populate Footing_Loads matrix with footing bearing pressure values
```

```

Footing_Loads["Footing1_Load"]=c(Footing1_Load)
Footing_Loads["Footing2_Load"]=c(Footing2_Load)
Footing_Loads["Footing3_Load"]=c(Footing3_Load)
Footing_Loads["Footing4_Load"]=c(Footing4_Load)
Footing_Loads["Footing5_Load"]=c(Footing5_Load)

```

```
#Calculate settlement for each footing based on non-linear undrained vertical displacement. Create matrix for each.
```

```

Footing1_Settlement = (B_1_prime*k1_1*Footing1_Load)/(q_stc_1*(1-
(k2_1*Footing1_Load/q_stc_1)))
Footing2_Settlement = (B_2_prime*k1_2*Footing2_Load)/(q_stc_2*(1-
(k2_2*Footing2_Load/q_stc_2)))
Footing3_Settlement = (B_3_prime*k1_3*Footing3_Load)/(q_stc_3*(1-
(k2_3*Footing3_Load/q_stc_3)))
Footing4_Settlement = (B_4_prime*k1_4*Footing4_Load)/(q_stc_4*(1-
(k2_4*Footing4_Load/q_stc_4)))
Footing5_Settlement = (B_5_prime*k1_5*Footing5_Load)/(q_stc_5*(1-
(k2_5*Footing5_Load/q_stc_5)))

```

```

Footing1_Settlement1 = matrix(c(Footing1_Settlement), n, 1)
Footing2_Settlement2 = matrix(c(Footing2_Settlement), n, 1)
Footing3_Settlement3 = matrix(c(Footing3_Settlement), n, 1)
Footing4_Settlement4 = matrix(c(Footing4_Settlement), n, 1)
Footing5_Settlement5 = matrix(c(Footing5_Settlement), n, 1)

```

```
#Revise settlement calculations to set maximum settlement equal to B (i.e., approx. settlement at bearing capacity failure)
```

```
#also revise for negative values that can arise from non-linear displacement equation at large values of displacement
```

```
#Footing 1
```

```

Footing1_Settlement_max = matrix(NA, n, 1)
  k=0
  for (i in 1:n) {
    k=k+1
    if(Footing1_Settlement1[i,]>B_1) {
      Footing1_Settlement_max[i,] = B_1
    } else {
      Footing1_Settlement_max[i,]=Footing1_Settlement1[i,]
    }
  }

  k=0
  for (i in 1:n) {
    k=k+1
    if(Footing1_Settlement_max[i,]<0) {
      Footing1_Settlement_max[i,] = B_1
    } else {
      Footing1_Settlement_max[i,]=Footing1_Settlement_max[i,]
    }
  }

rm(Footing1_Settlement1)
Footing1_Settlement1 = Footing1_Settlement_max

```

#Footing 2

```

Footing2_Settlement_max = matrix(NA, n, 1)
  k=0
  for (i in 1:n) {
    k=k+1
    if(Footing2_Settlement2[i,]>B_2) {
      Footing2_Settlement_max[i,] = B_2
    } else {
      Footing2_Settlement_max[i,]=Footing2_Settlement2[i,]
    }
  }

  k=0

```

```

for (i in 1:n) {
  k=k+1
  if(Footing2_Settlement_max[i,]<0) {
    Footing2_Settlement_max[i,] = B_2
  } else {
    Footing2_Settlement_max[i,]=Footing2_Settlement_max[i,]
  }
}

```

```

rm(Footing2_Settlement2)
Footing2_Settlement2 = Footing2_Settlement_max

```

#Footing 3

```

Footing3_Settlement_max = matrix(NA, n, 1)
  k=0
  for (i in 1:n) {
    k=k+1
    if(Footing3_Settlement3[i,]>B_3) {
      Footing3_Settlement_max[i,] = B_3
    } else {
      Footing3_Settlement_max[i,]=Footing3_Settlement3[i,]
    }
  }
}

```

```

  k=0
  for (i in 1:n) {
    k=k+1
    if(Footing3_Settlement_max[i,]<0) {
      Footing3_Settlement_max[i,] = B_3
    } else {
      Footing3_Settlement_max[i,]=Footing3_Settlement_max[i,]
    }
  }
}

```

```

rm(Footing3_Settlement3)
Footing3_Settlement3 = Footing3_Settlement_max

```

```
#Footing 4
```

```

Footing4_Settlement_max = matrix(NA, n, 1)
  k=0
  for (i in 1:n) {
    k=k+1
    if(Footing4_Settlement4[i,]>B_4) {
      Footing4_Settlement_max[i,] = B_4
    } else {
      Footing4_Settlement_max[i,]=Footing4_Settlement4[i,]
    }
  }

  k=0
  for (i in 1:n) {
    k=k+1
    if(Footing4_Settlement_max[i,]<0) {
      Footing4_Settlement_max[i,] = B_4
    } else {
      Footing4_Settlement_max[i,]=Footing4_Settlement_max[i,]
    }
  }

rm(Footing4_Settlement4)
Footing4_Settlement4 = Footing4_Settlement_max

```

```
#Footing 5
```

```

Footing5_Settlement_max = matrix(NA, n, 1)
  k=0
  for (i in 1:n) {
    k=k+1
    if(Footing5_Settlement5[i,]>B_5) {
      Footing5_Settlement_max[i,] = B_5
    } else {
      Footing5_Settlement_max[i,]=Footing5_Settlement5[i,]
    }
  }

```

```

k=0
for (i in 1:n) {
k=k+1
if(Footing5_Settlement_max[i,]<0) {
Footing5_Settlement_max[i,] = B_5
} else {
Footing5_Settlement_max[i,]=Footing5_Settlement_max[i,]
}
}
}

```

```
rm(Footing5_Settlement5)
```

```
Footing5_Settlement5 = Footing5_Settlement_max
```

```
#Populate Footing_Settlement matrix with results calculated above
```

```

Footing_Settlement[,"Footing1_Settlement"]=Footing1_Settlement1
Footing_Settlement[,"Footing2_Settlement"]=Footing2_Settlement2
Footing_Settlement[,"Footing3_Settlement"]=Footing3_Settlement3
Footing_Settlement[,"Footing4_Settlement"]=Footing4_Settlement4
Footing_Settlement[,"Footing5_Settlement"]=Footing5_Settlement5

```

```
write.table(Footing_Settlement, file = "E:\\All Sims\\Independent Footings
Settlement\\Footing Settlement COV=100 SOF=100.txt", row.names=FALSE)
```

```
write.table(OpenSees_trunc, file = "E:\\All Sims\\OpenSees Building Footing
Settlement\\OpenSees COV=100 SOF=100.txt", row.names=FALSE)
```

```
su_COV
```

```
SOF
```

**APPENDIX C: TABULATED FOOTING RESPONSE FROM  
OPENSEES ANALYSIS**

**OpenSees Results - Footing Displacements and Angular Distortion at Footing Elevation**

Calculated results from bearing pressure-settlement equation and simulated results with 50,000 simulations that include bearing pressure-settlement equation (with known dispersion of model parameters) and variable soil undrained shear strength across horizontal distance, x.

Soil Parameters		Displacement Model (Vertical Spring) Parameters			Footing Parameters	
		$k_1$	$k_2$	$M_{stc}$	$B_{1.5}$ (m)	$B_{3.4}$ (m)
$s_u$ (kPa)	= 70	0.013	0.701	0.643	1.675	
COV( $s_u$ )	= 0%	0.007	0.113	0.123	2.125	
Scale of Fluctuation, $\delta$ (m)	= 0.1	53.0	16.1	19.1	9.15	
$\gamma'$ (kN/m <sup>3</sup> )	= 19	Dist. = Gamma Inv. Gauss. Lognormal				

"calculated" values assume no variation in soil shear strength or spring parameters

"Allowable" Distortion = 1/500 = 0.002

	Displacement (mm)					Distortion (for 9.15 m on-center footing spacing)				
	Footing 1	Footing 2	Footing 3	Footing 4	Footing 5	Footings 1-2	Footings 2-3	Footings 3-4	Footings 4-5	
"Deterministic" estimate	23.2	30.3	30.5	28.9	23.7	7.2	0.13	1.5	5.2	"Deterministic" estimate
Simulated - mean	25.1	26.2	26.3	24.9	25.9	18.5	18.9	18.4	18.3	Simulated - mean
Simulated - median	21.3	22.2	22.2	21.3	21.9	14.3	14.5	14.2	14.2	Simulated - median
Simulated - Std Dev	17.0	17.7	17.9	16.8	17.6	16.3	16.6	16.2	16.1	Simulated - Std Dev
Simulated COV	0.68	0.68	0.68	0.67	0.68	0.88	0.88	0.88	0.88	Simulated COV
Minimum (neg. value is uplift)	0.31	0.26	0.34	0.38	0.18	0.000	0.000	0.001	0.002	Minimum
Maximum	178.4	251.3	187.4	196.7	181.4	235.0	241.9	171.4	164.4	Maximum
Prob exceeding "calculated" value	0.454	0.328	0.326	0.328	0.457	0.72	0.99	0.94	0.79	Prob of failure, $p_f$ =
Prob exceeding 12.5 mm	0.749	0.765	0.766	0.750	0.759	0.55	0.56	0.55	0.55	$\beta$ =
Prob exceeding 25 mm	0.411	0.434	0.435	0.411	0.427	0.27	0.28	0.26	0.26	0.26
Prob exceeding 50 mm	0.086	0.100	0.100	0.081	0.096	0.05	0.06	0.05	0.05	0.27

\*\*Note -  $p_f$  also equals the probability of exceeding approx. 18.3 mm of differential displacement

**OpenSees Results - Footing Displacements and Angular Distortion at Footing Elevation**

Calculated results from bearing pressure-settlement equation and simulated results with 50,000 simulations that include bearing pressure-settlement equation (with known dispersion of model parameters) and variable soil undrained shear strength across horizontal distance, x.

Soil Parameters		Displacement Model (Vertical Spring) Parameters				Footing Parameters					
$s_u$ (kPa)	= 70	$k_1$	$k_2$	$M_{stc}$	$B_{1,5}$ (m)						
COV( $s_u$ )	= 0%	$\mu$	0.013	0.701	0.643						
Scale of Fluctuation, $\delta$ (m)	= 0.2	$\sigma$	0.007	0.113	0.123	$B_{3,4}$ (m)	= 2.125				
$\gamma$ (kN/m <sup>3</sup> )	= 19	COV(%)	= 53.0	16.1	19.1	Beam Dist.(m)	= 9.15				
		Dist.	= Gamma	Inv. Gauss.	Lognormal						
"calculated" values assume no variation in soil shear strength or spring parameters											
"Allowable" Distortion = 1/500 = 0.002											
<b>Distortion (for 9.15 m on-center footing spacing)</b>											
		Displacement (mm)			Footing Displacement (mm)			Distortion			
		Footing 1	Footing 2	Footing 3	Footing 4	Footing 5	Footing 1-2	Footing 2-3	Footing 3-4	Footing 4-5	
"Deterministic" estimate		23.2	30.3	30.5	28.9	23.7	7.2	0.13	1.5	5.2	
Simulated - mean		25.3	26.4	26.2	25.0	25.8	18.7	19.0	18.5	18.3	
Simulated - median		21.4	22.5	22.3	21.2	21.9	14.3	14.5	14.2	14.1	
Simulated - Std Dev		17.1	17.9	17.9	17.0	17.5	16.4	16.8	16.3	16.1	
Simulated COV		0.68	0.68	0.68	0.68	0.68	0.88	0.88	0.88	0.88	
Minimum (neg. value is uplift)		0.40	0.36	0.36	0.23	0.41	0.000	0.000	0.001	0.000	
Maximum		163.9	230.5	178.9	179.4	170.7	208.5	204.2	153.9	159.8	
Prob exceeding "calculated" value		0.457	0.332	0.326	0.329	0.455	0.73	0.99	0.94	0.79	
Prob exceeding 12.5 mm		0.750	0.769	0.764	0.747	0.760	0.55	0.56	0.55	0.55	
Prob exceeding 25 mm		0.415	0.439	0.437	0.409	0.425	0.27	0.28	0.27	0.26	
Prob exceeding 50 mm		0.089	0.101	0.099	0.085	0.095	0.05	0.06	0.05	0.05	
Prob of failure, $p_f$		0.40		0.41		0.25		0.23		0.27	
$\beta$		0.25		0.23		0.26		0.26		0.27	

\*\*Note -  $p_f$  also equals the probability of exceeding approx. 18.3 mm of differential displacement



**OpenSees Results - Footing Displacements and Angular Distortion at Footing Elevation**

Calculated results from bearing pressure-settlement equation and simulated results with 50,000 simulations that include bearing pressure-settlement equation (with known dispersion of model parameters) and variable soil undrained shear strength across horizontal distance, x.

Soil Parameters		Displacement Model (Vertical Spring) Parameters				Footing Parameters						
		$k_1$	$k_2$	$M_{stc}$	$B_{1,5} (m)$	$B_{3,4} (m)$	Beam Dist.(m)					
$s_u (kPa)$	= 70	0.013	0.701	0.643	1.675							
$COV(s_u)$	= 0%	0.007	0.113	0.123	2.125							
Scale of Fluctuation, $\delta (m)$	= 0.5	53.0	16.1	19.1	9.15							
$\gamma' (kN/m^3)$	= 19	Dist. = Gamma Inv. Gauss. Lognormal										
"calculated" values assume no variation in soil shear strength or spring parameters												
"Allowable" Distortion = 1/500 = 0.002												
		Displacement (mm)			Differential Displacement (mm)			Distortion (for 9.15 m on-center footing spacing)				
		Footing 1	Footing 2	Footing 3	Footing 4	Footing 5	Footing 1-2	Footing 2-3	Footing 3-4	Footing 4-5		
"Deterministic" estimate		23.2	30.3	30.5	28.9	23.7	7.2	0.13	1.5	5.2	Deterministic* estimate	0.00078
Simulated - mean		25.3	26.2	26.3	24.9	25.9	18.6	19.0	18.6	18.4	Simulated - mean	0.00203
Simulated - median		21.5	22.4	22.3	21.2	21.9	14.3	14.6	14.3	14.2	Simulated - median	0.00160
Simulated - Std Dev		17.2	17.7	18.0	16.8	17.6	16.3	16.6	16.4	16.0	Simulated - Std Dev	0.00156
Simulated COV		0.68	0.67	0.68	0.68	0.68	0.88	0.88	0.88	0.87	Simulated COV	0.88
Minimum (neg. value is uplift)		0.30	0.31	0.21	0.47	0.40	0.001	0.000	0.001	0.001	Minimum	0.0000001
Maximum		225.6	246.2	203.7	191.1	184.4	215.4	227.4	192.6	171.7	Maximum	0.02354
Prob exceeding "calculated" value		0.460	0.329	0.329	0.329	0.456	0.72	1.00	0.94	0.79	Prob of failure, $p_f$	0.40
Prob exceeding 12.5 mm		0.752	0.766	0.764	0.746	0.761	0.55	0.56	0.55	0.55	$\beta$	0.26
Prob exceeding 25 mm		0.418	0.437	0.437	0.408	0.427	0.27	0.28	0.27	0.26		0.25
Prob exceeding 50 mm		0.089	0.099	0.101	0.084	0.096	0.05	0.05	0.05	0.05		0.26

\*\*Note -  $p_f$  also equals the probability of exceeding approx. 18.3 mm of differential displacement

**OpenSees Results - Footing Displacements and Angular Distortion at Footing Elevation**

Calculated results from bearing pressure-settlement equation and simulated results with 50,000 simulations that include bearing pressure-settlement equation (with known dispersion of model parameters) and variable soil undrained shear strength across horizontal distance, x.

Soil Parameters		Displacement Model (Vertical Spring) Parameters				Footing Parameters	
$s_u$ (kPa)	$\delta$ (mm)	$k_1$	$k_2$	$M_{stc}$	$B_{1-5}$ (m)	$B_{3-4}$ (m)	Beam Dist.(m)
70	0%	0.013	0.701	0.643	1.675		
COV( $s_u$ ) = 1	1	0.007	0.113	0.123	2.125		
Scale of Fluctuation, $\delta$ (mm) = 19		COV(%) = 53.0	18.1	19.1			
$\gamma$ (kN/m <sup>3</sup> ) = 19		Dist. = Gamma	Inv. Gauss.	Lognormal			

"calculated" values assume no variation in soil shear strength or spring parameters

"Allowable" Distortion = 1/500 = 0.002

	Displacement (mm)					Distortion (for 9.15 m on-center footing spacing)							
	Footing 1	Footing 2	Footing 3	Footing 4	Footing 5	Footings 1-2	Footings 2-3	Footings 3-4	Footings 4-5	Footings 1-2	Footings 2-3	Footings 3-4	Footings 4-5
"Deterministic" estimate	23.2	30.3	30.5	28.9	23.7	7.2	0.13	1.5	5.2	0.00078	0.00001	0.00017	0.00057
Simulated - mean	25.3	26.2	26.4	25.0	26.0	18.5	19.0	18.6	18.4	0.00203	0.00207	0.00203	0.00201
Simulated - median	21.5	22.2	22.3	21.3	22.0	14.3	14.7	14.2	14.2	0.00156	0.00160	0.00155	0.00155
Simulated - Std Dev	17.1	17.8	17.9	19.3	17.6	16.3	16.7	18.7	18.5	0.0018	0.0018	0.0020	0.0020
Simulated COV	0.68	0.68	0.68	0.77	0.68	0.88	0.88	1.00	1.01	0.88	0.88	1.00	1.01
Minimum (neg. value is uplift)	0.41	0.43	0.25	0.16	0.33	0.000	0.000	0.002	0.000	0.0000000	0.0000000	0.0000002	0.0000000
Maximum	218.4	177.6	250.5	2125.0	176.7	190.6	218.9	2062.2	2095.0	0.02084	0.02392	0.22538	0.22896
Prob exceeding "calculated" value	0.460	0.330	0.330	0.328	0.461	0.72	1.00	0.94	0.79	0.40	0.41	0.40	0.39
Prob exceeding 12.5 mm	0.752	0.766	0.766	0.749	0.762	0.55	0.56	0.55	0.55	0.26	0.23	0.26	0.27
Prob exceeding 25 mm	0.417	0.434	0.440	0.409	0.431	0.27	0.28	0.27	0.26	0.26	0.23	0.26	0.27
Prob exceeding 50 mm	0.086	0.099	0.103	0.085	0.097	0.05	0.05	0.05	0.05	0.26	0.23	0.26	0.27

Prob of failure,  $p_f$  = 0.40     $\beta$  = 0.26

\*\*Note -  $p_f$  also equals the probability of exceeding approx. 18.3 mm of differential displacement

**OpenSees Results - Footing Displacements and Angular Distortion at Footing Elevation**

Calculated results from bearing pressure-settlement equation and simulated results with 50,000 simulations that include bearing pressure-settlement equation (with known dispersion of model parameters) and variable soil undrained shear strength across horizontal distance, x.

Soil Parameters		Displacement Model (Vertical Spring) Parameters				Footing Parameters	
$s_u$ (kPa)	$k_z$	$k_1$	$k_2$	$M_{stc}$	$B_{1.5}$ (m)	$B_{3.4}$ (m)	Beam Dist.(m)
70	0.013	0.701	0.643	19.1	1.675	2.125	9.15
COV( $s_u$ ) = 0%	0.007	0.113	0.123	Inv. Guass.	"calculated" values assume no variation in soil shear strength or spring parameters		
Scale of Fluctuation, $\delta$ (m) = 2	53.0	16.1	19.1	Lognormal	"Allowable" Distortion = 1/500 = 0.002		
$\gamma'$ (kN/m <sup>3</sup> ) = 19							

	Displacement (mm)					Differential Displacement (mm)					Distortion (for 9.15 m on-center footing spacing)						
	Footing 1	Footing 2	Footing 3	Footing 4	Footing 5	Footing 1-2	Footing 2-3	Footing 3-4	Footing 4-5	Footing 1-2	Footing 2-3	Footing 3-4	Footing 4-5	Footing 1-2	Footing 2-3	Footing 3-4	Footing 4-5
"Deterministic" estimate	23.2	30.3	30.5	28.9	23.7	7.2	0.13	1.5	5.2	0.00078	0.00001	0.00017	0.00057	0.00078	0.00001	0.00017	0.00057
Simulated - mean	25.3	26.0	26.2	25.0	25.8	18.4	18.8	18.6	18.4	0.00202	0.00205	0.00203	0.00201	0.00202	0.00205	0.00203	0.00201
Simulated - median	21.5	22.2	22.2	21.2	22.0	14.2	14.5	14.4	14.2	0.00155	0.00158	0.00157	0.00155	0.00155	0.00158	0.00157	0.00155
Simulated - Std Dev	18.7	17.5	17.8	16.9	17.5	17.7	16.5	16.2	16.1	0.0019	0.0018	0.0018	0.0018	0.0019	0.0018	0.0018	0.0018
Simulated COV	0.74	0.67	0.68	0.68	0.68	0.96	0.88	0.87	0.87	0.96	0.88	0.87	0.87	0.96	0.88	0.87	0.87
Minimum (neg. value is uplift)	0.36	0.28	0.10	0.40	0.28	0.001	0.000	0.002	0.001	0.0000001	0.0000000	0.0000002	0.0000002	0.0000001	0.0000000	0.0000002	0.0000002
Maximum	1675.0	181.4	195.8	258.3	183.8	1668.1	162.3	214.7	250.2	0.18231	0.01774	0.02346	0.02734	0.18231	0.01774	0.02346	0.02734
Prob exceeding "calculated" value	0.458	0.327	0.326	0.329	0.459	0.72	0.99	0.94	0.79	0.40	0.40	0.24	0.40	0.40	0.40	0.25	0.25
Prob exceeding 12.5 mm	0.753	0.763	0.765	0.749	0.760	0.55	0.56	0.55	0.55	0.26	0.26	0.27	0.25	0.26	0.24	0.25	0.25
Prob exceeding 25 mm	0.417	0.434	0.435	0.411	0.430	0.27	0.27	0.27	0.27	0.05	0.05	0.05	0.05	0.05	0.05	0.05	0.05
Prob exceeding 50 mm	0.088	0.097	0.098	0.086	0.093	0.05	0.05	0.05	0.05	0.005	0.005	0.005	0.005	0.005	0.005	0.005	0.005

\*\*Note - p, also equals the probability of exceeding approx. 18.3 mm of differential displacement

**OpenSees Results - Footing Displacements and Angular Distortion at Footing Elevation**

Calculated results from bearing pressure-settlement equation and simulated results with 50,000 simulations that include bearing pressure-settlement equation (with known dispersion of model parameters) and variable soil undrained shear strength across horizontal distance, x.

Soil Parameters		Displacement Model (Vertical Spring) Parameters				Footing Parameters	
$s_u$ (kPa)	$k_z$	$k_1$	$k_2$	$M_{stc}$	$B_{1.5}$ (m)	$B_{3.4}$ (m)	Beam Dist.(m)
70	0.013	0.701	0.643	1.675	1.675	2.125	9.15
COV( $s_u$ ) = 0%	0.007	0.113	0.123				
Scale of Fluctuation, $\delta$ (m) = 5	53.0	16.1	19.1				
$\gamma'$ (kN/m <sup>3</sup> ) = 19	Dist. = Gamma	Inv. Gauss.	Lognormal				

"calculated" values assume no variation in soil shear strength or spring parameters

"Allowable" Distortion = 1/500 = 0.002

	Displacement (mm)					Differential Displacement (mm)					Distortion (for 9.15 m on-center footing spacing)						
	Footing 1	Footing 2	Footing 3	Footing 4	Footing 5	Footing 1-2	Footing 2-3	Footing 3-4	Footing 4-5	Footing 1-2	Footing 2-3	Footing 3-4	Footing 4-5	Footing 1-2	Footing 2-3	Footing 3-4	Footing 4-5
"Deterministic" estimate	23.2	30.3	30.5	28.9	23.7	7.2	0.13	1.5	5.2	0.00078	0.00001	0.00017	0.00057	0.00202	0.00001	0.00017	0.00057
Simulated - mean	25.2	26.1	26.2	25.0	25.9	18.5	18.9	18.5	18.3	0.00202	0.00206	0.00202	0.00200	0.00155	0.00159	0.00156	0.00155
Simulated - median	21.4	22.2	22.2	21.1	21.9	14.2	14.5	14.2	14.2	0.00155	0.00159	0.00156	0.00155	0.0018	0.0018	0.0018	0.0018
Simulated - Std Dev	17.1	17.7	17.9	16.9	17.6	16.2	16.5	16.3	16.0	0.0018	0.0018	0.0018	0.0018	0.88	0.87	0.88	0.87
Simulated COV	0.68	0.68	0.68	0.68	0.68	0.88	0.87	0.88	0.87	0.88	0.87	0.88	0.87	0.0000000	0.0000000	0.0000000	0.0000000
Minimum (neg. value is uplift)	179.4	170.4	170.4	174.6	244.0	0.000	0.000	0.000	0.000	0.01843	0.01721	0.01847	0.02001	0.40	0.41	0.40	0.40
Maximum	0.26	0.29	0.29	0.40	0.41	168.7	157.5	183.1	183.1	0.40	0.41	0.40	0.40	0.26	0.24	0.26	0.26
Prob exceeding "calculated" value	0.456	0.326	0.326	0.329	0.460	0.72	1.00	0.94	0.79	0.40	0.41	0.40	0.40	0.26	0.24	0.26	0.26
Prob exceeding 12.5 mm	0.751	0.765	0.764	0.746	0.758	0.55	0.56	0.55	0.55	0.27	0.27	0.27	0.26	0.26	0.26	0.26	0.26
Prob exceeding 25 mm	0.415	0.434	0.434	0.409	0.431	0.27	0.27	0.27	0.26	0.05	0.05	0.05	0.05	0.05	0.05	0.05	0.05
Prob exceeding 50 mm	0.089	0.098	0.101	0.085	0.097	0.05	0.05	0.05	0.05								

Prob of failure,  $p_f$  = 0.40     $\beta$  = 0.26

\*\*Note -  $p_f$  also equals the probability of exceeding approx. 18.3 mm of differential displacement

**OpenSees Results - Footing Displacements and Angular Distortion at Footing Elevation**

Calculated results from bearing pressure-settlement equation and simulated results with 50,000 simulations that include bearing pressure-settlement equation (with known dispersion of model parameters) and variable soil undrained shear strength across horizontal distance, x.

Soil Parameters	Displacement Model (Vertical Spring) Parameters					Footing Parameters		
	$s_u$ (kPa)	$k_1$	$k_2$	$M_{stc}$		$B_{1,5}$ (m)	$B_{3,4}$ (m)	Beam Dist.(m)
$s_u$ (kPa) =	70	0.013	0.701	0.643		1.675		
COV( $s_u$ ) =	0%	0.007	0.113	0.123		2.125		
Scale of Fluctuation, $\delta$ (m) =	10	53.0	16.1	19.1		9.15		
$\gamma$ (kN/m <sup>3</sup> ) =	19	Inv. Gauss.		Lognormal				

"calculated" values assume no variation in soil shear strength or spring parameters

"Allowable" Distortion = 1/500 = 0.002

	Displacement (mm)					Differential Displacement (mm)			Distortion (for 9.15 m on-center footing spacing)				
	Footing 1	Footing 2	Footing 3	Footing 4	Footing 5	Footing 1-2	Footing 2-3	Footing 3-4	Footing 4-5	Footing 1-2	Footing 2-3	Footing 3-4	Footing 4-5
"Deterministic" estimate	23.2	30.3	30.5	28.9	23.7	7.2	0.13	1.5	5.2	0.00078	0.00001	0.00017	0.00057
Simulated - mean	25.3	26.2	26.3	25.0	25.8	18.6	18.9	18.6	18.3	0.00203	0.00207	0.00203	0.00200
Simulated - median	21.5	22.2	22.3	21.1	21.9	14.4	14.6	14.3	14.1	0.00157	0.00159	0.00156	0.00154
Simulated - Std Dev	17.2	17.8	17.9	17.0	17.4	16.3	16.5	16.3	16.0	0.0018	0.0018	0.0018	0.0017
Simulated COV	0.68	0.68	0.68	0.68	0.68	0.88	0.88	0.88	0.87	0.88	0.88	0.88	0.87
Minimum (neg. value is uplift)	0.28	0.16	0.15	0.27	0.13	0.001	0.000	0.000	0.000	0.0000001	0.0000000	0.0000000	0.0000000
Maximum	193.9	188.1	212.4	216.9	193.5	167.6	195.7	197.3	189.4	0.01832	0.02138	0.02156	0.02179
Prob exceeding "calculated" value	0.457	0.326	0.331	0.329	0.456	0.73	1.00	0.94	0.79	0.40	0.41	0.40	0.39
Prob exceeding 12.5 mm	0.751	0.766	0.765	0.744	0.763	0.55	0.56	0.55	0.55	0.25	0.23	0.25	0.27
Prob exceeding 25 mm	0.416	0.434	0.441	0.409	0.428	0.27	0.27	0.27	0.27	0.25	0.23	0.25	0.27
Prob exceeding 50 mm	0.088	0.099	0.100	0.086	0.092	0.05	0.05	0.05	0.05	0.25	0.23	0.25	0.27

Prob of failure,  $p_f$  = 0.40 0.41 0.40 0.39

$\beta$  = 0.25 0.23 0.25 0.27

\*\*Note -  $p_f$  also equals the probability of exceeding approx. 18.3 mm of differential displacement

**OpenSees Results - Footing Displacements and Angular Distortion at Footing Elevation**

Calculated results from bearing pressure-settlement equation and simulated results with 50,000 simulations that include bearing pressure-settlement equation (with known dispersion of model parameters) and variable soil undrained shear strength across horizontal distance, x.

Soil Parameters		Displacement Model (Vertical Spring) Parameters				Footing Parameters	
$s_u$ (kPa)	$\delta$ (m)	$k_1$	$k_2$	$M_{stc}$	$B_{1-5}$ (m)	$B_{3-4}$ (m)	Beam Dist.(m)
70	0%	0.013	0.701	0.643	1.675	2.125	9.15
COV( $s_u$ ) =	20	0.007	0.113	0.123			
Scale of Fluctuation, $\delta$ (m) =	19	53.0	16.1	19.1			
$\gamma$ (kN/m <sup>3</sup> ) =		Dist. = Gamma	Inv. Gauss.	Lognormal			

"calculated" values assume no variation in soil shear strength or spring parameters

"Allowable" Distortion = 1/500 = 0.002

	Displacement (mm)					Distortion (for 9.15 m on-center footing spacing)							
	Footing 1	Footing 2	Footing 3	Footing 4	Footing 5	Footings 1-2	Footings 2-3	Footings 3-4	Footings 4-5	Footings 1-2	Footings 2-3	Footings 3-4	Footings 4-5
"Deterministic" estimate	23.2	30.3	30.5	28.9	23.7	7.2	0.13	1.5	5.2	0.00078	0.00001	0.00017	0.00057
Simulated - mean	25.4	26.2	26.3	25.0	25.8	18.6	19.0	18.6	18.3	0.00203	0.00207	0.00203	0.00200
Simulated - median	21.4	22.3	22.3	21.1	21.9	14.3	14.6	14.3	14.1	0.00156	0.00159	0.00157	0.00155
Simulated - Std Dev	17.1	17.8	20.2	16.9	17.4	16.3	19.0	18.7	16.0	0.0018	0.0021	0.0020	0.0017
Simulated COV	0.67	0.68	0.77	0.68	0.67	0.88	1.00	1.01	0.87	0.88	1.00	1.01	0.87
Minimum (neg. value is uplift)	0.38	0.22	0.33	0.44	0.25	0.000	0.001	0.000	0.001	0.0000000	0.0000001	0.0000001	0.0000001
Maximum	200.6	223.5	2125.0	204.0	178.6	217.2	2107.3	2079.2	187.2	0.02373	0.23030	0.22723	0.02046
Prob exceeding "calculated" value	0.459	0.329	0.329	0.328	0.457	0.72	0.99	0.94	0.79	0.40	0.41	0.40	0.39
Prob exceeding 12.5 mm	0.754	0.764	0.765	0.748	0.762	0.55	0.56	0.55	0.55	0.25	0.23	0.26	0.27
Prob exceeding 25 mm	0.420	0.435	0.438	0.410	0.429	0.27	0.28	0.27	0.26				
Prob exceeding 50 mm	0.089	0.097	0.101	0.085	0.095	0.05	0.05	0.05	0.05				

Prob of failure,  $p_f$  = 0.40     $\beta$  = 0.25     $\beta$  = 0.23     $\beta$  = 0.26     $\beta$  = 0.27

\*\*Note -  $p_f$  also equals the probability of exceeding approx. 18.3 mm of differential displacement

**OpenSees Results - Footing Displacements and Angular Distortion at Footing Elevation**

Calculated results from bearing pressure-settlement equation and simulated results with 50,000 simulations that include bearing pressure-settlement equation (with known dispersion of model parameters) and variable soil undrained shear strength across horizontal distance, x.

Soil Parameters		Displacement Model (Vertical Spring) Parameters				Footing Parameters	
		$k_1$	$k_2$	$M_{stc}$	$B_{1.5}$ (m)	$B_{3.4}$ (m)	
$s_u$ (kPa)	= 70	0.013	0.701	0.643	1.675		
COV( $s_u$ )	= 0%	0.007	0.113	0.123	2.125		
Scale of Fluctuation, $\delta$ (m)	= 30	53.0	16.1	19.1	9.15		
$\gamma'$ (kN/m <sup>3</sup> )	= 19	Inv. Gauss.		Lognormal			
		Dist. =					

	Displacement (mm)					Differential Displacement (mm)					Distortion (for 9.15 m on-center footing spacing)						
	Footing 1	Footing 2	Footing 3	Footing 4	Footing 5	Footing 1-2	Footing 2-3	Footing 3-4	Footing 4-5	Footing 1-2	Footing 2-3	Footing 3-4	Footing 4-5	Footing 1-2	Footing 2-3	Footing 3-4	Footing 4-5
"Deterministic" estimate	23.2	30.3	30.5	28.9	23.7	7.2	0.13	1.5	5.2	0.00078	0.00001	0.00017	0.00057	0.00202	0.00207	0.00201	0.00200
Simulated - mean	25.2	26.3	26.2	24.9	25.8	18.5	19.0	18.4	18.3	0.00156	0.00160	0.00155	0.00154	0.00156	0.00160	0.00155	0.00154
Simulated - median	21.3	22.3	22.1	21.1	21.8	14.3	14.7	14.2	14.1	0.0018	0.0018	0.0018	0.0017	0.0018	0.0018	0.0018	0.0017
Simulated - Std Dev	17.1	17.8	17.8	16.8	17.5	16.2	16.6	16.1	15.9	0.88	0.87	0.88	0.87	0.88	0.87	0.88	0.87
Simulated COV	0.68	0.68	0.68	0.67	0.68	0.88	0.87	0.88	0.87	0.88	0.87	0.88	0.87	0.88	0.87	0.88	0.87
Minimum (neg. value is uplift)	0.24	0.38	0.37	0.35	0.36	0.001	0.002	0.001	0.001	0.0000001	0.0000002	0.0000001	0.0000001	0.0000001	0.0000002	0.0000001	0.0000001
Maximum	173.2	234.6	182.8	181.5	167.2	225.2	193.6	175.3	184.4	0.02461	0.02116	0.01916	0.01797	0.02461	0.02116	0.01916	0.01797
Prob exceeding "calculated" value	0.456	0.330	0.327	0.327	0.456	0.72	0.99	0.94	0.79	0.40	0.41	0.40	0.39	0.40	0.41	0.40	0.39
Prob exceeding 12.5 mm	0.747	0.767	0.764	0.750	0.756	0.55	0.56	0.55	0.55	0.26	0.23	0.26	0.27	0.26	0.23	0.26	0.27
Prob exceeding 25 mm	0.416	0.438	0.433	0.407	0.427	0.27	0.28	0.27	0.26	0.05	0.05	0.05	0.05	0.05	0.05	0.05	0.05
Prob exceeding 50 mm	0.087	0.102	0.100	0.083	0.095	0.05	0.05	0.05	0.05								

\*\*Note - p, also equals the probability of exceeding approx. 18.3 mm of differential displacement

"calculated" values assume no variation in soil shear strength or spring parameters  
 "Allowable" Distortion = 1/500 = 0.002

**OpenSees Results - Footing Displacements and Angular Distortion at Footing Elevation**

Calculated results from bearing pressure-settlement equation and simulated results with 50,000 simulations that include bearing pressure-settlement equation (with known dispersion of model parameters) and variable soil undrained shear strength across horizontal distance, x.

Soil Parameters		Displacement Model (Vertical Spring) Parameters				Footing Parameters				
		$k_1$	$k_2$	$M_{stc}$	$B_{1.5}$ (m)	$B_{3.4}$ (m)	Beam Dist.(m)			
$s_u$ (kPa)	= 70	0.013	0.701	0.643	1.675					
COV( $s_u$ )	= 0%	0.007	0.113	0.123	2.125					
Scale of Fluctuation, $\delta$ (m)	= 50	53.0	16.1	19.1	9.15					
$\gamma'$ (kN/m <sup>3</sup> )	= 19	Dist. = Gamma Inv. Gauss. Lognormal								
"calculated" values assume no variation in soil shear strength or spring parameters										
"Allowable" Distortion = 1/500 = 0.002										
		Displacement (mm)			Differential Displacement (mm)			Distortion (for 9.15 m on-center footing spacing)		
		Footing 1	Footing 2	Footing 3	Footing 4	Footing 5	Footing 1-2	Footing 2-3	Footing 3-4	Footing 4-5
"Deterministic" estimate		23.2	30.3	30.5	28.9	23.7	7.2	0.13	1.5	5.2
Simulated - mean		25.3	26.3	26.3	25.1	25.9	18.6	18.8	18.5	18.3
Simulated - median		21.4	22.2	22.4	21.3	22.0	14.3	14.5	14.3	14.0
Simulated - Std Dev		17.2	17.8	17.7	17.0	17.5	16.3	16.6	16.2	16.1
Simulated COV		0.68	0.68	0.67	0.68	0.68	0.88	0.88	0.88	0.88
Minimum (neg. value is uplift)		0.20	0.26	0.42	0.47	0.31	0.000	0.000	0.000	0.001
Maximum		185.2	249.3	244.5	201.9	199.2	218.3	230.7	227.2	177.6
Prob exceeding "calculated" value		0.457	0.328	0.330	0.331	0.459	0.72	1.00	0.94	0.79
Prob exceeding 12.5 mm		0.750	0.767	0.768	0.751	0.759	0.55	0.55	0.55	0.54
Prob exceeding 25 mm		0.415	0.435	0.438	0.410	0.429	0.27	0.27	0.27	0.26
Prob exceeding 50 mm		0.088	0.101	0.101	0.085	0.095	0.05	0.05	0.05	0.05
		Prob of failure, $p_f$ =			$\beta$ =			Prob of failure, $p_f$ =		
		0.40			0.40			0.40		
		0.25			0.24			0.26		
		0.26			0.27			0.27		

\*\*Note -  $p_f$  also equals the probability of exceeding approx. 18.3 mm of differential displacement



**OpenSees Results - Footing Displacements and Angular Distortion at Footing Elevation**

Calculated results from bearing pressure-settlement equation and simulated results with 50,000 simulations that include bearing pressure-settlement equation (with known dispersion of model parameters) and variable soil undrained shear strength across horizontal distance, x.

Soil Parameters		Displacement Model (Vertical Spring) Parameters				Footing Parameters	
		$k_1$	$k_2$	$M_{stc}$	$B_{1.5}$ (m)	$B_{3.4}$ (m)	
$s_u$ (kPa)	= 70	0.013	0.701	0.643	1.675		
COV( $s_u$ )	= 0%	0.007	0.113	0.123	2.125		
Scale of Fluctuation, $\delta$ (m)	= 100	53.0	16.1	19.1	9.15		
$\gamma'$ (kN/m <sup>3</sup> )	= 19	Dist. = Gamma		Inv. Gauss. Lognormal			

"calculated" values assume no variation in soil shear strength or spring parameters

"Allowable" Distortion = 1/500 = 0.002

	Displacement (mm)					Distortion (for 9.15 m on-center footing spacing)				
	Footing 1	Footing 2	Footing 3	Footing 4	Footing 5	Footings 1-2	Footings 2-3	Footings 3-4	Footings 4-5	
"Deterministic" estimate	23.2	30.3	30.5	28.9	23.7	7.2	0.13	1.5	5.2	
Simulated - mean	25.2	26.3	26.4	24.9	25.9	18.6	19.0	18.6	18.3	"Deterministic" estimate
Simulated - median	21.5	22.3	22.5	21.1	21.9	14.2	14.7	14.3	14.1	Simulated - mean
Simulated - Std Dev	17.1	17.7	17.9	17.0	17.5	16.2	16.6	16.4	16.1	Simulated - median
Simulated COV	0.68	0.67	0.68	0.68	0.68	0.87	0.87	0.88	0.88	Simulated - Std Dev
Minimum (neg. value is uplift)	0.12	0.18	0.24	0.17	0.30	0.001	0.001	0.001	0.000	Simulated COV
Maximum	198.1	171.1	206.3	187.4	227.5	182.8	178.6	189.0	223.2	Minimum
Prob exceeding "calculated" value	0.456	0.332	0.333	0.326	0.459	0.73	0.99	0.94	0.79	Maximum
Prob exceeding 12.5 mm	0.749	0.770	0.766	0.744	0.761	0.55	0.56	0.55	0.54	Prob of failure, $p_f$ =
Prob exceeding 25 mm	0.414	0.438	0.440	0.408	0.430	0.27	0.28	0.27	0.26	$\beta$ =
Prob exceeding 50 mm	0.087	0.100	0.102	0.084	0.097	0.05	0.05	0.05	0.05	0.40
										0.26
										0.23
										0.25
										0.27

\*\*Note -  $p_f$  also equals the probability of exceeding approx. 18.3 mm of differential displacement

**OpenSees Results - Footing Displacements and Angular Distortion at Footing Elevation**

Calculated results from bearing pressure-settlement equation and simulated results with 50,000 simulations that include bearing pressure-settlement equation (with known dispersion of model parameters) and variable soil undrained shear strength across horizontal distance, x.

Soil Parameters		Displacement Model (Vertical Spring) Parameters				Footing Parameters	
		$k_1$	$k_2$	$M_{stc}$	$B_{1.5}$ (m)	$B_{3.4}$ (m)	
$s_u$ (kPa)	= 70	0.013	0.701	0.643	1.675		
COV( $s_u$ )	= 5%	0.007	0.113	0.123	2.125		
Scale of Fluctuation, $\delta$ (m)	= 0.1	53.0	16.1	19.1	9.15		
$\gamma'$ (kN/m <sup>3</sup> )	= 19	Dist. = Gamma Inv. Gauss. Lognormal					
"calculated" values assume no variation in soil shear strength or spring parameters							
"Allowable" Distortion = 1/500 = 0.002							
Distortion (for 9.15 m on-center footing spacing)							
		Footing 1-2		Footing 2-3	Footing 3-4	Footing 4-5	
"Deterministic" estimate		7.2	0.13	1.5	5.2		
Simulated - mean		18.5	19.0	18.5	18.4		
Simulated - median		14.3	14.5	14.3	14.2		
Simulated - Std Dev		16.2	16.8	16.2	16.0		
Simulated COV		0.88	0.88	0.88	0.87		
Minimum	(neg. value is uplift)	0.000	0.000	0.000	0.000		
Maximum		162.9	166.6	245.4	204.4		
Prob exceeding "calculated" value		0.461	0.328	0.330	0.331	0.453	
Prob exceeding 12.5 mm		0.753	0.766	0.768	0.748	0.759	
Prob exceeding 25 mm		0.420	0.437	0.439	0.412	0.424	
Prob exceeding 50 mm		0.087	0.099	0.102	0.084	0.094	
Differential Displacement (mm)							
		Footing 1-2		Footing 2-3	Footing 3-4	Footing 4-5	
"Deterministic" estimate		0.000	0.000	0.000	0.000		
Simulated - mean		0.72	0.72	0.99	0.94	0.80	
Simulated - median		0.55	0.55	0.56	0.55	0.55	
Simulated - Std Dev		0.27	0.28	0.28	0.27	0.27	
Simulated COV		0.005	0.005	0.06	0.05	0.05	
Minimum		0.000	0.000	0.000	0.000	0.000	
Maximum		0.01780	0.01780	0.01842	0.01842	0.02234	
Prob of failure, $p_f$		0.40	0.41	0.40	0.40	0.40	
$\beta$		0.26	0.23	0.26	0.26	0.26	

\*\*Note -  $p_f$  also equals the probability of exceeding approx. 18.3 mm of differential displacement

**OpenSees Results - Footing Displacements and Angular Distortion at Footing Elevation**

Calculated results from bearing pressure-settlement equation and simulated results with 50,000 simulations that include bearing pressure-settlement equation (with known dispersion of model parameters) and variable soil undrained shear strength across horizontal distance, x.

Soil Parameters		Displacement Model (Vertical Spring) Parameters				Footing Parameters				
		$k_1$	$k_2$	$M_{stc}$	$B_{1.5}$ (m)	$B_{3.4}$ (m)	Beam Dist.(m)			
$s_u$ (kPa)	= 70	0.013	0.701	0.643	1.675					
COV( $s_u$ )	= 5%	0.007	0.113	0.123	2.125					
Scale of Fluctuation, $\delta$ (m)	= 0.2	53.0	16.1	19.1	9.15					
$\gamma'$ (kN/m <sup>3</sup> )	= 19	Dist. = Gamma Inv. Gauss. Lognormal								
"calculated" values assume no variation in soil shear strength or spring parameters										
"Allowable" Distortion = 1/500 = 0.002										
		Displacement (mm)			Differential Displacement (mm)			Distortion (for 9.15 m on-center footing spacing)		
		Footing 1	Footing 2	Footing 3	Footing 4	Footing 5	Footing 1-2	Footing 2-3	Footing 3-4	Footing 4-5
"Deterministic" estimate		23.2	30.3	30.5	28.9	23.7	7.2	0.13	1.5	5.2
Simulated - mean		25.1	26.2	26.2	25.0	25.9	18.5	18.9	18.4	18.4
Simulated - median		21.2	22.3	22.3	21.2	22.0	14.3	14.6	14.2	14.1
Simulated - Std Dev		17.0	17.8	17.8	17.0	17.6	16.2	16.6	16.3	16.2
Simulated COV		0.68	0.68	0.68	0.68	0.68	0.87	0.88	0.88	0.88
Minimum (neg. value is uplift)		0.15	0.35	0.24	0.35	0.24	0.001	0.001	0.000	0.000
Maximum		220.2	213.1	190.5	194.4	313.1	209.8	161.8	189.0	283.1
Prob exceeding "calculated" value		0.453	0.329	0.327	0.326	0.459	0.73	1.00	0.94	0.79
Prob exceeding 12.5 mm		0.748	0.762	0.766	0.747	0.761	0.55	0.56	0.55	0.55
Prob exceeding 25 mm		0.412	0.436	0.435	0.410	0.429	0.27	0.28	0.26	0.26
Prob exceeding 50 mm		0.086	0.101	0.099	0.086	0.095	0.05	0.05	0.05	0.05
		Prob of failure, $p_f$ =			$\beta$ =			Prob of failure, $p_f$ =		
		0.40			0.41			0.39		
		0.25			0.24			0.27		
		0.27			0.27			0.27		
**Note - $p_f$ also equals the probability of exceeding approx. 18.3 mm of differential displacement										

**OpenSees Results - Footing Displacements and Angular Distortion at Footing Elevation**

Calculated results from bearing pressure-settlement equation and simulated results with 50,000 simulations that include bearing pressure-settlement equation (with known dispersion of model parameters) and variable soil undrained shear strength across horizontal distance, x.

Soil Parameters		Displacement Model (Vertical Spring) Parameters				Footing Parameters	
		$k_1$	$k_2$	$M_{stc}$	$B_{1,5}$ (m)	$B_{2,4}$ (m)	Beam Dist.(m)
$s_u$ (kPa)	= 70	0.013	0.701	0.643	1.675		
COV( $s_u$ )	= 5%	0.007	0.113	0.123	2.125		
Scale of Fluctuation, $\delta$ (m)	= 0.5	53.0	16.1	19.1			
$\gamma'$ (kN/m <sup>3</sup> )	= 19	Dist. = Gamma		Inv. Gauss.	Lognormal		

"calculated" values assume no variation in soil shear strength or spring parameters

"Allowable" Distortion = 1/500 = 0.002

	Displacement (mm)					Distortion (for 9.15 m on-center footing spacing)				
	Footing 1	Footing 2	Footing 3	Footing 4	Footing 5	Footing 1-2	Footing 2-3	Footing 3-4	Footing 4-5	
"Deterministic" estimate	23.2	30.3	30.5	28.9	23.7	7.2	0.13	1.5	5.2	
Simulated - mean	25.3	26.3	26.3	25.1	25.9	18.7	19.1	18.6	18.4	"Deterministic" estimate
Simulated - median	21.5	22.2	22.2	21.3	22.0	14.4	14.6	14.2	14.2	Simulated - mean
Simulated - Std Dev	17.1	18.0	20.3	17.0	17.7	16.4	19.3	18.8	16.2	Simulated - median
Simulated COV	0.67	0.69	0.77	0.68	0.68	0.88	1.01	1.01	0.88	Simulated - Std Dev
Minimum (neg. value is uplift)	0.29	0.40	0.15	0.33	0.26	0.001	0.000	0.002	0.000	Simulated COV
Maximum	202.5	204.6	2125.0	213.8	199.7	158.9	2119.6	2111.2	194.4	Minimum
Prob exceeding "calculated" value	0.461	0.327	0.327	0.328	0.460	0.73	0.99	0.94	0.79	Maximum
Prob exceeding 12.5 mm	0.752	0.766	0.766	0.750	0.758	0.55	0.56	0.55	0.55	Prob of failure, $p_f$ =
Prob exceeding 25 mm	0.419	0.435	0.436	0.410	0.430	0.27	0.28	0.27	0.26	$\beta$ =
Prob exceeding 50 mm	0.088	0.101	0.102	0.085	0.096	0.05	0.06	0.05	0.05	0.40
										0.25
										0.26
										0.26

\*\*Note -  $p_f$  also equals the probability of exceeding approx. 18.3 mm of differential displacement

**OpenSees Results - Footing Displacements and Angular Distortion at Footing Elevation**

Calculated results from bearing pressure-settlement equation and simulated results with 50,000 simulations that include bearing pressure-settlement equation (with known dispersion of model parameters) and variable soil undrained shear strength across horizontal distance, x.

Soil Parameters		Displacement Model (Vertical Spring) Parameters			Footing Parameters	
$s_u$ (kPa)	$k_1$	$k_2$	$M_{stc}$	$B_{1.5}$ (m)	$B_{3.4}$ (m)	Beam Dist.(m)
70	0.013	0.701	0.643	1.675		
COV( $s_u$ ) = 5%	0.007	0.113	0.123	2.125		
Scale of Fluctuation, $\delta$ (m) = 1	53.0	16.1	19.1	9.15		
$\gamma'$ (kN/m <sup>3</sup> ) = 19	Dist. = Gamma	Inv. Gauss.	Lognormal			

"calculated" values assume no variation in soil shear strength or spring parameters

"Allowable" Distortion = 1/500 = 0.002

	Displacement (mm)					Distortion (for 9.15 m on-center footing spacing)							
	Footing 1	Footing 2	Footing 3	Footing 4	Footing 5	Footings 1-2	Footings 2-3	Footings 3-4	Footings 4-5	Footings 1-2	Footings 2-3	Footings 3-4	Footings 4-5
"Deterministic" estimate	23.2	30.3	30.5	28.9	23.7	7.2	0.13	1.5	5.2	0.00078	0.00001	0.00017	0.00057
Simulated - mean	25.4	26.3	26.5	25.1	26.1	18.8	19.2	18.8	18.5	0.00206	0.00210	0.00205	0.00202
Simulated - median	21.4	22.2	22.4	21.3	22.1	14.4	14.7	14.4	14.2	0.00157	0.00161	0.00158	0.00156
Simulated - Std Dev	17.5	18.0	18.1	17.0	17.9	16.8	16.9	16.5	16.3	0.0018	0.0018	0.0018	0.0018
Simulated COV	0.69	0.69	0.68	0.68	0.69	0.89	0.88	0.88	0.88	0.89	0.88	0.88	0.88
Minimum (neg. value is uplift)	0.40	0.37	0.11	0.16	0.45	0.000	0.000	0.000	0.000	0.0000000	0.0000000	0.0000000	0.0000000
Maximum	318.5	188.1	178.9	198.7	203.3	294.6	178.7	160.7	182.7	0.03220	0.01853	0.01756	0.01997
Prob exceeding "calculated" value	0.457	0.329	0.333	0.330	0.462	0.72	1.00	0.94	0.79	0.40	0.41	0.40	0.40
Prob exceeding 12.5 mm	0.752	0.763	0.764	0.748	0.761	0.55	0.56	0.56	0.55	0.25	0.22	0.24	0.26
Prob exceeding 25 mm	0.416	0.434	0.440	0.412	0.432	0.27	0.28	0.27	0.26				
Prob exceeding 50 mm	0.090	0.103	0.104	0.085	0.100	0.05	0.06	0.05	0.05				

Prob of failure,  $p_f$  = 0.40     $\beta$  = 0.25

\*\*Note -  $p_f$  also equals the probability of exceeding approx. 18.3 mm of differential displacement

**OpenSees Results - Footing Displacements and Angular Distortion at Footing Elevation**

Calculated results from bearing pressure-settlement equation and simulated results with 50,000 simulations that include bearing pressure-settlement equation (with known dispersion of model parameters) and variable soil undrained shear strength across horizontal distance, x.

Soil Parameters		Displacement Model (Vertical Spring) Parameters				Footing Parameters	
$s_u$ (kPa)	$\delta$ (mm)	$k_1$	$k_2$	$M_{stc}$	$B_{1.5}$ (m)	$B_{3.4}$ (m)	Beam Dist.(m)
70	5%	0.013	0.701	0.643	1.675	2.125	9.15
COV( $s_u$ ) =	2	0.007	0.113	0.123			
Scale of Fluctuation, $\delta$ (mm) =	19	53.0	16.1	19.1			
$\gamma$ (kN/m <sup>3</sup> ) =		Dist. = Gamma	Inv. Gauss.	Lognormal			

"calculated" values assume no variation in soil shear strength or spring parameters

"Allowable" Distortion = 1/500 = 0.002

	Displacement (mm)					Differential Displacement (mm)					Distortion (for 9.15 m on-center footing spacing)						
	Footing 1	Footing 2	Footing 3	Footing 4	Footing 5	Footing 1-2	Footing 2-3	Footing 3-4	Footing 4-5	Footing 1-2	Footing 2-3	Footing 3-4	Footing 4-5	Footing 1-2	Footing 2-3	Footing 3-4	Footing 4-5
"Deterministic" estimate	23.2	30.3	30.5	28.9	23.7	7.2	0.13	1.5	5.2	0.00078	0.00001	0.00017	0.00057	0.00203	0.00208	0.00205	0.00202
Simulated - mean	25.4	26.2	26.3	25.1	25.9	18.6	19.0	18.8	18.5	0.00156	0.00161	0.00158	0.00154	0.00118	0.00118	0.00118	0.00118
Simulated - median	21.5	22.1	22.2	21.2	22.0	14.2	14.7	14.4	14.1	0.88	0.88	0.88	0.89	0.88	0.88	0.88	0.89
Simulated - Std Dev	17.1	17.9	18.1	17.2	17.8	16.5	16.8	16.6	16.4	0.001	0.001	0.001	0.001	0.001	0.001	0.001	0.001
Simulated COV	0.68	0.68	0.69	0.68	0.69	0.88	0.88	0.88	0.89	0.0000001	0.0000000	0.0000002	0.0000000	0.03214	0.03640	0.02806	0.01942
Minimum (neg. value is uplift)	0.23	0.15	0.22	0.35	0.27	0.001	0.000	0.002	0.000								
Maximum	173.5	338.3	267.1	191.9	200.2	294.1	333.1	256.7	177.7								
Prob exceeding "calculated" value	0.459	0.328	0.327	0.331	0.460	0.72	0.99	0.94	0.79	0.40	0.41	0.40	0.39	0.25	0.23	0.24	0.27
Prob exceeding 12.5 mm	0.754	0.763	0.763	0.745	0.758	0.55	0.56	0.55	0.55								
Prob exceeding 25 mm	0.418	0.433	0.437	0.409	0.431	0.27	0.28	0.27	0.27								
Prob exceeding 50 mm	0.089	0.101	0.102	0.087	0.097	0.05	0.06	0.05	0.05								

Prob of failure,  $p_f$  =  $\beta$  =

\*\*Note -  $p_f$  also equals the probability of exceeding approx. 18.3 mm of differential displacement

**OpenSees Results - Footing Displacements and Angular Distortion at Footing Elevation**

Calculated results from bearing pressure-settlement equation and simulated results with 50,000 simulations that include bearing pressure-settlement equation (with known dispersion of model parameters) and variable soil undrained shear strength across horizontal distance, x.

Soil Parameters		Displacement Model (Vertical Spring) Parameters				Footing Parameters	
$s_u$ (kPa)	$\delta$ (mm)	$k_1$	$k_2$	$M_{stc}$	$B_{1.5}$ (m)	$B_{3.4}$ (m)	Beam Dist.(m)
70	5%	0.013	0.701	0.643	1.675	2.125	9.15
COV( $s_u$ ) =	5	0.007	0.113	0.123			
Scale of Fluctuation, $\delta$ (mm) =	19	53.0	16.1	19.1			
$\gamma$ (kN/m <sup>3</sup> ) =		Dist. = Gamma	Inv. Gauss.	Lognormal			

"calculated" values assume no variation in soil shear strength or spring parameters

"Allowable" Distortion = 1/500 = 0.002

	Displacement (mm)					Distortion (for 9.15 m on-center footing spacing)				
	Footing 1	Footing 2	Footing 3	Footing 4	Footing 5	Footing 1-2	Footing 2-3	Footing 3-4	Footing 4-5	
"Deterministic" estimate	23.2	30.3	30.5	28.9	23.7	7.2	0.13	1.5	5.2	"Deterministic" estimate
Simulated - mean	25.4	26.3	26.6	25.1	26.0	18.9	19.3	18.8	18.6	Simulated - mean
Simulated - median	21.4	22.1	22.4	21.2	21.9	14.5	14.7	14.4	14.3	Simulated - median
Simulated - Std Dev	17.4	20.4	18.3	17.3	18.0	19.1	19.5	16.8	16.5	Simulated - Std Dev
Simulated COV	0.68	0.77	0.69	0.69	0.69	1.01	1.01	0.89	0.89	Simulated COV
Minimum (neg. value is uplift)	0.23	0.20	0.22	0.19	0.17	0.001	0.001	0.001	0.000	Minimum
Maximum	209.3	2125.0	186.1	175.0	239.4	2096.0	2099.2	167.6	202.1	Maximum
Prob exceeding "calculated" value	0.457	0.329	0.333	0.327	0.458	0.73	1.00	0.94	0.79	Prob of failure, $p_f$ =
Prob exceeding 12.5 mm	0.751	0.764	0.768	0.745	0.759	0.55	0.56	0.55	0.55	$\beta$ =
Prob exceeding 25 mm	0.417	0.434	0.441	0.407	0.429	0.28	0.28	0.27	0.27	0.24
Prob exceeding 50 mm	0.091	0.103	0.106	0.088	0.100	0.05	0.06	0.06	0.05	0.25

\*\*Note -  $p_f$  also equals the probability of exceeding approx. 18.3 mm of differential displacement

**OpenSees Results - Footing Displacements and Angular Distortion at Footing Elevation**

Calculated results from bearing pressure-settlement equation and simulated results with 50,000 simulations that include bearing pressure-settlement equation (with known dispersion of model parameters) and variable soil undrained shear strength across horizontal distance, x.

Soil Parameters		Displacement Model (Vertical Spring) Parameters				Footing Parameters	
$s_u$ (kPa)	$\delta$ (m)	$k_1$	$k_2$	$M_{stc}$	$B_{1.5}$ (m)	$B_{3.4}$ (m)	Beam Dist.(m)
70	5%	0.013	0.701	0.643	1.675	2.125	9.15
COV( $s_u$ ) =	10	0.007	0.113	0.123			
Scale of Fluctuation, $\delta$ (m) =	19	53.0	16.1	19.1			
$\gamma$ (kN/m <sup>3</sup> ) =		Dist. = Gamma	Inv. Gauss.	Lognormal			

"calculated" values assume no variation in soil shear strength or spring parameters

"Allowable" Distortion = 1/500 = 0.002

	Displacement (mm)					Differential Displacement (mm)					Distortion (for 9.15 m on-center footing spacing)						
	Footing 1	Footing 2	Footing 3	Footing 4	Footing 5	Footing 1-2	Footing 2-3	Footing 3-4	Footing 4-5	Footing 1-2	Footing 2-3	Footing 3-4	Footing 4-5	Footing 1-2	Footing 2-3	Footing 3-4	Footing 4-5
"Deterministic" estimate	23.2	30.3	30.5	28.9	23.7	7.2	0.13	1.5	5.2	0.00078	0.00001	0.00017	0.00057	0.00204	0.00208	0.00204	0.00203
Simulated - mean	25.4	26.2	26.5	25.1	26.0	18.6	19.1	18.6	18.6	0.00204	0.00208	0.00204	0.00203	0.00155	0.00160	0.00156	0.00156
Simulated - median	21.5	22.2	22.3	21.3	21.9	14.2	14.7	14.3	14.3	0.00155	0.00160	0.00156	0.00156	0.0018	0.0018	0.0018	0.0018
Simulated - Std Dev	17.4	17.8	18.2	17.1	17.9	16.5	16.8	16.5	16.3	0.89	0.88	0.89	0.88	0.89	0.88	0.89	0.88
Simulated COV	0.69	0.68	0.69	0.68	0.69	0.89	0.88	0.89	0.88	0.89	0.88	0.89	0.88	0.89	0.88	0.89	0.88
Minimum (neg. value is uplift)	0.16	0.17	0.24	0.29	0.26	0.000	0.000	0.000	0.001	0.0000000	0.0000000	0.0000000	0.0000000	0.02345	0.02369	0.01856	0.02187
Maximum	194.7	229.9	184.2	207.0	213.0	214.6	216.7	189.8	200.1	0.40	0.41	0.40	0.40	0.26	0.23	0.25	0.26
Prob exceeding "calculated" value	0.459	0.328	0.329	0.331	0.458	0.72	1.00	0.94	0.79	0.40	0.41	0.40	0.40	0.26	0.23	0.25	0.26
Prob exceeding 12.5 mm	0.751	0.766	0.765	0.748	0.759	0.55	0.56	0.55	0.55	0.26	0.23	0.25	0.26	0.26	0.23	0.25	0.26
Prob exceeding 25 mm	0.417	0.436	0.438	0.409	0.429	0.27	0.28	0.27	0.27	0.06	0.06	0.06	0.05	0.06	0.06	0.05	0.05
Prob exceeding 50 mm	0.091	0.099	0.104	0.089	0.100	0.06	0.06	0.06	0.05	0.00	0.00	0.00	0.00	0.00	0.00	0.00	0.00

Prob of failure,  $p_f$  = 0.40     $\beta$  = 0.26

\*\*Note -  $p_f$  also equals the probability of exceeding approx. 18.3 mm of differential displacement



**OpenSees Results - Footing Displacements and Angular Distortion at Footing Elevation**

Calculated results from bearing pressure-settlement equation and simulated results with 50,000 simulations that include bearing pressure-settlement equation (with known dispersion of model parameters) and variable soil undrained shear strength across horizontal distance, x.

Soil Parameters		Displacement Model (Vertical Spring) Parameters				Footing Parameters	
		$k_1$	$k_2$	$M_{stc}$	$B_{1.5}$ (m)	$B_{3.4}$ (m)	
$s_u$ (kPa)	= 70	0.013	0.701	0.643	1.675		
COV( $s_u$ )	= 5%	0.007	0.113	0.123	2.125		
Scale of Fluctuation, $\delta$ (m)	= 20	53.0	16.1	19.1	9.15		
$\gamma'$ (kN/m <sup>3</sup> )	= 19	Inv. Gauss.		Lognormal			
		Dist. = Gamma					
"calculated" values assume no variation in soil shear strength or spring parameters							
"Allowable" Distortion = 1/500 = 0.002							
		Displacement (mm)			Distortion (for 9.15 m on-center footing spacing)		
		Footing 1	Footing 2	Footing 3	Footing 4	Footing 5	
		23.2	30.3	30.5	28.9	23.7	
"Deterministic" estimate		25.4	26.3	26.5	25.1	26.1	
Simulated - mean		21.5	22.2	22.3	21.0	22.1	
Simulated - median		17.4	18.0	18.2	17.3	18.0	
Simulated - Std Dev		0.68	0.69	0.69	0.69	0.69	
Simulated COV		0.14	0.20	0.22	0.31	0.33	
Minimum (neg. value is uplift)		218.3	183.1	175.2	184.4	198.9	
Maximum		0.458	0.330	0.330	0.328	0.460	
Prob exceeding "calculated" value		0.754	0.764	0.765	0.744	0.761	
Prob exceeding 12.5 mm		0.418	0.435	0.438	0.407	0.432	
Prob exceeding 25 mm		0.088	0.102	0.104	0.088	0.100	
Prob exceeding 50 mm							
		Differential Displacement (mm)			Distortion (for 9.15 m on-center footing spacing)		
		Footing 1-2	Footing 2-3	Footing 3-4	Footing 4-5		
		7.2	0.13	1.5	5.2		
		18.7	19.1	18.7	18.6		
		14.4	14.7	14.2	14.2		
		16.5	17.0	16.6	16.6		
		0.88	0.89	0.89	0.89		
		0.001	0.000	0.000	0.000		
		194.4	170.5	165.7	185.3		
"Deterministic" estimate		0.00078	0.00001	0.00001	0.00001		
Simulated - mean		0.00204	0.00209	0.00204	0.00204		
Simulated - median		0.00157	0.00160	0.00156	0.00155		
Simulated - Std Dev		0.0018	0.0019	0.0018	0.0018		
Simulated COV		0.88	0.89	0.89	0.89		
Minimum		0.0000001	0.0000000	0.0000000	0.0000000		
Maximum		0.02124	0.01863	0.01811	0.02025		
		Prob of failure, $p_f$ =			0.40 0.41 0.40 0.40		
		$\beta$ =			0.26 0.23 0.26 0.26		
**Note - $p_f$ also equals the probability of exceeding approx. 18.3 mm of differential displacement							

**OpenSees Results - Footing Displacements and Angular Distortion at Footing Elevation**

Calculated results from bearing pressure-settlement equation and simulated results with 50,000 simulations that include bearing pressure-settlement equation (with known dispersion of model parameters) and variable soil undrained shear strength across horizontal distance, x.

Soil Parameters		Displacement Model (Vertical Spring) Parameters				Footing Parameters	
$s_u$ (kPa)	$\delta$ (mm)	$k_1$	$k_2$	$M_{stc}$	$B_{1.5}$ (m)	$B_{3.4}$ (m)	Beam Dist.(m)
70	30	0.013	0.701	0.643	1.675	2.125	9.15
COV( $s_u$ ) = 5%		0.007	0.113	0.123			
Scale of Fluctuation, $\delta$ (mm) = 19		53.0	16.1	19.1			
$\gamma$ (kN/m <sup>3</sup> ) = 19		Dist. = Gamma	Inv. Gauss.	Lognormal			

"calculated" values assume no variation in soil shear strength or spring parameters

"Allowable" Distortion = 1/500 = 0.002

	Displacement (mm)					Distortion (for 9.15 m on-center footing spacing)							
	Footing 1	Footing 2	Footing 3	Footing 4	Footing 5	Footings 1-2	Footings 2-3	Footings 3-4	Footings 4-5	Footings 1-2	Footings 2-3	Footings 3-4	Footings 4-5
"Deterministic" estimate	23.2	30.3	30.5	28.9	23.7	7.2	0.13	1.5	5.2	0.00078	0.00001	0.00017	0.00057
Simulated - mean	25.3	26.5	26.4	25.2	26.0	18.7	19.2	18.6	18.4	0.00205	0.00210	0.00204	0.00201
Simulated - median	21.3	22.3	22.2	21.4	22.0	14.3	14.7	14.2	14.2	0.00157	0.00160	0.00156	0.00155
Simulated - Std Dev	17.3	18.2	18.3	17.1	17.8	16.6	17.1	16.6	16.2	0.0018	0.0019	0.0018	0.0018
Simulated COV	0.68	0.69	0.69	0.68	0.69	0.89	0.89	0.89	0.88	0.89	0.89	0.89	0.88
Minimum (neg. value is uplift)	0.21	0.19	0.34	0.23	0.05	0.000	0.001	0.001	0.001	0.0000000	0.0000001	0.0000001	0.0000001
Maximum	176.7	241.6	211.0	204.7	201.0	229.9	189.3	208.7	171.1	0.02512	0.02068	0.02281	0.01870
Prob exceeding "calculated" value	0.455	0.334	0.329	0.332	0.460	0.72	1.00	0.94	0.79	0.40	0.41	0.40	0.40
Prob exceeding 12.5 mm	0.750	0.766	0.766	0.750	0.761	0.55	0.56	0.55	0.55	0.25	0.23	0.26	0.26
Prob exceeding 25 mm	0.414	0.439	0.437	0.413	0.430	0.27	0.28	0.27	0.26				
Prob exceeding 50 mm	0.089	0.104	0.103	0.087	0.097	0.05	0.06	0.05	0.05				

Prob of failure,  $p_f$  = 0.40     $\beta$  = 0.25

\*\*Note -  $p_f$  also equals the probability of exceeding approx. 18.3 mm of differential displacement

**OpenSees Results - Footing Displacements and Angular Distortion at Footing Elevation**

Calculated results from bearing pressure-settlement equation and simulated results with 50,000 simulations that include bearing pressure-settlement equation (with known dispersion of model parameters) and variable soil undrained shear strength across horizontal distance, x.

Soil Parameters		Displacement Model (Vertical Spring) Parameters				Footing Parameters	
$s_u$ (kPa)	$k_z$	$k_1$	$k_2$	$M_{stc}$	$B_{1.5}$ (m)	$B_{3.4}$ (m)	Beam Dist.(m)
70	0.013	0.701	0.643	1.675	1.675	2.125	9.15
COV( $s_u$ ) = 5%	0.007	0.113	0.123				
Scale of Fluctuation, $\delta$ (m) = 50	53.0	16.1	19.1				
$\gamma'$ (kN/m <sup>3</sup> ) = 19	Dist. = Gamma	Inv. Gauss.	Lognormal				

"calculated" values assume no variation in soil shear strength or spring parameters

"Allowable" Distortion = 1/500 = 0.002

	Displacement (mm)					Distortion (for 9.15 m on-center footing spacing)							
	Footing 1	Footing 2	Footing 3	Footing 4	Footing 5	Footings 1-2	Footings 2-3	Footings 3-4	Footings 4-5	Footings 1-2	Footings 2-3	Footings 3-4	Footings 4-5
"Deterministic" estimate	23.2	30.3	30.5	28.9	23.7	7.2	0.13	1.5	5.2	0.00078	0.00001	0.00017	0.00057
Simulated - mean	25.5	26.3	26.5	25.1	26.1	18.8	19.2	18.8	18.6	0.00206	0.00209	0.00205	0.00204
Simulated - median	21.5	22.1	22.4	21.1	22.0	14.3	14.7	14.5	14.3	0.00156	0.00161	0.00158	0.00157
Simulated - Std Dev	19.1	18.2	18.2	17.2	18.0	18.3	16.9	16.5	16.4	0.0020	0.0019	0.0018	0.0018
Simulated COV	0.75	0.69	0.69	0.69	0.69	0.97	0.88	0.88	0.88	0.97	0.88	0.88	0.88
Minimum (neg. value is uplift)	0.21	0.24	0.43	0.24	0.22	0.000	0.000	0.001	0.000	0.0000000	0.0000000	0.0000001	0.0000000
Maximum	1675.0	237.9	187.3	184.7	193.7	1650.9	213.2	165.2	166.2	0.18043	0.02330	0.01806	0.01817
Prob exceeding "calculated" value	0.459	0.326	0.333	0.330	0.459	0.72	1.00	0.94	0.79	0.40	0.41	0.40	0.40
Prob exceeding 12.5 mm	0.754	0.760	0.766	0.743	0.760	0.55	0.56	0.56	0.55	0.25	0.22	0.24	0.26
Prob exceeding 25 mm	0.417	0.431	0.440	0.410	0.431	0.27	0.28	0.27	0.27	0.10	0.09	0.10	0.10
Prob exceeding 50 mm	0.092	0.102	0.105	0.088	0.102	0.05	0.06	0.05	0.05	0.01	0.01	0.01	0.01

Prob of failure,  $p_f$  = 0.40     $\beta$  = 0.25

\*\*Note -  $p_f$  also equals the probability of exceeding approx. 18.3 mm of differential displacement

**OpenSees Results - Footing Displacements and Angular Distortion at Footing Elevation**

Calculated results from bearing pressure-settlement equation and simulated results with 50,000 simulations that include bearing pressure-settlement equation (with known dispersion of model parameters) and variable soil undrained shear strength across horizontal distance, x.

Soil Parameters		Displacement Model (Vertical Spring) Parameters				Footing Parameters	
		$k_1$	$k_2$	$M_{stc}$	$B_{1.5}$ (m)	$B_{3.4}$ (m)	Beam Dist.(m)
$s_u$ (kPa)	= 70	0.013	0.701	0.643	1.675		
COV( $s_u$ )	= 5%	0.007	0.113	0.123	2.125		
Scale of Fluctuation, $\delta$ (m)	= 100	53.0	16.1	19.1	9.15		
$\gamma'$ (kN/m <sup>3</sup> )	= 19	Dist. = Gamma		Inv. Gauss.	Lognormal		

"calculated" values assume no variation in soil shear strength or spring parameters

"Allowable" Distortion = 1/500 = 0.002

	Displacement (mm)					Distortion (for 9.15 m on-center footing spacing)				
	Footing 1	Footing 2	Footing 3	Footing 4	Footing 5	Footing 1-2	Footing 2-3	Footing 3-4	Footing 4-5	
"Deterministic" estimate	23.2	30.3	30.5	28.9	23.7	7.2	0.13	1.5	5.2	
Simulated - mean	25.3	26.4	26.4	25.1	26.0	18.6	19.1	18.7	18.4	"Deterministic" estimate
Simulated - median	21.4	22.2	22.3	21.1	21.9	14.2	14.7	14.2	14.1	Simulated - mean
Simulated - Std Dev	17.3	18.2	18.3	17.2	17.8	16.5	16.9	16.6	16.3	Simulated - median
Simulated COV	0.68	0.69	0.69	0.69	0.69	0.89	0.88	0.89	0.89	Simulated - Std Dev
Minimum (neg. value is uplift)	0.31	0.47	0.38	0.33	0.31	0.000	0.000	0.000	0.000	Simulated COV
Maximum	246.8	194.3	207.0	233.0	262.8	230.6	173.1	222.2	223.8	Minimum
Prob exceeding "calculated" value	0.457	0.331	0.328	0.327	0.457	0.72	1.00	0.94	0.79	Maximum
Prob exceeding 12.5 mm	0.750	0.764	0.765	0.746	0.761	0.55	0.56	0.55	0.55	Prob of failure, $p_f$ =
Prob exceeding 25 mm	0.415	0.436	0.437	0.407	0.427	0.27	0.28	0.27	0.26	$\beta$ =
Prob exceeding 50 mm	0.089	0.104	0.105	0.089	0.098	0.05	0.06	0.05	0.05	

\*\*Note -  $p_f$  also equals the probability of exceeding approx. 18.3 mm of differential displacement

**OpenSees Results - Footing Displacements and Angular Distortion at Footing Elevation**

Calculated results from bearing pressure-settlement equation and simulated results with 50,000 simulations that include bearing pressure-settlement equation (with known dispersion of model parameters) and variable soil undrained shear strength across horizontal distance, x.

Soil Parameters		Displacement Model (Vertical Spring) Parameters				Footing Parameters					
		$k_1$	$k_2$	$M_{stc}$	$B_{1,5} (m)$	$B_{3,4} (m)$	$B_{3,4} (m)$				
$s_u (kPa)$	= 70	0.013	0.701	0.643	1.675						
$COV(s_u)$	= 10%	0.007	0.113	0.123	2.125						
$Scale\ of\ Fluctuation,\ \delta (m)$	= 0.1	53.0	16.1	19.1	9.15						
$\gamma' (kN/m^3)$	= 19	Dist. = Gamma Inv. Gauss. Lognormal									
"calculated" values assume no variation in soil shear strength or spring parameters											
"Allowable" Distortion = 1/500 = 0.002											
		Displacement (mm)			Differential Displacement (mm)			Distortion (for 9.15 m on-center footing spacing)			
		Footing 1	Footing 2	Footing 3	Footing 4	Footing 5	Footing 1-2	Footing 2-3	Footing 3-4	Footing 4-5	
"Deterministic" estimate		23.2	30.3	30.5	28.9	23.7	7.2	0.13	1.5	5.2	
Simulated - mean		25.2	26.1	26.5	25.0	25.9	18.6	19.1	18.6	18.5	"Deterministic" estimate
Simulated - median		21.4	22.1	22.4	21.2	21.9	14.3	14.7	14.3	14.3	0.00017
Simulated - Std Dev		17.1	17.8	18.1	17.0	19.1	16.3	16.8	16.4	17.8	0.00203
Simulated COV		0.68	0.68	0.68	0.68	0.74	0.87	0.88	0.88	0.96	0.00156
Minimum (neg. value is uplift)		0.44	0.17	0.35	0.33	0.18	0.000	0.001	0.000	0.000	0.0019
Maximum		178.9	185.0	227.5	171.2	1675.0	173.1	202.8	192.9	1650.4	0.88
Prob exceeding "calculated" value		0.456	0.327	0.329	0.329	0.456	0.73	1.00	0.94	0.80	0.41
Prob exceeding 12.5 mm		0.752	0.761	0.768	0.748	0.761	0.55	0.56	0.55	0.55	0.40
Prob exceeding 25 mm		0.416	0.432	0.439	0.412	0.427	0.27	0.28	0.27	0.27	0.26
Prob exceeding 50 mm		0.088	0.098	0.104	0.084	0.096	0.05	0.06	0.05	0.05	0.26
										Prob of failure, $p_f$ = 0.40 $\beta$ = 0.25	
**Note - $p_f$ also equals the probability of exceeding approx. 18.3 mm of differential displacement											

**OpenSees Results - Footing Displacements and Angular Distortion at Footing Elevation**

Calculated results from bearing pressure-settlement equation and simulated results with 50,000 simulations that include bearing pressure-settlement equation (with known dispersion of model parameters) and variable soil undrained shear strength across horizontal distance, x.

Soil Parameters		Displacement Model (Vertical Spring) Parameters				Footing Parameters			
$s_u$ (kPa)	= 70	$k_1$	$k_2$	$M_{stc}$	$B_{1.5}$ (m)	$B_{3.4}$ (m)	$B_{4.5}$ (m)	$B_{5.2}$ (m)	
COV( $s_u$ )	= 10%	$\mu$	0.013	0.701	0.643	0.113	0.123	0.125	
Scale of Fluctuation, $\delta$ (m)	= 0.2	$\sigma$	0.007	18.1	19.1	16.1	19.1	9.15	
$\gamma'$ (kN/m <sup>3</sup> )	= 19	COV(%)	= 53.0	Inv. Gauss.	Lognormal	Beam Dist.(m)			
		Dist.	= Gamma						
"calculated" values assume no variation in soil shear strength or spring parameters									
"Allowable" Distortion = 1/500 = 0.002									
<b>Distortion (for 9.15 m on-center footing spacing)</b>									
		Footings 1-2	Footings 2-3	Footings 3-4	Footings 4-5				
"Deterministic" estimate		0.00078	0.00001	0.00001	0.00017				
Simulated - mean		0.00205	0.00209	0.00204	0.00202				
Simulated - median		0.00157	0.00161	0.00157	0.00155				
Simulated - Std Dev		0.0018	0.0018	0.0018	0.0018				
Simulated COV		0.88	0.88	0.88	0.88				
Minimum	(neg. value is uplift)	0.0000000	0.0000001	0.0000002	0.0000000				
Maximum		0.01852	0.02205	0.02293	0.01770				
<b>Prob of failure, <math>p_f</math> = 0.40 0.41 0.40 0.40</b>									
<b><math>\beta</math> = 0.25 0.23 0.25 0.26</b>									
**Note - $p_f$ also equals the probability of exceeding approx. 18.3 mm of differential displacement									
<b>Differential Displacement (mm)</b>									
		Footings 1-2	Footings 2-3	Footings 3-4	Footings 4-5				
"Deterministic" estimate		7.2	0.13	1.5	5.2				
Simulated - mean		18.8	19.1	18.7	18.5				
Simulated - median		14.4	14.7	14.3	14.2				
Simulated - Std Dev		16.6	16.8	16.5	16.3				
Simulated COV		0.88	0.88	0.88	0.88				
Minimum		0.000	0.001	0.002	0.000				
Maximum		169.4	201.8	209.8	161.9				
<b>Displacement (mm)</b>									
		Footing 1	Footing 2	Footing 3	Footing 4	Footing 5			
"Deterministic" estimate		23.2	30.3	30.5	28.9	23.7			
Simulated - mean		25.5	26.3	26.5	25.1	26.0			
Simulated - median		21.6	22.2	22.3	21.2	21.9			
Simulated - Std Dev		17.4	18.0	18.1	17.1	17.8			
Simulated COV		0.68	0.68	0.69	0.68	0.69			
Minimum		0.37	0.23	0.32	0.30	0.33			
Maximum		217.7	177.4	226.1	172.0	181.9			
<b>Prob exceeding "calculated" value</b>									
<b>Prob exceeding 12.5 mm</b>									
<b>Prob exceeding 25 mm</b>									
<b>Prob exceeding 50 mm</b>									
		0.463	0.329	0.331	0.330	0.456			
		0.757	0.763	0.767	0.748	0.760			
		0.420	0.433	0.439	0.409	0.427			
		0.090	0.102	0.104	0.087	0.097			
		0.73	0.99	0.94	0.79	0.79			
		0.55	0.56	0.55	0.55	0.55			
		0.27	0.28	0.27	0.27	0.27			
		0.05	0.06	0.05	0.05	0.05			

**OpenSees Results - Footing Displacements and Angular Distortion at Footing Elevation**

Calculated results from bearing pressure-settlement equation and simulated results with 50,000 simulations that include bearing pressure-settlement equation (with known dispersion of model parameters) and variable soil undrained shear strength across horizontal distance, x.

Soil Parameters		Displacement Model (Vertical Spring) Parameters				Footing Parameters					
		$k_1$	$k_2$	$M_{stc}$	$B_{1.5}$ (m)	$B_{3.4}$ (m)	Beam Dist.(m)				
$s_u$ (kPa)	= 70	0.013	0.701	0.643	1.675						
COV( $s_u$ )	= 10%	0.007	0.113	0.123	2.125						
Scale of Fluctuation, $\delta$ (m)	= 0.5	53.0	16.1	19.1	9.15						
$\gamma'$ (kN/m <sup>3</sup> )	= 19	Dist. = Gamma Inv. Gauss. Lognormal									
"calculated" values assume no variation in soil shear strength or spring parameters											
"Allowable" Distortion = 1/500 = 0.002											
		Displacement (mm)			Differential Displacement (mm)			Distortion (for 9.15 m on-center footing spacing)			
		Footing 1	Footing 2	Footing 3	Footing 4	Footing 5	Footing 1-2	Footing 2-3	Footing 3-4	Footing 4-5	
"Deterministic" estimate		23.2	30.3	30.5	28.9	23.7	7.2	0.13	1.5	5.2	
Simulated - mean		25.6	26.5	26.6	25.2	26.1	18.9	19.4	19.0	18.8	"Deterministic" estimate
Simulated - median		21.5	22.2	22.3	21.2	21.8	14.3	14.8	14.4	14.2	0.00207
Simulated - Std Dev		17.9	18.4	18.4	17.4	18.3	17.1	17.3	17.0	17.0	0.00156
Simulated COV		0.70	0.69	0.69	0.69	0.70	0.91	0.89	0.89	0.90	0.00161
Minimum (neg. value is uplift)		0.36	0.27	0.32	0.16	0.38	0.000	0.000	0.000	0.001	0.91
Maximum		420.7	222.9	236.1	214.4	602.4	415.5	228.6	183.4	555.5	0.0000000
Prob exceeding "calculated" value		0.459	0.329	0.333	0.331	0.454	0.72	1.00	0.94	0.79	0.40
Prob exceeding 12.5 mm		0.753	0.765	0.766	0.747	0.759	0.55	0.56	0.55	0.55	0.40
Prob exceeding 25 mm		0.417	0.436	0.440	0.413	0.426	0.27	0.28	0.27	0.27	0.25
Prob exceeding 50 mm		0.095	0.104	0.107	0.089	0.100	0.06	0.06	0.06	0.06	0.25
										Prob of failure, $p_f$ = 0.40 $\beta$ = 0.25	

\*\*Note -  $p_f$  also equals the probability of exceeding approx. 18.3 mm of differential displacement

**OpenSees Results - Footing Displacements and Angular Distortion at Footing Elevation**

Calculated results from bearing pressure-settlement equation and simulated results with 50,000 simulations that include bearing pressure-settlement equation (with known dispersion of model parameters) and variable soil undrained shear strength across horizontal distance, x.

Soil Parameters		Displacement Model (Vertical Spring) Parameters				Footing Parameters	
$s_u$ (kPa)	$k_z$	$k_1$	$k_2$	$M_{stc}$	$B_{1.5}$ (m)	$B_{3.4}$ (m)	Beam Dist.(m)
70	0.013	0.701	0.643	1.675	1.675	2.125	9.15
COV( $s_u$ ) = 10%	0.007	0.113	0.123				
Scale of Fluctuation, $\delta$ (m) = 1	53.0	16.1	19.1				
$\gamma$ (kN/m <sup>3</sup> ) = 19	Dist. = Gamma	Inv. Gauss.	Lognormal				

"calculated" values assume no variation in soil shear strength or spring parameters

"Allowable" Distortion = 1/500 = 0.002

	Displacement (mm)				Differential Displacement (mm)				Distortion (for 9.15 m on-center footing spacing)				
	Footing 1	Footing 2	Footing 3	Footing 4	Footing 5	Footing 1-2	Footing 2-3	Footing 3-4	Footing 4-5	Footing 1-2	Footing 2-3	Footing 3-4	Footing 4-5
"Deterministic" estimate	23.2	30.3	30.5	28.9	23.7	7.2	0.13	1.5	5.2	0.00078	0.00001	0.00017	0.00057
Simulated - mean	25.6	26.6	26.5	25.3	26.2	19.2	19.6	19.0	19.0	0.00209	0.00214	0.00208	0.00208
Simulated - median	21.4	22.2	22.2	21.2	21.8	14.6	14.8	14.3	14.5	0.00159	0.00162	0.00157	0.00158
Simulated - Std Dev	17.8	18.6	18.5	17.7	18.4	17.3	17.6	17.1	17.1	0.0019	0.0019	0.0019	0.0019
Simulated COV	0.70	0.70	0.70	0.70	0.70	0.91	0.90	0.90	0.90	0.91	0.90	0.90	0.90
Minimum (neg. value is uplift)	0.25	0.22	0.23	0.39	0.27	0.000	0.000	0.000	0.000	0.0000000	0.0000000	0.0000000	0.0000000
Maximum	205.2	296.1	229.7	189.0	199.1	286.7	263.4	178.7	179.2	0.03134	0.02879	0.01853	0.01958
Prob exceeding "calculated" value	0.458	0.330	0.329	0.332	0.457	0.72	0.99	0.94	0.80	0.41	0.42	0.40	0.40
Prob exceeding 12.5 mm	0.751	0.764	0.766	0.746	0.760	0.56	0.56	0.55	0.56	0.23	0.21	0.25	0.24
Prob exceeding 25 mm	0.417	0.437	0.433	0.412	0.428	0.28	0.29	0.27	0.27				
Prob exceeding 50 mm	0.094	0.108	0.106	0.092	0.104	0.06	0.06	0.06	0.06				

Prob of failure,  $p_f$  = 0.41     $\beta$  = 0.23

\*\*Note -  $p_f$  also equals the probability of exceeding approx. 18.3 mm of differential displacement



**OpenSees Results - Footing Displacements and Angular Distortion at Footing Elevation**

Calculated results from bearing pressure-settlement equation and simulated results with 50,000 simulations that include bearing pressure-settlement equation (with known dispersion of model parameters) and variable soil undrained shear strength across horizontal distance, x.

Soil Parameters		Displacement Model (Vertical Spring) Parameters				Footing Parameters	
		$k_1$	$k_2$	$M_{stc}$	$B_{1.5}$ (m)	$B_{3.4}$ (m)	Beam Dist.(m)
$s_u$ (kPa)	= 70	0.013	0.701	0.643	1.675		
COV( $s_u$ )	= 10%	0.007	0.113	0.123	2.125		
Scale of Fluctuation, $\delta$ (m)	= 2	53.0	16.1	19.1	9.15		
$\gamma'$ (kN/m <sup>3</sup> )	= 19	Dist. = Gamma		Inv. Gauss. Lognormal			

"calculated" values assume no variation in soil shear strength or spring parameters

"Allowable" Distortion = 1/500 = 0.002

	Displacement (mm)					Differential Displacement (mm)					Distortion (for 9.15 m on-center footing spacing)						
	Footing 1	Footing 2	Footing 3	Footing 4	Footing 5	Footing 1-2	Footing 2-3	Footing 3-4	Footing 4-5	Footing 1-2	Footing 2-3	Footing 3-4	Footing 4-5	Footing 1-2	Footing 2-3	Footing 3-4	Footing 4-5
"Deterministic" estimate	23.2	30.3	30.5	28.9	23.7	7.2	0.13	1.5	5.2	0.00078	0.00001	0.00017	0.00057	0.00215	0.00018	0.00211	0.00209
Simulated - mean	25.9	27.0	26.7	25.5	26.2	19.6	19.9	19.3	19.2	0.00215	0.00218	0.00211	0.00209	0.00162	0.00163	0.00157	0.00157
Simulated - median	21.6	22.4	22.3	21.2	21.9	14.9	14.9	14.4	14.4	0.00162	0.00163	0.00157	0.00157	0.0022	0.0022	0.0022	0.0021
Simulated - Std Dev	18.2	21.3	19.0	20.2	18.5	20.1	20.5	20.0	19.6	1.02	1.03	1.03	1.02	1.02	1.03	1.03	1.02
Simulated COV	0.70	0.79	0.71	0.79	0.70	1.02	1.03	1.03	1.02	1.02	1.03	1.03	1.02	1.02	1.03	1.03	1.02
Minimum (neg. value is uplift)	0.16	0.20	0.16	0.12	0.16	0.000	0.001	0.001	0.000	0.0000000	0.0000001	0.0000001	0.0000000	0.23055	0.23117	0.23156	0.22725
Maximum	242.4	2125.0	269.5	2125.0	185.8	2109.6	2115.2	2118.8	2079.4	0.42	0.42	0.41	0.41	0.21	0.21	0.21	0.24
Prob exceeding "calculated" value	0.461	0.338	0.329	0.335	0.455	0.73	1.00	0.94	0.80	0.42	0.42	0.41	0.41	0.21	0.21	0.21	0.24
Prob exceeding 12.5 mm	0.753	0.763	0.766	0.745	0.759	0.56	0.57	0.55	0.55	0.29	0.29	0.28	0.28	0.21	0.21	0.21	0.24
Prob exceeding 25 mm	0.421	0.441	0.437	0.413	0.428	0.29	0.29	0.28	0.28	0.07	0.07	0.06	0.06	0.07	0.07	0.07	0.06
Prob exceeding 50 mm	0.097	0.113	0.109	0.093	0.104	0.06	0.07	0.06	0.06								

Prob of failure,  $p_f$  = 0.42     $\beta$  = 0.21

\*\*Note -  $p_f$  also equals the probability of exceeding approx. 18.3 mm of differential displacement

**OpenSees Results - Footing Displacements and Angular Distortion at Footing Elevation**

Calculated results from bearing pressure-settlement equation and simulated results with 50,000 simulations that include bearing pressure-settlement equation (with known dispersion of model parameters) and variable soil undrained shear strength across horizontal distance, x.

Soil Parameters		Displacement Model (Vertical Spring) Parameters				Footing Parameters	
$s_u$ (kPa)	$k_z$	$k_1$	$k_2$	$M_{stc}$	$B_{1.5}$ (m)	$B_{3.4}$ (m)	Beam Dist.(m)
70	0.013	0.701	0.643	1.675	1.675	2.125	9.15
COV( $s_u$ ) = 10%	0.007	0.113	0.123				
Scale of Fluctuation, $\delta$ (m) = 5	53.0	16.1	19.1				
$\gamma$ (kN/m <sup>3</sup> ) = 19	Dist. = Gamma	Inv. Gauss.	Lognormal				

"calculated" values assume no variation in soil shear strength or spring parameters

"Allowable" Distortion = 1/500 = 0.002

	Displacement (mm)					Distortion (for 9.15 m on-center footing spacing)							
	Footing 1	Footing 2	Footing 3	Footing 4	Footing 5	Footings 1-2	Footings 2-3	Footings 3-4	Footings 4-5	Footings 1-2	Footings 2-3	Footings 3-4	Footings 4-5
"Deterministic" estimate	23.2	30.3	30.5	28.9	23.7	7.2	0.13	1.5	5.2	0.00078	0.00001	0.00017	0.00057
Simulated - mean	26.0	26.9	26.9	25.6	26.5	19.6	20.0	19.3	19.2	0.00215	0.00218	0.00211	0.00210
Simulated - median	21.6	22.4	22.5	21.3	22.0	14.7	15.1	14.5	14.5	0.00161	0.00165	0.00159	0.00159
Simulated - Std Dev	18.5	19.3	19.2	18.1	18.8	18.0	18.3	17.8	17.5	0.0020	0.0020	0.0019	0.0019
Simulated COV	0.71	0.72	0.71	0.71	0.71	0.92	0.92	0.92	0.91	0.92	0.92	0.92	0.91
Minimum (neg. value is uplift)	0.36	0.51	0.28	0.16	0.50	0.000	0.000	0.000	0.001	0.0000000	0.0000000	0.0000000	0.0000001
Maximum	257.5	273.7	398.0	228.6	225.4	251.8	377.7	368.9	219.0	0.02752	0.04128	0.04032	0.02393
Prob exceeding "calculated" value	0.462	0.335	0.334	0.335	0.461	0.73	1.00	0.94	0.80	0.41	0.42	0.41	0.41
Prob exceeding 12.5 mm	0.753	0.764	0.764	0.748	0.758	0.56	0.57	0.56	0.56	0.22	0.20	0.23	0.24
Prob exceeding 25 mm	0.421	0.440	0.442	0.412	0.433	0.29	0.29	0.28	0.28	0.07	0.07	0.07	0.06
Prob exceeding 50 mm	0.101	0.112	0.111	0.095	0.106	0.07	0.07	0.06	0.06				

Prob of failure,  $p_f$  = 0.41     $\beta$  = 0.22

\*\*Note -  $p_f$  also equals the probability of exceeding approx. 18.3 mm of differential displacement

**OpenSees Results - Footing Displacements and Angular Distortion at Footing Elevation**

Calculated results from bearing pressure-settlement equation and simulated results with 50,000 simulations that include bearing pressure-settlement equation (with known dispersion of model parameters) and variable soil undrained shear strength across horizontal distance, x.

Soil Parameters		Displacement Model (Vertical Spring) Parameters				Footing Parameters			
$s_u$ (kPa)	$\delta$ (mm)	$k_1$	$k_2$	$M_{stc}$	$B_{1.5}$ (m)	$B_{3.4}$ (m)	Beam Dist.(m)		
70	10%	0.013	0.701	0.643	1.675	2.125	9.15		
COV( $s_u$ ) = 10	10	0.007	0.113	0.123					
Scale of Fluctuation, $\delta$ (mm) = 19		COV(%) = 53.0	16.1	19.1					
$\gamma$ (kN/m <sup>3</sup> ) = 19		Dist. = Gamma	Inv. Gauss.	Lognormal					
"calculated" values assume no variation in soil shear strength or spring parameters									
"Allowable" Distortion = 1/500 = 0.002									
<b>Distortion (for 9.15 m on-center footing spacing)</b>									
		Footing 1-2		Footing 2-3		Footing 3-4		Footing 4-5	
"Deterministic" estimate		7.2	0.13	1.5	5.2				
Simulated - mean		19.5	19.9	19.4	19.3				
Simulated - median		14.7	14.9	14.6	14.6				
Simulated - Std Dev		17.8	18.3	17.9	17.8				
Simulated COV		0.91	0.92	0.92	0.92				
Minimum	(neg. value is uplift)	0.000	0.001	0.001	0.001				
Maximum		219.3	227.0	302.1	440.9				
Prob exceeding "calculated" value		0.459	0.337	0.334	0.463				
Prob exceeding 12.5 mm		0.753	0.765	0.745	0.759				
Prob exceeding 25 mm		0.417	0.443	0.413	0.436				
Prob exceeding 50 mm		0.099	0.113	0.096	0.109				
<b>Differential Displacement (mm)</b>									
		Footing 1-2		Footing 2-3		Footing 3-4		Footing 4-5	
"Deterministic" estimate		0.000	0.001	0.001	0.001				
Simulated - mean		0.73	1.00	0.94	0.80				
Simulated - median		0.56	0.57	0.56	0.56				
Simulated - Std Dev		0.28	0.29	0.28	0.28				
Simulated COV		0.06	0.07	0.06	0.06				
Minimum		0.000	0.001	0.001	0.001				
Maximum		219.3	227.0	302.1	440.9				
Prob of failure, $p_f$ =		0.41	0.42	0.41	0.41				
$\beta$ =		0.22	0.20	0.23	0.23				

\*\*Note -  $p_f$  also equals the probability of exceeding approx. 18.3 mm of differential displacement

**OpenSees Results - Footing Displacements and Angular Distortion at Footing Elevation**

Calculated results from bearing pressure-settlement equation and simulated results with 50,000 simulations that include bearing pressure-settlement equation (with known dispersion of model parameters) and variable soil undrained shear strength across horizontal distance, x.

Soil Parameters		Displacement Model (Vertical Spring) Parameters				Footing Parameters	
$s_u$ (kPa) =	70	$k_1$	0.013	$k_2$	0.701	$M_{stc}$	0.643
COV( $s_u$ ) =	10%	$\mu$ =	0.007	$\sigma$ =	0.113	$B_{1.5}$ (m) =	1.675
Scale of Fluctuation, $\delta$ (m) =	20	COV(%) =	53.0	Dist. =	Gamma	$B_{3.4}$ (m) =	2.125
$\gamma'$ (kN/m <sup>3</sup> ) =	19				Inv. Gauss.	Beam Dist.(m) =	9.15
					Lognormal		

"calculated" values assume no variation in soil shear strength or spring parameters

"Allowable" Distortion = 1/500 = 0.002

	Displacement (mm)					Distortion (for 9.15 m on-center footing spacing)				
	Footing 1	Footing 2	Footing 3	Footing 4	Footing 5	Footing 1-2	Footing 2-3	Footing 3-4	Footing 4-5	
"Deterministic" estimate	23.2	30.3	30.5	28.9	23.7	7.2	0.13	1.5	5.2	"Deterministic" estimate
Simulated - mean	25.9	26.9	27.2	25.8	26.6	19.4	19.9	19.5	19.2	Simulated - mean
Simulated - median	21.5	22.3	22.6	21.4	22.1	14.7	15.0	14.7	14.3	Simulated - median
Simulated - Std Dev	18.6	19.3	19.7	18.4	19.1	17.8	18.4	17.9	17.7	Simulated - Std Dev
Simulated COV	0.72	0.72	0.72	0.72	0.72	0.92	0.92	0.92	0.92	Simulated COV
Minimum (neg. value is uplift)	0.27	0.19	0.33	0.30	0.29	0.001	0.000	0.000	0.000	Minimum
Maximum	246.5	311.1	275.8	216.6	348.6	241.7	297.4	269.2	253.3	Maximum
Prob exceeding "calculated" value	0.460	0.334	0.340	0.339	0.462	0.73	0.99	0.94	0.79	Prob of failure, $p_f$ =
Prob exceeding 12.5 mm	0.751	0.765	0.766	0.747	0.763	0.56	0.57	0.56	0.55	$\beta$ =
Prob exceeding 25 mm	0.417	0.438	0.446	0.417	0.434	0.28	0.29	0.28	0.28	0.23
Prob exceeding 50 mm	0.100	0.114	0.114	0.099	0.108	0.06	0.07	0.06	0.06	0.22
										0.25

\*\*Note -  $p_f$  also equals the probability of exceeding approx. 18.3 mm of differential displacement

**OpenSees Results - Footing Displacements and Angular Distortion at Footing Elevation**

Calculated results from bearing pressure-settlement equation and simulated results with 50,000 simulations that include bearing pressure-settlement equation (with known dispersion of model parameters) and variable soil undrained shear strength across horizontal distance, x.

Soil Parameters		Displacement Model (Vertical Spring) Parameters				Footing Parameters	
		$k_1$	$k_2$	$M_{stc}$	$B_{1.5}$ (m)	$B_{3.4}$ (m)	Beam Dist.(m)
$s_u$ (kPa)	= 70	0.013	0.701	0.643	1.675		
COV( $s_u$ )	= 10%	0.007	0.113	0.123	2.125		
Scale of Fluctuation, $\delta$ (m)	= 30	53.0	16.1	19.1	9.15		
$\gamma'$ (kN/m <sup>3</sup> )	= 19	Dist. = Gamma		Inv. Gauss. Lognormal			

	Displacement (mm)				
	Footing 1	Footing 2	Footing 3	Footing 4	Footing 5
"Deterministic" estimate	23.2	30.3	30.5	28.9	23.7
Simulated - mean	25.8	27.0	27.0	25.6	26.6
Simulated - median	21.6	22.4	22.3	21.3	22.1
Simulated - Std Dev	18.3	19.5	19.5	18.4	19.3
Simulated COV	0.71	0.72	0.72	0.72	0.72
Minimum (neg. value is uplift)	0.25	0.20	0.31	0.18	0.13
Maximum	214.7	287.0	274.1	213.0	277.0

	Differential Displacement (mm)				
	Footings 1-2	Footings 2-3	Footings 3-4	Footings 4-5	
"Deterministic" estimate	7.2	0.13	1.5	5.2	
Simulated - mean	19.3	19.6	19.2	19.2	
Simulated - median	14.5	14.7	14.4	14.4	
Simulated - Std Dev	17.7	18.2	17.8	17.6	
Simulated COV	0.92	0.93	0.92	0.92	
Minimum	0.000	0.001	0.000	0.001	
Maximum	266.8	255.3	250.4	243.4	

	Distortion (for 9.15 m on-center footing spacing)				
	Footings 1-2	Footings 2-3	Footings 3-4	Footings 4-5	
"Deterministic" estimate	0.00078	0.00001	0.00017	0.00057	
Simulated - mean	0.00211	0.00215	0.00210	0.00210	
Simulated - median	0.00159	0.00160	0.00158	0.00158	
Simulated - Std Dev	0.0019	0.0020	0.0019	0.0019	
Simulated COV	0.92	0.93	0.92	0.92	
Minimum	0.0000000	0.0000001	0.0000000	0.0000001	
Maximum	0.02916	0.02790	0.02736	0.02660	

	Prob of failure, $p_f$ =	$\beta$ =
Prob exceeding 12.5 mm	0.41	0.40
Prob exceeding 25 mm	0.24	0.24
Prob exceeding 50 mm	0.07	0.06

"calculated" values assume no variation in soil shear strength or spring parameters

"Allowable" Distortion = 1/500 = 0.002

\*\*Note -  $p_f$  also equals the probability of exceeding approx. 18.3 mm of differential displacement

**OpenSees Results - Footing Displacements and Angular Distortion at Footing Elevation**

Calculated results from bearing pressure-settlement equation and simulated results with 50,000 simulations that include bearing pressure-settlement equation (with known dispersion of model parameters) and variable soil undrained shear strength across horizontal distance, x.

Soil Parameters		Displacement Model (Vertical Spring) Parameters				Footing Parameters	
$s_u$ (kPa)	$k_z$	$k_1$	$k_2$	$M_{stc}$	$B_{1.5}$ (m)	$B_{3.4}$ (m)	Beam Dist.(m)
70	0.013	0.701	0.643	19.1	1.675	2.125	9.15
COV( $s_u$ ) = 10%	0.007	0.113	0.123	19.1			
Scale of Fluctuation, $\delta$ (m) = 50	53.0	16.1					
$\gamma'$ (kN/m <sup>3</sup> ) = 19	Dist. = Gamma	Inv. Gauss.	Lognormal				

"calculated" values assume no variation in soil shear strength or spring parameters

"Allowable" Distortion = 1/500 = 0.002

	Displacement (mm)					Distortion (for 9.15 m on-center footing spacing)				
	Footing 1	Footing 2	Footing 3	Footing 4	Footing 5	Footing 1-2	Footing 2-3	Footing 3-4	Footing 4-5	
"Deterministic" estimate	23.2	30.3	30.5	28.9	23.7	7.2	0.13	1.5	5.2	
Simulated - mean	26.0	27.1	27.1	25.8	26.8	19.3	19.7	19.3	19.0	"Deterministic" estimate
Simulated - median	21.6	22.5	22.4	21.5	22.2	14.4	14.8	14.4	14.2	0.00211
Simulated - Std Dev	18.7	19.5	19.5	21.2	19.3	17.8	18.2	20.5	20.3	0.00158
Simulated COV	0.72	0.72	0.72	0.82	0.72	0.92	0.92	1.06	1.07	0.00155
Minimum (neg. value is uplift)	0.26	0.06	0.40	0.19	0.25	0.001	0.000	0.000	0.000	0.00022
Maximum	239.4	274.0	260.4	2125.0	325.5	245.3	259.0	2093.6	2037.7	1.06
Prob exceeding "calculated" value	0.463	0.337	0.335	0.339	0.465	0.73	1.00	0.94	0.79	0.41
Prob exceeding 12.5 mm	0.752	0.769	0.763	0.749	0.761	0.55	0.56	0.55	0.55	0.40
Prob exceeding 25 mm	0.422	0.441	0.443	0.418	0.436	0.28	0.29	0.28	0.27	0.26
Prob exceeding 50 mm	0.101	0.116	0.115	0.098	0.110	0.06	0.07	0.06	0.06	0.24
										0.21
										0.24

Prob of failure,  $p_f$  = 0.41     $\beta$  = 0.24

\*\*Note -  $p_f$  also equals the probability of exceeding approx. 18.3 mm of differential displacement

**OpenSees Results - Footing Displacements and Angular Distortion at Footing Elevation**

Calculated results from bearing pressure-settlement equation and simulated results with 50,000 simulations that include bearing pressure-settlement equation (with known dispersion of model parameters) and variable soil undrained shear strength across horizontal distance, x.

Soil Parameters		Displacement Model (Vertical Spring) Parameters				Footing Parameters	
$s_u$ (kPa)	$\delta$ (mm)	$k_1$	$k_2$	$M_{stc}$	$B_{1.5}$ (m)	$B_{3.4}$ (m)	Beam Dist.(m)
70	10%	0.013	0.701	0.643	1.675	2.125	9.15
COV( $s_u$ ) =	100	0.007	0.113	0.123			
Scale of Fluctuation, $\delta$ (mm) =	19	53.0	16.1	19.1			
$\gamma$ (kN/m <sup>3</sup> ) =		Dist. = Gamma	Inv. Gauss.	Lognormal			

"calculated" values assume no variation in soil shear strength or spring parameters

"Allowable" Distortion = 1/500 = 0.002

	Displacement (mm)					Distortion (for 9.15 m on-center footing spacing)							
	Footing 1	Footing 2	Footing 3	Footing 4	Footing 5	Footings 1-2	Footings 2-3	Footings 3-4	Footings 4-5	Footings 1-2	Footings 2-3	Footings 3-4	Footings 4-5
"Deterministic" estimate	23.2	30.3	30.5	28.9	23.7	7.2	0.13	1.5	5.2	0.00078	0.00001	0.00017	0.00057
Simulated - mean	26.1	27.0	27.1	25.7	26.7	19.2	19.7	19.3	19.1	0.00210	0.00215	0.00211	0.00209
Simulated - median	21.6	22.4	22.4	21.4	22.1	14.4	14.8	14.5	14.4	0.00158	0.00161	0.00158	0.00158
Simulated - Std Dev	18.8	19.6	19.7	18.4	19.3	17.9	18.4	17.8	17.6	0.0020	0.0020	0.0019	0.0019
Simulated COV	0.72	0.72	0.73	0.72	0.72	0.93	0.93	0.92	0.92	0.93	0.93	0.92	0.92
Minimum (neg. value is uplift)	0.26	0.12	0.37	0.08	0.22	0.000	0.001	0.001	0.001	0.0000000	0.0000001	0.0000001	0.0000001
Maximum	284.2	499.7	298.5	243.0	311.9	488.2	480.2	290.4	235.5	0.05336	0.05248	0.03173	0.02574
Prob exceeding "calculated" value	0.463	0.337	0.335	0.339	0.463	0.73	0.99	0.94	0.79	0.40	0.41	0.41	0.40
Prob exceeding 12.5 mm	0.752	0.766	0.764	0.746	0.759	0.55	0.56	0.56	0.55	0.24	0.22	0.24	0.24
Prob exceeding 25 mm	0.421	0.441	0.442	0.419	0.434	0.28	0.29	0.28	0.27	0.24	0.22	0.24	0.24
Prob exceeding 50 mm	0.102	0.113	0.114	0.098	0.108	0.06	0.07	0.06	0.06	0.24	0.22	0.24	0.24

Prob of failure,  $p_f$  = 0.40     $\beta$  = 0.24

\*\*Note -  $p_f$  also equals the probability of exceeding approx. 18.3 mm of differential displacement

**OpenSees Results - Footing Displacements and Angular Distortion at Footing Elevation**

Calculated results from bearing pressure-settlement equation and simulated results with 50,000 simulations that include bearing pressure-settlement equation (with known dispersion of model parameters) and variable soil undrained shear strength across horizontal distance, x.

Soil Parameters		Displacement Model (Vertical Spring) Parameters				Footing Parameters	
		$k_1$	$k_2$	$M_{stc}$	$B_{1.5}$ (m)	$B_{3.4}$ (m)	Beam Dist.(m)
$s_u$ (kPa)	= 70	0.013	0.701	0.643	1.675		
COV( $s_u$ )	= 20%	0.007	0.113	0.123	2.125		
Scale of Fluctuation, $\delta$ (m)	= 0.1	53.0	16.1	19.1	9.15		
$\gamma'$ (kN/m <sup>3</sup> )	= 19	Dist. = Gamma		Inv. Gauss.	Lognormal		

"calculated" values assume no variation in soil shear strength or spring parameters

"Allowable" Distortion = 1/500 = 0.002

	Displacement (mm)					Distortion (for 9.15 m on-center footing spacing)				
	Footing 1	Footing 2	Footing 3	Footing 4	Footing 5	Footing 1-2	Footing 2-3	Footing 3-4	Footing 4-5	
"Deterministic" estimate	23.2	30.3	30.5	28.9	23.7	7.2	0.13	1.5	5.2	"Deterministic" estimate
Simulated - mean	25.5	26.5	26.6	25.2	26.2	18.9	19.4	19.0	18.8	Simulated - mean
Simulated - median	21.4	22.3	22.4	21.4	21.9	14.4	14.7	14.6	14.3	Simulated - median
Simulated - Std Dev	17.6	18.4	18.6	17.2	18.2	17.0	17.5	16.8	16.7	Simulated - Std Dev
Simulated COV	0.69	0.70	0.70	0.68	0.70	0.90	0.90	0.89	0.89	Simulated COV
Minimum (neg. value is uplift)	0.30	0.23	0.31	0.31	0.21	0.000	0.001	0.000	0.001	Minimum
Maximum	174.8	208.6	310.4	232.4	202.1	200.9	299.2	268.1	216.6	Maximum
Prob exceeding "calculated" value	0.456	0.333	0.331	0.331	0.458	0.72	1.00	0.94	0.80	Prob of failure, $p_f$ =
Prob exceeding 12.5 mm	0.750	0.763	0.766	0.752	0.761	0.55	0.56	0.56	0.55	$\beta$ =
Prob exceeding 25 mm	0.416	0.439	0.439	0.412	0.429	0.27	0.28	0.28	0.27	0.24
Prob exceeding 50 mm	0.091	0.104	0.106	0.087	0.102	0.06	0.06	0.05	0.05	0.23
										0.25

\*\*Note -  $p_f$  also equals the probability of exceeding approx. 18.3 mm of differential displacement



**OpenSees Results - Footing Displacements and Angular Distortion at Footing Elevation**

Calculated results from bearing pressure-settlement equation and simulated results with 50,000 simulations that include bearing pressure-settlement equation (with known dispersion of model parameters) and variable soil undrained shear strength across horizontal distance, x.

Soil Parameters		Displacement Model (Vertical Spring) Parameters				Footing Parameters	
$s_u$ (kPa) =	70	$k_1$	0.013	0.701	0.643	$M_{stc}$	
COV( $s_u$ ) =	20%	$\mu$ =	0.007	0.113	0.123	$B_{1.5}$ (m) =	1.675
Scale of Fluctuation, $\delta$ (m) =	0.2	$\sigma$ =	53.0	16.1	19.1	$B_{3-4}$ (m) =	2.125
$\gamma'$ (kN/m <sup>3</sup> ) =	19	COV(%) =				Beam Dist.(m) =	9.15
		Dist. =	Gamma	Inv. Gauss.	Lognormal		

"calculated" values assume no variation in soil shear strength or spring parameters

"Allowable" Distortion = 1/500 = 0.002

	Displacement (mm)					Differential Displacement (mm)					Distortion (for 9.15 m on-center footing spacing)						
	Footing 1	Footing 2	Footing 3	Footing 4	Footing 5	Footing 1-2	Footing 2-3	Footing 3-4	Footing 4-5	Footing 1-2	Footing 2-3	Footing 3-4	Footing 4-5	Footing 1-2	Footing 2-3	Footing 3-4	Footing 4-5
"Deterministic" estimate	23.2	30.3	30.5	28.9	23.7	7.2	0.13	1.5	5.2	0.00078	0.00001	0.00017	0.00057	0.00213	0.00016	0.00211	0.00210
Simulated - mean	25.9	26.6	26.9	25.5	26.4	19.5	19.7	19.4	19.2	0.00213	0.00216	0.00211	0.00210	0.00160	0.00163	0.00159	0.00158
Simulated - median	21.5	22.2	22.5	21.3	22.0	14.7	14.9	14.6	14.4	0.00160	0.00163	0.00159	0.00158	0.00119	0.00122	0.00117	0.00116
Simulated - Std Dev	18.5	18.8	19.0	20.2	18.9	17.8	17.9	19.9	19.9	0.0019	0.0020	0.0022	0.0022	0.92	0.91	1.03	1.04
Simulated COV	0.71	0.71	0.70	0.79	0.71	0.92	0.91	1.03	1.04	0.92	0.91	1.03	1.04	0.92	0.91	1.03	1.04
Minimum (neg. value is uplift)	0.28	0.14	0.24	0.30	0.21	0.002	0.000	0.001	0.001	0.0000002	0.0000000	0.0000002	0.0000001	0.04005	0.03557	0.22907	0.23069
Maximum	384.7	349.2	323.1	2125.0	253.0	366.5	325.4	2096.0	2110.9	0.41	0.42	0.41	0.40	0.22	0.21	0.23	0.24
Prob exceeding "calculated" value	0.460	0.332	0.337	0.332	0.460	0.73	1.00	0.94	0.80	0.41	0.42	0.41	0.40	0.22	0.21	0.23	0.24
Prob exceeding 12.5 mm	0.751	0.764	0.767	0.747	0.761	0.56	0.57	0.56	0.55	0.22	0.21	0.23	0.24	0.22	0.21	0.23	0.24
Prob exceeding 25 mm	0.420	0.438	0.442	0.413	0.430	0.28	0.29	0.28	0.28	0.07	0.07	0.06	0.06	0.07	0.07	0.06	0.06
Prob exceeding 50 mm	0.099	0.109	0.110	0.092	0.105	0.06	0.07	0.06	0.06								

Prob of failure,  $p_f$  = 0.41     $\beta$  = 0.22

\*\*Note -  $p_f$  also equals the probability of exceeding approx. 18.3 mm of differential displacement

**OpenSees Results - Footing Displacements and Angular Distortion at Footing Elevation**

Calculated results from bearing pressure-settlement equation and simulated results with 50,000 simulations that include bearing pressure-settlement equation (with known dispersion of model parameters) and variable soil undrained shear strength across horizontal distance, x.

Soil Parameters		Displacement Model (Vertical Spring) Parameters				Footing Parameters					
		$k_1$	$k_2$	$M_{stc}$	$B_{1.5}$ (m)	$B_{3.4}$ (m)					
$s_u$ (kPa)	= 70	0.013	0.701	0.643	1.675						
COV( $s_u$ )	= 20%	0.007	0.113	0.123	2.125						
Scale of Fluctuation, $\delta$ (m)	= 0.5	53.0	16.1	19.1	9.15						
$\gamma'$ (kN/m <sup>3</sup> )	= 19	Dist. = Gamma Inv. Gauss. Lognormal									
"calculated" values assume no variation in soil shear strength or spring parameters											
"Allowable" Distortion = 1/500 = 0.002											
		Displacement (mm)		Differential Displacement (mm)		Distortion (for 9.15 m on-center footing spacing)					
		Footing 1	Footing 2	Footing 3	Footing 4	Footing 5	Footing 1-2	Footing 2-3	Footing 3-4	Footing 4-5	
"Deterministic" estimate		23.2	30.3	30.5	28.9	23.7	7.2	0.13	1.5	5.2	
Simulated - mean		26.6	27.6	27.7	26.2	27.4	20.8	21.1	20.5	20.4	
Simulated - median		21.6	22.6	22.6	21.5	22.2	15.2	15.4	15.1	14.9	
Simulated - Std Dev		21.8	20.8	22.9	19.5	21.3	21.9	22.6	21.9	20.3	
Simulated COV		0.82	0.75	0.83	0.74	0.78	1.05	1.07	1.07	0.99	
Minimum (neg. value is uplift)		1675.0	0.23	0.28	0.40	0.09	0.000	0.000	0.000	0.000	
Maximum			432.9	2125.0	283.5	559.0	1630.5	2110.9	2085.1	522.7	
Prob exceeding "calculated" value		0.463	0.344	0.341	0.343	0.466	0.74	1.00	0.94	0.80	
Prob exceeding 12.5 mm		0.747	0.764	0.765	0.751	0.760	0.57	0.58	0.57	0.56	
Prob exceeding 25 mm		0.423	0.447	0.446	0.420	0.437	0.30	0.31	0.30	0.29	
Prob exceeding 50 mm		0.111	0.121	0.123	0.105	0.118	0.08	0.08	0.07	0.08	
								Prob of failure, $p_f$ =		0.43	
								$\beta$ =		0.18	
										0.17	
										0.19	
										0.21	
										0.42	
										0.21	

\*\*Note -  $p_f$  also equals the probability of exceeding approx. 18.3 mm of differential displacement

**OpenSees Results - Footing Displacements and Angular Distortion at Footing Elevation**

Calculated results from bearing pressure-settlement equation and simulated results with 50,000 simulations that include bearing pressure-settlement equation (with known dispersion of model parameters) and variable soil undrained shear strength across horizontal distance, x.

Soil Parameters		Displacement Model (Vertical Spring) Parameters				Footing Parameters	
		$k_1$	$k_2$	$M_{stc}$	$B_{1.5}(m)$	$B_{3.4}(m)$	Beam Dist.(m)
$s_u (kPa)$	= 70	0.013	0.701	0.643	1.675		
$COV(s_u)$	= 20%	0.007	0.113	0.123	2.125		
Scale of Fluctuation, $\delta$ (m)	= 1	53.0	16.1	19.1	9.15		
$\gamma' (kN/m^3)$	= 19	Dist. = Gamma Inv. Gauss. Lognormal					

"calculated" values assume no variation in soil shear strength or spring parameters

"Allowable" Distortion = 1/500 = 0.002

	Displacement (mm)					Distortion (for 9.15 m on-center footing spacing)							
	Footing 1	Footing 2	Footing 3	Footing 4	Footing 5	Footings 1-2	Footings 2-3	Footings 3-4	Footings 4-5	Footings 1-2	Footings 2-3	Footings 3-4	Footings 4-5
"Deterministic" estimate	23.2	30.3	30.5	28.9	23.7	7.2	0.13	1.5	5.2	0.00078	0.00001	0.00017	0.00057
Simulated - mean	27.7	28.5	28.7	27.2	28.6	22.6	22.9	22.3	22.4	0.00247	0.00250	0.00244	0.00245
Simulated - median	21.7	22.8	22.8	21.7	22.3	15.6	16.0	15.6	15.4	0.00170	0.00174	0.00170	0.00168
Simulated - Std Dev	31.0	29.3	30.3	27.3	31.1	36.2	35.5	34.3	34.9	0.0040	0.0039	0.0037	0.0038
Simulated COV	1.12	1.03	1.05	1.01	1.09	1.61	1.55	1.54	1.56	1.61	1.55	1.54	1.56
Minimum (neg. value is uplift)	0.36	0.22	0.13	0.24	0.15	0.001	0.000	0.000	0.000	0.0000001	0.0000000	0.0000000	0.0000000
Maximum	1675.0	2125.0	2125.0	2125.0	1675.0	2115.7	2122.5	2112.5	2114.6	0.23123	0.23197	0.23087	0.23111
Prob exceeding "calculated" value	0.466	0.348	0.348	0.348	0.468	0.74	1.00	0.94	0.81	0.44	0.45	0.44	0.43
Prob exceeding 12.5 mm	0.749	0.764	0.766	0.751	0.758	0.58	0.59	0.58	0.58	0.16	0.13	0.16	0.17
Prob exceeding 25 mm	0.428	0.450	0.451	0.424	0.440	0.31	0.32	0.31	0.31	0.13	0.13	0.16	0.17
Prob exceeding 50 mm	0.119	0.129	0.131	0.114	0.130	0.09	0.10	0.09	0.09	0.13	0.13	0.16	0.17

Prob of failure,  $p_f$  = 0.44     $\beta$  = 0.16

\*\*Note -  $p_f$  also equals the probability of exceeding approx. 18.3 mm of differential displacement

**OpenSees Results - Footing Displacements and Angular Distortion at Footing Elevation**

Calculated results from bearing pressure-settlement equation and simulated results with 50,000 simulations that include bearing pressure-settlement equation (with known dispersion of model parameters) and variable soil undrained shear strength across horizontal distance, x.

Soil Parameters		Displacement Model (Vertical Spring) Parameters				Footing Parameters												
$s_u$ (kPa)	$k_1$	$k_2$	$M_{stc}$	$B_{1.5}$ (m)	$B_{3.4}$ (m)	Beam Dist.(m)												
70	0.013	0.701	0.643	1.675														
COV( $s_u$ ) = 20%	0.007	0.113	0.123	2.125														
Scale of Fluctuation, $\delta$ (m) = 2	53.0	16.1	19.1	9.15														
$\gamma'$ (kN/m <sup>3</sup> ) = 19	Dist. = Gamma	Inv. Gauss.	Lognormal															
"calculated" values assume no variation in soil shear strength or spring parameters																		
"Allowable" Distortion = 1/500 = 0.002																		
<b>Distortion (for 9.15 m on-center footing spacing)</b>																		
	Footing 1		Footing 2		Footing 3		Footing 4		Footing 5									
"Deterministic" estimate	23.2	30.3	30.5	28.9	28.9	23.7	7.2	0.13	1.5	5.2								
Simulated - mean	29.4	30.4	30.6	28.9	30.2	25.8	26.3	26.3	25.6	25.5								
Simulated - median	21.9	22.8	22.9	21.7	22.4	16.0	16.3	16.1	15.9	15.9								
Simulated - Std Dev	48.8	53.4	54.5	46.1	47.9	67.4	71.6	66.6	61.5	61.5								
Simulated COV	1.66	1.76	1.78	1.60	1.59	2.61	2.72	2.60	2.41	2.41								
Minimum (neg. value is uplift)	0.28	0.18	0.20	0.25	0.40	0.000	0.001	0.001	0.000	0.000								
Maximum	1675.0	2125.0	2125.0	2125.0	1675.0	2119.7	2123.4	2122.0	2120.1	2120.1								
Prob exceeding "calculated" value	0.471	0.352	0.357	0.355	0.471	0.75	1.00	0.94	0.81	0.81								
Prob exceeding 12.5 mm	0.749	0.764	0.765	0.747	0.758	0.59	0.60	0.59	0.58	0.58								
Prob exceeding 25 mm	0.433	0.454	0.457	0.430	0.444	0.33	0.33	0.33	0.33	0.33								
Prob exceeding 50 mm	0.130	0.139	0.141	0.126	0.138	0.11	0.11	0.11	0.10	0.10								
<b>Differential Displacement (mm)</b>								<b>Distortion (for 9.15 m on-center footing spacing)</b>										
	Footing 1		Footing 2		Footing 3		Footing 4		Footing 5		Footing 1-2		Footings 2-3		Footings 3-4		Footings 4-5	
"Deterministic" estimate	0.00078	0.00001	0.00001	0.00001	0.00001	0.00001	0.00001	0.00001	0.00001	0.00001	0.00001	0.00078	0.00017	0.00017	0.00017	0.00057		
Simulated - mean	0.00282	0.00287	0.00287	0.00280	0.00280	0.00280	0.00282	0.00282	0.00280	0.00280	0.00280	0.00282	0.00287	0.00280	0.00280	0.00278		
Simulated - median	0.00174	0.00178	0.00178	0.00176	0.00176	0.00176	0.00174	0.00174	0.00176	0.00176	0.00176	0.00174	0.00178	0.00176	0.00176	0.00173		
Simulated - Std Dev	0.0074	0.0078	0.0078	0.0073	0.0073	0.0073	0.0074	0.0074	0.0073	0.0073	0.0073	0.0074	0.0078	0.0073	0.0073	0.0067		
Simulated COV	2.61	2.72	2.72	2.60	2.60	2.60	2.61	2.61	2.60	2.60	2.60	2.61	2.72	2.60	2.60	2.41		
Minimum	0.0000000	0.0000001	0.0000001	0.0000001	0.0000001	0.0000001	0.0000000	0.0000000	0.0000000	0.0000000	0.0000000	0.0000000	0.0000001	0.0000001	0.0000001	0.0000000		
Maximum	0.23167	0.23206	0.23206	0.23191	0.23170	0.23170	0.23167	0.23167	0.23191	0.23170	0.23170	0.23167	0.23206	0.23191	0.23170	0.23170		
Prob of failure, $p_f$ =	0.45	0.46	0.46	0.45	0.45	0.45	0.45	0.45	0.45	0.45	0.45	0.45	0.46	0.45	0.45	0.45		
$\beta$ =	0.13	0.11	0.11	0.12	0.12	0.12	0.13	0.13	0.12	0.12	0.12	0.13	0.11	0.12	0.12	0.14		

\*\*Note -  $p_f$  also equals the probability of exceeding approx. 18.3 mm of differential displacement

**OpenSees Results - Footing Displacements and Angular Distortion at Footing Elevation**

Calculated results from bearing pressure-settlement equation and simulated results with 50,000 simulations that include bearing pressure-settlement equation (with known dispersion of model parameters) and variable soil undrained shear strength across horizontal distance, x.

Soil Parameters		Displacement Model (Vertical Spring) Parameters				Footing Parameters	
$s_u$ (kPa)	$k_z$	$k_1$	$k_2$	$M_{stc}$	$B_{1.5}$ (m)	$B_{3.4}$ (m)	Beam Dist.(m)
70	0.913	0.701	0.643	1.675	1.675	2.125	9.15
COV( $s_u$ ) = 20%	0.007	0.113	0.123				
Scale of Fluctuation, $\delta$ (m) = 5	53.0	16.1	19.1				
$\gamma'$ (kN/m <sup>3</sup> ) = 19	Dist. = Gamma	Inv. Gauss.	Lognormal				

"calculated" values assume no variation in soil shear strength or spring parameters

"Allowable" Distortion = 1/500 = 0.002

	Displacement (mm)					Differential Displacement (mm)					Distortion (for 9.15 m on-center footing spacing)						
	Footing 1	Footing 2	Footing 3	Footing 4	Footing 5	Footing 1-2	Footing 2-3	Footing 3-4	Footing 4-5	Footing 1-2	Footing 2-3	Footing 3-4	Footing 4-5	Footing 1-2	Footing 2-3	Footing 3-4	Footing 4-5
"Deterministic" estimate	23.2	30.3	30.5	28.9	23.7	7.2	0.13	1.5	5.2	0.00078	0.00001	0.00017	0.00057	0.00078	0.00001	0.00017	0.00057
Simulated - mean	30.9	32.7	32.7	30.6	32.4	28.9	30.0	28.7	28.8	0.00315	0.00328	0.00314	0.00315	0.00315	0.00328	0.00314	0.00315
Simulated - median	21.9	22.7	22.9	21.8	22.6	16.0	16.3	15.9	15.9	0.00175	0.00179	0.00174	0.00174	0.00175	0.00179	0.00174	0.00174
Simulated - Std Dev	62.2	75.9	76.5	69.7	70.0	92.9	102.9	98.3	93.4	0.0102	0.0112	0.0107	0.0102	0.0102	0.0112	0.0107	0.0102
Simulated COV	2.01	2.32	2.34	2.28	2.16	3.22	3.43	3.42	3.24	3.22	3.43	3.42	3.24	3.22	3.43	3.42	3.24
Minimum (neg. value is uplift)	0.18	0.39	0.33	0.23	0.32	0.001	0.000	0.000	0.001	0.0000001	0.0000000	0.0000000	0.0000001	0.0000001	0.0000000	0.0000000	0.0000001
Maximum	1675.0	2125.0	2125.0	2125.0	1675.0	2120.4	2122.3	2122.1	2121.9	0.23174	0.23195	0.23193	0.23190	0.23174	0.23195	0.23193	0.23190
Prob exceeding "calculated" value	0.472	0.357	0.356	0.355	0.476	0.75	1.00	0.94	0.81	0.45	0.46	0.45	0.45	0.45	0.46	0.45	0.45
Prob exceeding 12.5 mm	0.750	0.762	0.762	0.745	0.757	0.59	0.59	0.59	0.58	0.13	0.11	0.13	0.13	0.13	0.11	0.13	0.13
Prob exceeding 25 mm	0.435	0.454	0.455	0.429	0.449	0.33	0.34	0.33	0.33	0.11	0.12	0.11	0.11	0.11	0.12	0.11	0.11
Prob exceeding 50 mm	0.135	0.147	0.148	0.130	0.145	0.11	0.12	0.11	0.11								

Prob of failure,  $p_f$  = 0.45     $\beta$  = 0.13

\*\*Note -  $p_f$  also equals the probability of exceeding approx. 18.3 mm of differential displacement

**OpenSees Results - Footing Displacements and Angular Distortion at Footing Elevation**

Calculated results from bearing pressure-settlement equation and simulated results with 50,000 simulations that include bearing pressure-settlement equation (with known dispersion of model parameters) and variable soil undrained shear strength across horizontal distance, x.

Soil Parameters		Displacement Model (Vertical Spring) Parameters			Footing Parameters		
$s_u$ (kPa) =	70	$k_1$	0.213	$k_2$	0.701	$M_{stc}$	0.643
COV( $s_u$ ) =	20%	$\mu$ =	0.007	$\sigma$ =	0.113	$B_{1.5}$ (m) =	1.675
Scale of Fluctuation, $\delta$ (m) =	10	COV(%) =	53.0	Dist. =	Gamma	$B_{3.4}$ (m) =	2.125
$\gamma'$ (kN/m <sup>3</sup> ) =	19				Inv. Gauss.	Beam Dist.(m) =	9.15
					Lognormal		

"calculated" values assume no variation in soil shear strength or spring parameters  
 "Allowable" Distortion = 1/500 = 0.002

	Displacement (mm)					Differential Displacement (mm)					Distortion (for 9.15 m on-center footing spacing)						
	Footing 1	Footing 2	Footing 3	Footing 4	Footing 5	Footing 1-2	Footing 2-3	Footing 3-4	Footing 4-5	Footing 1-2	Footing 2-3	Footing 3-4	Footing 4-5	Footing 1-2	Footing 2-3	Footing 3-4	Footing 4-5
"Deterministic" estimate	23.2	30.3	30.5	28.9	23.7	7.2	0.13	1.5	5.2	0.00078	0.00001	0.00017	0.00057	0.00325	0.00034	0.00312	0.00314
Simulated - mean	31.8	33.6	33.2	31.2	33.0	29.7	30.5	28.6	28.7	0.00172	0.00174	0.00169	0.00170	0.00172	0.00174	0.00169	0.00170
Simulated - median	22.1	22.7	22.7	22.0	22.6	15.8	15.9	15.5	15.6	0.0111	0.0120	0.0108	0.0103	0.0111	0.0120	0.0108	0.0103
Simulated - Std Dev	69.2	85.9	79.5	72.8	73.4	101.5	109.7	98.4	94.4	3.42	3.59	3.44	3.29	3.42	3.59	3.44	3.29
Simulated COV	2.17	2.56	2.40	2.33	2.23	3.42	3.59	3.44	3.29	3.42	3.59	3.44	3.29	3.42	3.59	3.44	3.29
Minimum (neg. value is uplift)	0.22	0.10	0.08	0.14	0.41	0.001	0.000	0.000	0.000	0.0000001	0.0000000	0.0000000	0.0000000	0.0000001	0.0000000	0.0000000	0.0000000
Maximum	1675.0	2125.0	2125.0	2125.0	1675.0	2121.7	2119.7	2124.0	2121.0	0.23188	0.23166	0.23213	0.23181	0.23188	0.23166	0.23213	0.23181
Prob exceeding "calculated" value	0.477	0.355	0.353	0.358	0.476	0.74	1.00	0.94	0.80	0.44	0.45	0.44	0.44	0.44	0.45	0.44	0.44
Prob exceeding 12.5 mm	0.750	0.760	0.764	0.748	0.758	0.59	0.59	0.58	0.58	0.14	0.13	0.15	0.16	0.14	0.13	0.15	0.16
Prob exceeding 25 mm	0.439	0.451	0.451	0.434	0.450	0.33	0.33	0.32	0.32	0.11	0.12	0.11	0.11	0.11	0.12	0.11	0.11
Prob exceeding 50 mm	0.138	0.148	0.150	0.132	0.148	0.11	0.12	0.11	0.11								

Prob of failure,  $p_f$  = 0.44     $\beta$  = 0.14     $\beta$  = 0.15     $\beta$  = 0.16

\*\*Note -  $p_f$  also equals the probability of exceeding approx. 18.3 mm of differential displacement

**OpenSees Results - Footing Displacements and Angular Distortion at Footing Elevation**

Calculated results from bearing pressure-settlement equation and simulated results with 50,000 simulations that include bearing pressure-settlement equation (with known dispersion of model parameters) and variable soil undrained shear strength across horizontal distance, x.

Soil Parameters		Displacement Model (Vertical Spring) Parameters				Footing Parameters	
$s_u$ (kPa)	$k_z$	$k_1$	$k_2$	$M_{stc}$	$B_{1.5}$ (m)	$B_{3.4}$ (m)	Beam Dist.(m)
70	0.701	0.013	0.701	0.643	1.675	2.125	9.15
COV( $s_u$ ) = 20%	0.007	0.113	0.113	0.123			
Scale of Fluctuation, $\delta$ (m) = 20	53.0	16.1	19.1				
$\gamma'$ (kN/m <sup>3</sup> ) = 19	Dist. = Gamma	Inv. Gauss.	Lognormal				

"calculated" values assume no variation in soil shear strength or spring parameters

"Allowable" Distortion = 1/500 = 0.002

	Displacement (mm)					Distortion (for 9.15 m on-center footing spacing)				
	Footing 1	Footing 2	Footing 3	Footing 4	Footing 5	Footing 1-2	Footing 2-3	Footing 3-4	Footing 4-5	
"Deterministic" estimate	23.2	30.3	30.5	28.9	23.7	7.2	0.13	1.5	5.2	
Simulated - mean	31.8	35.1	34.6	31.7	33.9	29.6	31.3	28.9	28.9	"Deterministic" estimate
Simulated - median	22.0	22.9	23.1	21.9	22.7	15.4	15.9	15.2	15.2	0.00324
Simulated - Std Dev	70.4	98.2	90.8	78.7	80.3	107.4	118.1	104.8	100.0	0.00168
Simulated COV	2.21	2.80	2.62	2.48	2.37	3.62	3.77	3.63	3.47	0.0117
Minimum (neg. value is uplift)	0.23	0.37	0.12	0.30	0.24	0.002	0.000	0.000	0.000	3.62
Maximum	1675.0	2125.0	2125.0	2125.0	1675.0	2122.3	2120.5	2122.0	2114.3	0.000002
Prob exceeding "calculated" value	0.474	0.359	0.362	0.357	0.479	0.74	1.00	0.94	0.81	0.43
Prob exceeding 12.5 mm	0.749	0.763	0.765	0.749	0.761	0.57	0.58	0.57	0.57	0.45
Prob exceeding 25 mm	0.435	0.456	0.460	0.432	0.453	0.31	0.33	0.31	0.31	0.17
Prob exceeding 50 mm	0.136	0.149	0.153	0.132	0.148	0.10	0.11	0.10	0.10	0.13
										0.17
										0.17

Prob of failure,  $p_f$  = 0.43     $\beta$  = 0.13

\*\*Note -  $p_f$  also equals the probability of exceeding approx. 18.3 mm of differential displacement

**OpenSees Results - Footing Displacements and Angular Distortion at Footing Elevation**

Calculated results from bearing pressure-settlement equation and simulated results with 50,000 simulations that include bearing pressure-settlement equation (with known dispersion of model parameters) and variable soil undrained shear strength across horizontal distance, x.

Soil Parameters		Displacement Model (Vertical Spring) Parameters				Footing Parameters	
$s_u$ (kPa)	$k_z$	$k_1$	$k_2$	$M_{stc}$	$B_{1.5}$ (m)	$B_{3.4}$ (m)	Beam Dist.(m)
70	0.013	0.701	0.643	1.675	1.675	2.125	9.15
COV( $s_u$ ) = 20%	0.007	0.113	0.123				
Scale of Fluctuation, $\delta$ (m) = 30	COV(%) = 53.0	16.1	19.1				
$\gamma$ (kN/m <sup>3</sup> ) = 19	Dist. = Gamma	Inv. Gauss.	Lognormal				

"calculated" values assume no variation in soil shear strength or spring parameters

"Allowable" Distortion = 1/500 = 0.002

	Displacement (mm)					Differential Displacement (mm)					Distortion (for 9.15 m on-center footing spacing)						
	Footing 1	Footing 2	Footing 3	Footing 4	Footing 5	Footing 1-2	Footing 2-3	Footing 3-4	Footing 4-5	Footing 1-2	Footing 2-3	Footing 3-4	Footing 4-5	Footing 1-2	Footing 2-3	Footing 3-4	Footing 4-5
"Deterministic" estimate	23.2	30.3	30.5	28.9	23.7	7.2	0.13	1.5	5.2	0.00078	0.00001	0.00017	0.00057	0.00318	0.00336	0.00320	0.00308
Simulated - mean	32.9	35.1	35.3	32.1	33.7	29.1	30.7	29.2	28.2	0.00166	0.00170	0.00167	0.00165	0.0110	0.0126	0.0119	0.0104
Simulated - median	22.2	22.8	23.1	21.8	22.5	15.2	15.6	15.3	15.1	3.47	3.76	3.72	3.39	3.47	3.76	3.72	3.39
Simulated - Std Dev	76.1	98.1	95.8	83.2	78.8	100.9	115.4	108.7	95.6	0.0000001	0.0000000	0.0000000	0.0000001	0.23184	0.23113	0.23173	0.23132
Simulated COV	2.32	2.80	2.71	2.59	2.34	3.47	3.76	3.72	3.39	0.43	0.44	0.43	0.42	0.18	0.16	0.18	0.19
Minimum (neg. value is uplift)	0.47	0.25	0.21	0.17	0.27	0.001	0.000	0.000	0.001	0.43	0.44	0.43	0.42	0.18	0.16	0.18	0.19
Maximum	1675.0	2125.0	2125.0	2125.0	1675.0	2121.4	2114.8	2120.3	2116.5	0.43	0.44	0.43	0.42	0.18	0.16	0.18	0.19
Prob exceeding "calculated" value	0.477	0.357	0.363	0.358	0.473	0.73	0.99	0.94	0.80	0.43	0.44	0.43	0.42	0.18	0.16	0.18	0.19
Prob exceeding 12.5 mm	0.752	0.762	0.766	0.746	0.759	0.57	0.58	0.57	0.57	0.18	0.16	0.18	0.19	0.18	0.16	0.18	0.19
Prob exceeding 25 mm	0.439	0.455	0.461	0.432	0.447	0.31	0.32	0.31	0.31	0.11	0.11	0.10	0.10	0.11	0.10	0.10	0.10
Prob exceeding 50 mm	0.141	0.151	0.156	0.135	0.149	0.10	0.11	0.10	0.10								

Prob of failure,  $p_f$  = 0.43     $\beta$  = 0.18

\*\*Note -  $p_f$  also equals the probability of exceeding approx. 18.3 mm of differential displacement



**OpenSees Results - Footing Displacements and Angular Distortion at Footing Elevation**

Calculated results from bearing pressure-settlement equation and simulated results with 50,000 simulations that include bearing pressure-settlement equation (with known dispersion of model parameters) and variable soil undrained shear strength across horizontal distance, x.

Soil Parameters		Displacement Model (Vertical Spring) Parameters			Footing Parameters	
$s_u$ (kPa) =	70	$k_1$	$k_2$	$M_{stc}$	$B_{1.5}$ (m) =	1.675
COV( $s_u$ ) =	20%	$\mu$ =	0.013	0.701	0.643	0.0007
Scale of Fluctuation, $\delta$ (m) =	50	$\sigma$ =	0.007	0.113	0.123	2.125
$\gamma'$ (kN/m <sup>3</sup> ) =	19	COV(%) =	53.0	16.1	19.1	9.15
		Dist. =	Gamma	Inv. Gauss.	Lognormal	

"calculated" values assume no variation in soil shear strength or spring parameters  
 "Allowable" Distortion = 1/500 = 0.002

	Displacement (mm)					Differential Displacement (mm)					Distortion (for 9.15 m on-center footing spacing)						
	Footing 1	Footing 2	Footing 3	Footing 4	Footing 5	Footing 1-2	Footing 2-3	Footing 3-4	Footing 4-5	Footing 1-2	Footing 2-3	Footing 3-4	Footing 4-5	Footing 1-2	Footing 2-3	Footing 3-4	Footing 4-5
"Deterministic" estimate	23.2	30.3	30.5	28.9	23.7	7.2	0.13	1.5	5.2	0.00078	0.00001	0.00017	0.00057	0.00309	0.00328	0.00316	0.00307
Simulated - mean	32.7	35.2	36.0	33.3	33.8	28.3	30.0	29.0	28.0	0.00164	0.00168	0.00165	0.00165	0.0105	0.0122	0.0118	0.0106
Simulated - median	22.1	23.0	23.0	21.9	22.6	15.0	15.4	15.1	15.1	3.40	3.73	3.72	3.44	0.0000000	0.0000000	0.0000000	0.0000000
Simulated - Std Dev	76.6	97.9	104.7	94.9	79.7	96.0	112.0	107.6	96.5	0.0000000	0.0000000	0.0000000	0.0000000	0.23103	0.23156	0.23160	0.23171
Simulated COV	2.34	2.78	2.91	2.85	2.36	3.40	3.73	3.72	3.44	0.0000000	0.0000000	0.0000000	0.0000000	0.43	0.44	0.43	0.42
Minimum (neg. value is uplift)	0.14	0.19	0.36	0.24	0.11	0.000	0.000	0.000	0.000	0.0000000	0.0000000	0.0000000	0.0000000	0.18	0.16	0.18	0.19
Maximum	1675.0	2125.0	2125.0	2125.0	1675.0	2113.9	2118.8	2119.1	2120.2	0.0000000	0.0000000	0.0000000	0.0000000	0.43	0.44	0.43	0.42
Prob exceeding "calculated" value	0.475	0.360	0.361	0.360	0.476	0.73	0.99	0.94	0.80	0.0000000	0.0000000	0.0000000	0.0000000	0.43	0.44	0.43	0.42
Prob exceeding 12.5 mm	0.752	0.764	0.765	0.748	0.756	0.56	0.57	0.57	0.57	0.0000000	0.0000000	0.0000000	0.0000000	0.18	0.16	0.18	0.19
Prob exceeding 25 mm	0.437	0.458	0.459	0.434	0.450	0.31	0.32	0.31	0.30	0.0000000	0.0000000	0.0000000	0.0000000	0.18	0.16	0.18	0.19
Prob exceeding 50 mm	0.138	0.154	0.155	0.135	0.148	0.10	0.11	0.10	0.10	0.0000000	0.0000000	0.0000000	0.0000000	0.18	0.16	0.18	0.19

\*\*Note - p, also equals the probability of exceeding approx. 18.3 mm of differential displacement

**OpenSees Results - Footing Displacements and Angular Distortion at Footing Elevation**

Calculated results from bearing pressure-settlement equation and simulated results with 50,000 simulations that include bearing pressure-settlement equation (with known dispersion of model parameters) and variable soil undrained shear strength across horizontal distance, x.

Soil Parameters		Displacement Model (Vertical Spring) Parameters				Footing Parameters	
$s_u$ (kPa)	$k_z$	$k_1$	$k_2$	$M_{stc}$	$B_{1.5}$ (m)	$B_{3.4}$ (m)	Beam Dist.(m)
70	0.701	0.013	0.701	0.643	1.675	2.125	9.15
COV( $s_u$ ) = 20%	0.007	0.113	0.113	0.123			
Scale of Fluctuation, $\delta$ (m) = 100	53.0	16.1	19.1				
$\gamma$ (kN/m <sup>3</sup> ) = 19	Dist. = Gamma	Inv. Gauss.	Lognormal				

"calculated" values assume no variation in soil shear strength or spring parameters

"Allowable" Distortion = 1/500 = 0.002

	Displacement (mm)					Distortion (for 9.15 m on-center footing spacing)							
	Footing 1	Footing 2	Footing 3	Footing 4	Footing 5	Footings 1-2	Footings 2-3	Footings 3-4	Footings 4-5	Footings 1-2	Footings 2-3	Footings 3-4	Footings 4-5
"Deterministic" estimate	23.2	30.3	30.5	28.9	23.7	7.2	0.13	1.5	5.2	0.00078	0.00001	0.00017	0.00057
Simulated - mean	32.4	35.0	35.1	32.6	33.3	27.5	28.8	26.8	26.1	0.00300	0.00015	0.00293	0.00286
Simulated - median	22.1	22.8	22.8	21.9	22.7	15.0	15.3	14.7	14.7	0.00164	0.00167	0.00161	0.00160
Simulated - Std Dev	73.1	96.8	98.3	87.5	75.4	91.5	104.9	93.1	81.7	0.0100	0.0115	0.0102	0.0089
Simulated COV	2.26	2.76	2.80	2.68	2.26	3.33	3.65	3.47	3.13	3.33	3.65	3.47	3.13
Minimum (neg. value is uplift)	0.32	0.19	0.27	0.24	0.24	0.000	0.000	0.000	0.000	0.0000000	0.0000000	0.0000000	0.0000000
Maximum	1675.0	2125.0	2125.0	2125.0	1675.0	2116.0	2106.2	2117.8	2108.8	0.23126	0.23018	0.23145	0.23047
Prob exceeding "calculated" value	0.475	0.360	0.354	0.359	0.476	0.73	0.99	0.94	0.80	0.42	0.43	0.42	0.42
Prob exceeding 12.5 mm	0.747	0.761	0.761	0.747	0.759	0.57	0.57	0.56	0.56	0.19	0.17	0.21	0.21
Prob exceeding 25 mm	0.437	0.455	0.455	0.432	0.451	0.30	0.31	0.30	0.30				
Prob exceeding 50 mm	0.136	0.153	0.153	0.135	0.147	0.10	0.10	0.09	0.09				

Prob of failure,  $p_f$  = 0.42     $\beta$  = 0.19

\*\*Note -  $p_f$  also equals the probability of exceeding approx. 18.3 mm of differential displacement

**OpenSees Results - Footing Displacements and Angular Distortion at Footing Elevation**

Calculated results from bearing pressure-settlement equation and simulated results with 50,000 simulations that include bearing pressure-settlement equation (with known dispersion of model parameters) and variable soil undrained shear strength across horizontal distance, x.

Soil Parameters		Displacement Model (Vertical Spring) Parameters				Footing Parameters	
		$k_1$	$k_2$	$M_{stc}$	$B_{1.5}$ (m)	$B_{3.4}$ (m)	Beam Dist.(m)
$s_u$ (kPa)	= 70	0.013	0.701	0.643	1.675		
COV( $s_u$ )	= 30%	0.007	0.113	0.123	2.125		
Scale of Fluctuation, $\delta$ (m)	= 0.1	53.0	16.1	19.1	9.15		
$\gamma'$ (kN/m <sup>3</sup> )	= 19	Dist. = Gamma		Inv. Gauss. Lognormal			

	Displacement (mm)					Differential Displacement (mm)					Distortion (for 9.15 m on-center footing spacing)						
	Footing 1	Footing 2	Footing 3	Footing 4	Footing 5	Footing 1-2	Footing 2-3	Footing 3-4	Footing 4-5	Footing 1-2	Footing 2-3	Footing 3-4	Footing 4-5	Footing 1-2	Footing 2-3	Footing 3-4	Footing 4-5
"Deterministic" estimate	23.2	30.3	30.5	28.9	23.7	7.2	0.13	1.5	5.2	0.00078	0.00001	0.00017	0.00057	0.00216	0.00018	0.00212	0.00210
Simulated - mean	26.0	26.8	26.9	25.3	26.4	19.7	19.9	19.4	19.2	0.00216	0.00218	0.00212	0.00210	0.00162	0.00164	0.00159	0.00158
Simulated - median	21.5	22.3	22.4	21.1	22.0	14.8	15.0	14.6	14.5	0.00200	0.00200	0.00199	0.00199	0.00200	0.00200	0.00199	0.00199
Simulated - Std Dev	18.7	19.2	19.2	18.0	18.9	18.2	18.4	17.8	17.7	0.92	0.92	0.92	0.92	0.92	0.92	0.92	0.92
Simulated COV	0.72	0.71	0.71	0.71	0.71	0.92	0.92	0.92	0.92	0.92	0.92	0.92	0.92	0.92	0.92	0.92	0.92
Minimum (neg. value is uplift)	0.16	0.45	0.15	0.21	0.28	0.000	0.000	0.001	0.000	0.0000000	0.0000000	0.0000001	0.0000000	0.02695	0.03869	0.03922	0.03999
Maximum	273.4	254.7	371.4	249.9	397.5	246.6	354.0	358.9	365.9	0.42	0.42	0.42	0.41	0.42	0.42	0.41	0.40
Prob exceeding "calculated" value	0.461	0.332	0.334	0.328	0.460	0.73	0.99	0.94	0.80	0.21	0.21	0.20	0.23	0.21	0.20	0.23	0.24
Prob exceeding 12.5 mm	0.751	0.763	0.766	0.742	0.759	0.56	0.57	0.56	0.55	0.21	0.21	0.20	0.23	0.21	0.20	0.23	0.24
Prob exceeding 25 mm	0.422	0.437	0.442	0.409	0.433	0.29	0.29	0.28	0.27	0.07	0.07	0.07	0.06	0.07	0.07	0.06	0.06
Prob exceeding 50 mm	0.101	0.110	0.111	0.093	0.103	0.07	0.07	0.06	0.06	0.07	0.07	0.07	0.06	0.07	0.07	0.06	0.06

"Allowable" Distortion = 1/500 = 0.002

Prob of failure,  $p_f$  = 0.42 0.42 0.42 0.41 0.40 0.40

$\beta$  = 0.21 0.21 0.20 0.23 0.23 0.24

\*\*Note -  $p_f$  also equals the probability of exceeding approx. 18.3 mm of differential displacement

**OpenSees Results - Footing Displacements and Angular Distortion at Footing Elevation**

Calculated results from bearing pressure-settlement equation and simulated results with 50,000 simulations that include bearing pressure-settlement equation (with known dispersion of model parameters) and variable soil undrained shear strength across horizontal distance, x.

Soil Parameters		Displacement Model (Vertical Spring) Parameters				Footing Parameters	
		$k_1$	$k_2$	$M_{stc}$	$B_{1.5}$ (m)	$B_{3.4}$ (m)	Beam Dist.(m)
$s_u$ (kPa)	= 70	0.013	0.701	0.643	1.675		
COV( $s_u$ )	= 30%	0.007	0.113	0.123	2.125		
Scale of Fluctuation, $\delta$ (m)	= 0.2	53.0	16.1	19.1	9.15		
$\gamma'$ (kN/m <sup>3</sup> )	= 19						
		Dist. = Gamma	Inv. Gauss.	Lognormal			

"calculated" values assume no variation in soil shear strength or spring parameters

"Allowable" Distortion = 1/500 = 0.002

	Displacement (mm)					Distortion (for 9.15 m on-center footing spacing)				
	Footing 1	Footing 2	Footing 3	Footing 4	Footing 5	Footing 1-2	Footing 2-3	Footing 3-4	Footing 4-5	
"Deterministic" estimate	23.2	30.3	30.5	28.9	23.7	7.2	0.13	1.5	5.2	
Simulated - mean	26.9	27.4	27.8	26.2	27.5	20.9	21.0	20.6	20.8	"Deterministic" estimate
Simulated - median	21.7	22.4	22.6	21.5	22.2	15.1	15.4	15.1	15.1	Simulated - mean
Simulated - Std Dev	22.5	20.8	21.0	19.7	24.0	22.4	20.9	20.1	23.1	Simulated - median
Simulated COV	0.84	0.76	0.76	0.75	0.87	1.08	0.99	0.98	1.11	Simulated - Std Dev
Minimum (neg. value is uplift)	0.40	0.36	0.21	0.31	0.44	0.000	0.001	0.001	0.000	Simulated COV
Maximum	1675.0	855.4	470.3	482.2	1675.0	1627.5	846.7	451.7	1658.0	Minimum
Prob exceeding "calculated" value	0.467	0.337	0.343	0.342	0.465	0.73	1.00	0.94	0.80	Maximum
Prob exceeding 12.5 mm	0.750	0.764	0.767	0.748	0.756	0.57	0.58	0.57	0.57	Prob of failure, $p_f$ =
Prob exceeding 25 mm	0.427	0.439	0.448	0.420	0.438	0.30	0.31	0.30	0.30	$\beta$ =
Prob exceeding 50 mm	0.112	0.119	0.123	0.106	0.121	0.08	0.08	0.08	0.08	

\*\*Note -  $p_f$  also equals the probability of exceeding approx. 18.3 mm of differential displacement

**OpenSees Results - Footing Displacements and Angular Distortion at Footing Elevation**

Calculated results from bearing pressure-settlement equation and simulated results with 50,000 simulations that include bearing pressure-settlement equation (with known dispersion of model parameters) and variable soil undrained shear strength across horizontal distance, x.

Soil Parameters		Displacement Model (Vertical Spring) Parameters				Footing Parameters	
$s_u$ (kPa)	$\delta$ (m)	$k_1$	$k_2$	$M_{stc}$	$B_{1.5}$ (m)	$B_{3.4}$ (m)	Beam Dist.(m)
70	0.5	0.013	0.701	0.643	1.675	2.125	9.15
COV( $s_u$ ) = 30%		0.007	0.113	0.123			
Scale of Fluctuation, $\delta$ (m) = 0.5		53.0	16.1	19.1			
$\gamma$ (kN/m <sup>3</sup> ) = 19		Dist. = Gamma	Inv. Gauss.	Lognormal			

"calculated" values assume no variation in soil shear strength or spring parameters

"Allowable" Distortion = 1/500 = 0.002

	Displacement (mm)					Differential Displacement (mm)					Distortion (for 9.15 m on-center footing spacing)						
	Footing 1	Footing 2	Footing 3	Footing 4	Footing 5	Footing 1-2	Footing 2-3	Footing 3-4	Footing 4-5	Footing 1-2	Footing 2-3	Footing 3-4	Footing 4-5	Footing 1-2	Footing 2-3	Footing 3-4	Footing 4-5
"Deterministic" estimate	23.2	30.3	30.5	28.9	23.7	7.2	0.13	1.5	5.2	0.00078	0.00001	0.00017	0.00057	0.00305	0.00295	0.00283	0.00295
Simulated - mean	30.9	31.1	30.6	29.2	31.5	27.9	27.0	25.9	27.0	0.00179	0.00181	0.00177	0.00176	0.00179	0.00181	0.00177	0.00176
Simulated - median	22.1	22.8	22.8	21.8	22.5	16.4	16.5	16.2	16.1	0.0086	0.0078	0.0071	0.0079	0.0086	0.0078	0.0071	0.0079
Simulated - Std Dev	57.9	59.9	47.8	50.8	58.1	2.82	2.66	2.51	2.68	2.82	2.66	2.51	2.68	2.82	2.66	2.51	2.68
Simulated COV	1.87	1.93	1.56	1.74	1.84												
Minimum (neg. value is uplift)	0.18	0.33	0.13	0.37	0.29	0.001	0.001	0.000	0.000	0.0000001	0.0000001	0.0000000	0.0000000	0.0000001	0.0000001	0.0000000	0.0000000
Maximum	1675.0	2125.0	2125.0	2125.0	1675.0	2121.4	2121.4	2120.6	2122.0	0.23184	0.23184	0.23176	0.23191	0.23184	0.23185	0.23176	0.23191
Prob exceeding "calculated" value	0.475	0.355	0.355	0.357	0.473	0.75	0.99	0.94	0.81	0.46	0.46	0.46	0.45	0.46	0.46	0.45	0.45
Prob exceeding 12.5 mm	0.751	0.760	0.766	0.747	0.756	0.59	0.60	0.59	0.59	0.10	0.09	0.11	0.12	0.10	0.09	0.11	0.12
Prob exceeding 25 mm	0.437	0.455	0.455	0.430	0.446	0.34	0.34	0.33	0.33								
Prob exceeding 50 mm	0.138	0.141	0.145	0.126	0.142	0.12	0.12	0.11	0.11								

Prob of failure,  $p_f$  = 0.46     $\beta$  = 0.10

\*\*Note -  $p_f$  also equals the probability of exceeding approx. 18.3 mm of differential displacement

**OpenSees Results - Footing Displacements and Angular Distortion at Footing Elevation**

Calculated results from bearing pressure-settlement equation and simulated results with 50,000 simulations that include bearing pressure-settlement equation (with known dispersion of model parameters) and variable soil undrained shear strength across horizontal distance, x.

Soil Parameters		Displacement Model (Vertical Spring) Parameters				Footing Parameters												
$s_u$ (kPa)	$k_z$	$k_1$	$k_2$	$M_{stc}$	$B_{1.5}$ (m)	$B_{3.4}$ (m)	Beam Dist.(m)											
70	0.701	0.013	0.701	0.643	1.675													
COV( $s_u$ ) = 30%	0.007	0.113	0.113	0.123	2.125													
Scale of Fluctuation, $\delta$ (m) = 1	53.0	16.1	19.1		9.15													
$\gamma'$ (kN/m <sup>3</sup> ) = 19	Dist. = Gamma	Inv. Gauss.	Lognormal															
"calculated" values assume no variation in soil shear strength or spring parameters																		
"Allowable" Distortion = 1/500 = 0.002																		
<b>Distortion (for 9.15 m on-center footing spacing)</b>																		
		Footing 1-2			Footings 2-3			Footings 3-4			Footings 4-5							
"Deterministic" estimate		7.2	0.13	1.5	5.2													
Simulated - mean		44.8	45.3	43.0	44.7													
Simulated - median		17.4	17.6	17.3	17.1													
Simulated - Std Dev		169.9	180.8	171.2	168.7													
Simulated COV		3.79	3.99	3.98	3.77													
Minimum	(neg. value is uplift)	0.001	0.000	0.000	0.000													
Maximum		2123.0	2122.4	2123.8	2123.3													
		Footing 1			Footing 2			Footing 3			Footing 4			Footing 5				
"Prob exceeding "calculated" value		0.480	0.362	0.366	0.366	0.482	0.76	1.00	0.94	0.82	0.48	0.48	0.48	0.48	0.48	0.48	0.48	0.48
"Prob exceeding 12.5 mm		0.745	0.760	0.763	0.745	0.756	0.61	0.62	0.61	0.61	0.61	0.61	0.61	0.61	0.61	0.61	0.61	0.61
"Prob exceeding 25 mm		0.442	0.457	0.463	0.439	0.456	0.37	0.37	0.36	0.36	0.36	0.36	0.36	0.36	0.36	0.36	0.36	0.36
"Prob exceeding 50 mm		0.158	0.163	0.166	0.148	0.166	0.15	0.16	0.15	0.15	0.15	0.15	0.15	0.15	0.15	0.15	0.15	0.15
		Footing 1			Footing 2			Footing 3			Footing 4			Footing 5				
Minimum		0.33	0.20	0.31	0.36	0.15	0.001	0.000	0.000	0.000	0.000	0.000	0.000	0.000	0.000	0.000	0.000	0.000
Maximum		1675.0	2125.0	2125.0	2125.0	1675.0	2123.0	2122.4	2123.8	2123.3								
		Footing 1			Footing 2			Footing 3			Footing 4			Footing 5				
Prob of failure, $p_f$ =		0.48	0.49	0.49	0.48	0.48	0.48	0.48	0.48	0.48	0.48	0.48	0.48	0.48	0.48	0.48	0.48	0.48
$\beta$ =		0.05	0.03	0.03	0.05	0.03	0.05	0.03	0.05	0.03	0.05	0.03	0.05	0.03	0.05	0.03	0.05	0.03

\*\*Note -  $p_f$  also equals the probability of exceeding approx. 18.3 mm of differential displacement

**OpenSees Results - Footing Displacements and Angular Distortion at Footing Elevation**

Calculated results from bearing pressure-settlement equation and simulated results with 50,000 simulations that include bearing pressure-settlement equation (with known dispersion of model parameters) and variable soil undrained shear strength across horizontal distance, x.

Soil Parameters		Displacement Model (Vertical Spring) Parameters				Footing Parameters	
		$k_1$	$k_2$	$M_{stc}$	$B_{1.5}$ (m)	$B_{3.4}$ (m)	
$s_u$ (kPa) =	70	0.013	0.701	0.643	1.675		
COV( $s_u$ ) =	30%	0.007	0.113	0.123	2.125		
Scale of Fluctuation, $\delta$ (m) =	2	53.0	16.1	19.1	Beam Dist.(m) =	9.15	
$\gamma'$ (kN/m <sup>3</sup> ) =	19	Dist. = Gamma Inv. Gauss. Lognormal					

"calculated" values assume no variation in soil shear strength or spring parameters

"Allowable" Distortion = 1/500 = 0.002

	Displacement (mm)					Distortion (for 9.15 m on-center footing spacing)				
	Footing 1	Footing 2	Footing 3	Footing 4	Footing 5	Footing 1-2	Footing 2-3	Footing 3-4	Footing 4-5	
"Deterministic" estimate	23.2	30.3	30.5	28.9	23.7	7.2	0.13	1.5	5.2	
Simulated - mean	50.1	54.8	55.9	51.5	54.6	69.1	73.8	71.7	70.7	"Deterministic" estimate
Simulated - median	22.4	23.3	23.4	22.2	23.0	18.4	18.7	18.2	18.3	Simulated - mean
Simulated - Std Dev	168.6	204.0	212.0	197.4	183.2	256.4	284.6	281.4	260.6	Simulated - median
Simulated COV	3.36	3.73	3.79	3.84	3.35	3.71	3.86	3.92	3.69	Simulated - Std Dev
Minimum (neg. value is uplift)	0.14	0.24	0.17	0.18	0.24	0.000	0.000	0.000	0.000	Simulated COV
Maximum	1675.0	2125.0	2125.0	2125.0	1675.0	2123.5	2123.8	2123.9	2122.1	Minimum
Prob exceeding "calculated" value	0.484	0.376	0.377	0.375	0.486	0.77	1.00	0.95	0.83	Maximum
Prob exceeding 12.5 mm	0.745	0.762	0.761	0.742	0.755	0.63	0.63	0.62	0.62	Prob of failure, $p_f$ =
Prob exceeding 25 mm	0.447	0.467	0.469	0.443	0.460	0.39	0.40	0.39	0.39	$\beta$ =
Prob exceeding 50 mm	0.172	0.181	0.184	0.164	0.183	0.18	0.19	0.18	0.18	0.50
										0.01
										0.00

\*\*Note -  $p_f$  also equals the probability of exceeding approx. 18.3 mm of differential displacement

**OpenSees Results - Footing Displacements and Angular Distortion at Footing Elevation**

Calculated results from bearing pressure-settlement equation and simulated results with 50,000 simulations that include bearing pressure-settlement equation (with known dispersion of model parameters) and variable soil undrained shear strength across horizontal distance, x.

Soil Parameters		Displacement Model (Vertical Spring) Parameters				Footing Parameters	
$s_u$ (kPa)	$k_z$	$k_1$	$k_2$	$M_{stc}$	$B_{1.5}$ (m)	$B_{3.4}$ (m)	Beam Dist.(m)
70	0.701	0.013	0.701	0.643	1.675	2.125	9.15
COV( $s_u$ ) = 30%	0.007	0.113	0.123	19.1			
Scale of Fluctuation, $\delta$ (m) = 5	53.0	16.1					
$\gamma$ (kN/m <sup>3</sup> ) = 19	Dist. = Gamma	Inv. Gauss.	Lognormal				

"calculated" values assume no variation in soil shear strength or spring parameters

"Allowable" Distortion = 1/500 = 0.002

	Displacement (mm)					Distortion (for 9.15 m on-center footing spacing)							
	Footing 1	Footing 2	Footing 3	Footing 4	Footing 5	Footings 1-2	Footings 2-3	Footings 3-4	Footings 4-5	Footings 1-2	Footings 2-3	Footings 3-4	Footings 4-5
"Deterministic" estimate	23.2	30.3	30.5	28.9	23.7	7.2	0.13	1.5	5.2	0.00078	0.00001	0.00017	0.00057
Simulated - mean	64.9	73.9	74.3	67.9	68.4	97.9	106.2	101.8	96.2	0.01070	0.01160	0.01113	0.01051
Simulated - median	22.5	23.4	23.5	22.2	23.2	18.4	19.0	18.5	18.3	0.00202	0.00207	0.00202	0.00200
Simulated - Std Dev	224.1	279.8	279.3	264.7	232.1	337.4	373.4	364.6	331.7	0.0369	0.0408	0.0398	0.0363
Simulated COV	3.45	3.79	3.76	3.90	3.40	3.45	3.52	3.58	3.45	3.45	3.52	3.58	3.45
Minimum (neg. value is uplift)	0.16	0.03	0.12	0.27	0.22	0.000	0.000	0.000	0.000	0.0000000	0.0000000	0.0000000	0.0000000
Maximum	1675.0	2125.0	2125.0	2125.0	1675.0	2123.8	2124.3	2124.7	2124.1	0.23211	0.23216	0.23221	0.23214
Prob exceeding "calculated" value	0.487	0.383	0.384	0.379	0.490	0.77	1.00	0.95	0.82	0.50	0.51	0.50	0.50
Prob exceeding 12.5 mm	0.745	0.758	0.761	0.744	0.754	0.63	0.63	0.62	0.62	-0.01	-0.03	-0.01	0.00
Prob exceeding 25 mm	0.452	0.471	0.472	0.444	0.465	0.40	0.41	0.40	0.40				
Prob exceeding 50 mm	0.183	0.196	0.199	0.178	0.194	0.20	0.21	0.20	0.20				

Prob of failure,  $p_f$  = 0.50     $\beta$  = -0.01

\*\*Note -  $p_f$  also equals the probability of exceeding approx. 18.3 mm of differential displacement



**OpenSees Results - Footing Displacements and Angular Distortion at Footing Elevation**

Calculated results from bearing pressure-settlement equation and simulated results with 50,000 simulations that include bearing pressure-settlement equation (with known dispersion of model parameters) and variable soil undrained shear strength across horizontal distance, x.

Soil Parameters		Displacement Model (Vertical Spring) Parameters					Footing Parameters							
$s_u$ (kPa)	$k_z$	$k_1$	$k_2$	$M_{stc}$	$B_{1,5}$ (m)	$B_{3,4}$ (m)	Beam Dist.(m)							
70	0.701	0.013	0.701	0.643	1.675	2.125	9.15							
COV( $s_u$ ) = 30%	0.007	0.113	0.113	0.123										
Scale of Fluctuation, $\delta$ (m) = 10	53.0	16.1	19.1											
$\gamma'$ (kN/m <sup>3</sup> ) = 19	Dist. = Gamma	Inv. Gauss.	Lognormal											
"calculated" values assume no variation in soil shear strength or spring parameters														
"Allowable" Distortion = 1/500 = 0.002														
		Displacement (mm)					Distortion (for 9.15 m on-center footing spacing)							
		Footing 1	Footing 2	Footing 3	Footing 4	Footing 5	Footing 1-2	Footing 2-3	Footing 3-4	Footing 4-5				
"Deterministic" estimate		23.2	30.3	30.5	28.9	23.7	7.2	0.13	1.5	5.2	0.00078	0.00001	0.00017	0.00057
Simulated - mean		71.1	82.2	81.6	75.9	74.4	102.0	109.8	105.8	99.2	0.01115	0.01200	0.01156	0.01085
Simulated - median		22.6	23.5	23.7	22.5	23.1	18.0	18.1	17.8	17.7	0.00197	0.00198	0.00195	0.00193
Simulated - Std Dev		242.8	305.8	302.7	291.9	250.8	345.1	383.1	375.2	338.2	0.0377	0.0419	0.0410	0.0370
Simulated COV		3.41	3.72	3.71	3.84	3.37	3.38	3.49	3.55	3.41	3.38	3.49	3.55	3.41
Minimum (neg. value is uplift)		0.23	0.31	0.28	0.34	0.26	0.000	0.000	0.000	0.000	0.0000000	0.0000000	0.0000000	0.0000000
Maximum		1675.0	2125.0	2125.0	2125.0	1675.0	2124.2	2124.2	2124.1	2123.8	0.23215	0.23215	0.23215	0.23211
Prob exceeding "calculated" value		0.489	0.386	0.386	0.385	0.489	0.76	0.99	0.94	0.82	0.49	0.50	0.49	0.49
Prob exceeding 12.5 mm		0.743	0.757	0.759	0.741	0.750	0.62	0.62	0.61	0.61	0.01	0.01	0.02	0.03
Prob exceeding 25 mm		0.455	0.472	0.475	0.451	0.465	0.39	0.39	0.38	0.38				
Prob exceeding 50 mm		0.190	0.201	0.202	0.184	0.195	0.20	0.20	0.19	0.19				
"Prob of failure, $p_f$ = $\beta$ = 0.01														
**Note - $p_f$ also equals the probability of exceeding approx. 18.3 mm of differential displacement														

**OpenSees Results - Footing Displacements and Angular Distortion at Footing Elevation**

Calculated results from bearing pressure-settlement equation and simulated results with 50,000 simulations that include bearing pressure-settlement equation (with known dispersion of model parameters) and variable soil undrained shear strength across horizontal distance, x.

Soil Parameters		Displacement Model (Vertical Spring) Parameters				Footing Parameters	
$s_u$ (kPa)	$k_z$	$k_1$	$k_2$	$M_{stc}$	$B_{1.5}$ (m)	$B_{3.4}$ (m)	Beam Dist.(m)
70	0.701	0.013	0.701	0.643	1.675	2.125	9.15
COV( $s_u$ ) = 30%	0.007	0.113	0.123				
Scale of Fluctuation, $\delta$ (m) = 20	53.0	16.1	19.1				
$\gamma$ (kN/m <sup>3</sup> ) = 19	Dist. = Gamma	Inv. Gauss.	Lognormal				

	Displacement (mm)					Differential Displacement (mm)					Distortion (for 9.15 m on-center footing spacing)						
	Footing 1	Footing 2	Footing 3	Footing 4	Footing 5	Footing 1-2	Footing 2-3	Footing 3-4	Footing 4-5	Footing 1-2	Footing 2-3	Footing 3-4	Footing 4-5	Footing 1-2	Footing 2-3	Footing 3-4	Footing 4-5
"Deterministic" estimate	23.2	30.3	30.5	28.9	23.7	7.2	0.13	1.5	5.2	0.00078	0.00001	0.00017	0.00057	0.00078	0.00001	0.00017	0.00057
Simulated - mean	72.4	85.2	86.8	78.5	72.9	93.2	101.7	97.7	90.0	0.01019	0.01111	0.01068	0.00983	0.01019	0.01111	0.01068	0.00983
Simulated - median	22.7	23.4	23.6	22.0	22.9	17.1	17.1	16.5	16.6	0.00187	0.00186	0.00180	0.00181	0.00187	0.00186	0.00180	0.00181
Simulated - Std Dev	245.2	315.4	319.5	301.8	246.6	323.0	365.3	358.1	316.9	0.0353	0.0399	0.0391	0.0346	0.0353	0.0399	0.0391	0.0346
Simulated COV	3.39	3.70	3.68	3.84	3.38	3.46	3.59	3.67	3.52	3.46	3.59	3.67	3.52	3.46	3.59	3.67	3.52
Minimum (neg. value is uplift)	0.28	0.28	0.09	0.27	0.31	0.000	0.000	0.000	0.000	0.0000000	0.0000000	0.0000000	0.0000000	0.0000000	0.0000000	0.0000000	0.0000000
Maximum	1675.0	2125.0	2125.0	2125.0	1675.0	2122.8	2122.8	2122.9	2122.9	0.23201	0.23201	0.23201	0.23201	0.23201	0.23200	0.23201	0.23201
Prob exceeding "calculated" value	0.491	0.384	0.385	0.378	0.485	0.75	0.99	0.94	0.81	0.48	0.48	0.48	0.47	0.48	0.48	0.47	0.47
Prob exceeding 12.5 mm	0.744	0.755	0.757	0.737	0.747	0.60	0.60	0.59	0.59	0.06	0.06	0.06	0.09	0.06	0.06	0.09	0.09
Prob exceeding 25 mm	0.456	0.470	0.473	0.442	0.461	0.37	0.37	0.36	0.36	0.06	0.06	0.06	0.09	0.06	0.06	0.09	0.09
Prob exceeding 50 mm	0.195	0.201	0.204	0.181	0.196	0.18	0.18	0.17	0.18	0.06	0.06	0.06	0.09	0.06	0.06	0.09	0.09

\*\*Note - p, also equals the probability of exceeding approx. 18.3 mm of differential displacement

**OpenSees Results - Footing Displacements and Angular Distortion at Footing Elevation**

Calculated results from bearing pressure-settlement equation and simulated results with 50,000 simulations that include bearing pressure-settlement equation (with known dispersion of model parameters) and variable soil undrained shear strength across horizontal distance, x.

Soil Parameters		Displacement Model (Vertical Spring) Parameters				Footing Parameters			
$s_u$ (kPa)	$k_z$	$k_1$	$k_2$	$M_{stc}$	$B_{1.5}$ (m)	$B_{3.4}$ (m)	Beam Dist.(m)		
70	0.013	0.701	0.643		1.675	2.125	9.15		
COV( $s_u$ ) = 30%	0.007	0.113	0.123						
Scale of Fluctuation, $\delta$ (m) = 30	53.0	16.1	19.1						
$\gamma$ (kN/m <sup>3</sup> ) = 19	Dist. = Gamma	Inv. Gauss.	Lognormal						
"calculated" values assume no variation in soil shear strength or spring parameters									
"Allowable" Distortion = 1/500 = 0.002									
Displacement (mm)		Footing 2		Footing 3	Footing 4	Footing 5	Differential Displacement (mm)		
Footing 1	Footing 2	Footing 3	Footing 4	Footing 5	Footing 1-2	Footing 2-3	Footing 3-4	Footing 4-5	
23.2	30.3	30.5	28.9	23.7	7.2	0.13	1.5	5.2	
72.6	88.2	90.5	83.3	78.1	87.5	96.6	92.2	88.2	
22.9	23.4	23.7	22.5	23.2	16.7	16.6	16.2	16.6	
247.3	325.0	329.8	313.3	261.4	309.8	354.2	343.8	307.6	
3.41	3.68	3.65	3.76	3.35	3.54	3.67	3.73	3.49	
0.24	0.28	0.32	0.38	0.24	0.000	0.000	0.000	0.000	
1675.0	2125.0	2125.0	2125.0	1675.0	2123.8	2123.5	2123.9	2124.4	
"Deterministic" estimate	0.495	0.388	0.388	0.490	0.74	0.99	0.94	0.81	
Simulated - mean	0.748	0.755	0.758	0.743	0.59	0.59	0.58	0.59	
Simulated - median	0.462	0.472	0.476	0.452	0.36	0.36	0.35	0.36	
Simulated - Std Dev	0.192	0.204	0.209	0.191	0.17	0.17	0.17	0.17	
Simulated COV									
Minimum (neg. value is uplift)									
Maximum									
Prob exceeding "calculated" value									
Prob exceeding 12.5 mm									
Prob exceeding 25 mm									
Prob exceeding 50 mm									
"Deterministic" estimate		0.00078		0.00001		0.00017		0.00057	
Simulated - mean		0.00956		0.01056		0.01008		0.00964	
Simulated - median		0.00182		0.00181		0.00177		0.00181	
Simulated - Std Dev		0.00339		0.00387		0.00376		0.00338	
Simulated COV		3.54		3.67		3.73		3.49	
Minimum		0.0000000		0.0000000		0.0000000		0.0000000	
Maximum		0.23211		0.23207		0.23212		0.23218	
Prob of failure, $p_f$ =		0.47		0.47		0.46		0.47	
$\beta$ =		0.08		0.08		0.10		0.08	

\*\*Note -  $p_f$  also equals the probability of exceeding approx. 18.3 mm of differential displacement



**OpenSees Results - Footing Displacements and Angular Distortion at Footing Elevation**

Calculated results from bearing pressure-settlement equation and simulated results with 50,000 simulations that include bearing pressure-settlement equation (with known dispersion of model parameters) and variable soil undrained shear strength across horizontal distance, x.

Soil Parameters		Displacement Model (Vertical Spring) Parameters				Footing Parameters	
$s_u$ (kPa)	$k_z$	$k_1$	$k_2$	$M_{stc}$	$B_{1.5}$ (m)	$B_{3.4}$ (m)	Beam Dist.(m)
70	0.701	0.013	23.7	0.643	1.675	2.125	9.15
COV( $s_u$ ) = 30%	0.007	0.113	23.1	0.123			
Scale of Fluctuation, $\delta$ (m) = 100	53.0	16.1	19.1				
$\gamma$ (kN/m <sup>3</sup> ) = 19	Dist. = Gamma	Inv. Gauss.	Lognormal				

	Displacement (mm)					Differential Displacement (mm)					Distortion (for 9.15 m on-center footing spacing)						
	Footing 1	Footing 2	Footing 3	Footing 4	Footing 5	Footing 1-2	Footing 2-3	Footing 3-4	Footing 4-5	Footing 1-2	Footing 2-3	Footing 3-4	Footing 4-5	Footing 1-2	Footing 2-3	Footing 3-4	Footing 4-5
"Deterministic" estimate	23.2	30.3	30.5	28.9	23.7	7.2	0.13	1.5	5.2	0.00078	0.00001	0.00017	0.00057	0.00078	0.00001	0.00017	0.00057
Simulated - mean	73.6	90.3	91.5	83.1	77.6	70.2	70.6	67.2	66.4	0.00767	0.00772	0.00735	0.00725	0.00767	0.00772	0.00735	0.00725
Simulated - median	22.5	23.8	23.7	22.3	23.1	15.7	15.6	15.1	15.4	0.00172	0.00171	0.00165	0.00169	0.00172	0.00171	0.00165	0.00169
Simulated - Std Dev	251.2	329.9	333.3	314.5	259.5	254.6	280.0	271.6	240.2	0.0278	0.0306	0.0297	0.0263	0.0278	0.0306	0.0297	0.0263
Simulated COV	3.41	3.66	3.64	3.78	3.34	3.63	3.96	4.04	3.62	3.63	3.96	4.04	3.62	3.63	3.96	4.04	3.62
Minimum (neg. value is uplift)	0.13	0.14	0.28	0.15	0.20	0.000	0.000	0.000	0.001	0.0000000	0.0000000	0.0000000	0.0000001	0.0000000	0.0000000	0.0000000	0.0000001
Maximum	1675.0	2125.0	2125.0	2125.0	1675.0	2118.9	2120.1	2120.6	2122.7	0.23157	0.23171	0.23176	0.23199	0.23157	0.23171	0.23176	0.23199
Prob exceeding "calculated" value	0.486	0.391	0.389	0.384	0.488	0.73	0.98	0.92	0.80	0.45	0.44	0.43	0.44	0.45	0.44	0.43	0.44
Prob exceeding 12.5 mm	0.741	0.759	0.757	0.739	0.751	0.58	0.57	0.56	0.57	0.13	0.14	0.17	0.15	0.13	0.14	0.17	0.15
Prob exceeding 25 mm	0.452	0.478	0.476	0.446	0.464	0.34	0.34	0.33	0.34								
Prob exceeding 50 mm	0.191	0.207	0.207	0.188	0.202	0.16	0.15	0.14	0.15								

\*\*Note - p, also equals the probability of exceeding approx. 18.3 mm of differential displacement

"calculated" values assume no variation in soil shear strength or spring parameters

"Allowable" Distortion = 1/500 = 0.002

**OpenSees Results - Footing Displacements and Angular Distortion at Footing Elevation**

Calculated results from bearing pressure-settlement equation and simulated results with 50,000 simulations that include bearing pressure-settlement equation (with known dispersion of model parameters) and variable soil undrained shear strength across horizontal distance, x.

Soil Parameters		Displacement Model (Vertical Spring) Parameters				Footing Parameters	
		$k_1$	$k_2$	$M_{stc}$	$B_{1.5}$ (m)	$B_{2.4}$ (m)	
$s_u$ (kPa)	= 70	0.013	0.701	0.643	1.675		
COV( $s_u$ )	= 50%	0.007	0.113	0.123	2.125		
Scale of Fluctuation, $\delta$ (m)	= 0.1	53.0	16.1	19.1	9.15		
$\gamma'$ (kN/m <sup>3</sup> )	= 19	Dist. = Gamma		Inv. Gauss. Lognormal			

"calculated" values assume no variation in soil shear strength or spring parameters

"Allowable" Distortion = 1/500 = 0.002

	Displacement (mm)					Distortion (for 9.15 m on-center footing spacing)				
	Footing 1	Footing 2	Footing 3	Footing 4	Footing 5	Footings 1-2	Footings 2-3	Footings 3-4	Footings 4-5	
"Deterministic" estimate	23.2	30.3	30.5	28.9	23.7	7.2	0.13	1.5	5.2	
Simulated - mean	26.7	27.3	27.5	25.9	27.4	21.2	21.3	20.8	20.9	"Deterministic" estimate
Simulated - median	21.3	22.0	22.2	21.1	21.8	15.0	15.4	15.1	15.0	Simulated - mean
Simulated - Std Dev	26.0	23.5	22.4	20.3	25.0	28.0	24.3	21.9	24.4	Simulated - median
Simulated COV	0.87	0.86	0.81	0.78	0.91	1.32	1.14	1.05	1.17	Simulated - Std Dev
Minimum (neg. value is uplift)	0.22	0.28	0.35	0.21	0.35	0.001	0.000	0.000	0.000	Simulated COV
Maximum	1675.0	2125.0	912.7	1028.2	1675.0	2097.6	2107.4	1003.1	1658.0	Minimum
Prob exceeding "calculated" value	0.456	0.336	0.334	0.335	0.457	0.73	1.00	0.94	0.80	Maximum
Prob exceeding 12.5 mm	0.744	0.753	0.756	0.736	0.751	0.57	0.58	0.57	0.57	Prob of failure, $p_f$ =
Prob exceeding 25 mm	0.416	0.434	0.438	0.411	0.430	0.30	0.31	0.30	0.30	$\beta$ =
Prob exceeding 50 mm	0.111	0.119	0.119	0.103	0.121	0.08	0.08	0.08	0.08	0.42
										0.19
										0.19

\*\*Note -  $p_f$  also equals the probability of exceeding approx. 18.3 mm of differential displacement

**OpenSees Results - Footing Displacements and Angular Distortion at Footing Elevation**

Calculated results from bearing pressure-settlement equation and simulated results with 50,000 simulations that include bearing pressure-settlement equation (with known dispersion of model parameters) and variable soil undrained shear strength across horizontal distance, x.

Soil Parameters		Displacement Model (Vertical Spring) Parameters				Footing Parameters							
		$k_1$	$k_2$	$M_{stc}$	$B_{1.5}$ (m)	$B_{3.4}$ (m)							
$s_u$ (kPa)	= 70	0.313	0.701	0.643	1.675								
COV( $s_u$ )	= 50%	0.007	0.113	0.123	2.125								
Scale of Fluctuation, $\delta$ (m)	= 0.2	53.0	16.1	19.1	9.15								
$\gamma'$ (kN/m <sup>3</sup> )	= 19	Dist. = Gamma Inv. Gauss. Lognormal											
"calculated" values assume no variation in soil shear strength or spring parameters													
"Allowable" Distortion = 1/500 = 0.002													
		Displacement (mm)			Differential Displacement (mm)								
		Footing 1	Footing 2	Footing 3	Footing 4	Footing 5	Footing 1-2	Footing 2-3	Footing 3-4	Footing 4-5			
"Deterministic" estimate		23.2	30.3	30.5	28.9	23.7	7.2	0.13	1.5	5.2			
Simulated - mean		30.5	30.2	28.4	28.4	31.7	27.1	26.3	25.4	27.0			
Simulated - median		21.6	22.3	22.3	21.3	22.2	16.2	16.2	15.9	16.1			
Simulated - Std Dev		53.1	50.4	48.1	43.2	59.5	68.0	64.5	59.6	68.6			
Simulated COV		1.74	1.67	1.59	1.52	1.88	2.51	2.46	2.34	2.54			
Minimum (neg. value is uplift)		0.33	0.18	0.25	0.15	0.27	0.001	0.000	0.000	0.000			
Maximum		1675.0	2125.0	2125.0	2125.0	1675.0	2119.9	2120.6	2117.6	2123.5			
Prob exceeding "calculated" value		0.465	0.347	0.346	0.346	0.468	0.75	1.00	0.94	0.81			
Prob exceeding 12.5 mm		0.740	0.758	0.756	0.739	0.752	0.59	0.59	0.58	0.59			
Prob exceeding 25 mm		0.427	0.442	0.443	0.417	0.440	0.34	0.33	0.33	0.33			
Prob exceeding 50 mm		0.137	0.138	0.140	0.124	0.144	0.12	0.11	0.11	0.12			
		Distortion (for 9.15 m on-center footing spacing)			Distortion (for 9.15 m on-center footing spacing)			Distortion (for 9.15 m on-center footing spacing)					
		Footing 1-2			Footing 2-3			Footing 3-4			Footing 4-5		
		0.00078			0.00001			0.00017			0.00057		
"Deterministic" estimate		0.00297			0.00287			0.00278			0.00295		
Simulated - mean		0.00177			0.00177			0.00174			0.00176		
Simulated - median		0.0074			0.0071			0.0065			0.0075		
Simulated - Std Dev		2.51			2.46			2.34			2.54		
Simulated COV		0.0000001			0.0000000			0.0000000			0.0000000		
Minimum		0.23168			0.23176			0.23143			0.23208		
Maximum		0.46			0.45			0.45			0.45		
Prob of failure, $p_f$		0.11			0.11			0.13			0.12		
$\beta$		0.46			0.45			0.45			0.45		

\*\*Note -  $p_f$  also equals the probability of exceeding approx. 18.3 mm of differential displacement

**OpenSees Results - Footing Displacements and Angular Distortion at Footing Elevation**

Calculated results from bearing pressure-settlement equation and simulated results with 50,000 simulations that include bearing pressure-settlement equation (with known dispersion of model parameters) and variable soil undrained shear strength across horizontal distance, x.

Soil Parameters		Displacement Model (Vertical Spring) Parameters				Footing Parameters	
$s_u$ (kPa)	$k_z$	$k_1$	$k_2$	$M_{stc}$	$B_{1.5}$ (m)	$B_{3.4}$ (m)	Beam Dist.(m)
70	0.013	0.701	0.643	1.675	1.675	2.125	9.15
COV( $s_u$ ) = 50%	0.007	0.113	0.123				
Scale of Fluctuation, $\delta$ (m) = 0.5	53.0	16.1	19.1				
$\gamma$ (kN/m <sup>3</sup> ) = 19	Dist. = Gamma	Inv. Gauss.	Lognormal				

"calculated" values assume no variation in soil shear strength or spring parameters

"Allowable" Distortion = 1/500 = 0.002

	Displacement (mm)					Differential Displacement (mm)					Distortion (for 9.15 m on-center footing spacing)						
	Footing 1	Footing 2	Footing 3	Footing 4	Footing 5	Footing 1-2	Footing 2-3	Footing 3-4	Footing 4-5	Footing 1-2	Footing 2-3	Footing 3-4	Footing 4-5	Footing 1-2	Footing 2-3	Footing 3-4	Footing 4-5
"Deterministic" estimate	23.2	30.3	30.5	28.9	23.7	7.2	0.13	1.5	5.2	0.00078	0.00001	0.00017	0.00057	0.00078	0.00001	0.00017	0.00057
Simulated - mean	58.8	54.2	55.6	50.1	60.6	76.9	73.2	70.1	74.8	0.00841	0.00800	0.00767	0.00817	0.00841	0.00800	0.00767	0.00817
Simulated - median	22.3	23.0	23.1	21.9	22.7	19.0	19.4	18.8	18.7	0.00207	0.00212	0.00206	0.00205	0.00207	0.00212	0.00206	0.00205
Simulated - Std Dev	197.6	199.7	203.8	185.4	200.5	270.7	275.2	266.4	262.5	0.0296	0.0301	0.0291	0.0287	0.0296	0.0301	0.0291	0.0287
Simulated COV	3.36	3.68	3.66	3.70	3.31	3.52	3.76	3.80	3.51	3.52	3.76	3.80	3.51	3.52	3.76	3.80	3.51
Minimum (neg. value is uplift)	0.19	0.24	0.18	0.12	0.11	0.000	0.000	0.000	0.000	0.0000000	0.0000000	0.0000000	0.0000000	0.0000000	0.0000000	0.0000000	0.0000000
Maximum	1675.0	2125.0	2125.0	2125.0	1675.0	2123.9	2123.7	2124.1	2123.9	0.23212	0.23210	0.23214	0.23212	0.23212	0.23210	0.23214	0.23212
Prob exceeding "calculated" value	0.484	0.374	0.375	0.374	0.482	0.77	1.00	0.95	0.83	0.51	0.52	0.51	0.51	0.51	0.52	0.51	0.51
Prob exceeding 12.5 mm	0.740	0.752	0.752	0.739	0.747	0.63	0.64	0.63	0.63	-0.03	-0.05	-0.02	-0.02	-0.03	-0.05	-0.02	-0.02
Prob exceeding 25 mm	0.450	0.460	0.464	0.439	0.457	0.41	0.41	0.40	0.40								
Prob exceeding 50 mm	0.189	0.188	0.191	0.171	0.196	0.20	0.20	0.19	0.20								

Prob of failure,  $p_f$  = 0.51      $\beta$  = -0.02

\*\*Note -  $p_f$  also equals the probability of exceeding approx. 18.3 mm of differential displacement



**OpenSees Results - Footing Displacements and Angular Distortion at Footing Elevation**

Calculated results from bearing pressure-settlement equation and simulated results with 50,000 simulations that include bearing pressure-settlement equation (with known dispersion of model parameters) and variable soil undrained shear strength across horizontal distance, x.

Soil Parameters		Displacement Model (Vertical Spring) Parameters				Footing Parameters							
$s_u$ (kPa)	$\delta$ (m)	$k_1$	$k_2$	$M_{stc}$	$B_{1.5}$ (m)	$B_{3.4}$ (m)	Beam Dist.(m)						
70	50%	0.013	0.701	0.643	1.675	2.125	9.15						
COV( $s_u$ )		0.007	0.113	0.123									
Scale of Fluctuation, $\delta$ (m)		53.0	16.1	19.1									
$\gamma$ (kN/m <sup>3</sup> )		Inv. Gauss. Lognormal											
					"Allowable" Distortion = 1/500 = 0.002								
"calculated" values assume no variation in soil shear strength or spring parameters													
Displacement (mm)		Footing 2		Footing 3	Footing 4	Footing 5	Differential Displacement (mm)						
		Footing 1	Footing 2	Footing 3	Footing 4	Footing 5	Footing 1-2	Footing 2-3	Footing 3-4	Footing 4-5			
"Deterministic" estimate		23.2	30.3	30.5	28.9	23.7	7.2	0.13	1.5	5.2			
Simulated - mean		107.5	109.2	109.3	98.4	114.0	172.8	175.5	165.7	170.0			
Simulated - median		22.9	23.6	23.5	22.3	23.3	22.7	22.5	21.4	21.9			
Simulated - Std Dev		328.4	371.5	373.2	349.0	340.8	463.6	497.7	483.3	457.9			
Simulated COV		3.06	3.40	3.41	3.55	2.99	2.68	2.84	2.92	2.69			
Minimum (neg. value is uplift)		0.19	0.13	0.14	0.15	0.15	0.002	0.000	0.000	0.000			
Maximum		1675.0	2125.0	2125.0	2125.0	1675.0	2124.3	2124.2	2124.3	2124.0			
Prob exceeding "calculated" value		0.495	0.396	0.395	0.392	0.493	0.79	1.00	0.95	0.84			
Prob exceeding 12.5 mm		0.734	0.746	0.746	0.732	0.742	0.67	0.67	0.66	0.66			
Prob exceeding 25 mm		0.464	0.475	0.474	0.453	0.472	0.47	0.47	0.45	0.46			
Prob exceeding 50 mm		0.228	0.231	0.230	0.211	0.236	0.29	0.28	0.27	0.28			
Distortion (for 9.15 m on-center footing spacing)		Footing 1-2		Footing 2-3	Footing 3-4	Footing 4-5	"Deterministic" estimate		Footing 1-2		Footing 2-3	Footing 3-4	Footing 4-5
		0.00078	0.00001	0.00001	0.00017	0.00057	0.00078	0.00001	0.00017	0.00017	0.00017	0.00017	0.00057
		0.01888	0.01918	0.01811	0.01811	0.01858	0.01888	0.01918	0.01811	0.01811	0.01811	0.01811	0.01858
		0.00248	0.00246	0.00234	0.00234	0.00239	0.00248	0.00246	0.00234	0.00234	0.00234	0.00234	0.00239
		0.0507	0.0544	0.0528	0.0528	0.0500	0.0507	0.0544	0.0528	0.0528	0.0528	0.0528	0.0500
		2.68	2.84	2.84	2.92	2.69	2.68	2.84	2.84	2.92	2.92	2.92	2.69
		0.0000002	0.0000000	0.0000000	0.0000000	0.0000000	0.0000002	0.0000000	0.0000000	0.0000000	0.0000000	0.0000000	0.0000000
		0.23216	0.23216	0.23216	0.23216	0.23216	0.23216	0.23216	0.23216	0.23216	0.23216	0.23216	0.23216
		0.56	0.56	0.56	0.56	0.55	0.56	0.56	0.55	0.55	0.55	0.55	0.55
		-0.16	-0.15	-0.15	-0.12	-0.14	-0.16	-0.15	-0.12	-0.12	-0.12	-0.12	-0.14
Prob of failure, $p_f$ =		0.56		0.56	0.56	0.55	0.56	0.56	0.55	0.55	0.55	0.55	0.55
$\beta$ =		-0.16		-0.15	-0.12	-0.14	-0.16	-0.15	-0.12	-0.12	-0.12	-0.12	-0.14

\*\*Note -  $p_f$  also equals the probability of exceeding approx. 18.3 mm of differential displacement

**OpenSees Results - Footing Displacements and Angular Distortion at Footing Elevation**

Calculated results from bearing pressure-settlement equation and simulated results with 50,000 simulations that include bearing pressure-settlement equation (with known dispersion of model parameters) and variable soil undrained shear strength across horizontal distance, x.

Soil Parameters		Displacement Model (Vertical Spring) Parameters				Footing Parameters					
$s_u$ (kPa)	$k_z$	$k_1$	$k_2$	$M_{stc}$	$B_{1.5}$ (m)	$B_{3.4}$ (m)	Beam Dist.(m)				
70	0.013	0.701	0.643	1.675	1.675	2.125	9.15				
COV( $s_u$ ) = 50%	0.007	0.113	0.123								
Scale of Fluctuation, $\delta$ (m) = 2	53.0	16.1	19.1								
$\gamma'$ (kN/m <sup>3</sup> ) = 19	Dist. = Gamma	Inv. Gauss.	Lognormal								
"calculated" values assume no variation in soil shear strength or spring parameters											
"Allowable" Distortion = 1/500 = 0.002											
		Displacement (mm)		Differential Displacement (mm)		Distortion (for 9.15 m on-center footing spacing)					
		Footing 1	Footing 2	Footing 3	Footing 4	Footing 5	Footing 1-2	Footing 2-3	Footing 3-4	Footing 4-5	
"Deterministic" estimate		23.2	30.3	30.5	28.9	23.7	7.2	0.13	1.5	5.2	
Simulated - mean		152.8	172.3	177.1	166.5	156.9	268.8	290.1	284.1	267.4	
Simulated - median		23.1	24.0	24.2	22.9	23.7	25.3	25.1	24.6	24.7	
Simulated - Std Dev		414.7	502.8	511.3	496.3	420.5	592.9	655.6	650.1	591.5	
Simulated COV		2.71	2.92	2.89	2.88	2.68	2.21	2.26	2.29	2.21	
Minimum (neg. value is uplift)		0.18	0.18	0.21	0.19	0.12	0.000	0.000	0.000	0.000	
Maximum		1675.0	2125.0	2125.0	2125.0	1675.0	2124.6	2124.4	2124.5	2124.5	
Prob exceeding "calculated" value		0.498	0.412	0.413	0.409	0.499	0.81	0.99	0.95	0.85	
Prob exceeding 12.5 mm		0.733	0.747	0.745	0.729	0.738	0.69	0.69	0.68	0.68	
Prob exceeding 25 mm		0.470	0.485	0.487	0.464	0.479	0.50	0.50	0.49	0.50	
Prob exceeding 50 mm		0.250	0.258	0.258	0.244	0.258	0.34	0.33	0.33	0.33	
								Prob of failure, $p_f$ =		0.59	
										0.59	
								Prob $\beta$ =		-0.22	
										-0.22	
										0.58	
										-0.21	

\*\*Note -  $p_f$  also equals the probability of exceeding approx. 18.3 mm of differential displacement

**OpenSees Results - Footing Displacements and Angular Distortion at Footing Elevation**

Calculated results from bearing pressure-settlement equation and simulated results with 50,000 simulations that include bearing pressure-settlement equation (with known dispersion of model parameters) and variable soil undrained shear strength across horizontal distance, x.

Soil Parameters		Displacement Model (Vertical Spring) Parameters				Footing Parameters		
		$k_1$	$k_2$	$M_{stc}$	$B_{1.5}$ (m)	$B_{2.5,4}$ (m)	Beam Dist.(m)	
$s_u$ (kPa)	= 70	0.013	0.701	0.643	1.675			
COV( $s_u$ )	= 50%	0.007	0.113	0.123	2.125			
Scale of Fluctuation, $\delta$ (m)	= 5	53.0	16.1	19.1	9.15			
$\gamma'$ (kN/m <sup>3</sup> )	= 19	Dist. = Gamma		Inv. Gauss. Lognormal				
"calculated" values assume no variation in soil shear strength or spring parameters								
"Allowable" Distortion = 1/500 = 0.002								
<b>Distortion (for 9.15 m on-center footing spacing)</b>								
		Footing 1-2		Footing 2-3	Footing 3-4	Footing 4-5		
"Deterministic" estimate		0.00078	0.00001	0.00017	0.00017	0.00057		
Simulated - mean		0.03705	0.04015	0.03920	0.03630			
Simulated - median		0.00283	0.00278	0.00268	0.00283			
Simulated - Std Dev		0.0727	0.0806	0.0799	0.0718			
Simulated COV		1.96	2.01	2.04	1.98			
Minimum	(neg. value is uplift)	0.0000002	0.0000000	0.0000000	0.0000000			
Maximum		0.23219	0.23220	0.23219	0.23213			
<b>Prob of failure, <math>p_f</math> = <math>\beta</math></b>								
Prob exceeding 12.5 mm		0.59	0.58	0.58	0.59			
Prob exceeding 25 mm		-0.23	-0.21	-0.19	-0.22			
Prob exceeding 50 mm								
**Note - $p_f$ also equals the probability of exceeding approx. 18.3 mm of differential displacement								
<b>Differential Displacement (mm)</b>								
		Footing 1-2		Footing 2-3	Footing 3-4	Footing 4-5		
"Deterministic" estimate		7.2	0.13	1.5	5.2			
Simulated - mean		339.0	367.4	358.7	332.1			
Simulated - median		25.9	25.4	24.5	25.9			
Simulated - Std Dev		665.0	737.7	730.7	656.9			
Simulated COV		1.96	2.01	2.04	1.98			
Minimum		0.002	0.000	0.000	0.000			
Maximum		2124.5	2124.7	2124.6	2124.0			
<b>Displacement (mm)</b>								
		Footing 1	Footing 2	Footing 3	Footing 4	Footing 5		
"Deterministic" estimate		23.2	30.3	30.5	28.9	23.7		
Simulated - mean		197.4	238.6	237.5	226.3	199.6		
Simulated - median		23.2	24.2	24.4	23.0	23.9		
Simulated - Std Dev		483.9	608.4	606.2	593.0	485.9		
Simulated COV		2.45	2.55	2.62	2.43	2.43		
Minimum		0.18	0.22	0.31	0.12	0.04		
Maximum		1675.0	2125.0	2125.0	2125.0	1675.0		
<b>Prob of failure, <math>p_f</math> = <math>\beta</math></b>								
Prob exceeding "calculated" value		0.501	0.419	0.420	0.418	0.502		
Prob exceeding 12.5 mm		0.727	0.739	0.741	0.726	0.733		
Prob exceeding 25 mm		0.473	0.488	0.492	0.469	0.483		
Prob exceeding 50 mm		0.268	0.278	0.277	0.265	0.272		

**OpenSees Results - Footing Displacements and Angular Distortion at Footing Elevation**

Calculated results from bearing pressure-settlement equation and simulated results with 50,000 simulations that include bearing pressure-settlement equation (with known dispersion of model parameters) and variable soil undrained shear strength across horizontal distance, x.

Soil Parameters		Displacement Model (Vertical Spring) Parameters				Footing Parameters	
$s_u$ (kPa) =	70	$k_1$	0.013	0.701	0.643	$M_{stc}$	
COV( $s_u$ ) =	50%	$\mu$ =	0.007	0.113	0.123	$B_{1.5}$ (m) =	1.675
Scale of Fluctuation, $\delta$ (m) =	10	$\sigma$ =	53.0	16.1	19.1	$B_{2.5}$ (m) =	2.125
$\gamma'$ (kN/m <sup>3</sup> ) =	19	Dist. =	Gamma	Inv. Gauss.	Lognormal	Beam Dist. (m) =	9.15

"calculated" values assume no variation in soil shear strength or spring parameters

"Allowable" Distortion = 1/500 = 0.002

	Displacement (mm)					Differential Displacement (mm)					Distortion (for 9.15 m on-center footing spacing)						
	Footing 1	Footing 2	Footing 3	Footing 4	Footing 5	Footing 1-2	Footing 2-3	Footing 3-4	Footing 4-5	Footing 1-2	Footing 2-3	Footing 3-4	Footing 4-5	Footing 1-2	Footing 2-3	Footing 3-4	Footing 4-5
"Deterministic" estimate	23.2	30.3	30.5	28.9	23.7	7.2	0.13	1.5	5.2	0.00078	0.00001	0.00017	0.00057	0.00078	0.00001	0.00017	0.00057
Simulated - mean	214.1	261.2	264.4	248.5	222.2	327.1	346.6	343.4	318.4	0.03575	0.03787	0.03753	0.03480	0.03575	0.03787	0.03753	0.03480
Simulated - median	23.5	24.3	24.6	23.3	24.1	24.0	21.7	21.4	23.6	0.00263	0.00237	0.00234	0.00258	0.00263	0.00237	0.00234	0.00258
Simulated - Std Dev	506.1	639.7	644.2	624.7	515.4	649.4	722.3	719.7	637.2	0.0710	0.0789	0.0787	0.0696	0.0710	0.0789	0.0787	0.0696
Simulated COV	2.36	2.45	2.44	2.51	2.32	1.99	2.08	2.10	2.00	1.99	2.08	2.10	2.00	1.99	2.08	2.10	2.00
Minimum (neg. value is uplift)	0.13	0.09	0.13	0.28	0.25	0.000	0.000	0.000	0.000	0.0000000	0.0000000	0.0000000	0.0000000	0.0000000	0.0000000	0.0000000	0.0000000
Maximum	1675.0	2125.0	2125.0	2125.0	1675.0	2124.3	2124.6	2124.5	2124.4	0.23217	0.23220	0.23219	0.23217	0.23217	0.23220	0.23219	0.23217
Prob exceeding "calculated" value	0.505	0.424	0.425	0.424	0.506	0.79	0.97	0.92	0.84	0.57	0.54	0.54	0.57	0.57	0.54	0.54	0.57
Prob exceeding 12.5 mm	0.725	0.738	0.741	0.728	0.733	0.67	0.64	0.64	0.67	-0.17	-0.11	-0.10	-0.17	-0.17	-0.10	-0.10	-0.17
Prob exceeding 25 mm	0.477	0.491	0.494	0.473	0.487	0.49	0.46	0.46	0.49								
Prob exceeding 50 mm	0.276	0.283	0.286	0.270	0.283	0.35	0.32	0.32	0.34								

Prob of failure,  $p_f$  = 0.57     $\beta$  = -0.17

\*\*Note -  $p_f$  also equals the probability of exceeding approx. 18.3 mm of differential displacement

**OpenSees Results - Footing Displacements and Angular Distortion at Footing Elevation**

Calculated results from bearing pressure-settlement equation and simulated results with 50,000 simulations that include bearing pressure-settlement equation (with known dispersion of model parameters) and variable soil undrained shear strength across horizontal distance, x.

Soil Parameters		Displacement Model (Vertical Spring) Parameters				Footing Parameters	
$s_u$ (kPa) =	70	$k_1$	0.013	0.701	0.643	$M_{stc}$	
COV( $s_u$ ) =	50%	$\mu$ =	0.007	0.113	0.123	$B_{1.5}$ (m) =	1.675
Scale of Fluctuation, $\delta$ (m) =	20	$\sigma$ =	53.0	16.1	19.1	$B_{3.4}$ (m) =	2.125
$\gamma'$ (kN/m <sup>3</sup> ) =	19	Dist. =	Gamma	Inv. Gauss.	Lognormal	Beam Dist.(m) =	9.15

"calculated" values assume no variation in soil shear strength or spring parameters

"Allowable" Distortion = 1/500 = 0.002

	Displacement (mm)					Differential Displacement (mm)					Distortion (for 9.15 m on-center footing spacing)						
	Footing 1	Footing 2	Footing 3	Footing 4	Footing 5	Footing 1-2	Footing 2-3	Footing 3-4	Footing 4-5	Footing 1-2	Footing 2-3	Footing 3-4	Footing 4-5	Footing 1-2	Footing 2-3	Footing 3-4	Footing 4-5
"Deterministic" estimate	23.2	30.3	30.5	28.9	23.7	7.2	0.13	1.5	5.2	0.00078	0.00001	0.00017	0.00057	0.03060	0.03170	0.03089	0.03045
Simulated - mean	224.8	279.6	277.3	265.9	228.2	279.9	290.1	282.7	278.6	0.00233	0.00196	0.00192	0.00231	0.00233	0.00196	0.00192	0.00231
Simulated - median	23.4	24.2	24.3	23.2	24.2	21.3	17.9	17.6	21.1	0.0647	0.0726	0.0717	0.0644	0.0647	0.0726	0.0717	0.0644
Simulated - Std Dev	520.4	663.2	660.1	647.6	523.1	592.2	664.3	655.9	588.8	2.12	2.29	2.32	2.11	2.12	2.29	2.32	2.11
Simulated COV	2.31	2.37	2.38	2.44	2.29	2.12	2.29	2.32	2.11	2.12	2.29	2.32	2.11	2.12	2.29	2.32	2.11
Minimum (neg. value is uplift)	0.22	0.20	0.18	0.09	0.22	0.000	0.000	0.000	0.000	0.0000000	0.0000000	0.0000000	0.0000000	0.0000000	0.0000000	0.0000000	0.0000000
Maximum	1675.0	2125.0	2125.0	2125.0	1675.0	2124.8	2124.4	2124.0	2124.5	0.23222	0.23217	0.23213	0.23218	0.23222	0.23217	0.23213	0.23218
Prob exceeding "calculated" value	0.504	0.425	0.423	0.423	0.508	0.77	0.95	0.90	0.82	0.54	0.49	0.49	0.54	0.54	0.49	0.49	0.54
Prob exceeding 12.5 mm	0.725	0.738	0.736	0.723	0.734	0.64	0.59	0.59	0.64	-0.10	0.01	0.03	-0.10	-0.10	0.03	0.03	-0.10
Prob exceeding 25 mm	0.477	0.489	0.491	0.473	0.488	0.46	0.42	0.41	0.46								
Prob exceeding 50 mm	0.278	0.288	0.288	0.275	0.286	0.32	0.28	0.27	0.32								

Prob of failure,  $p_f$  = 0.54     $\beta$  = -0.10

\*\*Note -  $p_f$  also equals the probability of exceeding approx. 18.3 mm of differential displacement

**OpenSees Results - Footing Displacements and Angular Distortion at Footing Elevation**

Calculated results from bearing pressure-settlement equation and simulated results with 50,000 simulations that include bearing pressure-settlement equation (with known dispersion of model parameters) and variable soil undrained shear strength across horizontal distance, x.

Soil Parameters		Displacement Model (Vertical Spring) Parameters				Footing Parameters	
$s_u$ (kPa)	$k_z$	$k_1$	$k_2$	$M_{stc}$	$B_{1.5}$ (m)	$B_{3.4}$ (m)	Beam Dist.(m)
70	0.701	0.013	0.701	0.643	1.675	2.125	9.15
COV( $s_u$ ) = 50%	0.007	0.113	0.123	19.1			
Scale of Fluctuation, $\delta$ (m) = 30	53.0	16.1	19.1				
$\gamma$ (kN/m <sup>3</sup> ) = 19	Dist. = Gamma	Inv. Gauss.	Lognormal				

"calculated" values assume no variation in soil shear strength or spring parameters

"Allowable" Distortion = 1/500 = 0.002

	Displacement (mm)					Distortion (for 9.15 m on-center footing spacing)							
	Footing 1	Footing 2	Footing 3	Footing 4	Footing 5	Footings 1-2	Footings 2-3	Footings 3-4	Footings 4-5	Footings 1-2	Footings 2-3	Footings 3-4	Footings 4-5
"Deterministic" estimate	23.2	30.3	30.5	28.9	23.7	7.2	0.13	1.5	5.2	0.00078	0.00001	0.00017	0.00057
Simulated - mean	227.1	280.4	282.6	267.4	228.1	251.8	251.9	249.0	247.0	0.02751	0.02753	0.02721	0.02699
Simulated - median	23.3	24.4	24.5	23.1	24.0	19.7	16.3	16.0	19.6	0.00215	0.00179	0.00175	0.00215
Simulated - Std Dev	523.0	664.3	666.8	650.5	522.9	554.4	619.6	616.6	547.8	0.0606	0.0677	0.0674	0.0599
Simulated COV	2.30	2.37	2.36	2.43	2.29	2.20	2.46	2.48	2.22	2.20	2.46	2.48	2.22
Minimum (neg. value is uplift)	0.21	0.15	0.29	0.19	0.11	0.000	0.000	0.000	0.001	0.0000000	0.0000000	0.0000000	0.0000001
Maximum	1675.0	2125.0	2125.0	2125.0	1675.0	2124.2	2124.1	2123.7	2123.4	0.23215	0.23215	0.23210	0.23207
Prob exceeding "calculated" value	0.503	0.424	0.423	0.421	0.505	0.75	0.94	0.89	0.81	0.52	0.47	0.46	0.52
Prob exceeding 12.5 mm	0.723	0.736	0.739	0.724	0.730	0.62	0.57	0.57	0.62	-0.05	0.08	0.09	-0.04
Prob exceeding 25 mm	0.476	0.491	0.483	0.472	0.486	0.44	0.39	0.38	0.44				
Prob exceeding 50 mm	0.278	0.290	0.288	0.272	0.285	0.31	0.25	0.25	0.30				

Prob of failure,  $p_f$  = 0.52     $\beta$  = -0.05

\*\*Note -  $p_f$  also equals the probability of exceeding approx. 18.3 mm of differential displacement

**OpenSees Results - Footing Displacements and Angular Distortion at Footing Elevation**

Calculated results from bearing pressure-settlement equation and simulated results with 50,000 simulations that include bearing pressure-settlement equation (with known dispersion of model parameters) and variable soil undrained shear strength across horizontal distance, x.

Soil Parameters		Displacement Model (Vertical Spring) Parameters				Footing Parameters					
$s_u$ (kPa)	$\delta$ (m)	$k_1$	$k_2$	$M_{stc}$	$B_{1.5}$ (m)	$B_{3.4}$ (m)	Beam Dist.(m)				
70	50%	0.013	0.701	0.643	1.675	2.125	9.15				
COV( $s_u$ ) =	50	0.007	0.113	0.123							
Scale of Fluctuation, $\delta$ (m) =	19	53.0	16.1	19.1							
$\gamma$ (kN/m <sup>3</sup> ) =		Dist. = Gamma	Inv. Gauss.	Lognormal							
"calculated" values assume no variation in soil shear strength or spring parameters											
"Allowable" Distortion = 1/500 = 0.002											
		Displacement (mm)		Differential Displacement (mm)		Distortion (for 9.15 m on-center footing spacing)					
		Footing 1	Footing 2	Footing 3	Footing 4	Footing 5	Footing 1-2	Footing 2-3	Footing 3-4	Footing 4-5	
"Deterministic" estimate		23.2	30.3	30.5	28.9	23.7	7.2	0.13	1.5	5.2	
Simulated - mean		229.2	282.5	286.5	277.0	233.4	216.2	209.4	204.5	217.5	
Simulated - median		23.4	24.3	24.5	23.0	23.9	18.8	14.9	14.5	18.5	
Simulated - Std Dev		526.0	667.5	671.3	663.6	529.9	501.3	562.3	557.0	502.9	
Simulated COV		2.30	2.36	2.34	2.40	2.27	2.32	2.69	2.72	2.31	
Minimum (neg. value is uplift)		1675.0	0.20	0.28	0.12	0.10	0.001	0.000	0.000	0.001	
Maximum			2125.0	2125.0	2125.0	1675.0	2122.7	2124.1	2124.2	2123.8	
Prob exceeding "calculated" value		0.504	0.424	0.424	0.422	0.503	0.75	0.93	0.87	0.81	
Prob exceeding 12.5 mm		0.724	0.734	0.736	0.721	0.729	0.61	0.55	0.54	0.61	
Prob exceeding 25 mm		0.477	0.490	0.492	0.471	0.483	0.42	0.36	0.35	0.42	
Prob exceeding 50 mm		0.278	0.287	0.289	0.277	0.287	0.29	0.22	0.22	0.29	
		Prob of failure, $p_f$ =		0.44		0.51		0.44		0.50	
		$\beta$ =		-0.02		0.15		0.16		-0.01	

\*\*Note -  $p_f$  also equals the probability of exceeding approx. 18.3 mm of differential displacement

**OpenSees Results - Footing Displacements and Angular Distortion at Footing Elevation**

Calculated results from bearing pressure-settlement equation and simulated results with 50,000 simulations that include bearing pressure-settlement equation (with known dispersion of model parameters) and variable soil undrained shear strength across horizontal distance, x.

Soil Parameters		Displacement Model (Vertical Spring) Parameters				Footing Parameters					
$s_u$ (kPa)	$\delta$ (mm)	$k_1$	$k_2$	$M_{stc}$	$B_{1.5}$ (m)	$B_{3.4}$ (m)	Beam Dist.(m)				
70	50%	0.013	0.701	0.643	1.675						
COV( $s_u$ ) = 100	100	0.007	0.113	0.123	2.125						
Scale of Fluctuation, $\delta$ (mm) = 19		COV(%) = 53.0	16.1	19.1	9.15						
$\gamma'$ (kN/m <sup>3</sup> ) = 19		Dist. = Gamma	Inv. Gauss.	Lognormal							
"calculated" values assume no variation in soil shear strength or spring parameters											
"Allowable" Distortion = 1/500 = 0.002											
<b>Distortion (for 9.15 m on-center footing spacing)</b>											
		Footing 1-2		Footing 2-3		Footing 3-4		Footing 4-5			
"Deterministic" estimate		7.2	0.13	1.5	5.2	0.00078	0.00001	0.00017	0.00057		
Simulated - mean		179.7	155.9	156.4	178.6	0.01964	0.01704	0.01709	0.01951		
Simulated - median		17.8	13.5	13.2	17.3	0.00194	0.00148	0.00145	0.00190		
Simulated - Std Dev		436.8	477.1	479.3	436.1	0.0480	0.0521	0.0524	0.0477		
Simulated COV		2.44	3.06	3.07	2.44	2.44	3.06	3.07	2.44		
Minimum (neg. value is uplift)		0.001	0.000	0.000	0.001	0.0000001	0.0000000	0.0000000	0.0000001		
Maximum		2121.9	2124.5	2121.9	2123.9	0.23190	0.23219	0.23191	0.23212		
		Footing 1		Footing 2		Footing 3		Footing 4		Footing 5	
"Deterministic" estimate		30.3	30.5	28.9	23.7	30.5	28.9	23.7	23.7		
Simulated - mean		226.0	285.5	285.4	273.2	229.5	229.5	229.5	229.5		
Simulated - median		23.4	24.4	24.4	23.2	24.2	24.2	24.2	24.2		
Simulated - Std Dev		521.3	671.5	670.4	658.5	524.7	524.7	524.7	524.7		
Simulated COV		2.31	2.35	2.41	2.29	2.29	2.29	2.29	2.29		
Minimum (neg. value is uplift)		0.17	0.39	0.25	0.19	0.23	0.23	0.23	0.23		
Maximum		1675.0	2125.0	2125.0	2125.0	1675.0	1675.0	1675.0	1675.0		
Prob exceeding "calculated" value		0.503	0.425	0.423	0.508	0.74	0.91	0.86	0.80	0.41	
Prob exceeding 12.5 mm		0.726	0.736	0.722	0.736	0.60	0.52	0.52	0.59	0.41	
Prob exceeding 25 mm		0.477	0.491	0.483	0.473	0.41	0.33	0.32	0.40	0.27	
Prob exceeding 50 mm		0.281	0.288	0.289	0.274	0.27	0.19	0.19	0.27	0.27	
		Footing 1		Footing 2		Footing 3		Footing 4		Footing 5	
Prob of failure, $p_f$ =		0.49	0.41	0.41	0.41	0.41	0.41	0.41	0.41	0.48	
$\beta$ =		0.02	0.22	0.22	0.23	0.23	0.23	0.23	0.23	0.04	

\*\*Note -  $p_f$  also equals the probability of exceeding approx. 18.3 mm of differential displacement





**OpenSees Results - Footing Displacements and Angular Distortion at Footing Elevation**

Calculated results from bearing pressure-settlement equation and simulated results with 50,000 simulations that include bearing pressure-settlement equation (with known dispersion of model parameters) and variable soil undrained shear strength across horizontal distance, x.

Soil Parameters		Displacement Model (Vertical Spring) Parameters				Footing Parameters	
$s_u$ (kPa)	$\delta$ (m)	$k_1$	$k_2$	$M_{stc}$	$B_{1.5}$ (m)	$B_{3.4}$ (m)	Beam Dist.(m)
70	100%	0.013	0.701	0.643	1.675	2.125	9.15
COV( $s_u$ ) = 0.2		0.007	0.113	0.123			
Scale of Fluctuation, $\delta$ (m) = 0.2		53.0	16.1	19.1			
$\gamma$ (kN/m <sup>3</sup> ) = 19		Dist. = Gamma	Inv. Gauss.	Lognormal			

"calculated" values assume no variation in soil shear strength or spring parameters

"Allowable" Distortion = 1/500 = 0.002

	Displacement (mm)					Distortion (for 9.15 m on-center footing spacing)							
	Footing 1	Footing 2	Footing 3	Footing 4	Footing 5	Footing 1-2	Footing 2-3	Footing 3-4	Footing 4-5	Footing 1-2	Footing 2-3	Footing 3-4	Footing 4-5
"Deterministic" estimate	23.2	30.3	30.5	28.9	23.7	7.2	0.13	1.5	5.2	0.00078	0.00001	0.00017	0.00057
Simulated - mean	41.5	36.5	38.1	34.2	43.3	47.9	44.4	42.6	47.8	0.00524	0.00485	0.00466	0.00522
Simulated - median	18.9	19.3	19.8	18.5	19.5	15.7	15.8	15.3	15.7	0.00171	0.00173	0.00167	0.00172
Simulated - Std Dev	140.2	129.3	135.8	117.6	146.5	184.3	182.1	174.9	182.1	0.0201	0.0199	0.0191	0.0199
Simulated COV	3.38	3.55	3.56	3.44	3.38	3.84	4.10	4.11	3.81	3.84	4.10	4.11	3.81
Minimum (neg. value is uplift)	0.22	0.16	0.28	0.16	0.17	0.000	0.000	0.001	0.002	0.0000000	0.0000000	0.0000001	0.0000002
Maximum	1675.0	2125.0	2125.0	2125.0	1675.0	2124.0	2124.6	2123.4	2123.3	0.23214	0.23219	0.23207	0.23206
Prob exceeding "calculated" value	0.410	0.295	0.302	0.299	0.412	0.73	1.00	0.94	0.80	0.45	0.45	0.44	0.45
Prob exceeding 12.5 mm	0.677	0.690	0.696	0.674	0.689	0.58	0.58	0.57	0.58	0.13	0.13	0.16	0.13
Prob exceeding 25 mm	0.377	0.378	0.390	0.361	0.388	0.34	0.34	0.33	0.34				
Prob exceeding 50 mm	0.143	0.132	0.138	0.120	0.150	0.15	0.14	0.14	0.15				

Prob of failure,  $p_f$  = 0.45     $\beta$  = 0.13

\*\*Note -  $p_f$  also equals the probability of exceeding approx. 18.3 mm of differential displacement

**OpenSees Results - Footing Displacements and Angular Distortion at Footing Elevation**

Calculated results from bearing pressure-settlement equation and simulated results with 50,000 simulations that include bearing pressure-settlement equation (with known dispersion of model parameters) and variable soil undrained shear strength across horizontal distance, x.

Soil Parameters		Displacement Model (Vertical Spring) Parameters				Footing Parameters	
		$k_1$	$k_2$	$M_{stc}$	$B_{1,5} (m)$	$B_{2,4} (m)$	Beam Dist.(m)
$s_u (kPa)$	= 70	0.013	0.701	0.643	1.675		
$COV(s_u)$	= 100%	0.007	0.113	0.123	2.125		
Scale of Fluctuation, $\delta (m)$	= 0.5	53.0	16.1	19.1	9.15		
$\gamma' (kN/m^3)$	= 19	Inv. Gauss.		Lognormal			
		Dist. = Gamma					

"calculated" values assume no variation in soil shear strength or spring parameters

"Allowable" Distortion = 1/500 = 0.002

	Displacement (mm)					Distortion (for 9.15 m on-center footing spacing)				
	Footing 1	Footing 2	Footing 3	Footing 4	Footing 5	Footing 1-2	Footing 2-3	Footing 3-4	Footing 4-5	
"Deterministic" estimate	23.2	30.3	30.5	28.9	23.7	7.2	0.13	1.5	5.2	
Simulated - mean	129.4	120.5	123.5	111.3	131.7	207.3	201.1	195.5	200.4	"Deterministic" estimate
Simulated - median	20.4	20.7	20.7	19.7	20.9	22.3	21.2	20.7	21.6	Simulated - mean
Simulated - Std Dev	376.7	404.7	412.4	388.1	378.9	513.6	540.9	534.1	503.3	Simulated - median
Simulated COV	2.91	3.36	3.34	3.49	2.88	2.48	2.69	2.73	2.51	Simulated - Std Dev
Minimum (neg. value is uplift)	0.25	0.33	0.17	0.07	0.04	0.000	0.000	0.000	0.001	Simulated COV
Maximum	1675.0	2125.0	2125.0	2125.0	1675.0	2124.3	2124.6	2124.9	2124.5	Minimum
Prob exceeding "calculated" value	0.453	0.360	0.357	0.356	0.452	0.78	0.99	0.95	0.83	Maximum
Prob exceeding 12.5 mm	0.679	0.692	0.690	0.673	0.691	0.66	0.65	0.64	0.65	Prob of failure, $p_f$ =
Prob exceeding 25 mm	0.426	0.428	0.427	0.408	0.434	0.47	0.45	0.45	0.46	$\beta$ =
Prob exceeding 50 mm	0.230	0.219	0.216	0.202	0.234	0.30	0.28	0.28	0.30	

Prob exceeding 18.3 mm of differential displacement

\*\*Note -  $p_f$  also equals the probability of exceeding approx. 18.3 mm of differential displacement

**OpenSees Results - Footing Displacements and Angular Distortion at Footing Elevation**

Calculated results from bearing pressure-settlement equation and simulated results with 50,000 simulations that include bearing pressure-settlement equation (with known dispersion of model parameters) and variable soil undrained shear strength across horizontal distance, x.

Soil Parameters		Displacement Model (Vertical Spring) Parameters				Footing Parameters	
$s_u$ (kPa)	$\delta$ (mm)	$k_1$	$k_2$	$M_{stc}$	$B_{1,5}$ (m)	$B_{2,4}$ (m)	Beam Dist.(m)
70	100%	0.013	0.701	0.643	1.675	2.125	9.15
COV( $s_u$ ) =	1	0.007	0.113	0.123			
Scale of Fluctuation, $\delta$ (mm) =	19	53.0	16.1	19.1			
$\gamma'$ (kN/m <sup>3</sup> ) =		Dist. = Gamma Inv. Gauss. Lognormal					

	Displacement (mm)				
	Footing 1	Footing 2	Footing 3	Footing 4	Footing 5
"Deterministic" estimate	23.2	30.3	30.5	28.9	23.7
Simulated - mean	227.7	244.9	248.1	227.8	236.5
Simulated - median	21.4	22.2	22.1	20.9	22.0
Simulated - Std Dev	521.0	614.6	618.8	593.6	530.0
Simulated COV	2.29	2.51	2.49	2.61	2.24
Minimum (neg. value is uplift)	0.14	0.15	0.12	0.07	0.25
Maximum	1675.0	2125.0	2125.0	2125.0	1675.0

	Differential Displacement (mm)				
	Footing 1-2	Footing 2-3	Footing 3-4	Footing 4-5	
"Deterministic" estimate	7.2	0.13	1.5	5.2	
Simulated - mean	393.5	411.9	396.4	388.0	
Simulated - median	31.3	29.8	28.1	30.2	
Simulated - Std Dev	703.0	770.6	758.3	695.6	
Simulated COV	1.79	1.87	1.91	1.79	
Minimum	0.000	0.000	0.000	0.000	
Maximum	2124.7	2124.8	2124.9	2124.4	

	Distortion (for 9.15 m on-center footing spacing)				
	Footing 1-2	Footing 2-3	Footing 3-4	Footing 4-5	
"Deterministic" estimate	0.00078	0.00001	0.00017	0.00057	
Simulated - mean	0.04300	0.04501	0.04332	0.04240	
Simulated - median	0.00342	0.00325	0.00307	0.00330	
Simulated - Std Dev	0.0768	0.0842	0.0829	0.0760	
Simulated COV	1.79	1.87	1.91	1.79	
Minimum	0.0000000	0.0000000	0.0000000	0.0000000	
Maximum	0.23221	0.23222	0.23223	0.23218	

	$p_f$	$\beta$
Prob exceeding "calculated" value	0.474	0.403
Prob exceeding 12.5 mm	0.677	0.692
Prob exceeding 25 mm	0.451	0.460
Prob exceeding 50 mm	0.285	0.283

Prob of failure,  $p_f$  = 0.62 0.61 0.60 0.61 0.61  
 $\beta$  = -0.31 -0.28 -0.25 -0.25 -0.29

\*\*Note -  $p_f$  also equals the probability of exceeding approx. 18.3 mm of differential displacement

"calculated" values assume no variation in soil shear strength or spring parameters  
 "Allowable" Distortion = 1/500 = 0.002

**OpenSees Results - Footing Displacements and Angular Distortion at Footing Elevation**

Calculated results from bearing pressure-settlement equation and simulated results with 50,000 simulations that include bearing pressure-settlement equation (with known dispersion of model parameters) and variable soil undrained shear strength across horizontal distance, x.

Soil Parameters		Displacement Model (Vertical Spring) Parameters				Footing Parameters	
$s_u$ (kPa)	$\gamma$ (kN/m <sup>3</sup> )	$k_1$	$k_2$	$M_{stc}$	$B_{1,5}$ (m)	$B_{2,4}$ (m)	Beam Dist.(m)
70	19	0.013	0.701	0.643	1.675	2.125	9.15
COV( $s_u$ ) = 100%	2	0.007	0.113	0.123			
Scale of Fluctuation, $\delta$ (m) =		53.0	16.1	19.1			
		Dist. = Gamma	Inv. Gauss.	Lognormal			

"calculated" values assume no variation in soil shear strength or spring parameters

"Allowable" Distortion = 1/500 = 0.002

	Displacement (mm)					Differential Displacement (mm)					Distortion (for 9.15 m on-center footing spacing)						
	Footing 1	Footing 2	Footing 3	Footing 4	Footing 5	Footing 1-2	Footing 2-3	Footing 3-4	Footing 4-5	Footing 1-2	Footing 2-3	Footing 3-4	Footing 4-5	Footing 1-2	Footing 2-3	Footing 3-4	Footing 4-5
"Deterministic" estimate	23.2	30.3	30.5	28.9	23.7	7.2	0.13	1.5	5.2	0.00078	0.00001	0.00017	0.00057	0.06166	0.06581	0.06404	0.05995
Simulated - mean	324.7	380.0	379.1	360.2	330.5	564.2	602.1	585.9	548.5	0.00510	0.00430	0.00414	0.00491	0.00510	0.00430	0.00414	0.00491
Simulated - median	22.7	23.4	23.4	22.4	23.2	46.7	39.3	37.9	45.0	0.0882	0.0982	0.0973	0.0871	0.0882	0.0982	0.0973	0.0871
Simulated - Std Dev	619.5	765.7	764.6	747.9	624.1	807.5	898.4	890.1	796.7	1.43	1.49	1.52	1.45	1.43	1.49	1.52	1.45
Simulated COV	1.91	2.02	2.02	2.08	1.89	1.43	1.49	1.45	1.45	1.43	1.49	1.52	1.45	1.43	1.49	1.52	1.45
Minimum (neg. value is uplift)	0.12	0.19	0.18	0.11	0.11	0.000	0.000	0.000	0.000	0.0000000	0.0000000	0.0000000	0.0000000	0.0000000	0.0000000	0.0000000	0.0000000
Maximum	1675.0	2125.0	2125.0	2125.0	1675.0	2124.7	2124.8	2124.6	2124.9	0.23221	0.23222	0.23220	0.23223	0.23221	0.23222	0.23220	0.23223
Prob exceeding "calculated" value	0.494	0.431	0.430	0.431	0.494	0.83	0.97	0.93	0.86	0.66	0.64	0.63	0.66	0.66	0.64	0.63	0.66
Prob exceeding 12.5 mm	0.677	0.687	0.690	0.678	0.682	0.73	0.71	0.70	0.73	-0.41	-0.35	-0.34	-0.40	-0.41	-0.35	-0.34	-0.40
Prob exceeding 25 mm	0.474	0.481	0.481	0.470	0.480	0.60	0.58	0.57	0.60								
Prob exceeding 50 mm	0.331	0.330	0.330	0.320	0.335	0.49	0.46	0.46	0.48								

Prob of failure,  $p_f$  = 0.66     $\beta$  = -0.41     $\beta$  = -0.35     $\beta$  = -0.34     $\beta$  = -0.40

\*\*Note -  $p_f$  also equals the probability of exceeding approx. 18.3 mm of differential displacement

**OpenSees Results - Footing Displacements and Angular Distortion at Footing Elevation**

Calculated results from bearing pressure-settlement equation and simulated results with 50,000 simulations that include bearing pressure-settlement equation (with known dispersion of model parameters) and variable soil undrained shear strength across horizontal distance, x.

Soil Parameters		Displacement Model (Vertical Spring) Parameters					Footing Parameters	
$s_u$ (kPa)	$\delta$ (mm)	$k_1$	$k_2$	$M_{stc}$	$B_{1.5}$ (m)	$B_{3.4}$ (m)	Beam Dist.(m)	
70	100%	0.013	0.701	0.643	1.675	2.125	9.15	
COV( $s_u$ ) =	5	0.007	0.113	0.123				
Scale of Fluctuation, $\delta$ (mm) =	19	53.0	16.1	19.1				
$\gamma$ (kN/m <sup>3</sup> ) =		Gamma	Inv. Gauss.	Lognormal				

"calculated" values assume no variation in soil shear strength or spring parameters  
 "Allowable" Distortion = 1/500 = 0.002

	Displacement (mm)					Differential Displacement (mm)				
	Footing 1	Footing 2	Footing 3	Footing 4	Footing 5	Footing 1-2	Footing 2-3	Footing 3-4	Footing 4-5	
"Deterministic" estimate	23.2	30.3	30.5	28.9	23.7	7.2	0.13	1.5	5.2	
Simulated - mean	415.7	499.7	495.3	488.4	418.9	640.9	673.2	664.9	633.9	"Deterministic" estimate
Simulated - median	24.1	24.5	24.5	23.3	24.5	63.8	36.2	34.9	60.8	Simulated - mean
Simulated - Std Dev	689.7	862.9	859.4	855.7	691.1	831.7	936.5	932.9	827.3	Simulated - median
Simulated COV	1.66	1.73	1.74	1.75	1.65	1.30	1.39	1.40	1.31	Simulated - Std Dev
Minimum (neg. value is uplift)	0.11	0.16	0.21	0.12	0.16	0.003	0.000	0.000	0.000	Simulated COV
Maximum	1675.0	2125.0	2125.0	2125.0	1675.0	2124.8	2124.8	2124.8	2124.7	Minimum
Prob exceeding "calculated" value	0.510	0.450	0.450	0.449	0.508	0.82	0.93	0.89	0.86	Maximum
Prob exceeding 12.5 mm	0.678	0.687	0.687	0.672	0.682	0.73	0.67	0.67	0.73	Prob of failure, $p_f$ =
Prob exceeding 25 mm	0.492	0.494	0.495	0.482	0.495	0.62	0.55	0.55	0.61	$\beta$ =
Prob exceeding 50 mm	0.367	0.363	0.363	0.354	0.368	0.52	0.46	0.46	0.52	0.67
Location of min value	\$B\$34741	\$C\$35553	\$D\$4791	\$E\$19329	\$F\$53795					0.61
Location of max value	\$B\$336	\$C\$336	\$D\$335	\$E\$335	\$F\$338					0.60
										0.27
										-0.25
										-0.42

\*\*Note -  $p_f$  also equals the probability of exceeding approx. 18.3 mm of differential displacement

**OpenSees Results - Footing Displacements and Angular Distortion at Footing Elevation**

Calculated results from bearing pressure-settlement equation and simulated results with 50,000 simulations that include bearing pressure-settlement equation (with known dispersion of model parameters) and variable soil undrained shear strength across horizontal distance, x.

Soil Parameters		Displacement Model (Vertical Spring) Parameters				Footing Parameters	
$s_u$ (kPa)	$k_z$	$k_1$	$k_2$	$M_{stc}$	$B_{1,5}$ (m)	$B_{3,4}$ (m)	Beam Dist.(m)
70	0.701	0.013	0.701	0.643	1.675	2.125	9.15
COV( $s_u$ ) = 100%	0.007	0.113	0.123	19.1			
Scale of Fluctuation, $\delta$ (m) = 10	53.0	16.1					
$\gamma$ (kN/m <sup>3</sup> ) = 19	Dist. = Gamma	Inv. Gauss.	Lognormal				

"calculated" values assume no variation in soil shear strength or spring parameters  
 "Allowable" Distortion = 1/500 = 0.002

	Displacement (mm)				Differential Displacement (mm)				Distortion (for 9.15 m on-center footing spacing)				
	Footing 1	Footing 2	Footing 3	Footing 4	Footing 5	Footing 1-2	Footing 2-3	Footing 3-4	Footing 4-5	Footing 1-2	Footing 2-3	Footing 3-4	Footing 4-5
"Deterministic" estimate	23.2	30.3	30.5	28.9	23.7	7.2	0.13	1.5	5.2	0.00078	0.00001	0.00017	0.00057
Simulated - mean	446.3	556.1	561.9	541.6	454.2	588.0	600.8	601.0	581.5	0.06426	0.06566	0.06568	0.06355
Simulated - median	24.1	24.9	25.3	24.0	24.6	53.8	22.7	22.8	51.8	0.00588	0.00248	0.00249	0.00566
Simulated - Std Dev	710.1	899.8	903.6	892.6	714.2	798.4	907.9	908.9	793.5	0.0873	0.0992	0.0993	0.0867
Simulated COV	1.59	1.62	1.61	1.65	1.57	1.36	1.51	1.51	1.36	1.36	1.51	1.51	1.36
Minimum (neg. value is uplift)	0.18	0.19	0.12	0.20	0.08	0.000	0.000	0.000	0.001	0.0000000	0.0000000	0.0000000	0.0000001
Maximum	1675.0	2125.0	2125.0	2125.0	1675.0	2124.8	2124.7	2124.8	2124.8	0.23222	0.23221	0.23222	0.23222
Prob exceeding "calculated" value	0.509	0.458	0.459	0.459	0.510	0.80	0.89	0.84	0.84	0.64	0.53	0.54	0.63
Prob exceeding 12.5 mm	0.673	0.682	0.687	0.675	0.681	0.71	0.60	0.60	0.70	-0.36	-0.09	-0.09	-0.35
Prob exceeding 25 mm	0.492	0.499	0.502	0.491	0.486	0.59	0.49	0.49	0.59				
Prob exceeding 50 mm	0.372	0.379	0.378	0.369	0.376	0.51	0.40	0.40	0.50				
Location of min value	\$B\$48547	\$C\$48365	\$D\$49789	\$E\$16107	\$F\$16517								
Location of max value	\$B\$35	\$C\$37	\$D\$39	\$E\$36	\$F\$38								

Prob of failure,  $p_f$  = 0.64     $\beta$  = -0.36     $\beta$  = -0.09     $\beta$  = -0.09     $\beta$  = 0.63     $\beta$  = -0.35  
 \*\*Note -  $p_f$  also equals the probability of exceeding approx. 18.3 mm of differential displacement

**OpenSees Results - Footing Displacements and Angular Distortion at Footing Elevation**

Calculated results from bearing pressure-settlement equation and simulated results with 50,000 simulations that include bearing pressure-settlement equation (with known dispersion of model parameters) and variable soil undrained shear strength across horizontal distance, x.

Soil Parameters		Displacement Model (Vertical Spring) Parameters				Footing Parameters	
$s_u$ (kPa)	$k_z$	$k_1$	$k_2$	$M_{stc}$	$B_{1.5}$ (m)	$B_{3.4}$ (m)	Beam Dist.(m)
70	0.701	0.013	0.701	0.643	1.675	2.125	9.15
COV( $s_u$ ) = 100%	0.007	0.113	0.123				
Scale of Fluctuation, $\delta$ (m) = 20	53.0	16.1	19.1				
$\gamma$ (kN/m <sup>3</sup> ) = 19	Dist. = Gamma	Inv. Gauss.	Lognormal				

"calculated" values assume no variation in soil shear strength or spring parameters  
 "Allowable" Distortion = 1/500 = 0.002

	Displacement (mm)					Differential Displacement (mm)					Distortion (for 9.15 m on-center footing spacing)						
	Footing 1	Footing 2	Footing 3	Footing 4	Footing 5	Footing 1-2	Footing 2-3	Footing 3-4	Footing 4-5	Footing 1-2	Footing 2-3	Footing 3-4	Footing 4-5	Footing 1-2	Footing 2-3	Footing 3-4	Footing 4-5
"Deterministic" estimate	23.2	30.3	30.5	28.9	23.7	7.2	0.13	1.5	5.2	0.00078	0.00001	0.00017	0.00057	0.05441	0.05217	0.05187	0.05373
Simulated - mean	461.8	584.6	585.9	573.0	471.2	497.8	477.3	474.6	491.6	0.00413	0.00155	0.00154	0.00406	0.00413	0.00155	0.00154	0.00406
Simulated - median	24.3	25.0	25.4	24.0	24.8	37.8	14.2	14.1	37.1	0.0807	0.0918	0.0916	0.0800	0.0807	0.0918	0.0916	0.0800
Simulated - Std Dev	719.7	918.1	918.9	912.8	725.1	736.1	839.9	838.5	731.5	1.48	1.76	1.77	1.49	1.48	1.76	1.77	1.49
Simulated COV	1.56	1.57	1.57	1.59	1.54	1.48	1.76	1.77	1.49								
Minimum (neg. value is uplift)	0.23	0.10	0.22	0.04	0.08	0.000	0.000	0.000	0.000	0.0000000	0.0000000	0.0000000	0.0000000	0.0000000	0.0000000	0.0000000	0.0000000
Maximum	1675.0	2125.0	2125.0	2125.0	1675.0	2124.1	2124.7	2124.6	2124.5	0.23215	0.23220	0.23220	0.23219	0.23215	0.23220	0.23220	0.23219
Prob exceeding "calculated" value	0.511	0.459	0.462	0.460	0.511	0.77	0.85	0.79	0.82	0.60	0.46	0.45	0.60	0.60	0.46	0.45	0.60
Prob exceeding 12.5 mm	0.675	0.684	0.685	0.672	0.679	0.67	0.52	0.52	0.67	-0.26	0.11	0.12	-0.25	-0.26	0.11	0.12	-0.25
Prob exceeding 25 mm	0.493	0.500	0.504	0.491	0.486	0.55	0.41	0.40	0.55								
Prob exceeding 50 mm	0.376	0.382	0.383	0.374	0.381	0.47	0.33	0.32	0.47								
Location of min value	\$B\$14638	\$C\$45574	\$D\$31674	\$E\$42462	\$F\$25440												
Location of max value	\$B\$37	\$C\$38	\$D\$37	\$E\$37	\$F\$38												

\*\*Note - p, also equals the probability of exceeding approx. 18.3 mm of differential displacement



**OpenSees Results - Footing Displacements and Angular Distortion at Footing Elevation**

Calculated results from bearing pressure-settlement equation and simulated results with 50,000 simulations that include bearing pressure-settlement equation (with known dispersion of model parameters) and variable soil undrained shear strength across horizontal distance, x.

Soil Parameters		Displacement Model (Vertical Spring) Parameters				Footing Parameters	
$s_u$ (kPa)	$k_z$	$k_1$	$k_2$	$M_{stc}$	$B_{1.5}$ (m)	$B_{3.4}$ (m)	Beam Dist.(m)
70	0.701	0.013	0.701	0.643	1.675	2.125	9.15
COV( $s_u$ ) = 100%	0.007	0.113	0.123				
Scale of Fluctuation, $\delta$ (m) = 30	53.0	16.1	19.1				
$\gamma$ (kN/m <sup>3</sup> ) = 19	Dist. = Gamma	Inv. Gauss.	Lognormal				

	Displacement (mm)					Differential Displacement (mm)					Distortion (for 9.15 m on-center footing spacing)						
	Footing 1	Footing 2	Footing 3	Footing 4	Footing 5	Footing 1-2	Footing 2-3	Footing 3-4	Footing 4-5	Footing 1-2	Footing 2-3	Footing 3-4	Footing 4-5	Footing 1-2	Footing 2-3	Footing 3-4	Footing 4-5
"Deterministic" estimate	23.2	30.3	30.5	28.9	23.7	7.2	0.13	1.5	5.2	0.00078	0.00001	0.00017	0.00057	0.04880	0.04472	0.04456	0.04812
Simulated - mean	474.6	596.5	597.0	591.3	478.5	446.5	409.2	407.7	440.3	0.00360	0.00124	0.00122	0.00341	0.0759	0.0864	0.0863	0.0752
Simulated - median	24.6	25.3	25.3	23.9	24.9	32.9	11.4	11.2	31.2	0.0759	1.93	1.94	1.56	1.56	1.93	1.94	1.56
Simulated - Std Dev	726.8	925.3	925.3	923.3	729.3	694.4	790.9	789.9	688.3	0.0000000	0.0000000	0.0000000	0.0000001	0.23219	0.23220	0.23219	0.23217
Simulated COV	1.53	1.55	1.55	1.56	1.52	1.56	1.93	1.94	1.56	0.0000000	0.0000000	0.0000000	0.0000001	0.23219	0.23220	0.23219	0.23217
Minimum (neg. value is uplift)	0.10	0.10	0.10	0.14	0.16	0.000	0.000	0.000	0.001	0.0000000	0.0000000	0.0000000	0.0000001	0.23219	0.23220	0.23219	0.23217
Maximum	1675.0	2125.0	2125.0	2125.0	1675.0	2124.6	2124.6	2124.6	2124.3	0.0000000	0.0000000	0.0000000	0.0000001	0.23219	0.23220	0.23219	0.23217
Prob exceeding "calculated" value	0.513	0.462	0.461	0.460	0.512	0.76	0.82	0.77	0.81	0.58	0.41	0.41	0.58	0.58	0.41	0.41	0.58
Prob exceeding 12.5 mm	0.675	0.684	0.684	0.672	0.681	0.65	0.48	0.48	0.65	-0.21	0.22	0.23	-0.19	0.22	0.23	0.23	-0.19
Prob exceeding 25 mm	0.496	0.502	0.503	0.490	0.499	0.53	0.36	0.36	0.53								
Prob exceeding 50 mm	0.381	0.384	0.382	0.375	0.382	0.46	0.28	0.28	0.45								
Location of min value	\$B\$35694	\$C\$39270	\$D\$5799	\$E\$29890	\$F\$26223												
Location of max value	\$B\$36	\$C\$36	\$D\$36	\$E\$40	\$F\$36												

\*\*Note - p, also equals the probability of exceeding approx. 18.3 mm of differential displacement

**OpenSees Results - Footing Displacements and Angular Distortion at Footing Elevation**

Calculated results from bearing pressure-settlement equation and simulated results with 50,000 simulations that include bearing pressure-settlement equation (with known dispersion of model parameters) and variable soil undrained shear strength across horizontal distance, x.

Soil Parameters		Displacement Model (Vertical Spring) Parameters					Footing Parameters	
$s_u$ (kPa)	$\delta$ (mm)	$k_1$	$k_2$	$M_{stc}$	$B_{1.5}$ (m)	$B_{3.4}$ (m)	Beam Dist.(m)	
70	100%	0.013	0.701	0.643	1.675			
COV( $s_u$ ) =	50	0.007	0.113	0.123	2.125			
Scale of Fluctuation, $\delta$ (m) =	19	53.0	16.1	19.1	9.15			
$\gamma'$ (kN/m <sup>3</sup> ) =		Dist. = Gamma		Inv. Gauss.	Lognormal			

	Displacement (mm)					Differential Displacement (mm)					Distortion (for 9.15 m on-center footing spacing)						
	Footing 1	Footing 2	Footing 3	Footing 4	Footing 5	Footing 1-2	Footing 2-3	Footing 3-4	Footing 4-5	Footing 1-2	Footing 2-3	Footing 3-4	Footing 4-5	Footing 1-2	Footing 2-3	Footing 3-4	Footing 4-5
"Deterministic" estimate	23.2	30.3	30.5	28.9	23.7	7.2	0.13	1.5	5.2	0.00078	0.00001	0.00017	0.00057	0.04124	0.03582	0.03520	0.04137
Simulated - mean	480.3	605.5	603.7	593.7	477.8	377.3	327.8	322.0	378.5	0.04124	0.03582	0.03520	0.04137	0.00293	0.00100	0.00099	0.00282
Simulated - median	24.4	25.1	25.4	24.0	24.9	26.8	9.2	9.0	25.8	0.0686	0.0786	0.0779	0.0688	1.66	2.19	2.21	1.66
Simulated - Std Dev	731.0	930.9	929.1	925.1	728.9	627.9	718.9	713.2	629.4	0.0000000	0.0000000	0.0000000	0.0000000	0.23216	0.23216	0.23212	0.23217
Simulated COV	1.52	1.54	1.54	1.56	1.53	1.66	2.19	2.21	1.66	0.56	0.37	0.34	0.55	0.56	0.37	0.36	0.55
Minimum (neg. value is uplift)	0.15	0.28	0.19	0.11	0.10	0.000	0.000	0.000	0.000	0.56	0.37	0.34	0.55	0.56	0.37	0.36	0.55
Maximum	1675.0	2125.0	2125.0	2125.0	1675.0	2124.3	2124.3	2123.9	2124.4	0.56	0.37	0.34	0.55	0.56	0.37	0.36	0.55
Prob exceeding "calculated" value	0.512	0.461	0.463	0.461	0.511	0.74	0.80	0.74	0.79	0.56	0.37	0.34	0.55	0.56	0.37	0.36	0.55
Prob exceeding 12.5 mm	0.674	0.680	0.680	0.670	0.678	0.63	0.44	0.44	0.63	0.56	0.37	0.34	0.55	0.56	0.37	0.36	0.55
Prob exceeding 25 mm	0.495	0.501	0.503	0.491	0.499	0.51	0.32	0.31	0.50	0.56	0.37	0.34	0.55	0.56	0.37	0.36	0.55
Prob exceeding 50 mm	0.381	0.384	0.385	0.377	0.381	0.43	0.24	0.24	0.43	0.56	0.37	0.34	0.55	0.56	0.37	0.36	0.55
Location of min value	\$B\$22008	\$C\$24658	\$D\$48543	\$E\$8447	\$F\$8778												
Location of max value	\$B\$38	\$C\$38	\$D\$38	\$E\$38	\$F\$35												

"Allowable" Distortion = 1/500 = 0.002

\*\*Note - p, also equals the probability of exceeding approx. 18.3 mm of differential displacement

**OpenSees Results - Footing Displacements and Angular Distortion at Footing Elevation**

Calculated results from bearing pressure-settlement equation and simulated results with 50,000 simulations that include bearing pressure-settlement equation (with known dispersion of model parameters) and variable soil undrained shear strength across horizontal distance, X.

Soil Parameters		Displacement Model (Vertical Spring) Parameters			Footing Parameters	
$s_u$ (kPa) =	70	$k_1$	$k_2$	$M_{stc}$	$B_{1.5}$ (m) =	1.675
COV( $s_u$ ) =	100%	$\mu$ =	0.013	0.701	0.643	
Scale of Fluctuation, $\delta$ (m) =	100	$\sigma$ =	0.007	0.113	0.123	2.125
$\gamma$ (kN/m <sup>3</sup> ) =	19	COV(%) =	53.0	16.1	19.1	9.15
		Dist. =	Gamma	Inv. Gauss.	Lognormal	

"calculated" values assume no variation in soil shear strength or spring parameters  
 "Allowable" Distortion = 1/500 = 0.002

	Displacement (mm)					Differential Displacement (mm)					Distortion (for 9.15 m on-center footing spacing)						
	Footing 1	Footing 2	Footing 3	Footing 4	Footing 5	Footing 1-2	Footing 2-3	Footing 3-4	Footing 4-5	Footing 1-2	Footing 2-3	Footing 3-4	Footing 4-5	Footing 1-2	Footing 2-3	Footing 3-4	Footing 4-5
"Deterministic" estimate	23.2	30.3	30.5	28.9	23.7	7.2	0.13	1.5	5.2	0.00078	0.00001	0.00017	0.00057	0.03414	0.02670	0.02581	0.03397
Simulated - mean	480.1	607.2	604.3	596.6	487.0	312.4	244.3	236.1	310.8	0.03414	0.02670	0.02581	0.03397	0.00246	0.00084	0.00081	0.00246
Simulated - median	24.6	25.5	25.5	24.1	25.3	22.5	7.7	7.4	22.5	0.00246	0.00084	0.00081	0.00246	0.0603	0.0684	0.0673	0.0598
Simulated - Std Dev	731.4	931.4	929.8	927.4	733.9	551.4	625.7	616.1	547.4	1.77	2.56	2.61	1.76	1.77	2.56	2.61	1.76
Simulated COV	1.52	1.53	1.54	1.55	1.51	1.77	2.56	2.61	1.76	0.0000000	0.0000000	0.0000000	0.0000000	0.0000000	0.0000000	0.0000000	0.0000000
Minimum (neg. value is uplift)	0.15	0.13	0.14	0.19	0.07	0.000	0.000	0.000	0.000	0.0000000	0.0000000	0.0000000	0.0000000	0.0000000	0.0000000	0.0000000	0.0000000
Maximum	1675.0	2125.0	2125.0	2125.0	1675.0	2123.5	2123.6	2124.3	2123.9	0.23208	0.23209	0.23216	0.23212	0.54	0.32	0.32	0.53
Prob exceeding "calculated" value	0.513	0.464	0.464	0.461	0.514	0.72	0.78	0.71	0.78	0.61	0.40	0.39	0.61	-0.09	0.45	0.47	-0.09
Prob exceeding 12.5 mm	0.674	0.684	0.683	0.667	0.680	0.61	0.40	0.39	0.61	0.48	0.27	0.27	0.48				
Prob exceeding 25 mm	0.496	0.505	0.504	0.491	0.503	0.48	0.27	0.27	0.48	0.41	0.20	0.19	0.41				
Prob exceeding 50 mm	0.378	0.387	0.387	0.378	0.386	0.41	0.20	0.19	0.41								
Location of min value	\$B\$41273	\$C\$3131	\$D\$47333	\$E\$29078	\$F\$25517												
Location of max value	\$B\$41	\$C\$39	\$D\$36	\$E\$36	\$F\$36												

\*\*Note - p, also equals the probability of exceeding approx. 18.3 mm of differential displacement